VOLUME 26 / NUMBER 4
FEBRUARY 23, 1988
ACC. NOS. N88-12452 TO N88-13214

STAR

AN ABSTRACT JOURNAL

Scientific and Technical Aerospace Reports

PRODUCED BY THE
SCIENTIFIC AND TECHNICAL
INFORMATION
DIVISION

NASA

NATIONAL AERONAUTICS AND SPACE ADMINISTRATION

WHAT YOU CAN DO FOR *STAR*

All users of this abstract service are urged to forward reports to be considered for announcement in *STAR*. This will aid NASA in its efforts to provide the fullest possible coverage of all scientific and technical publications that might support aeronautics and space research and development. If you have prepared relevant reports (other than those that you will transmit to NASA, DoD, or DOE through the usual contract- or grant-reporting channels), please send them for consideration to the NASA Scientific and Technical Information Facility, P.O. Box 8757, B.W.I. Airport, Maryland 21240.

Reprints of journal articles, book chapters, and conference papers are also welcome. These will be considered for announcement in *STAR*'s companion journal, *International Aerospace Abstracts*.

You may specify a particular source to be included in a report announcement if you wish; otherwise the report will be placed on public sale at the National Technical Information Service. Copyrighted publications will be announced but not distributed or sold.

PURCHASE OF *STAR*

The semimonthly issues are available for sale by the Superintendent of Documents, U.S. Government Printing Office, Washington, D.C. 20402.

PUBLISHED BY:

UNITED STATES GOVERNMENT
NATIONAL AERONAUTICS AND SPACE ADMINISTRATION
SCIENTIFIC AND TECHNICAL INFORMATION DIVISION
Scientific and Technical Aerospace Reports, Volume 26, is prepared by the NASA Scientific and Technical Information Facility operated for the National Aeronautics and Space Administration by RMS Associates.

The Administrator of the National Aeronautics and Space Administration has determined that the publication of this periodical is necessary in the transaction of the public business required by law of this Agency. Use of funds for printing this periodical has been approved by the Director of the Office of Management and Budget through March 22, 1988.

US ISSN 0036-8741

INTRODUCTION

Scientific and Technical Aerospace Reports (STAR) is a major component of a comprehensive National Aeronautics and Space Administration information system covering aeronautics, space, and supporting disciplines. *STAR* is issued on the 8th and 23rd of each month and announces current publications of the following types:

- NASA, NASA contractor, and NASA grantee reports
- Reports issued by other U.S. Government Agencies, domestic and foreign institutions, universities, and private firms
- Translations in report form
- NASA-owned patents and patent applications
- Dissertations and theses

Journal, book, and conference literature, cover-to-cover journal translations, and certain foreign dissertations are announced in a companion journal, *International Aerospace Abstracts (IAA),* available on subscription from the American Institute of Aeronautics and Astronautics, Technical Information Service, 555 West 57th Street, 12th Floor, New York, New York 10019.

SUBJECT SCOPE

Subject scope of *STAR,* and *IAA* includes all aspects of aeronautics and space research and development, supporting basic and applied research, and applications. Aerospace aspects of earth resources, energy development, conservation, oceanography, environmental protection, urban transportation, and other topics of high national priority are also covered.

OTHER NASA PUBLICATIONS

Other NASA publications and information services are described in the publication, *The NASA Scientific and Technical Information System ... and How to Use It,* available without charge from the NASA Scientific and Technical Information Facility, P.O. Box 8757, B.W.I. Airport, Maryland 21240.

HOW TO USE *STAR* SUBJECT CATEGORIES

STAR is categorized by 10 major subject divisions divided into 76 specific subject categories and one general category/division. The major subject divisions are listed in the Table of Contents, together with a note for each that defines its scope and provides any cross-references. For example:

AERONAUTICS

Includes aeronautics (general); aerodynamics; air transportation and safety; aircraft communications and navigation; aircraft design, testing and performance; aircraft instrumentation; aircraft propulsion and power; aircraft stability and control; and research and support facilities (air).

For related information see also *Astronautics.*

Each major division is further divided into as many as nine specific categories, which are identified by category numbers.

Abstracts in *STAR* are grouped by specific category, the categories appearing in sequential order. Category breaks in the abstract section are identified by the category number and title, and a scope note. Cross-references to other categories are provided as appropriate. For example:

02 AERODYNAMICS

Includes aerodynamics of bodies, combinations, wings, rotors, and control surfaces; and internal flow in ducts and turbomachinery.

For related information see also *34 Fluid Mechanics and Heat Transfer.*

CROSS-REFERENCES

Individual *STAR* abstracts are not ordinarily cross-referenced, except for certain conference reports or book translations that have had separate abstracts written for their component papers or chapters. Citations and abstracts of the components follow immediately after those of the parent document. When the subject content of a component differs sufficiently from the general content of the parent, a cross-reference citation also is printed at the end of the category to which it normally would have been assigned if it were independent.

DOCUMENTS ON MICROFICHE

Documents on microfiche[1] are designated by a pound sign (#) following the accession number. The pound sign is used without regard to the source or quality of the microfiche.

AVAILABILITIES

One or more sources from which a document announced in *STAR* is available to the public is given in each citation. The most commonly indicated sources and their acronyms or abbreviations are listed below. If the publication is available from a source other than those listed, the publisher and his address will be displayed on the availability line or in combination with the corporate source line.

Avail: NTIS. Sold by the National Technical Information Service. Prices for hard copy (HC) and microfiche (MF) are indicated by a price code following the letters HC or MF in the *STAR* citation. Current values for the price codes are given in the tables on page vii.

Initially distributed microfiche under the NTIS SRIM (Selected Research in Microfiche) is available at greatly reduced unit prices. For this service and for information concerning subscription to NASA printed reports, consult the NTIS Subscription Section, Springfield, Va. 22161.

NOTE ON ORDERING DOCUMENTS: When ordering NASA publications (those followed by the * symbol), use the N accession number. NASA patent applications (only the specifications are offered) should be ordered by the US-Patent-Appl-SN number. Non-NASA publications (no asterisk) should be ordered by the AD, PB, or other *report number* shown on the last line of the citation, not by the N accession number. It is also advisable to cite the title and other bibliographic identification.

Avail: SOD (or GPO). Sold by the Superintendent of Documents, U.S. Government Printing Office, in hard copy. The current price and order number are given following the availability line. (NTIS will fill microfiche requests, as indicated above, for those documents identified by a # symbol.)

(1) A microfiche is a transparent sheet of film, 105 by 148 mm in size, containing as many as 60 to 98 pages of information reduced to micro images (not to exceed 26:1 reduction).

Avail: BLL (formerly NLL): British Library Lending Division, Boston Spa, Wetherby, Yorkshire, England. Photocopies available from this organization at the price shown. (If none is given, inquiry should be addressed to the BLL.)

Avail: DOE Depository Libraries. Organizations in U.S. cities and abroad that maintain collections of Department of Energy reports, usually in microfiche form, are listed in *Energy Research Abstracts*. Services available from the DOE and its depositories are described in a booklet, *DOE Technical Information Center - Its Functions and Services* (TID-4660), which may be obtained without charge from the DOE Technical Information Center.

Avail: ESDU. Pricing information on specific data, computer programs, and details on ESDU topic categories can be obtained from ESDU International Ltd. Requesters in North America should use the Virginia address while all other requesters should use the London address, both of which are on page vi.

Avail: Fachinformationszentrum, Karlsruhe. Sold by the Fachinformationszentrum Energie, Physik, Mathematik GMBH, Eggenstein Leopoldshafen, Federal Republic of Germany, at the price shown in deutschmarks (DM).

Avail: HMSO. Publications of Her Majesty's Stationery Office are sold in the U.S. by Pendragon House, Inc. (PHI), Redwood City, California. The U.S. price (including a service and mailing charge) is given, or a conversion table may be obtained from PHI.

Avail: NASA Public Document Rooms. Documents so indicated may be examined at or purchased from the National Aeronautics and Space Administration, Public Documents Room (Room 126), 600 Independence Ave., S.W., Washington, D.C. 20546, or public document rooms located at each of the NASA research centers, the NASA Space Technology Laboratories, and the NASA Pasadena Office at the Jet Propulsion Laboratory.

Avail: Univ. Microfilms. Documents so indicated are dissertations selected from *Dissertation Abstracts* and are sold by University Microfilms as xerographic copy (HC) and microfilm. All requests should cite the author and the Order Number as they appear in the citation.

Avail: US Patent and Trademark Office. Sold by Commissioner of Patents and Trademarks, U.S. Patent and Trademark Office, at the standard price of $1.50 each, postage free. (See discussion of NASA patents and patent applications below.)

Avail: (US Sales Only). These foreign documents are available to users within the United States from the National Technical Information Service (NTIS). They are available to users outside the United States through the International Nuclear Information Service (INIS) representative in their country, or by applying directly to the issuing organization.

Avail: USGS. Originals of many reports from the U.S. Geological Survey, which may contain color illustrations, or otherwise may not have the quality of illustrations preserved in the microfiche or facsimile reproduction, may be examined by the public at the libraries of the USGS field offices whose addresses are listed in this Introduction. The libraries may be queried concerning the availability of specific documents and the possible utilization of local copying services, such as color reproduction.

Avail: Issuing Activity, or Corporate Author, or no indication of availability. Inquiries as to the availability of these documents should be addressed to the organization shown in the citation as the corporate author of the document.

NASA PATENTS AND PATENT APPLICATIONS

Patents and patent applications owned by NASA are announced in *STAR* under appropriate subject categories and are referenced in the *STAR* indexes. In the Report/Accession Number Index, patents are indexed by the NASA Case Number (which appears in lieu of the report number in other indexes), the U.S. Patent Number, the U.S. Patent Application Serial Number, and the U.S. Patent Class. Patent applications for which patents have not yet been issued are indexed by the NASA Case Number and the U.S. Patent Application Serial Number.

NASA *patent application specifications* are sold in paper copy by the National Technical Information Service at price code A02. Microfiche are sold at price code A01. The US-Patent-Appl-SN- number should be used in ordering either paper copy or microfiche from NTIS. Printed copies of *patents* (which are not microfiched) are available for purchase at $1.50 per copy from:

Commissioner of Patents and Trademarks
U.S. Patent and Trademark Office
Washington, D.C. 20231

When ordering patents, the U.S. Patent Number should be used, and payment must be remitted in advance, preferably by money order or check payable to the Commissioner of Patents and Trademarks. Prepaid purchase coupons for ordering are also available from the Patent and Trademark Office. The patents and patent applications announced in *STAR* are owned by NASA and are available for royalty-free licensing. Requests for licensing terms and further information should be addressed to:

Associate General Counsel for Intellectual Property/Code GP
National Aeronautics and Space Administration
Washington, D.C. 20546

ELIGIBILITY AND REGISTRATION FOR NASA INFORMATION PRODUCTS AND SERVICES

A variety of services is available to organizations of the following types that have registered with NASA to receive specific services or products:

1. NASA offices, research centers, contractors, subcontractors, grantees, and consultants;
2. Other U.S. Government agencies and their contractors;
3. Libraries in the United States that have arrangements with NASA to maintain collections of NASA documents for public reference;
4. Other organizations in the United States having a need for NASA documents in work related to aeronautics and space research;
5. Organizations abroad that have established reciprocal document exchange arrangements with NASA.

Only the central service points or central points of document acquisition and control within qualified organizations are eligible to register for NASA products and services. Domestic organizations that may be eligible to receive various classes of NASA publications and services should address their requests for registration or for further information to:

NASA Scientific and Technical Information Facility
ATTN: Registration Activity
P.O. Box 8757
B.W.I. Airport, Maryland 21240

Organizations abroad should direct requests to the same address, but to the attention of: International Exchange Program.

AVAILABILITY OF *STAR* ABSTRACTS ON MICROFICHE

Microfiche of the abstract sections of this issue and other issues of *STAR* are available on annual subscription from NTIS as PB88-911300, Attn: Subscriptions, 5285 Port Royal Road, Springfield, Virginia 22161. Annual subscription rates are $70.00 North America; $140.00 foreign. Abstract sections for previous years retroactive to 1964 are available at the current rates. Microfiche for individual *STAR* issue abstract sections are not available.

PUBLIC COLLECTIONS OF NASA DOCUMENTS

DOMESTIC: NASA and NASA-sponsored documents and a large number of aerospace publications are available to the public for reference purposes at the library maintained by the American Institute of Aeronautics and Astronautics, Technical Information Service, 555 West 57th Street, 12th Floor, New York, New York 10019

EUROPEAN: An extensive collection of NASA and NASA-sponsored publications is maintained by the British Library Lending Division, Boston Spa, Wetherby, Yorkshire, England for public access. The British Library Lending Division also has available many of the non-NASA publications cited in *STAR*. European requesters may purchase facsimile copy or microfiche of NASA and NASA-sponsored documents, those identified by both the symbols # and * from ESA - Information Retrieval Service European Space Agency, 8-10 rue Mario-Nikis, 75738 Paris CEDEX 15, France.

FEDERAL DEPOSITORY LIBRARY PROGRAM

In order to provide the general public with greater access to U.S. Government publications, Congress established the Federal Depository Library Program under the Government Printing Office (GPO), with 50 regional depositories responsible for permanent retention of material, inter-library loan, and reference services. At least one copy of nearly every NASA and NASA-sponsored publication, either in printed or microfiche format, is received and retained by the 50 regional depositories. A list of the regional GPO libraries, arranged alphabetically by state, appears on the inside back cover. These libraries are *not* sales outlets. A local library can contact a Regional Depository to help locate specific reports, or direct contact may be made by an individual.

ADDRESSES OF ORGANIZATIONS

American Institute of Aeronautics and Astronautics
Technical Information Service
555 West 57th Street, 12th Floor
New York, New York 10019

British Library Lending Division,
Boston Spa, Wetherby, Yorkshire,
England

Commissioner of Patents and Trademarks
U.S. Patent and Trademark Office
Washington, D.C. 20231

Department of Energy
Technical Information Center
P.O. Box 62
Oak Ridge, Tennessee 37830

ESA-Information Retrieval Service
ESRIN
Via Galileo Galilei
00044 Frascati (Rome) Italy

ESDU International, Ltd.
1495 Chain Bridge Road
McLean, Virginia 22101

ESDU International, Ltd.
251-259 Regent Street
London, W1R 7AD, England

Fachinformationszentrum Energie, Physik, Mathematik GMBH
7514 Eggenstein Leopoldshafen
Federal Republic of Germany

Her Majesty's Stationery Office
P.O. Box 569, S.E. 1
London, England

NASA Scientific and Technical Information Facility
P.O. Box 8757
B.W.I. Airport, Maryland 21240

National Aeronautics and Space Administration
Scientific and Technical Information Division (NTT-1)
Washington, D.C. 20546

National Technical Information Service
5285 Port Royal Road
Springfield, Virginia 22161

Pendragon House, Inc.
899 Broadway Avenue
Redwood City, California 94063

Superintendent of Documents
U.S. Government Printing Office
Washington, D.C. 20402

University Microfilms
A Xerox Company
300 North Zeeb Road
Ann Arbor, Michigan 48106

University Microfilms, Ltd.
Tylers Green
London, England

U.S. Geological Survey Library
National Center - MS 950
12201 Sunrise Valley Drive
Reston, Virginia 22092

U.S. Geological Survey Library
2255 North Gemini Drive
Flagstaff, Arizona 86001

U.S. Geological Survey
345 Middlefield Road
Menlo Park, California 94025

U.S. Geological Survey Library
Box 25046
Denver Federal Center, MS914
Denver, Colorado 80225

NTIS PRICE SCHEDULES

(Effective January 1, 1988)

Schedule A
STANDARD PRICE DOCUMENTS AND MICROFICHE

PRICE CODE	PAGE RANGE	NORTH AMERICAN PRICE	FOREIGN PRICE
A01	Microfiche	$ 6.95	$13.90
A02	001-010	9.95	19.90
A03	011-050	12.95	25.90
A04-A05	051-100	14.95	29.90
A06-A09	101-200	19.95	39.90
A10-A13	201-300	25.95	51.90
A14-A17	301-400	32.95	65.90
A18-A21	401-500	38.95	77.90
A22-A25	501-600	44.95	89.90
A99	601-up	*	*
NO1		49.50	89.90
NO2		48.00	80.00

Schedule E
EXCEPTION PRICE DOCUMENTS AND MICROFICHE

PRICE CODE	NORTH AMERICAN PRICE	FOREIGN PRICE
E01	$ 8.50	17.00
E02	11.00	22.00
E03	12.00	24.00
E04	14.50	29.00
E05	16.50	33.00
E06	19.00	38.00
E07	21.50	43.00
E08	24.00	48.00
E09	26.50	53.00
E10	29.00	58.00
E11	31.50	63.00
E12	34.00	68.00
E13	36.50	73.00
E14	39.50	79.00
E15	43.00	86.00
E16	47.00	94.00
E17	51.00	102.00
E18	55.00	110.00
E19	61.00	122.00
E20	71.00	142.00
E99	*	*

*Contact NTIS for price quote.

IMPORTANT NOTICE

NTIS Shipping and Handling Charges
U.S., Canada, Mexico — ADD $3.00 per TOTAL ORDER
All Other Countries — ADD $4.00 per TOTAL ORDER

Exceptions — Does NOT apply to:
ORDERS REQUESTING NTIS RUSH HANDLING
ORDERS FOR SUBSCRIPTION OR STANDING ORDER PRODUCTS *ONLY*

NOTE: Each additional delivery address on an order requires a separate shipping and handling charge.

VOLUME 26 NUMBER 4 / FEBRUARY 23, 1988

TABLE OF CONTENTS

AERONAUTICS

Includes aeronautics (general); aerodynamics; air transportation and safety; aircraft communications and navigation; aircraft design, testing and performance; aircraft instrumentation; aircraft propulsion and power; aircraft stability and control; and research and support facilities (air).

For related information see also *Astronautics.*

01 AERONAUTICS (GENERAL) 393

02 AERODYNAMICS 393

Includes aerodynamics of bodies, combinations, wings, rotors, and control surfaces; and internal flow in ducts and turbomachinery.

For related information see also *34 Fluid Mechanics and Heat Transfer*

03 AIR TRANSPORTATION AND SAFETY 397

Includes passenger and cargo air transport operations; and aircraft accidents.

For related information see also *16 Space Transportation* and *85 Urban Technology and Transportation.*

04 AIRCRAFT COMMUNICATIONS AND NAVIGATION 397

Includes digital and voice communication with aircraft; air navigation systems (satellite and ground based); and air traffic control.

For related information see also *17 Space Communications, Spacecraft Communications, Command and Tracking* and *32 Communications and Radar.*

05 AIRCRAFT DESIGN, TESTING AND PERFORMANCE 398

Includes aircraft simulation technology.

For related information see also *18 Spacecraft Design, Testing and Performance* and *39 Structural Mechanics.* For land transportation vehicles see *85 Urban Technology and Transportation.*

06 AIRCRAFT INSTRUMENTATION 399

Includes cockpit and cabin display devices; and flight instruments.

For related information see also *19 Spacecraft Instrumentation* and *35 Instrumentation and Photography.*

07 AIRCRAFT PROPULSION AND POWER 400

Includes prime propulsion systems and systems components, e.g., gas turbine engines and compressors; and onboard auxiliary power plants for aircraft.

For related information see also *20 Spacecraft Propulsion and Power, 28 Propellants and Fuels,* and *44 Energy Production and Conversion.*

08 AIRCRAFT STABILITY AND CONTROL 400

Includes aircraft handling qualities; piloting; flight controls; and autopilots.

For related information see also *05 Aircraft Design, Testing and Performance.*

09 RESEARCH AND SUPPORT FACILITIES (AIR) 402

Includes airports, hangars and runways; aircraft repair and overhaul facilities; wind tunnels; shock tubes; and aircraft engine test stands.

For related information see also *14 Ground Support Systems and Facilities (Space).*

ASTRONAUTICS

Includes astronautics (general); astrodynamics; ground support systems and facilities (space); launch vehicles and space vehicles; space transportation; space communications, spacecraft communications, command and tracking; spacecraft design, testing and performance; spacecraft instrumentation; and spacecraft propulsion and power.

For related information see also *Aeronautics*

12 ASTRONAUTICS (GENERAL) 403

For extraterrestrial exploration see *91 Lunar and Planetary Exploration.*

13 ASTRODYNAMICS 404

Includes powered and free-flight trajectories; and orbital and launching dynamics.

14 GROUND SUPPORT SYSTEMS AND FACILITIES (SPACE) 404

Includes launch complexes, research and production facilities; ground support equipment, e.g., mobile transporters; and simulators.

For related information see also *09 Research and Support Facilities (Air).*

15 LAUNCH VEHICLES AND SPACE VEHICLES N.A.

Includes boosters; operating problems of launch/space vehicle systems; and reusable vehicles.

For related information see also *20 Spacecraft Propulsion and Power.*

16 SPACE TRANSPORTATION 406

Includes passenger and cargo space transportation, e.g., shuttle operations; and space rescue techniques.

For related information see also *03 Air Transportation and Safety* and *18 Spacecraft Design, Testing and Performance.* For space suits see *54 Man/System Technology and Life Support.*

17 SPACE COMMUNICATIONS, SPACECRAFT COMMUNICATIONS, COMMAND AND TRACKING N.A.

Includes telemetry; space communications networks; astronavigation and guidance; and radio blackout.

For related information see also *04 Aircraft Communications and Navigation* and *32 Communications and Radar.*

18 SPACECRAFT DESIGN, TESTING AND PERFORMANCE 407

Includes satellites; space platforms; space stations; spacecraft systems and components such as thermal and environmental controls; and attitude controls.

For life support systems see *54 Man/System Technology and Life Support.* For related information see also *05 Aircraft Design, Testing and Performance, 39 Structural Mechanics,* and *16 Space Transportation.*

19 SPACECRAFT INSTRUMENTATION N.A.

For related information see also *06 Aircraft Instrumentation* and *35 Instrumentation and Photography.*

20 SPACECRAFT PROPULSION AND POWER 408

Includes main propulsion systems and components, e.g. rocket engines; and spacecraft auxiliary power sources.

For related information see also *07 Aircraft Propulsion and Power, 28 Propellants and Fuels, 44 Energy Production and Conversion,* and *15 Launch Vehicles and Space Vehicles.*

CHEMISTRY AND MATERIALS

Includes chemistry and materials (general); composite materials; inorganic and physical chemistry; metallic materials; nonmetallic materials; propellants and fuels; and materials processing.

23 CHEMISTRY AND MATERIALS (GENERAL) 410

24 COMPOSITE MATERIALS 410

Includes physical, chemical, and mechanical properties of laminates and other composite materials.

For ceramic materials see *27 Nonmetallic Materials.*

25 INORGANIC AND PHYSICAL CHEMISTRY 412

Includes chemical analysis, e.g., chromatography; combustion theory; electrochemistry; and photochemistry.

For related information see also *77 Thermodynamics and Statistical Physics.*

26 METALLIC MATERIALS 414

Includes physical, chemical, and mechanical properties of metals, e.g., corrosion; and metallurgy.

27 NONMETALLIC MATERIALS 418

Includes physical, chemical, and mechanical properties of plastics, elastomers, lubricants, polymers, textiles, adhesives, and ceramic materials.

For composite materials see *24 Composite Materials.*

28 PROPELLANTS AND FUELS 422

Includes rocket propellants, igniters and oxidizers; their storage and handling procedures; and aircraft fuels.

For related information see also *07 Aircraft Propulsion and Power, 20 Spacecraft Propulsion and Power,* and *44 Energy Production and Conversion.*

29 MATERIALS PROCESSING 422

Includes space-based development of products and processes for commercial application.

For biological materials see *55 Space Biology.*

ENGINEERING

Includes engineering (general); communications and radar; electronics and electrical engineering; fluid mechanics and heat transfer; instrumentation and photography; lasers and masers; mechanical engineering; quality assurance and reliability; and structural mechanics.

For related information see also *Physics.*

31 ENGINEERING (GENERAL) 423

Includes vacuum technology; control engineering; display engineering; cryogenics; and fire prevention.

32 COMMUNICATIONS AND RADAR 430

Includes radar; land and global communications; communications theory; and optical communications.

For related information see also *04 Aircraft Communications and Navigation* and *17 Space Communications, Spacecraft Communications, Command and Tracking.* For search and rescue see *03 Air Transportation and Safety,* and *16 Space Transportation.*

33 ELECTRONICS AND ELECTRICAL ENGINEERING 438

Includes test equipment and maintainability; components, e.g., tunnel diodes and transistors; microminiaturization; and integrated circuitry.

For related information see also *60 Computer Operations and Hardware* and *76 Solid-State Physics.*

34 FLUID MECHANICS AND HEAT TRANSFER 441

Includes boundary layers; hydrodynamics; fluidics; mass transfer and ablation cooling.

For related information see also *02 Aerodynamics* and *77 Thermodynamics and Statistical Physics.*

35 INSTRUMENTATION AND PHOTOGRAPHY 446

Includes remote sensors; measuring instruments and gages; detectors; cameras and photographic supplies; and holography.

For aerial photography see *43 Earth Resources and Remote Sensing.* For related information see also *06 Aircraft Instrumentation* and *19 Spacecraft Instrumentation.*

36 LASERS AND MASERS 447

Includes parametric amplifiers.

For related information see also *76 Solid-State Physics.*

37 MECHANICAL ENGINEERING 450

Includes auxiliary systems (nonpower); machine elements and processes; and mechanical equipment.

38 QUALITY ASSURANCE AND RELIABILITY 453

Includes product sampling procedures and techniques; and quality control.

39 STRUCTURAL MECHANICS 453

Includes structural element design and weight analysis; fatigue; and thermal stress.

For applications see *05 Aircraft Design, Testing and Performance* and *18 Spacecraft Design, Testing and Performance.*

GEOSCIENCES

Includes geosciences (general); earth resources and remote sensing; energy production and conversion; environment pollution; geophysics; meteorology and climatology; and oceanography.

For related information see also *Space Sciences.*

42 GEOSCIENCES (GENERAL) 458

43 EARTH RESOURCES AND REMOTE SENSING 462

Includes remote sensing of earth resources by aircraft and spacecraft; photogrammetry; and aerial photography.

For instrumentation see *35 Instrumentation and Photography.*

44 ENERGY PRODUCTION AND CONVERSION 463

Includes specific energy conversion systems, e.g., fuel cells; global sources of energy; geophysical conversion; and windpower.

For related information see also *07 Aircraft Propulsion and Power, 20 Spacecraft Propulsion and Power,* and *28 Propellants and Fuels.*

45 ENVIRONMENT POLLUTION N.A.

Includes atmospheric, noise, thermal, and water pollution.

46 GEOPHYSICS 467

Includes aeronomy; upper and lower atmosphere studies; ionospheric and magnetospheric physics; and geomagnetism.

For space radiation see *93 Space Radiation.*

47 METEOROLOGY AND CLIMATOLOGY 469

Includes weather forecasting and modification.

48 OCEANOGRAPHY 471

Includes biological, dynamic, and physical oceanography; and marine resources.

For related information see also *43 Earth Resources and Remote Sensing.*

LIFE SCIENCES

Includes life sciences (general); aerospace medicine; behavioral sciences; man/system technology and life support; and space biology.

51 LIFE SCIENCES (GENERAL) 473

52 AEROSPACE MEDICINE 473

Includes physiological factors; biological effects of radiation; and effects of weightlessness on man and animals.

53 BEHAVIORAL SCIENCES 474

Includes psychological factors; individual and group behavior; crew training and evaluation; and psychiatric research.

54 MAN/SYSTEM TECHNOLOGY AND LIFE SUPPORT 475

Includes human engineering; biotechnology; and space suits and protective clothing.

For related information see also *16 Space Transportation.*

55 SPACE BIOLOGY N.A.

Includes exobiology; planetary biology; and extraterrestrial life.

MATHEMATICAL AND COMPUTER SCIENCES

Includes mathematical and computer sciences (general); computer operations and hardware; computer programming and software; computer systems; cybernetics; numerical analysis; statistics and probability; systems analysis; and theoretical mathematics.

59 MATHEMATICAL AND COMPUTER SCIENCES (GENERAL) 475

60 COMPUTER OPERATIONS AND HARDWARE 475

Includes hardware for computer graphics, firmware, and data processing.

For components see *33 Electronics and Electrical Engineering.*

61 COMPUTER PROGRAMMING AND SOFTWARE 476

Includes computer programs, routines, algorithms, and specific applications, e.g., CAD/CAM.

62 COMPUTER SYSTEMS 481

Includes computer networks and special application computer systems.

63 CYBERNETICS 482

Includes feedback and control theory, artificial intelligence, robotics and expert systems.

For related information see also *54 Man/System Technology and Life Support.*

64 NUMERICAL ANALYSIS 484

Includes iteration, difference equations, and numerical approximation.

65 STATISTICS AND PROBABILITY 486

Includes data sampling and smoothing; Monte Carlo method; and stochastic processes.

66 SYSTEMS ANALYSIS 487

Includes mathematical modeling; network analysis; and operations research.

67 THEORETICAL MATHEMATICS N.A.

Includes topology and number theory.

PHYSICS

Includes physics (general); acoustics; atomic and molecular physics; nuclear and high-energy physics; optics; plasma physics; solid-state physics; and thermodynamics and statistical physics.

For related information see also *Engineering.*

70 PHYSICS (GENERAL) 487

For precision time and time interval (PTTI) see *35 Instrumentation and Photography;* for geophysics, astrophysics or solar physics see *46 Geophysics, 90 Astrophysics,* or *92 Solar Physics.*

71 ACOUSTICS 487
Includes sound generation, transmission, and attenuation.
For noise pollution see *45 Environment Pollution.*

72 ATOMIC AND MOLECULAR PHYSICS 488
Includes atomic structure, electron properties, and molecular spectra.

73 NUCLEAR AND HIGH-ENERGY PHYSICS 489
Includes elementary and nuclear particles; and reactor theory.
For space radiation see *93 Space Radiation.*

74 OPTICS 490
Includes light phenomena and optical devices.
For lasers see *36 Lasers and Masers.*

75 PLASMA PHYSICS 490
Includes magnetohydrodynamics and plasma fusion.
For ionospheric plasmas see *46 Geophysics.* For space plasmas see *90 Astrophysics.*

76 SOLID-STATE PHYSICS 495
Includes superconductivity.
For related information see also *33 Electronics and Electrical Engineering* and *36 Lasers and Masers.*

77 THERMODYNAMICS AND STATISTICAL PHYSICS 500
Includes quantum mechanics; theoretical physics; and Bose and Fermi statistics.
For related information see also *25 Inorganic and Physical Chemistry* and *34 Fluid Mechanics and Heat Transfer.*

SOCIAL SCIENCES

Includes social sciences (general); administration and management; documentation and information science; economics and cost analysis; law, political science, and space policy; and urban technology and transportation.

80 SOCIAL SCIENCES (GENERAL) N.A.
Includes educational matters.

81 ADMINISTRATION AND MANAGEMENT 500
Includes management planning and research.

82 DOCUMENTATION AND INFORMATION SCIENCE 501
Includes information management; information storage and retrieval technology; technical writing; graphic arts; and micrography.
For computer documentation see *61 Computer Programming and Software.*

83 ECONOMICS AND COST ANALYSIS N.A.
Includes cost effectiveness studies.

84 LAW, POLITICAL SCIENCE AND SPACE POLICY N.A.
Includes NASA appropriation hearings; aviation law; space law and policy; international law; international cooperation; and patent policy.

85 URBAN TECHNOLOGY AND TRANSPORTATION 502
Includes applications of space technology to urban problems; technology transfer; technology assessment; and surface and mass transportation.
For related information see *03 Air Transportation and Safety, 16 Space Transportation,* and *44 Energy Production and Conversion.*

SPACE SCIENCES

Includes space sciences (general); astronomy; astrophysics; lunar and planetary exploration; solar physics; and space radiation.
For related information see also *Geosciences.*

88 SPACE SCIENCES (GENERAL) N.A.

89 ASTRONOMY 502
Includes radio, gamma-ray, and infrared astronomy; and astrometry.

90 ASTROPHYSICS 520
Includes cosmology; celestial mechanics; space plasmas; and interstellar and interplanetary gases and dust.
For related information see also *75 Plasma Physics.*

91 LUNAR AND PLANETARY EXPLORATION 524
Includes planetology; and manned and unmanned flights.
For spacecraft design or space stations see *18 Spacecraft Design, Testing and Performance.*

92 SOLAR PHYSICS 525
Includes solar activity, solar flares, solar radiation and sunspots.
For related information see *93 Space Radiation.*

93 SPACE RADIATION 526
Includes cosmic radiation; and inner and outer earth's radiation belts.
For biological effects of radiation see *52 Aerospace Medicine.* For theory see *73 Nuclear and High-Energy Physics.*

GENERAL

Includes aeronautical, astronautical, and space science related histories, biographies, and pertinent reports too broad for categorization; histories or broad overviews of NASA programs.

99 GENERAL N.A.

Note: N.A. means that no abstracts were assigned to this category for this issue.

SUBJECT INDEX I-1
PERSONAL AUTHOR INDEX I-47
CORPORATE SOURCE INDEX I-53
CONTRACT NUMBER INDEX I-63
REPORT/ACCESSION NUMBER INDEX I-65

TYPICAL CITATION AND ABSTRACT

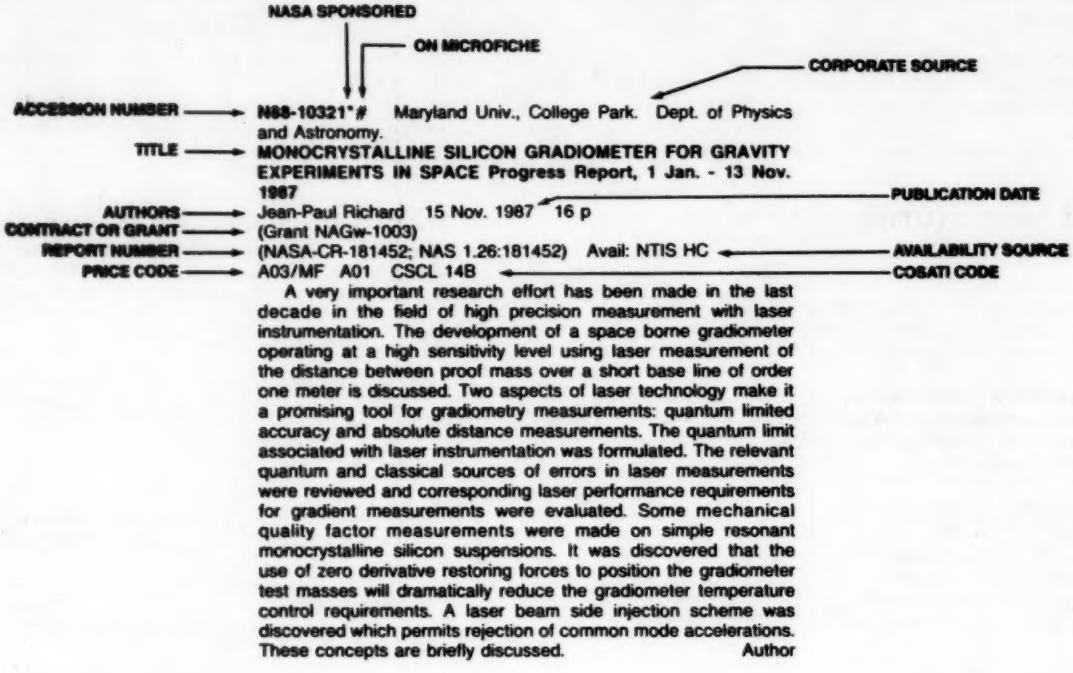
NASA SPONSORED
ON MICROFICHE
CORPORATE SOURCE
ACCESSION NUMBER
N88-10321*# Maryland Univ., College Park. Dept. of Physics and Astronomy.
TITLE
MONOCRYSTALLINE SILICON GRADIOMETER FOR GRAVITY EXPERIMENTS IN SPACE Progress Report, 1 Jan. - 13 Nov. 1987
PUBLICATION DATE
AUTHORS
Jean-Paul Richard 15 Nov. 1987 16 p
CONTRACT OR GRANT
(Grant NAGw-1003)
REPORT NUMBER
(NASA-CR-181452; NAS 1.26:181452) Avail: NTIS HC
AVAILABILITY SOURCE
PRICE CODE
A03/MF A01 CSCL 14B
COSATI CODE
A very important research effort has been made in the last decade in the field of high precision measurement with laser instrumentation. The development of a space borne gradiometer operating at a high sensitivity level using laser measurement of the distance between proof mass over a short base line of order one meter is discussed. Two aspects of laser technology make it a promising tool for gradiometry measurements: quantum limited accuracy and absolute distance measurements. The quantum limit associated with laser instrumentation was formulated. The relevant quantum and classical sources of errors in laser measurements were reviewed and corresponding laser performance requirements for gradient measurements were evaluated. Some mechanical quality factor measurements were made on simple resonant monocrystalline silicon suspensions. It was discovered that the use of zero derivative restoring forces to position the gradiometer test masses will dramatically reduce the gradiometer temperature control requirements. A laser beam side injection scheme was discovered which permits rejection of common mode accelerations. These concepts are briefly discussed. Author

VOLUME 26 NUMBER 4 / FEBRUARY 23, 1988

Scientific and Technical Aerospace Reports

A Semimonthly Publication of the National Aeronautics and Space Administration

01 AERONAUTICS (GENERAL)

N88-12452*# United Technologies Corp., East Hartford, Conn.
A FULL POTENTIAL FLOW ANALYSIS WITH REALISTIC WAKE INFLUENCE FOR HELICOPTER ROTOR AIRLOAD PREDICTION
T. Alan Egolf and S. Patrick Sparks Washington NASA Jan. 1987 69 p
(Contract NAS2-11150)
(NASA-CR-4007; NAS 1.26:4007; R86-915999-13) Avail: NTIS HC A04/MF A01 CSCL 01B

A 3-D, quasi-steady, full potential flow solver was adapted to include realistic wake influence for the aerodynamic analysis of helicopter rotors. The method is based on a finite difference solution of the full potential equation, using an inner and outer domain procedure for the blade flowfield to accommodate wake effects. The nonlinear flow is computed in the inner domain region using a finite difference solution method. The wake is modeled by a vortex lattice using prescribed geometry techniques to allow for the inclusion of realistic rotor wakes. The key feature of the analysis is that vortices contained within the finite difference mesh (inner domain) were treated with a vortex embedding technique while the influence of the remaining portion of the wake (in the outer domain) is impressed as a boundary condition on the outer surface of the finite difference mesh. The solution procedure couples the wake influence with the inner domain solution in a consistent and efficient solution process. The method has been applied to both hover and forward flight conditions. Correlation with subsonic and transonic hover airload data is shown which demonstrates the merits of the approach. Author

N88-12453*# Florida Univ., Gainesville. Dept. of Engineering Sciences.
REDUCED COMPLEXITY STRUCTURAL MODELING FOR AUTOMATED AIRFRAME SYNTHESIS
Prabhat Hajela May 1987 79 p
(Contract NCA2-IR240-401)
(NASA-CR-177440; NAS 1.26:177440) Avail: NTIS HC A05/MF A01 CSCL 01B

A procedure is developed for the optimum sizing of wing structures based on representing the built-up finite element assembly of the structure by equivalent beam models. The reduced-order beam models are computationally less demanding in an optimum design environment which dictates repetitive analysis of several trial designs. The design procedure is implemented in a computer program requiring geometry and loading information to create the wing finite element model and its equivalent beam model, and providing a rapid estimate of the optimum weight obtained from a fully stressed design approach applied to the beam. The synthesis procedure is demonstrated for representative conventional-cantilever and joined wing configurations. Author

02 AERODYNAMICS

Includes aerodynamics of bodies, combinations, wings, rotors, and control surfaces; and internal flow in ducts and turbomachinery.

For related information see also *34 Fluid Mechanics and Heat Transfer.*

N88-12454*# National Aeronautics and Space Administration. Langley Research Center, Hampton, Va.
PLANFORM EFFECTS ON THE SUPERSONIC AERODYNAMICS OF MULTIBODY CONFIGURATIONS
Naomi McMillin and Richard M. Wood [1987] 138 p
(NASA-TP-2762; L-16312; NAS 1.60:2762) Avail: NTIS HC A07/MF A01 CSCL 01A

An experimental and theoretical investigation of the effect of planform on the supersonic aerodynamics of low-fineness-ratio multibody configurations was conducted. Longitudinal and lateral-directional aerodynamic and flow visualization data were obtained on three multibody configurations. The data indicated that planform has a small effect on the zero lift drag of a multibody configuration. The longitudinal data obtained at lifting conditions showed a sensitivity to planform shape. Lateral-directional data obtained for all configurations did not uncover any unusual stability traits for this class of configuration. A comparison study was also made between the planform effects observed on single-body and multibody configurations. Results from this study indicate that the multibody concept appears to offer a mechanism for employing a low-sweep wing with no significant increase in zero-lift drag but still retaining high-performance characteristics at high-lift conditions. Evaluation of the linear-theory prediction methods revealed a general inability of the methods to predict the characteristics of low-fineness-ratio geometries. Author

N88-12455* National Aeronautics and Space Administration. Langley Research Center, Hampton, Va.
EFFECTS OF JET EXHAUST YAW VANE INSTALLATION AND OPERATION ON THE LONGITUDINAL AND LATERAL-DIRECTIONAL CHARACTERISTICS OF THE F-14 AIRPLANE
David E. Reubush and Bobby L. Berrier Dec. 1987 121 p
(NASA-TP-2769; L-16302; NAS 1.60:2769) Avail: NTIS HC A06/MF A01 CSCL 01A

A wind tunnel investigation was conducted in the Langley 16-Foot Transonic Tunnel to determine the effects of the installation and use of jet exhaust yaw vanes on the longitudinal and lateral-directional characteristics of the F-14 aircraft. The model was tested at Mach numbers from 0.70 to 1.25 at angles of attack from 0 deg to 4.3 deg. Compressed air was used to simulate nozzle exhaust flow from jet off up to a nozzle pressure ratio of 8. The results of the investigation show that the yaw vanes can augment the rudders to provide directional control, but further investigation will be necessary to optimize the deflection schedule associated with the various nozzle power settings. Author

N88-12456* National Aeronautics and Space Administration. Langley Research Center, Hampton, Va.
SEMIEMPIRICAL METHOD FOR PREDICTION OF AERODYNAMIC FORCES AND MOMENTS ON A STEADILY SPINNING LIGHT AIRPLANE

Bandu N. Pamadi (Vigyan Research Associates, Inc., Hampton, Va.) and Lawrence W. Taylor, Jr. Dec. 1987 89 p
(NASA-TM-4009; L-15654; NAS 1.15:4009) Avail: NTIS HC A05/MF A01 CSCL 01A

A semi-empirical method is presented for the estimation of aerodynamic forces and moments acting on a steadily spinning (rotating) light airplane. The airplane is divided into wing, body, and tail surfaces. The effect of power is ignored. The strip theory is employed for each component of the spinning airplane to determine its contribution to the total aerodynamic coefficients. Then, increments to some of the coefficients which account for centrifugal effect are estimated. The results are compared to spin tunnel rotary balance test data. Author

N88-12457*# Vigyan Research Associates, Inc., Hampton, Va.
THE DESIGN AND PRELIMINARY CALIBRATION OF A BOUNDARY-LAYER FLOW CHANNEL
Dhanvada M. Rao and Timmy T. Kariya (George Washington Univ., Washington, D.C.) Oct. 1987 37 p
(Contracts NAS1-17919; NCC1-24)
(NASA-CR-178399; NAS 1.26:178399) Avail: NTIS HC A03/MF A01 CSCL 01A

Design procedures for a new low-speed boundary-layer research channel are described. The channel is an open-circuit wind tunnel for the study of two-dimensional boundary layers under controlled pressure gradients, and follows design guidelines from published literature on blower tunnels with wide-angle diffusers. The contraction was arranged in a modular fashion permitting two different test sections of square and high-aspect-ratio cross section. A radical type of wide-angle diffuser was employed, and a stream-tube computer code (GE Streamtube Curvature Code) was used to check the contraction designs. The alternate test sections have the following specifications: 2- by 2-foot cross section with a fixed velocity of 23 ft/sec, and a boundary-layer section with a 0.5- by 2-foot cross section at a fixed velocity of approximately 89 ft/sec. Experimental techniques and data are described for the evaluation of diffuser effectiveness, boundary-layer channel characteristics, and overall performance of the facility. Author

N88-12458*# Kansas Univ. Center for Research, Inc., Lawrence. Flight Research Lab.
AN EXPERIMENTAL INVESTIGATION OF DYNAMIC GROUND EFFECT Final Report
Pai Hung Lee, C. Edward Lan, and Vincent U. Muirhead Washington Dec. 1987 85 p
(Grant NAG1-616)
(NASA-CR-4105; NAS 1.26:4105; CRING-FRL-717-1) Avail: NTIS HC A05/MF A01 CSCL 01A

A 60-degree delta wing, an F-106B, and an XB-70 model with and without flap deflections were tested in static and dynamic ground effect in the 36-by 51-inch subsonic wind tunnel at the University of Kansas. Dynamic ground effect was measured with movable sting support. For flow visualization, a tufted wire grid was mounted on the movable sting behind the model. Test results showed that lift and drag increments in dynamic ground effect were always lower than static values. Effect of the trailing edge flap deflections on lift increments was slight. The fuselage reduced the lift increments at a given ground height. From flow visualization under static conditions, the vortex core was seen to enlarge as the ground was approached. Author

N88-12459*# National Aeronautics and Space Administration. Langley Research Center, Hampton, Va.
AERODYNAMIC SENSITIVITIES FROM SUBSONIC, SONIC AND SUPERSONIC UNSTEADY, NONPLANAR LIFTING-SURFACE THEORY
E. Carson Yates, Jr. Sep. 1987 18 p
(NASA-TM-100502; NAS 1.15:100502) Avail: NTIS HC A03/MF A01 CSCL 01A

The technique of implicit differentiation has been used in combination with linearized lifting-surface theory to derive analytical expressions for aerodynamic sensitivities (i.e., rates of change of lifting pressures with respect to general changes in aircraft geometry, including planform variations) for steady or oscillating planar or nonplanar lifting surfaces in subsonic, sonic, or supersonic flow. The geometric perturbation is defined in terms of a single variable, and the user need only provide simple expressions or similar means for defining the continuous or discontinuous global or local perturbation of interest. Example expressions are given for perturbations of the sweep, taper, and aspect ratio of a wing with trapezoidal semispan planform. In addition to direct computational use, the analytical method presented here should provide benchmark criteria for assessing the accuracy of aerodynamic sensitivities obtained by approximate methods such as finite geometry perturbation and differencing. The present process appears to be readily adaptable to more general surface-panel methods. Author

N88-12460 Georgia Inst. of Tech., Atlanta.
A METHOD FOR THE EFFICIENT CALCULATION OF ELASTIC ROTOR BLADE DYNAMIC RESPONSE IN FORWARD FLIGHT Ph.D. Thesis
Dana James Taylor 1987 188 p
Avail: Univ. Microfilms Order No. DA8715823

A comprehensive set on nonlinear, integro-partial differential equations of motion are developed for an elastic rotor blade with nonuniform structural, geometric and aerodynamic properties, and chordwise offsets with flap, lag, and torsional degrees of freedom. The structural dynamic formulation parallels that derived by Hodges and Dowell and is extended for forward flight. The aerodynamic formulation parallels the development presented by Kaza and Kvaternik and is extended to consider linear inflow and unsteady aerodynamic approximations. The governing equations are solved in an efficient manner utilizing a modified Galerkin-generalized harmonic balance approach. Incorporated into the solution method is the capability of considering the elastic deformation of the rotor blade while calculating the control inputs. Results are presented which represent the response, shown in terms of nondimensional tip displacement as well as root loads, of an isolated articulated rotor whose blades possess nonuniform properties and chordwise offsets. The flight conditions considered are hover and forward flight at mu = 0.2 and m = 0.4. The quantitative effects of unsteady aerodynamics, linear inflow, and elastic trim are shown. It is concluded that the consideration of unsteady aerodynamics, nonuniform inflow and blade elasticity when calculating trim is dependent on the final use of the response. Dissert. Abstr.

N88-12461*# National Aeronautics and Space Administration. Lewis Research Center, Cleveland, Ohio.
APPLICATION OF RUNGE KUTTA TIME MARCHING SCHEME FOR THE COMPUTATION OF TRANSONIC FLOWS IN TURBOMACHINES
S. V. Subramanian and R. Bozzola (Avco Lycoming Div., Stratford, Conn.) [1987] 19 p Presented at the 21st Joint Propulsion Conference, Monterey, Calif., 8-10 Jul. 1985; sponsored by AIAA, SAE and ASME Previously announced in IAA as A85-39728
(NASA-TM-86997; E-2543; NAS 1.15:86997) Avail: NTIS HC A03/MF A01 CSCL 01A

Numerical solutions of the unsteady Euler equations are obtained using the classical fourth order Runge Kutta time marching scheme. This method is fully explicit and is applied to the governing equations in the finite volume, conservation law form. In order to determine the efficiency of this scheme for solving turbomachinery flows, steady blade-to-blade solutions are obtained for compressor and turbine cascades under subsonic and transonic flow conditions. Computed results are compared with other numerical methods and wind tunnel measurements. The study also focuses on other important numerical aspects influencing the performance of the algorithm and the solution accuracy such as grid types, boundary conditions and artificial viscosity. For this purpose, H, O, and C type computational grids as well as characteristic and extrapolation type boundary conditions are included in solution procedures. Author

N88-12462*# Textron Bell Helicopter, Fort Worth, Tex.
A 0.15-SCALE STUDY OF CONFIGURATION EFFECTS ON THE AERODYNAMIC INTERACTION BETWEEN MAIN ROTOR AND FUSELAGE
Ted Trept Jan. 1984 634 p
(Contract NAS2-11268)
(NASA-CR-166577; NAS 1.26:166577) Avail: NTIS HC A99/MF A01 CSCL 01A

Hover and forward flight tests were conducted to investigate the mutual aerodynamic interaction between the main motor and fuselage of a conventional helicopter configuration. A 0.15-scale Model 222 two-bladed teetering rotor was combined with a 0.15-scale model of the NASA Ames 40x80-foot wind tunnel 1500 horsepower test stand fairing. Configuration effects were studied by modifying the fairing to simulate a typical helicopter forebody. Separation distance between rotor and body were also investigated. Rotor and fuselage force and moment as well as pressure data are presented in graphical and tabular format. Data was taken over a range of thrust coefficients from 0.002 to 0.007. In forward flight speed ratio was varied from 0.1 to 0.3 with shaft angle varying from +4 to -12 deg. The data show that the rotors effect on the fuselage may be considerably more important to total aircraft performance than the effect of the fuselage on the rotor. Author

N88-12463*# Nielsen Engineering and Research, Inc., Mountain View, Calif.
CONCEPTS FOR RADICALLY INCREASING THE NUMERICAL CONVERGENCE RATE OF THE EULER EQUATIONS
David Nixon, Keh-Lih Tzuoo, Steven C. Caruso, Mohammad Farshchi, Goetz H. Klopfer, and Alfred Ayoub May 1987 85 p
(Contract NAS2-12129)
(NASA-CR-177456; NAS 1.26:177456; NEAR-TR-380) Avail: NTIS HC A05/MF A01 CSCL 01A

Integral equation and finite difference methods have been developed for solving transonic flow problems using linearized forms of the transonic small disturbance and Euler equations. A key element is the use of a strained coordinate system in which the shock remains fixed. Additional criteria are developed to determine the free parameters in the coordinate straining; these free parameters are functions of the shock location. An integral equation analysis showed that the shock is located by ensuring that no expansion shocks exist in the solution. The expansion shock appears as oscillations in the solution near the sonic line, and the correct shock location is determined by removing these oscillations. A second objective was to study the ability of the Euler equation to model separated flow. Author

N88-12464# Sandia National Labs., Albuquerque, N. Mex.
THE AERODYNAMICS OF SUPERSONIC PARACHUTES
C. W. Peterson Jun. 1987 29 p Presented at the Parachute Systems Technology: Fundamentals, Concepts, and Applications, Munich, Fed. Republic of Germany, 22 Jun. 1987
(Contract DE-AC04-76DP-00789)
(DE87-014846; SAND-87-1395C; CONF-8706165-3) Avail: NTIS HC A03/MF A01

A discussion of the aerodynamics and performance of parachutes flying at supersonic speeds is the focus of this paper. Typical performance requirements for supersonic parachute systems are presented, followed by a review of the literature on supersonic parachute configurations and their drag characteristics. Data from a recent supersonic wind tunnel test series is summarized. The value and limitations of supersonic wind tunnel data on hemisflo and 20-degree conical ribbon parachutes behind several forebody shapes and diameters are discussed. Test techniques were derived which avoided many of the opportunities to obtain erroneous supersonic parachute drag data in wind tunnels. Preliminary correlations of supersonic parachute drag with Mach number, forebody shape and diameter, canopy porosity, inflated canopy diameter and stability are presented. Supersonic parachute design considerations are discussed and applied to a M = 2 parachute system designed and tested at Sandia. It is shown that the performance of parachutes in supersonic flows is a strong function of parachute design parameters and their interactions with the payload wake. DOE

N88-12465*# Eloret Corp., Sunnyvale, Calif.
DEVELOPMENT AND APPLICATION OF COMPUTATIONAL AEROTHERMODYNAMICS FLOWFIELD COMPUTER CODES Technical Progress Report, 1 Sep. 1986 - 31 Oct. 1987
Ethiraj Venkatapathy 9 Dec. 1987 29 p
(Contract NCC2-420)
(NASA-CR-181534; NAS 1.26:181534) Avail: NTIS HC A03/MF A01 CSCL 01A

Multiple nozzle plume flow field is computed with a 3-D, Navier-Stokes solver. Numerical simulation is performed with a flux-split, two-factor, time asymptotic viscous flow solver of Ying and Steger. The two factor splitting provides a stable 3-D solution procedure under ideal-gas assumptions. An ad-hoc acceleration procedure that shows promise in improving the convergence rate by a factor of three for steady state problems is utilized. Computed solutions to generic problems at various altitude and flight conditions show flow field complexity and three-dimensional effects due to multiple nozzle jet interactions. Viscous, ideal gas solutions for the symmetric nozzle are compared with other numerical solutions. Author

N88-12466*# National Aeronautics and Space Administration. Ames Research Center, Moffett Field, Calif.
SOME EXPERIENCES WITH THE VISCOUS-INVISCID INTERACTION APPROACH
W. R. VanDalsem, J. L. Steger, and K. V. Rao (Iowa State Univ. of Science and Technology, Ames.) Nov. 1987 48 p
(NASA-TM-100015; A-87308; NAS 1.15:100015) Avail: NTIS HC A03/MF A01 CSCL 01A

Methods for simulating compressible viscous flow using the viscid-inviscid interaction approach are described. The formulations presented range from the more familiar full-potential/boundary-layer interaction schemes to a method for coupling Euler/Navier-Stokes and boundary-layer algorithms. An effort is made to describe the advantages and disadvantages of each formulation. Sample results are presented which illustrate the applicability of the methods. Author

N88-12467 Illinois Inst. of Tech., Chicago.
ON THE INSTABILITY OF THIN CIRCULAR SHEAR LAYERS Ph.D. Thesis
Azam Ahmadi-Moghadam 1987 178 p
Avail: Univ. Microfilms Order No. DA8717223

The hydrodynamic instability of thin circular shear layers, such as would occur in the near-lip region of a large Reynolds number incompressible jet, was investigated analytically and numerically. To leading order, the mean flow is the Blasius shear layer profile connecting a quiescent external region and a uniform flow in the jet core. Temporal and spatial linear inviscid stability calculations were performed allowing for nonaxisymmetric perturbations. The spatial calculations are in good agreement with reported experimental results. The linear growth rate decreases in magnitude with both the azimuthal wave number and the ratio of the momentum thickness to the local radius of the jet. The long wave case was investigated through an expansion in powers of the ratio of the shear layer thickness and the jet radius. Nonaxisymmetric secondary instability through parametric resonance was investigated. The analysis consists of an expansion and a multiple scaling technique in terms of the amplitude of the primary disturbance. A solvability condition gives the amplitude evolution equation for the secondary instability. Dissert. Abstr.

N88-12468 Colorado Univ., Boulder.
THREE-DIMENSIONAL UNSTEADY FLOW ELICITED BY FINITE WINGS AND COMPLEX CONFIGURATIONS Ph.D. Thesis
Jeffrey Clayton Ashworth 1987 191 p
Avail: Univ. Microfilms Order No. DA8716236

The spatial and temporal transport, accumulation and dissipation of vorticity on the surface of 3 wings varying only in sweep angles were examined using flow visualization and hot wire anemometry.

Identical geometric positions were tested on each wing for a variety of dynamic parameters. Each sweep geometry produced distinct, time dependent, spanwise and chordwise sites for vorticity accumulation into large scale leading edge and wingtip vortices. The wingtip and leading edge vortex interactions produced spanwise flow patterns uncharacteristic of 2 dimensional flows. Wing sweep is a dominant geometric parameter in analyzing the effects of unsteady wingtip flow. An initial investigation into the feasibility of unsteady flow application was performed on a model of the X-29 Forward Swept Wing Technology Demonstrator. This model geometry produces complex flow patterns but may be ideally suited for application of unsteady flow technology. These investigations provide initial insight into 3 dimensional flow behavior elicited by different sweep geometries and dynamic parameters. Dissert. Abstr.

N88-12469 Princeton Univ., N. J.
SOLUTION OF THE TWO-DIMENSIONAL EULER EQUATIONS ON UNSTRUCTURED TRIANGULAR MESHES Ph.D. Thesis
Dimitri James Mavriplis 1987 157 p
Avail: Univ. Microfilms Order No. DA8716898

Solutions of inviscid subsonic and transonic flows about multi-element airfoils are obtained using two-dimensional Euler equations. An edge-based data structure is adopted, where the simplest element of the mesh is taken as the edge rather than the triangular element itself. Two finite-volume discretization schemes are developed, one where the flow variables are stored at the center of each triangular element, and the other where the flow variables are stored at the vertices of the triangles. Convergence to a steady state is accelerated by local time-stepping, enthalpy-damping, and implicit residual-averaging. A novel multigrid algorithm for use on a sequence of completely unstructured, unrelated meshes is also developed. Solutions of both Euler schemes are compared to a variety of numerical results and experimental data and are found to exhibit similar accuracy to other existing Euler solvers. However, it was found that viscous effects on multi-element airfoils are most often non-negligible, e.g., drag is underpredicted by 10 to 15 percent for a particular case involving small regions of viscous flow. The use of unstructured meshes was found to result in substantially higher memory and CPU time requirements due to the indirect addressing needed and the use of shorter vector lengths. On the other hand, they enable the solution of the flow about arbitrarily shaped two-dimensional bodies. Dissert. Abstr.

N88-12470* National Aeronautics and Space Administration, Washington, D.C.
AERONAUTICAL ENGINEERING: A CONTINUING BIBLIOGRAPHY WITH INDEXES (SUPPLEMENT 219)
Nov. 1987 163 p
(NASA-SP-7037(219); NAS 1.21:7037(219)) Avail: NTIS HC A08; NTIS standing order as PB86-914100, $7.00 domestic, $14.00 foreign CSCL 01A

This bibliography lists 586 reports, articles, and other documents introduced into the NASA scientific and technical information system in October, 1987. Author

N88-12471*# Analytical Methods, Inc., Redmond, Wash.
INVESTIGATION OF LOW-SPEED TURBULENT SEPARATED FLOW AROUND AIRFOILS
Alan J. Wadcock Aug. 1987 66 p
(Contract NAS2-11601)
(NASA-CR-177450; NAS 1.26:177450) Avail: NTIS HC A04/MF A01 CSCL 01A

Described is a low-speed wind tunnel experiment to measure the flowfield around a two-dimensional airfoil operating close to maximum lift. Boundary layer separation occurs on the upper surface at x/c=0.85. A three-component laser velocimeter, coupled with a computer-controlled data acquisition system, was used to obtain three orthogonal mean velocity components and three components of the Reynolds stress tensor in both the boundary layer and wake of the airfoil. Pressure distributions on the airfoil, skin friction distribution on the upper surface of the airfoil, and integral properties of the airfoil boudary layer are also documented. In addition to these near-field flow properties, static pressure distributions, both upstream and downstream from the airfoil and on the walls of the wind tunnel, are also presented. Author

N88-12628# Joint Publications Research Service, Arlington, Va.
RENEWED INTEREST IN AIRSHIPS FOR INDUSTRY USE DISCUSSED
M. Ariye *In its* USSR Report: Engineering and Equipment 28 May 1987 p 61-62 Transl. into ENGLISH from Stroitelnaya Gazeta (Moscow, USSR), 23 Jan. 1987 p 3 (For primary document see N88-12621 04-31)
Copyright Avail: NTIS HC A06/MF A01

N88-12630# Joint Publications Research Service, Arlington, Va.
CALCULATION OF THREE-DIMENSIONAL STATIONARY TURBULENT BOUNDARY LAYER ON ROOT SECTION OF WING IGNORING COMPRESSIBILITY Abstract Only
G. A. Shchekin *In its* USSR Report: Engineering and Equipment 28 May 1987 p 89 Transl. into ENGLISH from Izvestiya Vysshikh Uchebnykh Zavedeniy: Aviatsionnaya Tekhnika (Kazan, USSR), no. 4, Oct. - Dec. 1985 p 72-76 (For primary document see N88-12621 04-31)
Copyright Avail: NTIS HC A06/MF A01

N88-12631# Joint Publications Research Service, Arlington, Va.
CALCULATION OF AERODYNAMIC CHARACTERISTICS OF THREE-DIMENSIONAL FINITE SPAN WINGS IN POTENTIAL INCOMPRESSIBLE FLOW Abstract Only
S. D. Yermolenko and Ye. A. Ryaguzov *In its* USSR Report: Engineering and Equipment 28 May 1987 p 90 Transl. into ENGLISH from Izvestiya Vysshikh Uchebnykh Zavedeniy: Aviatsionnaya Tekhnika (Kazan, USSR), no. 4, Oct. - Dec. 1985 p 43-48 (For primary document see N88-12621 04-31)
Copyright Avail: NTIS HC A06/MF A01

N88-12632# Joint Publications Research Service, Arlington, Va.
SOME ASYMPTOTIC MODES OF TRANSONIC VORTEX FLOW Abstract Only
A. G. Kuzmin *In its* USSR Report: Engineering and Equipment 28 May 1987 p 91 Transl. into ENGLISH from Vestnik Leningradskogo Universiteta, Seriya 1: Matematika, Mekhanika, Astronomiya (Leningrad, USSR), no. 2, Apr. 1986 p 61-65 Original language document was announced in IAA as A87-15553 (For primary document see N88-12621 04-31)
Copyright Avail: NTIS HC A06/MF A01

N88-12633# Joint Publications Research Service, Arlington, Va.
CONICAL WING WITH MAXIMUM LIFT-TO-DRAG RATIO IN SUPERSONIC GAS FLOW Abstract Only
V. I. Lapygin and P. V. Tretyakov *In its* USSR Report: Engineering and Equipment 28 May 1987 p 92 Transl. into ENGLISH from Izvestiya Akademii Nauk SSSR Mekhanika Zhidkosti i Gaza (Moscow, USSR), no. 3, May - Jun. 1986 p 128-133 Original language document was announced in IAA as A87-10615 (For primary document see N88-12621 04-31)
Copyright Avail: NTIS HC A06/MF A01

N88-12635# Joint Publications Research Service, Arlington, Va.
NUMERICAL STUDY OF SUPERSONIC FLOW AROUND BLUNT BODIES WITH EXTENDED NEEDLE NOSE Abstract Only
V. N. Karlovskiy and V. I. Sakharov *In its* USSR Report: Engineering and Equipment 28 May 1987 p 93 Transl. into ENGLISH from Izvestiya Akademii Nauk SSSR Mekhanika Zhidkosti i Gaza (Moscow, USSR), no. 3, May - Jun. 1986 p 119-127 (For primary document see N88-12621 04-31)
Copyright Avail: NTIS HC A06/MF A01

03 AIR TRANSPORTATION AND SAFETY

Includes passenger and cargo air transport operations; and aircraft accidents.

For related information see also *16 Space Transportation* and *85 Urban Technology and Transportation.*

N88-12472*# Hercules Aerospace Co., Magna, Utah.
FABRICATION AND TESTING OF FIRE RESISTANT GRAPHITE COMPOSITE PANELS
W. D. Roper Feb. 1986 57 p
(Contract NAS2-12039)
(NASA-CR-177397; NAS 1.26:177397) Avail: NTIS HC A04/MF A01 CSCL 01C

Eight different graphite composite panels were fabricated using four different resin matrices. The resin matrices included Hercules 71775, a blend of vinylpolystyrpyridine and bismaleimide, H795, a bismaleimide, Cycom 6162, a phenolic, and PSP 6022m, a polystyrylpyridine. Graphite panels were fabricated using fabric or unidirectional tape. Described are the processes for preparing these panels and some of their mechanical, thermal and flammability properties. Panel properties are compared with state-of-the-art epoxy fiberglass composite panels. Author

N88-12473*# National Aeronautics and Space Administration. Lewis Research Center, Cleveland, Ohio.
EXPERIMENTAL EVIDENCE FOR MODIFYING THE CURRENT PHYSICAL MODEL FOR ICE ACCRETION ON AIRCRAFT SURFACES
W. Olsen and E. Walker 1986 47 p Film supplement
(NASA-TM-87184; E-3658; NASA-MPD-1683; NAS 1.15:87184)
Avail: NTIS HC A03/MF A01; film supplement number NASA-MPD-1683 available from NASA Lewis Research Center, Phototgraphic and Printing Branch, Cleveland, Ohio CSCL 01C

Closeup movies, still photographs, and other experimental data suggest that the current physical model for ice accretion needs significant modification. At aircraft airspeeds there was no flow of liquid over the surface of the ice after a short initial flow, even at barely subfreezing temperatures. Instead, there were very large stationary drops on the ice surface that lose water from their bottoms by freezing and replenish their liquid by catching the microscopic cloud droplets. This observation disagrees with the existing physical model, which assumes there is a thin liquid film continuously flowing over the ice surface. With no such flow, the freezing-fraction concept of the model fails when a mass balance is performed on the surface water. Rime ice does, as the model predicts, form when the air temperature is low enough to cause the cloud droplets to freeze almost immediately on impact. However, the characteristic shapes of horn-glaze ice or rime ice are primarily caused by the ice shape affecting the airflow locally and consequently the droplet catch and the resulting ice shape. Ice roughness greatly increases the heat transfer coefficient, stops the movement of drops along the surface, and may also affect the airflow initially and thereby the droplet catch. At high subreezing temperatures the initial flow and shedding of surface drops have a large effect on the ice shape. At the incipient freezing limit, no ice forms. Author

N88-12526*# Air Force Wright Aeronautical Labs., Wright-Patterson AFB, Ohio. Aero Propulsion Lab.
AIRCRAFT FIRE SAFETY RESEARCH
Benito P. Botteri *In* NASA. Lewis Research Center, Spacecraft Fire Safety 1987 p 65-72 (For primary document see N88-12520 04-16)
Avail: NTIS HC A07/MF A01 CSCL 01C

04 AIRCRAFT COMMUNICATIONS AND NAVIGATION

Includes digital and voice communication with aircraft; air navigation systems (satellite and ground based); and air traffic control.

For related information see also *17 Space Communications, Spacecraft Communications, Command and Tracking* and *Communications and Radar.*

N88-12474# Maryland Univ., College Park. Center for Automation Research.
TWO DIMENSIONAL PATH PLANNING WITH OBSTACLES AND SHADOWS
Sunil Puri and Larry S. Davis Jan. 1987 44 p
(Contract DACA76-84-C-0004)
(AD-A184075; CAR-TR-255; CS-TR-1760; ETL-0452) Avail: NTIS HC A03/MF A01 CSCL 04B

A mobile robot navigates with a limited knowledge of its environment because of the restricted field of view and range of its sensors, and the occlusion of parts of the environment in any single image. Most path planning algorithms consider only free regions and obstacles in the robot's world for path planning. The objective of this report is to extend the classical path planning paradigm to include occluded regions. This introduces the new problem of deciding when (or whether) to employ the sensor system during the execution of the path to, potentially, reveal the occluded regions as obstacles or free space for the purpose of replanning. GRA

N88-12475# Hughes Research Labs., Malibu, Calif.
AUTONOMOUS LAND VEHICLE (ALV) PLANNING AND NAVIGATION SYSTEM Technical Report No. 1, 19 Sep. 1985 - 19 Oct. 1986
D. M. Keirsey, J. S. Mitchell, D. W. Payton, D. Y. Tseng, and V. S. Wong 6 Apr. 1987 74 p
(Contract DACA76-85-C-0017)
(AD-A184243; ETL-0465) Avail: NTIS HC A04/MF A01 CSCL 13F

The Hughes planning system is designed to achieve the reasoning requirements of the Autonomous Land Vehicle (ALV) for navigation in unconstrained outdoor environments. This system is designed specifically to handle diverse terrain with maximal speed, efficacy and versatility. The hierarchical architecture for this system is presented along with the detailed algorithms, heuristics, and planning methodologies for the component modules. The architecture is structured such that lower-level modules perform tasks requiring greatest immediacy while higher-level modules perform tasks involving greater assimilation of sensor data, making use of large amounts of a priori knowledge. GRA

N88-12476# Naval Postgraduate School, Monterey, Calif.
DYNAMIC POSITIONING AT SEA USING THE GLOBAL POSITIONING SYSTEM M.S. Thesis
Augusto M. Ezequiel Jun. 1987 123 p
(AD-A184453) Avail: NTIS HC A06/MF A01 CSCL 17G

Dynamic positioning of a moving platform is analyzed using data from the Global Positioning System (GPS) acquired in Phase II of the Seafloor Benchmark Experiment on R/V Point Sur in August 1986. GPS position determinations are compared to simultaneous Mini-Ranger fixes. The GPS positions computed using only broadcast ephemeris data were within 20 m from the Mini-Ranger fixes when data from four satellites were used and within 30 m when data from three satellites and a geoidal height constraint were used. It was found that the position accuracy is degraded when data from a satellite reaching culmination is used. GRA

N88-12477*# Theory and Applications Unlimited Corp., Los Gatos, Calif.
GPS VERTICAL AXIS PERFORMANCE ENHANCEMENT FOR HELICOPTER PRECISION LANDING APPROACH
Robert P. Denaro and Jacques Beser Sep. 1986 128 p

(Contract NAS2-11791)
(NASA-CR-177443; NAS 1.26:177443) Avail: NTIS HC
A07/MF A01 CSCL 17G

Several areas were investigated for improving vertical accuracy for a rotorcraft using the differential Global Positioning System (GPS) during a landing approach. Continuous deltaranging was studied and the potential improvement achieved by estimating acceleration was studied by comparing the performance on a constant acceleration turn and a rough landing profile of several filters: a position-velocity (PV) filter, a position-velocity-constant acceleration (PVAC) filter, and a position-velocity-turning acceleration (PVAT) filter. In overall statistics, the PVAC filter was found to be most efficient with the more complex PVAT performing equally well. Vertical performance was not significantly different among the filters. Satellite selection algorithms based on vertical errors only (vertical dilution of precision or VDOP) and even-weighted cross-track and vertical errors (XVDOP) were tested. The inclusion of an altimeter was studied by modifying the PVAC filter to include a baro bias estimate. Improved vertical accuracy during degraded DOP conditions resulted. Flight test results for raw differential results excluding filter effects indicated that the differential performance significantly improved overall navigation accuracy. A landing glidepath steering algorithm was devised which exploits the flexibility of GPS in determining precise relative position. A method for propagating the steering command over the GPS update interval was implemented. J.P.B.

N88-12478*# Analytical Mechanics Associates, Inc., Mountain View, Calif.
NAVSIM 2: A COMPUTER PROGRAM FOR SIMULATING AIDED-INERTIAL NAVIGATION FOR AIRCRAFT
William S. Bjorkman Mar. 1987 94 p
(Contract NAS2-10850)
(NASA-CR-177438; NAS 1.26:177438) Avail: NTIS HC
A05/MF A01 CSCL 17G

NAVSIM II, a computer program for analytical simulation of aided-inertial navigation for aircraft, is described. The description is supported by a discussion of the program's application to the design and analysis of aided-inertial navigation systems as well as instructions for utilizing the program and for modifying it to accommodate new models, constraints, algorithms and scenarios. NAVSIM II simulates an airborne inertial navigation system built around a strapped-down inertial measurement unit and aided in its function by GPS, Doppler radar, altimeter, airspeed, and position-fix measurements. The measurements are incorporated into the navigation estimate via a UD-form Kalman filter. The simulation was designed and implemented using structured programming techniques and with particular attention to user-friendly operation. Author

N88-12479*# Ohio State Univ., Columbus. ElectroScience Lab.
SIMULATION OF AN ENHANCED TCAS 2 SYSTEM IN OPERATION Semiannual Report
R. G. Rojas, P. Law, and W. D. Burnside Oct. 1987 79 p
(Grant NsG-1498)
(NASA-CR-181545; NAS 1.26:181545; ESL-716199-9) Avail:
NTIS HC A05/MF A01 CSCL 17G

Described is a computer simulation of a Boeing 737 aircraft equipped with an enhanced Traffic and Collision Avoidance System (TCAS II). In particular, an algorithm is developed which permits the computer simulation of the tracking of a target airplane by a Boeing 373 which has a TCAS II array mounted on top of its fuselage. This algorithm has four main components: namely, the target path, the noise source, the alpha-beta filter, and threat detection. The implementation of each of these four components is described. Furthermore, the areas where the present algorithm needs to be improved are also mentioned. Author

05 AIRCRAFT DESIGN, TESTING AND PERFORMANCE

Includes aircraft simulation technology.

For related information see also *18 Spacecraft Design, Testing and Performance* and *39 Structural Mechanics*.For land transportation vehicles see *85 Urban Technology and Transportation*.

N88-12480*# National Aeronautics and Space Administration. Langley Research Center, Hampton, Va.
EFFECT OF MOTION CUES DURING COMPLEX CURVED APPROACH AND LANDING TASKS: A PILOTED SIMULATION STUDY
Charles H. Scanlon (Arkansas State Univ., State University.) Dec. 1987 28 p
(Contract NCC1-107)
(NASA-TP-2773; L-16351; NAS 1.60:2773) Avail: NTIS HC
A03/MF A01 CSCL 01C

A piloted simulation study was conducted to examine the effect of motion cues using a high fidelity simulation of commercial aircraft during the performance of complex approach and landing tasks in the Microwave Landing System (MLS) signal environment. The data from these tests indicate that in a high complexity MLS approach task with moderate turbulence and wind, the pilot uses motion cues to improve path tracking performance. No significant differences in tracking accuracy were noted for the low and medium complexity tasks, regardless of the presence of motion cues. Higher control input rates were measured for all tasks when motion was used. Pilot eye scan, as measured by instrument dwell time, was faster when motion cues were used regardless of the complexity of the approach tasks. Pilot comments indicated a preference for motion. With motion cues, pilots appeared to work harder in all levels of task complexity and to improve tracking performance in the most complex approach task. Author

N88-12481# Advisory Group for Aerospace Research and Development, Neuilly-Sur-Seine (France). Flight Mechanics Panel.
DEVELOPMENTAL AIRDROP TESTING TECHNIQUES AND DEVICES
H. J. Hunter and R. K. Bogue, ed. Sep. 1987 97 p
(AGARD-AG-300-Vol-6; ISBN-92-835-1559-5) Copyright Avail:
NTIS HC A05/MF A01

The practical aspects of planning, conducting, and reporting on developmental airdrop tests made from cargo transport type aircraft are presented. Typical cargo aircraft aerial delivery systems, parachute extraction systems, and special devices and rigging techniques are described in detail. Typical instrumentation systems for obtaining aircraft and parachute systems force data are also described and piloting techniques for various airdrop methods are briefly discussed. A scenario of a typical parachute tow test is used to demonstrate the application of these techniques and the use of challenge and response checklists among the flight crewmembers. Finally the use of reports is discussed and appendices are included with many useful charts and calculations that are readily applicable in research and development airdrop testing. Author

N88-12482*# Sparta, Inc., Laguna Hills, Calif.
AN EVALUATION PLAN OF BUS ARCHITECTURES AND PROTOCOLS USING THE NASA AMES INTELLIGENT REDUNDANT ACTUATION SYSTEM
P. DeFeo and M. Chen Aug. 1987 34 p
(Contract NAS2-12081)
(NASA-CR-177458; NAS 1.26:177458) Avail: NTIS HC
A03/MF A01 CSCL 01C

Means for evaluating data bus architectures and protocols for highly integrated flight control system applications are needed. Described are the criteria and plans to do this by using the NASA/Ames Intelligent Redundant Actuation System (IRAS) experimental set-up. Candidate bus architectures differ from one another in terms of: topology, access control, message transfer

schemes, message characteristics, initialization. data flow control, transmission rates, fault tolerance, and time synchronization. The evaluation criteria are developed relative to these features. A preliminary, analytical evaluation of four candidate busses (MIL-STD-1553B, DATAC, Ethernet, and HSIS) is described. A bus must be exercised in a real-time environment to evaluate its dynamic characteristics. A plan for real-time evaluation of these four busses using a combination of hardware and simulation techniques is presented. Author

N88-12483*# Eloret Corp., Sunnyvale, Calif.
EXPERIMENTAL AEROTHERMODYNAMIC RESEARCH OF HYPERSONIC AIRCRAFT Technical Progress Report, 1 Mar. - 30 Sep. 1987
Joseph W. Cleary 9 Dec. 1987 28 p
(Contract NCC2-416)
(NASA-CR-181533; NAS 1.26:181533) Avail: NTIS HC A03/MF A01 CSCL 01C

The 2-D and 3-D advance computer codes being developed for use in the design of such hypersonic aircraft as the National Aero-Space Plane require comparison of the computational results with a broad spectrum of experimental data to fully assess the validity of the codes. This is particularly true for complex flow fields with control surfaces present and for flows with separation, such as leeside flow. Therefore, the objective is to provide a hypersonic experimental data base required for validation of advanced computational fluid dynamics (CFD) computer codes and for development of more thorough understanding of the flow physics necessary for these codes. This is being done by implementing a comprehensive test program for a generic all-body hypersonic aircraft model in the NASA/Ames 3.5 foot Hypersonic Wind Tunnel over a broad range of test conditions to obtain pertinent surface and flowfield data. Results from the flow visualization portion of the investigation are presented. Author

N88-12484*# Eloret Corp., Sunnyvale, Calif.
PERFORMANCE ANALYSIS OF ADVANCED SPACECRAFT TPS Technical Progress Report, 1 Mar. - 31 Oct. 1987
William C. Pitts 9 Dec. 1987 14 p
(Contract NCC2-434)
(NASA-CR-181532; NAS 1.26:181532) Avail: NTIS HC A03/MF A01 CSCL 01C

The analysis on the feasibility for using metal hydrides in the thermal protection system of cryogenic tanks in space was based on the heat capacity of ice as the phase change material (PCM). It was found that with ice the thermal protection system weight could be reduced by, at most, about 20 percent over an all LI-900 insulation. For this concept to be viable, a metal hydride with considerably more capacity than water would be required. None were found. Special metal hydrides were developed for hydrogen fuel storage applications and it may be possible to do so for the current application. Until this appears promising further effort on this feasibility study does not seem warranted. Author

N88-12485# Aeronautical Research Labs., Melbourne (Australia).
HOVERING HELICOPTER FLIGHT DYNAMICS: A STUDY OF VERTICAL MOTION
C. R. Guy Feb. 1987 47 p
(AR-004-526; ARL-AERO-TM-386) Copyright Avail: NTIS HC A03/MF A01

The flight dynamic characteristics of a hovering helicopter in response to collective stick inputs are examined. A mathematical model of the aerodynamics/kinetics and rotor system dynamics of a representative aircraft, linearized about the hovering flight condition, is used as a basis for the study. The dynamic behavior of this model is compared with flight test results for similar inputs and the coefficients are adjusted to improve model performance. The model structure is then modified by the incorporation of additional terms to improve its accuracy. Although no attempt is made to optimize the coefficients of the model using parameter identification techniques, the approach used here provides acceptable results. Author

N88-12486*# Kansas Univ. Center for Research, Inc., Lawrence.
AN INTEGRATED STUDY OF STRUCTURES, AERODYNAMICS AND CONTROLS ON THE FORWARD SWEPT WING X-29A AND THE OBLIQUE WING RESEARCH AIRCRAFT Final Report
Kenneth S. Dawson and Paul E. Fortin Dec. 1987 128 p
(Contract NCC2-396)
(NASA-CR-181548; NAS 1.26:181548) Avail: NTIS HC A07/MF A01 CSCL 01C

The results of an integrated study of structures, aerodynamics, and controls using the STARS program on two advanced airplane configurations are presented. Results for the X-29A include finite element modeling, free vibration analyses, unsteady aerodynamic calculations, flutter/divergence analyses, and an aeroservoelastic controls analysis. Good correlation is shown between STARS results and various other verified results. The tasks performed on the Oblique Wing Research Aircraft include finite element modeling and free vibration analyses. Author

N88-12622# Joint Publications Research Service, Arlington, Va.
A RELIABILITY CONCEPT FOR OPTIMIZING AIRCRAFT DESIGN Abstract Only
S. V. Arinchev and V. V. Bystrov *In its* USSR Report: Engineering and Equipment 28 May 1987 p 1 Transl. into ENGLISH from Izvestiya Vysshikh Uchebnykh Zavedeniy: Aviatsionnaya Tekhnika (Kazan, USSR), no. 4, Oct. - Dec. 1985 p 7-12 Original language document was announced in IAA as A86-35977 (For primary document see N88-12621 04-31)
Copyright Avail: NTIS HC A06/MF A01

N88-12623# Joint Publications Research Service, Arlington, Va.
OPTIMUM TAKE-OFF RUN OF AIRCRAFT ON GROUND AIRFIELDS Abstract Only
A. A. Badyagin *In its* USSR Report: Engineering and Equipment 28 May 1987 p 2 Transl. into ENGLISH from Izvestiya Vysshikh Uchebnykh Zavedeniy: Aviatsionnaya Tekhnika (Kazan, USSR), no. 4, Oct. - Dec. 1985 p 12-16 (For primary document see N88-12621 04-31)
Copyright Avail: NTIS HC A06/MF A01

N88-12625# Joint Publications Research Service, Arlington, Va.
EFFECT OF PERMISSIBLE VARIATIONS OF CENTER-OF-GRAVITY LOCATIONS OF CARGO AIRPLANE ON ITS MASS Abstract Only
V. P. Gogolin *In its* USSR Report: Engineering and Equipment 28 May 1987 p 4 Transl. into ENGLISH from Izvestiya Vysshikh Uchebnykh Zavedeniy: Aviatsionnaya Tekhnika (Kazan, USSR), no. 4, Oct. - Dec. 1985 p 24-28 (For primary document see N88-12621 04-31)
Copyright Avail: NTIS HC A06/MF A01

N88-12626# Joint Publications Research Service, Arlington, Va.
AIRCRAFT CLASSIFICATION BY TYPE OF PROPULSIVE DEVICES. DETERMINATION OF TYPE AND NUMBER OF CARRYING SOLUTIONS Abstract Only
M. A. Guryanov *In its* USSR Report: Engineering and Equipment 28 May 1987 p 5-6 Transl. into ENGLISH from Izvestiya Vysshikh Uchebnykh Zavedeniy: Aviatsionnaya Tekhnika (Kazan, USSR), no. 4, Oct. - Dec. 1985 p 33-39 (For primary document see N88-12621 04-31)
Copyright Avail: NTIS HC A06/MF A01

06 AIRCRAFT INSTRUMENTATION

Includes cockpit and cabin display devices; and flight instruments.

For related information see also *19 Spacecraft Instrumentation* and *35 Instrumentation and Photography.*

N88-12487*# National Aeronautics and Space Administration. Langley Research Center, Hampton, Va.
EFFECTS OF COMBINING VERTICAL AND HORIZONTAL INFORMATION INTO A PRIMARY FLIGHT DISPLAY

Terence S. Abbott, Mark Nataupsky, and George G. Steinmetz Dec. 1987 21 p
(NASA-TP-2783; L-16366; NAS 1.60:2783) Avail: NTIS HC A03/MF A01 CSCL 01D

A ground-based aircraft simulation study was conducted to determine the effects of combining vertical and horizontal flight information into a single display. Two display configurations were used in this study. The first configuration consisted of a Primary Flight Display (PFD) format and a Horizontal Situation Display (HSD) with the PFD displayed conventionally above the HSD. For the second display configuration, the HSD format was combined with the PFD format. Four subjects participated in this study. Data were collected on performance parameters, pilot-control inputs, auditory evoked response parameters (AEP), oculometer measurements (eye-scan), and heart rate. Subjective pilot opinion was gathered through questionnaire data and scorings for both the Subjective Workload Assessment Technique (SWAT) and the NASA Task Load Index (NASA-TLX). The results of this study showed that, from a performance and subjective standpoint, the combined configuration was better than the separate configuration. Additionally, both the eye-transition and eye-dwell times for the separate HSD were notably higher than expected, with a 46% increase in available visual time when going from double to single display configuration. Author

07 AIRCRAFT PROPULSION AND POWER

Includes prime propulsion systems and systems components, e.g., gas turbine engines and compressors; and onboard auxiliary power plants for aircraft.

For related information see also *20 Spacecraft Propulsion and Power, 28 Propellants and Fuels,* and *44 Energy Production and Conversion.*

N88-12488# Science and Engineering Associates, Inc., Seattle, Wash.
AIRCRAFT ENGINE EXHAUST PLUME DYNAMICS Final Report, Dec. 1984 - Aug. 1985
B. T. Delaney, Bryan A. Zetlen, Ronald C. Tai, Glenn D. Seitchek, and G. G. Elcock Oct. 1986 31 p
(Contract F08635-85-C-0036)
(AD-A184238; AFESC/ESL-TR-86-20) Avail: NTIS HC A03/MF A01 CSCL 21B

This report summarizes a research effort to remedy a known deficiency in the Air Quality Assessment Model dispersion calculation capability. Current methods use dispersion calculations and equations for vertical sources (i.e., power plants) resulting in inaccurate assumptions when applied to the horizontal source of an aircraft engine. This study examined the dispersion of aircraft engine exhaust by using infrared thermal imaging techniques. These results were compared to theoretical equations describing jet exhaust plumes. The resulting validation provided the necessary equations and support to mathematically model this phenomena. GRA

N88-12489# Toronto Univ. (Ontario). Inst. for Aerospace Studies.
NUMERICAL PREDICTION OF PROPELLER PERFORMANCE BY VORTEX LATTICE METHOD
Richard Shiu Wing Cheung Nov. 1987 128 p
(UTIAS-TN-265; ISSN-0082-5263) Avail: NTIS HC A07/MF A01

The vortex lattice methods of lifting line, and lifting surface with one and two layers of vortex elements were developed to analyze the performance of propellers. Comparison of the predicted thrust and power coefficients for NACA 109622, NACA 6623-A, NACA 6623-D straight blade propellers and NACA 4-(4)(06)-057-45A swept blade propeller gives close prediction with the experimental results by using the appropriate vortex lattice method. The vortex lattice method of lifting surface with two layers of vortex elements gives best accuracy among the three methods when it analyzes the performance of thick blade propellers. For thin blade propellers, the method becomes ill-conditioned, and the vortex lattice method of lifting surface with one layer of vortex elements is used, the thickness effect is excluded. Both of the above methods account for the camber of the blades. For thin blade propellers with no camber, the lifting line approach would give sufficient accuracy. Two dimensional airfoil drag data was included in the deviation of the equations of thrust and power coefficients. However, only a small improvement of the predicted results is observed. Author

N88-12490*# National Aeronautics and Space Administration. Lewis Research Center, Cleveland, Ohio.
PERFORMANCE AND COMBUSTION CHARACTERISTICS OF DIRECT-INJECTION STRATIFIED-CHARGE ROTARY ENGINES
Hung Lee Nguyen Dec. 1987 29 p
(NASA-TM-100134; E-3684; NAS 1.15:100134) Avail: NTIS HC A03/MF A01 CSCL 21A

Computer simulations of the direct-injection stratified-charge (DISC) Wankel engine have been used to calculate heat release rates and performance and efficiency characteristics of the 1007R engine. Engine pressure data have been used in a heat release analysis to study the effects of heat transfer, leakage, and crevice flows. Predicted engine performance data are compared with experimental test data over a range of engine speeds and loads. An examination of methods to improve the performance of the Wankel engine with faster combustion, reduced leakage, higher compression ratio, and turbocharging is presented. Author

N88-12509# Joint Publications Research Service, Arlington, Va.
NATIONAL AEROSPACE LABORATORY EXPERIMENT
Ryoji Yanagi *In its* JPRS Report: Science and Technology. Japan 24 Aug. 1987 p 25-28 Transl. into ENGLISH from Kogiken Nyusu (Tokyo, Japan), Nov. 1986 p 1-2 (For primary document see N88-12502 04-12)
Avail: NTIS A06/MF A01

N88-12512# Joint Publications Research Service, Arlington, Va.
SCRAM JET (SUPERSONIC COMBUSTION RAMJET) COMBUSTION EXPERIMENTS
In its JPRS Report: Science and Technology. Japan 24 Aug. 1987 p 33-35 Transl. into ENGLISH from Kogiken Nyusu (Tokyo, Japan), Nov. 1986 p 7-8 (For primary document see N88-12502 04-12)
Avail: NTIS HC A06/MF A01

08 AIRCRAFT STABILITY AND CONTROL

Includes aircraft handling qualities; piloting; flight controls; and autopilots.

For related information see also *05 Aircraft Design, Testing and Performance.*

N88-12491# School of Aerospace Medicine, Brooks AFB, Tex.
F-16 CONTROL STICK RESPONSE DURING +GZ-INDUCED LOSS OF CONSCIOUSNESS Interim Report, Dec. 1985 - Apr. 1986
James E. Whinnery Nov. 1986 21 p
(AD-A184107; USAFSAM-TR-86-26) Avail: NTIS HC A03/MF A01 CSCL 01D

The stick input has been analyzed during deliberate self-induced +Gz loss of consciousness (G-LOC) on the USAF School of Aerospace Medicine human centrifuge. An F-16A stick was utilized with output of + or - pitch, + or - roll, an on-off binary sensory being obtained in 1/8-s intervals during G-LOC and recovery. The results are applicable to emerging aircraft autorecovery technology. The currently known physiologic aspects of G-LOC and their time relationship are reviewed in relation to the potential use of stick force as a rather simplistic G-LOC physiologic monitoring technique. GRA

N88-12492# Army Aviation Engineering Flight Activity, Edwards AFB, Calif.
ENGINE/AIRFRAME RESPONSE EVALUATION OF THE HH-60A HELICOPTER EQUIPPED WITH THE T700-GE-701 TRANSIENT DROOP IMPROVEMENT ELECTRONIC CONTROL UNIT Final Report, 9 Jun. - 25 Aug. 1987
Gary L. Bender, James A. Adkins, and Roy A. Lockwood Oct. 1986 79 p
(AD-A184443; USAAEFA-86-02) Avail: NTIS HC A05/MF A01 CSCL 01C

The engine/drive train response was stable for all tests performed. The best configuration for magnitude of main rotors speed droop, rotor speed/power turbine speed droop recovery characteristics, and power turbine speed governing characteristics was the HH-60A with the T700-GE-401 engines equipped with the -401 transient droop improvement engine control unit. The HH-60A with the T700-GE-401 engine equipped with the -701 transient droop improvement engine control unit (with and without the collective potentiometer input) exhibited larger rotor speed droop, noticeable drive train oscillation during droop recovery, and less desirable power turbine speed governing characteristics. The undesirable engine/airframe characteristics of the HH-60A with the -701 transient droop improvement engine control unit is a shortcoming. The UH-60A with the T700-GE-700 engine demonstrated the largest main rotor speed droop but residual drive train oscillations were small, droop recovery characteristics were more predictable and power turbine speed governing was noticeably more stable than demonstrated by the T700-GE0-401 engines equipped with the -701 transient droop improvement engine control unit. The undesirable engine/airframe response (large main rotor speed droop) of the UH-60A with the T700-GE-700 engines is a previously identified shortcoming. Future designs for the UH-60 engine control units should include all the transient droop improvements of the -401 transient droop improvement engine control unit. Additionally, future designs of engine control units should have dynamics tailored to the particular helicopter in which the engines are to be installed. GRA

N88-12493*# Systems Technology, Inc., Mountain View, Calif.
SOME DATA PROCESSING REQUIREMENTS FOR PRECISION NAP-OF-THE-EARTH (NOE) GUIDANCE AND CONTROL OF ROTORCRAFT
Warren F. Clement, Duane T. McRuer, and Raymond E. Magdeleno Feb. 1987 224 p
(Contract NAS2-12364)
(NASA-CR-177453; NAS 1.26:177453; TR-1239-1) Avail: NTIS HC A10/MF A01 CSCL 01C

Nap-Of-the-Earth (NOE) flight in a conventional helicopter is extremely taxing for two pilots under visual conditions. Developing a single pilot all-weather NOE capability will require a fully automatic NOE navigation and flight control capability for which innovative guidance and control concepts were examined. Constrained time-optimality provides a validated criterion for automatically controlled NOE maneuvers if the pilot is to have confidence in the automated maneuvering technique. A second focus was to organize the storage and real-time updating of NOE terrain profiles and obstacles in course-oriented coordinates indexed to the mission flight plan. A method is presented for using pre-flight geodetic parameter identification to establish guidance commands for planned flight profiles and alternates. A method is then suggested for interpolating this guidance command information with the aid of forward and side looking sensors within the resolution of the stored data base, enriching the data content with real-time display, guidance, and control purposes. A third focus defined a class of automatic anticipative guidance algorithms and necessary data preview requirements to follow the vertical, lateral, and longitudinal guidance commands dictated by the updated flight profiles and to address the effects of processing delays in digital guidance and control system candidates. The results of this three-fold research effort offer promising alternatives designed to gain pilot acceptance for automatic guidance and control of rotorcraft in NOE operations. Author

N88-12494*# National Aeronautics and Space Administration. Ames Research Center, Moffett Field, Calif.
DIGITAL-FLIGHT-CONTROL-SYSTEM SOFTWARE WRITTEN IN AUTOMATED-ENGINEERING-DESIGN LANGUAGE: A USER'S GUIDE OF VERIFICATION AND VALIDATION TOOLS
Jim Saito Jan. 1987 95 p
(NASA-TM-88313; A-86282; NAS 1.15:88313) Avail: NTIS HC A05/MF A01 CSCL 01C

The user guide of verification and validation (V&V) tools for the Automated Engineering Design (AED) language is specifically written to update the information found in several documents pertaining to the automated verification of flight software tools. The intent is to provide, in one document, all the information necessary to adequately prepare a run to use the AED V&V tools. No attempt is made to discuss the FORTRAN V&V tools since they were not updated and are not currently active. Additionally, the current descriptions of the AED V&V tools are contained and provides information to augment the NASA TM 84276. The AED V&V tools are accessed from the digital flight control systems verification laboratory (DFCSVL) via a PDP-11/60 digital computer. The AED V&V tool interface handlers on the PDP-11/60 generate a Univac run stream which is transmitted to the Univac via a Remote Job Entry (RJE) link. Job execution takes place on the Univac 1100 and the job output is transmitted back to the DFCSVL and stored as a PDP-11/60 printfile. Author

N88-12495*# National Aeronautics and Space Administration. Ames Research Center, Moffett Field, Calif.
FLAP-LAG EQUATIONS OF MOTION OF RIGID, ARTICULATED ROTOR BLADES WITH THREE HINGE SEQUENCES
Robert T. N. Chen Nov. 1987 59 p
(NASA-TM-100023; A-87338; NAS 1.15:100023) Avail: NTIS HC A04/MF A01 CSCL 01C

A derivation of coupled flap-lag equations of motion for a rigid articulated rotor with hinge springs and viscous dampers is reported. Three different flapping-lag-pitch hinge sequences are considered and the Lagrange method is used to derive the equations. The effects of the complete six degrees-of-freedom aircraft motions are included and all the inertia dynamic terms are retained; no small-angle assumptions are used in the development. Comparisons of the results with those available in the literature are made. Sources of terms missing in previous analyses, especially those of the inertia dynamics, are identified. Author

N88-12624# Joint Publications Research Service, Arlington, Va.
AIRCRAFT DYNAMIC RESPONSE CALCULATION BASED ON DISCRETE-CONTINUAL MODEL Abstract Only
M. B. Vakhitov, A. S. Safonov, and I. A. Kuznetsov *In its* USSR Report: Engineering and Equipment 28 May 1987 p 3 Transl. into ENGLISH from Izvestiya Vysshikh Uchebnykh Zavedeniy: Aviatsionnaya Tekhnika (Kazan, USSR), no. 4, Oct. - Dec. 1985 p 16-20 (For primary document see N88-12621 04-31)
Copyright Avail: NTIS HC A06/MF A01

N88-12627# Joint Publications Research Service, Arlington, Va.
LOCAL-OPTIMAL CONTROL IN SYSTEMS WITH DELAY Abstract Only
G. L. Degtyaryov and S. A. Terentyev *In its* USSR Report: Engineering and Equipment 28 May 1987 p 7 Transl. into ENGLISH from Izvestiya Vysshikh Uchebnykh Zavedeniy: Aviatsionnaya Tekhnika (Kazan, USSR), no. 4, Oct. - Dec. 1985 p 39-42 (For primary document see N88-12621 04-31)
Copyright Avail: NTIS HC A06/MF A01

09 RESEARCH AND SUPPORT FACILITIES (AIR)

Includes airports, hangars and runways; aircraft repair and overhaul facilities; wind tunnels; shock tubes; and aircraft engine test stands.

For related information see also *14 Ground Support Systems and Facilities (Space).*

N88-12496*# National Aeronautics and Space Administration. Langley Research Center, Hampton, Va.
ANALYSIS OF 7- X 10-FOOT HIGH SPEED WIND TUNNEL SHAFT LOADS IN SUPPORT OF FAN BLADE FAILURE INVESTIGATION
Richard W. Faison Nov. 1987 49 p
(NASA-TM-100504; NAS 1.15:100504) Avail: NTIS HC A03/MF A01 CSCL 14B

This is a report of the investigation of the High-Speed 7- X 10-Foot Wind Tunnel at NASA Langley Research Center, which experienced a catastrophic failure of all 18 Sitka spruce fan blades during operation at 0.8 Mach number on 2 July 1985. The High-Speed Tunnel, a closed-circuit/single-return atmospheric wind tunnel, had been operated since 1945 to support a wide range of subsonic aerodynamic tests and studies. The failed blade set had been in use since 1975. In addition to blade loss, the most significant damage was a bent main drive shaft for a total estimated damage loss of 1.7 million dollars. An analysis of the natural frequency characteristics as well as loads, reactions, stresses, and deflections of the fan drive system resulting from steady-state and dynamic loads due to unbalance was performed. Transient load cases were simulated by step input and ramp input loading functions intended to simulate the loss of one to nine blades (maximum unbalance forces). Author

N88-12497*# Madison Magnetics, Inc., Wis.
REPULSIVE FORCE SUPPORT SYSTEM FEASIBILITY STUDY Progress Report, Sep. 1986 - Apr. 1987
R. W. Boom, M. K. Abdelsalam, Y. M. Eyssa, and G. E. McIntosh Oct. 1987 61 p
(Contract NAS1-18279)
(NASA-CR-178400; NAS 1.26:178400) Avail: NTIS HC A04/MF A01 CSCL 14B

A new concept in magnetic levitation and control is introduced for levitation above a plane. A set of five vertical solenoid magnets mounted flush below the plane supports and controls the model in five degrees of freedom. The compact system of levitation coils is contained in a space 2.4 m (96 in) diameter by 1 m (40 in) deep with the top of the levitation system 0.9 m (36 in) below the center line of the suspended model. The levitated model has a permanent magnet core held in position by the five parallel superconductive solenoids symmetrically located in a circle. The control and positioning system continuously corrects for model position in five dimensions using computer current pulses superimposed on the levitation coil base currents. The conceptual designs include: superconductive and Nd-Fe-B permanent magnet model cores and levitation solenoids of either superconductive, cryoresistive, or room temperature windings. Author

N88-12498*# Ohio State Univ., Columbus. ElectroScience Lab.
NEW MAIN REFLECTOR, SUBREFLECTOR AND DUAL CHAMBER CONCEPTS FOR COMPACT RANGE APPLICATIONS
C. W. I. Pistorius and W. D. Burnside Aug. 1987 350 p
(Grant NsG1-613)
(NASA-CR-181506; NAS 1.26:181506; OSU-716148-22) Avail: NTIS HC A15/MF A01 CSCL 14B

A compact range is a facility used for the measurement of antenna radiation and target scattering problems. Most presently available parabolic reflectors do not produce ideal uniform plane waves in the target zone. Design improvements are suggested to reduce the amplitude taper, ripple and cross polarization errors. The ripple caused by diffractions from the reflector edges can be reduced by adding blended rolled edges and shaping the edge contour. Since the reflected edge continues smoothly from the parabola onto the rolled surface, rather than being abruptly terminated, the discontinuity in the reflected field is reduced which results in weaker diffracted fields. This is done by blending the rolled edges from the parabola into an ellipse. An algorithm which enables one to design optimum blended rolled edges was developed that is based on an analysis of the continuity of the surface radius of curvature and its derivatives across the junction. Futhermore, a concave edge contour results in a divergent diffracted ray pattern and hence less stray energy in the target zone. Design equations for three-dimensional reflectors are given. Various examples were analyzed using a new physical optics method which eliminates the effects of the false scattering centers on the incident shadow boundaries. A Gregorian subreflector system, in which both the subreflector and feed axes are tilted, results in a substantial reduction in the amplitude taper and cross polarization errors. A dual chamber configuration is proposed to eliminate the effects of diffraction from the subreflector and spillover from the feed. A computationally efficient technique, based on ray tracing and aperture integration, was developed to analyze the scattering from a lossy dielectric slab with a wedge termination. Author

N88-12499# Naval Postgraduate School, Monterey, Calif.
AN INEXPENSIVE REAL-TIME INTERACTIVE THREE-DIMENSIONAL FLIGHT SIMULATION SYSTEM Summary Report, 1 Aug. 1986 - 31 Jul. 1987
Michael J. Zyda, Robert B. McGhee, Douglas B. Smith, and Dale G. Streyle 3 Aug. 1987 232 p
(AD-A184340; NPS52-87-034) Avail: NTIS HC A11/MF A01 CSCL 05I

A prototype flight simulator for the Fiber-Optically Guided Missile (FOG-M) is presented. This prototype demonstrates the practicability and feasibility of using low-cost graphics hardware to produce acceptable simulation of flight over terrain generated from Defense Mapping Agency (DMA) digital elevation data. The flight simulator displays a dynamic, three-dimensional, out-the-window view of the terrain in real-time while responding to operator control inputs. The total system cost (software and hardware) of the simulator is an order of magnitude less than most flight simulation systems in current use. GRA

N88-12500# Army Engineer Waterways Experiment Station, Vicksburg, Miss. Geotechnical Lab.
OPEN-GRADED BASES FOR AIRFIELD PAVEMENTS Final Report
Walter R. Barker Jul. 1987 76 p
(AD-A184461; WES/MP/GL-87-16) Avail: NTIS HC A05/MF A01 CSCL 13B

Water has long been recognized as a major contributor to pavement failures. To lessen the potential for damage due to water, the US Army Corps of Engineers established drainage criteria for bases and subbases in airfield pavements. Since the establishment of the drainage criteria, the use of dense-graded aggregate has become the most used material type for airfield pavement bases. Laboratory studies conducted in the late 1960's indicated that the dense-graded bases were almost impermeable and would not meet the drainage criteria. Bases constructed from a uniform size aggregate (an open-graded base) would provide the required permeability but do not have the stability of a denser graded base. A literature review and field survey on the use of open-graded bases and the results of a pilot test section to illustrate the structural capabilities of open-graded bases and follow-up on some ongoing studies are included in this report. GRA

12 ASTRONAUTICS (GENERAL)

For extraterrestrial exploration see *91 Lunar and Planetary Exploration.*

N88-12501*# TRW Defense and Space Systems Group, Redondo Beach, Calif.
STUDY OF PLASMA MOTOR GENERATOR (PMG) TETHER SYSTEM FOR ORBIT REBOOST Final Report
Sep. 1987 54 p
(Contract NAS9-17751)
(NASA-CR-172015; NAS 1.26:172015) Avail: NTIS HC A04/MF A01 CSCL 22A

Detailed designs were produced for a 2 kW plasma motor generator tether system based largely on existing hardware and hardware designs. Specifically, the hollow cathode design and electronics are derived from ion propulsion equipment. A prototype tether was constructed and will be tested for deployment, strength, resistance to breakage and abrasion and electrical properties. In addition, laboratory development models of the electronics will be used to operate two plasma motor generator hollow cathode assemblies with this tether to verify electrical performance parameters for the complete system. Results show that a low cost demonstration of a plasma motor generator tether system appears to be feasible by the middle of the 1990s. Author

N88-12502# Joint Publications Research Service, Arlington, Va.
JPRS REPORT: SCIENCE AND TECHNOLOGY. JAPAN
24 Aug. 1987 106 p Transl. into ENGLISH from various Japanese articles
(JPRS-JST-87-025) Avail: NTIS HC A06/MF A01

Open literature articles or summaries are presented in the areas of advanced materials, aerospace and civil aviation, automotive industry, defense industries, factory automation and robotics, telecommunications, and transportation. For individual titles, see N88-12503 through N88-12512.

N88-12503# Joint Publications Research Service, Arlington, Va.
ACTIVITIES AT GOVERNMENT RESEARCH LABORATORIES REPORTED c26
In its JPRS Report: Science and Technology. Japan 24 Aug. 1987 p 1-3 Transl. into ENGLISH from Nikko Materials (Tokyo, Japan), Feb. 1987 p 35 (For primary document see N88-12502 04-12)
Avail: NTIS HC A06/MF A01

New techniques for production of particle dispersion composites involve: (1) vortex mixing without preliminary treatment; and (2) pressurized casting by pouring molten metal among the particles filled in the mold beforehand. For vortex-mixing, a whirlpool is formed within the molten metal, and the nonmetallic particles are added and mixed within the whirlpool to form the composite materials. Extrusion processing removes air pockets and also strengthens the materials through the realignment of graphite particles in the direction of extrusion. Extrusion in the casting process makes it possible to improve performance, though brittleness becomes more of a problem as nonmetallic content increases. J.P.B.

N88-12504# Joint Publications Research Service, Arlington, Va.
SOLAR CONVERGING METHOD c44
In its JPRS Report: Science and Technology. Japan 24 Aug. 1987 p 3-5 Transl. into ENGLISH from Nikko Materials (Tokyo, Japan) Feb. 1987 p 35-36 (For primary document see N88-12502 04-12)
Avail: NTIS HC A06/MF A01

Reflective mirror segments have been developed to form the basis of the light-condensing units for solar condensers for space stations. One type (A), a carbon fiber reinforced plastic (CFRP) skin surrounding an aluminum honeycomb structure, aims for a high degree of precision in the mirror surface. A second type (B) is constructed from a surface skin alone and is extremely light in weight. For both, the surface roughness was 0.03. Reflectivity was 85.5 percent for Type A and 89.5 percent for Type B. In terms of condensivity, light traveling parallel to the mirror axis fell within a 3 by 3 mm area on a position detection sensor located 1,600 mm from the mirror surface for Type A, with most of the light falling within 1 mm from the center, while for Type B the light was concentrated within a 10 by 10 mm area. At this distance, the spreading of light waves due to spherical aberration is expected to be slightly under 2 mm for an ideal spherical surface, so that Type A shows a very good degree of precision. J.P.B.

N88-12505# Joint Publications Research Service, Arlington, Va.
CERAMICS THIN FILM c27
In its JPRS Report: Science and Technology. Japan 24 Aug. 1987 p 5-7 Transl. into ENGLISH from Nikko Materials (Tokyo, Japan), Feb. 1987 p 36-37 (For primary document see N88-12502 04-12)
Avail: NTIS HC A06/MF A01

A surface has been synthesized in which nitrogen atoms have been placed as if by tweezers into every fifth row of nickel atoms. To achieve this, an ultra-high-vacuum pulse molecular beam was designed for synthesizing new materials by vacuum evaporation of metal atoms in atom layer units, and alternately spraying the gas flow in beam form onto a substrate for extremely short intervals. A wide range of materials such as ceramics can be synthesized while the growth process is under direct observation, making possible highly accurate control of parameters such as membrane thickness. For example, after a one-atom layer of titanium atoms has been adsorbed under ultrahigh-vacuum conditions, oxygen molecules are blown across the substrate for a short period. The oxygen molecules are drawn to the titanium atoms already on the surface, and react with them to form a single layer of titanium oxide. This can be repeated a number of times to obtain a titanium oxide film of the desired thickness. The synthesis reactions progress automatically, entirely under computer control. J.P.B.

N88-12506# Joint Publications Research Service, Arlington, Va.
CARBON-FIBER REINFORCED PLASTICS c24
In its JPRS Report: Science and Technology. Japan 24 Aug. 1987 p 6-7 Transl. into ENGLISH from Ceramics Japan (Tokyo, Japan), Feb. 1987 p 157 (For primary document see N88-12502 04-12)
Avail: NTIS HC A06/MF A01

Results of theoretical testing on a carbon fiber reinforced plastic (CFRP) indicate that a thermal expansion coefficient of zero can be achieved in the direction of a monoelastic main axis. Lamination of fiber-directed materials of CFRP and diagonal monodirectional materials which show thermal expansion yield materials in which compression and expansion are effectively balanced, yielding the zero thermal expansion. Initial trials produced corroborative results. J.P.B.

N88-12507# Joint Publications Research Service, Arlington, Va.
CARBON-FIBER REINFORCED ALUMINUM c24
In its JPRS Report: Science and Technology. Japan 24 Aug. 1987 p 8-9 Transl. into ENGLISH from Ceramics Japan (Tokyo, Japan) Feb. 1987 p 157-158 (For primary document see N88-12502 04-12)
Avail: NTIS HC A06/MF A01

Methods of covering a carbon fiber surface with a protective film were investigated to prevent reactions which would weaken the fiber surface. A carbon fiber reinforced aluminum wire further strengthened by the coating fibers was produced. A metal carbide (SiC) was applied over the carbon fibers and the effect on fiber strength was investigated. The film-covered fiber showed a reduction in strength to 60 percent. Two-layer coatings in which a pure carbon film or a carbon film containing a trace of SiC was applied and then coated with a film of SiC alone worked well in maintaining original fiber strength. Since wetting by molten aluminum was poor for SiC coated fibers, a Ti-B coating was applied before passing the fibers through the molten aluminum. The role of the carbon film is in eliminating defects on the carbon fiber surface and increasing fiber strength, and preventing the propagation into the carbon fiber of cracks originating in brittle Ti-B or SiC films. J.P.B.

N88-12508# Joint Publications Research Service, Arlington, Va.
RESEARCH AND DEVELOPMENT ON HIGH STRENGTH CERAMIC HEATERS DISCUSSED **c27**
In its JPRS Report: Science and Technology. Japan 24 Aug. 1987 p 10-20 Transl. into ENGLISH from Kino Zairyo (Tokyo, Japan), Feb. 1987 p 16-13 (For primary document see N88-12502 04-12)
Avail: NTIS HC A06/MF A01

Some aspects are discussed of the state of the art in producing high-strength ceramic heaters made of alumina-metal carbides where ceramic material itself serves as an electroconductive heater. Characteristics of electroconductivity giving substances are reviewed, and the relationship between volume of electroconductivity giving substance and crystal size on the one hand and specific resistance on the other is discussed. Manufacturing methods are reviewed, including sintering and the hot-press (HP) and hot isostatic press (HIP) methods. Material, electric, thermal, and anti-corrosive properties of the ceramic heaters are discussed. Finally, a few sample applications in industry are mentioned. J.P.B.

N88-12509# Joint Publications Research Service, Arlington, Va.
NATIONAL AEROSPACE LABORATORY EXPERIMENT **c07**
Ryoji Yanagi *In its* JPRS Report: Science and Technology. Japan 24 Aug. 1987 p 25-28 Transl. into ENGLISH from Kogiken Nyusu (Tokyo, Japan), Nov. 1986 p 1-2 (For primary document see N88-12502 04-12)
Avail: NTIS HC A06/MF A01

An experiment was conducted in which turbine blades were cooled using steam in the composite cycle where steam turbines are connected at the last stage. An analysis of heat transmissivity indicated a linear direct correlation between heat transmissivity and the relative amount of steam in the cooling gas. A film cooling experiment revealed that, when the concentration of steam is high during the massive flow, massive flow velocity ratio is small and film cooling efficiency is attained; however, the efficiency curve reverses direction at high concentrations of steam with flow velocity ratio in excess of about 0.6. It is believed that the momentum of blow-off flow increases at high massive velocity ratios because the blow-off flow goes through the boundary layer of the main flow. J.P.B.

N88-12510# Joint Publications Research Service, Arlington, Va.
MOTION AND SPACE SICKNESS **c52**
Naoki Isu *In its* JPRS Report: Science and Technology. Japan 24 Aug. 1987 p 28-30 Transl. into ENGLISH from Kogiken Nyusu (Tokyo, Japan), Nov. 1986 p 2-4 (For primary document see N88-12502 04-12)
Avail: NTIS HC A06/MF A01

An experiment was conducted using 65 cats under anesthesia. After insertion of electrodes, neurone activities were recorded from nuclei vestibulares. Four kinds of vestibular secondary neurones of the posterior semicircular duct system were found, serving in part to control the motor nerve of contralateral cervical muscles. The existence of these neurones is believed to have advantageous functions, coordinating movements of the eyeballs and the neck. J.P.B.

N88-12511# Joint Publications Research Service, Arlington, Va.
NUMERICAL SIMULATION SYSTEM **c60**
In its JPRS Report: Science and Technology. Japan 24 Aug. 1987 p 30-33 Transl. into ENGLISH from Kogiken Nyusu (Tokyo, Japan), Nov. 1986 p 4-5 (For primary document see N88-12502 04-12)
Avail: NTIS HC A06/MF A01

A high-speed numerical simulation system for aviation and space research applications has been designed. The simulator consists of a FACOM VP-400 supercomputer, a high level graphic and image processing unit, remote subsystems based on smaller computers and remote input/output stations, and a high-speed communications network tying everything together. An automatic program is being developed to reduce energy consumption by completing start-up and shut-down with the touch of a button or on a timed basis. J.P.B.

N88-12512# Joint Publications Research Service, Arlington, Va.
SCRAM JET (SUPERSONIC COMBUSTION RAMJET) COMBUSTION EXPERIMENTS **c07**
In its JPRS Report: Science and Technology. Japan 24 Aug. 1987 p 33-35 Transl. into ENGLISH from Kogiken Nyusu (Tokyo, Japan), Nov. 1986 p 7-8 (For primary document see N88-12502 04-12)
Avail: NTIS HC A06/MF A01

An air-heating unit was used in scramjet experiments for the purpose of simulating air flows into an engine in hypersonic flight. The simulation was at an altitude of 20 to 40 km and speed from Mach 4 to Mach 6.7. The unit was connected with a testing combustor. Gaseous hydrogen was sprayed perpendicularly from the wall surface up or down in backward step between cylinders, or in parallel from the backward step on an axis. The hydrogen spontaneously ignited at temperatures equivalent to Mach 5.6 to 6. When the injection flow rate was low, wall pressure distribution moved downstream, indicating supersonic combustion. High wall pressure caused a sharp increase in the vicinity of the backward step, followed by a slow decrease, indicating a change in combustion speed into the subsonic. The different ejection systems showed a marked difference in fuel component rate distribution, with parallel injection resulting in a mixture that is unsatisfactory on initial injection. This combustor would be difficult to incorporate in an airframe because the fuel does not sufficiently reach the center of combustion. J.P.B.

13 ASTRODYNAMICS

Includes powered and free-flight trajectories; and orbital and launching dynamics.

N88-12680*# Jet Propulsion Lab., California Inst. of Tech., Pasadena.
A DEMONSTRATION OF HIGH PRECISION GPS ORBIT DETERMINATION FOR GEODETIC APPLICATIONS
S. M. Lichten and J. S. Border *In its* The Telecommunications and Data Acquisition Report 15 Nov. 1987 p 1-22 (For primary document see N88-12679 04-32)
Avail: NTIS HC A15/MF A01 CSCL 22A

N88-12682*# Jet Propulsion Lab., California Inst. of Tech., Pasadena.
PRECISE NEAR-EARTH NAVIGATION WITH GPS: A SURVEY OF TECHNIQUES
T. P. Yunck, S. C. Wu, and J. Wu *In its* The Telecommunications and Data Acquisition Report 15 Nov. 1987 p 29-45 (For primary document see N88-12679 04-32)
Avail: NTIS HC A15/MF A01 CSCL 22A

14 GROUND SUPPORT SYSTEMS AND FACILITIES (SPACE)

Includes launch complexes, research and production facilities; ground support equipment, e.g., mobile transporters; and simulators.

For related information see also *09 Research and Support Facilities (Air).*

N88-12513# Sandia National Labs., Albuquerque, N. Mex.
ULTIMATE VELOCITIES FOR INDUCTION LAUNCHERS
M. Cowan 1987 4 p Presented at the 6th IEEE Pulsed Power Conference, Washington, D.C., 29 Jun. 1987
(Contract DE-AC04-76DP-00789)
(DE87-012360; SAND-87-0642C; CONF-8706155-2) Avail: NTIS HC A02

The ultimate velocity achievable with railguns will probably be determined by how well one can manage to minimize barrel effects

associated with the need for sliding electrical contact between the rails and the armature. However, in principle, electromagnetic launchers can use levitated projectiles which are propelled by induced currents. Then barrel effects can be eliminated altogether, and the ultimate velocity is determined by ohmic heating of the projectile. In this paper, the velocity capabilities for these kinds of launchers - called induction launchers - are discussed. Requirements and pulsed power implications for achieving velocities in the 10 to 100 km/s range are developed. DOE

N88-12514# Los Alamos National Lab., N. Mex.
THERMAL ANALYSIS OF ELECTROMAGNETIC LAUNCHER RAILS
N. M. Schnurr Oct. 1987 15 p
(Contract W-7405-eng-36)
(DE88-000166; LA-11087-MS) Avail: NTIS HC A03/MF A01

A numerical technique has been developed to analyze the combined thermal and electric field diffusion in electromagnetic launcher rails. TOPAZ2D, a two-dimensional finite-element thermal analysis code, has been adapted for this purpose. The resulting code, TOPAZRG, was used to predict the temperature field in the rails of the Lethality Test System being constructed at Los Alamos. Results of those calculations indicate the possibility of localized melting at the rail corners under full-power conditions. A parametric study was made to determine the effect of using tungsten coatings to prevent the melting of rail surfaces. The results of those computations show that the time to melt for a given surface heat flux can be increased by a factor of 2.8. Optimum coating thicknesses were determined for a range of heat fluxes. DOE

N88-12515*# National Aeronautics and Space Administration. Lewis Research Center, Cleveland, Ohio.
OPTICAL ALIGNMENT OF CENTAUR'S INERTIAL GUIDANCE SYSTEM
Andrew L. Gordan Dec. 1987 108 p
(NASA-TM-88844; E-3226; NAS 1.15:88844) Avail: NTIS HC A06/MF A01 CSCL 14B

During Centaur launch operations the launch azimuth of the inertial platform's U-accelerometer input axis must be accurately established and maintained. This is accomplished by using an optically closed loop system with a long-range autotheodolite whose line of sight was established by a first-order survey. A collimated light beam from the autotheodolite intercepts a reflecting Porro prism mounted on the platform azimuth gimbal. Thus, any deviation of the Porro prism from its predetermined heading is optically detected by the autotheodolite. The error signal produced is used to torque the azimuth gimbal back to its required launch azimuth. The heading of the U-accelerometer input axis is therefore maintained automatically. Previously, the autotheodolite system could not distinguish between vehicle sway and rotational motion of the inertial platform unless at least three prisms were used. One prism was mounted on the inertial platform to maintain azimuth alignment, and two prisms were mounted externally on the vehicle to track sway. For example, the automatic azimuth-laying theodolite (AALT-SV-M2) on the Saturn vehilce used three prisms. The results of testing and modifying the AALT-SV-M2 autotheodolite to simultaneously monitor and maintain alignment of the inertial platform and track the sway of the vehicle from a single Porro prism. Author

N88-12516# Materials Research Labs., Melbourne (Australia).
ANALYSIS OF A SERIES OF ELECTROMAGNETIC LAUNCHER FIRINGS
V. Kowalenko Jun. 1987 95 p
(AR-005-131; MRL-R-1053) Avail: NTIS HC A05/MF A01

Theoretical aspects of electromagnetic launchers are presented in conjunction with an analysis of diagnostic measurements taken during the RAPID Plasma Intensity Profiles (RPIP) series of firings. These theoretical aspects deal with the current time behavior, the plasma temperature and the evaluation of railgun parameters such as the efficiency and effective inductance per unit length. The principal aims of the RPIP series were: (1) to see if different types and masses of plasma generating foils affected railgun performance and the diagnostic measurements taken during each firing, and (2) to compare some of the theoretical predictions of the Plasma Armature Rail Accelerator (PARA) simulation code with experimental results. Projectile displacement time results for the series were obtained by digitizing photographs from a streak camera and in order to verify the PARA predictions for plasma length behavior, light intensity profiles were produced from microdensiometer readings of the streak film. The experimental results were affected by plasma disruption, arcing ahead of the projectile and plasma leakage. These effects are also discussed. Author

N88-12517# Materials Research Labs., Melbourne (Australia).
EFFICIENCY ASPECTS OF SHORT, LOW VELOCITY RAILGUNS
C. I. Sach Jun. 1987 35 p
(AR-004-847; MRL-R-1029) Avail: NTIS HC A03/MF A01

The factors controlling the performance of short, low velocity railguns are studied and mathematical expressions defining the bounds of realizable efficiencies are obtained. The restrictions governing the validity of the expressions are discussed. The expressions are based on the proposition that during acceleration of the projectile in the railgun, the current fails almost linearly with time. Under the conditions discussed, it is shown that the maximum achievable efficiency is about 1.6 percent. Author

N88-12518# National Aeronautical Establishment, Ottawa (Ontario).
ACCESS TO MICROGRAVITY: A TECHNICAL DESCRIPTION OF THE NAE T-33 MICROGRAVITY FACILITY
J. F. Aitken Oct. 1987 43 p
(NAE-AN-47; NRC-26342) Avail: NTIS HC A03/MF A01

The National Aeronautical Establishment of Canada operates a T-33 aircraft as a facility for short duration microgravity experiments. Details covering available sensors, experiment electrical and mechanical requirements, package size constraints, power available, and requirements for interfacing experiments with the aircraft instrumentation system are provided for the microgravity experimenter. Author

N88-12519# Lawrence Livermore National Lab., Calif.
THE LLNL 150-mM EQUATION-OF-STATE GUN SYSTEM
F. Rienecker, C. Honodel, R. Waldron, E. Moor, S. Perfect, and R. Bast 22 Sep. 1987 35 p Presented at the 38th Meeting of the Aeroballistics Range Association, Tokyo, Japan, 6 Oct. 1987
(Contract W-7405-eng-48)
(DE88-000423; UCRL-97378; CONF-8710157-1) Avail: NTIS HC A03/MF A01

Lawrence Livermore National Laboratory is currently designing a large gun system for expanded studies of a wide range of materials, including samples of high explosives weighing up to 10 kg. In its initial configuration, the system will have a 150-mm bore, 20-m-long, single-stage gun that can fire a 10-kg projectile at velocities of 2.2 km/s. Future plans include conversion either to a two-stage gun, or to a single-stage 100-mm gun, and conversion to a ballistic range. The high-explosive samples will be contained in a stainless steel tank that is 3.8 m in diameter, 12.5-m long, and 89-mm thick. This paper emphasizes improvements in the gun design, including tube couplings that use large coupling nuts and elastic interference fits to achieve precise alignment, a rail support system that allows rapid changes of configuration without need for re-alignment, and a barrel venting experiment designed to reduce projectile tilt in free flight. In addition, a computer modeling experiment is discussed in which are examined the effects of stress and strain on one part of the gun, the breech. Results showed that peak stresses would cause the breech to deform, producing auto frettaged conditions. DOE

15 LAUNCH VEHICLES AND SPACE VEHICLES

Includes boosters; operating problems of launch/space vehicle systems; and reusable vehicles.

For related information see also *20 Spacecraft Propulsion and Power.*

No abstracts in this category.

16 SPACE TRANSPORTATION

Includes passenger and cargo space transportation, e.g., shuttle operations; and space rescue techniques.

For related information see also *03 Air Transportation and Safety* and *18 Spacecraft Design, Testing and Performance.* For space suits see *54 Man/System Technology and Life Support.*

N88-12520*# National Aeronautics and Space Administration. Lewis Research Center, Cleveland, Ohio.
SPACECRAFT FIRE SAFETY
Janice M. Margle, ed. (Pennsylvania State Univ., Abington.) 1987 134 p Workshop held in Cleveland, Ohio, 20-21 Aug. 1986
(NASA-CP-2476; E-3464; NAS 1.55:2476) Avail: NTIS HC A07/MF A01 CSCL 22B

Fire detection, fire standards and testing, fire extinguishment, inerting and atmospheres, fire-related medical science, aircraft fire safety, Space Station safety concerns, microgravity combustion, spacecraft material flammability testing, and metal combustion are among the topics considered. For individual titles, see N88-12521 through N88-12530.

N88-12521*# National Bureau of Standards, Gaithersburg, Md. Center for Fire Research.
TECHNIQUES FOR FIRE DETECTION **c31**
Richard W. Bukowski *In* NASA, Lewis Research Center, Spacecraft Fire Safety 1987 p 9-29 (For primary document see N88-12520 04-16)
Avail: NTIS HC A07/MF A01 CSCL 22B

An overview is given of the basis for an analysis of combustable materials and potential ignition sources in a spacecraft. First, the burning process is discussed in terms of the production of the fire signatures normally associated with detection devices. These include convected and radiated thermal energy, particulates, and gases. Second, the transport processes associated with the movement of these from the fire to the detector, along with the important phenomena which cause the level of these signatures to be reduced, are described. Third, the operating characteristics of the individual types of detectors which influence their response to signals, are presented. Finally, vulnerability analysis using predictive fire modeling techniques is discussed as a means to establish the necessary response of the detection system to provide the level of protection required in the application. Author

N88-12522*# National Bureau of Standards, Washington, D.C. Center for Fire Research.
FIRE-RELATED STANDARDS AND TESTING **c31**
Vytenis Babrauskas *In* NASA, Lewis Research Center, Spacecraft Fire Safety 1987 p 31-41 (For primary document see N88-12520 04-16)
Avail: NTIS HC A07/MF A01 CSCL 22B

The state of the art of flammability testing has been changing rapidly. Here, the progress in developing general test methods for solid materials and products exposed to an external fire are reviewed. The special requirements pertinent to environments of concern to NASA are examined and some suggestions for possible directions for future test method developments are given. Author

N88-12523*# Factory Mutual Research Corp., Norwood, Mass.
FIRE EXTINGUISHMENT AND INHIBITION IN SPACECRAFT ENVIRONMENTS
John deRis *In* NASA. Lewis Research Center, Spacecraft Fire Safety 1987 p 43-49 (For primary document see N88-12520 04-16)
Avail: NTIS HC A07/MF A01 CSCL 22B

It was concluded that it is essential that NASA develop a comprehensive approach to fire extinguishment and inerting in spacecraft environments. Electronic equipment might be easily protected through use of an onboard inert gas generating system. The use of Halon 1301 presents serious technological challenges for agent cleanup and removal of the toxic and corrosive products of combustion. Nitrogen pressurization, while effective, probably presents a serious weight penality. The use of liquid water sprays appears to be the most effective approach to general purpose spacecraft fire protection. Author

N88-12524*# Naval Research Lab., Washington, D.C.
INERTING AND ATMOSPHERES
Homer W. Carhart *In* NASA, Lewis Research Center, Spacecraft Fire Safety 1987 p 51-57 (For primary document see N88-12520 04-16)
Avail: NTIS HC A07/MF A01 CSCL 22B

It is argued that fires are dependent primarily on the concentration of oxygen, whereas life is dependent on the partial pressure of oxygen. It follows that in an inhabited capsule it should be possible to exercise a certain amount of willful control over fire and still maintain habitability by proper selection of the composition of the atmosphere. This leads to two concepts in the control of fires in confined spaces by controlling atmospheric composition: the first, to lower the overall potential hazard by maintaining the percent of oxygen in the capsule below that of air, and second, to provide for the emergency extinguishment of a fire by sudden flooding with nitrogen. Several relevant charts and graphs are presented. Author

N88-12525*# Naval Submarine Medical Research Lab., Groton, Conn.
FIRE-RELATED MEDICAL SCIENCE **c52**
Douglas R. Knight *In* NASA, Lewis Research Center, Spacecraft Fire Safety 1987 p 59-64 (For primary document see N88-12520 04-16)
Avail: NTIS HC A07/MF A01 CSCL 22B

Spacecraft fire safety may be improved by the use of a fire-retardant atmosphere in occupied spaces. Low concentrations of oxygen can protect humans from fire damage by reducing the rate and spread of combustion, but care must be taken to avoid the hypoxic effects of oxygen-lean atmospheres. Crews can live and work in 11 percent oxygen if barometric pressure were adjusted to maintain the partial pressure of oxygen above 16 kPa. Eleven percent oxygen should prevent most types of fires, since 15 percent oxygen retards the combustion of paper and 13 percent oxygen extinguishes pentane flames. Test results indicate that seated humans can perform mental tasks in atmospheres containing 11.5 percent oxygen. Although this strategy of fire safety is under consideration for submarines, it could be adapted to spacecraft once operational procedures define a maximum hyperbaric pressure and fire research defines the effects of reduced oxygen concentrations on combustion in low gravity environments. Author

N88-12526*# Air Force Wright Aeronautical Labs., Wright-Patterson AFB, Ohio. Aero Propulsion Lab.
AIRCRAFT FIRE SAFETY RESEARCH **c03**
Benito P. Botteri *In* NASA. Lewis Research Center, Spacecraft Fire Safety 1987 p 65-72 (For primary document see N88-12520 04-16)
Avail: NTIS HC A07/MF A01 CSCL 01C

During the past 15 years, very significant progress has been made toward enhancing aircraft fire safety in both normal and hostile (combat) operational environments. Most of the major aspects of the aircraft fire safety problem are touched upon here.

The technology of aircraft fire protection, although not directly applicable in all cases to spacecraft fire scenarios, nevertheless does provide a solid foundation to build upon. This is particularly true of the extensive research and testing pertaining to aircraft interior fire safety and to onboard inert gas generation systems, both of which are still active areas of investigation. Author

N88-12527*# National Aeronautics and Space Administration. Lyndon B. Johnson Space Center, Houston, Tex.
SPACE STATION INTERNAL ENVIRONMENTAL AND SAFETY CONCERNS
Matthew B. Cole *In* NASA. Lewis Research Center, Spacecraft Fire Safety 1987 p 73-87 (For primary document see N88-12520 04-16)
Avail: NTIS HC A07/MF A01 CSCL 22B

Space station environmental and safety concerns, especially those involving fires, are discussed. Several types of space station modules and the particular hazards associated with each are briefly surveyed. A brief history of fire detection and suppression aboard spacecraft is given. Microgravity fire behavior, spacecraft fire detector systems, space station fire suppression equipment and procedures, and fire safety in hyperbaric chambers are discussed. R.J.F.

N88-12528*# National Aeronautics and Space Administration. Lewis Research Center, Cleveland, Ohio.
MICROGRAVITY COMBUSTION FUNDAMENTALS c29
Kurt R. Sacksteder *In its* Spacecraft Fire Safety 1987 p 89-94 (For primary document see N88-12520 04-16)
Avail: NTIS HC A07/MF A01 CSCL 22A

A brief summary of some of the important physical processes involved in low gravity combustion is given. While the discussion is generally limited to the processes involved in the combustion of continuous, solid, nonmetallic fuels, much of the reasoning presented can be applied to other fuel types and configurations. Author

N88-12529*# McDonnell-Douglas Astronautics Co., Houston, Tex.
SPACECRAFT MATERIAL FLAMMABILITY TESTING AND CONFIGURATIONS c24
Paul W. Ledoux *In* NASA, Lewis Research Center, Spacecraft Fire Safety 1987 p 95-98 (For primary document see N88-12520 04-16)
Avail: NTIS HC A07/MF A01 CSCL 11D

Material and configuration testing for the Space Shuttle is mainly at 30 percent oxygen concentration at 70 kPa (10.2 psia). This is the worst case atmosphere during a mission and occurs 10 hours prior to extravehicular activity. The pressure is reduced from the nominal 101 kPa (14.7 paia) and the oxygen concentration is increased to 30 percent for medical reasons to prevent the bends during the extravehicular activity. NASA has tested many materials at 23.8, 25.9 and 30 percent oxygen levels for the Shuttle program. Data is given to show how flammability of material is affected by percentage of oxygen for those materials that would be considered for spacecraft applications. Author

N88-12530*# National Aeronautics and Space Administration. White Sands Test Facility, N. Mex.
IGNITION AND COMBUSTION OF METALS IN OXYGEN c26
Frank J. Benz and S. Zhu (Lockheed Engineering and Management Services Co., Inc., Las Cruces, N. Mex.) *In* NASA, Lewis Research Center, Spacecraft Fire Safety 1987 p 99-102 (For primary document see N88-12520 04-16)
Avail: NTIS HC A07/MF A01 CSCL 11F

Tests in which metals were rubbed against themselves in oxygen have revealed that increasing oxygen pressure does not always increase the potential for ignition. It is believed that there exists a specific pressure above which convective heat loss due to higher oxygen density will overcome the potential increase in the oxidation rate afforded by the increase in oxygen pressure. Test results have shown that, once a specific oxygen pressure is exceeded, greater rates of frictional energy were required for ignition of metals as pressure is increased. Other test results have indicated that as oxygen pressure is increased during the rubbing process, the bulk sample equilibrium temperatures decrease. These results support the belief that increases in convective heat loss as pressure is increased can raise the energy requirements for ignition of metals or lower their ignition potentials. Testing has also indicated that, when metals were exposed to a rubbing process and oxygen pressure was increased, metals such as carbon steel exhibited a decrease in their bulk ignition temperatures, whereas metals such as Monel showed bulk ignition temperatures independent of pressure. Author

17 SPACE COMM., SPACECRAFT COMM., COMMAND & TRACKING

Includes telemetry; space communications networks; astronavigation and guidance; and radio blackout.

For related information see also *04 Aircraft Communications and Navigation* and *32 Communications and Radar.*

N88-12683*# Jet Propulsion Lab., California Inst. of Tech., Pasadena.
SHORT BASELINE PHASE DELAY INTERFEROMETRY
C. D. Edwards *In its* The Telecommunications and Data Acquisition Report 15 Nov. 1987 p 46-56 (For primary document see N88-12679 04-32)
Avail: NTIS HC A15/MF A01 CSCL 09F

18 SPACECRAFT DESIGN, TESTING AND PERFORMANCE

Includes satellites; space platforms; space stations; spacecraft systems and components such as thermal and environmental controls; and attitude controls.

For life support systems see *54 Man/System Technology and Life Support.* For related information see also *05 Aircraft Design, Testing and Performance, 39 Structural Mechanics,* and *16 Space Transportation.*

N88-12531*# National Aeronautics and Space Administration. Langley Research Center, Hampton, Va.
STRUCTURAL ANALYSIS OF A BOLTED JOINT CONCEPT FOR THE SPACE SHUTTLE'S SOLID ROCKET MOTOR CASING
Michael C. Lindell and Winifred A. Stalnaker Sep. 1987 8 p Presented at the AIAA/SAE/ASME/ASEE 23rd Joint Propulsion Conference, San Diego, Calif., 29 Jun. - 2 Jul. 1987 Previously announced as A87-45340
(NASA-TM-89092; NAS 1.15:89092) Avail: NTIS HC A02/MF A01 CSCL 22B

The Space Shuttle Challenger accident is thought to have been caused by the failure of one of the tang-clevis joints joining together the casing segments of the Solid Rocket Motors (SRM). Excessive displacement between the tang and clevis, possibly unseating the O-ring seals, may have initiated the resulting accident. An effort was made at NASA Langley Research Center to design an alternative concept for mating the casing segments. A bolted flange joint concept was designed and analyzed to determine if the concept would effectively maintain a seal while minimizing joint weight and controlling stress levels. It is shown that under the loading conditions analyzed the seal area of the joint remains seated. The only potential stress problem is a stress concentration in the flange at the edge of the bolt hole, which is highly localized. While heavier than the existing joint, this concept does have some advantages making the bolted joint an attractive alternative. Author

N88-12532*# Science Applications International Corp., Huntsville, Ala.
OPTIMIZATION TECHNIQUES APPLIED TO PASSIVE MEASURES FOR IN-ORBIT SPACECRAFT SURVIVABILITY Final Report
Robert A. Mog and D. Marvin Price Nov. 1987 299 p
(Contract NAS8-37378)
(NASA-CR-179216; NAS 1.26:179216; HV410-12) Avail: NTIS HC A13/MF A01 CSCL 22B

Optimization techniques applied to passive measures for in-orbit spacecraft survivability, is a six-month study, designed to evaluate the effectiveness of the geometric programming (GP) optimization technique in determining the optimal design of a meteoroid and space debris protection system for the Space Station Core Module configuration. Geometric Programming was found to be superior to other methods in that it provided maximum protection from impact problems at the lowest weight and cost. Author

N88-12533*# Smithsonian Astrophysical Observatory, Cambridge, Mass.
ANALYTICAL INVESTIGATION OF THE DYNAMICS OF TETHERED CONSTELLATIONS IN EARTH ORBIT (PHASE 2) Quarterly Report No. 10, 1 Jul. - 30 Sep. 1987
Enrico C. Lorenzini Oct. 1987 64 p
(Contract NAS8-36606)
(NASA-CR-179218; NAS 1.26:179218) Avail: NTIS HC A04/MF A01 CSCL 22B

Simulation of two short distance crawling maneuvers of the elevator both with and without environmental perturbations acting upon the system is discussed. These simulation runs were performed in order to provide results useful for the interpretation of the data from the tests, on the ground, of a scaled down engineering model of the elevator. In these simulation runs the elevator crawls along the tether in accordance to the developed mirror image motion control law (MIMCL). Results from the simulation of the 4 km long maneuver run were compared to those obtained by adopting the modified hyperbolic tangent control law (MHTCL). A preprocessor was developed for setting up the initial conditions of a tethered system with L platforms, M longitudinal dampers, and N lumped masses (platforms plus tether beads). A short test run of the 4-platform system with 3 longitudinal dampers and 10 lumper mass without any perturbation acting upon the system is illustrated. In support of the Tether Applications Working Group, SAO is preparing a catalog of tether simulations, has prepared a set of simulator test cases, obtained results from SKYHOOK, and solicited results from simulators at other institutions, and prepared a paper on a specific analytic solution. B.G.

N88-12534 North Carolina State Univ., Raleigh.
NATURAL CONTROL OF FLEXIBLE SPACE STRUCTURES Ph.D. Thesis
Mark Harrison Morton 1987 145 p
Avail: Univ. Microfilms Order No. DA8718909

Families of structural control systems are characterized and the inherent properties that provide the essential motiviation behind the theory of Natural Control are revealed. First, the nature of Natural Control and the associated exponential stability characteristics of flexible space structures are described. Next the dynamics of freely non-rotating flexible spacecraft are reviewed and the results extended to rotating flexible spacecraft. Finally, the effect of using a limited number of forces to control the non-rotating spacecraft over the use of distributed control forces is characterized by a change in the magnitude of the control effort and a deterioration in the dynamic performance. Two numerical examples demonstrate the results. Dissert. Abstr.

N88-12535 Virginia Polytechnic Inst. and State Univ., Blacksburg.
NEW FEEDBACK DESIGN METHODOLOGIES FOR LARGE SPACE STRUCTURES: A MULTI-CRITERION OPTIMIZATION APPROACH Ph.D. Thesis
Dong-Won Rew 1987 228 p
Avail: Univ. Microfilms Order No. DA8719050

Three new feedback design algorithms are presented: (1) a generalized linear-quadratic regulator (LQR) formulation; (2) a generalized LQR formulation based on Lyapunov stability theorem; and (3) an eigenstructure assignment method using Sylvester's equation. In addition, a noniterative robust eigenstructure assignment algorithm via a projection method is introduced, which produces a fairly well-conditioned eigenvector matrix and provides an excellent starting solution for optimizations of various design criteria. Finally, two sets of numerical examples are adopted: 6th order mass-spring systems and various reduced order models of a flexible system. The numerical results confirm that the use of multi-criterion optimizations by using a minimum correction homotopy technique is a useful tool with significant potential for enhanced computer-aided design of control systems. The robust eigenstructure assignment algorithm is implemented and tested for a 24th reduced order model, which establishes the approach to be applicable to systems of at least moderate dimensionality. It is shown analytically and computationally that constraining closed-loop eigenvectors to equal open-loop eigenvectors generally does not lead to either optimal conditioning (robustness) of the closed-loop eigenvectors or minimum gain norm. Dissert. Abstr.

19 SPACECRAFT INSTRUMENTATION

For related information see also *06 Aircraft Instrumentation* and *35 Instrumentation and Photography.*

No abstracts in this category.

20 SPACECRAFT PROPULSION AND POWER

Includes main propulsion systems and components, e.g., rocket engines; and spacecraft auxiliary power sources.

For related information see also *07 Aircraft Propulsion and Power, 28 Propellants and Fuels, 44 Energy Production and Conversion,* and *15 Launch Vehicles and Space Vehicles.*

N88-12536# Stuttgart Univ. (West Germany). Inst. fuer Raumfahrtantriebe.
PLASMA THRUSTER DEVELOPMENT Final Report, Oct. 1984 - Sep. 1986
H. O. Schrade, M. Auweter-Kurtz, H. L. Kurtz, W. D. Merke, and P. C. Sleziona Jul. 1987 121 p
(Grant AF-AFOSR-0394-84)
(AD-A184173; IRS-87-P-10; AFAL-TR-87-053) Avail: NTIS HC A06/MF A01 CSCL 01C

Despite the present great lead of ion engines in development level, performance and life for sizes up to several kW, new interest in magnetoplasmadynamic (MPD) thrusters for higher power levels (up to hundreds of kW) has arisen in recent years. Mission studies showed specific impulse values between 1000 and 2000 s for orbit raising and orbit transfers for optimized mass savings and trip times, and advantages for MPD propulsion even with relatively low efficiencies. With the probable realization of the SP-100 nuclear space power plant, sufficient power would also be available for steady state MPD propulsion, so that the benefits of these thrusters versus pulsed ones could be utilized; i.e., the ruggedness and simplicity of power and propellant conditioning and the about 3 orders of magnitude smaller cathode erosion. But there are also disadvantages of steady state thrusters; e.g., with quasi-steady ones (but with other geometries) the achieved efficiencies and specific impulses were in some cases higher. The research work covered in this report deals with these and related problems: in chapter two, the experimental results with nozzle-type and

cylindrical thrusters are presented. The influence of cathode position, ambient pressure, anode gas injection and propellant type on the performance is investigated. The thruster design studies and the heat transfer calculations for the MPD thruster with a radiation-cooled anode are reported. GRA

N88-12537*# Rockwell International Corp., Canoga Park, Calif. Systems Dynamics.
FAILURE CONTROL TECHNIQUES FOR THE SSME Final Report
M. H. Taniguchi [1987] 187 p
(Contract NAS8-36305)
(NASA-CR-179224; NAS 1.26:179224; RI/RD86-165-Rev) Avail: NTIS HC A09/MF A01 CSCL 21H

Since ground testing of the Space Shuttle Main Engine (SSME) began in 1975, the detection of engine anomalies and the prevention of major damage have been achieved by a multi-faceted detection/shutdown system. The system continues the monitoring task today and consists of the following: sensors, automatic redline and other limit logic, redundant sensors and controller voting logic, conditional decision logic, and human monitoring. Typically, on the order of 300 to 500 measurements are sensed and recorded for each test, while on the order of 100 are used for control and monitoring. Despite extensive monitoring by the current detection system, twenty-seven (27) major incidents have occurred. This number would appear insignificant compared with over 1200 hot-fire tests which have taken place since 1976. However, the number suggests the requirement for and future benefits of a more advanced failure detection system. F.M.R.

N88-12538*# National Aeronautics and Space Administration. Lewis Research Center, Cleveland, Ohio.
COMPATABILITY OF DISPERSION-STRENGTHENED PLATINUM WITH RESISTOJET PROPELLANTS
Margaret V. Whalen and Michael V. Nathal Oct. 1987 29 p
(NASA-TP-2765; E-3738; NAS 1.60:2765) Avail: NTIS HC A03/MF A01 CSCL 21H

Resistojets for the Space Station require long life and multipropellant capability. The choice of available materials to meet these requirements is limited. Dispersion-strengthened platinum was selected. Past results indicated that it should be suffieiently inert in candidate propellant environments and should be capable of operating at moderate temperatures for extended periods. A series of propellant compatibility tests was done with platinum strengthened with either yttria or zirconia. Data presented included the results of 1000-hr tests in CO2, H2, ammonia (NH3), N2, steam, hydrazine (N2H4), and methane (CH4); and 2000-hr tests in H2 and NH3. The platinum samples were tested at 1400 C in CO2, H2, NH3, N2, steam, and N2H4; at 500 C in CH4; and at 800 C in N2H4. The mass-loss results indicated material life, exptrapolated from experimental mass-loss data, in excess of 100 000 hr in all environments except steam and N2H4, where it was greater than or =45000 hr. Generally, on the basis of mass loss, there were no compatibility concerns in any of the environments considered. Optical and scanning electron microscopy were used to determine the effect of propellants on the material surface and to evaluate material stability. Author

N88-12539*# National Aeronautics and Space Administration. Lewis Research Center, Cleveland, Ohio.
A TWO-DIMENSIONAL FINITE DIFFERENCE PROGRAM FOR THERMAL ANALYSIS OF ROCKET THRUST CHAMBERS
Mohammad H. Naraghi Sep. 1987 53 p
(Grant NAG3-672)
(NASA-TM-100191; E-3773; NAS 1.15:100191) Avail: NTIS HC A04/MF A01 CSCL 21H

A two-dimensional finite difference computer model for thermal analysis of rocket thrust chambers has been developed. The model uses an iterative scheme for calculating the temperature distribution within the chamber wall and implements a successive overrelaxation formula for a quick convergence. The inputs of the models are the dimensions of the thrust chamber wall, types of materials used, heat transfer coefficients and temperatures of the hot gas and the coolant. The resulting output of the program consists of the nodal temperature distribution, heat transfer to the coolant and heat transfer from the hot gas. Author

N88-12540*# National Aeronautics and Space Administration. Lyndon B. Johnson Space Center, Houston, Tex.
INTERPLANETARY PROPULSION USING INERTIAL FUSION
C. D. Orth, W. J. Hogan, N. Hoffman, K. Murray, G. Klein, and F. C. Diaz Jan. 1987 23 p Presented at the 4th Symposium on Space Nuclear Power Systems, Albuquerque, N. Mex., 12 Jan. 1987 Prepared in cooperation with Lawrence Livermore National Lab., Calif., Rockwell International Corp., Canoga Park, Calif. and JPL, Pasadena, Calif.
(Contract W-7405-eng-48)
(NASA-TM-89661; NAS 1.15:89661; DE87-014342; UCRL-95275-Rev-1; CONF-870102-29-Rev-1) Avail: NTIS HC A03/MF A01 CSCL 21C

Inertial fusion can be used to power spacecraft within the solar system and beyond. Such spacecraft have the potential for short-duration manned-mission performance exceeding other technologies. We are conducting a study to assess the systems aspects of inertial fusion as applied to such missions, based on the conceptual engine design of Hyde (1983) we describe the required systems for an entirely new spacecraft design called VISTA that is based on the use of DT fuel. We give preliminary design details for the power conversion and power conditioning systems for manned missions to Mars of total duration of about 100 days. Specific mission performance results will be published elsewhere, after the study has been completed. DOE

N88-12541*# Rockwell International Corp., Canoga Park, Calif. Rocketdyne Div.
SPACE STATION RESISTOJET SYSTEM REQUIREMENTS AND INTERFACE DEFINITION STUDY Final Report, Jun. 1986 - Jun. 1987
L. E. Finden Nov. 1987 120 p
(Grant NAS3-24658)
(NASA-CR-180832; NAS 1.26:180832; RI/RD-87-211) Avail: NTIS HC A06/MF A01 CSCL 21H

A conceptual design study of the resistojet orbital replacement unit (ORU) was conducted. The ORU consists of four 500-W multipropellant resistojets, fluid components downstream of the waste fluid storage subsystem, a power controller, structure, and micrometeorite shielding. The fluid components include latch valves, a water vaporizer, two pressure regulators or flow control valves, filters, check valves, fluid tubing, and interface couplings. Separate fluid components are provided for oxidizing fluids, reducing fluids and water. Different flow and power control methods were studied. The most promising methods consist of a constant pressure/on-off power control and a constant power/variable pressure control. The closed-loop power control incorporates a feedback signal which is proportional to resistojet heater temperature. Author

N88-12542*# National Aeronautics and Space Administration. Lewis Research Center, Cleveland, Ohio.
HIGH POWER ION THRUSTER PERFORMANCE
Vincent K. Rawlin and Michael J. Patterson 1987 14 p Presented at the Fourth Symposium on Space Nuclear Power Systems, Albuquerque, N. Mex., 12-16 Jan. 1987
(NASA-TM-100127; E-3676; NAS 1.15:100127) Avail: NTIS HC A03/MF A01 CSCL 21C

The ion thruster is one of several forms of space electric propulsion being considered for use on future SP-100-based missions. One possible major mission ground rule is the use of a single Space Shuttle launch. Thus, the mass in orbit at the reactor activation altitude would be limited by the Shuttle mass constraints. When the spacecraft subsystem masses are subtracted from this available mass limit, a maximum propellant mass may be calculated. Knowing the characteristics of each type of electric thruster allows maximum values of total impulse, mission velocity increment, and thrusting time to be calculated. Because ion thrusters easily operate at high values of efficiency (60 to 70%) and specific impulse

(3000 to 5000 sec), they can impart large values of total impulse to a spacecraft. They also can be operated with separate control of the propellant flow rate and exhaust velocity. This paper presents values of demonstrated and projected performance of high power ion thrusters used in an analysis of electric propulsion for an SP-100 based mission. Author

23 CHEMISTRY AND MATERIALS (GENERAL)

N88-12543*# National Aeronautics and Space Administration. Lewis Research Center, Cleveland, Ohio.
SURFACE CATALYTIC DEGRADATION STUDY OF TWO LINEAR PERFLUOROPOLYALKYLETHERS AT 345 C
Wilfredo Morales Nov. 1987 12 p
(NASA-TP-2774; E-3395; NAS 1.60:2774) Avail: NTIS HC A03/MF A01 CSCL 07A

Thin-liquid-film degradation studies of two commercially available perfluoropolyalkylether fluids (PFAE) were performed at 345 C, in nitrogen and air atmospheres, on iron and 440 C stainless steel surfaces. It was found that one fluid degraded on both iron and 440 C stainless steel surfaces in an air atmosphere, whereas the other fluid did not degrade. Chemical analysis revealed that the test fluid degraded to lower molecular weight products and that the degradation was accompanied by the formation of a brownish deposit on both the iron and 440 C stainless steel surfaces. Surface analysis of the deposit revealed a susbstantial amount of iron oxide (Fe2O3). It was hypothesized that the fluid which degraded did so because of its acetal structure. The other fluid, lacking the acetal structure, did not degrade. Author

24 COMPOSITE MATERIALS

Includes physical, chemical, and mechanical properties of laminates and other composite materials.
For ceramic materials see *27 Nonmetallic Materials*.

N88-12544*# National Aeronautics and Space Administration. Langley Research Center, Hampton, Va.
EFFECT OF LONG-TERM THERMAL AGING ON COATED CELION/LARC-160 COMPOSITES
James B. Nelson Oct. 1987 23 p
(NASA-TM-100495; NAS 1.15:100495) Avail: NTIS HC A03/MF A01 CSCL 11D

Coated and uncoated unidirectional laminates of Celion (Trademark)/LARC-160 graphite/polyimide were thermally aged in air at temperatures of 204, 260, and 316 C for various times up to 15,000 hours. Selected panels were coated with a high temperature coating resin (polyphenyl quinoxaline--PPQ): 1) edges only; 2) top and bottom only; 3)completely; or 4) not at all. Periodically during aging, panels were removed from the ovens, weighed, and short beam shear (SBS) specimens cut from selected locations in the panels. The protective coating did not influence the retention of SBS strength during thermal aging but did not lessen the amount of weight-loss incurred. The integrity of the PPQ coating was completely destroyed during aging at 316 C. Author

N88-12545 British Petroleum Co. Ltd., Sunbury-on-Thames (England).
THIXOTROPIC SURFACE COMPOSITION FOR PHENOLALDEHYDE RESIN LAMINATES Patent Application
Kenneth Leonard Forsdyke, inventor, Robert Stradling Francis, inventor, and Joseph Hunter, inventor 25 Mar. 1987 5 p Filed 4 Sep. 1986 priority 12 Sep. 1985 GB 8522757
(GB-Patent-2-180-251-A; GB-Patent-Appl-SN-8621355; Int-Patent-Class-C08L-61/06; Int-Patent-Class-C08J-5/00; ETN-87-90717) Avail: UK Patent Office, 25 Southampton Buildings, London WC2A 1AY, United Kingdom

A thixotropic composition and its use as a surface composition for preparing shaped laminated composites are described. The composition contains an acid hardenable phenol-aldehyde resole, a filler, and a viscosity modifier. The composition at 25 C has a viscosity of 200 to 800 poise measured using an RVT instrument, spindle 7 at 50 rpm. The use of the thixotropic surface composition gives laminated composites with a surface free of defects. ESA

N88-12546# United Technologies Research Center, East Hartford, Conn.
CARBON FIBER REINFORCED GLASS MATRIX COMPOSITES FOR SPACE BASED APPLICATIONS Annual Report, 1 Jul. 1986 - 30 Jun. 1987
William K. Tredway and Karl M. Prewo 31 Aug. 1987 89 p
(Contract N00014-85-C-0332)
(AD-A184355; UTRC/R87-917470-1) Avail: NTIS HC A05/MF A01 CSCL 11D

High elastic modulus (HMU) carbon fibers were combined with several different glass and glass ceramic matrix compositions. The importance of the fiber matrix interface in the control of composite performance was central to the investigation and was evaluated by correlating mechanical properties with microstructural and microchemical analysis of the interfacial region. Lithium aluminosilicate (LAS) glass-ceramic matrix composites were developed with tensile stress-strain behavior comparable to borosilicate glass matrix composites. Carbon fiber reinforced glass matrix composites of 0/90 deg orientation were found to be relatively notch insensitive. Lowering of the processing temperature of 7740/HMU composites was found to affect composite mechanical performance through matrix consolidation effects. Interfacial reactions between the carbon fiber and various matrix additives (nb205, mo03) were found to have a profound effect on composite mechanical behavior via formation of an interfacial carbide layer which increased fiber-matrix interfacial bond strength. GRA

N88-12547# Massachusetts Univ., Amherst. Dept. of Chemical Engineering.
MOLECULAR COMPOSITES: PROCESSING, POST-TREATMENT AND MECHANICS Final Report, May 1983 - Sep. 1986
M. F. Malone, C. F. Hwang, C. A. Gabriel, O. A. Nehme, and R. J. Farris Jul. 1987 98 p
(Contract F33615-83-K-5001)
(AD-A184458; AFWAL-TR-87-4048) Avail: NTIS HC A05/MF A01 CSCL 11D

Composites of poly(p-phenylene benzobisthiazole) (PBT) with nylons and with poly(ether ether ketone) (PEEK) were prepared in fiber and film form. Fiber and film spinning from dilute solutions in methane sulfonic acid (MSA) along with compression molding and sheet spinning were used to prepare materials for testing. Composite fibers of PBT and nylons exhibit tensile properties comparable to those previously reported for nylon/PBT materials. The mechanical and thermomechanical properties can be dramatically improved by post-treatment under tension at temperatures exceeding the melting point of the nylon. The torsional modulus is decreased somewhat by such post-processing and is in the range of 700 to 1000 GPa. Films of nylon/PBT material can be compression molded into larger articles, but the strength can be attributed to behavior of nylon alone. GRA

N88-12548# Boeing Military Airplane Development, Seattle, Wash.
FAILURE ANALYSIS OF COMPOSITE STRUCTURE MATERIALS Final Report, 1 Oct. 1985 - 31 Aug. 1986
Brian Smith and Ray Grove 27 May 1987 191 p
(Contract F33615-84-C-5010)
(AD-A184468; AFWAL-TR-87-4001) Avail: NTIS HC A09/MF A01 CSCL 11D

The objectives of the Failure Analysis for Composite Structural Materials program are to develop analytical and diagnostic techniques that can be used for determining the causes of failure in composite materials and to incorporate these results into a compendium of procedures that may be used as a reference

manual when conducting a postfailure analysis of a composite structure, given the failed part as the starting point of the investigation. Such techniques include flowcharts describing the logical arrangement of investigative operations along with diagnostic procedures that reveal the cause and mechanism of failure. To achieve these objectives, this program was divided into five tasks: (1) task 1-literature search and diagnostic technique selection, (2) task 2-specimen production and test, (3) task 3-diagnostic technique evaluations, (4) task 4-creation of a failure analysis compendium, and (5) task 5-evaluation and demonstration of techniques. This final report summarizes the progress and findings of activities carried out for tasks 1 through 5 that identified, organized, and examined a variety of postfailure analysis methods for composite materials. Because such failures may arise from a wide variety of causes, analysis techniques examined included four basic disciplines: nondestructive evaluation (NDE), stress analysis, fractography, and materials characterization. GRA

N88-12549*# Virginia Polytechnic Inst. and State Univ., Blacksburg. Center for Composite Materials and Structures.
INTERFACIAL STRENGTH DEVELOPMENT IN THERMOPLASTIC RESINS AND FIBER-REINFORCED THERMOPLASTIC COMPOSITES
Jeremy C. Howes and Alfred C. Loos Sep. 1987 148 p
(Grant NAG1-343)
(NASA-CR-181525; NAS 1.26:181525; CCMS-87-15; VPI-E-87-20) Avail: NTIS HC A07/MF A01 CSCL 11D

An experimental program to develop test methods to be used to characterize interfacial (autohesive) strength development in polysulfone thermoplastic resin and graphite-polysulfone prepreg during processing is reported. Two test methods were used to examine interfacial strength development in neat resin samples. These included an interfacial tension test and a compact tension (CT) fracture toughness test. The interfacial tensile test proved to be very difficult to perform with a considerable amount of data scatter. Thus, the interfacial test was discarded in favor of the fracture toughness test. Interfacial strength development was observed by measuring the refracture toughness of precracked compact tension specimens that were rehealed at a given temperature and contact time. The measured refracture toughness was correlated with temperature and contact time. Interfacial strength development in graphite-polysulfone unidirectional composites was measured using a double cantilever beam (DCB) interlaminar fracture toughness test. The critical strain energy release rate of refractured composite specimens was measured as a function of healing temperature and contact time. Author

N88-12550# Sandia National Labs., Albuquerque, N. Mex.
PARACHUTE MATERIALS
C. W. Peterson and D. W. Johnson Jun. 1987 72 p Presented at the Parachute Systems Technology: Fundamentals, Concepts, and Applications, Munich, Fed. Republic of Germany, 22 Jun. 1987
(Contract DE-AC04-76DP-00789)
(DE87-014845; SAND-87-1396C; CONF-8706165-4) Avail: NTIS HC A04/MF A01

The purpose of this paper is to present guidelines for the use of Kevlar and nylon materials in modern parachute systems. Nylon has been used in parachutes for many years, so this discussion will place emphasis upon Kevlar material properties and their application to parachute design and construction. Kevlar-29 is an aramid fiber manufactured by DuPont and is being used on parachute systems requiring high strength-to-weight ratios or sustained strength at high temperatures. Tests of parachutes using Kevlar webbing, braided cords, ribbons, and thread have demonstrated that these Kevlar materials can be used successfully in ribbon parachutes with no detrimental effects on performance. A few changes must be made in the design of a ribbon parachute to accommodate Kevlar's high modulus. Examples of parachutes that use Kevlar suspension lines, radials, ribbons, reefing lines, bridles, and skirt bands are presented to show that they are much lighter and more resistant to aerodynamic heating than all-nylon parachutes. Nylon continues to be an important material for high-performance parachute systems, however. New nylon weaves have resulted in lighter weight, stronger ribbon materials with excellent sewability characteristics. DOE

N88-12551*# National Aeronautics and Space Administration. Lewis Research Center, Cleveland, Ohio.
FREE-EDGE DELAMINATION: LAMINATE WIDTH AND LOADING CONDITIONS EFFECTS
P. L. N. Murthy (Cleveland State Univ., Ohio.) and C. C. Chamis Dec. 1987 28 p
(NASA-TM-100238; E-3862; NAS 1.15:100238) Avail: NTIS HC A03/MF A01 CSCL 11D

The width and loading conditions effects on free-edge stress fields in composite laminates are investigated using a three-dimensional finite element analysis. This analysis includes a special free-edge region refinement or superelement with progrssive substructuring (mesh refinement) and finite thickness interply layers. The different loading conditions include in-plane and out-of-plane bending, combined axial tension and in-plane shear, twisting, uniform temperature and uniform moisture. Results obtained indicate that: axial tension causes the smallest magnitude of interlaminar free edge stress compared to other loading conditions; free-edge delamination data obtained from laboratory specimens cannot be scaled to structural components; and composite structural components are not likely to delaminate. Author

N88-12552*# National Aeronautics and Space Administration. Lewis Research Center, Cleveland, Ohio.
COMPOSITE MECHANICS FOR ENGINE STRUCTURES
Christos C. Chamis [1987] 35 p Presented at the 32nd International Gas Turbine Conference and Exhibition, Anaheim, Calif., 31- May - 4 Jun. 1987; sponsored by ASME
(NASA-TM-100176; E-3750; NAS 1.15:100176) Avail: NTIS HC A03/MF A01 CSCL 11D

Recent research activities and accomplishments at Lewis Research Center on composite mechanics for engine structures are summarized. The activities focused mainly on developing procedures for the computational simulation of composite intrinsic and structural behavior. The computational simulation encompasses all aspects of composite mechanics, advanced three-dimensional finite-element methods, damage tolerance, composite structural and dynamic response, and structural tailoring and optimization. Author

N88-12553# California Univ., Berkeley. Lawrence Berkeley Lab.
A CREEP MEASUREMENT OF UNIDIRECTIONAL EPOXY-FIBERGLASS ROD
N. A. Munshi and R. C. Wolgast Jun. 1987 8 p Presented at the Conference on Advances in Cryogenic Engineering, St. Charles, Ill., 14 Jun. 1987
(Contract DE-AC03-76SF-00098)
(DE87-014812; LBL-23604; CONF-8706125-14) Avail: NTIS HC A02/MF A01

A creep measurement was made to prove the capability of a unidirectionally reinforced, epoxy-fiberglass rod to hold stable dimensions in compression over a 10 year period, during which operating temperatures of 40 C (104 F) could occur. This material has a high modulus of elasticity in tension and compression (approx.6 x 10 to the 6th psi) and strengths in excess of 100,000 psi. Its high strength and low thermal conductivity in the range from 300K to cryogenic temperatures make it ideally suited for cryogenic supports. The sample was tested in compression at 52 MPa (7500 psi) at 40 C for 1000 hours. The measured fractional deflection due to creep after 1000 hours was 3 x 10 to the -5 power. Extrapolation of the data to 10 years under the test load of 52 MPa predicts a fractional deflection of 6 x 10 to the -5 power. The low stress level was appropriate to a conservative design for the dipole magnet support struts for the Superconducting Super Collider cryostat (alternate design), an application requiring long-term accurate positioning of the magnet. The struts carry the weight of the magnet, at liquid helium temperature, to the base at ambient temperature. An elevated ambient standby or storage

temperature is the critical temperature for creep deflection in this case. DOE

N88-12554# Lawrence Livermore National Lab., Calif.
STUDY OF ZERO CTE (COEFFICIENTS OF THERMAL EXPANSION) OF GRAPHITE/EPOXY COMPOSITES
William W. Feng and Dale A. Schauer 14 Oct. 1986 14 p Presented at the Society of Mechanical Engineers Composites in Manufacturing 6th Conference, Anaheim, Calif., 19 Jan. 1987
(Contract W-7405-eng-48)
(DE87-013557; UCRL-95577; CONF-870189-1) Avail: NTIS HC A03/MF A01

The design of composites with very low coefficients of thermal expansion (CTE) is discussed. The magnitude of the CTE of a composite laminate is usually coupled with the mechanical properties. Here, the thermomechanical properties of multidirectional laminates, consisting of plies with arbitrary orientations and stacking sequences, are obtained by the laminate theory. Tests are performed to determine the thermomechanical properties of unidirectional composite laminates and to verify the analytical results for a variety of composite laminates. These tests measure the elastic moduli, Poisson's ratios and CTEs. In order to provide the required accuracies for measuring low CTEs, a differential dilatometer is used. All test results agree with the analytical predictions. DOE

N88-12506# Joint Publications Research Service, Arlington, Va.
CARBON-FIBER REINFORCED PLASTICS
In its JPRS Report: Science and Technology. Japan 24 Aug. 1987 p 6-7 Transl. into ENGLISH from Ceramics Japan (Tokyo, Japan), Feb. 1987 p 157 (For primary document see N88-12502 04-12)
Avail: NTIS HC A06/MF A01

N88-12507# Joint Publications Research Service, Arlington, Va.
CARBON-FIBER REINFORCED ALUMINUM
In its JPRS Report: Science and Technology. Japan 24 Aug. 1987 p 8-9 Transl. into ENGLISH from Ceramics Japan (Tokyo, Japan) Feb. 1987 p 157-158 (For primary document see N88-12502 04-12)
Avail: NTIS HC A06/MF A01

N88-12529*# McDonnell-Douglas Astronautics Co., Houston, Tex.
SPACECRAFT MATERIAL FLAMMABILITY TESTING AND CONFIGURATIONS
Paul W. Ledoux *In* NASA, Lewis Research Center, Spacecraft Fire Safety 1987 p 95-98 (For primary document see N88-12520 04-16)
Avail: NTIS HC A07/MF A01 CSCL 11D

N88-12646# Columbia Univ., New York, N.Y. Dept. of Civil Engineering and Engineering Mechanics.
SPATIAL STRENGTH VARIATION AND STATISTICAL SIZE EFFECT OF LAMINATED ORTHOTROPIC COMPOSITE MATERIALS
Elias Samaras and Masanobu Shinozuka *In* Army Materials Technology Lab., Work-in-Progress Presented at the Army Symposium on Solid Mechanics, 1986: Lightening of the Force Oct. 1986 p 3-5 (For primary document see N88-12644 04-31)
Avail: NTIS HC A04/MF A01 CSCL 11D

N88-12651# Ballistic Research Labs., Aberdeen Proving Ground, Md.
COMPOSITE MATERIALS APPLICATIONS PROGRAM AT THE US ARMY BALLISTIC RESEARCH LABORATORY: WORK IN PROGRESS
Richard B. Murray, Edward M. Patton, Larry W. Burton, and Robert P. Kaste *In* Army Materials Technology Lab., Work-in-Progress Presented at the Army Symposium on Solid Mechanics, 1986: Lightening of the Force Oct. 1986 p 29-31 (For primary document see N88-12644 04-31)
Avail: NTIS HC A04/MF A01 CSCL 11D

N88-12654# Transportation Systems Center, Cambridge, Mass. Structures and Dynamics Div.
CORROSION CONTROL BY COMPOSITE MATERIAL SUBSTITUTION WITH APPLICATION TO THE M-939 5-TON TRUCK
Tong Pin *In* Army Materials Technology Lab., Work-in-Progress Presented at the Army Symposium on Solid Mechanics, 1986: Lightening of the Force Oct. 1986 p 45-47 (For primary document see N88-12644 04-31)
Avail: NTIS HC A04/MF A01 CSCL 11D

25 INORGANIC AND PHYSICAL CHEMISTRY

Includes chemical analysis, e.g., chromatography; combustion theory; electrochemistry; and photochemistry.

For related information see also *77 Thermodynamics and Statistical Physics.*.

N88-12555# Foersvarets Forskingsansalt, Stockholm (Sweden).
EQUILIBRIUM CALCULATIONS OF IONIZATION IN TRACER FLAMES
S. E. Flygar and T. Liljegren Aug. 1986 24 p
In SWEDISH
(PB87-104154; FOA-C-20621-2.1) Avail: NTIS HC E03/MF E01 CSCL 21B

A theoretical study of ionization in tracer flames was performed to find compositions with low contents of free electrons. Thermochemical equilibrium calculations, including ionized species, were done for a great number of compositions based on oxidizer, magnesium, and binder. The results are reported in tables and diagrams. By using ammonium perchlorate instead of generally used strontium nitrate as oxidizer, the equilibrium content of electrons is decreased to at least on tenth of the content of conventional trancers. An addition of a small amount of an iodine compound gives further decrease of the electron content. If a colored flame is desired, a small part of ammonium perchlorate can be replaced by strontium nitrate or barium nitrate, resulting in only a small increase of the electron content. GRA

N88-12556# Army Construction Engineering Research Lab., Champaign, Ill.
CARBON DIOXIDE TREATMENT FOR SCALE REMOVAL AND CONTROL IN POTABLE WATER SYSTEMS Final Report
Temkar M. Prakash, Chester H. Neff, Richard J. Scholze, John T. Bandy, and Edgar D. Smith May 1987 59 p
(AD-A184346; CERL-TR-N-87-16) Avail: NTIS HC A04/MF A01 CSCL 13B

Carbon dioxide treatment for controlling and removing scale deposits in potable water systems has been investigated for potential application at Army installations. Scaling of water treatment systems is costly in terms of severe headloss and reduced carrying capacity of pipes, loss of heat transfer capacity in water heating systems, high operating costs due to inefficiencies, downtime and maintenance, and operational safety hazards. Conventional treatments for scale removal and control include mechanical and chemical methods. These methods are expensive and often ineffective; in addition, some chemical additives are unsafe, requiring special handling techniques and evacuation of building occupants during treatment. The Illinois State Water Survey has successfully field-tested a carbon dioxide treatment system. Treatment with controlled levels of carbon dioxide removed scale deposits safely and effectively; subsequent treatment kept the test pipes relatively scale-free while in service. However, one drawback is that overtreating a water system can result in corrosion due to dissolution of the scale and the protective coating on pipes. GRA

N88-12557*# Eloret Corp., Sunnyvale, Calif.
SIMULATION STUDIES FOR SURFACES AND MATERIALS STRENGTH Semiannual Progress Report, 1 May - 31 Oct. 1987

Timur Halicioglu 31 Oct. 1987 42 p
(Contract NCC2-297)
(NASA-CR-181535; NAS 1.26:181535) Avail: NTIS HC A03/MF A01 CSCL 07D

A realistic potential energy function comprising angle dependent terms was employed to describe the potential surface of the N+O2 system. The potential energy parameters were obtained from high level ab-initio results using a nonlinear fitting procedure. It was shown that the potential function is able to reproduce a large number of points on the potential surface with a small rms deviation. A literature survey was conducted to analyze exclusively the status of current small cluster research. This survey turned out to be quite useful in understanding and finding out the existing relationship between theoretical as well as experimental investigative techniques employed by different researchers. Additionally, the importance of the role played by computer simulation in small cluster research, was documented. Author

N88-12558# Brookhaven National Lab., Upton, N. Y.
THE ATOMIC WEIGHT AND ISOTOPIC COMPOSITION OF OXYGEN AND THEIR VARIATION IN NATURE
N. E. Holden 1987 18 p Presented at the 34th IUPAC General Assembly, Boston, Mass., 21 Aug. 1987
(Contract DE-AC02-76CH-00016)
(DE87-014397; BNL-NCS-39950; CONF-8708105-4) Avail: NTIS HC A03/MF A01

There is a problem with the absolute abundance measurements of oxygen. One of these calibrated measurements is in error, either oxygen in air, or oxygen in (V-SMOW), Vienna's standard mean ocean water reference material. Nier's measurement in air is probably wrong by three times his quoted error and his ratio for O-18/O-16 should be 0.002053 and not 0.002044. Fortunately, this has only a minor effect on the atomic weight. However, this error raises doubts on all O-17/O-16 values.Each O-17/-16 is determined using an enrichment factor, relative to the value of O-17/O-16 in the standard, which is the square root of the enrichment factor for O-18/O-16 relative to the standard. All standards, including V-SMOW, have O-17/O-16 values which have been derived originally from Nier's measurement of oxygen in air. In addition, a review of the literature provides isotopic abundance variations in various sources of oxygen. DOE

N88-12559# Pacific Northwest Labs., Richland, Wash.
RETENTION PROCESSES IN SUPERCRITICAL FLUID CHROMATOGRAPHY
C. R. Yonker and R. D. Smith May 1987 20 p Presented at the 193rd National Meeting of the American Chemical Society, Denver, Colo., 5 Apr. 1987
(Contract DE-AC06-76RL-01830)
(DE88-000079; PNL-SA-14421; CONF-870410-37) Avail: NTIS HC A03/MF A01

The understanding of retention processes in supercritical fluid chromatography is important for the continued growth and development of the analytical technique. Chromatographic retention has been studied using a simple thermodynamic model involving solute retention as a function of pressure and through assessment of the effect of density on the enthalpy of solute transfer between the supercritical mobile phase and bonded stationary phase. The solvatochromic behavior of solute probes in pure and binary supercritical fluids can be used to determine their polarity/polarizability as a function of density and related solvent effects on solute retention in supercritical fluid chromatography. DOE

N88-12560# Brigham Young Univ., Provo, Utah.
NOVEL MACROCYCLIC CARRIERS FOR PROTON-COUPLED LIQUID MEMBRANE TRANSPORT Progress Report, 1 Dec. 1986 - 31 Jul. 1987
J. D. Lamb, J. J. Christensen, R. M. Izatt, and J. W. Bradshaw 31 Aug. 1987 10 p
(Contract DE-FG02-86ER-13463)
(DE88-000636; DOE/ER-13463/T1) Avail: NTIS HC A02/MF A01

The objective of our research program is to elucidate the chemical principles which are responsible for the cation selectivity and permeability of liquid membranes containing macrocyclic carriers. A number of new carriers were synthesized, based on the inclusion of triazolo, pyridono, and sulfonamide groups in the principal macrocyclic ring. Many of these show interesting transport characteristics, especially with respect to Li(+), Ag(+), and Cs(+). Hydrophobic crown ethers were successfully incorporated into supported liquid membranes of the flat sheet and hollow fiber types. Hollow fiber transport demonstrated selectivities and permeabilities similar to those observed in the flat sheets. DOE

N88-12561# Mound Lab., Miamisburg, Ohio.
SIMULTANEOUS TG/DSC (THERMOGRAVIMETRY/DIFFERENTIAL SCANNING CALORIMETRY) AND TG/MS (THERMOGRAVIMETRY/MASS SPECTROMETRY) ANALYSES OF POLYMERIC AND ENERGETIC MATERIALS
R. B. Whitaker, C. R. Brown, C. Chang, J. A. McDaniel, and T. L. Shell 1987 18 p Presented at the 16th Annual Conference of the North American Thermal Analysis Society, Washington, D.C., 27 Sep. 1987
(Contract DE-AC04-76DP-00053)
(DE88-000727; MLM-3458(OP); CONF-870988-3) Avail: NTIS HC A02/MF A01

The utility of simultaneous thermal analysis techniques, such as TG/DSC and TG/MS, has been demonstrated for both energetic and polymeric materials. TG/DSC can assist in elucidating reaction mechanisms and determining weight losses for endothermic transitions which precede decomposition of energetic materials. The endothermic and exothermic nature of decomposition processes can be defined by TG/DSC and the decomposition products identified by TG/MS. DOE

N88-12562# Brigham Young Univ., Provo, Utah.
THERMODYNAMIC PROPERTIES OF SUPERCRITICAL MIXTURES Progress Report, 1 Sep. 1986 - 15 Sep. 1987
J. J. Christensen and R. M. Izatt 18 Sep. 1987 9 p
(Contract DE-FG02-85ER-13443)
(DE88-000809; DOE/ER-13443/2) Avail: NTIS HC A02/MF A01

The primary goal of this research effort is to gain increased understanding of the energetics associated with chemical and physical interactions involving supercritical and near-supercritical fluids. Emphasis has been placed on reactions involving CO2, fluorocarbons, and hydrocarbons. Heat of mixing(H/sup E/) values have been determined for several binary systems involving these three classes of compounds and manuscripts have been prepared which report the experimental results. The flow calorimeter and operating procedures have been modified to allow ternary systems to be studied. An extensive investigation of the ternary system, CO2 + n-hexane + toluene, has been completed over wide temperature and pressure ranges. In addition, the system (CO2 + hexane) has been studied as a function of temperature and pressure with the following additives present in the CO2 stream at five mole percent: CH3OH, octanol, n-octane. DOE

N88-12563# Physical Sciences, Inc., Andover, Mass.
EXPERIMENTAL AND THEORETICAL STUDY OF CONDENSATION IN MULTICOMPONENT MIXTURES Quarterly Report No. 11, 15 Aug. - 14 Nov. 1986
M. B. Frish, R. Waterhouse, and G. Wilemski Jul. 1987 18 p
(Contract DE-AC02-84ER-13154)
(DE88-000897; DOE/ER-13154/11; PSI-TR-154/710) Avail: NTIS HC A03/MF A01

This report covers work performed during the eleventh quarter of a multi-year program to study condensation in multi-component vapors. The program is primarily experimental, but a significant amount of theoretical work is also being performed. The experiments are studying the homogeneous nucleation and subsequent growth of mixed clusters formed during supersonic expansion of gas mixtures containing mutually condensible species. Herein we describe newly developed data analysis procedures for

determining particle sizes and number densities throughout the region of the nozzle where vapor condenses rapidly. These are the first experiments capable of obtaining this information without resorting to theoretical models and approximations. DOE

N88-12850# Joint Publications Research Service, Arlington, Va.
THERMOPHORESIS OF SPHERICAL AEROSOL PARTICLE AT ARBITRARY KNUDSEN NUMBERS Abstract Only
S. A. Beresnev and V. G. Chernyak *In its* USSR Report: Earth Sciences 22 Jul. 1986 p 53 Transl. into ENGLISH from Doklady Akademii Nauk SSSR (Moscow, USSR), v. 285, no. 6, Dec. 1985 p 1377-1381 Original language document was announced in IAA as A86-24317 (For primary document see N88-12831 04-42)
Avail: NTIS HC A05/MF A01

26 METALLIC MATERIALS

Includes physical, chemical, and mechanical properties of metals, e.g., corrosion; and metallurgy.

N88-12564# Pennsylvania State Univ., University Park. Dept. of Chemical Engineering.
CHARACTERIZATION OF CATALYSTS WITH METAL-SUPPORT EFFECTS AND OF THE SPECIES ADSORBED ON THEIR SURFACES Progress Report, 1 Sep. 1986 - 30 Aug. 1987
M. A. Vannice 28 May 1987 7 p
(Contract DE-FG02-84ER-13276)
(DE87-014636; DOE/ER-13276/T1) Avail: NTIS HC A02/MF A01

Pt crystallite size effects on H sub ad were investigated by varying particle sizes from 1.5 to 1500 nm on SiO2. This property for CO and H2 adsorption on Pt is much less affected by crystallite size than on Pd. We have completed our study of heats of adsorption on Pd. It also has provided insight into the H2-D2 exchange reaction on Pd. The study of C6H6 hydrogenation over Pd catalysts has been completed. We have found that the rate of acetone hydrogenation to isopropanol can be enhanced 100- to 1000-fold over TiO2-supported Pt. Ongoing studies of crotonaldehyde hydrogenation have provided evidence that selective hydrogenation of the C=O bond compared to the C=C bond can be induced by a metal-support effect. Only butyraldehyde is obtained over Pt on typical supports like SiO2 and Al2O3 whereas the use of TiO2 can produce over 35 percent crotyl alcohol. DOE

N88-12565# Sandia National Labs., Albuquerque, N. Mex.
THE EFFECT OF ORGANIC INHIBITORS ON THE ATMOSPHERIC CORROSION AND SOLDERABILITY OF COPPER
G. A. Poulter and N. R. Sorensen Aug. 1987 18 p
(Contract DE-AC04-76DP-00789)
(DE88-000261; SAND-87-0797) Avail: NTIS HC A03/MF A01

We found preliminary atmospheric exposure and solderability tests on uninhibited copper and copper inhibited with benzotriazole and tolyltriazole. Exposures were performed in humidity chambers at high relative humidity (RH), at 40° and 70°C. Inhibitors applied from both a methanol-based and a water-based solution effectively reduced oxidation. Oxidation was reduced by 35 percent after 70 days exposure to 70°C, 65 percent RH, and reduced by 80 percent after 67 days exposure to 40°C, 100 percent RH. We determined solderability of inhibited and uninhibited copper with a Hollis meniscometer, and a meniscograph. Inhibited copper exhibited enhanced equilibrium solder parameters, but solder kinetics were degraded. DOE

N88-12566# Naval Postgraduate School, Monterey, Calif.
A COMPARISON OF HIGH DAMPING SHAPE MEMORY ALLOYS WITH Cu-Mn-BASED AND Fe-Cr-BASED ALLOYS M.S. Thesis
Joseph T. Cronauer Jun. 1987 104 p
(AD-A184110) Avail: NTIS HC A06/MF A01 CSCL 11F

The strain dependence and temperature dependence of damping in the thermoelastic martensitic (shape memory) alloys titanium-nickel and copper zinc aluminum was compared to predetermined optimum damping behavior in the quiet alloys copper manganese aluminum and iron chromium molybdenum. Damping measurements were taken using a modified resonant dwell technique, in which cantilever beams were evaluated for damping at their first three resonant modes at temperatures between ambient and 110 C. Differential scanning calorimetry was used to correlate microstructural changes with damping capacity. All alloys that were conditioned for high damping showed a trend of low damping at low strains, a strain threshold, and increased damping with strains above the threshold. Damping was directly related to the progress of martensitic transformation in the titanium nickel alloy. The Copper, Zinc, Aluminum alloy was examined in a condition which did not develop high damping. Damping in the Iron, Chromium, Molybdenum, alloy was insensitive to temperature change. GRA

N88-12567# Naval Surface Weapons Center, Silver Spring, Md.
CORROSION BEHAVIOR OF P/M MECHANICALLY ALLOYED IN-9052.1: AN ELECTRO-CHEMICAL INVESTIGATION
P. A. Stone, J. F. McIntyre, and R. K. Garrett 1 Dec. 1986 70 p
(AD-A184191; NSWC/TR-86-412) Avail: NTIS HC A04/MF A01 CSCL 11F

The corrosion behavior of P/M mechanically alloyed IN-9052 is compared to AA-6061-T6. Electrochemical techniques are used to study these alloys exposed to 3.5% NaCl. Scanning electron microscopy is used to characterize the morphology of freely corroding samples. A mechanism for pit initiation on IN-9052 is proposed. GRA

N88-12568# Colorado School of Mines, Golden. Center for Welding Research.
THE NATURE OF METALLURGICAL REACTIONS IN UNDERWATER WELDING
S. Ibarra, D. L. Olson, and C. E. Grubbs Apr. 1987 7 p
(Contract DAAL03-86-K-0064)
(AD-A184464; ARO-23474.16-MS) Avail: NTIS HC A02/MF A01 CSCL 11F

The pyrometallurgical reactions are characterized as a function of depth for underwater wet welding. The influence of weld metal compositional variations with depth on weld metal microstructure are described. Metallurgical suggestions as to compositional modifications to underwater wet welding electrodes to achieve the desired microstructure and properties are given. Underwater welding has been recognized as a difficult and potentially cost saving engineering task that becomes more important with the maintenance of existing marine structures. Specifications for underwater welding which describe the mechanical requirements that load bearing weld deposits must meet are available. Christensen et. al. have introduced basic concepts for underwater weld metal chemistry and metallurgy. Their research was primarily on the influence of pressure on hyperbaric shielded metal arc weld metal compositions. Christensen's work did suggest that similar weld metal compositional variations should occur in wet underwater welding. Madator reported on the influences of parameters on the welding process and on the metallurgical reactions. GRA

N88-12569# Naval Surface Weapons Center, Silver Spring, Md.
ON THE STRESSING OF ANNEALED NITINOL: THE ELECTRICAL RESISTANCE AND CALORIMETRIC EFFECTS
David M. Goldstein Apr. 1987 28 p
(AD-A184465; NSWC/TR-87-126) Avail: NTIS HC A03/MF A01 CSCL 11F

The effects of stress on the electrical resistance and scanning calorimetry curves of NITINOL during its phase transformation are substantial. The generation of a peak occurs in the resistance curve, and an additional peak is generated in the calorimetry curve for the transformation during cooling, as compared to annealed metal. Explanation of the relation between stress and the formation of these peaks is presented for both cooling and heating cycles.

Straining the wire in the martensitic versus the austenitic condition also can result in differences in the subsequent phase transformation. These differences can be exploited for one-time higher temperature applications of this shape memory alloy. GRA

N88-12570# Universidade Federal de Sao Carlos (Brazil). Dept. de Fisica.
MODEL FOR ULTRASONIC ATTENUATION AND ELASTIC CONSTANT IN CHROMIUM AND ITS ALLOYS
E. P. Castro, G. E. Marques, and P. C. deCamargo 1987 26 p (DE87-703478; INIS-BR-726) Avail: NTIS (US Sales Only) HC A03/MF A01

A theory based on the thermodynamics of a magnetic system under applied acoustic field is proposed. The calculated attenuation and longitudinal elastic constant for pure chromium and its alloys with diluted vanadium, show a good agreement with the experimental values. DOE

N88-12571# Santa Catarina Univ., Florianopolis (Brazil).
MECHANICAL BEHAVIOR OF A CONTROLLED ROLLED HIGH-STRENGTH LOW ALLOY STEEL PLATE, MICROALLOYED WITH Nb and V
C. R. Maria, J. C. Bruno, D. T. Gomes, and K. K. Chawla 1986 4 p In PORTUGUESE; ENGLISH summary Presented at the 7th Brazilian Congress on Engineering and Materials Science, Florianopolis, Brazil, 10 Dec. 1986
(DE87-703507; INIS-BR-757; CONF-861299-3) Avail: NTIS (US Sales Only) HC A02/MF A01

The tension and fatigue behaviour of a controlled rolled high-strength low-alloy steel plate, microalloyed with Nb and V, was studied. It was verified that the material showed an anisotropic tensile behaviour. In spite of this anisotropy, it was verified that the fatigue crack propagation rates (da/Dn) in the L, T and S directions showed similar results with respect to the two levels of mean applied stress. DOE

N88-12572# Universidade Federale do Rio de Janeiro (Brazil). Coordenacao dos Programas de Pos-graduacao de Engenharia.
MECHANICAL PROPERTIES OF A MICROALLOYED STEEL WITH HIGH NIOBIUM CONTENT
H.-J. Kestenbach and I. N. daConceicao 1987 8 p In PORTUGUESE Presented at the 2nd Meeting on Technology and Utilization of Brazilian Steels, Rio de Janeiro, Brazil, 18 May 1987
(DE87-703545; INIS-BR-802; CONF-8705176-1) Avail: NTIS (US Sales Only) HC A02/MF A01

A higher-than-usual niobium content is being considered as a possible alternative to heavy low-temperature controlled rolling which is usually required in order to develop high strength and toughness in microalloyed steel. In the present study, the effect of 0.24% Nb dissolved in austenite on the strength and toughness of polygonal ferrite has been investigated. The niobium addition reduced the ferrite grain size but at the same time led to the deterioration of impact properties without raising yield strength. Electron microscope observations suggested that the decrease in toughness was caused by intercrystalline fracture due to preferential carbonitride precipitation at austenite grain boundaries. DOE

N88-12573# Universidade Federale do Rio de Janeiro (Brazil). Coordenacao dos Programas de Pos-graduacao de Engenharia.
SINTERED STEELS OF HIGH RESISTANCE ALLOYED TO Nb, Mo, Mn AND Si
A. N. Klein, I. K. Arroyo, and R. A. Salcedo 1987 8 p In PORTUGUESE Presented at the 2nd Meeting on Technology and Utilization of Brazilian Steels, Rio de Janeiro, Brazil, 18 May 1987
(DE87-703546; INIS-BR-804; CONF-8705176-2) Avail: NTIS (US Sales Only) HC A02/MF A01

Sinterability, homogenization and mechanical properties of Nb-Mo-Mn-Si alloyed steels obtained by means of compaction and sintering at 1250 C, are investigated on the basis of dilatometry, microstructural analysis, and tensile and hardness properties. The alloy components are combined into a single master alloy in proportions assuring easy dissolution, resulting in improvement of the kinetics of the sintering and homogenization processes. Optimal compositions show simultaneously excellent dimensional stability during sintering and strength superior to 920 MPa and up to 1250 MPa when an additional heat treatment is made. DOE

N88-12574# Universidade Federale do Rio de Janeiro (Brazil). Coordenacao dos Programas de Pos-graduacao de Engenharia.
MECHANICAL PROPERTIES OF AN ACICULAR FERRITE STEEL MICROALLOYED TO NIOBIUM AND VANADIUM
M. R. Palermo and J. C. Bruno 1987 9 p In PORTUGUESE Presented at the 2nd Meeting on Technology and Utilization of Brazilian Steels, Rio de Janeiro, Brazil, 18 May 1987
(DE87-703547; INIS-BR-805; CONF-8705176-3) Avail: NTIS (US Sales Only) HC A02/MF A01

Carbonitride precipitation hardening gas was studied in the acicular ferrite and bainite phases of a C-Mn-Nb-V steel. Precipitation hardening in the acicular ferrite phase was higher than in the bainite phase, although it was lower than expected. It was also observed that in both phases the fracture was ductile in as-cooled samples but became partially brittle after the samples were aged for 150 minutes at 550 C. DOE

N88-12575# Universidade Federale do Rio de Janeiro (Brazil). Coordenacao dos Programas de Pos-graduacao de Engenharia.
PARTIAL SUBSTITUTION OF VANADIUM BY NIOBIUM IN AISI H13 STEEL
A. ItmanFilho and O. Balancin 1987 7 p In PORTUGUESE Presented at the 2nd Meeting on Technology and Utilization of Brazilian Steels, Rio de Janeiro, Brazil, 18 May 1987
(DE87-703548; INIS-BR-806; CONF-8705176-4) Avail: NTIS (US Sales Only) HC A02/MF A01

The tempering resistence of AISI H13 steel, after partial substitution of vanadium by niobium, was studied. Four alloys of this steel were examined and in three of them the niobium was added to the extent of 0.2, 0.5 and 1.0%. Microstructural analysis was done to compare qualitatively the effect of the niobium in the various processing stages and heat treatment of the steels. Grain size measurements were made after austenitization; hardness measurements in prepared samples were made after quenching and tempering; tensile testing at elevated temperature was investigated as well as yield strength; and area reduction and elongation of the steel were calculated after fracturing. After these studies it was possible to certify that the partial substitution of vanadium by niobium did not alter significantly the basic mechanical properties of the AISI H13. GRA

N88-12576# Universidade Federale do Rio de Janeiro (Brazil). Coordenacao dos Programas de Pos-graduacao de Engenharia.
PROGRESS IN THE DEVELOPMENT OF NIOBIUM ALLOYED HIGH SPEED STEEL
J. R. C. Guimaraes 1987 8 p In PORTUGUESE Presented at the 2nd Meeting on Technology and Utilization of Brazilian Steels, Rio de Janeiro, Brazil, 18 May 1987
(DE87-703549; INIS-BR-808; CONF-8705176-5) Avail: NTIS (US Sales Only) HC A02/MF A01

The development of economy grades of niobium alloyed high speed steel is described. Both the metallurgical concepts behind the steel design and the results of performance tests are presented. DOE

N88-12577# Instituto de Pesquisas Energeticas e Nucleares, Sao Paulo (Brazil). Dept. de Metalurgia e Nucleares.
MECHANICAL STRENGTH AND NIOBIUM AND NIOBIUM-BASE ALLOYS SUBSTRUCTURES
W. A. Monteiro and A. H. P. deAndrade 1986 18 p In PORTUGUESE Presented at the 11th Annual Symposium of the ACIESP, Sao Paulo, Brazil, 13 Nov. 1986

(DE87-703692; INIS-BR-701; CONF-8611184-2) Avail: NTIS (US Sales Only) HC A03/MF A01

Niobium and some of its alloys have been used in several fields of technological applications such as the aerospace, chemical and nuclear industries. This is due to its excellent mechanical strength at high temperatures and reasonable ductility at low temperatures. In this work, we review mechanical strength and substructure in niobium and its alloys, taking into account the presence of impurities, the influence of initial thermal and thermo - mechanical treatments as well as the irradiation by energetic particles. DOE

N88-12578# Instituto de Pesquisas Tecnologicas, Sao Paulo (Brazil).
CORROSION STRENGTH OF NIOBIUM AND ITS ALLOYS
N. Alonso and C. Takano 1986 13 p In PORTUGUESE Presented at the 11th Annual Symposium of the ACIESP, Sao Paulo, Brazil, 13 Nov. 1986
(DE87-703693; INIS-BR-702; CONF-8611184-3) Avail: NTIS (US Sales Only) HC A03/MF A01

The main aspects of corrosion strength of the niobium and its alloys in acid and alkaline aqueous solution, in liquid metals and in an oxidizing atmosphere are described. In some cases the strength corrosion was compared to other materials. DOE

N88-12579# Universidade Federale do Rio de Janeiro (Brazil). Coordenacao dos Programas de Pos-graduacao de Engenharia.
HADFIELD STEELS WITH Nb AND Ti CARBIDES
J. Vatavuk and H. Goldenstein 1987 10 p In PORTUGUESE Presented at the 2nd Meeting on Technology and Utilization of Brazilian Steels, Rio de Janeiro, Brazil, 18 May 1987
(DE87-703706; INIS-BR-803; CONF-8705176-6) Avail: NTIS (US Sales Only) HC A02/MF A01

The Hadfield Steels and the mechanisms responsible for its high strain hardening rate were reviewed. Addition of carbide forming alloying elements to the base compostion was discussed, using the matrix steel concept. Three experimental crusher jaws were cast, with Nb and Nb + Ti added to the usual Hadfield compostion, with enough excess carbon to allow the formation of MC carbides. Samples for metallographic analysis were prepared from both as cast and worn out castings. The carbic morphology was described. Partition of alloying elements was qualitatively studied, using Energy Dispersive Expectroscopy in SEM. The structure of the deformed layer near the worn surface was studied by optical metallography and microhardness measurements. The results showed that fatigue cracking is one of the wear mechanisms in operation in association with the cyclic work hardening of the surface of worn crusher jaws. DOE

N88-12580# Universidade Federale do Rio de Janeiro (Brazil). Coordenacao dos Programas de Pos-graduacao de Engenharia.
INFLUENCE OF SOME PARAMETERS ON THE STRESS CORROSION OF A ABNT 304 STAINLESS STEEL IN MgCl/SUB 2/
L. C. Candido, R. M. Schroeder, and I. L. Mueller 1987 7 p In PORTUGUESE Presented at the 2nd Meeting on Technology and Utilization of Brazilian Steels, Rio de Janeiro, Brazil, 18 May 1987
(DE87-703707; INIS-BR-807; CONF-8705176-7) Avail: NTIS (US Sales Only) HC A02/MF A01

The susceptibility to stress corrosion cracking of the austenitic stainless steel AISI 304 in MgCl2 solution was studied, such as surface changes caused by a prepassivation of the steel in HNO3 solution or chromate solution or even a previous cathodic reduction. An addition of NaCl or MgCl2 was also used in such a way that the cation influence on the stress corrosion process could be analyzed. Results show that the surface layer seems to have great importance in the stress corrosion mechanism and that addition of Na(+) ions inhibit cracks at the corrosion potential. DOE

N88-12581# Lehigh Univ., Bethlehem, Pa.
SOME STOCHASTIC ASPECTS OF INTERGRANULAR CREEP CAVITATION
S. J. Fariborz, J. P. Farris, D. G. Harlow, and T. J. Delph Oct. 1987 12 p Presented at the International Seminar on High Temperature Fracture Mechanisms and Mechanics, Dourdan, France, 13 Oct. 1987
(Contract DE-FG02-84ER-45088)
(DE88-000065; CONF-8710123-2) Avail: NTIS HC A03/MF A01

Presented are results obtained from a simplified stochastic model of intergranular creep cavitation. The probabilistic features of the model arise from the inclusion of random cavity placement on the grain boundary and time-discrete stochastic cavity nucleation. Among the predictions of the model are Weibull-distributed creep rupture failure times and a Weibull distribution of cavity radii. Both of these predictions have qualitative experimental support. DOE

N88-12582# Oak Ridge National Lab., Tenn.
WELDING AND WELDABILITY OF DUCTILE INTERMETALLIC ALLOYS
S. A. David, M. L. Santella, and G. M. Goodwin 1987 14 p Presented at the Annual North American Welding Research Seminar, Columbus, Ohio, 29 Sep. 1987
(Contract DE-AC05-84OR-21400)
(DE87-014061; CONF-870981-2) Avail: NTIS HC A03/MF A01

Successful welds have been produced in several nickel aluminide (Ni3Al) alloys. Weldability has been found to be a strong function of boron, other alloying additions, and welding speed. Cracking during welding observed in some of the aluminides was predominantly in the heat-affected zone (HAZ) and was always intergranular. Additions of iron promote the formation of a second phase. The observed HAZ cracking in some of these alloys resulted from thermal stresses imposed on this region of the weldment at elevated temperature and from grain boundary weakness. Sound welds were produced in sheets of (Fe,Ni)3(V,Ti) and (Fe,Co)3(V,Ti) ordered alloys. Welds of (Fe,Ni)3(V,Ti) were disordered, but the tensile properties were not adversely affected. A reordering heat treatment restored the weldment properties to those of the base metal. Welds of (Fe,Co)3(V,Ti) remained ordered after the weld thermal cycle. Factors that seem to influence the weldment properties include ordered domain size and precipitation of carbide. DOE

N88-12583# Los Alamos National Lab., N. Mex.
EXPERIMENTAL PERSPECTIVES ON HEAVY ELECTRON METALS
Z. Fisk, H. R. Ott, and G. Aeppli 1987 6 p Presented at the 18th Conference on Low Temperature Physics, Kyoto, Japan, 20 Aug. 1987 Prepared in cooperation with Eidgenoessische Technische Hochschule, Zurich, Switzerland and Bell Telephone Labs., Murray Hill, N.J.
(Contract W-7405-eng-36)
(DE87-014766; LA-UR-87-2805; CONF-870873-15) Avail: NTIS HC A02/MF A01

We motivate the description of heavy electron metals in terms of concepts from the Kondo problem. These concepts are used to discuss magnetism and superconductivity in heavy electron systems. Particular attention is given to what we view as the principal outstanding questions in this field and direction in which the field is developing. This will include consideration of the differences between Ce and U heavy electron compounds, as well as the occurrence of very small ordered magnetic moments. DOE

N88-12584# Georgia Univ., Athens. Dept. of Physics.
A STUDY OF MECHANISMS OF HYDROGEN DIFFUSION IN SEPARATION DEVICES Final Report
M. H. Lee 20 Aug. 1987 27 p
(Contract DE-AS09-77ER-01023)
(DE88-000328; DOE/ER-01023/7) Avail: NTIS HC A03/MF A01

Physical properties of hydrogen diffusion in transition metals show considerable potential for technical applications. Towards developing a quantum statistical theory of diffusion, we have constructed and developed a microscopic, dynamic model appropriate for hydrogen in a transition metal. Our work is based on the notion that the basic aggregates of transport are spin clusters of either Fermi or Bose type. Our theory is able to encompass much of the known basic facts including the reversed isotope effect in diffusion. Our model also provides new information on long-time behavior in the velocity autocorrelation function, intrinsic mobility and diffusion which can grow anomalously. To obtain time-dependent properties of our model, we developed a new technique called the method of recurrence relations. This method is a general mathematical technique appropriate for solving time-dependent many-body problems. DOE

N88-12585# Oak Ridge National Lab., Tenn.
CORROSION OF FERRITIC STEELS BY MOLTEN LITHIUM: INFLUENCE OF COMPETING THERMAL GRADIENT MASS TRANSFER AND SURFACE PRODUCT REACTIONS
P. F. Tortorelli Oct. 1987 20 p Presented at the 3rd International Conference on Fusion Reactor Materials, Karlsruhe, Fed. Republic of Germany, 4 Oct. 1987
(Contract DE-AC05-84OR-21400)
(DE88-000334; CONF-871036-5) Avail: NTIS HC A03/MF A01

An Fe-12Cr-1MoVW steel was exposed to thermally convective lithium for 6962 h. Results showed that the weight change profile of Fe-12Cr-1MoVW steel changed substantially as the maximum loop temperature was raised from 500 to 600°C. Furthermore, for a particular loop experiment, changes in the structure and composition of the exposed surfaces did not reflect typical thermal gradient mass transfer effects for all elements: the surface concentration of chromium was often a maximum at intermediate temperatures, while nickel (present at low concentrations in the starting material) tended to be transported to the coldest part of the loop. Such data were interpreted in terms of a qualitative model in which there are different dominant reactions or the various constituents of the ferritic steels (surface product formation involving nitrogen and/or carbon and solubility-driven elemental transport). This competition among different reactions is important in evaluating overall corrosion behavior and the effects of temperature. The overall corrosion rate of the 12Cr-1MoVW steel was relatively low when compared to that for austenitic stainless steel exposed under similar conditions. DOE

N88-12586# Central Electricity Generating Board, London (England). Inst. for Metal Materials.
EFFECTS OF STRESS-RELIEVING ON THE MECHANICAL PROPERTIES AND THE STRUCTURE OF SPECIMENS OF HIGH-TEMPERATURE FINE-GRAINED STRUCTURAL STEELS HEAT-TREATED TO SIMULATE WELDING
K. Detert, R. Banga, and W. Bertram [1987] 24 p Transl. into ENGLISH of conference paper presented at the 110th Plenary Session of the Materials Committee of the German Iron and Steel Federation, 1987 Session held in Fed. Republic of Germany, 15 Dec. 1987
(BLL-CE-Trans-8258-(9022.09); Rept-1794) Avail: British Library Lending Div., Boston Spa, United Kingdom

The properties of the coarse-grained structure in the heat affected zone (HAZ) beside a weld on specimens heat-treated to simulate welding of six fine-grained structural steels were investigated. The transition temperature for notch toughness, fracture toughness, and crack propagation rate and the conditions for the development of cracks during stress relief heat treatment were determined. The relationship between creep rupture notch sensitivity, creep rupture elongation, relaxation behavior, and stress relief cracking was examined. Clarification of the metallurgical causes of cracking during stress relieving were sought. The test methods used were creep and mechanical fracture tests. In addition the crack propagation rate under threshold loading in the HAZ was measured in comparison with the parent material. The purpose of the investigation was to answer the question whether cracking is linked to brittleness of this particular structural composition or whether the explanation must be looked for elsewhere. B.G.

N88-12587# National Aeronautical Lab., Bangalore (India). Materials Science Div.
ANALYSIS OF FREE CUTTING BRASS BY A.C. POLAROGRAPHY
S. Sreepathy, Aithu Poojary, Bharathi Bai J Basu, and S. R. Rajagopalan Aug. 1987 15 p
(PD-MT-8728) Avail: NTIS HC A03/MF A01

The analysis of lead as well as the major components copper and zinc is very important in the quality control of free cutting brass. The charging current eliminated AC polarograph and the phase selective AC polarograph are employed for this purpose. Author

N88-12588# National Aeronautical Lab., Bangalore (India). Materials Science Div.
STUDIES ON ESTIMATION OF NICKEL IN ZINC BASE DIE CASTING BY D.C. POLAROGRAPHY
S. Sreepathy, Aithu Poojary, and S. R. Rajagopalan Aug. 1987 10 p
(PD-MT-8729) Avail: NTIS HC A02/MF A01

Pure nickel gives good wave in alkaline cyanide supporting electrolyte. In the presence of a large amount of zinc (e.g. Mazac alloy) Ni does not give a well-defined wave. Experiments show that the presence of zinc up to 100mM enhances the nickel wave height, the enhancement being proportional to zinc concentration. The effect of nitrate ions and pH are studied and a suitable method for mazac analysis by DC polarography is suggested. Author

N88-12589# Central Electricity Generating Board, London (England).
INFLUENCE OF CREEP ON THE PRECIPITATE STRUCTURE UNDER CONDITIONS OF LONG-TERM CREEP. 4: EXPERIMENTS ON 10 CrMo 9 10 STEEL
Otto Schulz and Gerhard Sauthoff [1987] 18 p Transl. into ENGLISH from Arch. Eisenhuettenwes (Fed. Republic of Germany), v. 55, no. 2, Feb. 1984
(BLL-CE-Trans-8256-(9022.09)) Avail: British Library Lending Div., Boston Spa, United Kingdom

The creep and the precipitation behavior of the steel 10 CrMo 9 10 (2.5 percent Cr 1 percent Mo) was investigated at 600 C with loads between 80 and 190 MN/sq m. The carbide phases which precipitate during the carbide sequence in this steel are distributed inhomogeneously, from which a domain structure results with different carbides occupying different domains. During aging the domains with the more stable carbides grow at the expense of the other domains. This domain coarsening was measured as a function of aging time with and without loading. A noticeable influence of the creep on the domain coarsening was found only under special circumstances when there was initially a martensitic structure and when the creep rate was high during the early stages of carbide sequence. Such effects are not expected under practicable conditions of long-term creep. Author

N88-12590# Oak Ridge National Lab., Tenn.
THE AGING BEHAVIOR OF TYPES 308 AND 308CRE STAINLESS STEELS AND ITS EFFECT ON MECHANICAL PROPERTIES
J. M. Vitek and S. A. David 1987 37 p Presented at the Symposium on Technology of Glass, Ceramic, or Glass-Ceramic to Metal Sealing, Boston, Mass., 13 Dec. 1987
(Contract DE-AC05-84OR-21400)
(DE87-012541; CONF-871207-11) Avail: NTIS HC A03/MF A01

Aging of 308 and 308CRE SS was studied at 475 to 850 C for aging times up to 10,000 hours. Above 550 C, aging of 308 steel resulted in precipitation of carbides and the transformation of ferrite to sigma phase or the formation of sigma phase in initially ferrite-free material. The elevated-temperature aging of 308CRE steel resulted in the precipitation of titanium-rich carbides, nitrides, and sulfides, and the transformation of ferrite to sigma

phase. The distribution of precipitates was affected by the initial condition of the materials. The elevated-temperature creep properties, and in particular the improved properties of 308CRE, were related to the precipitate distribution. Below 550 C, aging of welded type 308 steel, precipitation of G-phase within the ferrite was observed, as well as the decomposition of ferrite into alpha and alpha prime. With the help of a novel mechanical properties microprobe, which was capable of determining the hardness of the minor constituent ferrite phase, the hardness behavior as a function of aging could be related to the microstructures. These results are interpreted in terms of the potential susceptibility of these alloys to 475 C embirrlement. DOE

N88-12591# Mound Lab., Miamisburg, Ohio.
METALLOGRAPHY OF MARAGING 350 STEEL
S. M. Hutson and C. W. Merten 1987 9 p Presented at the International Metallurgical Society Symposium, Monterey, Calif., 27 Jul. 1987
(Contract DE-AC04-76DP-00053)
(DE87-013746; MLM-3447(OP); CONF-8707113-1) Avail: NTIS HC A02/MF A01

A technique for etching maraging 350 steel with Glyceregia is described. Surface activation procedures are integral to this technique. Microstructural features revealed by this technique are compared with those obtained with Kalling's reagent, Fry's reagent, and 5% Nital, three etchants commonly used to reveal microstructures of maraging steels. Features which may be simultaneously revealed using Glyceregia include prior austenite grain boundaries, martensitic structure, precipitates, titanium carbo-nitrides, and reverted austenite. The other etchants examined in this investigation typically reveal only a few of the microstructural features detailed above at any one time. DOE

N88-12503# Joint Publications Research Service, Arlington, Va.
ACTIVITIES AT GOVERNMENT RESEARCH LABORATORIES REPORTED
In its JPRS Report: Science and Technology. Japan 24 Aug. 1987 p 1-3 Transl. into ENGLISH from Nikko Materials (Tokyo, Japan), Feb. 1987 p 35 (For primary document see N88-12502 04-12)
Avail: NTIS HC A06/MF A01

N88-12530*# National Aeronautics and Space Administration. White Sands Test Facility, N. Mex.
IGNITION AND COMBUSTION OF METALS IN OXYGEN
Frank J. Benz and S. Zhu (Lockheed Engineering and Management Services Co., Inc., Las Cruces, N. Mex.) *In* NASA, Lewis Research Center, Spacecraft Fire Safety 1987 p 99-102 (For primary document see N88-12520 04-16)
Avail: NTIS HC A07/MF A01 CSCL 11F

N88-12655# Air Force Wright Aeronautical Labs., Wright-Patterson AFB, Ohio.
DURABILITY OF POWDERED ALUMINUM STRUCTURES
Karen Severyna and Margery Artley *In* Army Materials Technology Lab., Work-in-Progress Presented at the Army Symposium on Solid Mechanics, 1986: Lightening of the Force Oct. 1986 p 49-52 (For primary document see N88-12644 04-31)
Avail: NTIS HC A04/MF A01 CSCL 11F

27 NONMETALLIC MATERIALS

Includes physical, chemical, and mechanical properties of plastics, elastomers, lubricants, polymers, textiles, adhesives, and ceramic materials.

For composite materials see *24 Composite Materials.*

N88-12592# Royal Naval Engineering Coll., Manadon (England).
DETERMINATION OF THROUGH-PLANE SHEAR MODULI FOR GLASS-REINFORCED PLASTICS
R. T. Hartshorn, M. D. Smith, and J. Summerscales Sep. 1983 12 p
(PB87-106274) Avail: NTIS HC E04/MF E04 CSCL 11B

The characterization of the mechanical properties of an orthotropic composite material requires nine elastic constants; although this may be reduced to six in the case of a square symmetric laminate. The three Young's moduli and the three Poisson's ratios may be determined with relative ease, but the three shear moduli pose a more complex problem. Numerous test rigs have been described for the determination of the in-plane shear modulus, but the through-plane shear moduli have been largely neglected. The paper describes experiments to determine the through-plane shear moduli of thick glass reinforced plastic (GRP) plates. GRA

N88-12593 British Petroleum Co. Ltd., Sunbury-on-Thames (England).
THERMOPLASTIC ELASTOMER COMPOSITIONS Patent Application
David Joseph Anzini, inventor and Charles Dains Shedd, inventor 10 Dec. 1986 17 p Filed 15 May 1986 Priority 21 May 1985 US 736547
(EP-Patent-0-204-453-A1; EP-Patent-Appl-SN-86303727.1; Int-Patent-Class-C08L-33/08; Int-Patent-Class-C08L-23/04; ETN-87-90719) Avail: UK Patent Office, 25 Southampton Buildings, London WC2A 1A4, United Kingdom

A thermoplastic elastomer composition was obtained by blending together and partially curing an acrylate rubber and a polyolefin resin in a weight ratio of acrylate rubber to polyolefin of from 95:5 to 50:50. The compositions may be filled with aluminum trihydrate to provide thermoplastic elastomer compositions having low smoke, and flame retardant properties. Such compositions are suitable for use as jacketing for cables. ESA

N88-12594 British Petroleum Co. Ltd., Sunbury-on-Thames (England).
POLYMER COMPOSITION Patent Application
Jeffrey David Umpleby, inventor 29 Oct. 1986 11 p Filed 6 Mar. 1986 Priority 12 Mar. 1985 GB 8506304
(EP-Patent-0-199-444-A1; EP-Patent-Appl-SN-86301608.5; Int-Patent-Class-H01B-7/28; Int-Patent-Class-C08K-5/54; Int-Patent-Class-H01B-3/44; Int-Patent-Class-H01B-3/46; ETN-87-90721) Avail: UK Patent Office, 25 Southampton Buildings, London WC2A 1A4, United Kingdom

A polymer composition suitable for use as cable insulation and exhibiting a reduced tendency to form water-trees under the influence of medium or high voltage was developed. The composition comprises a polymeric component, for example polyethylene or ethylene copolymer and, as a water-tree retardant, a defined organo-silicon compound having at least one substituent comprising a chain of three amino-alkyl units. ESA

N88-12595# Connecticut Univ., Storrs. Inst. of Materials Science.
STRUCTURE OF THERMOTROPIC POLYESTERS WITH LARGE SUBSTITUENTS Technical Report No. 4, 1-27 Aug. 1987
H. H. Chin, L. V. Azaroff, A. Furukawa, and R. W. Lenz 27 Aug. 1987 12 p
(Contract N00014-86-K-0772)
(AD-A184086) Avail: NTIS HC A03/MF A01 CSCL 07C

Thermotropic aromatic polyesters were aligned by drawing from nematic melts and by quenching in a magnetic field of 15 tesla and subsequently examined by x ray diffraction. The degree of alignment obtained depended slightly on the substituent (H, F, C1, Br, CH3, NO2) present with the highest degree of alignment observed when the arylsulfonyl substituted group contained in the para-position H or F and the lowest when it contained Br or CH3. GRA

N88-12596# Northwestern Univ., Evanston, Ill. Dept. of Chemistry.
SYNTHESIS, NMR CHARACTERIZATION AND ELECTRICAL PROPERTIES OF SILOXANE-BASED POLYMER ELECTROLYTES Interim Technical Report

R. Spindler and D. F. Shriver 24 Aug. 1987 32 p
(Contract N00014-80-C-0532)
(AD-A184184; Rept-015) Avail: NTIS HC A03/MF A01 CSCL 07C

A crosslinked siloxane-based polymer has been prepared by the reaction of Poly(methyl hudrosiloxane), monomethyl ether poly(ethylene glycol), and poly(ethylene glycol). The polymer, which has been structurally characterized by 29 Si NMR, forms complexes with LISO CF3 that exhibit good ionic conductivities (for a LiSO3CF3 15 wt% complex). The polymer and its salt complexes have been characterized by elemental analysis, 29 Si NMR powder diffraction X-ray powder diffraction, DSC, and AC complex impedance spectroscopy. The dependence of the ionic conductivity was investigated as a function of temperature, salt concentration (91 wt % to 25 wt %), and alkali metal cation (Li, Na, K, Rb, and Cs). GRA

N88-12597# Massachusetts Inst. of Tech., Cambridge.
CONDUCTIVE POLYMERS VIA REACTIVE ALIGOMER Final Report
G. E. Wnek and S. C. Arnold 30 Jan. 1987 40 p
(Contracts N62269-85-C-0297; DA Proj. R00-0001)
(AD-A184270; NADC-87038-60) Avail: NTIS HC A03/MF A01 CSCL 07C

This report summarizes the efforts that have been made towards synthesizing a processible conducting polymer. Low molecular weight flexible chain telechelic polymers, such as sebacyl chloride or PEG, are endcapped, via acylation and esterification, with a-terthiophene groups. Although the synthesis of these prepolymers is simple and straight-forward; high yield and purity, and which is essential for their polymerization, have not yet been attained. Although polymerization can presumably be carried out through many of the oxidative coupling routes that are available, either through chemical or electrochemical means, it is felt that the lack of synthetic control of these reactions could obscure the structure of the product. By brominating the prepolymer at the terminal 2-thienyl positions, the mono-Grignard reagent can be prepared and polymerized with a Ni(II) catalyst similar to Yamamoto's technique. This polymerization route offers a higher degree of control due to the exact placement of the coupling links. Furthermore, if the thiophene hexamers in the alternating block copolymer are not of sufficient conjugation length for high conductivity, the Grignard-coupling technique allows for additional terthiophene units to be incorporated into the thienyl blocks. GRA

N88-12598# University of Southern Mississippi, Hattiesburg. Dept. of Polymer Science.
SOLID STATE C-13 NMR CHARACTERIZATION OF TEXTILES: QUALITATIVE AND QUANTITATIVE ANALYSIS Technical Report No. 3, Aug. 1986 - Aug. 1987
Ronald F. Colletti and Lon J. Mathias 27 Aug. 1987 16 p
(Contract N00014-86-K-0659)
(AD-A184349) Avail: NTIS HC A03/MF A01 CSCL 11E

Cross-polarization magic angle spinning (CP/MAS) carbon 13 NMR was used to qualitatively characterize textiles of various compositions. Rapid and accurate determination of cotton/polyester blends was accomplished with minimal sample preparation. Qualitative identification was demonstrated for various fiber blends including mislabeled samples. This technique demonstrates the ability to characterize as-obtained fibers and fabrics and should extend to composite reinforcing materials and prepregs. GRA

N88-12599# Massachusetts Univ., Amherst.
THERMOPLASTIC ELASTOMERS AS LOVA (LOW VULNERABILITY AMMUNITION) BINDERS Annual Report, Jan. - Dec. 1986 - Dec. 1986
James C. Chien, Richard J. Farris, C. P. Lillya, and H. H. Winter 1986 46 p
(Contract N00014-85-K-0680)
(AD-A184350) Avail: NTIS HC A03/MF A01 CSCL 19A

From promesogens - Conventional mesogenic compounds have high Tm which limits the conditions for processing. In this work, low melting promesogens were used to synthesize liquid crystalline compounds and polymers. Alkyl-4(4'-alkoxybenzoyloxy)benzoates (with C1-C-10 alkyl and alkoxy groups) are monotropic compounds which melt directly to isotropic liquids. Twin liquid crystalline compounds, TLCC, of alkoxybenzoyloxybenzoic acid have been synthesized. The TLCC with methoxy end groups and trioxyethylene spacer is weakly mesogenic; but replacement of the methoxy with an n-butoxy end group results in a smectic mesophase. From Mesogens Azo and azoxy aromatic systems are currently being investigated to test the feasibility of this project. 4,4-Azoxy benzoic acid has been prepared by a reduction nitrobenzoic acid with sodium hydroxide in methanol. This purified material was then converted to the diacid chloride by treatment with thionyl chloride. The azoxy benzoyl chloride was purified by recrystallization in good yields. GRA

N88-12600# Army Lab. Command, Watertown, Mass. Material Technology Lab.
EFFECT OF TIME AND TEMPERATURE ON TRANSFORMATION TOUGHENED ZIRCONIAS Final Report
Liselotte J. Schioler Jun. 1987 107 p
(Contract DE-AI05-840R-21411)
(AD-A184356; MTL-TR-87-29) Avail: NTIS HC A06/MF A01 CSCL 11B

The effects of exposure to elevated temperatures (900 to 1300 C) for times ranging from 50 to 500 hours on toughened oxide ceramics intended for use in heat engines were examined. The materials were magnesia stabilized transformation toughened zirconia, yttria stabilized tetragonal zirconia polycrystal, and zirconia toughened alumina, as well as untoughened zirconias for comparison. The materials were heat treated, and physical and mechanical properties were then measured at room temperature. High temperature mechanical tests performed were stress rupture and stepped temperature stress rupture. The results of the tests indicate that the mechanical properties of magnesia stabilized transformation toughened zirconia degrade substantially after relatively short times at the moderate temperatures expected in low heat rejection diesel engines. The yttria stabilized tetragonal zirconia polycrystal and the untoughened partially stabilized zirconia materials appear to be more stable against the effects of time at temperature. GRA

N88-12601# University of Southern Mississippi, Hattiesburg. Dept. of Polymer Science.
A LOW VOLUME INSERT FOR SOLID STATE MAGIC ANGLE SPINNING NMR OF SMALL SAMPLES Technical Report No. 5, Aug. 1986 - Aug. 1987
Lon J. Mathias, Douglas G. Powell, and James L. Bridges 27 Aug. 1987 11 p
(Contract N00014-86-K-0659)
(AD-A184359) Avail: NTIS HC A03/MF A01 CSCL 14B

Easily machined ceramic inserts with low volume capacities were compared to standard rotors packed completely with samples or with silica gel-diluted samples of adamantane and glycine. A disc shaped sample cavity gave better signal-to-noise than a cylindrically-shaped one for comparable sample size and number of scans, and gave the narrower peak widths than even the full rotor. The inserts are inexpensive and easy to use while facilitating high-speed rotor spin-up and recovery of the noncontaminated samples. GRA

N88-12602# Instituto de Pesquisas Energeticas e Nucleares, Sao Paulo (Brazil).
STUDIES OF ALUMINA ADDITIONS IN ZIRCONIA - MAGNESIA
R. Muccillo 1987 13 p In PORTUGUESE; ENGLISH summary Presented at the 31st Brazilian Congress on Ceramics, Brasilia, Brazil, 24 May 1987
(DE87-703500; INIS-BR-749; CONF-8705175-1) Avail: NTIS (US Sales Only) HC A03/MF A01

Ionic conductivity measurements have been carried out in the 500 sup 0 C - 1000 sup 0 C temperature range in Mg - PSZ

(Partially Stabilized Zirconia) with 0.5 to 10 mol % alumina additions. All specimens were prepared by pressing followed by pre - and sintering at 1000 sup 0 C 2h and 1450 sup 0 C 4h, respectively. Thermal hysteresis of the ionic conductivity have been detected, probably due to phase changes in the Mg-PSZ samples. The results show that alumina additions up to 2.1% enhance densification with no major variations in electrical resistivity values. DOE

N88-12603# Sandia National Labs., Albuquerque, N. Mex.
MOLECULAR ENGINEERING OF CERAMICS
J. E. Martin 1987 10 p Presented at the Conference on Atomic and Molecular Processing of Electronic and Ceramic Materials: Preparation, Characterization and Properties, Seattle, Wash., 31 Aug. 1987
(Contract DE-AC04-76DP-00789)
(DE88-000174; SAND-87-2098C; CONF-870878-1) Avail: NTIS HC A02/MF A01

We discussed some recent advances in the study of silica sol-gels, including the kinetics of growth of the sol beneath the gel point, the fractal structure of the sol and the observation of a spatial correlation length in undiluted gels. We attempted to connect these results to popular theories, but were not able to paint a definitive picture of the sol-gel transition. In part, this is due to the paucity of experimental data in this field. A few tentative conclusions can be drawn: (1) The static structure of the fractionated and unfractionated sol seems to be fairly well accounted for by the percolation model if swelling is taken into account. (2) The divergences of the average cluster mass and radius are stronger than predicted by the percolation model, and much stronger than the Flory-Stockmayer predictions. (3) The static structure observed in the undiluted, low-density silica gels are in reasonable agreement with either an equilibrium model, such as correlated percolation, or a kinetic growth model. Discrepancies exist in either case. DOE

N88-12604# Georgia Inst. of Tech., Atlanta. Research Inst.
DEVELOPMENT OF ADVANCED FIBER REINFORCED CERAMICS Final Report
T. L. Starr and J. N. Harris 1987 98 p
(Contract DE-AC05-84OR-21400)
(DE88-000779; ORNL/Sub-83-43369/01) Avail: NTIS HC A05/MF A01

A fundamental problem in the processing of ceramic composites is the fact that the incorporated fibers tend to reinforce the green structure, preventing the volume reduction and densification that usually is obtained during free sintering. Hot pressing is one approach to overcoming this problem, providing the necessary densification by application of pressure. An alternative approach is to maximize the green density of composite preforms and to utilize volume filling techniques to achieve high density. This type of process is more suitable for fabrication of large and complex shapes. Development of such processing is the primary thrust of this research program. The results of this program are organized into four topics. A review of models for the physical properties of composites is given. New understanding of cast and sinter processing of fiber/powder blends was gained and used to produce consistent, dense composites. These results are broadly applicable to many composite systems. Development work on silica and silicon nitride matrix composites is reported. The silica composites were fabricated using a precursor resin infiltration process to increase the sintered density. Silicon nitride composites were processed using reaction sintering of silicon powder/fiber preforms. In both cases, composites were produced with densities comparable to monolithic materials and using fabrication techniques suitable for large, complex components. This emphasis on scale-able processing is an important theme running throughout this work. DOE

N88-12605# Oak Ridge National Lab., Tenn.
CERAMIC TECHNOLOGY FOR ADVANCED HEAT ENGINES PROJECT Semiannual Progress Report, Oct. 1986 - Mar. 1987
Aug. 1987 428 p
(Contract DE-AC05-84OR-21400)
(DE88-001520; ORNL/TM-10469) Avail: NTIS HC A19/MF A01

This report contains four subelements: (1) Monolithics, (2) Ceramic Composites, (3) Thermal and Wear Coatings, and (4) Joining. Ceramic research conducted within the Monolithics subelement currently includes work activities on green state ceramic fabrication, characterization, and densification and on structural, mechanical, and physical properties of these ceramics. Research conducted within the Ceramic Composites subelement currently includes silicon carbide and oxide-based composites, which, in addition to the work activities cited for Monolithics, include fiber synthesis and characterization. Research conducted in the Thermal and Wear Coatings subelement is currently limited to oxide-based coatings and invloves coating synthesis, characterization, and determination of the mechanical and physical properties of the coatings. Research conducted in the Joining subelement currently includes studies of processes to produce strong stable joints between zirconia ceramics and iron-based alloys. A major objective of the research in the Materials and Processing project element is to systematically advance the understanding of the relationships between ceramic raw materials such as powders and reactant gasses, the processing variables involved in producing the ceramic materials, and the resultant microstructures and physical and mechanical properties of the ceramic materials. Success in meeting this objective will provide economical highly reliable ceramic components for advanced heat engines. DOE

N88-12606# National Aeronautical Lab., Bangalore (India). Materials Science Div.
THERMAL EXPANSION OF SOME Ge-Se-Te GLASSES
Sudha Mahadevan, A. Giridhar, and A.K. Singh Jul. 1987 22 p
(PD-MT-8722) Avail: NTIS HC A03/MF A01

Results of the measurement of thermal expansion coefficient (from 50 C to the softening temperature) are reported for eight glass compositions of the Ge-Se-Te system. For the (GeSe2) sub 100-2x Se sub 30-x Te sub x glasses, an increase of T sub g and of Delta alpha is seen with decreasing SeTe content. For (GeSe2) sub 23.33 Se sub 30-x Te sub x glasses, alpha, T sub g, and Delta alpha are invariant with composition. The results obtained, when examined along with those obtained for other chalcogenide glasses, show that chalcogenide glasses are not necessarily in a state of isofree volume during glass transition. Values ranging from 0.024 to 0.167 are obtained for the free volume of some chalcogenide glasses. Author

N88-12607# National Aeronautical Lab., Bangalore (India). Materials Science Div.
STUDIES ON SOME Ge-Se-Te GLASSES
Sudha Mahadevan, A. Giridhar, and A.K. Singh Jun. 1987 52 p
(PD-MT-8721) Avail: NTIS HC A04/MF A01

Results of measurements of the glass transition temperature (T sub g), electrical conductivity (sigma) and density (d) are reported for eight glass compositions of the Ge-Se-Te system. For (GeSe2)(100-2x)Se(x)Te(x) glasses, a monotonic increase of sigma and d with increase in Te content is seen. The T sub g of these glasses shows a decrease with increaseing Te content. For the (GeSe2)23.33Se(30-x)Te(x) glasses, the T sub g does not vary with composition because the effective connectedness remains the same. Sigma and delta E show a smooth variation across the tie line composition Ge23.33Se61.67Te15 prime while a kink is seen at this composition for density and molar volume. The composition Ge23.33Se51.67Te25 is found to exhibit microphase separation and reigsters double T sub g and double T sub C. The compositions of the two phases are found to be approximately Ge25Se62.5Te12.5 (residual glass) and approximately Ge22.5Se46.3Te31.2 in the approximate weight ratio of 1:2. On partial crystallization the sigma and d of this glass are found to decrease before they register an increase on complete crystallization of the glass. A model where Te crystallizes out from the first glassy phase and is found to be dispersed

discontinuously in a semiconducting glassy matrix consisting of essentially GeSe2 and the residual glass is found to account for the variations of sigma and the density during crystallization of this composition. On complete crystallization, when GeSe2, GeTe and additional Te are all crystallized, an increase in density and a steep increase of sigma are seen. Author

N88-12608# Los Alamos National Lab., N. Mex.
SYNTHESIS OF THE MONOCLINIC YTTRIA BY THERMAL PLASMA PROCESSING
G. J. Vogt 1987 17 p Presented at the 172nd Meeting of the Electrochemical Society, Honolulu, Hawaii, 18 Oct. 1987
(Contract W-7405-eng-36)
(DE88-000496; LA-UR-87-3149; CONF-871027-34) Avail: NTIS HC A03/MF A01

Submicron powders of monoclinic yttria were prepared by thermal plasma processing of commercial yttria powder. The starting yttria powder was vaporized in the hot tail flame of a thermal argon plasma and the resulting vapor was quenched with hydrogen gas to form yttria particles with a 21-nm mean diameter. The synthesis of yttria by oxidizing yttrium carbide in the plasma was also examined. The plasma powders were characterized by powder x-ray diffraction, transmission electron microscopy, and differential thermal analysis. DOE

N88-12609# Pacific Northwest Labs., Richland, Wash.
REAL-TIME RAMAN DETECTION OF MOLECULAR CHANGES IN CERAMICS UNDERGOING SLIDING FRICTION
G. J. Exarhos and M. S. Donley Feb. 1987 13 p Presented at the 22nd Annual Meeting of the Microbeam Analysis Society, Kailua-Kona, Hawaii, 13 Jul. 1987
(Contract DE-AC06-76RL-01830)
(DE88-000558; PNL-SA-14794; CONF-870725-12) Avail: NTIS HC A03/MF A01

Time-resolved Raman spectroscopy was used to probe the wear track caused by contact between a rotating ceramic disk (boron nitride or silicon carbide) and either a steel ball bearing or a silicon carbide wedge. The visco-elastic response of the hexagonal phase of boron nitride, used as a solid lubricant, was evaluated on a millisecond timescale. Vibrational spectra indicate that this material actually becomes a better lubricant under conditions of increased force between the wear tip and spinning disk. Similar studies involving wear between a silicon carbide disk and silicon carbide wear tip indicated that decomposition and/or segregation of elemental silicon and carbon occurred at high wear rates. The surface temperature near the wear tip was determined from measured vibrational spectra and the temperature profile around the wear track was evaluated. Evidence for oxidation of carbon at the surface was inferred from measured spectra. Application of this laser-based technique to tribological studies provides information relating to localized heating, relaxation dynamics, and phase transformation/decomposition phenomena useful for understanding the fundamental mechanisms of friction and wear. DOE

N88-12610# Los Alamos National Lab., N. Mex.
ADVANCES IN INHERENTLY CONDUCTING POLYMERS
M. Aldissi Sep. 1987 20 p Presented at the 1st European Polymer Symposium, Lyon, France, 14 Sep. 1987
(Contract W-7405-eng-36)
(DE88-000501; LA-UR-87-3019; CONF-8709138-1) Avail: NTIS HC A03

The discovery of polyacetylene as the prototype material led to extensive research on its synythesis and characterization. The techniques that emerged as the most important and promising ones are those that dealt with molecular orientation and that resulted in conductivities almost as high as that of copper. The study of dozens of other materials followed. Interest in conducting polymers stems from their nonclassical optical and electronic properties as well as their potential technological applications. However, some of the factors currently limiting their use are the lack of long-term stability and the need to develop conventional low-cost techniques for easy processing. Therefore, research was extended toward solving these problems, and progress has been recently made in that direction. The synthesis of new materials such as stable and easily processable alkylthiophenes, water-soluble polymers, and multicomponent systems, including copolymers and composites, constitutes an important step forward in the area of synthetic metals. However, a full understanding of materials chemistry and properties requires more work in the years to come. DOE

N88-12611# Los Alamos National Lab., N. Mex.
CONDUCTING HYBRID POLYMERIC SYSTEMS
M. Aldissi, J. W. White, S. Agnew, and B. S. Jorgensen Sep. 1987 10 p Presented at the 1st European Polymer Symposium, Lyon, France, 14 Sep. 1987 Prepared in cooperation with Australian National Univ., Canberra
(Contract W-7405-eng-36)
(DE88-000527; LA-UR-87-3048; CONF-8709138-2) Avail: NTIS HC A02/MF A01

The studies took advantage of the opportunities offered by copolymerization for gaining insight into electrical conduction, morphology, phase separation, polymer-polymer interfaces, and solubility. Copolymerization is technologically important for it allows one to tailor-make products with specifically desired properties. However, the utility of copolymerization involving conjugated, rigid components could be different from that of conventional polymers. This paper is focused on the synthesis and properties of various materials: Rod-coil systems such as polyisoprene/polyacetylene diblock copolymers (resonance raman and small angle neutron scattering studies correlated to conductivity); and alternating copolymers such as poly (arylpyrroles) (electrochemical synthesis and characterization). DOE

N88-12612# Pennsylvania State Univ., University Park. Polymer Science Section.
PROTON ABSTRACTION AS A ROUTE TO CONDUCTIVE POLYMERS
Lawrence F. Hancock, Brian L. Hilker, William Chapman, and Bernard Gordon, III 1 Aug. 1987 4 p
(Contract N00014-85-K-0899)
(AD-A184019; TR-1) Avail: NTIS HC A02/MF A01 CSCL 07D

Proton abstraction doping has been demonstrated as a viable alternate procedure for the synthesis of electrically conductive polymers through the preparation of poly(phenylene pentadienylene). Additional procedures being used for the synthesis of proton abstraction doping precursors include sulfur ylide and Grignard condensations; details will be presented. These systems offer tremendous advantages for the study of effects arising from dopant density and conjugation length in organic conductors. One interesting result involves the conductivity of 1,5-diphenypentadine, a low molecular weight model for poly(p-phenylene pentadienylene). 1,5-diphenyl pentadienyl anion displays a conductivity of 8s/cm which supports the conclusion that polymeric delocalization of charge is not a necessity. GRA

N88-12505# Joint Publications Research Service, Arlington, Va.
CERAMICS THIN FILM
In its JPRS Report: Science and Technology. Japan 24 Aug. 1987 p 5-7 Transl. into ENGLISH from Nikko Materials (Tokyo, Japan), Feb. 1987 p 36-37 (For primary document see N88-12502 04-12)
Avail: NTIS HC A06/MF A01

N88-12508# Joint Publications Research Service, Arlington, Va.
RESEARCH AND DEVELOPMENT ON HIGH STRENGTH CERAMIC HEATERS DISCUSSED
In its JPRS Report: Science and Technology. Japan 24 Aug. 1987 p 10-20 Transl. into ENGLISH from Kino Zairyo (Tokyo, Japan), Feb. 1987 p 16-13 (For primary document see N88-12502 04-12)
Avail: NTIS HC A06/MF A01

28 PROPELLANTS AND FUELS

Includes rocket propellants, igniters, and oxidizers; their storage and handling procedures; and aircraft fuels.

For related information see also *07 Aircraft Propulsion and Power, 20 Spacecraft Propulsion and Power,* and *44 Energy Production and Conversion.*

N88-12613# Foersvarets Forskingsansalt, Stockholm (Sweden).
TEST NUMBER 2 OF PROPELLANT FOR ROCKET MOTOR MK52
A. Schwartz May 1987 28 p
(PB87-226155; FOA-C-20660-2.1) Avail: NTIS HC A03/MF A01 CSCL 21I

Tensile tests have been done on propellants taken from two MK52 rocket motors. Samples of propellant from near the motor wall had higher strength than propellant near the bore. Also the age of rocket motors influences the tensile strength which decreases with increasing age. The tensile strength of propellant cast in cardboard decreased a little compared with previous measurements. This is valid for low temperatures. Measures of moisture in motor propellants indicates that about 0.25 to 0.35% moisture is to be found in the propellant. The moisture may be conducive to some decrease of strength with time. A desiccator could eventually be placed in the nozzle in order to limit the decomposing effect on propellant of moisture during storage.
GRA

N88-12614# Argonne National Lab., Ill.
EMERGING ENVIRONMENTAL CONSTRAINTS ON THE USE OF GASOLINE AND DIESEL FUEL AND TRADEOFFS ASSOCIATED WITH THE USE OF ALTERNATIVE FUELS
M. K. Singh, C. L. Saricks, S. J. LaBelle, and D. O. Moses (Department of Energy, Washington, D. C.) 1987 20 p Presented at the Air Pollution Control Association International Specialty Conference on Mobile Sources/Emerging Issues, Windsor, Ontario, 22 Mar. 1987 Prepared in cooperation with USDOE Assistant Secretary for Environment, Safety and Health, Washington, D.C. Office of Environmental Analysis
(Contract W-31109-eng-38)
(DE87-011504; CONF-8703157-1) Avail: NTIS HC A03/MF A01

In this era of stable to declining oil prices, the economic incentive for turning to alternative fuels for transportation has obviously decreased. Other incentives may lead to the use of alternative transportation fuels. This paper presents preliminary results of a study examining whether an inability of highway vehicles to comply fully with mobile source emission regulations might constrain the use of gasoline and diesel fuels, and thus catalyze penetration of alternative fuels into the transportation market. The study found that while compliance challenges exist, it is unlikely that they alone will force manufacturers to turn to alternative-fueled vehicles. Based on projected household and vehicle characteristics over the next 10 years, a forecast of alternative-fueled vehicle penetration and impact on national emissions has been developed under a set of optimistic but plausible assumptions about future availability and price of alternative fuels. It is estimated that by 1997 under 2% of personal vehicle miles driven could be in methanol-fueled cars and light trucks, the alternative-fueled vehicles most likely to penetrate first. This level of penetration would lead to a reduction of less than 1 percent in RHC and NO/sub x/ from all transportation sources in 1997. DOE

N88-12615# Princeton Combustion Research Labs., Inc., Monmouth Junction, N.J.
HIGH PRESSURE STRAND BURN RATE TESTS OF POLYVINYLNITRATE/NITRAMINE PROPELLANTS Final Technical Report, Feb. - Dec. 1986
Neale A. Messina, Larry S. Ingram, Gustave F. Konig, Martin Summerfield, and W. Crawford 10 Jun. 1987 70 p
(Contract DAAA21-86-C-0067)
(AD-A184178; PCRL-FR-87-004) Avail: NTIS HC A04/MF A01 CSCL 19A

One approach to solving the problem of the erratic burning behavior, i.e., slope break, of nitramine gun propellants is to complex the nitramine propellant with polyvinylnitrate (PVN) binder material, i.e., hydrogen bond the RDX or HMX with the unesterified hydroxyl groups in the binder. The objective of the current effort was to conduct independent high pressure strand burn rate tests of this new class of PVN/nitramine propellant, as distinct from high pressure closed bomb burn rate tests. Comparisons of strand burn rate data of solution processed PVN/nitramine complexed formulations with conventionally processed control formulations have been conducted. Also, comparisons of strand burn rate data and closed bomb burn rate data have been conducted. GRA

N88-12616# Department of Energy, Washington, D. C. Office of Operational Safety.
DOE EXPLOSIVES SAFETY MANUAL
Aug. 1987 99 p
(DE88-000831; DOE/EV-06194/3-Rev-3) Avail: NTIS HC A05/MF A01

This manual is applicable to all DOE facilities engaged in operations of development, manufacturing, handling, storage, transportation (on site), processing, or testing of explosives, or assemblies containing explosives. It contains guidelines and standards for these operations in order to safeguard personnel and to prevent property damage. Criteria established by this manual are specific to high explosives but also apply to propellants and pyrotechnics when these materials can undergo explosive reactions. The standards of this manual deal with the operations involving explosives and the safe management of such operations. Design criteria for facilities used in conjunction with explosives operations are addressed only indirectly. Design criteria for explosives facilities are contained in DOE 6430.1, 'General Design Criteria Manual.' It is not intended that existing physical facilities be changed arbitrarily to comply with this manual's provisions, except as required by law. Facility conditions determined to be noncompliant shall be resolved among the DOE Field Operations Office (FOO), Program Ofice, and the Office of Operational Safety. (FOO), Program Office, and the Office of Operational Safety (OOS). The standards are presented as either mandatory or advisory. Mandatory standards, denoted by the words "shall," "must," or "will," are requirements that must be followed unless written authority for deviation is granted as an exemption by the DOE. Advisory standards denoted by "should" are standards that may be deviated from with a waiver granted by facility management.
DOE

29 MATERIALS PROCESSING

Includes space-based development of products and processes for commercial applications.

For biological materials see *55 Space Biology.*

N88-12617*# Sundstrand Corp., Rockford, Ill. Energy Systems.
A STUDY OF TWO-PHASE FLOW IN A REDUCED GRAVITY ENVIRONMENT Final Report
D. Hill and Robert S. Downing 16 Oct. 1987 173 p
(Contract NAS9-17195)
(NASA-CR-172035; NAS 1.26:172035; DRL-T-1884; DRD-TM-478T) Avail: NTIS HC A08/MF A01 CSCL 22A

A test loop was designed and fabricated for observing and measuring pressure drops of two-phase flow in reduced gravity. The portable flow test loop was then tested aboard the NASA-JSC KC135 reduced gravity aircraft. The test loop employed the Sundstrand Two-Phase Thermal Management System (TPTMS) concept which was specially fitted with a clear two-phase return line and condenser cover for flow observation. A two-phase (liquid/vapor) mixture was produced by pumping nearly saturated liquid through an evaporator and adding heat via electric heaters. The quality of the two-phase flow was varied by changing the evaporator heat load. The test loop was operated on the ground before and after the KC135 flight tests to create a one-gravity data base. The ground testing included all the test points run

during the reduced gravity testing. Two days of reduced gravity tests aboard the KC135 were performed. During the flight tests, reduced-gravity, one-gravity, and nearly two-gravity accelerations were experienced. Data was taken during the entire flight which provided flow regime and pressure drop data for the three operating conditions. The test results show that two-phase pressure drops and flow regimes can be accurately predicted in zero-gravity. Author

N88-12618*# Virginia Univ., Charlottesville. Dept. of Chemical Engineering.
MICROGRAVITY NUCLEATION AND PARTICLE COAGULATION EXPERIMENTS SUPPORT Status Report, 1 Jun. - Nov. 30 1987
L. U. Lilleleht and F. T. Ferguson Dec. 1987 38 p Original contains color illustrations
(Grant NAG5-865)
(NASA-CR-181540; NAS 1.26:181540; UVA/528260/CHE88/102) Avail: NTIS HC A03/MF A01 CSCL 22A

A preliminary model for diffusion between concentric hemispheres was adapted to the cylindrical geometry of a microgravity nucleation apparatus, and extended to include the effects of radiation and conduction through the containment walls. Computer programs were developed to calculate first the temperature distribution and then the evolving concentration field using a finite difference formulation of the transient diffusion and radiation processes. The following estimations are made: (1) it takes approximately 35 minutes to establish a steady temperature field; (2) magnesium vapors released into the argon environment at the steady temperature distribution will reach a maximum supersaturation ratio of approximately 10,000 in the 20-second period at a distance of 15 cm from the source of vapors; and (3) approximately 750W electrical power will be required to maintain steady operating temperatures within the chamber. Author

N88-12619*# Virginia Univ., Charlottesville. Dept. of Chemical Engineering.
MICROGRAVITY NUCLEATION AND PARTICLE COAGULATION EXPERIMENTS SUPPORT Status Report, 1 Jan. - 31 May 1987
L. U. Lilleleht and T. J. Lass Dec. 1987 89 p
(Grant NAG5-865)
(NASA-CR-181541; NAS 1.26:181541; UVA/528260/CHE88/101) Avail: NTIS HC A05/MF A01 CSCL 22A

A hollow sphere model is developed to predict the range of supersaturation ratio values for refractory metal vapors in a proposed experimental nucleation apparatus. Since the experiments are to be carried out in a microgravity environment, the model neglects the effects of convection and assumes that the only transfer of vapors through an inert gas atmosphere is by conduction and molecular diffusion. A consistent set of physical properties data is assembled for the various candidate metals and inert ambient gases expected to be used in the nucleation experiments. Transient partial pressure profiles are computed for the diffusing refractory species for two possible temperature distributions. The supersaturation ratio values from both candidate temperature profiles are compared with previously obtained experimetnal data on a silver-hydrogen system. The model is used to simulate the diffusion of magnesium vapor through argon and other inert gas atmospheres over ranges of initial and boundary conditions. These results identify different combinations of design and operating parameters which are liekly to produce supersaturation ratio values high enough to induce homogeneous nucleation in the apparatus being designed for the microgravity nucleation experiments. Author

N88-12620# Pacific Northwest Labs., Richland, Wash.
LOW GRAVITY FLUID-THERMAL EXPERIMENTS
W. J. Krotiuk and J. M. Cuta Jun. 1987 18 p Presented at the 3rd Pathways to Space Experimentation Workshop, Orlando, Fla., 3 Jun. 1987
(Contract DE-AC06-76RL-01830)
(DE88-000553; PNL-SA-15084; CONF-8706214-1) Avail: NTIS HC A03/MF A01

Pacific Northwest Laboratory (PNL) is the lead laboratory for the thermal-hydraulic research in the US Department of Energy Multimegawatt Space Nuclear Power Program. PNL must provide the tools necessary to analyze proposed space reactor concepts, which include single- and two-phase alkali metal and gas-cooled designs. PNL has divided its activities for this task into three basic areas: computer code development, thermal-hydraulic modeling, and experimentation. The subject of this paper is the low-gravity experimental program currently underway at PNL in support of the MMW Program. DOE

N88-12528*# National Aeronautics and Space Administration. Lewis Research Center, Cleveland, Ohio.
MICROGRAVITY COMBUSTION FUNDAMENTALS
Kurt R. Sacksteder *In its* Spacecraft Fire Safety 1987 p 89-94 (For primary document see N88-12520 04-16)
Avail: NTIS HC A07/MF A01 CSCL 22A

31 ENGINEERING (GENERAL)

Includes vacuum technology; control engineering; display engineering; cryogenics; and fire prevention.

N88-12621# Joint Publications Research Service, Arlington, Va.
USSR REPORT: ENGINEERING AND EQUIPMENT
28 May 1987 120 p Transl. into ENGLISH from various Russian articles
(JPRS-UEQ-87-008) Copyright Avail: NTIS HC A06/MF A01

Numerous topics related to engineering and equipment are discussed. Aeronautics and space technology, nuclear energy, electric power plants, industrial technology, turbines, engine design, fluid mechanics, the mechanics of solids, and materials testing are among the topics covered. For individual titles, see N88-12622 through N88-12641.

N88-12622# Joint Publications Research Service, Arlington, Va.
A RELIABILITY CONCEPT FOR OPTIMIZING AIRCRAFT DESIGN Abstract Only c05
S. V. Arinchev and V. V. Bystrov *In its* USSR Report: Engineering and Equipment 28 May 1987 p 1 Transl. into ENGLISH from Izvestiya Vysshikh Uchebnykh Zavedeniy: Aviatsionnaya Tekhnika (Kazan, USSR), no. 4, Oct. - Dec. 1985 p 7-12 Original language document was announced in IAA as A86-35977 (For primary document see N88-12621 04-31)
Copyright Avail: NTIS HC A06/MF A01

A multidimensional quantile of the parameters of a system of a given order is adopted as a reliability function of the system. A lower bound on the multidimensional quantile is obtained in terms of the one-dimensional quantiles, and a relationship is established between the lower bound and the known upper bound of multidimensional probability. The possibility of using this estimate as an optimization function in flight vehicle design is illustrated through numerical modeling. Author

N88-12623# Joint Publications Research Service, Arlington, Va.
OPTIMUM TAKE-OFF RUN OF AIRCRAFT ON GROUND AIRFIELDS Abstract Only c05
A. A. Badyagin *In its* USSR Report: Engineering and Equipment 28 May 1987 p 2 Transl. into ENGLISH from Izvestiya Vysshikh Uchebnykh Zavedeniy: Aviatsionnaya Tekhnika (Kazan, USSR), no. 4, Oct. - Dec. 1985 p 12-16 (For primary document see N88-12621 04-31)
Copyright Avail: NTIS HC A06/MF A01

Conditions under which the most favorable for take off attack angle is small were clarified. It has been alleged by another author that a drawback of this takeoff method was a rather long takeoff run, especially in the case of poor ground. Here, the opposite result was obtained: the more the resistance coefficient of ground (the poorer the ground), the larger are the optimum attack angle and the aircraft lift coefficient during takeoff. It was explained from the physical standpoint by the fact that aerodynamic wing relief not only makes it possible to realize the well known effect

of reducing ground resistance forces, but also to reduce the coefficient of resistance to wheel movement. Author

N88-12624# Joint Publications Research Service, Arlington, Va.
AIRCRAFT DYNAMIC RESPONSE CALCULATION BASED ON DISCRETE-CONTINUAL MODEL Abstract Only c08
M. B. Vakhitov, A. S. Safonov, and I. A. Kuznetsov *In its* USSR Report: Engineering and Equipment 28 May 1987 p 3 Transl. into ENGLISH from Izvestiya Vysshikh Uchebnykh Zavedeniy: Aviatsionnaya Tekhnika (Kazan, USSR), no. 4, Oct. - Dec. 1985 p 16-20 (For primary document see N88-12621 04-31)
Copyright Avail: NTIS HC A06/MF A01

A numerical procedure for the determination of stresses and deformations in cantilevered thin-wall aircraft lifting surfaces under a varying in time load is generalized to take into account the motion of the structure in the aircraft systems as a whole. It was assumed that the aircraft was located in a subsonic compressible flow. Equations of its perturbed motion were derived, only taking into account deformations of its lifting surfaces. External non-stationary aerodynamic loads on deformable lifting surfaces and on a non-deformable aircraft body were determined using the discrete vortex method. The set of equations for deriving parameters of dynamic stress-strain state of aircraft lifting surfaces, of displacements of an aircraft as a whole and of a non-stationary dynamic load consisted of three groups of equations describing the dynamic reaction of the aircraft. Initial conditions for solving these equations are presented. Author

N88-12625# Joint Publications Research Service, Arlington, Va.
EFFECT OF PERMISSIBLE VARIATIONS OF CENTER-OF-GRAVITY LOCATIONS OF CARGO AIRPLANE ON ITS MASS Abstract Only c05
V. P. Gogolin *In its* USSR Report: Engineering and Equipment 28 May 1987 p 4 Transl. into ENGLISH from Izvestiya Vysshikh Uchebnykh Zavedeniy: Aviatsionnaya Tekhnika (Kazan, USSR), no. 4, Oct. - Dec. 1985 p 24-28 (For primary document see N88-12621 04-31)
Copyright Avail: NTIS HC A06/MF A01

In order to meet the requirements for stability and controllability and for the operational range of center of gravity locations, parameters of horizontal tail surfaces that determine the aft and forward limits of center-of-gravity location were chosen. At chosen parameters of the shape of airplane components, the permissible range of variations of operational center-of-gravity locations determined relationships between empennage and wing dimensions. If it is possible to narrow the range of operational center-of-gravity locations by means of design changes that require expenditures of mass (for instance, installing a fuel tank in the tail fin), the problem of determining the maximum permissible value of these expenditures comes up. This problem was solved, based on the concept of coefficients of increase of airplane mass. The derived solution was applied to a hypothetical airplane, similar, as far as its characteristics were concerned, to the TU-134 airplane. Author

N88-12626# Joint Publications Research Service, Arlington, Va.
AIRCRAFT CLASSIFICATION BY TYPE OF PROPULSIVE DEVICES. DETERMINATION OF TYPE AND NUMBER OF CARRYING SOLUTIONS Abstract Only c05
M. A. Guryanov *In its* USSR Report: Engineering and Equipment 28 May 1987 p 5-6 Transl. into ENGLISH from Izvestiya Vysshikh Uchebnykh Zavedeniy: Aviatsionnaya Tekhnika (Kazan, USSR), no. 4, Oct. - Dec. 1985 p 33-39 (For primary document see N88-12621 04-31)
Copyright Avail: NTIS HC A06/MF A01

The objective was to trace qualitative development of aircraft population and to demonstrate that in order to convert this development into a purposeful creative process it is sufficient to derive laws of formation of known kinds and types of aircraft, using the dialectic epistemology method and well studied processes of formation of populations of substances, plants and animals. The proposed method makes it possible to constantly monitor development of aircraft populations and propulsive devices. Author

N88-12627# Joint Publications Research Service, Arlington, Va.
LOCAL-OPTIMAL CONTROL IN SYSTEMS WITH DELAY Abstract Only c08
G. L. Degtyaryov and S. A. Terentyev *In its* USSR Report: Engineering and Equipment 28 May 1987 p 7 Transl. into ENGLISH from Izvestiya Vysshikh Uchebnykh Zavedeniy: Aviatsionnaya Tekhnika (Kazan, USSR), no. 4, Oct. - Dec. 1985 p 39-42 (For primary document see N88-12621 04-31)
Copyright Avail: NTIS HC A06/MF A01

The problem of determining parameters of the control mechanism in aircraft stabilization systems with the delay that develops in measuring and servosystems is one of the most important problems in developing control systems in modern aircraft. Optimum control was sought as a function of current and previous measurements of the state of the system. Results obtained earlier were expanded. Equations for simulating aircraft movement and for optimum control were proposed. An equation of system motion was derived. Based on conditions of local optimality, a set of equations for determination of controller coefficients was derived. Solving the set makes it possible to derive the optimal parameters. Author

N88-12628# Joint Publications Research Service, Arlington, Va.
RENEWED INTEREST IN AIRSHIPS FOR INDUSTRY USE DISCUSSED c02
M. Ariye *In its* USSR Report: Engineering and Equipment 28 May 1987 p 61-62 Transl. into ENGLISH from Stroitelnaya Gazeta (Moscow, USSR), 23 Jan. 1987 p 3 (For primary document see N88-12621 04-31)
Copyright Avail: NTIS HC A06/MF A01

The use and development of airships in the U.S.S.R is discussed. The unique combination of features possessed by these machines (vertical takeoff and landing, large lift capacity, distance and duration of flight, and safety of operation) are noted. The development of a plan for a combined aerostatic airship of a semi-rigid type with a lift capacity of up to 30 tons is discussed. Author

N88-12629# Joint Publications Research Service, Arlington, Va.
MULTIPATH GEAR-FRICTION PLANETARY TRANSMISSIONS Abstract Only c37
L. M. Ivachev *In its* USSR Report: Engineering and Equipment 28 May 1987 p 70-71 Transl. into ENGLISH from Vestnik Mashinostroyeniya (Moscow, USSR), no. 12, Dec. 1986 p 18-21 (For primary document see N88-12621 04-31)
Copyright Avail: NTIS HC A06/MF A01

A new trend has developed, multipath gear-friction planetary transmissions, in which each of the parallel power paths includes friction elements for uniform distribution of torque among all of the power paths and compensation of various errors in manufacture, assembly, operating wear, etc. The number of power paths is significantly increased by placement of satellites around the circumference of the central axis and along the central axis. Author

N88-12630# Joint Publications Research Service, Arlington, Va.
CALCULATION OF THREE-DIMENSIONAL STATIONARY TURBULENT BOUNDARY LAYER ON ROOT SECTION OF WING IGNORING COMPRESSIBILITY Abstract Only c02
G. A. Shchekin *In its* USSR Report: Engineering and Equipment 28 May 1987 p 89 Transl. into ENGLISH from Izvestiya Vysshikh Uchebnykh Zavedeniy: Aviatsionnaya Tekhnika (Kazan, USSR), no. 4, Oct. - Dec. 1985 p 72-76 (For primary document see N88-12621 04-31)
Copyright Avail: NTIS HC A06/MF A01

A method for calculating a three dimensional steady state turbulent boundary layer is proposed. It is based on a general method for calculating three dimensional compressible laminar and turbulent boundary layers on arbitrary wings. Boundary conditions on the surface and on the external boundary of the boundary

layer were formulated. In the transition region, the coefficient of turbulent viscosity increases in direct proportion to the longitudinal coefficient of intermittency. After transformations, the initial set of equations was solved numerically using the Petukhov finite differences method. For solving the set of equations on a computer, a computer program, written in FORTRAN, was written. Components of the local coefficient of friction resistence, projected onto the chord and wing span directions, the displacement of thickness of the three dimensional boundary layer, and the boundary of the separation region were calculated. Expressions for calculating these parameters are presented. Author

N88-12631# Joint Publications Research Service, Arlington, Va.
CALCULATION OF AERODYNAMIC CHARACTERISTICS OF THREE-DIMENSIONAL FINITE SPAN WINGS IN POTENTIAL INCOMPRESSIBLE FLOW Abstract Only c02
S. D. Yermolenko and Ye. A. Ryaguzov *In its* USSR Report: Engineering and Equipment 28 May 1987 p 90 Transl. into ENGLISH from Izvestiya Vysshikh Uchebnykh Zavedeniy: Aviatsionnaya Tekhnika (Kazan, USSR), no. 4, Oct. - Dec. 1985 p 43-48 (For primary document see N88-12621 04-31)
Copyright Avail: NTIS HC A06/MF A01

A simpler and less time consuming method for calculating the aerodynamic characteristics of three dimensional finite span wings in potential incompressible flow is given. It is based on the application of the discrete vortex method which earlier proved to be effective in solving two dimensional problems. A non-separating potential incompressible flow was examined under the assumption that the wing surface was specified, wherein the left hand side of the wing was symmetrical to its right hand side, its leading and trailing edges were straight, and its ends were flat and there was no slippage. Wing profile could vary across the span and had a geometric twist. The method for constructing a vortex model was explained. Intensities of vortices were determined. Formulae for reduced flow velocity and static pressure coefficient in reference points were derived. Examples of pressure distribution in the root, end and mid-sections of thick wings, calculated in accordance with the proposed method and the authors' methods were presented. These results were compared to wind tunnel tests of the wings. Design and experimental data were in good agreement. Author

N88-12632# Joint Publications Research Service, Arlington, Va.
SOME ASYMPTOTIC MODES OF TRANSONIC VORTEX FLOW Abstract Only c02
A. G. Kuzmin *In its* USSR Report: Engineering and Equipment 28 May 1987 p 91 Transl. into ENGLISH from Vestnik Leningradskogo Universiteta, Seriya 1: Matematika, Mekhanika, Astronomiya (Leningrad, USSR), no. 2, Apr. 1986 p 61-65 Original language document was announced in IAA as A87-15553 (For primary document see N88-12621 04-31)
Copyright Avail: NTIS HC A06/MF A01

Steady state plane parallel vortex flows of an ideal gas are investigated analytically. In particular, a study is made of the qualitative flow patterns in the vicinity of a point where the sonic line is orthogonal with respect to the velocity vector and in the vicinity of a point on the sonic line where acceleration is equal to zero. Together with the results of Shifrin (1966), the results obtained here provide information on all possible flow patterns near the point where the sonic line is orthogonal to the velocity vector and demonstrate a large variety of possible flow patterns near the zero acceleration point. Author

N88-12633# Joint Publications Research Service, Arlington, Va.
CONICAL WING WITH MAXIMUM LIFT-TO-DRAG RATIO IN SUPERSONIC GAS FLOW Abstract Only c02
V. I. Lapygin and P. V. Tretyakov *In its* USSR Report: Engineering and Equipment 28 May 1987 p 92 Transl. into ENGLISH from Izvestiya Akademii Nauk SSSR Mekhanika Zhidkosti i Gaza (Moscow, USSR), no. 3, May - Jun. 1986 p 128-133 Original language document was announced in IAA as A87-10615 (For primary document see N88-12621 04-31)
Copyright Avail: NTIS HC A06/MF A01

A theoretical analysis of conical wings at Mach numbers greater than 2 shows that maximum lift-to-drag ratio is possessed by wings with a flat lower surface. Simple analytical relationships are obtained determining the wing aerodynamic characteristics at angles of attack up to the separation of the bow shock from the leading edges. Author

N88-12634# Joint Publications Research Service, Arlington, Va.
EXCITATION OF NATURAL OSCILLATIONS OF A BOUNDARY LAYER BY AN EXTERNAL ACOUSTIC FIELD Abstract Only c34
A. A. Maslov and N. V. Semenov *In its* USSR Report: Engineering and Equipment 28 May 1987 p 92 Transl. into ENGLISH from Izvestiya Akademii Nauk SSSR Mekhanika Zhidkosti i Gaza (Moscow, USSR), no. 3, May - Jun. 1986 p 74-78 Previously announced as X87-71990 (For primary document see N88-12621 04-31)
Copyright Avail: NTIS HC A06/MF A01

Experimental studies of the susceptibility of the supersonic boundary layer to undergo the transition from laminar to turbulent flow were undertaken. It was found that there are areas on the plate of most effective conversion of external acoustic disturbances to natural oscillations of the supersonic boundary layer. The leading edge of the plate, acoustical branch of the neutral curve and lower branch of the curve of neutral stability are such areas. Experiments were performed in a T-325 supersonic wind tunnel with reduced turbulence in a 200 by 200 mm cross-section. Author

N88-12635# Joint Publications Research Service, Arlington, Va.
NUMERICAL STUDY OF SUPERSONIC FLOW AROUND BLUNT BODIES WITH EXTENDED NEEDLE NOSE Abstract Only c02
V. N. Karlovskiy and V. I. Sakharov *In its* USSR Report: Engineering and Equipment 28 May 1987 p 93 Transl. into ENGLISH from Izvestiya Akademii Nauk SSSR Mekhanika Zhidkosti i Gaza (Moscow, USSR), no. 3, May - Jun. 1986 p 119-127 (For primary document see N88-12621 04-31)
Copyright Avail: NTIS HC A06/MF A01

A method was developed for the calculation of supersonic flow of an ideal gas around axisymmetrical blunted bodies with extended needle noses. A study is made of the flow around a truncated cone with a spherical blunted cylindrical needle as a function of the ratio of needle length to diameter of the end portion of the body and Mach number of the incident stream. Several steady flow modes were obtained, including one with circulation zones in the shock layer and internal shock wave. The installation of a needle in advance of the truncated cone can reduce its resistance by 40 to 50 percent. A full study of the change in drag as a function of ratio of needle length is performed for Mach 3. Author

N88-12636# Joint Publications Research Service, Arlington, Va.
DYNAMICS OF REVERSE FLOWS AT PUMP INLET Abstract Only c34
N. S. Yershov *In its* USSR Report: Engineering and Equipment 28 May 1987 p 93 Transl. into ENGLISH from Izvestiya Vysshikh Uchebnykh Zavedeniy: Aviatsionnaya Tekhnika (Kazan, USSR), no. 4, Oct. - Dec. 1985 p 49-53 (For primary document see N88-12621 04-31)
Copyright Avail: NTIS HC A06/MF A01

Under stationary conditions, due to the effect of cavitation on the aerodynamics between the blading and the flow, the length of the zone of reverse flows decreases and the field of velocities in each section is distorted. The boundary of reverse flows is a place where the reverse flow and an unperturbed flow meet at the inlet pipe wall. An equation was derived that gives a mathematical description of a phenomenon which was observed in the case of self-excited oscillations, when at a certain stage of the process the length of the reverse flows increases. This phenomenon was in contradiction with earlier conceptions. The derived equations could be used for construction of a pump operating with reverse flows. Author

N88-12637# Joint Publications Research Service, Arlington, Va.
SOLUTION OF GEOMETRICALLY NONLINEAR PROBLEM FOR REINFORCED SHELL OF REVOLUTION HAVING ARBITRARY SHAPE Abstract Only **c39**
V. V. Kuzmin *In its* USSR Report: Engineering and Equipment 28 May 1987 p 95 Transl. into ENGLISH from Izvestiya Vysshikh Uchebnykh Zavedeniy: Aviatsionnaya Tekhnika (Kazan, USSR), no. 4, Oct. - Dec. 1985 p 53-59 Original language document was announced in IAA as A86-35987 (For primary document see N88-12621 04-31)
Copyright Avail: NTIS HC A06/MF A01

A discrete energy method for solving geometrically nonlinear problems has been developed which employs a coupled gradient method with restoration and analytical determination of the gradient components of the function being minimized. The model used for solving the axisymmetric problem for a reinforced shell of revolution closely approximates real shell structures and their loading. As an example, results are presented for a hinged smooth cylindrical titanium shell under compression. Author

N88-12638# Joint Publications Research Service, Arlington, Va.
RATIONAL REINFORCEMENT OF CYLINDRICAL SHELLS WITH VARIABLE STIFFNESS FRAMES SUBJECTED TO EXTERNAL PRESSURE Abstract Only **c39**
A. S. Gorbatov and Yu. M. Pochtman *In its* USSR Report: Engineering and Equipment 28 May 1987 p 96 Transl. into ENGLISH from Izvestiya Vysshikh Uchebnykh Zavedeniy: Aviatsionnaya Tekhnika (Kazan, USSR), no. 4, Oct. - Dec. 1985 p 29-33 Original language document was announced in IAA as A86-35982 (For primary document see N88-12621 04-31)
Copyright Avail: NTIS HC A06/MF A01

A mathematical model for the weight optimization of reinforced cylindrical shells is developed with allowance for the moment nature of the subcritical state and the discrete nature of the reinforcement. The resulting nonlinear programming problem is solved on a computer using a random search method. Recommendations are given concerning the use of the results in shell design. Author

N88-12639# Joint Publications Research Service, Arlington, Va.
FINITE DEFORMATIONS OF SHELL WITH RIGID INCLUSION Abstract Only **c39**
B. A. Antufyev *In its* USSR Report: Engineering and Equipment 28 May 1987 p 97 Transl. into ENGLISH from Izvestiya Vysshikh Uchebnykh Zavedeniy: Aviatsionnaya Tekhnika (Kazan, USSR), no. 4, Oct. - Dec. 1985 p 3-7 (For primary document see N88-12621 04-31)
Copyright Avail: NTIS HC A06/MF A01

An approximate solution of the problem of deformation of a radially loaded flexible shell with non-negative Gaussian curvature that has a rigid inclusion of an arbitrary shape was sought. A sloping, rectangular at the top view model of a shell panel, reinforced by means of a rigid inclusion, was examined. The system was loaded with a distributed normal load. Nonlinear deformation of the panel were described by equations of the theory of flexible sloping shells. Displacements of the rigid inclusions were determined by the shift and angles of rotation relative to the coordinate axes. The problem was reduced to a set of equations consisting of two nonlinear differential equations of a flexible shell, three integral inclusion equilibrium equations and two shell and inclusion compatibility equations. The unknown quantities were normal displacements, the shell stress function, two interaction reactions and three constants. The set of nonlinear equations was solved using the successive approximation method and the Bubnov method, thus reducing the problem to solving linear algebraic equations. The process of solving nonlinear equations as a sequence of linear problems was repeated until solutions of two successive approximations coincided with a given degree of accuracy. Author

N88-12640# Joint Publications Research Service, Arlington, Va.
FATIGUE FAILURE OF THIN POROUS STRIPS **c39**
G. G. Gugunishvili, G. V. Kiziriya, and L. I. Rozentur *In its* USSR Report: Engineering and Equipment 28 May 1987 p 98-100 Transl. into ENGLISH from Soobshcheniya Akademii Nauk Gruzinskoy SSR (Tbilisi, USSR), v. 124, no. 1, Oct. 1986 p 49-51 (For primary document see N88-12621 04-31)
Copyright Avail: NTIS HC A06/MF A01

This work is devoted to researching the fatigue failure of thin (about 0.0001 meters) porous plates depending on the number of cycles needed for the specimen to fail, the plate's geometric dimensions, and the amount of stress applied. The specimens were thin drawn strips of bands obtained from the rolling of mixtures consisting of PNK-1 powered nickel and finely ground Ni(NO sub 3) sub 2 6H sub 2 O salt in a ratio of 9:1 with subsequent sintering in a hydrogen atmosphere for one hour at a temperature of 1023 degrees Kelvin. The longitudinal axis of the specimen coincided with the direction of the band rolling. One end of the strip was fastened and the other was deflected measurably in both directions. Author

N88-12641# Joint Publications Research Service, Arlington, Va.
OPTIMAL RIBBING OF LONG PLATE MADE OF COMPOSITE MATERIAL **c39**
E. V. Belubekyan and A. Z. Darbinyan *In its* USSR Report: Engineering and Equipment 28 May 1987 p 101-105 Transl. into ENGLISH from Doklady Akademii Nauk Armyanskoy SSR (Yerevan, USSR), v. 82, no. 5, 1986 p 214-217 (For primary document see N88-12621 04-31)
Copyright Avail: NTIS HC A06/MF A01

A long rectangular plate strengthened by means of equidistant stiffening ribs, hinged along the edges and subjected to transverse pressure is discussed. The construction is of monolayers of a composite fibrous material placed at an angle to the axis in the plates between ribs and along the axis of the ribs. Author

N88-12642 British Petroleum Co. Ltd., Sunbury-on-Thames (England).
PROCESS FOR PRODUCING SANDWICH MOULDINGS Patent Application
Peter Stewart Allan, inventor and Michael John Bevis, inventor 20 Aug. 1986 10 p Filed 11 Feb. 1986 Priority 13 Feb. 1985 GB 8503695
(EP-Patent-0-191-623-A2; EP-Patent-Appl-SN-86300904.9; Int-Patent-Class-B29C-45/16; Int-Patent-Class-B29C-45/57; Int-Patent-Class-B29C-37/00; ETN-87-90720) Avail: UK Patent Office, 25 Southampton Buildings, London WC2A 1A4, United Kingdom

A process is described for producing sandwich molding comprised of the sequential introduction into a mold a first material capable of forming the surface layer or skin of the sandwich molding followed by a second material capable of forming the core of the sandwich molding. After filling the mold, an oscillating pressure is applied to the material in the mold at least during the initial cooling of the melt and concurrently therewith additional thermoplastic material is introduced into the mold. ESA

N88-12643# Lawrence Livermore National Lab., Calif.
INTERACTIONS BETWEEN SCIENCE AND PRECISION ENGINEERING
D. P. Atkinson, E. R. McClure, and T. T. Saito Nov. 1987 10 p Presented at the International Conference on Precision Engineering, Osaka, Japan, 1 Nov. 1987
(Contract W-7405-eng-48)
(DE87-010873; UCRL-96700; CONF-871134-1) Avail: NTIS HC A02

The history of scientific progress is intertwined intimately with precision engineering. Precision engineering and science have synergistically interacted in stimulating each other to significant advances. Furthermore, tangible benefits to the quality of human life, through often unexpected industrial applications, occur. High energy lasers, astrophysical telescopes, and anamorphic optics, along with developments in ultraprecision machining and measurement, are discussed as examples of evolution in science and precision engineering. Possibilities for ultimate by-products for mankind's welfare are explored. DOE

N88-12644# Army Materials Technology Lab., Watertown, Mass.

WORK-IN-PROGRESS PRESENTED AT THE ARMY SYMPOSIUM ON SOLID MECHANICS, 1986: LIGHTENING OF THE FORCE Final Report

Oct. 1986 62 p Symposium held at West Point, N.Y., 7-9 Oct. 1986

(AD-A184791; MTL-MS-86-3) Avail: NTIS HC A04/MF A01 CSCL 20K

This document contains the extended abstracts of works in progress selected for presentation at the symposium. The theme lightening of the force represents a major Army priority in order to enhance both fighting capability on the battlefield and the capability for rapid deployment of fighting forces to remote locations. Some representative titles include: Computed neutron tomography and coded aperture holography from real time neutron images; Spatial strength variation and statistical size of laminated orthotropic composite materials; Plastic strain localization between voids in shear deformation fields; and Durability of powdered aluminum structures. For individual titles, see N88-12645 through N88-12655.

N88-12645# Virginia Univ., Charlottesville.

COMPUTED NEUTRON TOMOGRAPHY AND CODED APERTURE HOLOGRAPHY FROM REAL TIME NEUTRON IMAGES **c72**

Mark F. Sulcoski *In* Army Materials Technology Lab., Work-in-Progress Presented at the Army Symposium on Solid Mechanics, 1986: Lightening of the Force Oct. 1986 p 1-2 (For primary document see N88-12644 04-31)

Avail: NTIS HC A04/MF A01 CSCL 20H

The uses of neutron tomography and holography for nondestructive evaluation applications are developed and investigated. The use of a real time neutron imaging system coupled with a image processing system to obtain neutron tomographs. Experiments utilized a Thomson-CSF neutron camera coupled to a computer based system used for image processing. Experiments included a configuration of a reactor neutron beam port for neutron imaging, development and implementation of a convolution method tomographic algorithm suitable for neutron imaging. Results to date have demonstrated the proof of principle of this neutron tomography system. Coded aperture neutron holography is under investigation using a cadmium Fresnel zone plate as the coded aperture and the real time imaging system as the detection and holographic reconstruction system. Coded aperture imaging utilizes the zone place to encode scattered radiation pattern recorded at the detector is used as input data to a convolution algorithm which reconstructs the scattering source. This technique has not yet been successfully implemented and is still under development. Author

N88-12646# Columbia Univ., New York, N.Y. Dept. of Civil Engineering and Engineering Mechanics.

SPATIAL STRENGTH VARIATION AND STATISTICAL SIZE EFFECT OF LAMINATED ORTHOTROPIC COMPOSITE MATERIALS **c24**

Elias Samaras and Masanobu Shinozuka *In* Army Materials Technology Lab., Work-in-Progress Presented at the Army Symposium on Solid Mechanics, 1986: Lightening of the Force Oct. 1986 p 3-5 (For primary document see N88-12644 04-31)

Avail: NTIS HC A04/MF A01 CSCL 11D

Emphasis is placed on the probabilistic model for spatial variation of material strength and on the corresponding statistical size effect. The material strength can be idealized as a multidimensional random field. This interpretation together with the recently developed method of digital simulation of multidimensional random fields by use of ARMA models makes it possible to demonstrate the statistical size effect in terms of numerical examples. The ARMA model method uses a recursive equation whose coefficient matrices are determined in accordance with the prescribed autocorrelation function of the multidimensional random field. Using the recursive equation with these coefficient matrices sample functions of the field are generated over a large 2 or 3 dimensional domain. An alternative method for the digital simulation of multidimensional random fields is the Fast Fourier Transform method. Author

N88-12647# Honeywell, Inc., Edina, Minn. Defense Systems Div.

A DIRECT METHOD TO OBTAIN CONSTITUTIVE MODEL CONSTANTS FROM CYLINDER IMPACT TEST RESULTS **c39**

Tim J. Holmquist and Gordon R. Johnson *In* Army Materials Technology Lab., Work-in-Progress Presented at the Army Symposium on Solid Mechanics, 1986: Lightening of the Force Oct. 1986 p 7-11 (For primary document see N88-12644 04-31)

Avail: NTIS HC A04/MF A01 CSCL 20K

Since the cylinder impact test was introduced, the merits of the test have been debated. Some argue that this test should not be used to obtain constitutive data because a wide range of unknown strains, strain rates, temperatures, and stresses vary throughout the test specimen, and throughout the duration of the test. Other argue that dynamic tension, compression, and/or torsion tests require expensive test facilities and that these tests are limited in their ability to achieve the range of strains and strain rates of interest. An explicit method (as opposed to previous trial and error methods) was developed to obtain constants for computational constitutive models. The method consists of applying a given equation in an iterative manner until a satisfactory set of constants is attained. It is demonstrated that it is possible to directly obtain constitutive model constants from cylinder impact test results. Author

N88-12648# Army Materials Technology Lab., Watertown, Mass.

PLASTIC STRAIN LOCALIZATION BETWEEN VOIDS IN SHEAR DEFORMATION FIELDS **c39**

D. H. Tracey, C. E. Freese, and P. J. Perrone *In its* Work-in-Progress Presented at the Army Symposium on Solid Mechanics, 1986: Lightening of the Force Oct. 1986 p 13-21 (For primary document see N88-12644 04-31)

Avail: NTIS HC A04/MF A01 CSCL 20K

Metallographic studies have shown that crack propagation occurs by a plastic shear instability mechanism in high strength martensitic alloy steels. This study was conducted in support of an alloy development program attempting to produce an ultra-high strength steel alloy with fracture toughness sufficiently high to allow a wide range of structural applications. A quantitative understanding was established of the void softening mechanism in shear. The key to understanding how microscopic voids deteriorate a plastically deforming metal is knowledge of the void region stress/strain elevation over the uniform levels that would exist in the absence of voids. A set of elastic plastic finite element analyses were conducted to establish the local field between a pair of voids close enough to produce significant interactions. The analyses were conducted using an elastic plastic finite element formulation for nonhardening Prandtl-Reuss constitutive theory. The plasticity results for the test cases studied are consistent with experimental observations of void sheet development in shear and void growth in tension. Author

N88-12649# Little (Arthur D.), Inc., Cambridge, Mass.

A STUDY OF THE CRACK TIP PARAMETERS THAT GOVERN ENVIRONMENTALLY ASSISTED CRACKING BY USE OF THE RISING DISPLACEMENT TEST **c39**

R. Mayville, T. Warren, and P. Hilton *In* Army Materials Technology Lab., Work-in-Progress Presented at the Army Symposium on Solid Mechanics, 1986: Lightening of the Force Oct. 1986 p 23-26 (For primary document see N88-12644 04-31)

Avail: NTIS HC A04/MF A01 CSCL 20K

There is an increasing interest in the use of rising displacement or load tests, similar to K-R or J-R resistance curve tests, to characterize environmentally assisted cracking (EAC) in metal environment systems. This was a study of the effect a wide range of applied displacement rates has on EAC for AISI 4340 with sigma sub 0 to 1095 MPa (159 ksi) in flowing synthetic seawater. Cantilever beam (constant load) tests were performed to obtain K

sub IEAC to 98 MPa. Rising displacement tests were performed over 4 orders of magnitude with 25 mm thick compact tension specimens under ambient conditions and in environment to generate J-R curves and to determine crack velocities. Under ambient conditions the 4340 exhibits substantial stable tearing. In environment, the J-R curves were identical to the ambient J-R curve except for the slowest test, which lasted over a week. Two experiments were also performed in environment in which displacement was held constant after some stable crack extension had occurred. The crack velocities from these and the other compact tension tests are plotted against K sub I. Author

N88-12650# Army Materials Technology Lab., Watertown, Mass.

EXPLICIT AND IMPLICIT SOIL MODELLING FOR DYNAMIC SOIL-STRUCTURE INTERACTION PROBLEMS

Aaron DasGupta *In its* Work-in-Progress persented at the Army Symposium on Solid Mechanics, 1986: Lightening of the Force Oct. 1986 p 27-28 (For primary document see N88-12644 04-31)

Avail: NTIS HC A04/MF A01 CSCL 13B

Increased application of nonlinear viscoelastic materials in structures and consideration of operating environments require modeling of interaction of such structures with the surrounding soil medium which significantly influences the dynamic response when subjected to an impulse or blast overpressure loading. The need is accentuated by the rapid advances in numerical modeling of dynamic problems using either finite difference or finite element techniques of structural analysis. An explicit modeling technique is recommended whereby a few layers of soil surrounding the base of the structure are modeled as an assembly of elements in contact with the structure. The interfacing contact elements for both structure and soil are allowed to stick, slide or separate from each other to simulate the appropriate boundary conditions. The explicit modeling technique using a finite element code requires characterization of constitutive relationship of geological materials from shock compression behavior of such materials and their Hugoniot characteristics. The characterization technique used here is currently restricted to materials with linear Hugoniot characteristics at all pressure ranges. Author

N88-12651# Ballistic Research Labs., Aberdeen Proving Ground, Md.

COMPOSITE MATERIALS APPLICATIONS PROGRAM AT THE US ARMY BALLISTIC RESEARCH LABORATORY: WORK IN PROGRESS **c24**

Richard B. Murray, Edward M. Patton, Larry W. Burton, and Robert P. Kaste *In* Army Materials Technology Lab., Work-in-Progress Presented at the Army Symposium on Solid Mechanics, 1986: Lightening of the Force Oct. 1986 p 29-31 (For primary document see N88-12644 04-31)

Avail: NTIS HC A04/MF A01 CSCL 11D

The Army is provided design techniques and prediction methodologies specifically aimed at the problems peculiar to using composite materials in Army systems. These problems include high rates of loading, including ballistic loadings and blast loadings; high and low cycle fatigue; corrosion and erosion resistance; and the necessity to predict structural response of thick sections to all loading environments. Three aspects of composite material behavior were selected as the most critical predictive techniques for composite materials. They are: structural response to high rates of loading, predicting structural response of thick sections of laid-up laminated structures, and failure criteria for thick laminates. The work in progress in these three critical areas is discussed. Author

N88-12652# Army Materials Technology Lab., Watertown, Mass.

EFFECTIVE TREATMENT OF MEMBRANE AND SHEAR LOCKING PHENOMENA IN CURVED SHEAR-DEFORMABLE AXISYMMETRIC SHELL ELEMENT **c39**

A. Tessler and L. Spiridigliozzi *In its* Work-in-Progress Presented at the Army Symposium on Solid Mechanics, 1986: Lightening of the Force Oct. 1986 p 33-35 (For primary document see N88-12644 04-31)

Avail: NTIS HC A04/MF A01 CSCL 20K

Wide varieties of structural shells exhibit geometric and material symmetry. As such, they are best modeled by appropriate shell of revolution finite elements which are usually one dimensional. Design requirements for thin and moderately thick shells and in particular those made of laminated organic composite materials necessitate accurate modeling of the shell geometry and proper account of the effects due to shear deformation and rotary inertia. A difficulty intrinsic to shear deformable bending elements is due to a mathematical deficiency called shear locking. A simple effective 2 node, displacement type, axisymmetric shell element derived from Naghdi's refined shell theory with the aid of the Marguerre shallowness equation is presented. The anisoparametric kinematic approximations is adopted which employ different degree polynomials for the kinematic variabes. Owing to these approximations, both the membrane and shear strains, which serve as penalty constraints in the thin element regime, possess admissible penalty modes. Only the axisymmetric response of linearly elastic isotopic shells is considered. The main features of the 2 node, 6 deg of freedom shell element are summarized and discussed. Author

N88-12653# Kaman Sciences Corp., Colorado Springs, Colo.

ANALYSIS AND TESTING OF PREDAMAGED SHELL STRUCTURES **c39**

Richard E. Keeffe and Eric Reece (Sandia National Labs., Albuquerque, N. Mex.) *In* Army Materials Technology Lab., Work-in-Progress Presented at the Army Symposium on Solid Mechanics, 1986: Lightening of the Force Oct. 1986 p 41-43 (For primary document see N88-12644 04-31)

(Contract DASG60-85-C-0051)

Avail: NTIS HC A04/MF A01 CSCL 20K

A predamaged shell structure may undergo a reduction in load carrying capacity, dependent upon the location, size, and shape of the damaged area. Analytic and experimental methods for evaluation of these effects are investigated. Of primary concern are thin walled cylindrical and conical shell frustra which have locally damaged areas. Three basic loading conditions are of interest: (1) axial tension; (2) axial compression; and (3) lateral bending. The basic analysis tool being considered for these studies involves application of the nonlinear finite element code ABAQUS. The code capabilities include static and dynamic modeling of solid, beam, and shell elements, and provides accurate modeling for arbitrary magnitudes of displacement, rotation, and strain. Preliminary test of the applicability of the ABAQUS formulation was applied to tension and compression test results obtained on 6061-T6 seamless aluminum cylinders. Author

N88-12654# Transportation Systems Center, Cambridge, Mass. Structures and Dynamics Div.

CORROSION CONTROL BY COMPOSITE MATERIAL SUBSTITUTION WITH APPLICATION TO THE M-939 5-TON TRUCK **c24**

Tong Pin *In* Army Materials Technology Lab., Work-in-Progress Presented at the Army Symposium on Solid Mechanics, 1986: Lightening of the Force Oct. 1986 p 45-47 (For primary document see N88-12644 04-31)

Avail: NTIS HC A04/MF A01 CSCL 11D

In an effort to improve the corrosion resistance of a 5 ton truck and to lighten its weight, the Army is evaluating the replacement of structural components which have high potential for environmental deterioration with equivalent composite components. Several graphite epoxy chassis were designed and fabricated to match the strength and stiffness characteristics of steel chassis and to weight about 50 percent less. The prototype chassis was evaluated both as fabricated and as installed in the truck for corrosion resistance, structural integrity, and damage tolerance. Of interest is the sensitivity of the composite frame mechanical details to stress concentrations, fracture, shock and vibration and environmentally produced degradation particularly from moisture and abrasion. The method of evaluation involves

identifying stress sensitive locations, characterizing static strength and dynamic flexibility of the composite frame, and evaluating the in service stresses. Author

N88-12655# Air Force Wright Aeronautical Labs., Wright-Patterson AFB, Ohio.
DURABILITY OF POWDERED ALUMINUM STRUCTURES c26
Karen Severyna and Margery Artley *In* Army Materials Technology Lab., Work-in-Progress Presented at the Army Symposium on Solid Mechanics, 1986: Lightening of the Force Oct. 1986 p 49-52 (For primary document see N88-12644 04-31)
Avail: NTIS HC A04/MF A01 CSCL 11F

Many high strength, low density powdered metals are being developed for aerospace applications. Powdered metallurgy (P/M) offers significant improvements in material properties over ingot metallurgy (I/M). Properties of P/M alloys are promising greater load carrying capability and/or reduced weight in high stress, fracture critical airframe applications. This research program investigates the characteristic properties of extruded bar stock of a first generation high strength P/M aluminum. Four tensile tests were administered to determine the mechanical properties, along with 94 fatigue crack growth tests of constant and variable amplitudes load histories. The results of tests are presented and discussed. Author

N88-12656# California Univ., Berkeley. Lawrence Berkeley Lab.
STUDIES ON HIGH-SPEED ELECTROFORMING Ph.D. Thesis
D. P. Barkey Aug. 1987 163 p
(Contract DE-AC03-76SF-00098)
(DE88-001395; LBL-23880) Avail: NTIS HC A08/MF A01

Studies on high-speed electroforming were undertaken to evaluate the potential for electroforming at rates comparable to those of mechanical forming. A rotating cylindrical cathode was used to provide intense turbulent convective transport. Transport in the cylindrical cell equipped with radial baffles was characterized by direct measurement of limiting currents of high rate copper deposition. Copper electroforms of thicknesses of several hundred micrometers were produced by deposition at rates of up to 7.5 A/sq cm corresponding to 160 microns per minute. A quantitative theory of morphological stability, accounting for transport, kinetic and ohmic effects, was formulated for copper deposition at high rates. Surfaces of deposits produced in the electroforming experiments were characterized by surface profilometry, and digitalized profiles were analyzed by Fourier transform for comparison with predictions of the stability theory. Decrease in roughness protrusion spacing with both increasing current density and increasing fraction of limiting current is correctly predicted. Differences between expected and observed roughness characteristics are attributed to constraints on protrusion size and spacing imposed by nucleation of growths sites. DOE

N88-12657# Toronto Univ. (Ontario). Inst. for Aerospace Studies.
IDEAL-VISCOPLASTIC EXTRUSION MODEL WITH APPLICATION TO DEFORMING PISTONS IN LIGHT-GAS GUNS
C. P. T. Groth, J. J. Gottlieb, and C. Bourget Nov. 1987 109 p
(UTIAS-TN-266; ISSN-0082-5263) Avail: NTIS HC A06/MF A01

An approximate, one-dimensional, ideal viscoplastic model of the axisymmetric extrusion process through rigid circular-cross section channels is presented. The ideal viscoplastic model incorporates the fundamental effects associated with the physical phenomenon of inertia, plastic deformation, strain-rate behavior, and surface friction. By using the Bingham body constitutive relations, employing quasi-steady kinematically-admissible approximations to actual flow fields, and making various relevant simple first-order approximations for small area gradients, this semi-analytic, one-dimensional, extrusion model can be used to quite quickly solve the flows of extruding, incompressible, solid materials without resorting to often complex two and three dimensional numerical solution procedures. The ideal viscoplastic model is applied to a number of different extrusion problems and the model's predictions of the various components of the velocity and stress fields, as well as the combined forces acting on the extruding material, compare very favorably with other experimental and finite element method results. Although the ideal viscoplastic extrusion model is shown to have certain limitations, this analysis appears to be a powerful and economical tool for the solution of many different problems related to extrusion processes such as wire drawing, rod extrusion, and piston deformation in light-gas guns. Author

N88-12658# Pittsburgh Univ., Pa. Dept. of Chemical and Petroleum Engineering.
PIPE AND BEND EROSION BY PNEUMATIC TRANSPORT OF SOLIDS AT HIGH TEMPERATURE Quarterly Report, Mar. - Jun. 1987
G. E. Klinzing 1987 5 p
(Contract DE-FG22-85PC-80524)
(DE88-001345; DOE/PC-80524/T8) Avail: NTIS HC A02/MF A01

The test series using slag as erodent have begun. Special attention is given to the effect of temperature on the erosion rates. Three tests runs have been completed. DOE

N88-12659# Department of Energy, Washington, D. C. Office of Basic Energy Sciences.
MATERIALS SCIENCES PROGRAMS: FISCAL YEAR 1987
Sep. 1987 297 p
(DE88-000672; DOE/ER-0348) Avail: NTIS HC A13/MF A01

Purpose of this report is to provide a convenient compilation and index of the DOE Materials Sciences Division programs. This compilation is primarily intended for use by administrators, managers, and scientists to help coordinate research. The report is divided into seven sections. Section A contains all Laboratory projects, Section B has all contract research projects, Section C has projects funded under the Small Business Innovation Research Program, Sections D and E have information on DOE collaborative research centers, gives distribution of funding, and Section G has various indexes. DOE

N88-12660# Argonne National Lab., Ill.
PROCEEDINGS OF THE FIFTH SYMPOSIUM ON ENERGY ENGINEERING SCIENCES: INSTRUMENTATION, DIAGNOSTICS, AND MATERIAL BEHAVIOR
Jun. 1987 271 p Symposium held in Argonne, Ill., 17 Jun. 1987
(Contract W-31-109-eng-38)
(DE88-001479; CONF-8706187) Avail: NTIS HC A12/MF A01

Separate abstracts were prepared for the individual papers in this report on the Proceedings of the 5th Symposium on Energy Engineering Sciences. DOE

N88-12521*# National Bureau of Standards, Gaithersburg, Md. Center for Fire Research.
TECHNIQUES FOR FIRE DETECTION
Richard W. Bukowski *In* NASA, Lewis Research Center, Spacecraft Fire Safety 1987 p 9-29 (For primary document see N88-12520 04-16)
Avail: NTIS HC A07/MF A01 CSCL 22B

N88-12522*# National Bureau of Standards, Washington, D.C. Center for Fire Research.
FIRE-RELATED STANDARDS AND TESTING
Vytenis Babrauskas *In* NASA, Lewis Research Center, Spacecraft Fire Safety 1987 p 31-41 (For primary document see N88-12520 04-16)
Avail: NTIS HC A07/MF A01 CSCL 22B

N88-12690*# Jet Propulsion Lab., California Inst. of Tech., Pasadena.
A COLD EJECTOR FOR CLOSED-CYCLE HELIUM REFRIGERATORS
D. L. Johnson and D. L. Daggett (San Jose State Univ., Calif.) *In its* The Telecommunications and Data Acquisition Report

15 Nov. 1987 p 102-111 (For primary document see N88-12679 04-32)
Avail: NTIS HC A15/MF A01 CSCL 13B

N88-12709*# Jet Propulsion Lab., California Inst. of Tech., Pasadena.
TWO-WATT, 4-KELVIN CLOSED CYCLE REFRIGERATOR PERFORMANCE
M. Britcliffe *In its* The Telecommunications and Data Acquisition Report 15 Nov. 1987 p 312-317 (For primary document see N88-12679 04-32)
Avail: NTIS HC A15/MF A01 CSCL 13B

32 COMMUNICATIONS AND RADAR

Includes radar; land and global communications; communications theory; and optical communications.

For related information see also *04 Aircraft Communications and Navigation* and *17 Space Communications, Spacecraft Communications, Command and Tracking.* For search and rescue see *03 Air Transportation and Safety,* and *16 Space Transportation.*

N88-12661# Technische Hogeschool, Delft (Netherlands). Afdeling der Elektrotechniek.
PROGRAMMABLE REAL-TIME DIGITAL VIDEO IMAGE PROCESSING
G. Kirana Nov. 1985 131 p
(PB87-104162; Rept-1985-20) Avail: NTIS HC E06/MF E01 CSCL 17B

The possibility of developing a relatively small image processing system for video signals is described. With this system video images can be manipulated in real-time. The manipulation includes: image expansion, image compression, multi-pictures, and mirror effects. In fact the picture can be controlled down to manipulation of any given picture element (pixel), so that virtually any visual effect becomes possible. To process pictorial information, images usually are digitized into large arrays of picture elements, which require large computer memories for storage and long computer time for processing. Different possibilities of parallel microprocessor configurations are considered, before the best architecture design is chosen. This system architecture is then implemented in hardware and software. It is based on a microprogram and pipeline architecture design. GRA

N88-12662# National Telecommunications and Information Administration, Boulder, Colo. Inst. for Telecommunication Sciences.
GENERAL THEORY OF RADIO PROPAGATION THROUGH A STRATIFIED ATMOSPHERE
G. Hufford Jul. 1987 39 p
(PB87-226197; NTIA-87-219) Avail: NTIS HC A03/MF A01 CSCL 20N

When wave propagation through a stratified atmosphere is formulated in operator theoretic terms, it becomes evident that the problem does not follow the guide of the usual examples of mathematical physics. Nevertheless, such a formulation is useful to reveal why many of the usual procedures are valid and where they may be deficient. In particular, even if the refractivity profile is merely required to belong to a general class of perhaps badly discontinuous functions, the problem always has a well-behaved solution that may be subjected to a modal analysis. On the other hand, the resulting mode series converges neither rapidly nor uniformly, and, as the asymptotic behavior of the modes shows, one is advised to use that series with caution. GRA

N88-12663# Newcastle-upon-Tyne Univ. (England). Computing Lab.
MULTICAST GATEWAY DESIGN CONSIDERATIONS
F. L. Hughes [1987] 19 p
(PB87-219960; NTU-CL/TRS-231) Avail: NTIS HC E03/MF E03 CSCL 17B

Several of the problems associated with multicast communications between netwoks are examined. As part of the study, some of the different kinds of multicast gateways that have been described in the literature over the past several years are discussed. In addition, a particular type of multicast gateway developed at the Computing Laboratory is discussed in detail. Finally, some of the different benefits of the different designs are considered. Author

N88-12664# National Physical Lab., Teddington (England). Div. of Information Technology and Computing.
INPUT DEVICES FOR TASKS USING INTERACTIVE VIDEO
C. Thomas and S. Milan [1987] 38 p
(PB87-220018; NPL-DITC-87/87) Copyright Avail: NTIS HC E04/MF E04 CSCL 17B

Two experiments and a literature review were carried out in an attempt to discover the optimum devices needed to enter information into a computer when using interactive video in a variety of contexts. In both the experiments, novice and expert subjects performed different types of tasks using a number of different devices. The tasks were object manipulation, large area selection, small area selection, artwork, and menu selection. The devices compared were the mouse, touchscreen, cursor keys, and concept keyboard. The touch methods seemed to be the best devices for most of the tasks. There were also differences in performance and preference between novices and experts. The second experiment was carried out in an attempt to refine and validate the findings of the first. Author

N88-12665# Los Alamos National Lab., N. Mex.
PARTICLE INJECTION AND COSMIC RAY ACCELERATION AT COLLISIONLESS PARALLEL SHOCKS
K. B. Quest 1987 24 p Presented at the 6th Meeting of Solar Wind, Estes Park, Colo., 24 Aug. 1987
(Contract W-7405-eng-36)
(DE88-000507; LA-UR-87-2977; CONF-8708141-1) Avail: NTIS HC A03/MF A01

The structure of collisionless parallel shocks is studied using one-dimensional hybrid simulations, with emphasis on particle injection into the first-order Fermi acceleration process. It is argued that for sufficiently high Mach number shocks, and in the absence of wave turbulence, the fluid firehose marginal stability condition will be exceeded at the interface between the upstream, unshocked, plasma and the heated plasma downstream. As a consequence, nonlinear, low-frequency, electromagnetic waves are generated and act to slow the plasma and provide dissipation for the shock. It is shown that large amplitude waves at the shock ramp scatter a small fraction of the upstream ions back into the upstream medium. These ions, in turn, resonantly generate the electromagnetic waves that are swept back into the shock. As these waves propagate through the shock they are compressed and amplified, allowing them to non-resonantly scatter the bulk of the plasma. Moreover, the compressed waves back-scatter a small fraction of the upstream ions, maintaining the shock structure in a quasi-steady state. The back-scattered ions are accelerated during the wave generation process to 2 to 4 times the ram energy and provide a likely seed population for cosmic rays. DOE

N88-12666# Ohio State Univ., Columbus. Electroscience Lab.
ON M-ARY SEQUENTIAL HYPOTHESES TESTING FOR THE CLASSIFICATION OF RADAR SIGNALS
Ismail Jouny and F. D. Garber Jul. 1987 99 p
(Contract N00014-85-K-0321)
(AD-A184094; ESL-717220-4) Avail: NTIS HC A05/MF A01 CSCL 17I

This report is concerned with the performance of M-ARY sequential hypothesis tests applied to the classification of radar signals. In the first part of this report, several available M-ARY sequential algorithms are considered. These include the algorithms due to Reed, Armitage and Palmer. Modifications of the existing algorithm are considered and their effects on the average number of required measurements and the resulting error performance are examined. Three other techniques are also proposed, a tree

algorithm and a sequential maximum a posteriori test as well as a sequential version of the various algorithms by means of Monte-Carlo simulations of the radar signal observations. The performance of these techniques is compared and the relative merits of each algorithm are discussed. GRA

N88-12667# Naval Surface Weapons Center, Silver Spring, Md.
AUTOMATED MICROWAVE DIELECTRIC CONSTANT MEASUREMENT Technical Progress Report, Feb. 1985 - Jan. 1986
Brian C. Glancy and Albert Krall 9 Mar. 1987 40 p
(AD-A184182; NSWC/TR-86-46) Avail: NTIS HC A03/MF A01 CSCL 14B

The tedious and often difficult measurement of dielectric constants as a function of microwave frequency has been simplified using an automated testing apparatus. This automated procedure is based on the use of a slotted line to take measurements. It also includes the automatic application of a numeric solution to a transcendental equation to determine the dielectric constant. The computer program for automation of data acquisition and the overall experimental setup are fully discussed. Experimental data taken using this apparatus are presented in graphic form for porous beds of inerts (including aluminized inerts) and explosives. An equation previously derived in the literature, describing the variation of dielectric constant with density, is used to fit the data. Also, additional applications of this automated apparatus are proposed including the use of this system, and the equation describing the variation of dielectric material mixtures, to estimate the dielectric constant of conductive materials. GRA

N88-12668# George Mason Univ., Fairfax, Va. Dept. of Operations Research and Applied Statistics.
HETEROGENEOUS MULTI-TRUNKING QUEUEING SYSTEMS
Martin J. Fischer and Carl M. Harris Sep. 1987 29 p
(Contract N00014-86-K-0029)
(AD-A184255; GMU/22461/103) Avail: NTIS HC A03/MF A01 CSCL 17B

In a packet switched network, several types of transmission may connect a pair of nodes of the network. The delay characteristics of each type of transmission may be significantly different and so a single queue to the node pair operating under a first-come, first-served rule may not be best. This paper develops both exact and approximate mathematical models that determine various system-level performance measures for a (K,N) scheme. Under this scheme arriving packets are placed in the queue for one type of transmission until the size reaches K, whereupon arriving packets are diverted to the other transmission system. When the number of packets at the first system drops to N(is less than K), arriving packets are placed in the first queue. GRA

N88-12669# American Society for Engineering Education, Washington, D. C.
ON A CIRCULAR CORRELATION TECHNIQUE FOR FILTERING RANDOMLY NOISY DATA
S. Giles, C. D. Taylor, E. Harper, and R. McCloskey 1987 33 p
(Contract N00014-83-D-0689)
(AD-A184317) Avail: NTIS HC A03/MF A01 CSCL 20C

This paper introduces a technique of smoothing high frequency random fluctuations from noisy data. An optimum lowpass filter is developed by using the circular serial correlation statistic to minimize the random noise content in serial data. The procedure is applicable for statistically mild data. All the basic aspects of the new filter technique are discussed and are applied to both simulated noisy data and actual measured data of unknown noise reduction, but it also appears to provide a means to reconstruct undersampled data. GRA

N88-12670# Air Force Geophysics Lab., Hanscom AFB, Mass.
MICROWAVE REFRACTIVE INDEX STRUCTURE FUNCTION PROFILES (Cn2) MEASURED FROM A SMALL AIRCRAFT Final Report, 1985 - 1987
James F. Morrissey, Yutaka Izumi, and Owen R. Cote 5 Mar. 1987 29 p
(AD-A184343; AFGL-TR-87-0080; AFGL-ERP-969) Avail: NTIS HC A03/MF A01 CSCL 04A

Measurements of the microwave refractive index structure function (Cn2) obtained with a microwave refractometer on a small aircraft are presented. Thin layers (< 300 m) of highly enhanced Cn2 were observed on several flights, usually associated with an inversion. Results from two refractometers about 4 m apart are shown for several flights. The double measurements are discussed from the point of view of the validity of the measurements themselves. GRA

N88-12671# Lawrence Livermore National Lab., Calif.
APPLICATION OF LATTICE FILTERING TECHNIQUES TO CW MEASURED TIME DOMAIN DATA Final Technical Report
S. Giles, H. G. Hudson, S. R. Parker, and R. J. King Jan. 1987 26 p
(Contract N00014-83-D-0689)
(AD-A184351) Avail: NTIS HC A03/MF A01 CSCL 09A

This paper concerns the application of lattice filtering techniques to discrete frequency domain data. Time domain models for two different antennas are found, the monopole and cavity-back spiral. Lattice models and a layered medium model are obtained. GRA

N88-12672# Naval Postgraduate School, Monterey, Calif.
METEOR-BURST COMMUNICATIONS: IS THIS WHAT THE NAVY NEEDS? M.S. Thesis
Gretchen A. Helweg Jun. 1987 115 p
(AD-A184433) Avail: NTIS HC A06/MF A01 CSCL 17B

This thesis evaluates the limitations of meteor-burst communications for Navy requirements. The author examines the basic physics of the meteor-burst concept and the history of meteor-burst systems to determine inherent or persistent shortcomings. These findings are then compared to ongoing research and Navy applications for this communications medium. Limitations of meteor-burst communications are discussed with respect to potential Navy applications. Recommendations of possible applications of this technology are provided. GRA

N88-12673# Texas Univ., Austin. Microwave Lab.
A STUDY OF SCATTERING FROM E-PLANE CIRCUIT ELEMENTS
Qiu Zhang and Tatsuo Itoh May 1987 108 p
(Contract DAAG29-84-K-0076)
(AD-A184473; MW-87-P-5; ARO-21438.37-EL) Avail: NTIS HC A06/MF A01 CSCL 09A

This study contains two parts. In part one, a new analytical technique is introduced to characterize the scattering phenomena of a number of planar E-plane obstacles. This technique is based on the spectral domain method combined with residue calculus. This is the first time the spectral domain method has been used to solve a waveguide excitation problem. It provides some attractive features. For instance, it can handle a wide non-touching E-plane fin on a dielectric substrate; the method deals with inhomogeneous algebraic equations instead of integral equations; and also the spectral domain Green's functions have simple closed-form expressions. The calculated results for a simplified case are compared with existing data, and are in good agreement. Several curves, useful for E-plane configurations, are included. Part two presents an analysis and design of an evanescent mode bandpass waveguide filter with non-touching E-plane fins. The theoretical analysis is based on the generalized scattering matrix technique in conjunction with the spectral domain approach, which is described in part one, and mode matching method. The method used in this study takes into account the dominant as well as the higher order mode effects. The measured filter responses in Ka band (26.5 to 40.0 GHz) are in good agreement with those obtained by this analysis. Author (GRA)

N88-12674# Sandia National Labs., Albuquerque, N. Mex.
HIGH EFFICIENCY GENERATION OF 130-nm RADIATION FROM SUM-FREQUENCY MIXING IN Hg
G. R. Hadley, A. V. Smith, and W. J. Alford 1987 3 p Presented at the SDIO/DARPA Services Annual Propagation Review,

Monterey, Calif., 29 Sep. 1987
(Contract DE-AC04-76DP-00789)
(DE87-013714; SAND-87-2383C; CONF-8709146-3) Avail: NTIS HC A02/MF A01

The formation of an upper atmospheric ionization channel for electron beam propagation, as envisioned in the DELPHI program, requires high-intensity laser sources to accomplish the ionization of atomic oxygen. For one of the ionization schemes being examined, a strong source at 130.2 nm is required in order to excite oxygen atoms into the ^5S state, from which they are easily ionized using more readily available and lower-power lasers. We are presently investigating the use of two-photon-resonant four-wave mixing in atomic Hg vapor as a means of efficiently generating the necessary 130 nm light. This particular system is attractive primarily because the relevant oscillator strengths are high enough to allow reasonable (greater than 10 percent) conversion efficiencies without resorting to focused geometries. Thus, the results of laboratory experiments may be directly scaled to higher powers. DOE

N88-12675 Meteorological Office, London (England).
STUDY OF AN AIRBORNE DOPPLER RADAR: PROJECT ASTERIX
Jacques Testud, F. Baudin, and P. Amayenc [1987] 44 p
Transl. into ENGLISH of report (Paris, France, CNRS), 1987
(BLL-MO-Trans-1667-(9022.552); CRPE/159) Avail: British Library Lending Div., Boston Spa, United Kingdom

Specifications for an airborne Doppler radar for meteorological applications are given. The following areas are covered: (1) principle for measuring three-dimensional speed field; (2) pulse pattern and detectability; (3) antenna; (4) processing of data; (5) analog system; (6) data control and recording; (7) attitude control and vibrations; and (8) logistics. J.P.B.

N88-12676 British Broadcasting Corp., Kingswood (England). Engineering Div.
ACCOMMODATING THE RESIDUE OF PROCESSED OR COMPUTED DIGITAL VIDEO SIGNALS WITHIN THE 8 BIT CCIR RECOMMENDATION 601
M. G. Croll, V. G. Devereux, and M. Weston Sep. 1987 14 p
(BBC-RD-1987/12) Avail: Issuing Activity

A method is described for rounding down the number of bits in a digital video signal in such a manner that the resulting quantizing errors have a lower visibility than that of errors given by simple truncation. In particular, it avoids the generation of visible contours when the quantizing resolution is reduced to 8 bits. It is relevant to digital video processes such as fading and filtering where lower order bits are generated prior to an 8-bit interface. It can also be used in the synthetic generation of video signals. Systems employing the method of rounding described here have been found to exhibit a more noise like and subjectively less distracting quantization effect than where simple truncation is applied after digital processes. Author

N88-12677 British Broadcasting Corp., Kingswood (England). Engineering Div.
BAND 2 VHF ANTENNA FOR HOME CONSTRUCTION
S. Wakeling Sep. 1987 21 p
(BBC-RD-1987/13) Avail: Issuing Activity

A wideband Band 2 Yagi antenna, suitable for home construction, has been designed using computer techniques. The antenna is intended for use as a domestic receiving antenna for VHF/FM sound broadcasting at frequencies in the range of 88 to 108 MHz. Scale-model antennas were constructed and measured to verify the performance predicted by the computer. Finally, a full-scale Yagi antenna was constructed and its radiation patterns measured. The measurements on the new antenna and on some commercially made antennas, all of which had performances inferior to the new antenna, throw doubt on the practability or usefulness of the directivity characteristic in CCIR Recommendation 599. Author

N88-12678*# Nebraska Univ., Lincoln. Dept. of Electrical Engineering.
DESIGN OF SOURCE CODERS AND JOINT SOURCE/CHANNEL CODERS FOR NOISY CHANNELS Semiannual Status Report, 15 May - 15 Nov. 1987
Khalid Sayood, Martin C. Rost, and Alan Michels 15 Nov. 1987 27 p
(Grant NAG5-916)
(NASA-CR-181547; NAS 1.26:181547) Avail: NTIS HC A03/MF A01 CSCL 17B

A theory behind a proposed joint source/channel coding approach is developed and a variable rate design approach which provides substantial improvement over current joint source/channel coder designs is obtained. The Rice algorithm as applied to the output of the Gamma Ray Detector of the Mars Orbiter is evaluated. An alternative algorithm is obtained which outperforms the Rice both in terms of data compression and noisy channel performance. A high-fidelity low-rate image compression algorithm is developed which provides almost distortionless compression of high resolution images. Author

N88-12679*# Jet Propulsion Lab., California Inst. of Tech., Pasadena.
THE TELECOMMUNICATIONS AND DATA ACQUISITION REPORT Progress Report, Jul. - Sep. 1987
E. C. Posner, ed. 15 Nov. 1987 336 p
(NASA-CR-181546; JPL-TDA-PR-42-91; NAS 1.26:181546) Avail: NTIS HC A15/MF A01 CSCL 17B

This quarterly publication (July-September 1987) provides archival reports on developments in programs managed by JPL's Office of Telecommunications and Data Acquisition (TDA). In space communications, radio navigation, radio science, and ground-based radio astronomy, it reports on activities of the Deep Space Network (DSN) and its associated Ground Communications Facility (GCF) in planning, in supporting research and technology, in implementation, and in operations. This work is performed for NASA's Office of Space Tracking and Data Systems (OSTDS). In geodynamics, the publication reports on the application of radio interferometry at microwave frequencies for geodynamic measurements. In the Search for Extraterrestrial Intelligence (SETI), it reports on implementation and operations for searching the microwave spectrum. The latter two programs are performed for NASA's Office of Space Science and Applications (OSSA). For individual titles, see N88-12680 through N88-12711.

N88-12680*# Jet Propulsion Lab., California Inst. of Tech., Pasadena.
A DEMONSTRATION OF HIGH PRECISION GPS ORBIT DETERMINATION FOR GEODETIC APPLICATIONS c13
S. M. Lichten and J. S. Border *In its* The Telecommunications and Data Acquisition Report 15 Nov. 1987 p 1-22 (For primary document see N88-12679 04-32)
Avail: NTIS HC A15/MF A01 CSCL 22A

High precision orbit determination of Global Positioning System (GPS) satellites is a key requirement for GPS-based precise geodetic measurements and precise low-earth orbiter tracking, currently under study at JPL. Different strategies for orbit determination have been explored at JPL with data from a 1985 GPS field experiment. The most successful strategy uses multi-day arcs for orbit determination and includes fine tuning of spacecraft solar pressure coefficients and station zenith tropospheric delays using the GPS data. Average rms orbit repeatability values for 5 of the GPS satellites are 1.0, 1.2, and 1.7 m in altitude, cross-track, and down-track componenets when two independent 5-day fits are compared. Orbit predictions up to 24 hours outside the multi-day arcs agree within 4 m of independent solutions obtained with well tracked satellites in the prediction interval. Baseline repeatability improves with multi-day as compared to single-day arc orbit solutions. When tropospheric delay fluctuations are modeled with process noise, significant additional improvement in baseline repeatability is achieved. For a 246-km baseline, with 6-day arc solutions for GPS orbits, baseline repeatability is 2 parts in 100 million (0.4-0.6 cm) for east, north, and length components and 8

parts in 100 million for the vertical component. For 1314 and 1509 km baselines with the same orbits, baseline repeatability is 2 parts in 100 million for the north components (2-3 cm) and 4 parts in 100 million or better for east, length, and vertical components. Author

N88-12681*# Jet Propulsion Lab., California Inst. of Tech., Pasadena.
ROBUST STATISTICAL METHODS FOR AUTOMATED OUTLIER DETECTION c65
J. R. Jee *In its* The Telecommunications and Data Acquisition Report 15 Nov. 1987 p 23-28 (For primary document see N88-12679 04-32)
Avail: NTIS HC A15/MF A01 CSCL 12A

The computational challenge of automating outlier, or blunder point, detection in radio metric data requires the use of nonstandard statistical methods because the outliers have a deleterious effect on standard least squares methods. The particular nonstandard methods most applicable to the task are the robust statistical techniques that have undergone intense development since the 1960s. These new methods are by design more resistant to the effects of outliers than standard methods. Because the topic may be unfamiliar, a brief introduction to the philosophy and methods of robust statistics is presented. Then the application of these methods to the automated outlier detection problem is detailed for some specific examples encountered in practice. Author

N88-12682*# Jet Propulsion Lab., California Inst. of Tech., Pasadena.
PRECISE NEAR-EARTH NAVIGATION WITH GPS: A SURVEY OF TECHNIQUES c13
T. P. Yunck, S. C. Wu, and J. Wu *In its* The Telecommunications and Data Acquisition Report 15 Nov. 1987 p 29-45 (For primary document see N88-12679 04-32)
Avail: NTIS HC A15/MF A01 CSCL 22A

The tracking accuracy of the low earth orbiters (below about 3000 km altitude) can be brought below 10 cm with a variety of differential techniques that exploit the Global Positioning System (GPS). All of these techniques require a precisely known global network of GPS ground receivers and a receiver aboard the user satellite, and all simultaneously estimate the user and GPS satellite orbits. Three basic approaches are the geometric, dynamic, and nondynamic strategies. The last combines dynamic GPS solutions with a geometric user solution. Two powerful extensions of the nondynamic strategy show considerable promise. The first uses an optimized synthesis of dynamics and geometry in the user solution, while the second uses a novel gravity-adjustment method to exploit data from repeat ground tracks. These techniques will offer sub-decimeter accuracy for dynamically unpredictable satellites down to the lowesst possible altitudes. Author

N88-12683*# Jet Propulsion Lab., California Inst. of Tech., Pasadena.
SHORT BASELINE PHASE DELAY INTERFEROMETRY c17
C. D. Edwards *In its* The Telecommunications and Data Acquisition Report 15 Nov. 1987 p 46-56 (For primary document see N88-12679 04-32)
Avail: NTIS HC A15/MF A01 CSCL 09F

The high precision of the phase delay data type allows angular navigation accuracy on relatively short baselines to compete with the angular accuracy achieved with long baseline group delay measurements. Differential phase delay observations of close quasar pairs on both a 5.9-km baseline (DSS 12-DSS 13) and a 253-km baseline (DSS 13-Owens Valley Radio Observatory) have been performed to study the potential navigational precision and accuracy of the short baseline interferometry. As a first step toward demonstration of a connected element system at Goldstone, the DSS 12-DSS 13 baseline was operated coherently, distributing a common frequency reference via a recently installed fiber optic cable. The observed phase delay residuals of about 10 psec or less on both baselines appear to be dominated by short term troposphere fluctuations, and correspond to navigational accuracies of well below 50 nrad for the 253-km baseline. Additional experiments will be required to probe the full range of systematic errors. Author

N88-12684*# Jet Propulsion Lab., California Inst. of Tech., Pasadena.
NON-LINEARITY IN MEASUREMENT SYSTEMS: EVALUATION METHOD AND APPLICATION TO MICROWAVE RADIOMETERS c61
C. T. Stelzried *In its* The Telecommunications and Data Acquisition Report 15 Nov. 1987 p 57-66 (For primary document see N88-12679 04-32)
Avail: NTIS HC A15/MF A01 CSCL 09B

A simple method for determination and correction of nonlinaearity in measurement systems is presented. The technique is applicable to a wide range of measuring systems. The basic concept, an analysis, and a sample application are given. Nonlinearity of the Goldstone DSS 13 low noise HEMT 2.3 GHz (S-band) radiometer system results in noise temperature measurement errors. These errors are successfully correct with this method. Author

N88-12685*# Jet Propulsion Lab., California Inst. of Tech., Pasadena.
ATOMIC FREQUENCY STANDARDS FOR ULTRA-HIGH-FREQUENCY STABILITY c36
L. Maleki, J. D. Prestage, and G. J. Dick *In its* The Telecommunications and Data Acquisition Report 15 Nov. 1987 p 67-72 (For primary document see N88-12679 04-32)
Avail: NTIS HC A15/MF A01 CSCL 20E

The general features of the Hg-199(+) trapped-ion frequency standard are outlined and compared to other atomic frequency standards, especially the hydrogen maser. The points discussed are those which make the trapped Hg-199(+) standard attractive: high line Q, reduced sensitivity to external magnetic fields, and simplicity of state selection, among others. Author

N88-12686*# Jet Propulsion Lab., California Inst. of Tech., Pasadena.
MEASUREMENT AND ANALYSIS OF CRYOGENIC SAPPHIRE DIELECTRIC RESONATORS AND DROS c33
G. J. Dick *In its* The Telecommunications and Data Acquisition Report 15 Nov. 1987 p 73-80 (For primary document see N88-12679 04-32)
Avail: NTIS HC A15/MF A01 CSCL 09C

Presented are the experimental and computational results of a study on a new kind of dielectric resonator oscillator (DRO). It consists of a cooled, cylindrically symmetric sapphire resonator surrounded by a metallic shield and is capable of higher Q's than any other dielectric resonator. Isolation of fields to the sapphire by the special nature of the electromagnetic mode allows the very low loss of the sapphire itself to be expressed. Calculations show that the plethora of modes in such resonators can be effectively reduced through the use of a ring resonator with appropriate dimensions. Experimental results show Q's ranging from 3 x 10 to the 8th at 77 K to 10 to the 9th at 4.2 K. Performance is estimated for several types of DROs incorporating these resonators. Phase noise reductions in X-band sources are indicated at values substantially lower than those previously available. Author

N88-12687*# Jet Propulsion Lab., California Inst. of Tech., Pasadena.
INDUCTANCE EFFECTS IN THE HIGH-POWER TRANSMITTER CROWBAR SYSTEM c33
J. Daeges and A. Bhanji *In its* The Telecommunications and Data Acquisition Report 15 Nov. 1987 p 81-88 (For primary document see N88-12679 04-32)
Avail: NTIS HC A15/MF A01 CSCL 09C

The effective protection of a klystron in a high-power transmitter requires the diversion of all stored energy in the protected circuit through an alternate low-impedance path, the crowbar, such that less than 1 joule of energy is dumped into the klystron during an internal arc. A scheme of adding a bypass inductor in the

crowbar-protected circuit of the high-power transmitter was tested using computer simulations and actual measurements under a test load. Although this scheme has several benefits, including less power dissipation in the resistor, the tests show that the presence of inductance in the portion of the circuit to be protected severely hampers effective crowbar operation. Author

N88-12688*# Jet Propulsion Lab., California Inst. of Tech., Pasadena.
LOW-NOISE CRYOGENIC TRANSMISSION LINE c33
D. Norris *In its* The Telecommunications and Data Acquisition Report 15 Nov. 1987 p 89-93 (For primary document see N88-12679 04-32)
Avail: NTIS HC A15/MF A01 CSCL 09C

New low-noise cryogenic input transmission lines have been developed for the Deep Space Network (DSN) at 1.668 GHz for cryogenically cooled Field Effect Transistors (FET) and High Electron Mobility Transistor (HEMT) amplifiers. These amplifiers exhibit very low noise temperatures of 5 K to 15 K, making the requirements for a low-noise input transmission line critical. Noise contribution to the total amplifier system from the low-noise line is less than 0.5 K for both the 1.668-GHz and 2.25-GHz FET systems. The 1.668-GHz input line was installed in six FET systems which were implemented in the DSN for the Venus Balloon Experiment. The 2.25-GHz input line has been implemented in three FET systems for the DSN 34-m HEF antennas, and the design is currently being considered for use at higher frequencies. Author

N88-12689*# Jet Propulsion Lab., California Inst. of Tech., Pasadena.
A 2.3-GHz CRYOGENICALLY COOLED HEMT AMPLIFIER FOR DSS 13 c33
L. Tanida *In its* The Telecommunications and Data Acquisition Report 15 Nov. 1987 p 94-101 (For primary document see N88-12679 04-32)
Avail: NTIS HC A15/MF A01 CSCL 09C

A prototype 2.3 GHz (S band) high electron mobility transistor (HEMT) amplifier/closed cycle refrigerator (CCR) system was installed in the DDS-13 feedcone, replacing the 2.3 GHz maser. The amplifier is cryogenically cooled to a physical temperature of 12 K and provides 31.5 K antenna system noise temperature and 29 dB of gain. The HEMT device used in the amplifier is a prototype. Author

N88-12690*# Jet Propulsion Lab., California Inst. of Tech., Pasadena.
A COLD EJECTOR FOR CLOSED-CYCLE HELIUM REFRIGERATORS c31
D. L. Johnson and D. L. Daggett (San Jose State Univ., Calif.) *In its* The Telecommunications and Data Acquisition Report 15 Nov. 1987 p 102-111 (For primary document see N88-12679 04-32)
Avail: NTIS HC A15/MF A01 CSCL 13B

The test results are presented of an initial cold helium ejector design that can be installed on a closed cycle refrigerator to provide refrigeration at temperatures below 4.2 K. The ejector, test apparatus, instrumentation, and test results are described. Tests were conducted both at room temperature and at cryogenic temperatures to provide operational experience with the ejector as well as for future use in the subsequent design of an ejector that will provide refrigeration at temperatures below 3 K. Author

N88-12691*# Jet Propulsion Lab., California Inst. of Tech., Pasadena.
FREQUENCY DOUBLING CONVERSION EFFICIENCIES FOR DEEP SPACE OPTICAL COMMUNICATIONS
D. L. Robinson and R. L. Shelton *In its* The Telecommunications and Data Acquisition Report 15 Nov. 1987 p 112-123 (For primary document see N88-12679 04-32)
Avail: NTIS HC A15/MF A01 CSCL 17B

The theory of optical frequency doubling conversion efficiency is analyzed for the small signal input case along with the strong signal depleted input case. Angle phase matching and beam focus spot size are discussed and design trades are described which maximize conversion efficiency. Experimental conversion efficiencies from the literature, which are less than theoretical results at higher input intensities due to saturation, reconversion, and higher order processes, are applied to a case study of an optical communications link from Saturn. Double pass conversion efficiencies as high as 45 percent are expected. It is believed that even higher conversion efficiencies can be obtained using multipass conversion. Author

N88-12692*# Jet Propulsion Lab., California Inst. of Tech., Pasadena.
THE ATMOSPHERE OF MARS AND OPTICAL COMMUNICATIONS c91
J. Annis *In its* The Telecommunications and Data Acquisition Report 15 Nov. 1987 p 124-132 (For primary document see N88-12679 04-32)
Avail: NTIS HC A15/MF A01 CSCL 03B

The effects of the Martian atmosphere on an optical communication link are analyzed using Mariner 9, Viking Orbiter, and Viking Lander data. Clouds are found to have minimal effect because of their scarcity and thinness. Dust (from dust storms) has the dominant impact on opacity. However, periods of reduced visibility are infrequent and more closely resemble the effects of thin clouds on the earth. A simple argument is presented which suggests that the Martian atmosphere has fewer turbulence related effects (i.e., Mars has better resolution, lower image wander, and less scintillation) than the best of the earth's ground based locations. Author

N88-12693*# Jet Propulsion Lab., California Inst. of Tech., Pasadena.
A NEAR-EARTH OPTICAL COMMUNICATIONS TERMINAL WITH A COREVOLVING PLANETARY SUN SHIELD
E. L. Kerr *In its* The Telecommunications and Data Acquisition Report 15 Nov. 1987 p 133-140 (For primary document see N88-12679 04-32)
Avail: NTIS HC A15/MF A01 CSCL 17B

The umbra of a planet may serve as a sun shield for a space based optical communications terminal or for a space based astronomical observatory. An orbit that keeps the terminal or observatory within the umbra is desirable. There is a corevolution point behind every planet. A small body stabilized at the planet corevolution point will revolve about the sun at the same angular velocity as the planet, always keeping the planet between itself and the sun. This corevolution point is within the umbra of Mars but beyond the end of the umbra for Mercury, Venus, and earth. The Mars corevolution point is an ideal location for an astronomical observatory. There Mars obstruct less than 0.00024 percent of the sky at any time, and it shades the observatory completely from the sun. At the earth corevolution point, between 51 and 84 percent of the solar disk area is blocked, as is up to 92 percent of the sunlight. This provides a reduction from 3 dB to 11 dB in sunlight that could interfere with optical communications if scattered directly into the detectors. The variations is caused by revolution of the earth about the earth-moon barycenter. Author

N88-12694*# Jet Propulsion Lab., California Inst. of Tech., Pasadena.
OPTIMIZED TRACKING OF RF CARRIERS WITH PHASE NOISE, INCLUDING PIONEER 10 RESULTS
V. A. Vilnrotter, W. J. Hurd, and D. H. Brown *In its* The Telecommunications and Data Acquisition Report 15 Nov. 1987 p 141-157 (For primary document see N88-12679 04-32)
Avail: NTIS HC A15/MF A01 CSCL 17B

The ability to track very weak signals from distant spacecraft is limited by the phase instabilities of the received signal and of the local oscillator employed by the receiver. These instabilities ultimately limit the minimum loop bandwidth that can be used in a phase-coherent receiver, and hence limit the ratio of received carrier power to noise spectral density which can be tracked phase coherently. A method is presented for near real time estimation

of the received carrier phase and additive noise spectrum, and optimization of the phase locked loop bandwidth. The method was used with the breadboard Deep Space Network (DSN) Advanced Receiver to optimize tracking of very weak signals from the Pioneer 10 spacecraft, which is now more distant that the edge of the solar system. Tracking with bandwidths of 0.1 Hz to 1.0 Hz reduces tracking signal threshold and increases carrier loop signal to noise ratio (SNR) by 5 dB to 15 dB compared to the 3 Hz bandwidth of the receivers now used operationally in the DSN. This will enable the DSN to track Pioneer 10 until its power sources fails near the end of the century. Author

N88-12695*# Jet Propulsion Lab., California Inst. of Tech., Pasadena.
DETECTION OF SIGNALS BY THE DIGITAL INTEGRATE-AND-DUMP FILTER WITH OFFSET SAMPLING
R. Sadr and W. J. Hurd *In its* The Telecommunications and Data Acquisition Report 15 Nov. 1987 p 158-173 (For primary document see N88-12679 04-32)
Avail: NTIS HC A15/MF A01 CSCL 17B

The Integrate and Dump Filter (IDF) is used as a matched filter for the detection of signals in additive white Gaussian noise. The performance of the digital integrate and dump filter is evaluated. The case considered is when symbol times are known and the sampling clock is free running at a constant rate, i.e., the sampling clock is not phase locked to the symbol clock. Degradations in the output signal to noise ratio of the digital implementation due to sampling rate, sampling offset, and finite bandwidth, resulting from the anti-aliasing low pass prefilter, are computed and compared with those of the analog counterpart. It is shown that the digital IDF performs within 0.6 dB of the ideal analog IDF whenever the prefilter bandwidth exceeds four times the symbol rate and when sampling is performed at the Nyquist rate. The loss can be reduced to 0.3 dB by doubling the sampling rate, where 0.2 dB loss results from finite bandwidth and 0.1 dB results from the digital IDF. Author

N88-12696*# Jet Propulsion Lab., California Inst. of Tech., Pasadena.
DETECTION OF SIGNALS BY WEIGHTED INTEGRATE-AND-DUMP FILTER
R. Sadr *In its* The Telecommunications and Data Acquisition Report 15 Nov. 1987 p 174-185 (For primary document see N88-12679 04-32)
Avail: NTIS HC A15/MF A01 CSCL 17B

A Weighted Integrate and Dump Filter (WIDF) is presented that results in reducing those losses in telemetry symbol signal to noise ratio (SNR) which occur in digital Integrate and Dump Filters (IDFs) when the samples are not phase locked to the input data symbol clock. The Minimum Mean Square Error (MMSE) criterion is used to derive a set of weights for approximating the analog integrate and dump filter, which is the matched filter for detection of signals in additive white Gaussian noise. This new digital matched filter results in considerable performance improvement compared to unweighted digital matched filters. An example is presented for a sampling rate of four times the symbol rate. As the sampling offset (or phase) varies with respect to the data symbol boundaries, the output SNR varies 1 dB for an unweighted IDF, but only 0.3 dB for the optimum WIDF, averaged over random data patterns. This improvement in performance relative to unweighted IDF means that significantly lower sampling and processing rates can be used for given telemetry symbol rates, resulting in reduced system cost. Author

N88-12697*# Jet Propulsion Lab., California Inst. of Tech., Pasadena.
THE DESIGN PLAN OF A VLSI SINGLE CHIP (255, 223) REED-SOLOMON DECODER
I. S. Hsu, H. M. Shao, and L. J. Deutsch *In its* The Telecommunications and Data Acquisition Report 15 Nov. 1987 p 186-199 (For primary document see N88-12679 04-32)
Avail: NTIS HC A15/MF A01 CSCL 17B

The very large-scale integration (VLSI) architecture of a single chip (255, 223) Reed-Solomon decoder for decoding both errors and erasures is described. A decoding failure detection capability is also included in this system so that the decoder will recognize a failure to decode instead of introducing additional errors. This could happen whenever the received word contains too many errors and erasures for the code to correct. The number of transistors needed to implement this decoder is estimated at about 75,000 if the delay for received message is not included. This is in contrast to the older transform decoding algorithm which needs about 100,000 transistors. However, the transform decoder is simpler in architecture than the time decoder. It is therefore possible to implement a single chip (255, 223) Reed-Solomon decoder with today's VLSI technology. An implementation strategy for the decoder system is presented. This represents the first step in a plan to take advantage of advanced coding techniques to realize a 2.0 dB coding gain for future space missions. Author

N88-12698*# Jet Propulsion Lab., California Inst. of Tech., Pasadena.
A SIMPLIFIED PROCEDURE FOR CORRECTING BOTH ERRORS AND ERASURES OF A REED-SOLOMON CODE USING THE EUCLIDEAN ALGORITHM c64
T. K. Truong, I. S. Hsu, W. L. Eastman, and I. S. Reed (University of Southern California, Los Angeles.) *In its* The Telecommunications and Data Acquisition Report 15 Nov. 1987 p 200-212 (For primary document see N88-12679 04-32)
Avail: NTIS HC A15/MF A01 CSCL 12A

It is well known that the Euclidean algorithm or its equivalent, continued fractions, can be used to find the error locator polynomial and the error evaluator polynomial in Berlekamp's key equation needed to decode a Reed-Solomon (RS) code. A simplified procedure is developed and proved to correct erasures as well as errors by replacing the initial condition of the Euclidean algorithm by the erasure locator polynomial and the Forney syndrome polynomial. By this means, the errata locator polynomial and the errata evaluator polynomial can be obtained, simultaneously and simply, by the Euclidean algorithm only. With this improved technique the complexity of time domain RS decoders for correcting both errors and erasures is reduced substantially from previous approaches. As a consequence, decoders for correcting both errors and erasures of RS codes can be made more modular, regular, simple, and naturally suitable for both VLSI and software implementation. An example illustrating this modified decoding procedure is given for a (15, 9) RS code. Author

N88-12699*# Jet Propulsion Lab., California Inst. of Tech., Pasadena.
MORE ON THE DECODER ERROR PROBABILITY FOR REED-SOLOMON CODES c64
K.-M. Cheung *In its* The Telecommunications and Data Acquisition Report 15 Nov. 1987 p 213-223 (For primary document see N88-12679 04-32)
Avail: NTIS HC A15/MF A01 CSCL 12A

The decoder error probability for Reed-Solomon codes (more generally, linear maximum distance separable codes) is examined. McEliece and Swanson offered an upper bound on P sub E (u), the decoder error probability given that u symbol errors occurs. This upper bound is slightly greater than Q, the probability that a completely random error pattern will cause decoder error. By using a combinatoric technique, the principle of inclusion and exclusion, an exact formula for P sub E (u) is derived. The P sub e (u) for the (255, 223) Reed-Solomon Code used by NASA, and for the (31,15) Reed-Solomon code (JTIDS code), are calculated using the exact formula, and the P sub E (u)'s are observed to approach the Q's of the codes rapidly as u gets larger. An upper bound for the expression is derived, and is shown to decrease nearly exponentially as u increases. This proves analytically that P sub E (u) indeed approaches Q as u becomes large, and some laws of large numbers come into play. Author

N88-12700*# Jet Propulsion Lab., California Inst. of Tech., Pasadena.
ON THE VLSI DESIGN OF A PIPELINE REED-SOLOMON DECODER USING SYSTOLIC ARRAYS **c33**
H. M. Shao, L. J. Deutsch, and I. S. Reed (University of Southern California, Los Angeles.) *In its* The Telecommunications and Data Acquisition Report 15 Nov. 1987 p 224-234 (For primary document see N88-12679 04-32)
Avail: NTIS HC A15/MF A01 CSCL 09C

A new very large scale integration (VLSI) design of a pipeline Reed-Solomon decoder is presented. The transform decoding technique used in a previous article is replaced by a time domain algorithm through a detailed comparison of their VLSI implementations. A new architecture that implements the time domain algorithm permits efficient pipeline processing with reduced circuitry. Erasure correction capability is also incorporated with little additional complexity. By using a multiplexing technique, a new implementation of Euclid's algorithm maintains the throughput rate with less circuitry. Such improvements result in both enhanced capability and significant reduction in silicon area. Author

N88-12701*# Jet Propulsion Lab., California Inst. of Tech., Pasadena.
A PROCEDURAL METHOD FOR THE EFFICIENT IMPLEMENTATION OF FULL-CUSTOM VLSI DESIGN **c33**
P. Belk and N. Hickey *In its* The Telecommunications and Data Acquisition Report 15 Nov. 1987 p 235-246 (For primary document see N88-12679 04-32)
Avail: NTIS HC A15/MF A01 CSCL 09C

An imbedded language system for the layout of very large scale integration (VLSI) circuits is examined. It is shown that through the judicious use of this system, a large variety of circuits can be designed with circuit density and performance comparable to traditional full-custom design methods, but with design costs more comparable to semi-custom design methods. The high performance of this methodology is attributable to the flexibility of procedural descriptions of VLSI layouts and to a number of automatic and semi-automatic tools within the system. Author

N88-12702*# Jet Propulsion Lab., California Inst. of Tech., Pasadena.
A NEW STATE SPACE MODEL FOR THE NASA/JPL 70-METER ANTENNA SERVO CONTROLS **c37**
R. E. Hill *In its* The Telecommunications and Data Acquisition Report 15 Nov. 1987 p 247-264 (For primary document see N88-12679 04-32)
Avail: NTIS HC A15/MF A01 CSCL 13I

A control axis referenced model of the NASA/JPL 70-m antenna structure is combined with the dynamic equations of servo components to produce a comprehansive state variable (matrix) model of the coupled system. An interactive Fortran program for generating the linear system model and computing its salient parameters is described. Results are produced in a state variable, block diagram, and in factored transfer function forms to facilitate design and analysis by classical as well as modern control methods. Author

N88-12703*# Jet Propulsion Lab., California Inst. of Tech., Pasadena.
X-BAND UPLINK GROUND SYSTEMS DEVELOPMENT: PART 2
C. E. Johns *In its* The Telecommunications and Data Acquisition Report 15 Nov. 1987 p 265-268 (For primary document see N88-12679 04-32)
Avail: NTIS HC A15/MF A01 CSCL 17B

The prototype X-band exciter testing has been completed. Stability and single-sideband phase noise measurements have been made on the X-band exciter signal (7.145-7.235 GHz) and on the coherent X- and S-band receiver test signals (8.4-8.5 GHz and 2.29-2.3 GHz) generated within the exciter equipment. Outputs are well within error budgets. Author

N88-12704*# Jet Propulsion Lab., California Inst. of Tech., Pasadena.
ANALYSIS OF THE ICE COMBINER FOR MULTIPLE ANTENNA ARRAYING
C. Foster and M. Marina *In its* The Telecommunications and Data Acquisition Report 15 Nov. 1987 p 269-277 (For primary document see N88-12679 04-32)
Avail: NTIS HC A15/MF A01 CSCL 20N

The passage of the International Cometary Explorer (ICE) through the tail of comet Giacobini-Zinner took place on September 11, 1985, at approximately 11:04 GMT. The signal-to-noise ratio of the data received from the ICE spacecraft during the comet encounter was improved by arraying the 64-m antenna channels A and B (RCP and LCP) with the two 34-m antennas. Specially designed combiners were built to combine the signals received by the three antennas at the different DSN sites to ensure that the spacecraft's weak signal was received. Although the ICE spacecraft was built with a 5-W transmitter and with a small antenna designed to provide data from no farther than 1 million miles, these combiners provided enough signal margin during the encounter to receive the ICE transmitted data from within the tail of comet Giacobini-Zinner, 44 million miles from earth. Author

N88-12705*# Jet Propulsion Lab., California Inst. of Tech., Pasadena.
THE 8.4-GHz LOW-NOISE MASER PUMP SOURCE ASSEMBLY **c36**
R. Cardenas *In its* The Telecommunications and Data Acquisition Report 15 Nov. 1987 p 278-284 (For primary document see N88-12679 04-32)
Avail: NTIS HC A15/MF A01 CSCL 20E

Improved pump source assemblies and new 8.4-GHz low noise traveling-wave masers (TWMs) were installed at the same time at Deep Space Stations 14 and 43 as part of the Mark IVA DSCC Antenna Microwave Subsystems upgrade. The pump source assemblies are part of the new 8.4-GHz TWMs, which are identified as Block IIA Low-Noise TWMs. Improved reliability of the pump source assemblies was required to meet stress analysis criteria. Author

N88-12706*# Jet Propulsion Lab., California Inst. of Tech., Pasadena.
A MODERN CONTROL THEORY BASED ALGORITHM FOR CONTROL OF THE NASA/JPL 70-METER ANTENNA AXIS SERVOS **c37**
R. E. Hill *In its* The Telecommunications and Data Acquisition Report 15 Nov. 1987 p 285-294 (For primary document see N88-12679 04-32)
Avail: NTIS HC A15/MF A01 CSCL 13I

A digital computer-based state variable controller was designed and applied to the 70-m antenna axis servos. The general equations and structure of the algorithm and provisions for alternate position error feedback modes to accommodate intertarget slew, encoder referenced tracking, and precision tracking modes are descibed. Development of the discrete time domain control model and computation of estimator and control gain parameters based on closed loop pole placement criteria are discussed. The new algorithm was successfully implemented and tested in the 70-m antenna at Deep Space Network station 63 in Spain. Author

N88-12707*# Jet Propulsion Lab., California Inst. of Tech., Pasadena.
FAST AUTOTUNING OF A HYDROGEN MASER BY CAVITY Q MODULATION **c36**
G. J. Dick and T. K. Tucker *In its* The Telecommunications and Data Acquisition Report 15 Nov. 1987 p 295-303 (For primary document see N88-12679 04-32)
Avail: NTIS HC A15/MF A01 CSCL 20E

A new fast autotuner for the hydrogen maser was implemented. By modulating the cavity, a phase shift in the maser output signal is induced which is proportional to the cavity tuning error. The phase shift is detected and fed back to a varactor tuner to stabilize the cavity against long-term drifts. Also, a PIN-diode cavity

modulator which gives no incidental frequency shift over a very wide range of operation was developed. Modulated at over 200 Hz, it allows variations in maser cavity frequency to be compensated with a loop gain greater than 1000. Compensation of incidental amplitude modulation of the output was demonstrated. Author

N88-12708*# Jet Propulsion Lab., California Inst. of Tech., Pasadena.
TRAVELING-WAVE MASER CLOSED-CYCLE REFRIGERATOR DATA ACQUISITION AND DISPLAY SYSTEM **c36**
L. Fowler and M. Britcliffe *In its* The Telecommunications and Data Acquisition Report 15 Nov. 1987 p 304-311 (For primary document see N88-12679 04-32)
Avail: NTIS HC A15/MF A01 CSCL 20E

A data acquisition and display system that automatically monitors the performance of the 4.5-K closed-cycle refrigerators used to cryogenically cool traveling-wave masers is described. The system displays and stores operating parameters for the purpose of providing status information, failure prediction, and analysis. A prototype of this system will be installed at Deep Space Network 12 in the near future. The advantages of using commercial data acquisition hardware with installed operating systems and BASIC programs for this application are discussed. Author

N88-12709*# Jet Propulsion Lab., California Inst. of Tech., Pasadena.
TWO-WATT, 4-KELVIN CLOSED CYCLE REFRIGERATOR PERFORMANCE **c31**
M. Britcliffe *In its* The Telecommunications and Data Acquisition Report 15 Nov. 1987 p 312-317 (For primary document see N88-12679 04-32)
Avail: NTIS HC A15/MF A01 CSCL 13B

A 2-watt, 4-K helium refrigerator using the Gifford-McMahon/Joule Thomson cycle is described. The unit features a removable displacer cylinder and high-efficiency, low-pressure drop heat exchangers. These improvements result in a 100 percent increase in cooling power over the existing Deep Space Network system. The effects of the heat exchanger efficiency and Gifford-McMahon expander performance on refrigerator capacity are also discussed. Author

N88-12710*# Jet Propulsion Lab., California Inst. of Tech., Pasadena.
TAU RANGING REVISITED
R. C. Tausworthe *In its* The Telecommunications and Data Acquisition Report 15 Nov. 1987 p 318-324 (For primary document see N88-12679 04-32)
Avail: NTIS HC A15/MF A01 CSCL 17B

It is shown that a ranging receiver with a sufficient and reasonable number of correlators is competitive with the current sequential component ranging system by some 1.5 to 2.5 dB. The optimum transmitter code, the optimum receiver, and a near-maximum-likelihood range-estimation algorithm are presented. Author

N88-12711*# Jet Propulsion Lab., California Inst. of Tech., Pasadena.
POWER DENSITY MEASUREMENTS IN THE NEAR FIELD OF THE DSS 13 26-METER ANTENNA
E. B. Jackson and M. J. Klein *In its* The Telecommunications and Data Acquisition Report 15 Nov. 1987 p 325-329 (For primary document see N88-12679 04-32)
Avail: NTIS HC A15/MF A01 CSCL 20N

ower density measurements were made at Deep Space Station (DSS) 13 in the near field of the 26-m antenna to determine if radio frequency (rf) fields generated by the 20-kW transmitters could be responsible for the failure of three solid state rf amplifiers. These amplifiers are used in the Search for Extraterrestrial Intelligence (SETI) Radio Spectrum Surveillance System, which is currently located at the site. Measurements were made independently for one transmitter at 7150 MHz, and both transmitters together. Measurement results are tabulated and compared with predicted power densities under the measurement conditions. The results agree with the predictions within a factor of two. The predictions appear to give worst case values. Measurements indicated that amplifier failures are not attributable to the transmitter. Author

N88-12712*# Hawaii Univ., Honolulu. Dept. of Electrical Engineering.
BANDWIDTH EFFICIENT BLOCK CODES FOR M-ary PSK MODULATION
Shu Lin 31 Dec. 1987 48 p
(Grant NAG5-931)
(NASA-CR-181543; NAS 1.26:181543) Avail: NTIS HC A03/MF A01 CSCL 17B

A class of bandwidth efficient block codes for M-ary PSK modulation is presented. A soft-decision decoding for this class of codes is devised. Some specific short codes for Quad Phase Shift Key (QPSK), 8-PSK and 16-PSK modulations are constructed. These codes have good minimum squared Euclidean distances and provide 2 to 5.8 dB coding gains over uncoded QPSK modulation without (or with little) bandwidth expansion. The complete weight distributions of these specific codes are determined. Based on these weight distributions, their error probabilities are evaluated. Some of these codes have simple trellis structures and hence can be decoded by Viterbi decoding algorithm with relatively simple implementation. Moreover, the codes are very suitable for use as inner codes for various cascaded coding schemes with Reed-Solomon codes as outer codes. Author

N88-12713# Sandia National Labs., Albuquerque, N. Mex.
AN EXCITATION-TERM MODIFICATION FOR A CERTAIN CLASS OF ELECTROMAGNETIC APERTURE-COUPLING PROBLEMS
D. J. Riley and L. D. Bacon Sep. 1987 31 p
(Contract DE-AC04-76DP-00789)
(DE88-000260; SAND-87-0889) Avail: NTIS HC A03/MF A01

A simple technique is presented for modifying electromagnetic aperture-coupling integral equations that are based on an infinite-ground-plane assumption, to partially account for excitation modifications which result from plane-wave interaction with a side of an actual three-dimensional scatterer. The technique is based on incorporating the solution for a conducting wedge into the integral equations. Results are presented for coupling to coaxial connectors which are more consistent with experimental observations. DOE

N88-12714# Lawrence Livermore National Lab., Calif.
PULSE-MODE EXPANSIONS AND REFRACTIVE INDICES IN PLANE-WAVE PROPAGATION
B. W. Shore, R. Sacks, T. Karr, J. Morris, J. A. Paisner, and J. H. Eberly (Rochester Univ., N. Y.) 20 Jun. 1987 44 p
(Contract W-7405-eng-48)
(DE88-001328; UCID-21062) Avail: NTIS HC A03/MF A01

This memo presents basic background theory for treating simultaneous propagation of electromagnetic pulses of various colors, directed along a common ray, through a molecular vapor. The memo discusses some techniques for expanding the positive frequency part of the transverse electric field into pulse modes, characterized by carrier frequencies within a modulated envelope. We discuss, in the approximation of plane waves with slowly varying envelopes, a set of uncoupled envelope equations in which a polarization mode-envelope acts as a source for an electric-field envelope. These equations, when taken with a prescription for the polarization field, are the basic equations of plane-wave pulse propagation through a molecular medium. We discuss two ways of treating dispersive media, one based upon expansions in the frequency domain and the other based in the time domain. In both cases we find envelope equations that involve group velocities. This memo represents a portion of a more extensive treatment of propagation to be presented separately. Many of the equations presented have been described before. They are treated here as a summary and review of contemporary theory been described in

various books and articles. They are collected and described here as a summary and review of contemporary theory. DOE

N88-12715# California Univ., Berkeley. Lawrence Berkeley Lab.
A NEW APPROACH TO MODELING AND INTERPRETING ELECTROMAGNETIC SOUNDING DATA
K. H. Lee May 1987 14 p Presented at the Mexican Geophysical Union Conference, Ensenada, Mexico, 10 Nov. 1987
(Contract DE-AC03-76SF-00098)
(DE88-000460; LBL-23544; CONF-871164-1) Avail: NTIS HC A02/MF A01

A major impediment to the application and acceptance of controlled-source electromagnetics has been the difficulty of processing, displaying, and intepreting the data. Our goal has been to develop a method for imaging the subsurface conductivity distribution. We have sought a representation that would provide some direct visualization of the subsurface conductivity contrasts that give rise to the observed or calculated fields. We have discovered a new method for calculating the electromagnetic response of inhomogeneous conducting media that is not only computationally efficient but promises to provide the inverse solutions we have long sought. The method can be used to: (1) model EM problems (the forward solution) with a speed at least two orders of magnitude faster than conventional methods; and (2) provide reflectivity images of subsurface conductivity contrasts similar to those obtained in reflection seismic methods. DOE

33 ELECTRONICS AND ELECTRICAL ENGINEERING

Includes test equipment and maintainability; components, e.g., tunnel diodes and transistors; microminiaturization; and integrated circuitry.

For related information see also *60 Computer Operations and Hardware* and *76 Solid-State Physics.*

N88-12716# Technical Research Centre of Finland, Espoo.
DESIGN OF DIGITAL FILTERS FOR ELECTRONIC INSTRUMENTATION
K. P. Estola 1986 88 p
(PB87-100418; VTT/PUB-30; ISBN-951-38-2604-X) Avail: NTIS HC E03/MF E01 CSCL 09A

The design of digital filters for electronic instrumentation is considered. The overall design and realization problem addressed can be divided into five subproblems: sampling and reconstruction; digital equalization; digital filtering and noise rejection; sampling rate alteration; and digital coding and transmission. The basic discriminating feature compared with other related studies is the requirement of the preservation of the time domain characteristics. Design methods are presented both for recursive and nonrecursive digital filters covering a wide range of electronic instrumentation. Medical signal processing was the major field of application requiring the most delicate signal processing to preserve the clinically important time domain characteristics. However, the design problems considered and results achieved are general and can be applied to any signal processing task bearing similar principal constraints. GRA

N88-12717# Technical Research Centre of Finland, Espoo.
DESIGN OF EFFICIENT FIR FILTERS WITH MINIMAL DELAY
K. P. Estola 1986 23 p
(PB87-100434; VTT/RR-403; ISBN-951-38-2580-9) Avail: NTIS HC E03/MF E01 CSCL 09A

A design method for approximately linear phase narrow-band and highpass FIR filters is presented. Also an efficient filter structure is introduced for realizing the designed filters. The structure is based on a cascade of linear and nonlinear phase FIR filters having transfer functions expressable as integer powers of the unit delay. The overall implementation requires significantly less multiplications than conventional direct form FIR filters. Moreover, the delay of the filters is only fractions of what can be attained using pure linear-phase FIR filters. It is shown by means of an example that the design method and realization results in virtually linear phase FIR highpass filters which are computationally efficient and have short response times. GRA

N88-12718# Technische Hogeschool, Delft (Netherlands). Afdeling der Elektrotechniek.
PROGRAMMABLE LOGIC ARRAYS (PLA's) DESIGN FOR TESTABILITY M.S. Thesis
M. M. Ligthart Aug. 1985 67 p
(PB87-102935) Avail: NTIS HC E04/MF E01 CSCL 09A

In testing integrated circuits for fabrication failures, Programmable Logic Arrays (PLAs) have to be treated differently from random logic. There are two main reasons for this different treatment. First, due to the high reconvergent fanout in PLAs, the existing test pattern algorithms developed for random logic are hard to use. Second, the single stuck-at fault model, normally used for random logic, is inadequate for PLAs. Many attempts have been made to develop dedicated test pattern algorithms for PLAs. Design for testability approaches for PLAs are in progress. In the report, a fault model for PLAs is derived from literature. The fault model contains multiple stuck-at faults and multiple extra and multiple missing crosspoint defects. GRA

N88-12719# Cambridge Univ. (England). Dept. of Engineering.
DEPARTMENTAL REPORT ON PROGRAM EMTP-MACHINE WINDINGS SURGE TRANSIENTS: TRAVELLING WAVE METHOD
M. H. AbdelRahman [1986] 33 p
(PB87-123733; CUED/B-ELECT/TR-73) Avail: Issuing Activity CSCL 09A

The program may be used for the calculation of transient voltage distributions in machine windings caused by steep-fronted surges impinging upon the machine windings. The program uses a multi-conductor transmission line model to represent machine windings and is based on the traveling wave equations of a transmission line being an extension of the Lattice-Diagram Method due to Bewley. Whereas in two conductor transmission line calculations, the reflection and refraction coefficients at discontinuities are calculated from the simple line surge impedance of the sections on either side of the discontinuity for multi-conductor calculations, these individual surge impedances are replaced by surge impedance matrices which include the mutual effects between the conductors which make up the coil side. Author

N88-12720# Bradford Univ. (England). Postgraduate School of Electrical and Electronic Engineering.
PERFORMANCE OPTIMIZATION OF ELECTRONIC NETWORKS IN THE FREQUENCY DOMAIN
A. R. Elobeid Sep. 1986 9 p
(PB87-123873; UB/PSEEE-389) Avail: NTIS HC E03/MF E03 CSCL 09C

A unified approach is presented for the optimization of linear electronic networks in the frequency domain. Based on adjoint-network development, this employs a performance parameter which is a function of the network responses and the upper frequency limit. Redefining the performance function and constraint relation allows computationally economical post-design bandwidth adjustment. Author

N88-12721# Stanford Univ., Calif. Computer Systems Lab.
RESEARCH IN VLSI (VERY LARGE SCALE INTEGRATION) SYSTEMS Technical Progress Report, Dec. 1986 - Mar. 1987
John Hennessy and James Plummer Mar. 1987 30 p
(Contracts MDA903-84-K-0062; MDA903-83-C-0335)
(AD-A184089) Avail: NTIS HC A03/MF A01 CSCL 09A

This report summarizes progress in the DARPA funded VLSI Systems Research Projects from December 1986 to March 1987. The major areas under investigation have included: analysis and synthesis design aids, applications of VLSI, special purpose chip design, VLSI computer architectures, reliability studies, manufacturing science, and VLSI fabrication. The major research problems are introduced and progress is discussed; the Appendix

contains a list of published research papers from these projects.
Author (GRA)

N88-12722# Minnesota Univ., Minneapolis. Dept. of Chemical Engineering and Materials Science.
APPLICATIONS OF MULTIVALENT IONIC CONDUCTORS TO POLYMERIC ELECTROLYTE BATTERIES Technical Report No. 12, Mar. 1986 - Aug. 1987
J. Y. Cherng, Boone B. Owens, W. H. Smyrl, and M. Z. Munshi 10 Aug. 1987 18 p
(Contract N00014-85-K-0634)
(AD-A184252) Avail: NTIS HC A03/MF A01 CSCL 09A

The feasibility of solid state cells based upon lithium ion conducting polymer electrolytes has been demonstrated. In the present paper a preliminary investigation of sodium and magnesium ion conductors in polymer electrolyte cells is summarized. Cell types were Li/V6O13, Na/V6O13, and Mg/V6O13 with polymer electrolytes based on polyethylene oxide and salts of the anode element. GRA

N88-12723# Illinois Univ., Urbana. Coordinated Science Lab.
MUTUAL ADMITTANCE BETWEEN SLOTS IN CYLINDERS OF ARBITRARY SHAPE
A. F. Peterson and R. Mittra Aug. 1987 127 p
(Contract N00014-84-C-0149)
(AD-A184254; UILU-ENG-87-2247) Avail: NTIS HC A07/MF A01 CSCL 09A

A numerical procedure to estimate the mutual admittance between finite slots in infinite, conducting cylinders of arbitrary cross-sectional shape is described. The problem formulation involves a Fourier transform and the numerical solution of integral equations. Additional issues addressed include the large amount of required computation, remedies for non-uniqueness problems associated with the integral equations, and the overall accuracy of the procedure. Good agreement is obtained between the numerical results and exact eigenfunction data for slots in circular cylinders. Several other cylindrical shapes are investigated. GRA

N88-12724# Massachusetts Inst. of Tech., Cambridge. Dept. of Chemistry.
CHEMICALLY MODIFIED MICROELECTRODE ARRAYS. NEW KINDS OF ELECTRONIC DEVICES
Mark S. Wrighton, Shuchi Chao, Oliver M. Chyan, E. T. Jones, and Nicholas Leventis 5 Aug. 1987 29 p
(Contract N00014-84-K-0553)
(AD-A184389; AD-F000100; TR-18) Avail: NTIS HC A03/MF A01 CSCL 09A

Modification of closely spaced (approx 1.5 micron) microelectrodes (approx 2.5 microns wide x 50 microns long x 0.1 microns high) with electroactive materials gives rise to a variety of new kinds of electronic devices. Surface modification of microelectrode arrays with metal oxides, e.g., WO3, conventional redox polymers, e.g., viologen-based polymers, and so-called conducting redox polymers, e.g., poly(3-methylthiophene), allows demonstration of a variety of microelectrochemical transistors having properties that depend on the electroactive material. While the response time of such devices is slow by solid state electronics standards, chemically sensitive transistors can be envisioned as sensitive, specific sensors. Solid state microelectrochemical devices can be made that involve the use of ionic conducting polymers as the solvent/electrolyte system. Solid state microelectrochemical transistors can be designed to be sensitive to certain gases. GRA

N88-12725# Massachusetts Inst. of Tech., Cambridge. Research Lab. of Electronics.
PHASE-COHERENT ASTROMETRIC INTERFEROMETRY Annual Report, 1 Feb. 1986 - 31 Jan. 1987
David H. Staelin, J. W. Barrett, L. D. Clark, and B. E. Hines 17 Aug. 1987 10 p
(Contract N00014-86-C-2114)
(AD-A184428) Avail: NTIS HC A02/MF A01 CSCL 03A

This year involved continuation of the development of the Mark III stellar interferometer, which is a fringe-tracking long-baseline Michelson interferometer designed primarily for wide-angle astrometry at the milli-arcsecond level. It also is useful for measuring stellar diameters and as an initial test bed for concepts relevant to aperture synthesis imaging. It is being constructed on Mount Wilson, California. GRA

N88-12726# Utah Univ., Salt Lake City. Dept. of Electrical Engineering.
RAMAN SCATTERING AS A DIAGNOSTIC TECHNIQUE FOR CATHODE CHARACTERIZATION Final Technical Report, Sep. 1982 - Sep. 1985
Robert E. Benner, J. R. Mitchell, and R. W. Grow Jun. 1987 38 p
(Contracts F30602-82-C-0161; F30602-84-C-0153)
(AD-A184434; UTEC-MD-87-002; RADC-TR-87-67) Avail: NTIS HC A03/MF A01 CSCL 07D

The feasibility of using the optical technique of Raman scattering to determine the chemical composition of cathode surfaces has been investigated. Reference Raman spectra have been obtained for many of the chemical compounds expected to be present at the surface of dispenser cathodes. In addition, spectra obtained from 5-3-2 impregnant and several cathode surfaces are presented. The potential advantages of the approach are discussed. GRA

N88-12727*# National Aeronautics and Space Administration. Lewis Research Center, Cleveland, Ohio.
AN ANALYTICAL AND EXPERIMENTAL STUDY OF INJECTION-LOCKED TWO-PORT OSCILLATORS
Jon C. Freeman and Alan N. Downey Jul. 1987 39 p
(NASA-TM-100119; E-3663; NAS 1.15:100119) Avail: NTIS HC A03/MF A01 CSCL 09A

A Ku-band IMPATT oscillator with two distinct output power ports was injection-locked alternately at both ports. The transmission locking bandwidth was nearly the same for either port. The lower free running power port had a reflection locking bandwidth that was narrower than its transmission locking one. Just the opposite was found at the other port. A detailed analytical model for two-port injection-locked oscillators is presented, and its results agree quite well with the experiments. A critique of the literature on this topic is included to clear up misconceptions and errors. It is concluded that two-port injection-locked oscillators may prove useful in certain communication systems. Author

N88-12728# Sandia National Labs., Albuquerque, N. Mex.
IMPEDANCE OF PASSIVE LITHIUM ANODES IN SOCl2 SOLUTIONS UNDER LOW-FIELD POLARIZATION
F. M. Delnick 1987 17 p Presented at the 172nd Meeting of the Electrochemical Society, Honolulu, Hawaii, 18 Oct. 1987
(Contract DE-AC04-76DP-00789)
(DE88-000922; SAND-87-1106C; CONF-871027-35) Avail: NTIS HC A02/MF A01

Passive films on lithium anodes in Li/SOCl2 batteries inhibit the kinetic response of the batteries. Under potentiostatic polarization, passive lithium anodes exhibit current delay; and under galvanostatic polarization, they exhibit voltage delay. In this report, low-field potentiostatic polarization and complex impedance measurements are used to determine the mechanism of current delay. The time-dependent transition in the current is caused by the injection of excess cation defects into the film. These excess defects decrease the film resistance and repartition the overvoltage to the LiCl/SOCl2 interface. The enhanced defect concentration at this interface and/or the enhanced field accelerate the dissipation of the film. DOE

N88-12729# Lawrence Livermore National Lab., Calif.
GENERATING MESHES FOR FINITE-DIFFERENCE ANALYSIS USING A SOLID MODELER
G. W. Laguna, W. T. White, and B. K. Cabral Sep. 1987 83 p
(Contract W-7405-eng-48)
(DE88-001458; UCID-21189) Avail: NTIS HC A05/MF A01

One tool used by the Engineering Research Division of LLNL to help analyze the behavior of electronic systems in hostile environments is 3D finite-difference time-domain (FDTD) computation. FDTD codes solve Maxwell's equations,the differential equations of electromagnetism, on a uniform lattice of points. It is this uniform lattice, or mesh, that distinguishes finite-difference codes from other codes. The simple mesh makes FDTD codes computationally more efficient than other codes, which enables them to run larger problems and to run faster (up to thirty times faster than finite-element codes, for example). Therefore, within the Engineering Department at LLNL, Electronics Engineering (EE) has initiated a project to develop a mesh generator that will provide meshes suitable for FDTD analysis. This report describes the results of the first year of EE's FDTD Mesh Generation Project. During this year a preliminary version of an automated mesh generator was built and used to create a mesh of an object of interest to the High-Power Microwave Program, namely an electrically detonatable land mine. The code was verified by meshing basic solids such as spheres and cylinders. Because of the design of the code, there is no software limitation to the size of meshes that can be accommodated. The algorithm with a mesh space of approximately 500,000 cells has been demonstrated. The mesh generator can detect certain objects with walls that are thinner than the width of a cell. The code has internal graphics for viewing objects as they appear prior to being converted to a finite-difference representation. Additionally, via data files, the code is coupled to two external graphics packages for visually checking the meshes, namely TAURUS on the Cray and a new code, IMAGE, on the Silicon Graphics IRIS workstation. DOE

N88-12730*# Jet Propulsion Lab., California Inst. of Tech., Pasadena.
INTERFEROMETRY THEORY FOR THE BLOCK 2 PROCESSOR
J. B. Thomas 15 Oct. 1987 101 p
(Contract NAS7-918)
(NASA-CR-181551; NAS 1.26:181551; JPL-Pub-87-29) Avail: NTIS HC A06/MF A01 CSCL 09C

Presented is the interferometry theory for the Block 2 processor, including a high-level functional description and a discussion of data structure. The analysis covers the major processing steps: cross-correlation, fringe counter-rotation, transformation to the frequency domain, phase calibration, bandwidth synthesis, and extraction of the observables of amplitude, phase, phase rate, and delay. Also included are analyses for fractional bitshift correction, station clock error, ionosphere correction, and effective frequencies for the observables. Author

N88-12731# California Univ., Berkeley. Electronics Research Lab.
THE PIERCE DIODE WITH AN EXTERNAL CIRCUIT. PART 1: SIMULATIONS IN THE LINEAR REGIME
W. S. Lawson 22 Jul. 1987 17 p
(Contract DE-FG03-86ER-53220)
(DE88-000413; UCB/ERL-M-87/51) Avail: NTIS HC A03/MF A01

The linear theory for the eigenfrequencies of the extended Pierce diode for resistive, capacitive, and inductive external circuits is tested via computer simulation with the PDW1 code, and is verified to within the accuracy of the simulation (between 1% and .01% depending on the circumstances). The simulations were remarkably inexpensive in terms of computer time, and could have been performed on a personal computer. DOE

N88-12732# Ames Lab., Iowa.
ALTERNATING CURRENT CIRCUIT THEORY AND PULSED NMR (NUCLEAR MAGNETIC RESONANCE)
B. C. Gerstein Jun. 1987 37 p
(Contract W-7405-eng-82)
(DE88-000641; IS-4924) Avail: NTIS HC A03/MF A01

Pulsed NMR, by definition, deals with time varying excitations. These excitations, supplied by resonant circuits which provide a pulse of radiofrequency (frequencies in the megahertz region) power to a resonant circuit containing, among other things, a coil of wire, or inductor, in which a sample under investigation is placed for purposes of the nuclear magnetic resonance experiment. There are therefore two features of the pulse NMR experiment. First is the fact that we have available a source of continuous wave (CW) alternating current at some angular frequency, omega, measured in radians per second. This source is generally supplied by an ultrastable device called a frequency synthesizer. The second feature of the pulsed NMR experiment is that the sample is not continuously irradiated, but a pulse of radiofrequency oscillation is applied to the sample. This report discusses alternating current theory, resonant circuits and the equipment used in this experiment. DOE

N88-12733# Fermi National Accelerator Lab., Batavia, Ill.
RESISTOR COOLING IN A VACUUM
R. Crittenden and J. Krider 31 Jul. 1987 6 p
(Contract DE-AC02-76CH-03000)
(DE88-000696; FNAL-TM-1468) Avail: NTIS HC A02/MF A01

This note describes thermal measurements which were done on a resistor operating both in air at one atmosphere pressure and in a vacuum of a few milliTorr. The motivation for this measurement was our interest in operating a BGO crystal-photomultiplier tube-base assembly in a vacuum, as a synchrotron radiation detector to tag electrons in the MT beam. We wished to determine what fraction of the total resistor power was dissipated by convection in air, in order to know whether there would be excessive heating of the detector assembly in a vacuum. DOE

N88-12734# Sandia National Labs., Albuquerque, N. Mex. Corrosion Div.
CORROSION SUSCEPTIBILITY STUDY OF CANDIDATE PIN MATERIALS FOR ALTC (ACTIVE LITHIUM/THIONYL CHLORIDE) BATTERIES
Francine S. Bovard and Wendy R. Cieslak Sep. 1987 38 p
(Contract DE-AC04-76DP-00789)
(DE88-001449; SAND-87-0707) Avail: NTIS HC A03/MF A01

The corrosion susceptibilities of eight alternate battery pin material candidates for ALTC (Active Lithium/Thionyl Chloride) batteries in 1.5M LiAlCl4/SOCl2 electrolyte have been investigated using ampule exposure and electrochemical tests. The thermal expansion coefficients of these candidate materials are expected to match Sandia-developed Li-corrosion resistant glasses. The corrosion resistances of the candidate materials, which included three stainless steels (15-5 PH, 17-4 PH, and 446), three Fe-Ni glass sealing alloys (Kovar, Alloy 52, and Niromet 426), a Ni-based alloy (Hastelloy B-2) and a zirconium-based alloy (Zircaloy), were compared to the reference materials Ni and 316L SS. All of the candidate materials showed some evidence of corrosion and, therefore, did not perform as well as the reference materials. The Hastelloy B-2 and Zircaloy are clearly unacceptable materials for this application. Of the remaining alternate materials, the 446 SS and Alloy 52 are the most promising candidates. DOE

N88-12735# Sandia National Labs., Albuquerque, N. Mex. Exploratory Batteries Div.
RELIABILITY OF LI/SO2 CELLS FOR LONG-LIFE APPLICATIONS
Samuel C. Levy 1987 6 p Presented at the 172nd Meeting of the Electrochemical Society, Honolulu, Hawaii, 18 Oct. 1987
(Contract DE-AC04-76DP-00789)
(DE88-001360; SAND-87-0924C; CONF-871027-37) Avail: NTIS HC A02/MF A01

Commercial Li/SO2 cells and cells with various modifications to improve long-life performance and reliability were placed on a real-time test of up to six years duration. Analysis of the results has indicated the primary mode of failure to be corrosion of the glass in the glass-to-metal seal. Use of a corrosion-resistant glass has resulted in a significant improvement in both performance and reliability. Units deployed in the field have demonstrated a reliability of greater than 0.999 using cells containing all the Sandia developed modifications. DOE

N88-12686*# Jet Propulsion Lab., California Inst. of Tech., Pasadena.
MEASUREMENT AND ANALYSIS OF CRYOGENIC SAPPHIRE DIELECTRIC RESONATORS AND DROS
G. J. Dick *In its* The Telecommunications and Data Acquisition Report 15 Nov. 1987 p 73-80 (For primary document see N88-12679 04-32)
Avail: NTIS HC A15/MF A01 CSCL 09C

N88-12687*# Jet Propulsion Lab., California Inst. of Tech., Pasadena.
INDUCTANCE EFFECTS IN THE HIGH-POWER TRANSMITTER CROWBAR SYSTEM
J. Daeges and A. Bhanji *In its* The Telecommunications and Data Acquisition Report 15 Nov. 1987 p 81-88 (For primary document see N88-12679 04-32)
Avail: NTIS HC A15/MF A01 CSCL 09C

N88-12688*# Jet Propulsion Lab., California Inst. of Tech., Pasadena.
LOW-NOISE CRYOGENIC TRANSMISSION LINE
D. Norris *In its* The Telecommunications and Data Acquisition Report 15 Nov. 1987 p 89-93 (For primary document see N88-12679 04-32)
Avail: NTIS HC A15/MF A01 CSCL 09C

N88-12689*# Jet Propulsion Lab., California Inst. of Tech., Pasadena.
A 2.3-GHz CRYOGENICALLY COOLED HEMT AMPLIFIER FOR DSS 13
L. Tanida *In its* The Telecommunications and Data Acquisition Report 15 Nov. 1987 p 94-101 (For primary document see N88-12679 04-32)
Avail: NTIS HC A15/MF A01 CSCL 09C

N88-12700*# Jet Propulsion Lab., California Inst. of Tech., Pasadena.
ON THE VLSI DESIGN OF A PIPELINE REED-SOLOMON DECODER USING SYSTOLIC ARRAYS
H. M. Shao, L. J. Deutsch, and I. S. Reed (University of Southern California, Los Angeles.) *In its* The Telecommunications and Data Acquisition Report 15 Nov. 1987 p 224-234 (For primary document see N88-12679 04-32)
Avail: NTIS HC A15/MF A01 CSCL 09C

N88-12701*# Jet Propulsion Lab., California Inst. of Tech., Pasadena.
A PROCEDURAL METHOD FOR THE EFFICIENT IMPLEMENTATION OF FULL-CUSTOM VLSI DESIGNS
P. Belk and N. Hickey *In its* The Telecommunications and Data Acquisition Report 15 Nov. 1987 p 235-246 (For primary document see N88-12679 04-32)
Avail: NTIS HC A15/MF A01 CSCL 09C

34 FLUID MECHANICS AND HEAT TRANSFER

Includes boundary layers; hydrodynamics; fluidics; mass transfer; and ablation cooling.

For related information see also *02 Aerodynamics* and *77 Thermodynamics and Statistical Physics.*

N88-12736# Helsinki Univ. (Finland). Dept. of Mechanical Engineering.
THEORY OF ONE AND TWO-PASS CROSS-FLOW HEAT EXCHANGER
J. Saastamoinen Jun. 1987 18 p Prepared in cooperation with Technical Research Centre of Finland, Helsinki
(PB87-225157; Rept-25; ISBN-951-754-179-1) Avail: NTIS HC A03/MF A01 CSCL 20D

There are numerous ways to connect heat exchangers. The fluids may be mixed or unmixed between heat exchangers and inside them. The heat exchangers may be connected in counterflow or in cocurrent flow. The efficiency of the cross-flow system and the efficiency charts are usually calculated by using numerical methods. Analytical solutions are valuable. New analytical solutions for the two-pass cross-flow heat exchangers are derived. GRA

N88-12737# Technische Hogeschool, Delft (Netherlands). Onderafdeling der Wiskunde en Informatica.
TOTAL LINEARISATION METHOD FOR SOLVING VISCOUS FREE BOUNDARY FLOW PROBLEMS BY THE FINITE ELEMENT METHOD
N. P. Kruyt, C. Cuvelier, A. Segal, and J. vanderZanden 1986 24 p
(PB87-222337; Rept-86-30) Copyright Avail: NTIS HC A03/MF A01 CSCL 20D

A Total Linearization Method is derived for solving steady viscous free boundary flow problems (including capillary effects) by the finite element method. It is shown that the influence of the geometrical unknown in the totally linearized weak formulation can be expressed in terms of boundary elements. This means that the implementation of the method is simple. Numerical experiments show that the iterative method gives accurate results and converges very fast. GRA

N88-12738# Brookhaven National Lab., Upton, N. Y.
OPTIMIZED GROUND COUPLED HEAT PUMP MECHANICAL PACKAGE
M. A. Catan 1987 8 p
(Contracts DE-AC02-76CH-00016; DE-AC05-84OR-21400)
(DE87-014899; BNL-36225) Avail: NTIS HC A02/MF A01

This project addresses the question of how well a ground coupled heat pump system could perform with a heat pump which was designed specifically for such systems operating in a northern climate. Conventionally, systems are designed around water source heat pumps which are not designed for ground coupled heat pump application. The objective of the project is to minimize the life cycle cost for a ground coupled system given the freedom to design the heat pump and the ground coil in concert. In order to achieve this objective a number of modeling tools were developed which will likely be of interest in their own right. DOE

N88-12739# Lawrence Livermore National Lab., Calif.
FULLY DEVELOPED TURBULENCE VIA FEIGENBAUM'S PERIOD-DOUBLING BIFURCATIONS
M. Duong-van Aug. 1987 35 p Presented at the International Conference on Physics of Chaos and Systems Far From Equilibrium, Monterey, Calif., 11 Jan. 1987
(Contract W-7405-eng-48)
(DE88-000242; UCRL-97268; CONF-870159-3) Avail: NTIS HC A03/MF A01

Since its publication in 1978, Feigenbaum's predictions of the onset of turbulence via period-doubling bifurcations have been thoroughly borne out experimentally. In this paper, Feigenbaum's theory is extended into the regime in which we expect to see fully developed turbulence. We develop a method of averaging that imposes correlations in the fluctuating system generated by this map. With this averaging method, the field variable is obtained by coarse-graining, while microscopic fluctuations are preserved in all averaging scales. Fully developed turbulence will be shown to be a result of microscopic fluctuations with proper averaging. Furthermore, this model preserves Feigenbaum's results on the physics of bifurcations at the onset of turbulence while yielding additional physics both at the onset of turbulence and in the fully developed turbulence regime. DOE

N88-12740# Army Military Personnel Center, Alexandria, Va.
USE OF A THERMODYNAMIC ANALOG FOR PNEUMATIC TRANSPORT IN HORIZONTAL PIPES Final Report
Craig A. Myler Aug. 1987 304 p
(AD-A184076) Avail: NTIS HC A14/MF A01 CSCL 13G

A study of pneumatic transport of solids in 0.0254 m and 0.0504 m diameter pipes was conducted. Measurements included particle velocities and pressure drop. A model based on thermodynamic analogy was employed to describe the phase behavior of horizontal flows. Electrostatic effects to include equipment damaging discharges were discussed. A new design equation for particle velocity and pressure drop was presented. GRA

N88-12741# Naval Postgraduate School, Monterey, Calif.
NUMERICAL SIMULATION OF UNSTEADY SEPARATED FLOWS Ph.D. Thesis
Samir I. Mostafa Jun. 1987 141 p
(AD-A184132) Avail: NTIS HC A07/MF A01 CSCL 20D

Two unsteady flows dominated by the occurrence of separation are simulated through the use of the discrete vortex model. The first of these is a sinusoidally oscillating flow about a circular cylinder at a Keulegan-Carpenter number of K = 10. The vortex model has been combined with the boundary layer calculations and the positions of the separation and stagnation points, the evolution of the wake, the velocity and pressure distributions, and the instantaneous forces have been calculated and compared, whenever possible, with those obtained experimentally. The model has successfully simulated the occurrence of the transverse half Karman vortex street. The calculated positions of the vortices are in good agreement with those obtained experimentally. The measured and calculated in-line forces and the differential pressure distributions showed reasonably good agreement. The second simulation dealt with a rapidly decelerating flow about a two-dimensional sharp-edged camber. An extensive study of the velocity field in the vicinity of the singular points led to the development of a novel method for the introduction of vorticity at variable time intervals. The measured and calculated characteristics of the flow, such as the evolution of the wake and the forces acting on the camber, were found to be in excellent agreement. GRA

N88-12742# Texas Univ., Austin. Aerosol Research Lab.
PLUME MECHANICS AND AEROSOL GROWTH PROCESSES Contractor Report, Aug. 1983 - Jul. 1986
J. R. Brock Jul. 1987 221 p
(Contract DAAK11-83-K-0006)
(AD-A184467; CRDEC-CR-87084) Avail: NTIS HC A10/MF A01 CSCL 19A

Results of research on major topics in aerosol science and technology are summarized. These include: (1) Formation of liquid and solid particles by nucleation and growth; (2) Influence of smoke plume/puff dispersion on aerosol growth; (3) Nonlinear interactions of laser beams with aerosols; and (4) Aerosol filtration. GRA

N88-12743# Los Alamos National Lab., N. Mex.
THE TAB METHOD FOR NUMERICAL CALCULATION OF SPRAY DROPLET BREAKUP
P. J. ORourke and A. A. Amsden 1987 12 p Presented at the International Fuels and Lubricants Meeting and Exposition, Toronto, Ontario, 2 Nov. 1987
(Contract W-7405-eng-36)
(DE87-011756; LA-UR-87-2105-Rev; CONF-871142-1-Rev)
Avail: NTIS HC A03/MF A01

A short history is given of the major milestones in the development of the stochastic particle method for calculating liquid fuel sprays. The most recent advance has been the discovery of the importance of drop breakup in engine sprays. A new method, called TAB, for calculating drop breakup is presented. Some theoretical properties of the method are derived; its numerical implementation in the computer program KIVA is described; and comparisons are presented between TAB-method calculations and experiments and calculations using another breakup model. DOE

N88-12744# Catholic Univ. of America, Washington, D.C.
OPTICAL INSTRUMENTATION AND STUDY OF GAS-SOLID SUSPENSION FLOWS
S. C. Ling and H. P. Pao 1987 16 p Presented at the 18th Annual Meeting of the Fine Particle Society, Boston, Mass., 3 Aug. 1987
(Contract DE-FG22-86PC-90956)
(DE88-000147; CONF-8708134-2) Avail: NTIS HC A03/MF A01

The study of the mechanics of solid-suspension flows is performed by a darkfield optical technique using micro-glass spheres as the suspension solid. The unique specular-reflection characteristic of the glass sphere is utilized for local measurements of the particle size, concentration, and velocity in the flow field. This technique permits one to obtain a more complete knowledge concerning the nature of suspended solid flows. A comprehensive description of both the instrumentation technique and the mechanics of low concentration solid-suspension flow is presented. The recent discovery of the existence of micro-hairpin vortices in the intermediate sublayer-flow may have an important relationship to the transport of solid particles. DOE

N88-12745# Lawrence Livermore National Lab., Calif.
A FREE-LAGRANGE METHOD FOR 2-D COMPRESSIBLE FLOWS
W. P. Crowley Aug. 1987 24 p Presented at the Workshop on Particle Methods in Fluid Dynamics and Plasma Physics, Los Alamos, N. Mex., 13 Apr. 1987
(Contract W-7405-eng-48)
(DE88-000216; UCRL-97323; CONF-8704168-4) Avail: NTIS HC A03/MF A01

Numerical algorithms for solving fluid flow problems are traditionally constructed in either an Eulerian or a Lagrangian reference frame. In the Lagrangian formulation, the mesh follows the fluid motion and this automatically guarantees the accurate treatment of interfaces. However, when large relative motions occur in the flow, the mesh becomes tangled and the problem must be repaired before it can continue. The Free-Lagrange method overcomes this difficulty by automatically reconnecting the mesh when necessary during run time. The main advantage of the Free-Lagrange formulation is that problems are completed in a minimum amount of calendar time with an accurate solution. Another advantage is that the general mesh structure permits a great deal of flexibility in generating the initial mesh. The disadvantage is that solutions may be more expensive in terms of CPU time because the general structure of the mesh means that gather/scatter parts of the code are not vectorized. Recent hardware developments help ameliorate this consideration. DOE

N88-12746# Southwest Research Inst., San Antonio, Tex.
EXPERIMENTS ON DENSELY-LOADED NON-NEWTONIAN SLURRIES IN LAMINAR AND TURBULENT PIPE FLOWS Quarterly Technical Progress Report No. 4
J. T. Park, R. J. Mannheimer, T. A. Grimley, and T. B. Morrow 15 Oct. 1987 42 p
(Contract DE-FG22-86PC-90962)
(DE88-000719; DOE/PC-90962/T4) Avail: NTIS HC A03/MF A01

An experimental description of the flow structure of non-Newtonian slurries in the laminar, transitional, and full turbulent pipe flow regimes is the primary objective of this research. Measurements include rheological characterization of the fluid and local fluid velocity measurements with a laser Doppler velocimeter (LDV). Optical access to the flow is gained through a test section and model slurry which are both transparent. The model slurry is formulated from silica gel particles and hydrocarbon liquid mixture whose indices of refraction are matched so that light is not scattered from the particles. Experiments are being conducted in a large-scale pipe slurry flow facility with an inside pipe diameter of 51 mm (2 inches). Detailed flow measurements including turbulence quantities such as Reynolds stress will be taken with a two-component two-color LDV. The present research indicates that non-Newtonian slurries are possible with concentrations of a few percent by weight of small particles whose sizes are one micron or less. A non-Newtonian slurry from small particles could maintain large particles (100 micron size) at high concentrations in

suspension almost indefinitely. Such a slurry would prevent particle fallout and its associated problems. DOE

N88-12747*# Hughes Aircraft Co., Torrance, Calif. Electron Dynamics Div.
ADVANCED RADIATOR CONCEPTS UTILIZING HONEYCOMB PANEL HEAT PIPES Final Technical Report, Jun. 1982 - Jun. 1987
G. L. Fleischman, S. J. Peck, and H. J. Tanzer Oct. 1987 107 p
(Contract NAS9-16581; NASA Order W-30746)
(NASA-CR-172017; NAS 1.26:172017) Avail: NTIS HC A06/MF A01 CSCL 20D

The feasibility of fabricating and processing moderate temperature range vapor chamber type heat pipes in a low mass honeycomb panel configuration for highly efficient radiator fins for potential use on the space station was investigated. A variety of honeycomb panel facesheet and core-ribbon wick concepts were evaluated within constraints dictated by existing manufacturing technology and equipment. Concepts evaluated include type of material, material and panel thickness, wick type and manufacturability, liquid and vapor communication among honeycomb cells, and liquid flow return from condenser to evaporator facesheet areas. A thin-wall all-welded stainless steel design with methanol as the working fluid was the initial prototype unit. It was found that an aluminum panel could not be fabricated in the same manner as a stainless steel panel due to diffusion bonding and resistance welding considerations. Therefore, a formed and welded design was developed. The prototype consists of ten panels welded together into a large panel 122 by 24 by 0.15 in., with a heat rejection capability of 1000 watts and a fin efficiency of essentially 1.0. Author

N88-12748*# Alabama Univ., Huntsville. Dept. of Mechanical Engineering.
STUDIES OF PRESSURE-VELOCITY COUPLING SCHEMES FOR ANALYSIS OF INCOMPRESSIBLE AND COMPRESSIBLE FLOWS M.S. Thesis
Gregory Wayne Burgreen [1987] 95 p
(Grants NAG8-092; NAG8-053; NGT01-008-803)
(NASA-CR-181526; NAS 1.26:181526) Avail: NTIS HC A05/MF A01 CSCL 20D

Two pressure-velocity coupling schemes, both of which solve the fully implicit discretized equations governing the flow of fluids were examined, and the capability of performing large Reynolds number, low Mach number compressible flow calculations were assessed. The semi-implicit iterative SIMPLE algorithm is extended to handle transient compressible flow calculations. This extension takes into account a strong coupling between the pressure and temperature through a correction procedure, based on the equations of state. Results obtained from the extended SIMPLE algorithm are then compared to similar results obtained from the non-iterative PISO algorithm. Both time-dependent and steady state calculations were performed using an axisymmetric 2:1 pipe expansion geometry and laminar flow conditions corresponding to Reynolds number of 1000 and Mach number of 2.0. For calculations simulating a time-dependent compression/expansion process, both schemes exhibit transient features in excellent agreement with each other, and moreover, the PISO method shows a significant computational time reduction of 60 percent over the SIMPLE scheme, regardless of the time step size or grid size employed. The effects of numerical diffusion are shown to be significant in these calculations. For steady state compressible flows, however, the SIMPLE algorithm displays increasing computational efficiency over the PISO method as the time step sizes employed to reach steady state conditions are decreased. Author

N88-12749# Los Alamos National Lab., N. Mex.
THREE-DIMENSIONAL, FREE-LAGRANGE HYDRODYNAMICS
H. Trease 1987 22 p Presented at the Numerical Applications for Particle Methods Meeting, Los Alamos, N. Mex., 6 Apr. 1987
(Contract W-7405-eng-36)
(DE88-000494; LA-UR-87-3163; CONF-8704208-1) Avail: NTIS HC A03/MF A01

This paper describes the algorithms that make up a 3-D version of the Free-Lagrange Method. The basic method involves the explicit integration of the fluid flow equations over control volumes formed by Voronoi cells. A Voronoi cell is an arbitrary, convex polyhedron that has plane polygon faces. The nearest neighbors of any given mass point are identified by noting the mass point that lies on the opposite side of a given Voronoi face. The nearest neighbors of a mass point are allowed to change in response to the (Lagrange) motion of the mass points. This implies that the mesh reorganizes itself as the mass points move with the fluid motion. DOE

N88-12750# Sandia National Labs., Albuquerque, N. Mex.
NACHOS 2: A FINITE ELEMENT COMPUTER PROGRAM FOR INCOMPRESSIBLE FLOW PROBLEMS. PART 2: USER'S MANUAL
D. K. Gartling Sep. 1987 129 p
(Contract DE-AC04-76DP-00789)
(DE88-001451; SAND-86-1817) Avail: NTIS HC A07

Complete user instructions are given for the finite element, fluid mechanics and heat transfer code, NACHOS II. DOE

N88-12751# Sandia National Labs., Livermore, Calif.
TOPAZ: THE TRANSIENT ONE-DIMENSIONAL PIPE FLOW ANALYZER: AN UPDATE ON CODE IMPROVEMENTS AND INCREASED CAPABILITIES
W. S. Winters Sep. 1987 39 p
(Contract DE-AC04-76DR-00789)
(DE88-001781; SAND-87-8225) Avail: NTIS HC A03/MF A01

TOPAZ is a user-friendly computer code for modeling the one-dimensional, transient physics of multi-species gas transfer in arbitrary arrangements of pipes, valves, vessels, and flow branches. This report, the fourth in a series of reports documenting TOPAZ, discusses coding improvements and the addition of new capabilities. These improvements make the current version of TOPAZ considerably more versatile than the original version which was distributed last year. For example, the new version does not restrict the user to modeling only hydrogen and helium isotope flows. Users now have the capability of modeling arbitrary gas mixture flows. In addition users may define time-dependent functions for mass generation, energy deposition, flow area, and maximum integration time step. Parallel flow paths and flows through channels having noncircular cross-sections may now be simulated. Improvements in TOPAZ mesh generation have been made which permit users to add additional plumbing to existing models without renumbering the mesh. DOE

N88-12752*# National Aeronautics and Space Administration. Lewis Research Center, Cleveland, Ohio.
SIMILAR SOLUTIONS FOR VISCOUS HYPERSONIC FLOW OVER A SLENDER THREE-FOURTHS-POWER BODY OF REVOLUTION
Chin-Shun Lin Dec. 1987 23 p
(NASA-TM-100205; ICOMP-87-7; E-3803; NAS 1.15:100205)
Avail: NTIS HC A03/MF A01 CSCL 20D

For hypersonic flow with a shock wave, there is a similar solution consistent throughout the viscous and inviscid layers along a very slender three-fourths-power body of revolution The strong pressure interaction problem can then be treated by the method of similarity. Numerical calculations are performed in the viscous region with the edge pressure distribution known from the inviscid similar solutions. The compressible laminar boundary-layer equations are transformed into a system of ordinary differential equations. The resulting two-point boundary value problem is then solved by the Runge-Kutta method with a modified Newton's method for the corresponding boundary conditions. The effects of wall temperature, mass bleeding, and body transverse curvature are investigated. The induced pressure, displacement thickness, skin friction, and heat transfer due to the previously mentioned parameters are estimated and analyzed. Author

N88-12753# National Aeronautical Lab., Bangalore (India). Fluid Mechanics Div.
OBSERVATIONS ON THE HYDRODYNAMIC FLOW VISUALIZATION AT ONERA
S. Sundaram May 1987 24 p
(PD-FM-8718) Avail: NTIS HC A03/MF A01

Flow visualization serves a useful purpose in developing better geometrical shapes for both airborne and ground vehicles. In particular, it can indicate onset of flow separation and vortice formation. Visualization in water has found more widespread application than that in air because of the large range of available techniques. Some important observations made on the flow visualization technique employed in the hydrodynamic flow visualization facilities at ONERA (France) are described. Details regarding tunnel design, techniques used, and other related data are given. Author

N88-12754*# Universities Space Research Association, Huntsville, Ala. Systems Dynamics Lab.
A MULTIPLE-TIME-SCALE TURBULENCE MODEL BASED ON VARIABLE PARTITIONING OF TURBULENT KINETIC ENERGY SPECTRUM Final Report
S.-W. Kim and C.-P. Chen (Alabama Univ., Huntsville.) Nov. 1987 42 p
(Contract NAS8-35918)
(NASA-CR-179222; NAS 1.26:179222) Avail: NTIS HC A03/MF A01 CSCL 20D

A multiple-time-scale turbulence model of a single point closure and a simplified split-spectrum method is presented. In the model, the effect of the ratio of the production rate to the dissipation rate on eddy viscosity is modeled by use of the multiple-time-scales and a variable partitioning of the turbulent kinetic energy spectrum. The concept of a variable partitioning of the turbulent kinetic energy spectrum and the rest of the model details are based on the previously reported algebraic stress turbulence model. Example problems considered include: a fully developed channel flow, a plane jet exhausting into a moving stream, a wall jet flow, and a weakly coupled wake-boundary layer interaction flow. The computational results compared favorably with those obtained by using the algebraic stress turbulence model as well as experimental data. The present turbulence model, as well as the algebraic stress turbulence model, yielded significantly improved computational results for the complex turbulent boundary layer flows, such as the wall jet flow and the wake boundary layer interaction flow, compared with available computational results obtained by using the standard kappa-epsilon turbulence model. Author

N88-12755 California Univ., Berkeley.
BLOWUP FOR A NONLINEAR EVOLUTION EQUATION AND SELF-REPRODUCING STRAINED SHEAR LAYERS Ph.D. Thesis
Robert Andrew Palais 1986 279 p
Avail: Univ. Microfilms Order No. DA8718112

A nonlinear nonlocal evolution equation modeling the dynamics of stretched vortices in an incompressible fluid was studied. An equation was derived by John Neu for perturbations to the Burgers' strained vortex layer steady solution of the 3D Navier-Stokes equations. The blowup results are also presented as consequences of a general theorem which is applicable to many other evolution equations. The theorem is proved by a method using a comparison principle for the Fourier transform of certain solutions. In the context of Neu's paper it inidicates that a strained shear layer can be a self-reproducing structure in the turbulent mixing layer.
Dissert. Abstr.

N88-12756 Syracuse Univ., N. Y.
COMPARATIVE STUDIES IN THE NEAR-FIELD OF TURBULENT TRANSPORTS OF HEATED AND UNHEATED JETS NORMAL TO A CROSS STREAM Ph.D. Thesis
Xiong He 1986 422 p
Avail: Univ. Microfilms Order No. DA8717031

A new velocity vector measurement technology is developed with a specially designed slant rotating hot wire and an optimally selected set of measurement orientations. A directional measurement validity checking procedure is proposed to solve some ambiguities in the determination of the velocity direction from the rotational symmetry. Experiments were performed in the near field of turbulent unheated and heated jets issuing normal to a cross stream of the velocity vector, temperature, and fluctuation fields. The wake vortex shedding was extracted from the fluctuation spectrum. Attention was paid to the dynamics of linear momentum and angular momentum on control volumes and surfaces. A unified mechanics based on the vorticity dynamics was proposed for the interaction between the jet fluid and its surroundings. This mechanics was supported by independent measurements. The development of the jet body shape, the entrainment of mass flux and momentum, the balance of momentum force were analyzed based on this mechanics. A consistent explanation for the jet vortex roll up and tail vortex formation was presented from this view point. Dissert. Abstr.

N88-12757 Marquette Univ., Milwaukee, Wis.
ANALYTICAL STUDIES OF AXIALLY SYMMETRIC MOTION OF AN INCOMPRESSIBLE VISCOUS FLUID BETWEEN TWO CONCENTRIC ROTATING SPHERES Ph.D. Thesis
John Charles Gagliardi 1987 270 p
Avail: Univ. Microfilms Order No. DA8716861

The equations of motion for a viscous incompressible fluid in a rotating spherical annulus, subject to case study boundary conditions were develped. The specific boundary conditions were: one or both spheres rotates with prescribed constant angular velocities; and one sphere rotates under the action of an applied constant or impulsive torque. The solution of the stream and circumferential functions were obtained in the form of a series of powers of the Reynolds number. The number of independent variables in the perturbation equations were reduced by specifying the meridional dependence with Gegenbauer functions and then employing the concept of orthogonality. Time dependent fluid flow for radius ratios (R sub 2/R sub 1) equal to 0.2, 0.5, and 0.9 were studied. Accurate results for the perturbation solution were obtained for smaller values of Re as the gap size was increased. Transient profiles were obtained for the dimensionaless torque, dimensionaless angular velocity of the rotating sphere, and the dimensionaless angular momentum of the fluid. These values were found to be strongly dependent on boundary conditions, physical ratios and weakly dependent on Re for Re is less than or equal to 100. Dissert. Abstr.

N88-12758 Brown Univ., Providence, R. I.
EQUILIBRIA, LATTICES AND CHAOTIC DYNAMICS OF POINT VORTICES Ph.D. Thesis
James Bernard Kadtke 1987 161 p
Avail: Univ. Microfilms Order No. DA8715516

Three separate and somewhat unrelated problems involving two-dimensional, inviscid Hamiltonian point vortices are examined. A method is presented for analytically determining stationary configurations for point vortices, for systems which may have arbitrary numbers and strengths of vortices. A technique is explained for exactly calculating the energy of a two-dimensional lattice of vortices, for a Bravais lattice with arbitrary cell parameters and arbitrary numbers of vortices in the primitive cell. The Hamiltonian and dynamical equations are also calculated, and these are used to implement a numerical relaxation technique to determine minimum energy configurations corresponding to stable or metastable lattices. The integrability of the motion of a vortex system in two types of bounded domains, the ellipse and the rectangle, was investigated. The Green's functions for these two domains are calculated using conformal mapping techniques, and these are used to construct the Hamiltonian and dynamical equations. Numerical experiments are then performed to determine the regularity of the motion of a two-vortex system in both boundary geometries, and in both cases these systems are stochastic, indicating the absence of a second global integral for either boundary. Finally, a numerical experiment is performed to investigate some of the structure of the phase space, by perturbing

a period-one torus and examining the behavior around the resulting hyperbolic fixed point. Dissert. Abstr.

N88-12759 Johns Hopkins Univ., Baltimore, Md.
TURBULENT MIXING IN A ROTATING, STRATIFIED FLUID Ph.D. Thesis
Yigh Noh 1987 226 p
Avail: Univ. Microfilms Order No. DA8716640

An experimental study was described of the effect of rotation on turbulent mixing when the turbulence in the mixed layer is generated by an oscillation-grid. Two types of experiments were performed: one in which deepening of the upper mixed layer in a stable, two-fluid system was investigated; and one in which a stabilizing buoyancy flux was imposed to form a steady pycnocline. In the first experiment, it was found that rotatin suppresses entrainment to the depth D sub b and the results were interpreted qualitatively by considering the inertial wave propagation to the lower layer under rotation. It was observed that vortices were generated rather abruptly in the lower layer as the mixed layer deepened, and the depth of the mixed layer at the time of the appearance of the vortices was comparable to the Ekman length. In the second experiment, the formation of steady mixed layer was observed and its depth represented as D = L(sub Q)f(X), where X = (L sub Q/L sub E) squared. The depth of transition from three-dimensional turbulence to rotation-dominated two-dimensional turbulence was found to be the same as the Ekman length (L sub E) in homogeneous, rotating turbulence. Dissert. Abstr.

N88-12760 Princeton Univ., N. J.
AN EXPERIMENTAL INVESTIGATION OF UNSTEADINESS IN SWEPT SHOCK WAVE/TURBULENT BOUNDARY LAYER INTERACTIONS Ph.D. Thesis
Triet Thuong Tran 1987 223 p
Avail: Univ. Microfilms Order No. DA8716903

The unsteadiness of various swept shock wave/turbulent boundary layer interactions was examined by measuring wall pressure fluctuations using multiple, high frequency responses, pressure transducers mounted flush with the test surface. The interactions were generated by a variety of test models to study the effect of shock strength and model geometry on the unsteadiness. Tests with nominally 2-D interactions generated by compression ramps were also made for comparison with the results of swept interactions. The unsteadiness is characterized by an intermittent region of relatively low frequency and large amplitude pressure fluctuations, accompanied by a local rms pressure peak at the beginning of the interactions. Results further indicate that the level of the rms peak, for either swept or 2-D interactions, can be understood in terms of the motion of the initial pressure gradient and the spatial extent of the intermittent region. These results lead to the observation, for the first time, that local conical scaling law can also be applied to statistical quantities. Results of the two-point correlation and VITA analyses show that the swept and 2-D ramp interactions are inherently different. Results further show these large scale structures have a small effect on unsteadiness, suggesting that other mechanisms are responsible for unsteadiness in interactions. Dissert. Abstr.

N88-12761 Colorado State Univ., Fort Collins.
CONTINUATION FINITE ELEMENT ANALYSIS OF VISCOELASTIC FLUIDS Ph.D. Thesis
Tai-Whang Chow 1987 126 p
Avail: Univ. Microfilms Order No. DA8717132

A finite element procedure using a mixed formulation and a predictor-corrector type continuation algorithm for the analysis of two dimensional steady state flows of viscoelastic fluids is described. As a simple but nontrivial test example, radial flow immenating from a line by the numerical discretization and believed to be the cause for previous numerical failures, are shown and branch solution paths are followed by step length adjustment and by convergent tolerance relaxation. A technique for jumping over bifurcation points is presented and used to increase the Weissenberg number with no apparent limit for the radial flow problem. A second example related to extrusion of viscoelastic material is also analyzed. Steady state velocity fields, deviatoric stress distributions and pressure distributions for several different Weissenberg numbers are presented with bifurcation points and turning points noted. Dissert. Abstr.

N88-12762 Texas Univ., Austin.
OPTIMIZATION OF EXPLICIT TIME-STEPPING ALGORITHMS AND STREAM-FUNCTION-COORDINATE (SFC) CONCEPT FOR FLUID DYNAMICS PROBLEMS Ph.D. Thesis
Chung-Yuan Huang 1987 149 p
Avail: Univ. Microfilms Order No. DA8717434

A new formulation of the stream function based on a stream function coordinate (SFC) concept for inviscid flow field calculations is presented. In addition, a new method is developed not only to accelerate, but also to stabilize the iterative schemes for steady and unsteady, linear and non-linear, scalar and system of coupled, partial differential equations. With this theory, the limitation on the time step size of an explicit scheme for solving unsteady problems and the limitation on the relaxation factors of an iterative scheme for solving steady state problems could be analytically determined. Moreover, this theory allows the determination of the optimal time steps for explicit time-stepping schemes and the optimal values of the acceleration factors for iterative schemes, if the transient behavior is immaterial. Dissert. Abstr.

N88-12763*# National Aeronautics and Space Administration. Lewis Research Center, Cleveland, Ohio.
EXPERIMENTAL STUDY OF THERMOCAPILLARY FLOWS IN A THIN LIQUID LAYER WITH HEAT FLUXES IMPOSED ON THE FREE SURFACE
Chun-Liang Lai, Paul S. Greenberg, and An-Ti Chai 1988 13 p Presented at the Second International Symposium on Experimental Methods for Microgravity Material Science Research, Phoenix, Ariz., 25-28 Jan. 1988
(NASA-TM-100252; E-3831; NAS 1.15:100252) Avail: NTIS HC A03/MF A01 CSCL 20D

To study thermocapillary flows in a two-dimensional thin liquid layer with heat fluxes imposed on the free surface experimentally, a long tray configuration was employed to simulate the infinite layer. The surface temperature distribution due to thermocapillary convective for different flow regimes was measured and compared with theoretical predictions. A short tray configuration was also employed to study the end wall effects (insulating or conducting). The results show that for a strong convection flow with an insulating wall as the boundary the surface temperature distribution became quite uniform. Consequently, the thermocapillary driving force was greatly reduced. On the other hand, a strong fluid motion always existed adjacent to the conducting wall because of the large surface temperature gradient near the wall. Author

N88-12764# Brown Univ., Providence, R. I. Div. of Engineering.
GEOMETRIC ANALYSIS OF ENSEMBLE OF SOLUTIONS IN TWO-PHASE FLOW AND COMPLETE RESOLUTION OF PROBLEM OF CHOKING Final Report, Feb. 1984 - Apr. 1987
J. Kestin Aug. 1987 8 p
(Contract DE-AC02-84ER-13167)
(DE88-001687; DOE/ER-13167/1) Avail: NTIS HC A02/MF A01

The search for choking 'criteria' was abandoned in the conviction that the onset of choking and the appropriate conditions for its occurrence, must be obtained as logical consequences of the mathematical model of the two-phase flow employed by the analyst. Second, it was determined that the preponderant majority of mathematical models for steady-state flows (those germane to the problem of choking) consist of a number, n greater than or equal to 2, of nonlinear ordinary differential equations in n unknowns and in a single independent variable - the space coordinate z. Third, it was recognized that the preceding schema dominates the analysis of dynamical systems which have been the subject of intensive and fruitful mathematical studies. The latter have achieved remarkable progress in the understanding of the nature of the problem and of its handling by topological-geometric

methods. The application of these methods to two-phase flow models constitutes the prime achievement of this project; it led to the formulation of an analytic supplement which determines the existence of choking and the location of the critical cross section. DOE

N88-12634# Joint Publications Research Service, Arlington, Va.
EXCITATION OF NATURAL OSCILLATIONS OF A BOUNDARY LAYER BY AN EXTERNAL ACOUSTIC FIELD Abstract Only
A. A. Maslov and N. V. Semenov *In its* USSR Report: Engineering and Equipment 28 May 1987 p 92 Transl. into ENGLISH from Izvestiya Akademii Nauk SSSR Mekhanika Zhidkosti i Gaza (Moscow, USSR), no. 3, May - Jun. 1986 p 74-78 Previously announced as X87-71990 (For primary document see N88-12621 04-31)
Copyright Avail: NTIS HC A06/MF A01

N88-12636# Joint Publications Research Service, Arlington, Va.
DYNAMICS OF REVERSE FLOWS AT PUMP INLET Abstract Only
N. S. Yershov *In its* USSR Report: Engineering and Equipment 28 May 1987 p 93 Transl. into ENGLISH from Izvestiya Vysshikh Uchebnykh Zavedeniy: Aviatsionnaya Tekhnika (Kazan, USSR), no. 4, Oct. - Dec. 1985 p 49-53 (For primary document see N88-12621 04-31)
Copyright Avail: NTIS HC A06/MF A01

N88-12838# Joint Publications Research Service, Arlington, Va.
ASYMPTOTIC FORM OF STATIONARY SOLUTIONS OF THE NAVIER-STOKES EQUATIONS FOR LARGE REYNOLDS NUMBERS Abstract Only
S. I. Chernyshenko *In its* USSR Report: Earth Sciences 22 Jul. 1986 p 15 Transl. into ENGLISH from Doklady Akademii Nauk SSSR (Moscow, USSR), v. 285, no. 6, Dec. 1985 p 1353-1355 Original language document was announced in IAA as A86-24313 Prev. announced as X87-71987 1987 (For primary document see N88-12831 04-42)
Avail: NTIS HC A05/MF A01

N88-12842# Joint Publications Research Service, Arlington, Va.
DISPERSION EQUATION FOR PLANE CAPILLARY-GRAVITY WAVE ON FREE SURFACE OF VISCOUS INCOMPRESSIBLE FLUID Abstract Only
P. N. Antonyuk *In its* USSR Report: Earth Sciences 22 Jul. 1986 p 20 Transl. into ENGLISH from Doklady Akademii Nauk SSSR (Moscow, USSR), v. 286, no. 6, Feb. 1986 p 1324-1328 (For primary document see N88-12831 04-42)
Avail: NTIS HC A05/MF A01

N88-12851# Joint Publications Research Service, Arlington, Va.
THEORY OF HEAT AND MOISTURE EXCHANGE BETWEEN FINELY DISPERSE STORM-GENERATED SPRAY AND TURBULENT AIR FLOW Abstract Only
Ye. P. Borisenkov and M. A. Kuznetsov *In its* USSR Report: Earth Sciences 22 Jul. 1986 p 54 Transl. into ENGLISH from Izvestiya Akademii Nauk SSSR: Fizika Atmosfery i Okeana (Moscow, USSR), v. 21, no. 11, Nov. 1985 p 1191-1197 (For primary document see N88-12831 04-42)
Avail: NTIS HC A05/MF A01

35 INSTRUMENTATION AND PHOTOGRAPHY

Includes remote sensors; measuring instruments and gages; detectors; cameras and photographic supplies; and holography.

For aerial photography see *43 Earth Resources and Remote Sensing*. For related information see also *06 Aircraft Instrumentation*, and *19 Spacecraft Instrumentation*.

N88-12765# Pacific Northwest Labs., Richland, Wash.
NONCONTACT TEMPERATURE MEASUREMENTS OF HOT STEEL BODIES USING AN ELECTROMAGNETIC ACOUSTIC TRANSDUCER (EMAT)
D. M. Boyd and P. D. Sperline Jul. 1987 9 p Presented at the Review of Progress in Quantitative NDE, Williamsburg, Va., 21 Jun. 1987
(Contract DE-AC06-76RL-01830)
(DE88-000560; PNL-SA-14791; CONF-870691-3) Avail: NTIS HC A02/MF A01

A noncontacting sensor system for measuring the average internal temperature of hot steel objects has been developed. The system uses a pulsed ruby laser for the generation of the acoustic wave and a pulsed Electromagnetic Acoustic Transducer (EMAT) as the receiver in a through-transmission technique. The pulsed EMAT design has been successfully tested to 1300° Celsius on a nine-inch-long stainless steel sample. The system measures the time-of-flight of the acoustic wave, which is coupled with the part dimension to determine the average acoustic velocity. From a calibrated relationship between velocity and temperature, the average sample temperature is determined. DOE

N88-12766# Sandia National Labs., Albuquerque, N. Mex.
TRACKING THROUGH TURBULENCE AT THE TONOPAH TEST RANGE
J. D. Weiss Sep. 1987 36 p
(Contract DE-AC04-76DP-00789)
(DE88-001448; SAND-87-1111) Avail: NTIS HC A03/MF A01

This report discusses the deleterious effects of turbulence on tracking images at the Tonopah Test Range and the means to overcome them. After reviewing the existing technologies used to compensate for optical aberrations in real-time and trying to restore sample images by using computer algorithms, we have concluded that raising the camera 20 to 30 ft is a simple, and probably the only, expedient available to overcome most of the turbulence problem at that facility. Previous experimental and theoretical studies, as well as our own photographic study, support that conclusion. DOE

N88-12767# Oak Ridge Gaseous Diffusion Plant, Tenn. Quality and Technical Services Div.
EVALUATION OF THE SENSIDYNE TOXIC GAS SENSOR FOR HF (HYDROGEN FLUORIDE) VAPOR
W. D. Bostick, E. C. Angel, and T. H. Hamilton Sep. 1987 37 p
(Contract DE-AC05-84OT-21400)
(DE88-000647; K/PS-5076) Avail: NTIS HC A03/MF A01

A diffusion-type electrochemical sensor is evaluated for the detection of hydrogen fluoride (HF) vapor, both for use as an area monitor safety device and as a stack gas monitor. Response characteristics of individual sensor assemblies are variable, but with frequent, proper calibration, the Sensidyne HF Toxic Alert device is demonstrated to provide accurate, sensitive, and relatively rapid response to this contaminant. We describe a calibration flow cell and gas permeation apparatus capable of delivering a predictable (and easily confirmed) concentration of contaminant to the sensor in a safe manner. DOE

N88-12768# Fermi National Accelerator Lab., Batavia, Ill.
SOME NEW IDEAS IN LIQUID DETECTORS
D. F. Anderson Aug. 1987 15 p Presented at the Conference on Position-Sensitive Detectors, London, United Kingdom, 7 Sep. 1987

(Contract DE-AC02-76CH-03000)
(DE88-000732; FNAL/C-87/127; CONF-8709153-1) Avail: NTIS HC A03/MF A01

Three new techniques for the detection and imaging of the energy deposited in liquid detectors are discussed. These are electrostatic imaging in liquid argon doped with methane, photon mediated charge amplification in liquid xenon containing photosensitive dopants, and electron extraction from liquid argon and 2,2,4,4-TMP with charge amplifiction in the gas phase. DOE

N88-12769# Mound Lab., Miamisburg, Ohio.
OPTIMIZATION OF DILATOMETER TEST PROCEDURES
W. R. Henderson and D. A. Waker 14 Sep. 1987 32 p
(Contract DE-AC04-76DP-00053)
(DE87-014998; MLM-3452) Avail: NTIS HC A03/MF A01

An investigation was conducted to determine the best methods for obtaining the most accurate and precise data from a Theta dual pushrod dilatometer. The dilatometer uses computer-acquired data for both temperature and differential expansion measurements. Various potential sources of error were examined to determine their actual effects. It is learned that the type of thermocouple, thermocouple location, ramp rate, method of data acquisition, statistical deviations of multiple sample runs, and measuring head temperature stability all had large effects on the data. In addition, the linear variable differential transformer, errors in measuring sample lengths, and errors in algorithms used for reference expansion had insignificant effects. These tests were based on sample expansions typically used in production glass-ceramic samples (50-250 x E-07 in./in./deg C). DOE

36 LASERS AND MASERS

Includes parametric amplifiers.
For related information see also *76 Solid-State Physics*.

N88-12770# Sandia National Labs., Albuquerque, N. Mex.
RO-VIBRATIONAL LASER SPECTROSCOPY OF ESD NEUTRALS FROM CHEMISORBED SPECIES
A. R. Burns, E. B. Stechel, and D. R. Jennison 1987 7 p Presented at the 3rd International Workshop on Desorption Induced by Electronic Transitions, Shelter Island, N.Y., 20 May 1987
(Contract DE-AC04-76DP-00789)
(DE87-013011; SAND-87-0644C; CONF-8705194-1) Avail: NTIS HC A02/MF A01

Ever since the introduction of intense tunable laser radiation, the fields of molecular spectroscopy and dynamics have expanded tremendously. Indeed, with each technical improvement in laser resolution and output power, new applications have emerged with correspondingly increased levels of sophistication and information. In the field of electron-stimulated desorption (ESD), not only has the utilization of lasers resulted in the detection of neutral species, which were previously difficult to observe without specially-designed analyzers, but also the quantum-specific nature of the resonant laser interaction with the neutrals has yielded valuable information concerning internal energies. In this article, we will discuss some of the experimental methods in the application of laser resonance-ionization spectroscopy (RIS) to the study of the ESD of neutrals, in particular, chemisorbed NO and CO desorption from Pt(111). We will also show how the detailed information obtained in these experiments has identified a new desorption mechanism. DOE

N88-12771# Los Alamos National Lab., N. Mex.
SPECTRAL EVOLUTION EQUATION FOR THE SIDEBAND INSTABILITY IN A FREE-ELECTRON LASER OSCILLATOR
P. J. Channell 1987 17 p Presented at the 9th International Free-Electron Laser Conference, Williamsburg, Va., 14 Sep. 1987
(Contract W-7405-eng-36)
(DE88-000510; LA-UR-87-2961; CONF-8709110-7) Avail: NTIS HC A03

Assuming that the light remains in the optical system while the electrons pass through and are lost, we have derived the evolution equation for an arbitrary optical spectrum in a free-electron laser oscillator. The resulting integrodifferential equation includes the effects of linear optical system losses (due to either mirror reflectivity or clipping), the usual small signal gain term, and a quadratic nonlinear term that includes the effects of saturation and coupling to sideband modes. The effects of detuning and particle beam current and energy variations can easily be included. Results of numerical solutions of the equations for various conditions will be presented. DOE

N88-12772# OptiMetrics, Inc., Burlington, Mass.
REVIEW OF INVERSION TECHNIQUES FOR SPACEBORNE LIDAR SYSTEMS Report, Apr. - Sep. 1986
Derek W. Gallon and John R. Hummel Dec. 1986 89 p
(Contract F19628-85-C-0178)
(AD-A184164; OMI-181; AFGL-TR-86-0266; SR-2) Avail: NTIS HC A05/MF A01 CSCL 20F

An examination of inversion techniques applicable for a spaceborne lidar system has been made. The purpose has been to recommend a technique that could be used with the lidar system under development by AFGL. In a Rayleigh atmosphere with no or minimal gaseous absorption, a power law relationship between backscattering and extinction exists in which k=1. In an atmosphere with aerosols and clouds, the assumption of a power law relationship is tenuous at best. An examination of the literature leads us to conclude that the power law relationship has no physical basis to support its extensive use. For any application probing different regions of the atmosphere and different types of aerosols, one cannot assume a single set of power law parameters for the entire atmosphere. GRA

N88-12773# Naval Research Lab., Washington, D.C.
THE FREE ELECTRON LASER SIDEBAND INSTABILITY RECONSIDERED Interim Report
S. Riyopoulos and C. M. Tang 12 Aug. 1987 53 p
(AD-A184269; NRL-MR-6028) Avail: NTIS HC A04/MF A01 CSCL 09C

The problem of sideband growth in a free electron laser (FEL) is studied using canonical formalism. The exact unperturbed orbits, without sidebands, are obtained in action-angle variables for all particles. Integration of the linearized Vlasov equation with perturbing sidebands over the unperturbed orbits yields the sideband growth for both trapped and untrapped particles. The unperturbed distribution f sub o is in an equilibrium with the main signal field. It is found that upper and lower sidebands that are symmetric relative to the FEL frequency have opposite growth rates. There is no differentiation in the magnitude of the growth between upper and lower sidebands. The stability is determined by the sign of df sub o/d(omega sub b), i.e., the relative population of oscillation quanta (h-bar)(omega sub b), omega sub b = bounce frequency around resonance. The shear d (omega sub b)/dj, where J is the action variable, is stabilizing and distributions with gradients df sub o/dJ localized near the separatrix have the minimum growth rates. The structure and scaling of the unstable spectrum are different from previous results obtained for electrons localized at the bottom of the pondermotive well. GRA

N88-12774# HY-Tech Research Corp., Radford, Va.
LASER INDUCED FLUORESCENT STUDY OF RELATIVISTIC ELECTRON BEAMS Final Report, 28 Apr. 1983 - 31 Jan. 1986
Edward J. Yadlowsky and Robert C. Hazelton Jun. 1987 69 p
(Contract F29601-83-C-0024)
(AD-A184456; AFWL-TR-85-140) Avail: NTIS HC A04/MF A01 CSCL 20G

The magnetic fields associated with a relativistic electron beam propagating in a gas provide information about the net current distribution in the beam and the stability of the beam with respect to hose, hollowing, and flute instabilities. In principle, these magnetic fields can be measured using Faraday rotation techniques, or by measuring the Zeeman splitting of atomic/ionic transitions using emission spectroscopy. This work investigates the measurement of magnetic field contours by optically pumping atoms/ions with a narrow band dye laser tuned to a Zeeman

shifted electronic transition, and recording the fluorescence radiation emitted perpendicular to the excitation laser. This technique has important advantages because the dye laser is the frequency selective element and the magnetic field measurement is reduced to an intensity measurement with the spatial resolution determined by the irradiated volume viewed by the collection optics. The studies were carried out in a high current discharge operated in neon and neon/nitrogen mixtures at pressures of 0.1 to 2 kPa. A grazing incidence flash lamp pumped dye laser having a band width of 0.004 to 0.009-nm was used to fluoresce the 585.25-nm transition in neutral neon. The frequency spectrum of the radiation was recorded with a photomultiplier by scanning the laser frequency. The measurements reveal an LIF spectrum which is double-humped under certain conditions. The overall width of the spectrum is consistent with the Stark broadened line width anticipated for the plasma condition, and the minimum at the line center cannot be attributed to self absorption in the plasma. GRA

N88-12775# Los Alamos National Lab., N. Mex.
HIGH-POWER RF-PULSED MODULATORS FOR THE LOS ALAMOS FREE-ELECTRON LASER
W. J. D. Johnson, M. T. Lynch, P. J. Tallerico, D. R. Keffeler, and J. O. Hornkohl Sep. 1987 10 p Presented at the 9th International Free-Electron Laser Conference, Williamsburg, Va., 14 Sep. 1987
(Contract W-7405-eng-36)
(DE88-000514; LA-UR-87-2911; CONF-8709110-9) Avail: NTIS HC A02/MF A01

In the RF-driven free-electron laser (FEL) at the Los Alamos National Laboratory, there are two pulsed-power RF modulators as sources for two tandem, side-coupled 20-MeV linear accelerators. The RF power used to control the cavity fields is supplied by two 5.5-MW modulating anode klystrons operating at a center frequency of 1300.2 MHz. The modulation of the 125 kV klystron is achieved by using a triode switch tube that provides a pulse width up to 300 microns and a pulse repetition rate up to 10 Hz. This paper describes the present configuration of these two duplicate systems and presents plans for meeting the requirements of future RF FEL experiments at Los Alamos. DOE

N88-12776# Los Alamos National Lab., N. Mex.
THE LASERTRON RF GENERATOR FOR FEL (FREE-ELECTRON LASER) APPLICATIONS
P. J. Tallerico Sep. 1987 11 p Presented at the 9th International Free-Electron Laser Conference, Williamsburg, Va., 14 Sep. 1987
(Contract W-7405-eng-36)
(DE88-000515; LA-UR-87-2910; CONF-8709110-8) Avail: NTIS HC A03/MF A01

The lasertron RF generator uses an RF-modulated laser beam to generate a tightly bunched electron beam that is accelerated by a dc power supply to the fractional megawatt region. The tightly bunched beam then crosses an output cavity where most of the kinetic energy may be extracted. The bunching is so good that efficient microwave generation at 3 GHz and above is feasible, and three projects worldwide are under way for these frequencies. All three existing projects focus on the linear collider application of high peak power with good efficiency, short output pulses, and low average power. A short review of these projects is presented. The purpose of this paper is to discuss the lasertron as the RF generator for free-electron laser (FEL) RF systems. The author has developed a ring model of the lasertron device that shows excellent dc-to-RF conversion efficiency at high output power over the 400- to 1700-MHz frequency range. The issue of the lasertron advantages at higher average output power is also explored. First-order estimates of the weight versus frequency and power are also made. An experiment using the Los Alamos photoinjector to make a lasertron is discussed. DOE

N88-12777# Los Alamos National Lab., N. Mex.
LONG-RANGE PULSELENGTH SCALING OF 351nm LASER DAMAGE THRESHOLDS
S. R. Foltyn and L. J. Jolin 1986 14 p Presented at the Boulder Damage Symposium, Boulder, Colo., 3 Nov. 1986
(Contract W-7405-eng-36)
(DE87-014754; LA-UR-87-2856; CONF-8611154-2) Avail: NTIS HC A03

In a series of experiments incorporating 351nm pulselength of 9, 26, 54, and 625ns, it was found that laser damage thresholds increased as (pulselength)/sup x/, and that the exponent averaged 0.36 and ranged, for different samples, from 0.23 to 0.48. Similar results were obtained when only catastrophic damage was considered. Samples included Al2O3/SiO2 in both AR and HR multilayers, HR's of Sc2O3/SiO2 and HfO2/SiO2, and Al-on-pyrex mirror; 9ns thresholds were between 0.2 to 5.6 J/sq cm. When these data were compared with a wide range of other results - for wavelengths from 0.25 to 10.6 microns and pulselengths down to 4ps - a remarkably consistent picture emerged. Damage thresholds, on average, increase approximately as the cube-root of pulselength from picoseconds to nearly a microsecond, and do so regardless of wavelength or material under test. DOE

N88-12778# Los Alamos National Lab., N. Mex.
ANALYSIS OF SIDEBAND SPECTRA FROM UNTAPERED UNDULATOR USING ANALYTICAL TECHNIQUE
H. Takeda 1987 25 p Presented at the 9th International Free-Electron Laser Conference, Williamsburg, Va., 14 Sep. 1987
(Contract W-7405-eng-36)
(DE87-014763; LA-UR-87-2808; CONF-8709110-10) Avail: NTIS HC A03/MF A01

The sideband spectrum appearing in the free-electron laser is analyzed. For an untapered undulator, we predict the wavelengths of local peaks arising from the sidebands; they are compared with numerical simulations. In our analytical theory, three laser-driving terms are derived: one term does not chirp in frequency, drives a number of sidebands simultaneously, and is always the strongest term with a fixed strength. The other two driving terms, which also drive multiple frequencies, chirp to both directions from a resonant frequency. We assume that the sidebands originate from a dipole oscillation of average electron energy where the average energy oscillates with the synchrotron oscillation frequency. DOE

N88-12779# Lawrence Livermore National Lab., Calif.
XUV EMISSION FEATURES FROM THE LIVERMORE SOFT X-RAY LASER EXPERIMENTS
M. J. Eckart, J. H. Scofield, and A. U. Hazi Sep. 1987 6 p Presented at the International Colloquium on UV and X-ray Spectroscopy, Beaulieu-Sur-Mer, France, 9 Sep. 1987
(Contract W-7405-eng-48)
(DE88-000420; UCRL-96494; CONF-8709143-1) Avail: NTIS HC A02/MF A01

The measured wavelengths in the soft x-ray region for 3p to 3s and 3d to 3p transitions in neon-, sodium-, and magnesium-like selenium are presented. The experimental results for the neon-like ions are compared to theoretical wavelength values and with values extrapolated along the isoelectronic sequence. The ions were contained in a plasma heated in a line-focus of a Nd-glass laser. The measurements were made with a time-gated microchannel-plate-intensified grazing incidence spectrograph. DOE

N88-12780# Lawrence Livermore National Lab., Calif.
THERMAL STRESS IN THE EDGE CLADDING OF NOVA GLASS LASER DISKS
J. H. Pitts, M. K. Kong, and M. A. Gerhard 28 Sep. 1987 6 p Presented at the Symposium on Fusion Engineering, Monterey, Calif., 12 Oct. 1987
(Contract W-7405-eng-48)
(DE88-000425; UCRL-96662; CONF-871007-3) Avail: NTIS HC A02

We calculated thermal stresses in Nova glass laser disks having light-absorbing edge cladding glass attached to the periphery with an epoxy adhesive. Our closed-form solutions indicated that, because the epoxy adhesive is only 25 microns across, it does not significantly affect the thermal stress in the disk or cladding glass. Our numerical results showed a peak tensile stress in the

cladding glass of 24 MPa when the cladding glass had a uniform absorption coefficient of 7.5/cm. This peak value is reduced to 19 MPa if surface parasitic oscillation heating is eliminated by tilting the disk edges. The peak tensile stresses exceed the typical 7 to 14-MPa working stress for glass; however, we have not observed any disk or cladding glass failures at peak Nova fluences of 20 J/sq cm . We have observed delamination of the epoxy adhesive bond at fluences several times that which would occur on Nova. Replacement laser disks will incorporate cladding with a reduced absorption coefficient of 4.5/cm. Recent experiments show that this reduced absorption coefficient is satisfactory. DOE

N88-12781# Oak Ridge Gaseous Diffusion Plant, Tenn. Enrichment Technology Applications Center.
CALIBRATION OF A LASER-PUMPED, THERMOGRAPHIC PHOSPHOR REMOTE THERMOMETRY SYSTEM
S. W. Allison, M. R. Cates, L. J. Dowell, G. T. Gillies, W. N. Lutz, and R. C. Ritter Aug. 1987 20 p Presented at the International Congress on Applications of Lasers and Electro Optics, Washington, D.C., 1 Nov. 1986 Prepared in cooperation with Virginia Univ., Charlottesville
(Contract DE-AC05-84OT-21400)
(DE88-000452; K/ETAC-8; CONF-8611137-3) Avail: NTIS HC A03/MF A01

Remote thermometry via laser-induced fluorescence (LIF) of a thermographic phosphor (doped refractory oxide) is a sensitive and potentially high-precision technique of growing usefulness in thermal metrology. A typical LIF measurement system consists of detection, waveguide, and signal analysis hardware. The systematic errors due to each of these components must be evaluated in order to arrive at an overall error budget for the measurement. In this paper, we consider the problems arising in calibration and characterization of the instrumentation used to monitor a fluorescing Y2O3 : Eu phosphor. DOE

N88-12782# Los Alamos National Lab., N. Mex.
ENERGY BALANCE IN LASER-IRRADIATED VAPORIZING DROPLETS
A. Zardecki and R. L. Armstrong Sep. 1987 7 p Presented at the CRDEC Scientific Conference on Obscuration and Aerosol Research, Aberdeen, Md., 1 Jun. 1987 Prepared in cooperation with New Mexico State Univ., Las Cruces
(Contract W-7405-eng-36)
(DE88-000525; LA-UR-87-3056; CONF-8706199-3) Avail: NTIS HC A02/MF A01

We analyze the interactions of atmospheric aerosols with a high-energy laser beam. The energy balance equation allows us to compute the conversion of the pulse energy into temperature increase, vaporization, conduction, and convection. We also include the shrinkage term whose significance has recently been discussed by Davies and Brock. DOE

N88-12783# California Univ., Berkeley. Lawrence Berkeley Lab.
CENTER FOR X-RAY OPTICS, 1986
Jul. 1987 30 p
(Contract DE-AC03-76SF-00098)
(DE88-000715; LBL-23795) Avail: NTIS HC A03/MF A01

The Center for X-Ray Optics has made substantial progress during the past year on the development of very high resolution x-ray technologies, the generation of coherent radiation at x-ray wavelengths, and, based on these new developments, had embarked on several scientific investigations that would not otherwise have been possible. The investigations covered in this report are topics on x-ray sources, x-ray imaging and applications, soft x-ray spectroscopy, synchrotron radiation, advanced light source and magnet structures for undulators and wigglers. DOE

N88-12784 Rice Univ., Houston, Tex.
GAMMA-RAY OPTICS OF MULTI-BEAM BORRMANN MODES WITH POSSIBLE APPLICATIONS TO NUCLEAR LASING Ph.D. Thesis
J. Timothy Hutton 1986 179 p
Avail: Univ. Microfilms Order No. DA8718729

There is a possibility that an isomer can be found which could be used to obtain enough population inversion density to bring about nuclear lasing. If realized, a gamma ray laser will be a new source of radiation in the approx. 1 A region of unexcelled spectral brightness and coherence. The results of research is that the effects of crystallinity are of crucial importance in considerations regarding gamma ray lasers, bringing in new elements to laser theory. Certain multibeam Borrmann eigenmodes of the radiation field in a perfect crystal have much stronger coupling to the emitting nuclei, and much less photoabsorption, than modes in the amorphous case. A crystal containing emitters would require orders of magnitude less population inversion density in order to lase than would an amorphous sample of similar material. Multibeam Borrmann modes also have several applications to single photon optics, particularly the problem of anomalous emission of a gamma ray by an internal source of multipolarity M1 or higher. While this effect can occur for a 2 beam Borrmann mode, even stronger anormalous emission is possible into multibeam Borrmann modes. Dissert. Abstr.

N88-12785# Mound Lab., Miamisburg, Ohio.
STORING PHOTOMICROGRAPHS ON OPTICAL LASER DISKS
M. H. Ransick 1987 14 p Presented at the International Metallurgical Society Symposium, Monterey, Calif., 27 Jul. 1987
(Contract DE-AC04-76DP-00053)
(DE87-013747; MLM-3449(OP); CONF-8707113-2) Avail: NTIS HC A03/MF A01

Storing duplicate photomicrographs is a common practice at many service laboratories and is a requirement for many programs performed for the government. In a large service lab, storing photographs permanently or for a period of years requires a significant amount of storage space and the film is usually expensive. An alternate method of storing photographs is to digitize the image with a PC and store the photograph on an optical laser disk drive. These disks are based on a write once read many times (WORM) technology and cannot be erased or overwritten. Each 5-1/4in disk can store 400 Mbytes of data, or about 1600 photographs, at approximately 5% of the cost of standard 4x5in instant film. DOE

N88-12786# Los Alamos National Lab., N. Mex.
OUTPUT POWER ENHANCEMENT OF AC RAMAN FREE-ELECTRON LASER
Y. T. Yan 1987 19 p Presented at the 9th International Free Electron Laser Conference, Williamsburg, Va., 14 Sep. 1987
(Contract W-7405-eng-36)
(DE88-000503; LA-UR-87-3013; CONF-8709140-1) Avail: NTIS HC A03/MF A01

The ac free-electron laser (ac FEL) uses an ac (temporally oscillating but spatially uniform) field as the pump source with the hope that electromagnetic radiation will be produced with wavelength shorter than that generated by a conventional magnet FEL. The ac field can be provided by a superconducting cavity or by a plasma wave. In this note, the effects of the thermal motion of the electron beam on the linear gain and the nonlinear saturated output power in a Raman-regime ac FEL with the launch of an electromagnetic signal wave by particle-in-cell simulations are investigated. The output power enhancement of the ac FEL either by imposing an appropriate axial electric field at the time of radiation saturation or by properly tapering the strength or the frequency of the ac pump is discussed. DOE

N88-12787# Los Alamos National Lab., N. Mex.
THE GENERATION AND SUPPRESSION OF SYNCHROTRON SIDEBANDS
R. W. Warren and J. C. Goldstein 1987 26 p Presented at the 9th International Free-Electron Laser Conference, Williamsburg, Va., 14 Sep. 1987
(Contract W-7405-eng-36)
(DE88-000532; LA-UR-87-3035; CONF-8709110-4) Avail: NTIS HC A03/MF A01

Computer simulations of FEL lasing differ in the degree to which they approximate real experiments. One of the FEL codes used extensively at Los Alamos takes account of the features of each electron micropulse and follows the growth and saturation of the optical micropulse. With no additional adjustments, this code displays the development of sidebands and demonstrates their control when optical filters of various kinds are used. Other codes that do not include a description of the micropulse do not automatically display sidebands but need to have artificial noise of some kind added. This is not unexpected because sidebands are generated by an FEL instability; instabilities, in general, need some kind of initiating disturbance. In this paper we: identify the disturbance that triggers the instability in the pulse code; discuss a practical way to suppress the instability without using filters; compare these results with experiments; and discuss these findings. DOE

N88-12788# Lawrence Livermore National Lab., Calif.
J = O TASK FORCE Interim Report
B. L. Whitten, A. U. Hazi, C. J. Keane, R. A. London, B. J. MacGowan, T. W. Phillips, M. D. Rosen, and D. A. Whelen 25 Aug. 1987 51 p
(Contract W-7405-eng-48)
(DE88-001326; UCID-21152) Avail: NTIS HC A04/MF A01

The J = O task force was instituted to analyze the theoretical and experimental information available which is relevant to solving the J = O anomaly in the neon-like selenium x-ray laser. We summarize what is presently known about neon-like x-ray lasers from experiments at LLNL and NRL, and what is known about the plasma conditions of the x-ray laser plasma. We propose several hypotheses to explain the J = O anomaly, and discuss the arguments for and against each. Finally, we propose a series of experiments to further elucidate the solution to this problem. DOE

N88-12789# Los Alamos National Lab., N. Mex.
COMPARISON OF SIDEBAND SPECTRA OBTAINED FROM ANALYTICAL FORMULA AND FROM NUMERICAL SIMULATION IN FREE-ELECTRON LASER
H. Takeda 1987 14 p Presented at the 19th Fluid dynamics, Plasma Dynamics and Laser Conference, Honolulu, Hawaii, 8 Jun. 1987
(Contract W-7405-eng-36)
(DE88-000521; LA-UR-87-1268; CONF-870622-10) Avail: NTIS HC A03

The sideband spectrum appearing in the free-electron laser is analyzed. For an untapered undulator, we predict the wavelengths of local peaks arising from the sidebands; they are compared with numerical simulations. In our analytical theory, three laser-driving terms are derived. One term does not chirp in frequency, drives a number of frequencies simultaneously, and is always the strongest term with a fixed strength. The other two driving terms, which also drive multiple frequencies, chirp to both directions from a resonant frequency. It is assumed that the sidebands originate from a dipole oscillation of average electron energy. This oscillation frequency is equal to the synchrotron oscillation frequency. The theory predicts that the strength of the chirping terms is proportional to the amplitude of the dipole moment. DOE

N88-12790# Lawrence Livermore National Lab., Calif.
PROCEEDINGS: SDIO/DARPA WORKSHOP ON LASER PROPULSION. VOLUME 3: VIEWGRAPHS
J. T. Kare, ed. Aug. 1987 246 p Workshop held in Livermore, Calif., 7 Jul. 1986
(Contract W-7405-eng-48)
(DE88-000964; CONF-860778-Vol-3) Avail: NTIS HC A11/MF A01

Discussed is the concept of laser propulsion with regard to rockets and space vehicles. Topics covered are: laser propulsion to earth orbit; adaptive optics; free electron lasers; the Mercury Lightcraft concept; laser thermal propulsion; the ten-meter telescope; laser steering concepts; cw laser propulsion; and detonation-wave rockets. DOE

N88-12685*# Jet Propulsion Lab., California Inst. of Tech., Pasadena.
ATOMIC FREQUENCY STANDARDS FOR ULTRA-HIGH-FREQUENCY STABILITY
L. Maleki, J. D. Prestage, and G. J. Dick *In its* The Telecommunications and Data Acquisition Report 15 Nov. 1987 p 67-72 (For primary document see N88-12679 04-32)
Avail: NTIS HC A15/MF A01 CSCL 20E

N88-12705*# Jet Propulsion Lab., California Inst. of Tech., Pasadena.
THE 8.4-GHz LOW-NOISE MASER PUMP SOURCE ASSEMBLY
R. Cardenas *In its* The Telecommunications and Data Acquisition Report 15 Nov. 1987 p 278-284 (For primary document see N88-12679 04-32)
Avail: NTIS HC A15/MF A01 CSCL 20E

N88-12707*# Jet Propulsion Lab., California Inst. of Tech., Pasadena.
FAST AUTOTUNING OF A HYDROGEN MASER BY CAVITY Q MODULATION
G. J. Dick and T. K. Tucker *In its* The Telecommunications and Data Acquisition Report 15 Nov. 1987 p 295-303 (For primary document see N88-12679 04-32)
Avail: NTIS HC A15/MF A01 CSCL 20E

N88-12708*# Jet Propulsion Lab., California Inst. of Tech., Pasadena.
TRAVELING-WAVE MASER CLOSED-CYCLE REFRIGERATOR DATA ACQUISITION AND DISPLAY SYSTEM
L. Fowler and M. Britcliffe *In its* The Telecommunications and Data Acquisition Report 15 Nov. 1987 p 304-311 (For primary document see N88-12679 04-32)
Avail: NTIS HC A15/MF A01 CSCL 20E

N88-12857# Joint Publications Research Service, Arlington, Va.
CONSIDERING REFRACTION IN LEVELING WITH LASER PLANE Abstract Only
Yu. S. Galkin and G. G. Pobedinskiy *In its* USSR Report: Earth Sciences 22 Jul. 1986 p 58 Transl. into ENGLISH from Geodeziya i Kartografiya (Moscow, USSR), no. 2, Feb. 1986 p 17-21 (For primary document see N88-12831 04-42)
Avail: NTIS HC A05/MF A01

37 MECHANICAL ENGINEERING

Includes auxiliary systems (nonpower); machine elements and processes; and mechanical equipment.

N88-12791# Air Force Academy, Colo.
CALCULATION OF THE TRIBOLOGICAL PROPERTIES OF SURFACES BY SEMI-EMPIRICAL METHODS
Jon T. Swanson and James J. Stewart Jul. 1987 10 p
(AD-A184283; FJSRL-TR-87-0005) Avail: NTIS HC A02/MF A01 CSCL 11H

One method of increasing the performance of aircraft engines is to operate the engines at higher temperatures. A critical technology in this application is lubrication at high temperatures. A thorough understanding of solid lubrication of ceramic materials is therefore required. This report details our initial attempts at preparing a semi-empirical quantum chemical model of solid lubricants. In our initial study we focused on two areas of the problem. The first area was to determine the best approach to treating a model surface or lubricant. The selection was governed by providing a reasonable model without requiring an unreasonable amount of computer time for each calculation. The second area concerned obtaining an estimate of the ability of the above models to calculate the relatively weak interactions which occur between surfaces and lubricants, and between the lubricants themselves.

Our first concern was to reproduce the trends, rather than obtain the absolute values in these interactions. GRA

N88-12792# Army Lab. Command, Watertown, Mass. Material Technology Lab.
WELDABILITY OF 2219-T851 AND 2519-T87 ALUMINUM ARMOR ALLOYS FOR USE IN ARMY VEHICLE SYSTEMS Final Report
Thomas D. Wolfe and Steven A. Gedeon Jun. 1987 27 p
(AD-A184296; MTL-TR-87-28) Avail: NTIS HC A03/MF A01 CSCL 19D

A preliminary study of the weldability of 2219-T851 and 2519-T87 aluminum armor alloys was undertaken to determine the feasibility of their use in U.S. Army vehicle systems. Weldability was assessed in terms of weldment tensile strength, fatigue endurance limit, resistance to stress corrosion cracking, and ballistic shock integrity. Results show that 2519-T87 is a candidate material for replacing 5083-H131 or 7039-T64 due to high tensile strength and resistance to stress corrosion cracking. The initial weldments failed ballistic qualification to MIL-STD-1946, but the results were encouraging. It is felt that, with recent joint design changes and alterations to the critical velocity requirements in MIL-STD-1946, 2519-T87 weldments can exhibit sufficient ballistic integrity. GRA

N88-12793# Massachusetts Univ., Amherst. Dept. of Polymer Science and Engineering.
THE MODELLING OF ORIENTATION IN PLANAR POLYMER WELDING FLOWS
James C. Chien and Kung-Hwa Wei 1 Jul. 1987 3 p
(Contract N00014-85-K-0880)
(AD-A184404; TR-20) Avail: NTIS HC A02/MF A01 CSCL 13H

Welding flows occur in many important polymer processing operations. When two streams of molten polymers meet and form a weld interface, the macromolecules near the interface can be highly oriented due to the flow history. Weld interfaces would vanish very quickly in a low molecular weight material. However, macromolecules need a long time to diffuse across the interface induced orientation on the welding process is largely unknown. This work establishes a mathematical model quantifying orientation development in two-dimensional welding flows of polymer liquids and tests the model experimentally. The modelling consists of three phases: 1. Determination of the approximate kinematics by using a finite element analysis. 2. Integration of the deformation history by tracking material elements based on continuum mechanics. 3. Calculation of the stress by using a memory integral constitutive equation. The modelling applies to molten homopolymers. GRA

N88-12794# Rockwell International Corp., Golden, Colo.
LOW-COST TELEOPERATOR-CONTROLLED VEHICLE FOR DAMAGE ASSESSMENT AND DOSE MEASUREMENT
W. H. Tyree, ed. and R. L. Thomas, ed. Aug. 1987 9 p
(Contract DE-AC04-76DP-03533)
(DE88-000713; RFP-4029) Avail: NTIS HC A02/MF A01

A low-cost, disposable, radio-controlled, remote-reading, ionizing radiation and surveillance teleoperator re-entry vehicle has been built. The vehicle carries equipment, measures radiation levels, and evaluates building conditions. The system includes a black-and-white video camera to observe the environment surrounding the vehicle. The camera is mounted on a vertical elevator extendable to 11 feet above the floor. The present vehicle uses a video camera with an umbilical cord between the vehicle and the operators. Video monitoring equipment is part of the operator control system. Power for the vehicle equipment is carried on board and supplied by sealed lead-acid batteries. Radios are powered by 9-V alkaline batteries. Battery supplies for locomotion, camera, and lights are separate to ensure well-defined vehicle battery capacity while the camera and lights are in use. The radio control receiver, servo drivers, high-power amplifier and 49-MHz FM transceivers were irradiated at moderate rates with neutron and gamma doses to 3000 Rem and 300 Rem, respectively, to ensure system operation. These units performed normally during and after being exposed to these doses. DOE

N88-12795# Clemson Univ., S.C. Dept. of Electrical and Computer Engineering.
STATIC STANDING AND DYNAMIC WALKING OF A PRACTICAL BIPED ROBOT
Yuan F. Zheng and M. Rao 1987 114 p
(Contract DE-AC09-76SR-00001)
(DE88-001367; CORR-86-00241) Avail: NTIS HC A06/MF A01

The study of static standing and dynamic walking of a practical biped robot is presented in this research report. A systematic method for describing the kinematic behavior of a biped robot is first developed. The development is based on the well-known Denavit-Hartenburg convention. As a result, the method is basically the same as the one used for robot manipulators, except for some considerations given to the unique functions and structure of a biped robot. The static standing of a biped robot is then studied. It is argued that static standing capability is very important if a biped robot is to be employed in an industrial environment. In order to measure the performance of the biped in static standing in terms of its stability, two parameters, stable margin and stable index, are introduced. Based on these parameters, optimal stability of the biped robot with one-foot and two-foot standing cases are discussed. For dynamic walking, a mathematical treatment is first described. Conclusion is reached that by proper positioning of the landing, stable dynamic walking can be realized. A practical biped robot is introduced in the final part of the report. Experimental results of static standing and dynamic walking of the biped robot are presented, to verify the theoretical results. DOE

N88-12796*# National Aeronautics and Space Administration. Lewis Research Center, Cleveland, Ohio.
MEASURED PERFORMANCE OF THE HEAT EXCHANGER IN THE NASA ICING RESEARCH TUNNEL UNDER SEVERE ICING AND DRY-AIR CONDITIONS
W. Olsen, J. VanFossen, and R. Nussle Dec. 1987 29 p
(NASA-TM-100116; E-3661; NAS 1.15:100116) Avail: NTIS HC A03/MF A01 CSCL 13I

Measurements were made of the pressure drop and thermal perfomance of the unique refrigeration heat exchanger in the NASA Lewis Icing Research Tunnel (IRT) under severe icing and frosting conditions and also with dry air. This data will be useful to those planning to use or extend the capability of the IRT and other icing facilities (e.g., the Altitude Wind Tunnel-AWT). The IRT heat exchanger and refrigeration system is able to cool air passing through the test section down to at least a total temperature of -30 C (well below icing requirements), and usually up to -2 C. The system maintains a uniform temperature across the test section at all airspeeds, which is more difficult and time consuming at low airspeeds, at high temperatures, and on hot, humid days when the cooling towers are less efficient. The very small surfaces of the heat exchanger prevent any icing cloud droplets from passing through it and going through the tests section again. The IRT heat exchanger was originally designed not to be adversely affected by severe icing. During a worst-case icing test the heat exchanger iced up enough so that the temperature uniformaity was no worse than about +/- 1 deg C. The conclusion is that the heat exchanger design performs well. Author

N88-12797*# National Aeronautics and Space Administration. Lewis Research Center, Cleveland, Ohio.
ON DYNAMIC LOADS IN PARALLEL SHAFT TRANSMISSIONS. 1: MODELLING AND ANALYSIS
Edward Hsiang-Hsi Lin, Ronald L. Huston, and John J. Coy (Army Aviation Research and Development Command, Cleveland, Ohio.) Dec. 1987 16 p
(NASA-TM-100180; E-3756; NAS 1.15:100180; AVSCOM-TM-87-C-2) Avail: NTIS HC A03/MF A01 CSCL 13I

A model of a simple parallel-shaft, spur-gear transmission is presented. The model is developed to simulate dynamic loads in

power transmissions. Factors affecting these loads are identified. Included are shaft stiffness, local compliance due to contact stress, load sharing, and friction. Governing differential equations are developed and a solution procedure is outlined. A parameter study of the solutions is presented in NASA TM-100181 (AVSCOM TM-87-C-3). Author

N88-12798*# National Aeronautics and Space Administration. Lewis Research Center, Cleveland, Ohio.
ON DYNAMIC LOADS IN PARALLEL SHAFT TRANSMISSIONS. 2: PARAMETER STUDY
Edward Hsiang-Hsi Lin, Ronald L. Huston, and John J. Coy (Army Aviation Research and Development Command, Cleveland, Ohio.) Dec. 1987 13 p
(NASA-TM-100181; E-3756; NAS 1.15:100181; AVSCOM-TM-87-C-3) Avail: NTIS HC A03/MF A01 CSCL 13I

Solutions to the governing equations of a spur gear transmission model, developed in NASA TM-100180 (AVSCOM TM-87-C-2), are presented. Factors affecting the dynamic load are identified. It is found that the dynamic load increases with operating speed up to a system natural frequency. At operating speeds beyond the natural frequency the dynamic load decreases dramatically. Also. it is found that the applied load and shaft inertia have little effect on the dynamic load. Damping and friction decrease the dynamic load. Finally, tooth stiffness has a significant effect on dynamic loading; the higher the stiffness, the lower the dynamic loading. Also, the higher the stiffness the higher the rotating speed required for dynamic response. Author

N88-12799 Virginia Polytechnic Inst. and State Univ., Blacksburg.
NONLINEAR AXIAL STIFFNESS CHARACTERISTICS OF AXISYMMETRIC BOLTED JOINTS Ph.D. Thesis
Ian Royce Grosse 1987 173 p
Avail: Univ. Microfilms Order No. DA8719008

A critical assessment of the current design theory for bolted joints which is based on a linear, one-dimensional stiffness analysis is presented. A detailed nonlinear finite element analysis of a bolted joint conforming to ANSI standards was performed. The finite element results are presented in the classical bolted joint diagram and compared with the linear theory. The results revealed that the joint stiffness is highly dependent on the magnitude of the applied load. The joint stiffness changes continuously from extremely high for small applied loads to extremely low for large applied loads, contrary to the constant joint stiffness of the linear theory. The linear theory is shown to be extremely inadequate in characterizing the joint stiffness. The significance of the results in terms of the failure of bolted joints is discussed. Straight forward analytical procedures are proposed for establishing estimates of the nonlinear stiffness description and the associated bolt loading in fatigue environments. The two-dimensional, axisymmetric finite element model includes bilinear gap elements to model the interfaces. Special orthotropic elements were used to model the bolt/nut interaction. A free-body diagram approach was taken by applying loads to the outer diameter of the joint model which correspond to internal, uniformly distributed line-shear and line-moment loads in the joint. A number of convergence studies were performed to validate the solution. Dissert. Abstr.

N88-12800# Du Pont de Nemours (E. I.) and Co., Aiken, S.C. Savannah River Lab.
EXPERT ROBOTS IN NUCLEAR PLANTS
J. S. Byrd, J. J. Fisher, K. R. DeVries, and T. P. Martin 1987 11 p Presented at the Topical Meeting on Artificial Intelligence and Other Innovative Computer Applications in the Nuclear Industry, Snowbird, Utah, 31 Aug. 1987
(Contract DE-AC09-76SR-00001)
(DE87-014839; DP-MS-87-6; CONF-870832-6) Avail: NTIS HC A03/MF A01

Expert mobile robots will enhance safety and operations in nuclear plants, i.e., in nuclear applications at the Savannah River Plant. Knowledge-based expert systems are being evaluated to simplify operator control, to assist in navigation and manipulation functions, and to analyze sensory information. Development work using two research vehicles is underway to demonstrate semiautonomous, intelligent, expert robot system operation in process areas. A description of the mechanical equipment, control systems, and operating modes is presented, including the integration of onboard sensors. A control hierarchy that uses modest computational methods is being used to allow mobile robots to autonomously navigate and perform tasks in known environments without the need for large computer systems. DOE

N88-12801# Los Alamos National Lab., N. Mex.
CONTROLLING ROBOTS WITH SPOKEN COMMANDS
T. Beugelsdijk and P. Phelan Oct. 1987 12 p Presented at the 5th International Symposium on Laboratory Robotics, Hopkinton, Mass., 18 Oct. 1987
(Contract W-7405-eng-36)
(DE88-000537; LA-UR-87-3115; CONF-8710151-1) Avail: NTIS HC A03/MF A01

A robotic system for handling radioactive materials has been developed at Los Alamos National Laboratory. Because of safety considerations, the robot must be under the control of a human operator continuously. In this paper we describe the implementation of a voice-recognition system that makes such control possible, yet permits the robot to perform preprogrammed manipulations without the operator's intervention. We also describe the training given both the operator and the voice recognition-system, as well as practical problems encountered during routine operation. A speech synthesis unit connected to the robot's control computer provides audible feedback to the operator. Thus, when a task is completed or if an emergency develops, the computer provides an appropriate spoken message. Implementation and operation of this commercially available hardware are discussed. DOE

N88-12802# Sandia National Labs., Albuquerque, N. Mex.
TRIBOLOGICAL PROPERTIES OF RF-SPUTTERED MoS2 COATINGS
J. K. G. Panitz, L. E. Pope, C. R. Hills, J. E. Lyons, and D. J. Staley Aug. 1987 29 p
(Contract DE-AC04-76DP-00789)
(DE88-000266; SAND-86-2825) Avail: NTIS HC A03/MF A01

A two-part study is completed of the effects of: 1) substrate temperature; 2) substrate bias; 3) post-deposition annealing; and 4) the presence of a Cr3Si2 undercoating on the tribological properties of 300 to 500 nm MoS2 coatings which were deposited on annealed 304 stainless steel substrates. Two-level factorial statistical analysis was used to identify the relative importance of and parametric interactions between the above parameters. A Cr3Si2 undercoating and substrate bias are the most important individual factors in order to obtain MoS2 coatings with low coefficients of friction, 0.07, in lab air. The highest coefficients of friction, 0.12, occurred for coatings which were not heated during deposition nor annealed afterwards and which were deposited onto substrates that were not biased during deposition or precoated with Cr3Si2. The coatings which were deposited onto substrates that were precoated with Cr3Si2, subjected to deposition temperatures of 300 C, biased during deposition and annealed afterwards were the most wear resistant. In the second part of this study, we used the three deposition conditions that resulted in superior MoS2 coatings (300 C substrate temperature, a Cr3Si2 underlayer and post-deposition vacuum annealing) and systematically varied the substrate bias from 0 to -150 V to determine the optimal bias voltage. This indicated that the best MoS2 coatings with regards to both the coefficient of friction and wear life occurred for substrate biases ranging from -50 to -100 V. DOE

N88-12629# Joint Publications Research Service, Arlington, Va.
MULTIPATH GEAR-FRICTION PLANETARY TRANSMISSIONS Abstract Only
L. M. Ivachev *In its* USSR Report: Engineering and Equipment 28 May 1987 p 70-71 Transl. into ENGLISH from Vestnik

Mashinostroyeniya (Moscow, USSR), no. 12, Dec. 1986 p 18-21 (For primary document see N88-12621 04-31)
Copyright Avail: NTIS HC A06/MF A01

N88-12702*# Jet Propulsion Lab., California Inst. of Tech., Pasadena.
A NEW STATE SPACE MODEL FOR THE NASA/JPL 70-METER ANTENNA SERVO CONTROLS
R. E. Hill *In its* The Telecommunications and Data Acquisition Report 15 Nov. 1987 p 247-264 (For primary document see N88-12679 04-32)
Avail: NTIS HC A15/MF A01 CSCL 13I

N88-12706*# Jet Propulsion Lab., California Inst. of Tech., Pasadena.
A MODERN CONTROL THEORY BASED ALGORITHM FOR CONTROL OF THE NASA/JPL 70-METER ANTENNA AXIS SERVOS
R. E. Hill *In its* The Telecommunications and Data Acquisition Report 15 Nov. 1987 p 285-294 (For primary document see N88-12679 04-32)
Avail: NTIS HC A15/MF A01 CSCL 13I

38 QUALITY ASSURANCE AND RELIABILITY

Includes product sampling procedures and techniques; and quality control.

N88-12803# Brookhaven National Lab., Upton, N. Y.
PRAAGE: AN INTERACTIVE IBM-PC CODE FOR UNRELIABILITY/AGING ANALYSIS
R. R. Fullwood, R. E. Hall, and J. H. Taylor 1987 6 p Presented at the Joint Meeting of the American Nuclear Society and the Atomic Industrial Forum, Los Angeles, Calif., 15 Nov. 1987 Prepared in cooperation with Nuclear Regulatory Commission, Washington, D.C.
(Contract DE-AC02-76CH-00016)
(DE87-012124; BNL-NUREG-39923; CONF-871101-51) Avail: NTIS HC A02/MF A01

The more redundant a system is, the faster its unavailability increases with aging. Normally a highly redundant system has a small unavailability contribution, but aging may make it significant. This is due to the fact that, as assumed in this study, aging degradation drives up the failure rate of all redundant trains and causes a rapid loss in the effectiveness of the redundancy in reducing the unavailability. Thus aging, if allowed to cross trains, can be a significant contributor to unavailability. This conclusion demonstrates the usefulness of PRAAGE for interactive systems analysis. DOE

N88-12804# Oak Ridge Y-12 Plant, Tenn.
DEVELOPMENT OF AN ACOUSTIC EMISSION MONITOR AND MONITORING TECHNIQUES FOR LONG-TERM MONITORING OF U-0.8TI ELECTRON-BEAM WELDMENTS FOR POSTWELD CRACKING
J. W. Whittaker and M. W. Richey Jul. 1987 17 p
(Contract DE-AC05-84OS-21400)
(DE88-000819; Y-2387) Avail: NTIS HC A03/MF A01

An acoustic emission (AE) monitor and data analysis techniques have been developed for long-term monitoring to detect delayed weldment cracking. The monitor, which comprises multiple identical channels of standard electronic instruments, is capable of measuring the total AE activity in a weldment and the relative energy content of individual AE pulses. The monitor was used to detect the onset of hydrogen-assisted cracking (HAC) in U-0.8Ti electron-beam weldments. Use led to the conclusions that the monitor is adequate to study delayed-cracking phenomena, such as HAC; weldments of the U-0.8Ti alloy do produce AE after welding and intensive AE production coincides with the appearance of macrocracks and their extension; the time-dependency of HAC can be determined from the AE record; and the monitor is a valuable tool for studies of delayed-cracking behavior, such as HAC and stress-corrosion cracking. Recommendations are made to upgrade the monitor to enhance utility and data analysis efficiency and to use the monitor in stress-corrosion cracking studies. The monitor is in regular use on continuing studies of HAC in several alloys. DOE

N88-12805# Central Electricity Generating Board, London (England).
METHOD FOR THE ULTRASONIC INSPECTION OF THE SOUNDNESS OF THE METAL IN WELD JOINTS IN TWO-PLY PIPES
V. S. Grebennik and V. I. Radko [1977] 9 p Transl. into ENGLISH from Svarochnoe Proizvodstvo (USSR), no. 8, 1984 p 34-35
(BLL-CE-Trans-8265-(9022.09)) Avail: British Library Lending Div., Boston Spa, United Kingdom

In the structures belonging to thermal power engineering plant, use is made of two-ply pipes fabricated from type 20 steel. In order to ensure the desired quality of weld joints involving two-ply steels it is necessary, in addition to the ultrasonic inspection of the metal in the reinforced part of the seam, to carry out ultrasonic inspection for the purpose of detecting cracks, incomplete fusion, and lack of fusion in the root and neighboring zone in the anti-corrosion facing. Technological recommendations for the ultrasonic inspection of weld seams comprising two-ply steels were developed and put into effect under industrial conditions. The method developed can be used for periodically inspecting the metal in pipework in the course of operation. B.G.

N88-12806# Central Electricity Generating Board, London (England).
ULTRASONIC METHOD OF IMSPECTING AUSTENITIC WELD JOINTS IN NUCLEAR POWER STATION EQUIPMENT
V. I. Lantukh, V. S. Grebennik, E. V. Kardinov, N. A. Kesler, and I. F. Shchedrin [1987] 20 p Transl. into ENGLISH from Elektricheskie Stantsii (USSR), no. 1, 1987 p 9-13
(BLL-CE-Trans-8281-(9022.09)) Avail: British Library Lending Div., Boston Spa, United Kingdom

Inspection technology is optimized by using a special probe and standard flaw detectors to locate defects in the form of cracks, incomplete fusion, faulty fusion, large pores, and slag inclusions in annular butt-welds in pipes having a diameter of not less than 100 mm and in longitudinal weld joints in vessels having a diameter of 1000 mm and above, fabricated without backing rings and having a reinforcing bead and ground out excavations in the vicinity of the seam. The ultrasonic method developed is intended for detecting defects, which are dangerous in operation, in the entire weld joint section, because at present the visual and penetrant inspection methods enable defects to be found only on the outside surface of a pipe or vessel. The procedures are discussed. B.G.

39 STRUCTURAL MECHANICS

Includes structural element design and weight analysis; fatigue; and thermal stress.

For applications see *05 Aircraft Design, Testing and Performance* and *18 Spacecraft Design, Testing and Performance.*

N88-12807 British Petroleum Co. Ltd., Sunbury-on-Thames (England).
DETECTION OF DEFECTS ON STRUCTURES Patent Application
Robert Longley-Cook, inventor 4 Feb. 1987 13 p Filed 17 Jul. 1986 Priority 23 Jul. 1985 GB 8518578
(EP-Patent-0-210-794-A2; EP-Patent-Appl-SN-86305526.5; Int-Patent-Class-G01N-27/84; ETN-87-90718) Avail: UK Patent Office, 25 Southampton Buildings, London WC2A 1A4, United Kingdom

A method for detecting defects in metal structures and welds, especially underwater structures was developed. The method

involves applying to the surface of the suspected area of the defective structure a fast curing, cold cure impression material, curing the impression material into a solid cast, and lifting off the cured cast as a three dimensional profile of the defect. The impression material may be used with a magnetic ink which forms on the defective surface a cluster of magnetic particles, termed indication, simulating the defect and this indication can be lifted off on a cast of the impression material as previously. The preferred impression material is maleinized polybutadiene. ESA

N88-12808# Los Alamos National Lab., N. Mex.
NUMERICAL MODELING OF SLOW SHOCKS
D. Winske 1987 21 p Presented at the 6th Meeting of Solar Wind, Estes Park, Colo., 24 Aug. 1987
(Contract W-7405-eng-36)
(DE87-014768; LA-UR-87-2803; CONF-8708141-3) Avail: NTIS HC A03/MF A01

This paper reviews previous attempts and the present status of efforts to understand the structure of slow shocks by means of time dependent numerical calculations. Studies carried out using MHD or hybrid-kinetic codes have demonstrated qualitative agreement with theory. A number of unresolved issues related to hybrid simulations of the internal shock structure are discussed in some detail. DOE

N88-12809# New Mexico Univ., Albuquerque. Bureau of Engineering Research.
THERMOMECHANICAL CRACKING IN COATED MEDIA DUE TO HIGH SPEED ASPERITY EXCITATION Technical Report, Jan. 1986 - Jun. 1987
Frederick D. Ju and Jew-Chy Liu Apr. 1987 82 p
(Contract N00014-84-K-0252)
(AD-A184176; ME-142(87)ONR-233-3) Avail: NTIS HC A05/MF A01 CSCL 11C

This investigation considers the thermo-mechanical effects of an asperity traversing at a high speed over a semi-infinite medium with a thin hard coating surface. The general analytical solutions of the mechanical stress state, the temperature field and the thermal stress state are obtained and expressed in Fourier transform space. The asperity speed is sufficiently high such that the thermal stress is much larger than that caused by the mechanical traction of asperity pressure and friction. The analysis emphasizes the heating effect of the friction force, which leads to the initiation of the thermo-mechanical cracking, or heat-cracking in the surface layer, the substrate or their interface. For hard coating layers, the initiation of a crack will occur at a depth eta sub max (where the maximum principal thermal stresses occur). The depth is found to be controlled principally by the Peclet number. GRA

N88-12810# Ballistic Research Labs., Aberdeen Proving Ground, Md.
STEADY SHEARING IN A VISCOPLASTIC SOLID
Thomas W. Wright Jun. 1987 39 p
(AD-A184341; BRL-TR-2810) Avail: NTIS HC A03/MF A01 CSCL 20K

Steady shearing solutions are found as quadratures within the context of a simple theory of viscoplasticity which includes thermal softening and heat conduction. The solutions are illustrated by numerical examples for four commonly used versions of viscoplasticity, where each version has first been calibrated against the same hypothetical data set. It is found that, although they give results that differ in detail, the four flow laws predict qualitatively similar morphology and appear to give rough agreement with physical measurements of adiabatic shear bands. The conjecture is made that steady solutions correspond to central boundary layers for the full unsteady theory. GRA

N88-12811# Virginia Polytechnic Inst. and State Univ., Blacksburg. Dept. of Engineering Science and Mechanics.
A REFINED NONLINEAR ANALYSIS OF LAMINATED COMPOSITE PLATES AND SHELLS Final Technical Report, 1985 - 1987
J. N. Reddy Aug. 1987 50 p
(Contract DAAG29-85-K-0007)
(AD-A184436; ARO-21203.7-MA) Avail: NTIS HC A03/MF A01 CSCL 20K

This final technical report summarizes in a compact from the results of a two-year research program on the development of refined shear deformation theories of plates and shells, and their analytical solutions. The detailed results are reported in various reports and technical papers during the course of the project. A third-order, nonlinear shear deformation shell theory and finite element model that accounts for parabolic distribution of transverse shear stresses through thickness and the von Karman nonlinear strains was developed during an investigation sponsored by NASA Langley Research Center during the first year of this research. The most significant contributions of this research are: (1) the development of analytical solutions of the linear theory for various boundary conditions (the space-time concept is used to develop such solutions); and (2) the development of element models for first-ply and post-first-ply failure analysis. GRA

N88-12812# Sandia National Labs., Albuquerque, N. Mex.
MECHANICAL SHOCK TEST SPECIFICATION USING NONSTATIONARY RANDOM EXCITATION MODELS
T. J. Baca and T. L. Paez 1987 6 p Presented at the SEM Fall Meeting, Savannah, Ga., 25 Oct. 1987
(Contract DE-AC04-76DP-00789)
(DE87-013650; SAND-87-0166C; CONF-8710135-3) Avail: NTIS HC A02/MF A01

A test specification procedure is described which characterizes an operational mechanical shock environment in terms of the parameters of a nonstationary random process. These parameters define the shock test input which will be applied to a structure in the laboratory using an electro-dynamic shaker. Both the model and the procedure for identifying the model parameters are described. The technique is demonstrated by deriving test specifications from both simulated and actual shock data. The method provides a test specification technique which will allow more realistic simulation of actual mechanical shock environments in the laboratory. DOE

N88-12813# Sandia National Labs., Albuquerque, N. Mex.
A DISSIPATION PRINCIPLE AND ITS CONSEQUENCES FOR STRUCTURED SHOCK WAVES IN THERMOELASTIC MATERIALS
J. E. Dunn and R. Fosdick 1987 5 p Presented at the 5th Topical Conference of the American Physical Society on Shockwaves in Condensed Matter, Monterey, Calif., 20 Jul. 1987 Prepared in cooperation with Minnesota Univ., Minneapolis
(Contract DE-AC05-84OR-21400)
(DE87-013723; SAND-87-0967C; CONF-870753-73) Avail: NTIS HC A02/MF A01

The main purpose of this paper is to discuss how supersonic-subsonic conditions arise as a natural manifestation of the entropy inequality for any Rayleigh trajectory, whether or not the global a priori constitutive inequalities hold. Also sketched in this paper is a proof of a fundamental theorem for a steady structured shock wave of a Rayleigh trajectory. DOE

N88-12814# California Univ., Berkeley. Lawrence Berkeley Lab.
THE ACCOMMODATION OF PRECIPITATE PLATES MODELLED AS A TENSILE TEST
U. Dahmen and K. H. Westmacott Jul. 1987 13 p Presented at the 2nd International Conference on Phase Transformations in Solids, Cambridge, United Kingdom, 6 Jul. 1987
(Contract DE-AC03-76SF-00098)
(DE88-000207; LBL-23811; CONF-870719-5) Avail: NTIS HC A03/MF A01

Thin-plate precipitates in transformations with principal stains of mixed sign are approximately in a state of uniaxial stress if the interface contains an invariant line. This similarity to a tensile test can be used for the prediction of coherent and semicoherent plate habits; to relieve the uniaxial stress the tensile axis must lie in an

elastically soft direction for coherent plates and at approximately 45 degrees to the operative slip system for semicoherent plates. The habit plane is the plane that contains both the invariant line and tensile axis. Predictions of this simple model are shown to be in excellent agreement with available experimental observations on plate precipitates in several bcc interstitial alloys. DOE

N88-12815# Allied Bendix Aerospace, Kansas City, Mo.
SMALL-DIAMETER WIRE TENSILE TESTING
P. M. Mizik Sep. 1987 24 p
(Contract DE-AC04-76DP-00613)
(DE88-000835; BDX-613-3710) Avail: NTIS HC A03/MF A01

Tests were conducted on small-diameter wire (0.025 cm) per AMS 5834 to determine effects on yield and tensile strengths. Straight and coiled wire samples were heat-treated in vacuum, nitrogen, and hydrogen atmospheres to compare their effects on tensile properties. Surface flaws, strain rate sensitivity, and extensometer effects were also studied. Eight samples were included in scanning electron microscopy (SEM) fractography to document fracture mode variations. DOE

N88-12816# Lawrence Livermore National Lab., Calif.
INFLUENCE OF STRAIN RATE AND NOTCH DEPTH ON TENSILE PROPERTIES OF HITCO 6250
R. J. Sanchez, A. Goldberg, and D. R. Lesuer 20 Aug. 1987 19 p
(Contract W-7405-eng-48)
(DE88-001324; UCID-21188) Avail: NTIS HC A03/MF A01

Stress-strain data were obtained for HITCO 6250 material tested in uniaxial tension at nominal strain rates ranging from 0.15 to 400 in./in./s. Both double-edge-notched and notch-free specimens were tested. The effects of strain rate and notch depth are discussed. DOE

N88-12817*# North Carolina Univ., Charlotte. Dept. of Electrical Engineering.
COMBINED PROBLEM OF SLEW MANEUVER CONTROL AND VIBRATION SUPPRESSION
Y. P. Kakad [1987] 11 p
(Grant NAG1-535)
(NASA-CR-181537; NAS 1.26:181537) Avail: NTIS HC A03/MF A01 CSCL 20K

The combined problem of slew maneuver control and vibration suppression of NASA Spacecraft Control Laboratory Experiment (SCOLE) is considered. The coupling between the rigid body modes and the flexible modes together with the effect of the control forces on the flexible antenna is discussed. The nonlinearities in the equations are studied in terms of slew maneuver angular velocities. Author

N88-12818# Advisory Group for Aerospace Research and Development, Paris (France). Structures and Materials Panel.
STANDARD FATIGUE TEST SPECIMENS FOR FASTENER EVALUATION
Robin Cook (Royal Aircraft Establishment, Farnborough, England) Nov. 1987 66 p
(AGARD-AG-304; ISBN-92-835-0429-1) Copyright Avail: NTIS HC A04/MF A01

An AGARD coordinated program which examines the fatigue performance and joint characteristics of a number of mechanically fastened joints with (1) no or low secondary bending and (2) with high secondary bending. In part 1, three types of joint are assessed which exhibit no, low, and high amounts of load transfer by the fastener. The no-load transfer joint was rejected and low and high load transfer joint were considered to be equivalent in rating fastener systems. In part 2, three types of single shear joint are considered. They are compared on the basis of load transfer and secondary bending characteristics and also on the fatigue endurance with a range of fastener systems installed. Only one joint, the UK designed Q-joint, adequately fulfilled the requirements of a standard joint for fastener evaluation purposes. Author

N88-12819# National Aeronautical Establishment, Ottawa (Ontario).
THE EFFECT OF MASS, WIND ANGLE AND ERECTION TECHNIQUE ON THE AEROELASTIC BEHAVIOUR OF A CABLE-STAYED BRIDGE MODEL
S. J. Zan Sep. 1987 65 p
(NAE-AN-46; NRC-28207) Avail: NTIS HC A04/MF A01

Results are presented of an aeroelastic investigation into the dynamic response of a cable-stayed bridge to wind loading. This is a continuation of an earlier study in which the deck response was investigated for nine deck sections in three different flows. The present effort used a plate girder section only and was concerned with the effects of mass, yawed winds and erection phases on the response of the bridge to buffeting and torsional instability. The model, built at a geometric scale of 1:75, was tested in the NAE 9 m X 9 m low-speed wind tunnel. Author

N88-12820 Ohio State Univ., Columbus.
HIGHER ORDER THEORY ANALYSIS OF A MODIFIED FREE-EDGE DELAMINATION SPECIMEN Ph.D. Thesis
Howard William Brown, III 1987 149 p
Avail: Univ. Microfilms Order No. DA8717610

A high order theory of laminated plates based on assumption of in-plane displacements varying linearly over the thickness of sublaminates is specialized to the problem of the modified free-edge delamination specimen and a procedure is developed for determination of the energy release rate associated with delamination. The method includes the effects of interlaminar stresses yielding better estimates of displacements and energy release rates than was possible with the classical plate theory. The theory and procedures developed are implemented in a computer program that needs only a physical and material description of a laminate in order to compute the displacement field. The energy release rate of a modified free-edge delamination specimen is calculated within the program using the displacement solution. The displacement and stress fields from the displacement procedure compare favorably with solutions derived by Pagano from a totally different set of assumptions. The methods of energy release rates computation described in earlier research are shown to be a specialization of the general procedure introduced. Dissert. Abstr.

N88-12821 California Univ., Berkeley.
KINEMATIC FORMULATION OF FINITE ELEMENTS FOR PLATE BENDING Ph.D. Thesis
George Robert Morris 1986 142 p
Avail: Univ. Microfilms Order No. DA8718091

A finite element formulation is developed for the computer analysis of flat plate bending behavior. The formulation is derived by the displacement approach, and is based on the Mindlin theory for plates. This permits the analysis of thin to moderately thick plates. Attention is restricted to homogeneous, isotropic, linear elastic materials. The extension to orthotropic materials is direct. Shear and bending deformations are allowed, and they are approximated so as to be kinematically independent of one another. Construction of the bending field in the distorted space of the element helps reduce the sensitivity of this formulation to geometric distortion. Integrability constraints must be imposed on the element to assure complete kinematic compatibility. The degree of imcompatibility in a relaxed element can be measured for error analysis. The proposed integrated bending field formulation is specifically applied to the common isoparametric family of elements. The method is sufficiently general, however, to work with other interpolation schemes and element types. Full integration of the stiffness matrix is allowed, and no spurious kinematic modes are produces. Numerical results are presented which show the accuracy, reliability, and efficiency of the proposed element for modeling bending and shear deformations. Comparisons are made with other prevalent formulations to show the advanatages and disadvantages of the present method. Dissert. Abstr.

N88-12822 Ohio State Univ., Columbus.
VIBRATION AND BUCKLING OF GEOMETRICALLY IMPERFECT LAMINATED CYLINDRICAL SHELLS Ph.D. Thesis
Hung-Yih Isaac Du 1987 171 p
Avail: Univ. Microfilms Order No. DA8717625

The influence of geometric imperfections on the linear vibration frequencies of thin, laminated angle-ply, simply supported antisymmetric cylindrical panels under axial compression and lateral pressure is considered. The effects of axial geometric imperfections on the fundamental vibration frequencies of cross-ply simply supported oval cylindrical shells are examined. The initial postbuckling behavior of antisymmetric cross-ply closed cylindrical shells under torsion is treated. The theoretical postbuckling behavior and imperfection sensitivity of antisymmetrically laminated open, long, cylindrical panels under shear loads is examined. Finally, the buckling and initial postbuckling behavior and imperfection sensitivity of stiffened cylindrical shells under torsion is examined. Dissert. Abstr.

N88-12823 California Univ., Berkeley.
VIBRATION AND PARAMETRIC EXCITATION IN ROTATING ASYMMETRIC CIRCULAR PLATES Ph.D. Thesis
Ray-Chung Yu 1986 122 p
Avail: Univ. Microfilms Order No. DA8718221

Rotating circular plates are the fundamental elements in many machines such as steam turbines, circular saws, and computer memory discs. Both unavoidable and intentional imperfections in the geometry, material properties, and initial stress in circular plates create asymmetry that substantially alters the vibration of the plates. Large transverse vibration of circular plates due to parametric excitation can lead to failure. It is therefore crucial to understand how the imperfections generate the parametric excitation. The natural frequencies and modes of transverse vibration of circular plates containing small imperfections are determined through a functional perturbation method. The distinction between the split and repeated vibration modes in an asymmetric circular plate is fundamental to the parametric excitation mechanism. The vibration of a plate, containing any number of thin slots cut into it at the rim and rotating past any number of stationary linear springs, is analyzed. Parametric instability can be excited in the split mode by the springs, but it can not be excited in the split modes. The traveling wave or fixed vibration of the plate at parametric resonance is discussed. The response of asymmetric circular plates subjected to a moving concentrated harmonic load is also analyzed. The theoretical predictions of split and repeated vibration modes and the excitation of parametric instability are confirmed by experiments. Dissert. Abstr.

N88-12824 Johns Hopkins Univ., Baltimore, Md.
EXTREMUM METHODS OF STRUCTURAL ANALYSIS FOR SYSTEM RELIABILITY ASSESSMENT Ph.D. Thesis
Avinash Madhukar Nafday 1987 102 p
Avail: Univ. Microfilms Order No. DA8716636

Discrete extremum methods of systems analysis are demonstrated as a tool for structural system reliability assessment. Specifically, linear and multiobjective linear programming based procedures are developed for structural analysis of ductile frames under proportional and multiparameter loading, respectively. Kinematic and static approaches for rigid plastic analysi from a primal-dual pair in each of these models and have a polyhedral format. Duality relations link extreme points and hyperplanes of these polyhedra and lead naturally to dual methods for computing system reliability, depending upon the treatment of uncertainty. Random events-based procedures require enumeration of the failure modes, and these are identified as the extreme points of the convex polytope for the kinematic model. An algorithmic procedure is used for the generation of the multiple failure modes of frames under proportional loading in ascending order of their collapse loads. Random variable methods proceed from the limit surface demarcating the safe and unsafe regions. An approach for the estimation of structural system reliability based on the random variable approach is presented. The proposed method replaces the safe region of the structure with an analytically tractable region of equivalent volume, where this volume may be of different order and dimensions. The system reliability can be computed form the properties of the substituted region. Dissert. Abstr.

N88-12825*# National Aeronautics and Space Administration. Lewis Research Center, Cleveland, Ohio.
CREEP LIFE PREDICTION BASED ON STOCHASTIC MODEL OF MICROSTRUCTURALLY SHORT CRACK GROWTH
Takayuki Kitamura and Ryuichi Ohtani (Kyoto Univ., Japan) 1988 23 p Proposed for presentation to the Summer Annual Meeting of the American Society of Mechanical Engineers, Berkeley, Calif., 20-22 Jun. 1988
(NASA-TM-100245; E-3867; NAS 1.15:100245) Avail: NTIS HC A03/MF A01 CSCL 20K

A nondimensional model of microstructurally short crack growth in creep is developed based on a detailed observation of the creep fracture process of 304 stainless steel. In order to deal with the scatter of small crack growth rate data caused by microstructural inhomogeneity, a random variable technique is used in the model. A cumulative probability of the crack length at an arbitary time, G(bar a, bar t), and that of the time when a crack reaches an arbitary length, F(bar t, bar a), are obtained numerically by means of a Monte Carlo method. G(bar a, bar t), and F(bar t, bar a) are the probabilities for a single crack. However, multiple cracks generally initiate on the surface of a smooth specimen from the early stage of creep life to the final stage. TAking into account the multiple crack initiations, the actual crack length distribution observed on the surface of a specimen is predicted by the combination of probabilities for a single crack. The prediction shows a fairly good agreement with the experimental result for creep of 304 stainless steel at 923 K. The probability of creep life is obtained from an assumption that creep fracture takes place when the longest crack reaches a critical length. The observed and predicted scatter of the life is fairly small for the specimens tested. Author

N88-12826# Sandia National Labs., Albuquerque, N. Mex.
THE EVOLUTION OF PLASTIC STRAIN IN STEADY, PLASTIC SHOCK WAVES
J. E. Dunn 1987 5 p Presented at the 5th Topical Conference of the American Physical Society on Shockwaves in Condensed Matter, Monterey, Calif., 20 Jul. 1987
(Contract DE-AC04-76DP-00789)
(DE87-013812; SAND-87-0966C; CONF-870753-77) Avail: NTIS HC A02/MF A01

This study is a brief summary of some recent efforts to understand the constitutive implications of empirical relations like the following: P(sub D) = k times the absolute value of (d epsilon(sub m)dt)(sup 1/4), where P(sub D) is the impact needed to create a plastic shock wave, k is a material constant, and d epsilon(sub M /dt (sup 1/4) is the peak strain rate in that wave. This is in the context of viscoplasticity theories that introduce an internal state variable for the plastic strain and a companion rate law for its evolution. DOE

N88-12827# Sandia National Labs., Albuquerque, N. Mex.
IMPLEMENTATION OF A NEW SHOCK TESTING PROCEDURE USING NONSTATIONARY RANDOM EXCITATION
T. L. Paez and T. J. Baca 1987 6 p Presented at the SEM Fall Meeting, Savannah, Ga., 25 Oct. 1987
(Contract DE-AC04-76DP-00789)
(DE87-014643; SAND-87-0165C; CONF-8710135-2) Avail: NTIS HC A02/MF A01

A new approach for the specification and performance of shock tests is described in this paper. Many field shock sources are nonstationary random processes. When a mechanical system will be subjected, in field use, to a shock drawn from a nonstationary random process source, it is best to test the system in the laboratory using a test shock drawn from the same random process source. It is shown that when a nonstationary random process is specified, realizations of the random process can be digitally

generated and then reproduced on an electrodynamic shaker. Examples are presented. DOE

N88-12828# Oak Ridge Gaseous Diffusion Plant, Tenn.
DAMPING CHARACTERISTICS OF A COMPOSITE-REINFORCED STAINLESS-STEEL PLATE
J. B. Andriulli and H. J. Grimsby Sep. 1987 11 p
(Contract DE-AC05-84OT-21400)
(DE88-000303; K/ETAC-31) Avail: NTIS HC A03/MF A01

The investigation of damping characteristics of composite-steel laminates was initiated for the Naval Underwater Systems in March 1987. Phase 2 of the Composite Damping Task consists of fabricating a composite laminated stainless-steel plate and comparing the damping characteristics to that of a bare stainless-steel plate. This report summarizes the activities initiated under Phase 2 of this project performed at the Enrichment Technology Applications Center, Martin Marietta Energy Systems, Inc. DOE

N88-12829# Sandia National Labs., Albuquerque, N. Mex. Modal and Structural Mechanics Div.
A COMPARISON OF STRUCTURAL FREQUENCY RESPONSE FUNCTIONS MEASURED WITH FORCES FROM 500 TO 250,000 LB
V. I. Bateman Sep. 1987 17 p
(Contract DE-AC04-76DP-00789)
(DE88-000668; SAND-87-0632) Avail: NTIS HC A03/MF A01

Modal analysis of structural systems is typically performed at low force levels (10's or 100's of pounds). Often, in their intended use environment, the systems encounter much higher service loads, and linearity of their responses must be assumed. This work describes a technique to dynamically characterize structural systems with force levels in excess of 100 klb. A hollow steel bar (6 in. in dia and 60 in. long) was instrumented with strain gages at an axial distance of 41.25 in. A frequency response function for the bar was determined from the strain gage measurements in response to a transient force of a few hundred pounds. A Reverse Hopkinson Bar technique was used to generate a force input at 150 and 250 klb for the same hollow steel bar. A frequency response function was calculated for this high-force input that simulates a field test environment. The two frequency response functions are compared. DOE

N88-12830# Oak Ridge National Lab., Tenn.
PULSED EDDY-CURRENT INSPECTION OF THIN-WALLED STAINLESS STEEL TUBING
C. V. Dodd, D. W. Koerner, W. E. Deeds, and C. A. Pickett Sep. 1987 118 p
(Contract DE-AC05-84OR-21400)
(DE88-001492; ORNL-6408) Avail: NTIS HC A06/MF A01

A pulsed eddy-current system has been developed for production inspection of small, thin-wall, non-ferromagnetic tubing. To detect and accurately size both outer and bore-side flaws required an operating frequency higher than available from present commercial equipment. A pulsed eddy-current instrument was designed and constructed that used 3.2 MHz square waves, with a bandwidth of 20 MHz. The system is able to reliably detect flaws as small as 0.015 mm (0.6 mils) on either the inner or outer surface of the tube. A computer controls the scanning of the tube, recording, analyzing, and plotting the data. The computer programs and instrument details are given. DOE

N88-12637# Joint Publications Research Service, Arlington, Va.
SOLUTION OF GEOMETRICALLY NONLINEAR PROBLEM FOR REINFORCED SHELL OF REVOLUTION HAVING ARBITRARY SHAPE Abstract Only
V. V. Kuzmin *In its* USSR Report: Engineering and Equipment 28 May 1987 p 95 Transl. into ENGLISH from Izvestiya Vysshikh Uchebnykh Zavedeniy: Aviatsionnaya Tekhnika (Kazan, USSR), no. 4, Oct. - Dec. 1985 p 53-59 Original language document was announced in IAA as A86-35987 (For primary document see N88-12621 04-31)
Copyright Avail: NTIS HC A06/MF A01

N88-12638# Joint Publications Research Service, Arlington, Va.
RATIONAL REINFORCEMENT OF CYLINDRICAL SHELLS WITH VARIABLE STIFFNESS FRAMES SUBJECTED TO EXTERNAL PRESSURE Abstract Only
A. S. Gorbatov and Yu. M. Pochtman *In its* USSR Report: Engineering and Equipment 28 May 1987 p 96 Transl. into ENGLISH from Izvestiya Vysshikh Uchebnykh Zavedeniy: Aviatsionnaya Tekhnika (Kazan, USSR), no. 4, Oct. - Dec. 1985 p 29-33 Original language document was announced in IAA as A86-35982 (For primary document see N88-12621 04-31)
Copyright Avail: NTIS HC A06/MF A01

N88-12639# Joint Publications Research Service, Arlington, Va.
FINITE DEFORMATIONS OF SHELL WITH RIGID INCLUSION Abstract Only
B. A. Antufyev *In its* USSR Report: Engineering and Equipment 28 May 1987 p 97 Transl. into ENGLISH from Izvestiya Vysshikh Uchebnykh Zavedeniy: Aviatsionnaya Tekhnika (Kazan, USSR), no. 4, Oct. - Dec. 1985 p 3-7 (For primary document see N88-12621 04-31)
Copyright Avail: NTIS HC A06/MF A01

N88-12640# Joint Publications Research Service, Arlington, Va.
FATIGUE FAILURE OF THIN POROUS STRIPS
G. G. Gugunishvili, G. V. Kiziriya, and L. I. Rozentur *In its* USSR Report: Engineering and Equipment 28 May 1987 p 98-100 Transl. into ENGLISH from Soobshcheniya Akademii Nauk Gruzinskoy SSR (Tbilisi, USSR), v. 124, no. 1, Oct. 1986 p 49-51 (For primary document see N88-12621 04-31)
Copyright Avail: NTIS HC A06/MF A01

N88-12641# Joint Publications Research Service, Arlington, Va.
OPTIMAL RIBBING OF LONG PLATE MADE OF COMPOSITE MATERIAL
E. V. Belubekyan and A. Z. Darbinyan *In its* USSR Report: Engineering and Equipment 28 May 1987 p 101-105 Transl. into ENGLISH from Doklady Akademii Nauk Armyanskoy SSR (Yerevan, USSR), v. 82, no. 5, 1986 p 214-217 (For primary document see N88-12621 04-31)
Copyright Avail: NTIS HC A06/MF A01

N88-12647# Honeywell, Inc., Edina, Minn. Defense Systems Div.
A DIRECT METHOD TO OBTAIN CONSTITUTIVE MODEL CONSTANTS FROM CYLINDER IMPACT TEST RESULTS
Tim J. Holmquist and Gordon R. Johnson *In* Army Materials Technology Lab., Work-in-Progress Presented at the Army Symposium on Solid Mechanics, 1986: Lightening of the Force Oct. 1986 p 7-11 (For primary document see N88-12644 04-31)
Avail: NTIS HC A04/MF A01 CSCL 20K

N88-12648# Army Materials Technology Lab., Watertown, Mass.
PLASTIC STRAIN LOCALIZATION BETWEEN VOIDS IN SHEAR DEFORMATION FIELDS
D. H. Tracey, C. E. Freese, and P. J. Perrone *In its* Work-in-Progress Presented at the Army Symposium on Solid Mechanics, 1986: Lightening of the Force Oct. 1986 p 13-21 (For primary document see N88-12644 04-31)
Avail: NTIS HC A04/MF A01 CSCL 20K

N88-12649# Little (Arthur D.), Inc., Cambridge, Mass.
A STUDY OF THE CRACK TIP PARAMETERS THAT GOVERN ENVIRONMENTALLY ASSISTED CRACKING BY USE OF THE RISING DISPLACEMENT TEST
R. Mayville, T. Warren, and P. Hilton *In* Army Materials Technology Lab., Work-in-Progress Presented at the Army Symposium on Solid Mechanics, 1986: Lightening of the Force Oct. 1986 p 23-26 (For primary document see N88-12644 04-31)
Avail: NTIS HC A04/MF A01 CSCL 20K

N88-12652# Army Materials Technology Lab., Watertown, Mass.
EFFECTIVE TREATMENT OF MEMBRANE AND SHEAR LOCKING PHENOMENA IN CURVED SHEAR-DEFORMABLE AXISYMMETRIC SHELL ELEMENT
A. Tessler and L. Spiridigliozzi *In its* Work-in-Progress Presented at the Army Symposium on Solid Mechanics, 1986: Lightening of the Force Oct. 1986 p 33-35 (For primary document see N88-12644 04-31)
Avail: NTIS HC A04/MF A01 CSCL 20K

N88-12653# Kaman Sciences Corp., Colorado Springs, Colo.
ANALYSIS AND TESTING OF PREDAMAGED SHELL STRUCTURES
Richard E. Keeffe and Eric Reece (Sandia National Labs., Albuquerque, N. Mex.) *In* Army Materials Technology Lab., Work-in-Progress Presented at the Army Symposium on Solid Mechanics, 1986: Lightening of the Force Oct. 1986 p 41-43 (For primary document see N88-12644 04-31)
(Contract DASG60-85-C-0051)
Avail: NTIS HC A04/MF A01 CSCL 20K

42 GEOSCIENCES (GENERAL)

N88-12831# Joint Publications Research Service, Arlington, Va.
USSR REPORT: EARTH SCIENCES
22 Jul. 1986 77 p Transl. into ENGLISH from various Russian articles
(JPRS-UES-86-006) Avail: NTIS HC A05/MF A01

The complete text or abstracts of articles addressing various topics in the earth sciences are compiled. General subject areas include meteorology, oceanography, terrestrial geophysics, atmospheric physics, and arctic and antarctic research. For individual titles, see N88-12832 through N88-12857.

N88-12832# Joint Publications Research Service, Arlington, Va.
COMPUTER MODELING AIDS STUDIES OF PRECIPITATION FORMATION Abstract Only **c47**
V. Korneyev *In its* USSR Report: Earth Sciences 22 Jul. 1986 p 1 Transl. into ENGLISH from Izvestiya (USSR), no. 82(21524), 23 Mar. 1986 p 3 (For primary document see N88-12831 04-42)
Avail: NTIS HC A05/MF A01

Cloud physics research in progress at the Central Aerological Observatory (USSR) is described along with the methods utilized for the studies. Scientists are trying to determine the ratio of ice crystals to cloud volume which is optimal for the formation of precipitation. Methods being used in this research include both field observations and laboratory experiments, including digital modeling of clouds. Such experiments have been necessitated by the complexity of measurements which must be made inside clouds and the limited capabilities of equipment available for this purpose. Airborne equipment alone cannot provide all of the information which researchers need. Computer modeling has made it possible to clarify many aspects of precipitation formation processes in extensive cloud fields associated with cyclones. Author

N88-12833# Joint Publications Research Service, Arlington, Va.
PROGRESS IN IMPROVING WEATHER FORECASTING VIEWED Abstract Only **c47**
Andrey Prainikov *In its* USSR Report: Earth Sciences 22 Jul. 1986 p 2 Transl. into ENGLISH from Nedelya (USSR), no. 1 (1345), 30 Dec. 1985 p 23 (For primary document see N88-12831 04-42)
Avail: NTIS HC A05/MF A01

Weather monitoring and forecasting methods currently in use by researchers of the Hydrometeorological Scientific Research Center (USSR) are discussed along with progress in heightening the accuracy of forecasts and work aimed at improving long-term forecasting. Short-term weather forecasting has become substantially more accurate thanks to the introduction of computer aided processing of data gathered by ground and aerospace observation equipment. Modern computers make it possible to predict processes of circulation in the atmosphere for five to seven days in advance; one-month forecasts are now being made with a reliability of about 65%. The accuracy of long-term forecasting can and will be heightened still further through more extensive use of satellite data. Computers with speeds of billions of operations a second are needed for processing if the network of satellite aided weather observations is to be expanded. Author

N88-12834# Joint Publications Research Service, Arlington, Va.
NEW PRECIPITATION MAP OF WORLD OCEAN Abstract Only **c47**
E. G. Bogdanova *In its* USSR Report: Earth Sciences 22 Jul. 1986 p 3 Transl. into ENGLISH from Izvestiya Akademii Nauk SSSR: Seriya Geograficheskaya (Moscow, USSR), no. 1, Jan. - Feb. 1986 p 37-49 (For primary document see N88-12831 04-42)
Avail: NTIS HC A05/MF A01

During recent years great amounts of data have become available concerning precipitation over the world ocean, dictating revision of maps published in past years. Accordingly, maps of the quantity and intensity of precipitation over the oceans have been compiled. Their reliability was evaluated by comparison with corresponding data obtained by independent methods. The maps were analyzed in order to clarify new distribution patterns or details. Only directly collected data were used; no data were extrapolated from islands or the mainland. The computation parameters used were temperature, wind and humidity; the distribution of precipitation fully corresponds to the patterns of atmospheric circulation and ocean currents. Since calculations of the quantity and intensity of precipitation were made at the level of their monthly values, any characteristics of their intra-annual variability can be obtained. The computation procedures used were simple, particularly in comparison with the unwieldy processing method used by G. B. Tucker (1961). The accuracy of the new maps is somewhat compromised by errors in the indirect computation of intensity and determination of duration using data on the frequency of recurrence of precipitation. Author

N88-12835# Joint Publications Research Service, Arlington, Va.
DROUGHT, SOLAR ACTIVITY LINK ESTABLISHED BY LENINGRAD GEOPHYSICISTS Abstract Only **c47**
In its USSR Report: Earth Sciences 22 Jul. 1986 p 4 Transl. into ENGLISH from TASS (Moscow, USSR), 28 Feb. 1986 (For primary document see N88-12831 04-42)
Avail: NTIS HC A05/MF A01

Scientists of the Main Geophysical Observatory in Leningrad have succeeded in establishing a link between extreme weather conditions and solar activity. The main subject is droughts, whose distribution is related to solar activity cycles. For some regions of the earth a 22-year cycle applies, and for others, including the USSR, an 11-year cycle. Even though people cannot avert droughts, by knowing when they are due to begin they can prepare for them. Author

N88-12836# Joint Publications Research Service, Arlington, Va.
COMPLEX FOR OCEAN STUDY FROM SPACE AND HYDROACOUSTIC STATIONS **c48**
In its USSR Report: Earth Sciences 22 Jul. 1986 p 9 Transl. into ENGLISH from Sovetskaya Estoniya (Tallinn, USSR), 18 Feb. 1986 p 1 (For primary document see N88-12831 04-42)
Avail: NTIS HC A05/MF A01

In collaboration with other USSR academy and industry institutes, the Institute of Automation and Control Processes (IAPU) is working on the development of information support for oceanological research. In particular, research is being done on principles of remote study of the ocean from space stations and hydroacoustic stations. In connection with this, the development of a software-hardware complex called DISTERM is being completed; it is intended for automated gathering, storage and processing of data from hydrometeorological observations made

on ships and satellites. A copy of this system was installed on the scientific research ship Akademik Sergey Korolev, where experiments with its operation are being conducted. The use of DISTERM is expected to provide information which scientists, weather forecasters and fishermen need quickly. Author

N88-12837# Joint Publications Research Service, Arlington, Va.
CAUCHY PROBLEM FOR LINEARIZED SYSTEM OF NAVIER-STOKES EQUATIONS CONSIDERING COMPRESSIBILITY Abstract Only **c48**
A. K. Shatov *In its* USSR Report: Earth Sciences 22 Jul. 1986 p 15 Transl. into ENGLISH from Doklady Akademii Nauk SSSR (Moscow, USSR), v. 285, no. 6, Dec. 1985 p 1374-1376 Original language document was announced in IAA as A86-24316 (For primary document see N88-12831 04-42)
Avail: NTIS HC A05/MF A01

The Cauchy problem is formulated for a linearized system of Navier-Stokes equations for a homogeneous (in steady state) compressible fluid whose physical characteristics, such as the adiabatic velocity of sound, specific heat, thermal conductivity coefficient, and shear viscosity remain constant with time. The convergence of the solution to the solution for the degenerate case (i.e., where the thermal conductivity coefficient and shear viscosity are zero) is demonstrated. Author

N88-12838# Joint Publications Research Service, Arlington, Va.
ASYMPTOTIC FORM OF STATIONARY SOLUTIONS OF THE NAVIER-STOKES EQUATIONS FOR LARGE REYNOLDS NUMBERS Abstract Only **c34**
S. I. Chernyshenko *In its* USSR Report: Earth Sciences 22 Jul. 1986 p 15 Transl. into ENGLISH from Doklady Akademii Nauk SSSR (Moscow, USSR), v. 285, no. 6, Dec. 1985 p 1353-1355 Original language document was announced in IAA as A86-24313 Prev. announced as X87-71987 1987 (For primary document see N88-12831 04-42)
Avail: NTIS HC A05/MF A01

An attempt is made to construct an internally noncontradictory asymptotic series expansion of solutions to the Navier-Stokes equations for large Reynolds numbers. It is shown that such a solution can be obtained in a class of complex functions for some cases where attempts to obtain a real-valued asymptotic expansion fail. Author

N88-12839# Joint Publications Research Service, Arlington, Va.
STEADY DISTORTION OF SHAPE OF GEOID AND NORMAL GRAVITY FIELD UNDER INFLUENCE OF TIDAL POTENTIAL Abstract Only **c48**
S. S. Ivanov *In its* USSR Report: Earth Sciences 22 Jul. 1986 p 16 Transl. into ENGLISH from Doklady Akademii Nauk SSSR (Moscow, USSR), v. 285, no. 6, Dec. 1985 p 1356-1359 (For primary document see N88-12831 04-42)
Avail: NTIS HC A05/MF A01

An expression for the tidal potential is studied. Expressions for the diurnal and semidiurnal components of the tidal potential include the cosines of the single and double hour angle of the star, causing their mean value to equal zero over the period of rotation. This is not the case for the long-period tidal potential. The distortion is computed to be about 10 cm at the equator, 20 cm at the poles, and 0 and +/- 35.16 deg. The full amplitude of steady distortion of the normal gravity field of the earth due to the long-period tidal potential is approximately 0.2 mGal. Author

N88-12840# Joint Publications Research Service, Arlington, Va.
EXPERIMENTAL STUDY OF TURBULENT DIFFUSION PARAMETERS IN OCEAN Abstract Only **c48**
V. V. Anikiyev, O. V. Zaytsev, T. V. Zaytseva, and V. V. Yarosh *In its* USSR Report: Earth Sciences 22 Jul. 1986 p 16-17 Transl. into ENGLISH from Izvestiya Akademii Nauk SSSR: Fizika Atmosfery i Okeana (Moscow, USSR), v. 21, no. 11, Nov. 1985 p 1226-1229 (For primary document see N88-12831 04-42)
Avail: NTIS HC A05/MF A01

In research on turbulent diffusion in the ocean carried out in the Black Sea, North Sea, Baltic Sea and in the Atlantic Ocean it was impossible to deduce any universal laws of development of spots or streams of tracers being used to ascertain patterns of turbulent diffusion. In each case these patterns are highly dependent on hydrometeorological and morphometric parameters. A dependence of rate of expansion of such spots on wave height and velocity of the mean current was noted. Bottom relief, shore configuration and structure of currents exert a marked influence on spot configuration in coastal and shallow water areas. In the coastal waters of Japan, China and South Korea tidal currents are also a highly important factor. The same is true of monsoons, passage of typhoons and powerful currents. All these factors were taken into account in studying the laws of turbulent diffusion in the coastal region of the Sea of Japan and in the open part of the Pacific Ocean by release of dye. Spot evaluation was investigated using an aerial survey and a towed submersible fluorometer. The law expressing the increase in effective area with time obtained earlier for the coastal zone was confirmed, but the increase in anisotropy was slower. The role of velocity gradients in spot diffusion was less in the tropical parts of the ocean than in coastal zones. Author

N88-12841# Joint Publications Research Service, Arlington, Va.
INFLUENCE OF STRATIFICATION IN NEAR-SURFACE WATER LAYER ON INTENSITY OF GAS EXCHANGE BETWEEN ATMOSPHERE AND WATER Abstract Only **c46**
V. F. Brekhovskikh and V. I. Bratkov *In its* USSR Report: Earth Sciences 22 Jul. 1986 p 17 Transl. into ENGLISH from Izvestiya Akademii Nauk SSSR: Fizika Atmosfery i Okeana (Moscow, USSR), v. 21, no. 11, Nov. 1985 p 1198-1205 (For primary document see N88-12831 04-42)
Avail: NTIS HC A05/MF A01

Little is known concerning the influence of the temperature field in the near-water layer on gas exchange between the atmosphere and water. During periods of calm the transfer of oxygen from the air to water is sometimes impeded and large numbers of fish may die. A laboratory experiment was carried out in glass thermostated containers, in each of which the temperature was maintained with great accuracy. One was heated to 39 to 40 C; another was cooled to 12 to 13 C; a third was kept at ambient temperature. In each case the aeration coefficient and rate of mass transfer were computed. Air and water temperatures were varied to determine temperature gradients in the near-water and near-surface layers. A copper constantan thermocouple was used in measuring temperatures above and below the interface. The influence of petroleum films on the rate of mass transfer was also determined. The rate of evaporation at different temperatures was ascertained. The greatest influence was observed in experiments with cooled air. It was found that temperature stratification in the near-surface water layer exerts a considerable influence on water-air gas exchange. In certain cases a petroleum film increases the temperature gradient and causes an even greater decrease in mass transfer rate. Author

N88-12842# Joint Publications Research Service, Arlington, Va.
DISPERSION EQUATION FOR PLANE CAPILLARY-GRAVITY WAVE ON FREE SURFACE OF VISCOUS INCOMPRESSIBLE FLUID Abstract Only **c34**
P. N. Antonyuk *In its* USSR Report: Earth Sciences 22 Jul. 1986 p 20 Transl. into ENGLISH from Doklady Akademii Nauk SSSR (Moscow, USSR), v. 286, no. 6, Feb. 1986 p 1324-1328 (For primary document see N88-12831 04-42)
Avail: NTIS HC A05/MF A01

A parametric representation is obtained at a dispersion equation for a plane capillary-gravity wave on the free surface of a viscous incompressible fluid in real form, allowing exhaustive investigation of the influence of viscosity on plane capillary-gravity waves. The existence of both periodic and aperiodic modes, alternating at a certain critical wavelength, is established. Author

N88-12843# Joint Publications Research Service, Arlington, Va.
INFLUENCE OF SURFACTANTS ON DAMPING OF GRAVITY-CAPILLARY WAVES. 1: FREQUENCY DEPENDENCE Abstract Only **c46**

A. A. Lazarev and K. V. Pokazeyev *In its* USSR Report: Earth Sciences 22 Jul. 1986 p 24 Transl. into ENGLISH from Okeanologiya (Moscow, USSR), v. 26, no. 1, Jan. - Feb. 1986 p 46-50 (For primary document see N88-12831 04-42)
Avail: NTIS HC A05/MF A01

A study was made of the influence of surfactants on the damping of regular gravity-capillary waves in the range 2.5 to 16.0 Hz. Since the dissipation of these waves is dependent on surfactant characteristics, the results can be used in determining the type of pollution. Research was done on the damping of these waves in pure water and in the presence of surfactants of five different types. These included three which are insoluble (oleic acid, palmitic acid, dodecyl alcohol) and two which are soluble (sodium dodecyl sulfate and potassium laurate). An effort was made to simulate pollutants actually observed in the sea. The experiment was in a flume 7 meters in length, 49 cm in width and 20 cm in depth. Computations agree well with experimental data and reveal the existence of a quasi-resonant dependence of the relative damping coefficient on the frequency of gravity-capillary waves. The damping effect of insoluble surfactants is somewhat less than for soluble surfactants. Author

N88-12844# Joint Publications Research Service, Arlington, Va.
INTENSIVE SYNOPTIC EDDIES AND QUASIGEOSTROPHIC APPROXIMATION Abstract Only c48
Z. I. Kizner *In its* USSR Report: Earth Sciences 22 Jul. 1986 p 24-25 Transl. into ENGLISH from Okeanologiya (Moscow, USSR), v. 26, no. 1, Jan. - Feb. 1986 p 28-35 (For primary document see N88-12831 04-42)
Avail: NTIS HC A05/MF A01

A baroclinic Rossby soliton with axial symmetry was described by G. R. Flierl (1979) and an approximate solution for the equation for a quasi-geostrophic eddy on a beta plane was obtained. This general problem was reexamined in order to ascertain the conditions for applicability of the equation for a quasi-geostrophic eddy for the description of well-developed synoptic currents (like rings, whose velocity of movement is much less than the orbital velocities of fluid particles) in a continuously stratified ocean. It was found that if in the expansion of the sought-for variables into power series for the Kibel number the zero approximation has circular symmetry relative to an arbitrary vertical axis, the horizontal components of current velocity are described with an error on the order of 0(Ki squared). The results obtained by Flierl are distinctly different from the results obtained in this analysis in that the Flierl soliton moved westward with a phase velocity exceeding the phase velocities of linear Rossby waves, whereas the elongated wave revealed in the present study travels eastward and it can have any phase velocity. Author

N88-12845# Joint Publications Research Service, Arlington, Va.
DYNAMICS OF ISOLATED INTRATHERMOCLINE EDDY Abstract Only c48
G. I. Shapiro *In its* USSR Report: Earth Sciences 22 Jul. 1986 p 25 Transl. into ENGLISH from Okeanologiya (Moscow, USSR), v. 26, no. 1, Jan. - Feb. 1986 p 21-27 (For primary document see N88-12831 04-42)
Avail: NTIS HC A05/MF A01

There is a definite analogy between the dynamics of eddy lenses and solitary Rossby waves, but there are also very significant differences which make it possible to apply the theory of nonlinear Rossby waves to such lenses. Accordingly, an in-depth study was made of this problem. Specifically, an investigation was made of the dynamics of a thin, density homogeneous, vortical fluid lens floating on a free surface, on the bottom or at the interface in a two-layer stratified fluid. A beta plane approximation was used. An asymptotic method was used in deriving an equation describing the dynamics of a stationary moving lenticular eddy. A precise analytical solution was found and the conditions under which a solution actually exists were determined. The limitations which the unperturbed (computed in the f-plane approximation) characteristics of the lens must be satisfied were ascertained and specific examples of fluid circulation in a lens were described. It was demonstrated that in contrast to the dynamics of solitary, almost axisymmetric waves, under the influence of the beta effect lenses always move toward the west; slow solitary Rossby waves move only to the east. Author

N88-12846# Joint Publications Research Service, Arlington, Va.
INFLUENCE OF SECONDARY EDDY CURRENTS ON SCATTERING OF ADMIXTURE IN ZONAL FLOW Abstract Only c48
V. N. Yeremeyev, L. M. Ivanov, I. A. Neyelov, and V. I. Smelyanskiy *In its* USSR Report: Earth Sciences 22 Jul. 1986 p 28 Transl. into ENGLISH from Izvestiya Akademii Nauk SSSR: Fizika Atmosfery i Okeana (Moscow, USSR), v. 22, no. 1, Jan. 1986 p 78-86 (For primary document see N88-12831 04-42)
Avail: NTIS HC A05/MF A01

Data on the drift of Sofar floats can be used for finding dynamic characteristics of the ocean in the range of synoptic-spatial scales, but there are serious difficulties in the interpretation of these data. The contribution of movements of different scales to the drift of such floats is difficult to discriminate and certain assumptions must be made concerning the statistical nature of float movements in order to ascertain the energy and other characteristics of hydrodynamic fields along the trajectories of floats. An effort has been made to overcome these difficulties. The approach used was numerical analysis of movement and an admixture in nonstationary eddy fields. It was important to take into account that in the prediction of drifting floats an important role is played by baroclinically unstable currents of a jet character and the secondary eddy currents generated by them. The study was based on hydrodynamic fields computed using a numerical model describing an unstable zonal flow for analysis of dispersal of tracer particles. Numerical experiments were conducted for time intervals of about 5 to 6 months, comparable with the lifetime of an individual eddy. Computations were made in a grid with intervals 20 km with examination of five layers with depths of 100 to 2,000 m and a time interval of 20 min. Two processes of eddy disappearance were found: decay of eddies into zonal currents and decay of large eddies into smaller ones. It was found that some characteristics of the eddy field can be determined from Sofar data. Conclusions can be drawn concerning the barotropization of the eddy field. Zones of upwelling and subsidence of water masses in eddies can be determined. Author

N88-12847# Joint Publications Research Service, Arlington, Va.
STUDIES OF THIN SURFACE FILMS AIM AT SEEING DEEP OCEAN PROCESSES Abstract Only c48
A. Zabotin *In its* USSR Report: Earth Sciences 22 Jul. 1986 p 32-33 Transl. into ENGLISH from Sotsialisticheskaya Industriya (Moscow, USSR), 3 Apr. 1986 p 4 (For primary document see N88-12831 04-42)
Avail: NTIS HC A05/MF A01

The effects of liquid films on sea surface dynamics and the potential use of artificial films to control surface characteristics and air-water interactions are discussed. It is speculated that surface films may be used to protect harbors against rough seas, to contain oil spills for easier clean-up, and possibly to prevent tropical hurricanes by inhibiting sea surface evaporation. Analysis of film coated waters may also reveal characteristics of internal waves and other subsurface dynamics. M.G.

N88-12848# Joint Publications Research Service, Arlington, Va.
SOLUTION OF THREE-DIMENSIONAL INVERSE PROBLEM OF GRAVIMETRY IN CONTACT SURFACES CLASS BY LOCAL CORRECTIONS METHOD Abstract Only c48
I. L. Prutkin *In its* USSR Report: Earth Sciences 22 Jul. 1986 p 50 Transl. into ENGLISH from Izvestiya Akademii Nauk SSSR: Seriya Fizika Zemli (Moscow, USSR), no. 1, Jan. 1986 p 67-77 (For primary document see N88-12831 04-42)
Avail: NTIS HC A05/MF A01

A local corrections method for approximate solution of nonlinear inverse problems is proposed. The method does not utilize nonlinear minimization, allowing computer time to be reduced by an order of magnitude. The method was previously applied in

solving nonlinear three-dimensional inverse problems of gravimetry and magnetometry in a class of limited objects. The local corrections method is now applied to solution of inverse problems in the contact surfaces class. It is emphasized that the three-dimensional inverse problem is solved in its full, nonlinear formulation, and that the method can be used to construct one or several contact surfaces. The amount of machine time required for solution of the problem is the same as for the solution of the inverse problem in its linearized formulation by a simple method, while the quality of solution obtained is much better. A regularization method for solution of the problem is suggested. Author

N88-12849# Joint Publications Research Service, Arlington, Va.
LASERS MEASURE ATMOSPHERE Abstract Only **c46**
In its USSR Report: Earth Sciences 22 Jul. 1986 p 52 Transl. into ENGLISH from TASS (Moscow, USSR), 27 Apr. 1986 (For primary document see N88-12831 04-42)
Avail: NTIS HC A05/MF A01

The development and application of laser based instruments by Belorussian scientists is discussed. Laser detection and ranging instruments have helped in the drafting of a design for a resort on Lake Naroch by identifying areas of especially pure air impregnated with the scent of pine. Several types of optical quantum generators have been developed which operate on a mixture of helium and neon and also on solutions of organic dyes. Such instruments have been successfully used for sounding the sea, plasma diagnostics and acceleration of reactions. Lasers have also been used to identify high-yielding varieties of frost resistant cereal crops. Author

N88-12850# Joint Publications Research Service, Arlington, Va.
THERMOPHORESIS OF SPHERICAL AEROSOL PARTICLE AT ARBITRARY KNUDSEN NUMBERS Abstract Only **c25**
S. A. Beresnev and V. G. Chernyak *In its* USSR Report: Earth Sciences 22 Jul. 1986 p 53 Transl. into ENGLISH from Doklady Akademii Nauk SSSR (Moscow, USSR), v. 285, no. 6, Dec. 1985 p 1377-1381 Original language document was announced in IAA as A86-24317 (For primary document see N88-12831 04-42)
Avail: NTIS HC A05/MF A01

Most of the results reported in the literature on the problem of the motion of an aerosol particle in a temperature gradient field (thermophoresis) concern flows with Knudsen numbers either much less than 1 or approaching infinity. Here, a solution to the problem of the thermophoresis of a spherical solid particle in a monoatomic gas is presented for arbitrary Knudsen numbers. The problem is solved for the steady-state case using linearized kinetic equations with molecular collision operators in the form of the BGK and S models. Author

N88-12851# Joint Publications Research Service, Arlington, Va.
THEORY OF HEAT AND MOISTURE EXCHANGE BETWEEN FINELY DISPERSE STORM-GENERATED SPRAY AND TURBULENT AIR FLOW Abstract Only **c34**
Ye. P. Borisenkov and M. A. Kuznetsov *In its* USSR Report: Earth Sciences 22 Jul. 1986 p 54 Transl. into ENGLISH from Izvestiya Akademii Nauk SSSR: Fizika Atmosfery i Okeana (Moscow, USSR), v. 21, no. 11, Nov. 1985 p 1191-1197 (For primary document see N88-12831 04-42)
Avail: NTIS HC A05/MF A01

The expressions describing heat and moisture exchange between finely disperse spray and a turbulent air flow were improved. The requirements on description of the motion of fine particles were reduced and it was found that in a definite part of the spectrum of spray particle sizes there is no need to compute particle flight time, thereby greatly simplifying the determination of heat and moisture exchange during storms. Salinity plays a major role in this process. An increase in salinity results in a slowing of evaporation and its subsequent cessation. It is essential that salinity be taken into account for droplets with D less than 100 microns. The mean temperature of spray particles is extremely close to the air temperature in the near water layer; there is no dependence on water temperature. With the expressions derived it is possible to predict the sizes of aerosol particles entering the atmosphere when there are moderate or strong winds. The number of heavy spray particles in the total flux is small and can be neglected in calculating energy exchange. Further progress along these lines is impossible without much more experimental data on turbulence parameters in the near-surface water layer. Nevertheless, these important findings and clarifications improve computations of total energy exchange between the ocean and atmosphere. Author

N88-12852# Joint Publications Research Service, Arlington, Va.
MULTIWAVE LASER SOUNDINGS OF ATMOSPHERIC AEROSOL: EXPERIMENTAL RESEARCH (REVIEW) Abstract Only **c46**
A. P. Chaikovskiy *In its* USSR Report: Earth Sciences 22 Jul. 1986 p 55 Transl. into ENGLISH from Zhurnal Prikladnoy Spektroskopii (Minsk, USSR), v. 44, no. 2, Feb. 1986 p 183-197 (For primary document see N88-12831 04-42)
Avail: NTIS HC A05/MF A01

The Soviet and Western literature on multiple wavelength laser soundings of atmospheric aerosols is reviewed. Primary attention is given to practical implementation of the method and analysis of the capabilities of its application for determination of the microstructure of aerosol in a number of specific situations. The amount of information obtained by multiple wavelength laser soundings can be increased by expanding the spectral band of the lidars. This is quite possible at present, but the creation of such apparatus would be a complex technical problem requiring commitment of significant resources. It is therefore often more desirable to perform multiwave soundings in combination with other optical and microphysical measurements to achieve the same results. Author

N88-12853# Joint Publications Research Service, Arlington, Va.
USE OF ELECTRON BEAM INSTRUMENTS TO DETERMINE FLUCTUATIONS IN VERTICAL REFRACTION PARTIAL ANGLE Abstract Only **c72**
A. S. Kolos *In its* USSR Report: Earth Sciences 22 Jul. 1986 p 55-56 Transl. into ENGLISH from Geodeziya i Kartografiya (Moscow, USSR), no. 2, Feb. 1986 p 21-23 (For primary document see N88-12831 04-42)
Avail: NTIS HC A05/MF A01

An analysis was made of the possibility of determining fluctuations in the partial angle of vertical refraction based on fluctuations of an image on the screen of a cathode ray tube. Determination of the partial angle of vertical refraction and consideration of leveled refraction requires highly accurate measurement of the maximum amplitude of image fluctuation over a certain period. Experimental observations were made over distances of 150 and 200 m over a homogeneous road surface. The use of fiber optic screens resulted in an increase in image resolution and contrast, allowing work to be done on a bright sunny day. Author

N88-12854# Joint Publications Research Service, Arlington, Va.
LIDAR-RADIOMETRIC METHOD FOR DETERMINING LIQUID-WATER CONTENT OF CIRRUS CLOUDS Abstract Only **c47**
V. A. Zhuravleva and O. K. Kostko *In its* USSR Report: Earth Sciences 22 Jul. 1986 p 56 Transl. into ENGLISH from Izvestiya Akademii Nauk SSSR: Fizika Atmosfery i Okeana (Moscow, USSR), v. 22, no. 1, Jan. 1986 p 44-52 Original language document was announced in IAA as A86-29318 (For primary document see N88-12831 04-42)
Avail: NTIS HC A05/MF A01

A lidar-radiometric method for determining the ice water content (IWC) and integrated IWC of cirrus clouds is described and grounded. The method is based on the measurement of the emissivity of cirrus clouds in the 8 to 13 micron range and a mean statistical model of the microphysical characteristics. The observed values of integrated IWC and IWC varied in the ranges 5 to 30 g/sq m and 0.005 to 0.03 g/cu m, respectively, with mean values of 12 g/sq m and 0.013 g/cu m. An analysis of vertical profiles of IWC showed that the lower part of a cirrus

cloud has the greatest IWC. In addition, it is found that the IWC of cirrus clouds increases with increasing temperature. Author

N88-12855# Joint Publications Research Service, Arlington, Va.
ABSORPTION OF FAR IR-RADIATION BY H2O-N2 COMPLEXES UNDER ATMOSPHERIC CONDITIONS Abstract Only **c46**
A. A. Vigasin and G. V. Chlenova *In its* USSR Report: Earth Sciences 22 Jul. 1986 p 56-57 Transl. into ENGLISH from Izvestiya Akademii Nauk SSSR: Fizika Atmosfery i Okeana (Moscow, USSR), v. 22, no. 1, Jan. 1986 p 30-35 Original language document was announced in IAA as A86-29316 (For primary document see N88-12831 04-42)
Avail: NTIS HC A05/MF A01

The envelope of the low-frequency intermolecular vibrational spectrum of H2O-N2 hydrogen-bonded complexes is calculated. In addition, the molar part of these complexes is estimated. It is shown that part of the atmospheric excess continuum long-wavelength IR absorption which is linear with respect to the partial pressure of water vapor may be connected with the H2O-N2 complexes. The concentration of these complexes in the atmosphere is estimated. Author

N88-12856# Joint Publications Research Service, Arlington, Va.
STRUCTURE OF STABLY STRATIFIED ATMOSPHERIC SURFACE LAYER IN PRESENCE OF HEAT-RELEASING ADMIXTURE Abstract Only **c46**
L. Kh. Ingel *In its* USSR Report: Earth Sciences 22 Jul. 1986 p 57 Transl. into ENGLISH from Izvestiya Akademii Nauk SSSR: Fizika Atmosfery i Okeana (Moscow, USSR), v. 22, no. 1, Jan. 1986 p 10-16 (For primary document see N88-12831 04-42)
Avail: NTIS HC A05/MF A01

A nonlinear semi-empirical model of a horizontally homogeneous stably stratified surface layer is presented in which the atmosphere contains a weightless heat-releasing admixture simulating an aerosol which absorbs solar radiation. The heat source was assumed to be proportional to the partial density of the admixture. First a background stationary solution is found for the pertinent system of equations in the absence of a heat-releasing admixture and then appropriate boundary conditions are selected for solving the final problem. In a stationary case it was possible to find a general analytical solution of a system of equations for the balance of turbulent energy in Kolmogorov form, transfer of heat, admixture and momentum. However, stationary solutions are possible only in some range of values of parameters of the problem. It was found that there is a critical value of the flux of admixture through the surface layer above which stationary solutions are impossible. As heat release continues stratification becomes increasingly stable, resulting in a suppression of turbulent exchange. The heat flux first increases a little in absolute value and only then decreases. Author

N88-12857# Joint Publications Research Service, Arlington, Va.
CONSIDERING REFRACTION IN LEVELING WITH LASER PLANE Abstract Only **c36**
Yu. S. Galkin and G. G. Pobedinskiy *In its* USSR Report: Earth Sciences 22 Jul. 1986 p 58 Transl. into ENGLISH from Geodeziya i Kartografiya (Moscow, USSR), no. 2, Feb. 1986 p 17-21 (For primary document see N88-12831 04-42)
Avail: NTIS HC A05/MF A01

The practical experience gained in studying the influence of refraction on the accuracy of measurement of the heights of pickets in a topographic survey is analyzed. Heights were determined by leveling of a reference laser plane using an automatic altimeter over distances of about 800 m, sometimes up to 1300 m. Studies on the Moscow area in 1984 using the proposed method over a base of 600 m indicated an error of 2 mm in an agricultural area on a cloudy day with intermittent showers. The method, based on refraction by the registry of laser beam fluctuations, is said to be the simplest to implement and equal in accuracy to traditional methods. Author

43 EARTH RESOURCES AND REMOTE SENSING

Includes remote sensing of earth resources by aircraft and spacecraft; photogrammetry; and aerial photography.

For instrumentation see *35 Instrumentation and Photography.*

N88-12858# Technical Research Centre of Finland, Espoo. Rakenneteknikan Lab.
HUURRE EXPEDITION TO THE NORTH POLE IN 1984
O. P. Nordlund 1987 57 p
(PB87-220935; VTT/RN-685; ISBN-951-38-2668-6) Copyright
Avail: NTIS HC A04/MF A01 CSCL 08L

Five research papers based on the experiences and measurements made during and after the Huurre Expedition to the North Pole in 1984 are reported. Two deal with snow studies. Snow samples were collected and analyzed for inorganic ions and organochlorine pollutants. Another report deals with ice research. Ice observations were made by man and satellite. Two final studies deal with the human body. One researches clothing and heat loss from the body. The other treats the cold acclimatization of the three explorers. GRA

N88-12859# Los Alamos National Lab., N. Mex.
A MINERAL RECONNAISSANCE SAMPLING MANUAL FOR COSTA RICA: CENTRAL AMERICAN ENERGY AND RESOURCE PROJECT
S. Bolivar Jun. 1987 30 p In ENGLISH and SPANISH
(Contract W-7405-eng-36)
(DE87-014997; LA-10945-M) Avail: NTIS HC A03/MF A01

This manual describes field procedures for the collection of stream-sediment and rock samples as part of the Mineral Resource Assessment of Costa Rica. It provides guidelines to be followed by personnel collecting, treating, or otherwise handling samples taken as part of this program. The objectives of the manual are to ensure that all samples are collected uniformly and consistent techniques are employed throughout the program. If this is done, the data from this study can be used to identify areas with potential for mineralization. This manual can also be used as a guideline for future geochemical sampling programs in Costa Rica. DOE

N88-12860# Naval Postgraduate School, Monterey, Calif.
A MULTIBODY DYNAMIC ANALYSIS OF THE N-ROSS (NAVY REMOTE OCEAN SENSING SYSTEM) SATELLITE ROTATING FLEXIBLE REFLECTOR USING KANE'S METHOD M.S. Thesis
Natalie F. Heffernan Jun. 1987 128 p
(AD-A184452) Avail: NTIS HC A07/MF A01 CSCL 22B

The Navy Remote Ocean Sensing System (N-ROSS) satellite is being developed to supply accurate data on ocean parameters for fleet operations. A Low Frequency Microwave Radiometer (LFMR), a large flexible reflector attached to an angled flexible boom, is a sea surface temperature sensor on this satellite which rotates at 15 rpm. The dynamic interaction between the reflector and the boom, and the effects of the reflector orientation and flexibility on the pointing error of the LFMR during a spin-up procedure are investigated by performing dynamic simulations. Dynamical equations of this flexible multibody system are formulated using Kane's method. Efficient computer simulations were achieved by developing a FORTRAN program and using Dynamic Simulation Language (DSL). GRA

N88-12861 Ohio State Univ., Columbus.
RADIAL ORBIT ERROR REDUCTION AND SEA SURFACE TOPOGRAPHY DETERMINATION USING SATELLITE ALTIMETRY Ph.D. Thesis
Theodossios Engelis 1987 190 p
Avail: Univ. Microfilms Order No. DA8717631

A method is presented in satellite altimetry that attempts to simultaneously determine the geoid and sea surface topography with minimum wavelengths of about 500 km and to reduce the radial orbit errors caused by geopotential errors. The modeling of the radial orbit error is made using the linearized Lagrangian

perturbation theory. Secular and second order effects are also included. A Fourier series formulation allows for easier computation of different statistics. Numerical estimates for the radial orbit error and geoid undulation error are computed using the differences of two geopotential models as potential coefficient errors, for a Seasat orbit. To provide statistical estimates of the radial distances and the geoid, a covariance propagation is made based on the full geopotential covariances. Accuracy estimates for the Seasat orbits are given which agree quite well with the already published results. Observation equations are developed using sea surface heights and crossover discrepancies as observeable. The potential of the method is demonstrated in a solution where simulated geopotential errors and the Levitus sea surface topography are used to generate the observables for a three day Seasat arc. The simulation results show that the method can be used to effectively reduce the radial orbit error and recover the sea surface topography.
Dissert. Abstr.

N88-12862 Ohio State Univ., Columbus.
ACCURACY POTENTIAL OF NON-METRIC CAMERAS IN CLOSE-RANGE PHOTOGRAMMETRY Ph.D. Thesis
Mostafa Seyed Madani 1987 211 p
Avail: Univ. Microfilms Order No. DA8717680

Techniques of self calibration and quality control are used to obtain the highest possible accuracy from nonmetric cameras. Two nonmetric cameras, the Hasselblad C/M 500 and the Minolta XC5 are used along with a Wild P32 metric camera for comparison purposes. A progressive data snooping technique is used in a sequential model to detect and locate the erroneous observations. For a system having at least four convergent, overlapping photographs and having a dense image point distribution, extra-correlation was found to be of marginal use. However, inter-correlation was helpful in locating blunders in a data set. Three different error models are analyzed for compensation of systematic errors. Their parameters are treated as photo-invariant and/or block-invariant, based on the characteristics of the physical sources and the geometry of the computing units in on-line triangulation. It was found that block-invariant and mixed photo/block-invariant additional parameters (APs) provide similar results for precision and accuracy indicators. Determinability and significance of APs are also studied. Several measures and a decision table are suggested for checking the determinability of APs.
Dissert. Abstr.

N88-12863 Miami Univ., Fla.
MESOSCALE EDDY DYNAMICS BY THE METHOD OF POINT VORTICES Ph.D. Thesis
Stanford Baird Hooker 1987 173 p
Avail: Univ. Microfilms Order No. DA8716167

The subject of mesoscale eddies is considered from the vantage of vorticity dynamics in a numerical model based on the point vortex model developed by Christiansen. Barotropic and equivalent baratropic inviscid eddies on a f-plane are considered; full baroclinic and planetary effects are not included. A wide parameter range is considered to describe and demonstrate under which circumstances the separate and combined effects of adjacent vortices, mean flow (jet), and nearby topography (sidewalls) can alter the translation and evolution of an isolated eddy. The interaction of equivalent barotropic eddies is seen to be similar to their 2-dimensional counterparts, but with an important difference: the scale at which the vortices interact is reduced. This is a consequence of the weakening strain field associated with introducing the vertical stretching contribution to the potential vorticity. The interaction of an eddy with a jet usually results in an upstream motion of the eddy. The controlling factor for this motion is the formation of a vortex that forms from the adjacent shear vorticity of the jet.
Dissert. Abstr.

N88-12864 Minnesota Univ., Minneapolis.
TWO-LAYER STRATIFIED FLOW ANALYSIS OF GRAVITY CURRENTS AND TURBIDITY CURRENTS IN LAKES, RESERVOIRS AND THE OCEAN Ph.D. Thesis
Juichiro Akiyama 1987 302 p
Avail: Univ. Microfilms Order No. DA8718606

Suspension gravity currents (turbidity currents) occurring in lakes, reservoirs, and the ocean are investigated theoretically. When the turbid water, a mixture of suspended particles and clear water, is introduced in a quiescent body of clear water, the turbid mixture flows downslope due to its larger density. The governing equations which describe the movement of gradually varied steady-state turbidity currents occurring in sloping channels with constant as well as variable widths are developed. In order to incorporate the mechanism of sediment exchange into the model, the sediment entrainment function is derived by utilizing data for suspended sediment transport in free-surface open channel flows and is applied to the analysis. The model is alo applied to actual field sites. Such turbidity currents can be originated by various processes when large amounts of sediment are put into suspension. One mechanism investigated both theoretically and experimentally is the direct inflow of a dense river water into a reservoir. This phenomenon is sometimes referred to as plunging flow.
Dissert. Abstr.

N88-12865*# Arizona Univ., Tucson. Committee on Remote Sensing.
RADIOMETRIC CALIBRATION OF THE EARTH OBSERVING SYSTEM'S IMAGING SENSORS Semiannual Report, May - Nov. 1987
P. N. Slater Dec. 1987 35 p
(Grant NAGw-896)
(NASA-CR-181542; NAS 1.26:181542) Avail: NTIS HC A03/MF A01 CSCL 14B

Philosophy, requirements, and methods of calibration of multispectral space sensor systems as applicable to the Earth Observing System (EOS) are discussed. Vicarious methods for calibration of low spatial resolution systems, with respect to the Advanced Very High Resolution Radiometer (AVHRR), are then summarized. Finally, a theoretical introduction is given to a new vicarious method of calibration using the ratio of diffuse-to-global irradiance at the Earth's surfaces as the key input. This may provide an additional independent method for in-flight calibration. Author

44 ENERGY PRODUCTION AND CONVERSION

Includes specific energy conversion systems, e.g., fuel cells; global sources of energy; geophysical conversion; and windpower.

For related information see also *07 Aircraft Propulsion and Power, 20 Spacecraft Propulsion and Power,* and *28 Propellants and Fuels.*

N88-12866# Commission of the European Communities (Luxembourg)
SOLAR ENERGY: EUROPEAN RESEARCH AND DEVELOPMENT
W. Palz 1985 341 p
(PB87-107645; EUR-9374-EN; ISBN-92-825-5307-8) Avail: NTIS HC E12/MF E12; customers in the European Community Countries should apply to the Office for Official Publications of the European Communities, B.P. 2985, Luxembourg CSCL 10A

The catalog contains two-page summaries of the results obtained in the contracts on solar energy R and D, i.e., solar radiation data, solar heating, the Eurelios solar tower power plant, photovoltaic power generation, which were concluded between the Commission of the European Communities, Directorate General for Science, Research and Development, Brussels, and a number of public and private research institutions of the European Community;.
GRA

N88-12867# Technische Hogeschool, Delft (Netherlands). Lab. voor Koudetechniek en Klimaatregeling.
TECHNICAL EVALUATION OF A SOLAR-POWERED ABSORPTION COOLING SYSTEM (LiBr-H2O)

J. P. vanSchie Apr. 1983 143 p In Dutch
(PB87-108254; ST-201) Avail: Issuing Activity CSCL 10A

The report contains a technical evaluation of a solar-powered absorption cooling system in which lithium bromide and water are the solvent and coolant, respectively. The goal of the evaluation is the optimization of existing systems. To this end, a computer model is developed based on the mathematical description of the physical process using the mass and energy balances in the individual components of the cooling system. GRA

N88-12868# California Univ., Berkeley. Lawrence Berkeley Lab.
TECHNOLOGY BASE RESEARCH PROJECT FOR ELECTROCHEMICAL ENERGY STORAGE Annual Report, 1986
K. Kinoshita, ed. Jul. 1987 61 p
(Contract DE-AC03-76SF-00098)
(DE88-000649; LBL-23495) Avail: NTIS HC A04/MF A01

The US DOE Office of Energy Storage and Distribution provides continuing support for an Energy Storage Program, which includes R and D on advanced electrochemical energy storage and conversion systems. A major goal of this program is to develop electrochemical power sources suitable for application in electric vehicles and/or electric load-leveling devices. The program centers on advanced secondary batteries and fuel cells that offer the potential for high performance and low life-cycle costs. The Technology Base Research Project is divided into three major project elements: Exploratory Research, Applied Science Research, and Air Systems Research. Highlights of each project element are summarized according to the appropriate battery system or electrochemical research area. Cells covered include molten salt, lithium, alkaline, zinc/halogen, alkali/sulfur, nonaqueous, metal/air, fuel cell. DOE

N88-12869# Systems Research Labs., Inc., Dayton, Ohio. Research Applications Div.
NITROGEN ENERGY TRANSFER STUDY Final Report, 10 Sep. 1984 - 31 Dec. 1986
D. F. Grosjean Aug. 1987 88 p
(Contract F33615-84-C-2441)
(AD-A184457; AFWAL-TR-87-2038) Avail: NTIS HC A05/MF A01 CSCL 07D

The use of Nitrogen as an energy transfer medium between an electrical discharge and a target molecule was investigated experimentally. Efforts were concentrated primarily upon the attainment of a high density of N2 metastable molecules in a flowing afterglow arrangement. Excitation techniques utilized were microwave surface-wave discharges and dielectric-barrier discharges at pressures of 3 to 760 Torr in N2 and Argon Nitrogen mixtures. Although the radiative lifetime of Nitrogen (Active state) is long, the effective lifetime at high pressures was found to be much too short for use in a flowing system. GRA

N88-12870*# Boeing Aerospace Co., Seattle, Wash.
LIGHT FUNNEL CONCENTRATOR PANEL FOR SOLAR POWER Final Report
May 1987 60 p
(Contract NAS8-36463)
(NASA-CR-179223; NAS 1.26:179223; D180-30473-1) Avail: NTIS HC A04/MF A01 CSCL 10B

The solar concentrator design concept provides a theoretical concentration efficiency of 96 percent with power-to-weight ratios as high as 50 W/kg. Further, it eliminates the need for fragile reflective coatings and is very tolerant to pointing inaccuracies. The concept differs from conventional reflective mirrors and lens design in that is uses the principle of total internal reflection in order to funnel incident sunlight into a concentrator photovoltaic cell. The feasibility of the light funnel concentrator concept was determined through a balanced approach of analysis, development, and fabrication of prototypes, and testing of components. A three-dimensional optical model of the light funnel concentrator and photovoltaic cell was developed in order to assess the ultimate performance of such systems. In addition, a thermal and structural analysis of a typical unit was made. Techniques of fabricating the light funnel cones, optically coupling them to GaAs concentrator cells, bonding the funnels to GaAs cells, making electrical interconnects, and bonding substrates was explored and a prototype light funnel concentrator unit was fabricated and tested. Testing of the system included measurements of optical concentrating efficiency, optical concentrator to cell coupling efficiency, and electrical efficiency. B.G.

N88-12871# Institute of Gas Technology, Chicago, Ill.
INTERNAL REFORMING DEVELOPMENT FOR SOLID OXIDE FUEL CELLS Final Report
A. L. Lee Feb. 1987 194 p
(Contract DE-AC21-85MC-22045)
(DE87-006518; DOE/MC-22045/2364) Avail: NTIS HC A09/MF A01

Internal reforming of natural gas within a solid oxide fuel cell (SOFC) should simplify the overall system design and make the SOFC an attractive means for producing electrical power. This program was undertaken to investigate the catalytic properties of nickel cermets, which are prime candidates for SOFC anodes. The initial task in this program was an extensive literature search for information on steam reforming of light hydrocarbons. The second task was to modify and calibrate the reactor systems that were used in the experimental kinetic studies. Two systems were used in this investigation; a continuously stirred tank reactor system (CSTR) and a plug flow reactor system (PFR). In the third task, 16 nickel-zirconia cermets were prepared using four procedures, tape casting, Westinghouse slurry, incorporation of performers, and granulation. The catalytic behavior of three cermets was determined in the fourth task. The reaction was first order with respect to methane and -1.25 for steam. Ethane and propane in the feed did not affect the methane conversion rate. The cermet has a higher initial tolerance for sulfur than standard nickel reforming catalysts. The final task was a mechanistic study of the steam reforming reaction on nickel and nickel-zirconia catalysts. DOE

N88-12872# Sandia National Labs., Albuquerque, N. Mex.
A HYDROGEN/NICKEL OXIDE BATTERY FOR REMOTE APPLICATIONS
D. M. Bush and J. F. Sindorf 1987 10 p Presented at the 172nd Meeting of the Electrochemical Society, Honolulu, Hawaii, 18 Oct. 1987 Prepared in cooperation with Johnson Controls, Inc., Milwaukee, Wis.
(Contract DE-AC04-76DP-00789)
(DE87-009048; SAND-87-0996C; CONF-871027-8) Avail: NTIS HC A02/MF A01

A hydrogen/nickel oxide battery is being developed for terrestrial applications. The main purpose has been to reduce the cost of the aerospace technology, with only minimal changes in the performance characteristics. The latest design consists of individual prismatic cells in a sealed common pressure vessel; thus, the battery is essentially maintenance free. The development work has been conducted at Comsat Laboratories and Johnson Controls, Inc., under a cost sharing contract with Sandia National Laboratories. Contract deliverables include cells and batteries. Testing of one of the batteries connected in parallel with a photovoltaic array and a constant current load is described. Only minimal controls are necessary since gases recombine internally on overcharge. The state-of-charge can be monitored continuously by measuring the hydrogen pressure. DOE

N88-12873# Pacific Northwest Labs., Richland, Wash.
INPUT TURBULENCE FEATURES AT A MEGAWATT-SIZE WIND TURBINE, MEDICINE BOW, WYOMING
J. R. Connell, V. R. Morris, and M. E. Hinchee Dec. 1986 14 p Presented at the 10th Energy Sources Technology Conference and Exhibition, Dallas, Tex., 15 Feb. 1987
(Contract DE-AC06-76RL-01830)
(DE88-000098; PNL-SA-14517; CONF-870210-2) Avail: NTIS HC A03

In response to recent observations that wind turbulence has a strong effect on wind turbine fatigue life, measurements of turbulent wind velocity profiles have been made at the Medicine

Bow, Wyoming, WTS-4 wind turbine site. These measurements were taken at seven levels spanning the WTS-4 rotor height on a single meteorological tower 1.75 rotor diameters upstream of the turbine. Concurrent measurements of rotor response were also made. Analysis of the winds at the Medicine Bow site reveals the influence of atmospheric and geographic conditions on what may at first glance appear to be a classic, simple, flat terrain case. The turbulence data are then analyzed to: (1) characterize the wind in terms of fixed-point, single-tower properties, and (2) model the wind properties as they would be experienced by points on rotating turbine blades. The STRS-2 model, developed by the Pacific Northwest Laboratory, is used to convert single-tower wind characteristics into those that would be measured from an array of towers arranged in a crosswind line covering the rotor disk. A response function for the flatwise root bending moment of one of the WTS-4 turbine blades is computed using the turbine data and the STRS-2 data. The STRS-2 model provides a substantially improved correlation with wind turbine blade bending moment over other single-tower estimation methods. DOE

N88-12874# Pacific Northwest Labs., Richland, Wash.
PERFORMANCE ANALYSIS OF SOLAR THERMAL POWER SYSTEMS
T. A. Williams and J. A. Dirks Apr. 1987 12 p Presented at the Conference of the American Solar Energy Society, Boulder, Colo., 12 Jul. 1987
(Contract DE-AC06-76RL-01830)
(DE88-000563; PNL-SA-14588; CONF-8707117-1) Avail: NTIS HC A03/MF A01

Methods of analyzing and predicting the performance of solar thermal power plants for electric applications are discussed, and insight provided into the major energy loss mechanisms for solar thermal systems. The efficiency of each component in a solar thermal plant is discussed as are the plant parasitic losses and plant availability. This is followed by a discussion of the computer simulation which is needed to derive reasonable projections of component annual efficiencies and parasitic losses. Finally, plant design considerations and annual system performance estimates are made. DOE

N88-12875*# Hughes Aircraft Co., Long Beach, Calif.
DESIGN DESCRIPTION REPORT FOR A PHOTOVOLTAIC POWER SYSTEM FOR A REMOTE SATELLITE EARTH TERMINAL
N. A. Marshall and G. J. Naff Jan. 1987 136 p
(Contract NAS3-23862)
(NASA-CR-179586; NAS 1.26:179586) Avail: NTIS HC A07/MF A01 CSCL 10B

A photovoltaic (PV) power system has been installed as an adjunct to an agricultural school at Wawatobi on the large northern island of the Republic of Indonesia. Its purpose is to provide power for a satellite earth station and a classroom. The renewable energy developed supports the video and audio teleconferencing systems as well as the facility at large. The ground station may later be used to provide telephone service. The installation was made in support of the Agency for International Development's Rural Satellite Program, whose purpose is to demonstrate the use of satellite communications for rural development assistance applications. The objective of this particular PV power system is to demonstrate the suitability of a hybrid PV engine-generator configuration for remote satellite earth stations. F.M.R.

N88-12876# Sandia National Labs., Albuquerque, N. Mex.
MEASUREMENTS AND CALCULATIONS OF AERODYNAMIC TORQUES FOR A VERTICAL-AXIS WIND TURBINE
R. E. Akins, D. E. Berg, and W. T. Cyrus Oct. 1987 43 p
(Contract DE-AC04-76DP-00789)
(DE88-001783; SAND-86-2164) Avail: NTIS HC A03/MF A01

This report describes measurements of aerodynamic torque on a vertical-axis wind turbine. Accelerometers mounted at the equator of the rotor and a torque meter mounted at the base of the rotor were used to compute the net aerodynamic torque acting on the rotor. Assumptions concerning blade-response symmetry were required to achieve blade torque as a function of rotor position on each half of a revolution for a two-bladed rotor. Results are presented for tip-speed ratios from 2.5 to 8.0 for two turbine rotational speeds. Evidence of dynamic stall is observed at low tip-speed ratios. DOE

N88-12877*# National Aeronautics and Space Administration. Lewis Research Center, Cleveland, Ohio.
PERFORMANCE OF GaAs AND SILICON CONCENTRATOR CELLS UNDER 37 MeV PROTON IRRADIATION
Henry B. Curtis and Clifford K. Swartz 1987 10 p Presented at the 19th Photovoltaic Specialists Conference, New Orleans, La., 4-8 May 1987; sponsored by IEEE
(NASA-TM-100144; E-3696; NAS 1.15:100144) Avail: NTIS HC A02/MF A01 CSCL 10A

Gallium arsenide concentrator cells from three sources and silicon concentrator cells from one source were exposed to 37 MeV protons at fluences up to 2.8 x 10 to the 12th protons/sq cm. Performance data were taken after several fluences, at two temperatures (25 and 80 C), and at concentration levels from 1 to about 150 x AMO. Data at one sun and 25 C were taken with an X-25 xenon lamp solar simulator. Data at concentration were taken using a pulsed solar simulator with the assumption of a linear relationship between short circuit current and irradiance. The cells are 5 x 5 mm with a 4-mm diameter illuminated area. Author

N88-12878*# National Aeronautics and Space Administration. Lewis Research Center, Cleveland, Ohio.
RADIATION PERFORMANCE OF AlGaAs CONCENTRATOR CELLS AND EXPECTED PERFORMANCE OF CASCADE STRUCTURES
Henry B. Curtis, Clifford K. Swartz, and Russell E. Hart, Jr. [1987] 11 p Presented at the 19th Photovoltaic Specialists Conference, New Orleans, La., 4-8 May 1987; sponsored by IEEE
(NASA-TM-100145; E-3697; NAS 1.15:100145) Avail: NTIS HC A03/MF A01 CSCL 10A

Aluminum gallium arsenide, GaAs, silicon and InGaAs cells have been irradiated with 1 MeV electrons and 37 MeV protons. These cells are candidates for individual cells in a cascade structure. Data is presented for both electron and proton irradiation studies for one sun and a concentration level of 100X AMO. Results of calculations on the radiation resistance of cascade cell structures based on the individual cell data are also presented. Both series connected and separately connected structures are investigated. Author

N88-12879# Sandia National Labs., Albuquerque, N. Mex.
INTERNATIONAL ENERGY AGENCY (IEA) SMALL SOLAR POWER SYSTEMS (SSPS) SODIUM CAVITY AND EXTERNAL RECEIVER PERFORMANCE COMPARISON
A. F. Baker Oct. 1987 43 p
(Contract DE-AC04-76DR-00789)
(DE88-001310; SAND-87-8021) Avail: NTIS HC A03/MF A01

Experimental data is used to compare the performance of two sodium cooled solar central receivers operated at the International Energy Agency Small Solar Power Systems project near Almeria, Spain. Performance includes point-in-time steady state efficiency, average efficiency, start-up time, and operation time. Point-in-time steady state efficiency calculations were based on the statistical method of least squares using receiver incident and absorbed powers. One receiver, a cavity type, showed a peak steady state receiver efficiency of 87% +/- 5% and an average efficiency of about 67%. The other receiver, an external billboard type, had a peak steady state receiver efficiency of 96% +/- 4% and an average efficiency of about 79%. The original design peak steady state efficiency predictions for both receivers were within the experimentally determined 95% probability interval. Thermal loss test data were evaluated for the external receiver to confirm its point-in-time steady state efficiency independent of the receiver incident power. The thermal loss, which includes emitted radiation, convection, and conduction from the external receiver, was less than 100 kW(sub t) with the receiver operating at normal design

conditions and having an absorbed power of over 2200 kW/sub t/. DOE

N88-12880# Sandia National Labs., Albuquerque, N. Mex.
CHARACTERISTICS OF CURRENT SOLAR CENTRAL RECEIVER PROJECTS
A. F. Baker and A. C. Skinrood Oct. 1987 34 p
(Contract DE-AC04-76DR-00789)
(DE88-001314; SAND-86-8058) Avail: NTIS HC A03/MF A01

This report summarizes the characteristics and status of six experimental solar central receiver projects. These are Eurelios (located in Italy), CESA-I (Spain), International Energy Agency Small Solar Power Systems Project (Spain), Sunshine (Japan), Themis (France), and Solar One (US). DOE

N88-12881# Pacific Northwest Labs., Richland, Wash.
USING A NEW CHARACTERIZATION OF TURBULENT WIND FOR ACCURATE CORRELATION OF WIND TURBINE RESPONSE WITH WIND SPEED
J. R. Connell and R. L. George Sep. 1987 44 p
(Contract DE-AC06-76RL-01830)
(DE88-001453; PNL-6283) Avail: NTIS HC A03/MF A01

The turbulence encountered by a point on a rotating wind turbine blade has characteristics that in some important respects are different from those measured by a stationary anemometer. The conventional one-peaked continuous spectrum becomes, broadly, a two-peaked spectrum that in addition contains a set of narrow-band spikes of turbulence energy, one centered on the frequency of rotor rotation and the others centered on multiples of that frequency. The rotational sampling effect on wind spectra is quantified using measurements of wind velocity by anemometers on stationary crosswind circular arrays. Characteristics of fluctuating wind are compared to measured fluctuations of bending moments of the rotor blades and power output fluctuations of a horizontal-axis wind turbine at the same site. The wind characteristics and the correlations between wind fluctuations and wind turbine fluctuations provide a basis for improving turbine design, siting, and control. DOE

N88-12882# Oak Ridge National Lab., Tenn.
A STUDY OF THE OPTIMAL TRANSITION TEMPERATUE OF PCM (PHASE CHANGE MATERIAL) WALLBOARD FOR SOLAR ENERGY STORAGE
J. B. Drake Sep. 1987 19 p
(Contract DE-AC05-84OR-21400)
(DE88-001522; ORNL/TM-10210) Avail: NTIS HC A02/MF A01

The performance of wallboard impregnated with phase change material (PCM) is considered. An ideal setting is assumed and several measures of performance discussed. With a definition of optimal performance given, the performance with respect to variation of transition temperature is studied. Results are based on computer simulations of PCM wallboard with a standard stud wall construction. The diurnal heat capacity was found to be to be overly sensitive to numerical errors for use in PCM applications. The other measures of performance, diurnal effectiveness, net collected to storage ratio, and absolute discharge flux, all indicate similar trends. It is shown that the optimal transition temperature of the PCM is strongly influenced by the amount of solar flux absorbed. DOE

N88-12883# California Univ., Berkeley. Lawrence Berkeley Lab.
PROCEEDINGS OF THE ELEVENTH DOE SOLAR PHOTOCHEMISTRY RESEARCH CONFERENCE
Jul. 1987 202 p Conference held in Tahoe City, Calif., 7 Jun. 1987
(Contract DE-AC03-76SF-00098)
(DE88-000678; LBL-23453; CONF-870666-Summa) Avail: NTIS HC A10/MF A01

The program of the Eleventh DOE Solar Photochemistry Research Conference, the abstracts of 28 formal presentations and 42 posters, a record of the often lively questions and answers following each presentation, and a list of the 93 attendees are presented. DOE

N88-12884# Sandia National Labs., Albuquerque, N. Mex.
THE DEVELOPMENTAL STATUS OF SOLAR THERMOCHEMICAL HYDROGEN PRODUCTION
C. W. Pretzel and J. E. Funk Sep. 1987 114 p
(Contract DE-AC04-76DR-00789)
(DE88-001778; SAND-86-8056) Avail: NTIS HC A06/MF A01

This report discusses the status of development on solar thermochemical hydrogen production. It discusses the results of recent experiments of components for the solar interface. Various process designs that have been proposed are examined and areas of technical concern are discussed. The process has the potential for having the highest efficiency for producing hydrogen from water. Development has consisted of process flowsheet designs for using nuclear heat sources, several solar interface conceptual designs, and experiments for solar central receiver components. Conceptually, the flowsheets show how the chemical process plant is to actually be built. Each stream is identified and temperature, pressure, and composition are specified. The function of each piece of process equipment - reactors, heat exchangers - is defined. Design requirements such as conversion, heat transfer, etc., and materials of construction are established. While many uncertainties still exist, we have identified no major technical problems that will prevent the production of solar thermochemical hydrogen if additional analysis and experimentation are completed. DOE

N88-12885# Cranfield Inst. of Tech., Bedford (England). School of Mechanical Engineering.
DESIGN AND DEVELOPMENT OF ABSORPTION HEAT PUMPS Final Report
I. E. Smith 1986 67 p
(DE88-900082; EUR-10808-EN) Avail: NTIS (US Sales Only) HC A04/MF A01

The aim of the research was to demonstrate an absorption heat pump capable of accepting heat from ambient air at building design temperatures, typically -1 C, and elevating it typically to 70 C to supply hydronic central heating systems. An absorbent consisting of a mixture of sodium and potassium hydroxide has been investigated with water as the working fluid and it has been demonstrated that it will accept heat at -5 C and deliver heat 68 degrees higher. If the condenser of the heat pump was operated at temperatures of around 80 C then the heat pump system would meet the above requirement. Liquid water, containing an anti-freeze component has successfully been evaporated at -5 C, and heat transfer coefficients for evaporation at these, and lower temperatures, have been measured. Both film flash evaporation have been investigated in a quantitative manner. The important matter of constructional materials has been investigated through literature review and consultation and no insuperable problems have been identified. DOE

N88-12504# Joint Publications Research Service, Arlington, Va.
SOLAR CONVERGING METHOD
In its JPRS Report: Science and Technology. Japan 24 Aug. 1987 p 3-5 Transl. into ENGLISH from Nikko Materials (Tokyo, Japan) Feb. 1987 p 35-36 (For primary document see N88-12502 04-12)
Avail: NTIS HC A06/MF A01

45 ENVIRONMENT POLLUTION

Includes atmospheric, noise, thermal, and water pollution.

No abstracts in this category.

46 GEOPHYSICS

Includes aeronomy; upper and lower atmosphere studies; ionospheric and magnetospheric physics; and geomagnetism.

For space radiation see *93 Space Radiation.*

N88-12886# Commission of the European Communities (Luxembourg).

STATISTICAL DISTRIBUTION OF SOLAR RADIATION (HOURLY SUMS): CUMULATIVE FREQUENCY CURVES PREPARATION OF A EUROPEAN DATA SET AND DIRECTION FOR USE

B. Bourges and F. Lasnier 1985 166 p

(PB87-107454; EUR-10203-EN) Avail: NTIS HC E07/MF E07; customers in the European Community countries should apply to the Office for Official Publications of the European Communities, B.P. 2985, Luxembourg CSCL 04A

The monthly statistical distribution of solar irradiance, as Cumulative Frequency Curves (CFC), is a particularly well suited meteorological input for solar system design tools. (The ESM method for Solar Active Space Heating Systems is a good example of these methods.) The present report contains: generalities on CFCs (characteristics, use in simplified methods, way of fitting); CFCs of global irradiance on horizontal plane (statistical method used to derive empirical formulas, comparison with the so-called utilizability); CFCs of global irradiance on inclined surfaces (reconstitution of irradiance on inclined surface from measurements, global and diffuse, on horizontal plane); available data sets.

GRA

N88-12887# Army Cold Regions Research and Engineering Lab., Hanover, N. H.

DISTURBANCE AND RECOVERY OF ARCTIC ALASKAN TUNDRA TERRAIN. A REVIEW OF RECENT INVESTIGATIONS Report, 1976 - 1983

Donald A. Walker, David Cate, Jerry Brown, and Charles Racine Jul. 1987 72 p

(AD-A184442; CRREL-87-11) Avail: NTIS HC A04/MF A01 CSCL 08F

This report summarizes over a decade of CRREL-managed research regarding disturbance and recovery in northern Alaska. Themes emphasized include: (1) Most anthropogenic disturbances have natural analogs, which can provide much inexpensive information that can be related to modern disturbances and their rates of recovery. (2) Most single-event disturbances will heal and develop a functioning ecosystem within a human life span, but a return to the original ecosystem can rarely be expected for major impacts. (3) The concept of recovery must be based on consistent terminology that recognizes the distinction between ecosystem resistance (the ability to withstand impact) and resilience (the ability to return to the previous undisturbed state) and also the distinction between complete recovery (a return to the original ecosystem) and functional recovery (the development of a functional ecosystem different from the original). In permafrost regions with massive ground ice, recovery of the vegetation is limited by alterations to the permafrost regime.

GRA

N88-12888# Teledyne Geotechnical, Alexandria, Va.

MULTICHANNEL DECONVOLUTION OF P WAVES AT SEISMIC ARRAYS AND THREE COMPONENT STATIONS Annual Report, 1 Oct. 1985 - 1 Oct. 1986

Z. A. Der, A. C. Lees, R. H. Shumway, T. W. McElfresh, and M. E. Marshall 30 Oct. 1986 116 p

(Contract F08606-86-C-0006; ARPA Order 4511)

(AD-A184450; TGAL-86-6) Avail: NTIS HC A06/MF A01 CSCL 08K

The results of a new multichannel method, applied to array recordings and three component station networks for teleseismic P waves, are presented and interpreted in terms of possible surface reflections and other arrivals from the Nevada Test Site (NTS), Novaya Zemlya, and Eastern Kazakh Test Site (EKTS) nuclear explosions. The deconvolution method utilizes the well known fact that P wave spectra can be decomposed into source and receiver spectral factors. The source functions obtained in the deconvolution process provide a better picture of the nature of explosion source time functions, and in particular of the presence or lack of secondary arrivals following the P wave such as pP or spall. The presence of such secondary arrivals and their effects on the first cycle of the P wave are very important in yield estimation. For most events at the eastern part of EKTS the source time functions appear to contain a pP arrival but they also show later, unexplained arrivals and other complexities. At other test sites often there are no clearly identifiable pP phases in the deconvolved traces. Joint deconvolution of central EKTS data using all AWRE arrays indicated strong azimuthal asymmetries in the body wave radiation. Deconvolutions of NTS events were considerably degraded by the limited signal bandwidth due to strong mantle attenuation under this test site. The site functions are also complex in most cases. Site and source effects contribute about equally to the energy observed in the P codas of the events analyzed.

GRA

N88-12889# Lower Mississippi River Forecast Center, Slidell, La. Center for Atmospheric Research.

HIGH LATITUDE F-REGION DRIFT STUDIES Technical Report, Oct. 1985 - Sep. 1986

Bodo W. Reinisch, Jurgen Buchau, Edward J. Weber, Claude G. Dozois, and Klaus Bibl Dec. 1986 28 p

(Contract F19628-83-C-0092)

(AD-A184466; ULRF-436/CAR; AFGL-TR-87-0154; SR-7) Avail: NTIS HC A03/MF A01 CSCL 04A

The large scale, high latitude ionospheric convection pattern is driven by the interaction of the solar wind and the interplanetary magnetic field with the Earth's magnetosphere. Ground-based digital ionosondes, with spaced receiving antennas, have been developed and deployed at the high latitude stations of Thule, Greenland and Goose Bay, Labrador. Results from these stations demonstrate that the ionospheric convection can be measured for the bottomside ionosphere. Data from Thule consistently show the predominant antisunward convection. The data from Goose Bay indicate the sunward return flows of the polar plasma convection and the switch over when the station rotates from the dusk into the dawn cell. These data also illustrate the potential for systematic study of the convection patterns that is possible with a network of ground-based digital ionosondes.

Author (GRA)

N88-12890*# Scripps Institution of Oceanography, La Jolla, Calif. Inst of Geophysics and Planetary Physics.

STATISTICS OF THE GEOMAGNETIC SECULAR VARIATION FOR THE PAST 5Ma

C. G. Constable and R. L. Parker [1986] 54 p

(Grant NAG5-883)

(NASA-CR-181558; NAS 1.26:181558) Avail: NTIS HC A04/MF A01 CSCL 08N

A new statistical model is proposed for the geomagnetic secular variation over the past 5Ma. Unlike previous models, the model makes use of statistical characteristics of the present day geomagnetic field. The spatial power spectrum of the non-dipole field is consistent with a white source near the core-mantle boundary with Gaussian distribution. After a suitable scaling, the spherical harmonic coefficients may be regarded as statistical samples from a single giant Gaussian process; this is the model of the non-dipole field. The model can be combined with an arbitrary statistical description of the dipole and probability density functions and cumulative distribution functions can be computed for declination and inclination that would be observed at any site on Earth's surface. Global paleomagnetic data spanning the past 5Ma are used to constrain the statistics of the dipole part of the field. A simple model is found to be consistent with the available data. An advantage of specifying the model in terms of the spherical harmonic coefficients is that it is a complete statistical description of the geomagnetic field, enabling us to test specific properties for a general description. Both intensity and directional data distributions may be tested to see if they satisfy the expected model distributions.

Author

N88-12891 Ohio State Univ., Columbus.
AN ALGORITHMIC APPROACH TO CRUSTAL DEFORMATION ANALYSIS Ph.D. Thesis
Huseyin Baki Iz 1987 127 p
Avail: Univ. Microfilms Order No. DA8717651

In recent years the analysis of crustal deformation measurements has become important as a result of current improvements in geodetic methods and an increasing amount of theoretical and observational data provided by several earth sciences. A first-generation data analysis algorithm which combines a priori information with current geodetic measurements was proposed. Prior information is the unifying feature of this algorithm. Some of the problems which may arise through the use of a priori information in this analysis were indicated and preventive measures were demonstrated. Six different estimators which employ a priori information were examined. Emphasis was put on the case when the prior information is wrong and analytical expressions for possible improvements under incompatible prior information were derived. Dissert. Abstr.

N88-12892 Rice Univ., Houston, Tex.
BANDED ION MORPHOLOGY Ph. D. Thesis
Rudy Allan Frahm 1987 236 p
Avail: Univ. Microfilms Order No. DA8718712

Bands of ions were observed at constant pitch angle by the Dynamics Explorer High and Low Altitude Plasma Instruments at auroral latitudes. The observed ion dispersion pattern shows lower energy ions toward the equatorward side of the band and higher energy ions toward the poleward side of the band. Ion bands have their highest energy flux at small pitch angles. The observed bands were correlated with storm phase (by Dst) and substorm phase (by AE). Two models have the potential of producing ion signatures that are similar to the band features. Simulations were performed on ions under the influence of the time-of-flight and convective dispersion mechanisms. Using the measured drifts on a satellite pass which shoed a band, ions were traced from one hemisphere to the other. A composite of arrival latitudes from an inverted V simulated source in the opposite hemisphere, nearly approximates the banded ion pattern. Thus, it was concluded tht convective dispersion is the correct mechanism for formation of ion bands. Dissert. Abstr.

N88-12893 State Univ. of New York, Stony Brook.
THE EFFECTS OF MINOR TRACE GASES ON THE TRANSFER OF THERMAL INFRARED RADIATION THROUGH THE EARTH'S ATMOSPHERE Ph.D. Thesis
David Paul Kratz 1987 224 p
Avail: Univ. Microfilms Order No. DA8717343

The ability of narrow-band models to calculate accurately the radiative effects of infrared-active molecules is investigated. The models are employed to investigate the radiative effects which minor trace gases have on the transfer of thermal infrared radiation through the atmosphere. Results show that, in general, the Malkmus narrow-band model with an interval width of 5/cm is fairly accurate in reproducing the total band absorptance results as calculated for a homogeneous gas by the reference line-by-line procedure. The Curtis-Godson scaling procedure when employed with a narrow-band model provides an accurate means of accounting for atmospheric temperature and pressure variations for a gas with an altitude invariant mixing ratio. The transmissivity multiplication property when utilized by a random-line narrow-band model is a valid technique to account for the overlap of the absorption bands of different gases. There are notable exceptions to these results. It is demonstrated that a doubling of the minor trace gases will collectivley yield a radiative effect comparable to a doubling of CO2. On a per molecule basis, the minor trace gases possess a far greater radiative effect than CO2. Dissert. Abstr.

N88-12894 Denver Univ., Colo.
RELATIVISTIC ELECTRON PRECIPITATIONS IN A PULSATING AURORA Ph.D. Thesis
Karl D. Hudnut 1987 153 p
Avail: Univ. Microfilms Order No. DA8717205

Data from scintillation and solid state detectors flown on rockets in Norway are used to examine the temporal and energetic characteristics of relativistic electrons precipitated during a pulsating post breakup aurora in the morning sector. Electron bursts with mildly relativistic energies discovered from the data are discribed in detail. Temporal features of these bursts showing periodic components on a time scale of 10 ms are described. These observations constitute a new regime of time and energy for electrons in morningside aurorae. A region within approximately 1 earth radius above the ionosphere on the L = 6.6 magnetic field line is determined as the point of acceleration of the electrons. These temporal, energetic and spatial characteristics are compared to the electron cyclotron resonance theory which was proposed to explain pulsating electron precipitation in a morningside aurorae. The theoretical model is shown to adequately explain some but not all of the observations. Suggestions for further theoretical and experimental treatments of this problem are made.
Dissert. Abstr.

N88-12895# California Univ., Berkeley. Lawrence Berkeley Lab.
SLOW-MODE SHOCKS IN THE EARTH'S MAGNETOSPHERE
W. C. Feldman 1987 41 p Presented at the 6th Meeting of Solar Wind, Estes Park, Colo., 24 Aug. 1987
(Contract W-7405-eng-36)
(DE88-000483; LA-UR-87-3261; CONF-8708141-2) Avail: NTIS HC A03/MF A01

The locations and structure of slow-mode shocks in the earth's magnetosphere are reviewed. To date, such shocks have only been identified along the high latitude portions of the lobe-plasma sheet boundary of the geomagnetic tail. Although their intrinsic thickness is of the order of the upstream ion inertial length, they affect the internal state of a relatively much larger volume of surrounding plasma. In particular, they support a well-developed foreshock very similar to that observed upstream of the earth's bow shock, and a turbulent, strongly convecting downstream flow. They also figure importantly in the energy budget of geomagnetic substorms and produce effects which are closely analogous to much of the phenomenology known from solar observations to be associated with two-ribbon flares. DOE

N88-12896# Department of Energy, Washington, D. C. Engineering and Geosciences Div.
SUMMARIES OF PHYSICAL RESEARCH IN THE GEOSCIENCES
Sep. 1987 133 p
(DE88-000833; DOE/ER-0349) Avail: NTIS HC A07/MF A01

The Department of Energy supports research in the geosciences in order to provide a sound foundation of fundamental knowledge in those areas that are germane to the Department of Energy's many missions. The summaries in this document, prepared by the investigators, describe the scope of the individual programs. The Geoscience Research Program includes research in geology, petrology, geophysics, geochemistry, solar-terrestrial relationships, aeronomy, seismology, and natural resource analysis, including their various subdivisions and interdisciplinary areas. All such research is related either directly or indirectly to the Department of Energy's technological needs. DOE

N88-12841# Joint Publications Research Service, Arlington, Va.
INFLUENCE OF STRATIFICATION IN NEAR-SURFACE WATER LAYER ON INTENSITY OF GAS EXCHANGE BETWEEN ATMOSPHERE AND WATER Abstract Only
V. F. Brekhovskikh and V. I. Bratkov *In its* USSR Report: Earth Sciences 22 Jul. 1986 p 17 Transl. into ENGLISH from Izvestiya Akademii Nauk SSSR: Fizika Atmosfery i Okeana (Moscow, USSR), v. 21, no. 11, Nov. 1985 p 1198-1205 (For primary document see N88-12831 04-42)
Avail: NTIS HC A05/MF A01

N88-12843# Joint Publications Research Service, Arlington, Va.
INFLUENCE OF SURFACTANTS ON DAMPING OF GRAVITY-CAPILLARY WAVES. 1: FREQUENCY DEPENDENCE Abstract Only
A. A. Lazarev and K. V. Pokazeyev *In its* USSR Report: Earth Sciences 22 Jul. 1986 p 24 Transl. into ENGLISH from Okeanologiya (Moscow, USSR), v. 26, no. 1, Jan. - Feb. 1986 p 46-50 (For primary document see N88-12831 04-42)
Avail: NTIS HC A05/MF A01

N88-12848# Joint Publications Research Service, Arlington, Va.
SOLUTION OF THREE-DIMENSIONAL INVERSE PROBLEM OF GRAVIMETRY IN CONTACT SURFACES CLASS BY LOCAL CORRECTIONS METHOD Abstract Only
I. L. Prutkin *In its* USSR Report: Earth Sciences 22 Jul. 1986 p 50 Transl. into ENGLISH from Izvestiya Akademii Nauk SSSR: Seriya Fizika Zemli (Moscow, USSR), no. 1, Jan. 1986 p 67-77 (For primary document see N88-12831 04-42)
Avail: NTIS HC A05/MF A01

N88-12849# Joint Publications Research Service, Arlington, Va.
LASERS MEASURE ATMOSPHERE Abstract Only
In its USSR Report: Earth Sciences 22 Jul. 1986 p 52 Transl. into ENGLISH from TASS (Moscow, USSR), 27 Apr. 1986 (For primary document see N88-12831 04-42)
Avail: NTIS HC A05/MF A01

N88-12852# Joint Publications Research Service, Arlington, Va.
MULTIWAVE LASER SOUNDINGS OF ATMOSPHERIC AEROSOL: EXPERIMENTAL RESEARCH (REVIEW) Abstract Only
A. P. Chaikovskiy *In its* USSR Report: Earth Sciences 22 Jul. 1986 p 55 Transl. into ENGLISH from Zhurnal Prikladnoy Spektroskopii (Minsk, USSR), v. 44, no. 2, Feb. 1986 p 183-197 (For primary document see N88-12831 04-42)
Avail: NTIS HC A05/MF A01

N88-12855# Joint Publications Research Service, Arlington, Va.
ABSORPTION OF FAR IR-RADIATION BY H2O-N2 COMPLEXES UNDER ATMOSPHERIC CONDITIONS Abstract Only
A. A. Vigasin and G. V. Chlenova *In its* USSR Report: Earth Sciences 22 Jul. 1986 p 56-57 Transl. into ENGLISH from Izvestiya Akademii Nauk SSSR: Fizika Atmosfery i Okeana (Moscow, USSR), v. 22, no. 1, Jan. 1986 p 30-35 Original language document was announced in IAA as A86-29316 (For primary document see N88-12831 04-42)
Avail: NTIS HC A05/MF A01

N88-12856# Joint Publications Research Service, Arlington, Va.
STRUCTURE OF STABLY STRATIFIED ATMOSPHERIC SURFACE LAYER IN PRESENCE OF HEAT-RELEASING ADMIXTURE Abstract Only
L. Kh. Ingel *In its* USSR Report: Earth Sciences 22 Jul. 1986 p 57 Transl. into ENGLISH from Izvestiya Akademii Nauk SSSR: Fizika Atmosfery i Okeana (Moscow, USSR), v. 22, no. 1, Jan. 1986 p 10-16 (For primary document see N88-12831 04-42)
Avail: NTIS HC A05/MF A01

47 METEOROLOGY AND CLIMATOLOGY

Includes weather forecasting and modification.

N88-12897*# Electro Magnetic Applications, Inc., Denver, Colo.
EXPERIMENTAL AND ANALYTIC STUDIES OF THE TRIGGERED LIGHTNING ENVIRONMENT OF THE F106B
Terence Rudolph, Calvin C. Easterbrook, Poh H. Ng, Robert W. Haupt, and Rodney A. Perala Washington Dec. 1987 122 p
(Contract NAS1-17748)
(NASA-CR-4104; NAS 1.26:4104; EMA-87-R-37) Avail: NTIS HC A06/MF A01 CSCL 04B

The triggered lightning environment of the F106B aircraft is investigated. Scale modeling of the F106B with a metallized model was done to measure electric field enhancement factors on the aircraft and on canonically shaped conducting objects. These are then compared to numerically determined quantities. Detailed numerical modeling is done of the development of the triggered lightning channel. This is done using nonlinear air chemistry models to model a variety of physical phenomena which occur in a triggered lightning event. The effect of a triggered lightning strike on internal wires in the F106B is investigated using finite difference models and transmission line models to calculate the electromagnetic coupling of lightning currents through seams and joints of the aircraft to internal cables. Time domain waveforms are computed and compared to measured waveforms. The effect of thunderstorm particles on the initial triggering of a lightning strike is investigated. The electric field levels needed to cause air breakdown in the presence and absence of thunderstorm particles are calculated. This is done as a function of the size, shape, and density of the particles. Author

N88-12898# National Weather Service, Silver Spring, Md. Office of Meteorology.
NWS (NATIONAL WEATHER SERVICE) WATCH/WARNING VERIFICATION FLASH FLOOD, WINTER STORM AND HIGH WIND, JANUARY 1980 - JUNE 1986
R. E. LaPlante Jul. 1987 43 p
(PB87-223053; NOAA-TM-NWS-FCST-32) Avail: NTIS HC A03/MF A01 CSCL 04B

The study presents flash flood, winter storm, and high wind watch and warning statistics of lead time, probability of detection, false alarm ratio, and critical success index. The period of record is 1980 through 1985 for flash floods and 1980 through June 1986 for winter storms and high winds. Several years of data that were obtained under similar procedures are presented so that trends in watch/warning performance can be established. Two years of detailed statistics, not previously published, of flash floods, winter storms, and high winds are contained in an appendix. GRA

N88-12899# National Center for Atmospheric Research, Boulder, Colo.
USER'S GUIDE TO NCAR (NATIONAL CENTER FOR ATMOSPHERIC RESEARCH) CCM1
L. M. Bath, M. A. Dias, D. L. Williamson, G. S. Williamson, and R. J. Wolski Jun. 1987 186 p
(Grant NSF-ATM-82-17015)
(PB87-224366; NCAR/TN-286/1A) Avail: NTIS HC A09/MF A01 CSCL 04B

Described are the program design, data organization, and operation of the version of the National Center for Atmospheric Research Community Climate Model designated CCM1, and is intended to provide in-depth and easy-to-use information about running CCM1, as well as a description of the model structure and data organization in enough detail that a user can begin to add to or modify the code for his own research. The document, along with a report describing individual subroutines of the model and a report describing the model equations, physical parameterizations, and computational aspects, is intended to provide sufficient documentation to allow users to understand, modify and use the model. GRA

N88-12900# National Oceanic and Atmospheric Administration, Boulder, Colo. Wave Propagation Lab.
MEASUREMENTS OF VAPOR FLUX, LIQUID WATER CONTENTS, PRECIPITATION RATES AND RIMING IN A UTAH MOUNTAIN CLOUD SYSTEM
T. Uttal, R. A. Kropfli, and J. B. Snider Sep. 1986 6 p Presented at the 23rd Conference on Radar Meteorology and the Conference on Cloud Physics, Snowmass, Colo., 22-26 Sep. 1986 Submitted for publication
(PB87-224945) Avail: NTIS HC A02/MF A01 CSCL 04B

In recent years the Utah Department of Water Resources has been conducting a series of weather modification field projects in the Tushar Mountains near Beaver, Utah. The purpose of these projects is to investigate the dynamic and microphysical characteristics of clouds for further planning and evaluation of

weather modification activities. An important part of the 1985 field project, distinguishing it from earlier projects, was inclusion of a suite of remote sensing instruments. The paper presents the calculated vapor fluxes for the March 2-3 storm and the February 8-9 storm,from the 1985 Beaver field season. GRA

N88-12901# National Center for Atmospheric Research, Boulder, Colo.
NATIONAL CENTER FOR ATMOSPHERIC RESEARCH Annual Report, fiscal year 1986
Jun. 1987 86 p
(Grant NSF ATM-82-17015)
(PB87-228391; NCAR/AR-86) Avail: NTIS HC A05/MF A01 CSCL 04B

Described are ongoing research activities and the most significant recent achievements of the National Center for Atmospheric Research, which is operated by the 54-member University Corporation for Atmospheric Research, under the sponsorship of the National Science Foundation. A section of directories lists the scientific and technical staff, organizational structure, financial statements, visitors and publications. Abundant illustrations and photographs, and a semitechnical narrative makes the report accessible to a wide readership of science administrators, decision makers, students, and interested laypeople. GRA

N88-12902# Pacific Northwest Labs., Richland, Wash.
VARIABILITY OF WIND POWER NEAR OKLAHOMA CITY AND IMPLICATIONS FOR SITING OF WIND TURBINES
E. Kessler and R. Eyster Sep. 1987 116 p
(Contracts DE-AI06-81RL-10336; DE-AC06-76RL-01830)
(DE88-000444; DOE/RL-10336/1; PNL-6293) Avail: NTIS HC A06/MF A01

Data from five sites near Oklahoma City were examined to assess wind power availability. Wind turbines of identical manufacture were operated at three of the sites, one of which was also equipped with anemometers on a 100-ft tower. Comprehensive anemometric data were available from the other two sites. The study indicates that the average wind speed varies substantially over Oklahoma's rolling plains, which have often been nominally regarded as flat for purposes of wind power generation. Average wind differences may be as much as 5 mph at 20 ft above ground level, and 7 mph at 100 ft above ground level for elevation differences of about 200 ft above mean sea level, even in the absence of substantial features of local terrain. Local altitude above mean sea level seems to be as influential as the shape of local terrain in determining the average wind speed. The wind turbine used at a meteorologically instrumented site in the study produced the power expected from it for the wind regime in which it was situated. The observed variations of local wind imply variations in annual kWh of as much as a factor of four between identical turbines located at similar heights above ground level in shallow valleys and on hilltops or elevated extended flat areas. DOE

N88-12903# Naval Oceanography Command Center/Joint Typhoon Warning Center, FPO San Francisco, Calif.
ANNUAL TROPICAL CYCLONE REPORT, 1986
Charles G. Steinbruck, Carl W. Hoffman, and Vernon G. Patterson 1986 181 p
(AD-A184082) Avail: NTIS HC A09/MF A01 CSCL 04B

The mission of the Joint Typhoon Warning Center (JTWC) is multi-faceted and includes: (1) Continuous monitoring of all tropical weather activity in the Northern and Southern Hemispheres, from 180 degrees longitude westward to the east coast of Africa, and prompt issuance of appropriate advisories and alerts when tropical cyclone development is anticipated. (2) Issuing warnings on all significant tropical cyclones in the above area of responsibility. (3) Determination of reconnaissance requirements for tropical cyclone surveillance and assignment of appropriate priorities. (4) Post-storm analysis of all significant tropical cyclones occurring within the western North Pacific and North Indian Oceans, which includes an in-depth analysis of tropical cyclones of note and all typhoons. (5) Cooperation on the operational evaluation of tropical cyclone models and forecast aids, and the development of new techniques to support operational forecast scenarios. GRA

N88-12904# Flow Analysis Associates, Ithaca, N.Y.
HEAT AND MOISTURE TRANSPORT IN THE ATMOSPHERIC BOUNDARY LAYER Final Report, 23 Jan. 1983 - 31 Dec. 1986
Sidney Leibovich, John L. Lumley, and J. C. Hunt 5 Jan. 1987 292 p
(Contract F19628-83-C-0018)
(AD-A184222; AFGL-TR-87-0011) Avail: NTIS HC A13/MF A01 CSCL 04B

The goal of this contract is the establishment of practical methods for the prediction of three-dimensional turbulent atmospheric flow over complex terrain, when environmental conditions at the boundaries of the flow volume are prescribed. Development is made of analytical and computational approaches to turbulent, stratified shear flows and complex terrain, with turbulent transport of latent and sensible heat. GRA

N88-12905 Wisconsin Univ., Madison.
ON THE INTERANNUAL VARIABILITY OF SOUTH AMERICAN CLIMATE AND THE SOUTHERN OSCILLATION Ph.D. Thesis
Patricio Aceituno 1987 151 p
Avail: Univ. Microfilms Order No. DA8713133

The Southern Oscillation (SO) is studied through analyses of SO-related anomalies in various surface and upper-air fields which reveal the three-dimensional characteristics of the SO over South America and the surrounding ocean. Correlation analyses are complemented by case studies of extreme episodes. Anomalies related to the negative SO phase include: (1) low pressure and high sea surface temperature (SST) over the eastern Pacific; (2) warm water in the tropical eastern Pacific; and (3) abundant winter rainfall in central Chile. Positive-SO anomalies include: (1) excessive rainfall along the Ecuador-Peru littoral; (2) wind, pressure, and temperature anomalies in the tropical North Atlantic during the austral summer; and (3) dry summer conditions over South America with the exception of relative wetness in southern northeast Brazil and the Parana river basin. Dissert. Abstr.

N88-12906 Wisconsin Univ., Madison.
MEASUREMENT OF CIRRUS CLOUD OPTICAL PROPERTIES BY HIGH SPECTRAL RESOLUTION LIDAR Ph.D. Thesis
Christian John Grund 1987 102 p
Avail: Univ. Microfilms Order No. DA8713152

The High Spectral Resolution Lidar (HSRL) was used to observe the optical properties and occurrence of cirrus clouds. Significant improvements in instrument and calibration technique were accomplished which enabled the HSRL to perform optical property measurements at cirrus cloud altitudes. Eye-safe measurements were achieved during both day and night conditions using only 50 mW of average power at an 8 kHz repetition rate. Range-time indicator displays of the lidar backscatter signal were generated which depict the height, occurrence and layer thickness of the clouds. Calibrated backscatter cross section profiles were produced as well as time and range averaged values of extinction and backscatter phase function. Backscatter phase functions ranged from .027 to .045/sr with no apparent dependence on in-situ temperature. Backscatter cross section profiles indicated that cirrus cloud-top structures often diminish slowly with height. Theoretical calculations were made which demonstrated that clouds of significant total optical thickness exhibiting realistic extinction profiles which diminished with height could be invisible to nadir viewing space borne simple lidar systems. Dissert. Abstr.

N88-12907 Colorado Univ., Boulder.
INTERACTIONS BETWEEN THE ASIAN MONSOONS, THE TROPICAL PACIFIC AND THE SOUTHERN HEMISPHERE EXTRATROPICS Ph.D. Thesis
Gerald Allen Meehl 1987 174 p
Avail: Univ. Microfilms Order No. DA8716270

Relatively strong and weak years of Indian monsoon rainfall are selected and used as a starting point to follow the evolution of the annual cycle of precipitation in the tropical Indian and Pacific

sectors. Analysis of observations shows that the dynamically coupled ocean atmosphere system in the Indian-Pacific region produces Southern Oscillation type signals in atmosphere and ocean in many years, with extremes being manifested as Warm and Cold Events. Four different GCM simulations are analyzed. One is run with the specified annual cycle of observed sea surface temperatures (SPEC SST), and two are coupled to a single 50 m deep slab ocean model with present (1 x CO2) and doubled (2 x CO2) amounts of atmospheric CO2. The 50 m slab ocean model acts as a simple heat reservoir with no provision for currents or upwelling. Due to these inherent limitations, the SPEC SST simulation most closely represents observed mean conditions, while the 1 x CO2 and 2 x CO2 integrations produce a progressively more Warm Event type of response in the tropics. The high southern latitudes in these model runs show internally consistent circulation anomalies in the 2 x CO2 compared with the 1 x CO2 and SPEC SST. Dissert. Abstr.

N88-12908*# Colorado Univ., Boulder. Cooperative Inst. for Research in Environmental Sciences.
CLOUD COVER DETERMINATION IN POLAR REGIONS FROM SATELLITE IMAGERY Semiannual Report
R. G. Barry, J. A. Maslanik, and J. R. Key 29 Dec. 1987 35 p (Grant NAG5-898)
(NASA-CR-181544; NAS 1.26:181544) Avail: NTIS HC A03/MF A01 CSCL 04B

A definition is undertaken of the spectral and spatial characteristics of clouds and surface conditions in the polar regions, and to the creation of calibrated, geometrically correct data sets suitable for quantitative analysis. Ways are explored in which this information can be applied to cloud classifications as new methods or as extensions to existing classification schemes. A methodology is developed that uses automated techniques to merge Advanced Very High Resolution Radiometer (AVHRR) and Scanning Multichannel Microwave Radiometer (SMMR) data, and to apply first-order calibration and zenith angle corrections to the AVHRR imagery. Cloud cover and surface types are manually interpreted, and manual methods are used to define relatively pure training areas to describe the textural and multispectral characteristics of clouds over several surface conditions. The effects of viewing angle and bidirectional reflectance differences are studied for several classes, and the effectiveness of some key components of existing classification schemes is tested. Author

N88-12909# Argonne National Lab., Ill.
A REVIEW OF PARAMETERIZATIONS OF MICROPHYSICAL PROCESSES IN CLOUDS FOR APPLICATION IN MODELS OF REGIONAL ATMOSPHERIC DEPOSITION
I. Y. Lee and M. S. Hong Aug. 1987 49 p
(Contract W-31-109-eng-38)
(DE88-000451; ANL-87-32) Avail: NTIS HC A03/MF A01

The literature on parameterizations of cloud microphysical processes was reviewed to examine the theoretical bases of those parameterizations and to evaluate their applicability to regional models. New parameterizations were produced by multiple regression upon the solution fields derived from simulations of a cloud model incorporating sophisticated microphysics. The currently available rates for cloud microphysical interactions were generally derived under the assumption that the size distribution functions for various hydrometeors are given. Such parameterizations must therefore be applied with caution because the spectral evolution of various types of hydrometeors in reality varies significantly during the stages of cloud development. Uncertainties exist in assigning values for aerodynamic properties such as the bulk collection efficiency, and the growth processes for various types of ice crystals are not well enough known for accurate multiphase cloud-microphysics parameterizations. The new parameterizations, in general, compare favorably with those currently available and are more efficient and applicable to regional models. DOE

N88-12832# Joint Publications Research Service, Arlington, Va.
COMPUTER MODELING AIDS STUDIES OF PRECIPITATION FORMATION Abstract Only
V. Korneyev *In its* USSR Report: Earth Sciences 22 Jul. 1986 p 1 Transl. into ENGLISH from Izvestiya (USSR), no. 82(21524), 23 Mar. 1986 p 3 (For primary document see N88-12831 04-42)
Avail: NTIS HC A05/MF A01

N88-12833# Joint Publications Research Service, Arlington, Va.
PROGRESS IN IMPROVING WEATHER FORECASTING VIEWED Abstract Only
Andrey Pralnikov *In its* USSR Report: Earth Sciences 22 Jul. 1986 p 2 Transl. into ENGLISH from Nedelya (USSR), no. 1 (1345), 30 Dec. 1985 p 23 (For primary document see N88-12831 04-42)
Avail: NTIS HC A05/MF A01

N88-12834# Joint Publications Research Service, Arlington, Va.
NEW PRECIPITATION MAP OF WORLD OCEAN Abstract Only
E. G. Bogdanova *In its* USSR Report: Earth Sciences 22 Jul. 1986 p 3 Transl. into ENGLISH from Izvestiya Akademii Nauk SSSR: Seriya Geograficheskaya (Moscow, USSR), no. 1, Jan. - Feb. 1986 p 37-49 (For primary document see N88-12831 04-42)
Avail: NTIS HC A05/MF A01

N88-12835# Joint Publications Research Service, Arlington, Va.
DROUGHT, SOLAR ACTIVITY LINK ESTABLISHED BY LENINGRAD GEOPHYSICISTS Abstract Only
In its USSR Report: Earth Sciences 22 Jul. 1986 p 4 Transl. into ENGLISH from TASS (Moscow, USSR), 28 Feb. 1986 (For primary document see N88-12831 04-42)
Avail: NTIS HC A05/MF A01

N88-12854# Joint Publications Research Service, Arlington, Va.
LIDAR-RADIOMETRIC METHOD FOR DETERMINING LIQUID-WATER CONTENT OF CIRRUS CLOUDS Abstract Only
V. A. Zhuravleva and O. K. Kostko *In its* USSR Report: Earth Sciences 22 Jul. 1986 p 56 Transl. into ENGLISH from Izvestiya Akademii Nauk SSSR: Fizika Atmosfery i Okeana (Moscow, USSR), v. 22, no. 1, Jan. 1986 p 44-52 Original language document was announced in IAA as A86-29318 (For primary document see N88-12831 04-42)
Avail: NTIS HC A05/MF A01

48 OCEANOGRAPHY

Includes biological, dynamic, and physical oceanography; and marine resources.

For related information see also *43 Earth Resources and Remote Sensing.*

N88-12910# Institute of Oceanographic Sciences, Wormley (England).
RRS DISCOVERY CRUISE 160, 30 JUNE-25 JULY, 1986. GEOCHEMICAL SAMPLING OVER THE MADEIRA AND PORCUPINE ABYSSAL PLAINS
J. Thomson [1986] 32 p
(PB87-222030; IOS/CRUISE-187) Avail: NTIS HC E05/MF E05 CSCL 08C

The main purpose of the cruise was to obtain samples of sediment pore waters for geochemical research. The primary objectives were: to sample the sediments in the 10 km by 10 km abyssal plain area centered on 31 degrees 17 min N, 25 degrees 24 min W to obtain solid phase and pore water material for geochemical characterization of the sediment column; to investigate pore water advection by sampling where the abyssal plain laps on to local relief; to sample an area of the plain where the uppermost turbidite is missing for further investigation of the oxidation front phenomena; and to undertake a number of activities related to non-geological programs. Author

N88-12911# Naval Postgraduate School, Monterey, Calif.
COUPLED ACOUSTIC AND OCEAN THERMODYNAMIC MODEL M.S. Thesis
Jacques M. Fourniol Jun. 1987 101 p
(AD-A184357) Avail: NTIS HC A06/MF A01 CSCL 08A

An acoustic ray tracing algorithm is developed and coupled with a thermodynamic upper ocean mixed layer model. For a test case, the coupled mixed layer-acoustic model is applied to a specific area in the western Mediterranean Sea. Climatological atmospheric forcing is used time during different seasons. The response of the acoustic model to the predicted changes in the sound-speed profile is analyzed to show dependence of acoustic propagation upon the surface atmospheric forcing and the season. The atmospheric factors such as wind, rain, and solar irradiation have almost no effect on the propagation of rays emanating from a deep transmitter. In the case of a shallow source, the wind is the most dominating factor which influences the acoustic propagation. The effect of heavy rain with light wind is also examined. GRA

N88-12912# Naval Postgraduate School, Monterey, Calif.
EFFECTS OF RAINFALL ON THE SEASONAL THERMOCLINE M.S. Thesis
Galo H. Garzon Jun. 1987 70 p
(AD-A184432) Avail: NTIS HC A04/MF A01 CSCL 08C

An oceanic planetary boundary layer model is used to determine the effects of fresh water flux on the seasonal pycnocline and mixed layer at Ocean Station P (50 N, 145 W). First sensitivity of the model was tested by constant forcing with a range of values of precipitation minus evaporation. Then realistic forcing with daily average evaporation, monthly average precipitation values, observed winds and heat fluxes were applied to the model for a simulation of the year 1967. The sensitivity study revealed that precipitation and evaporation have a significant impact on the seasonal evolution of mixed layer depth and temperature, even though the surface heat flux is not changed. The use of realistic forcing indicates the importance of having realistic initial salinity profiles in such models. This is especially true in the autumn and winter seasons when rainfall reduces seasonal mixed layer deepening by as much as 25 meters, representing a 20% change. For the simulation of the year 1967, the model-predicted values of salinity very closely follow climatology for the first half of the year. During the late summer and fall, predicted salinity is greater than suggested by the climatology and may be due to unrealistically steady values of precipitation. Author (GRA)

N88-12913# Lawrence Livermore National Lab., Calif.
SEA LEVEL CHANGES
R. W. Buddemeier 21 Aug. 1987 11 p Presented at the CCOP/SOPAC Workshop on Coastal Processes in the South Pacific Island Nations, Lae, Papua New Guinea, 5 Oct. 1987
(Contract W-7405-eng-48)
(DE87-014357; UCRL-97278; CONF-8710150-1) Avail: NTIS HC A03/MF A01

The paper develops an approach to the issues relating to sea level change that will assist the non-scientist and the applied scientist in making the most effective use of our existing and developing knowledge. The human perception of sea level and how that changes as societies change and develop are discussed. After some practical perspectives on the relationships between societies and sea levels are developed, an approach to developing the best available local prediction of sea level changes is outlined, and finally present knowledge and uncertainties about the future course of events that will influence sea level as defined in the practical sense is discussed. DOE

N88-12914 Georgia Inst. of Tech., Atlanta.
GROUP ANALYSIS OF EQUATIONS ARISING IN OCEAN ACOUSTICS Ph.D Thesis
Pamela Jane Childs Richards 1987 120 p
Avail: Univ. Microfilms Order No. DA8718462

Equations arising in oceanic acoustics are studied from a group-theoretic perspective. These equations include the two-dimensional Helmholtz equation p sub rr + (1/r)p sub r + p sub zz + G(r,z)p = 0, the three-dimensional Helmholtz equation p sub rr + (1/r)p sub r + p sub zz + (1/r squared)p sub theta theta + F(r, theta, z)p = 0, and the standard parabolic approximation to the two-dimensional Helmholtz equation u sub r = K(r,z)u + (alpha sub 0) u sub zz. The one-parameter family of invariant transformation groups is derived for each equation. A restricted full group is obtained for the three-dimensional Helmholtz equation. Symmetry considerations yield conditions on the functional forms of G, F, and K. Exact solutions are found by utilizing results of the full group analysis. The method results in a reduction in the number of independent variables in the original equation. Examples are given for several different types of invariant transformations. Dissert. Abstr.

N88-12836# Joint Publications Research Service, Arlington, Va.
COMPLEX FOR OCEAN STUDY FROM SPACE AND HYDROACOUSTIC STATIONS
In its USSR Report: Earth Sciences 22 Jul. 1986 p 9 Transl. into ENGLISH from Sovetskaya Estoniya (Tallinn, USSR), 18 Feb. 1986 p 1 (For primary document see N88-12831 04-42)
Avail: NTIS HC A05/MF A01

N88-12837# Joint Publications Research Service, Arlington, Va.
CAUCHY PROBLEM FOR LINEARIZED SYSTEM OF NAVIER-STOKES EQUATIONS CONSIDERING COMPRESSIBILITY Abstract Only
A. K. Shatov *In its* USSR Report: Earth Sciences 22 Jul. 1986 p 15 Transl. into ENGLISH from Doklady Akademii Nauk SSSR (Moscow, USSR), v. 285, no. 6, Dec. 1985 p 1374-1376 Original language document was announced in IAA as A86-24316 (For primary document see N88-12831 04-42)
Avail: NTIS HC A05/MF A01

N88-12839# Joint Publications Research Service, Arlington, Va.
STEADY DISTORTION OF SHAPE OF GEOID AND NORMAL GRAVITY FIELD UNDER INFLUENCE OF TIDAL POTENTIAL Abstract Only
S. S. Ivanov *In its* USSR Report: Earth Sciences 22 Jul. 1986 p 16 Transl. into ENGLISH from Doklady Akademii Nauk SSSR (Moscow, USSR), v. 285, no. 6, Dec. 1985 p 1356-1359 (For primary document see N88-12831 04-42)
Avail: NTIS HC A05/MF A01

N88-12840# Joint Publications Research Service, Arlington, Va.
EXPERIMENTAL STUDY OF TURBULENT DIFFUSION PARAMETERS IN OCEAN Abstract Only
V. V. Anikiyev, O. V. Zaytsev, T. V. Zaytseva, and V. V. Yarosh *In its* USSR Report: Earth Sciences 22 Jul. 1986 p 16-17 Transl. into ENGLISH from Izvestiya Akademii Nauk SSSR: Fizika Atmosfery i Okeana (Moscow, USSR), v. 21, no. 11, Nov. 1985 p 1226-1229 (For primary document see N88-12831 04-42)
Avail: NTIS HC A05/MF A01

N88-12844# Joint Publications Research Service, Arlington, Va.
INTENSIVE SYNOPTIC EDDIES AND QUASIGEOSTROPHIC APPROXIMATION Abstract Only
Z. I. Kizner *In its* USSR Report: Earth Sciences 22 Jul. 1986 p 24-25 Transl. into ENGLISH from Okeanologiya (Moscow, USSR), v. 26, no. 1, Jan. - Feb. 1986 p 28-35 (For primary document see N88-12831 04-42)
Avail: NTIS HC A05/MF A01

N88-12845# Joint Publications Research Service, Arlington, Va.
DYNAMICS OF ISOLATED INTRATHERMOCLINE EDDY Abstract Only
G. I. Shapiro *In its* USSR Report: Earth Sciences 22 Jul. 1986 p 25 Transl. into ENGLISH from Okeanologiya (Moscow, USSR), v. 26, no. 1, Jan. - Feb. 1986 p 21-27 (For primary document see N88-12831 04-42)
Avail: NTIS HC A05/MF A01

N88-12846# Joint Publications Research Service, Arlington, Va.
INFLUENCE OF SECONDARY EDDY CURRENTS ON SCATTERING OF ADMIXTURE IN ZONAL FLOW Abstract Only
V. N. Yeremeyev, L. M. Ivanov, I. A. Neyelov, and V. I. Smelyanskiy *In its* USSR Report: Earth Sciences 22 Jul. 1986 p 28 Transl. into ENGLISH from Izvestiya Akademii Nauk SSSR: Fizika Atmosfery i Okeana (Moscow, USSR), v. 22, no. 1, Jan. 1986 p 78-86 (For primary document see N88-12831 04-42)
Avail: NTIS HC A05/MF A01

N88-12847# Joint Publications Research Service, Arlington, Va.
STUDIES OF THIN SURFACE FILMS AIM AT SEEING DEEP OCEAN PROCESSES Abstract Only
A. Zabotin *In its* USSR Report: Earth Sciences 22 Jul. 1986 p 32-33 Transl. into ENGLISH from Sotsialisticheskaya Industriya (Moscow, USSR), 3 Apr. 1986 p 4 (For primary document see N88-12831 04-42)
Avail: NTIS HC A05/MF A01

51 LIFE SCIENCES (GENERAL)

N88-12915# Joint Publications Research Service, Arlington, Va.
JPRS REPORT: SCIENCE AND TECHNOLOGY. USSR: LIFE SCIENCES
5 Aug. 1987 103 p Transl. into ENGLISH from various Russian articles
(JPRS-ULS-87-009) Avail: NTIS HC A06/MF A01

Articles from the open literature are presented or summarized on the following topics: aerospace medicine, agricultural science, biochemistry, biotechnology, epidemiology, genetics, immunology, industrial medicine, laser bioeffects, medicine, microbiology, military medicine, nonionizing radiation effects, pharmacology and toxicology, physiology, public health, radiation biology, and virology. Recent research in the U.S.S.R. is the focus. For individual titles, see N88-12916 through N88-12917.

N88-12916# Joint Publications Research Service, Arlington, Va.
CHANGE IN FUNCTIONAL ACTIVITY OF CORTICAL BRAIN STRUCTURES AND THEIR BLOOD SUPPLY IN ALERT RABBITS IN RESPONSE TO ROCKING
V. F. Maksimuk and N. A. Skoromnyy *In its* JPRS Report: Science and Technology. USSR: Life Sciences 5 Aug. 1987 p 1 Transl. into ENGLISH from Fiziologicheskiy Zhurnal SSSR imeni I. M. Sechenova (Leningrad, USSR), v. 72, no. 7, Jul. 1986 p 881-887 Original language document was announced in IAA as A87-25198 (For primary document see N88-12915 04-51)
Avail: NTIS HC A06/MF A01

Chronic experiments on alert rabbits studied the dynamics of changes in EEG, EMG, pulse rate, blood pressure, general and local circulation of the brain during rocking and its aftereffect to determine the peculiarities of individual reactions of the animals. Experiments were performed on 18 rabbits of both sexes with implanted platinum electrodes to record local blood flow by the hydrogen clearance method in several segments of the cerebral hemispheres. Steel subcutaneous electrodes in the cervical and subscapular areas were used to record EMG and EKG. The dynamics of changes in bioelectric activity of the various segments of the cerebral hemispheres, pulse rate, blood pressure, local and total brain blood flow and muscular tonus had features in common plus some specific features. One hour of rocking resulted in persistent changes in the status of all parameters studied, particularly the frequency components of the EEG. Local and total brain blood flow increased. EKG changes, bradycardia and hypotension were observed. Changes were greater in winter than in summer, indicating significant reserve capacity of the regulatory centers of the brain in summer. Author

N88-12917# Joint Publications Research Service, Arlington, Va.
STUDY OF CERTAIN BIOLOGICAL CHARACTERISTICS OF BACTERIA DURING THE FRENCH-SOVIET CYTOS-2 SPACE EXPERIMENT
S. N. Zaloguyev, A. F. Moroz, N. G. Antsiferova, L. I. Glatman, V. L. Popov, V. K. Ilyin, F. M. Kirillova, L. N. Kats, M. P. Bragina, and V. M. Shilov *In its* JPRS Report: Science and Technology. USSR: Life Sciences 5 Aug. 1987 p 2 Transl. into ENGLISH from Zhurnal Mikrobiologii, Epidemiologii i Immunobiologii (Moscow, USSR), no. 8, Aug. 1985 p 3-7 (For primary document see N88-12915 04-51)
Avail: NTIS HC A06/MF A01

The major purpose of the studies reported in this article was to determine the antibiotic sensitivity of opportunistic microorganisms among the autoflora of astronauts by in vitro cultivation in orbital flight. Experiments were performed on the Salyut-7 spacecraft during a visit by a French astronaut utilizing S. aureus and E. coli isolated from the astronaut before the flight. Antibiotic sensitivity of the microorganisms was determined by double serial dilution. S. aureus were tested with oxacillin, chloramphenicol and erythromycin, E. coli--with kanamycin and colistin. The toxicity, immunogenicity and serotype membership of three strains of Pseudomonas aeruginosa were also determined. The antibiotic sensitivity of the microorganisms was found to be slightly higher under orbital conditions. Ultrastructural studies performed after the flight showed no significant morphologic changes in the E. coli, but some thickening of the cell walls, particularly in S. aureus. Characteristics of the P. aeruginosa were found to be stable and unaltered by space flight. Author

52 AEROSPACE MEDICINE

Includes physiological factors; biological effects of radiation; and effects of weightlessness on man and animals.

N88-12918# Los Alamos National Lab., N. Mex.
LATENCY DIFFERENCES AND EFFECTS OF SELECTIVE ATTENTION TO GRATINGS IN THE CENTRAL AND RIGHT VISUAL FIELDS: 2
C. J. Aine, J. S. George, and E. R. Flynn 1987 5 p Presented at the 6th International Conference on Biomagnetism, Tokyo, Japan, 27 Aug. 1987
(Contract W-7405-eng-36)
(DE87-014730; LA-UR-87-2683-2; CONF-8708121-1) Avail: NTIS HC A02/MF A01

The goals were to examine the temporal sequence in which visual information (such as visual field, spatial frequency) are processed and to determine whether different neural sources are activated when such features are attended versus not attended. These issues are basic to current models of visual selective attention. DOE

N88-12919# Los Alamos National Lab., N. Mex.
VISUAL EVOKED RESPONSES TO SINUSOIDAL GRATINGS PRESENTED IN CENTRAL AND RIGHT VISUAL FIELDS: 1
J. S. George, C. J. Aine, and E. R. Flynn 1987 5 p Presented at the 6th International Conference on Biomagnetism, Tokyo, Japan, 27 Aug. 1987
(Contract W-7405-eng-36)
(DE87-014731; LA-UR-87-2682-1; CONF-8708121-2) Avail: NTIS HC A02/MF A01

The present study applies neuromagnetic measurement techniques to probe the neurophysiological processing of spatial frequency (SF) by normal human observers. By exploiting the temporal and spatial resolution of neuromagnetic measurements, we hope to discriminate and characterize underlying neural functions and explore their correlation with perceptual or behavioral performance measures. Spatial frequency analysis has proven a useful paradigm for the study of visual perception and has been applied in psychophysical studies as well as invasive anatomical and physiological studies of experimental animals. These approaches have produced evidence of specialized neural activity

and network structure for the analysis of spatial frequency information. Because the encoding of spatial frequency is a function of neuronal receptive-field size and since receptive-field size varies as a function of retinal location, we have also examined effects of visual field on responses to stimuli of defined spatial frequency content. DOE

N88-12920# California Univ., Irvine. Center for the Neurobiology of Learning and Memory.
LARGE-SCALE NEURONAL CIRCUITS FOR SELECTIVE STORAGE AND RECOGNITION OF COMPLEX STIMULI, A PILOT STUDY Final Report
1 Jul. 1987 3 p
(Contract N00014-85-K-0650)
(AD-A184134) Avail: NTIS HC A02/MF A01 CSCL 06D

Studies are undertaken on the nature and behavior of neural circuits based on the known anatomical and physiological characteristics of cortical circuits in rat brain. They are focused on olfactory (piriform) cortex, for a number of reasons, including the fact that piriform cortex is phylogenetically old, and significantly simpler than neocortical areas, and that piriform receives its inputs monosynaptically from the olfactory bulb, which in turn receives inputs monosynaptically from the nasal epithelium, directly in response to chemical olfactory inputs. This offers an unusual opportunity to study cortical mechanisms operating on inputs that have only minimally been preprocessed, in contrast to the inputs to other cortical areas (even sensory cortical areas) that receive extensive preprocessing before reaching the cortex. GRA

N88-12921# Connecticut Univ., Farmington. School of Medicine.
THE TOXICOLOGY AND METABOLISM OF NICKEL COMPOUNDS Final Technical Progress Report, 1 Dec. 1985 - 31 Aug. 1987
F. W. Sunderman, Jr. 1 Sep. 1987 9 p
(Contract DE-AC02-76EV-03140)
(DE87-014801; DOE/EV-03140/10) Avail: NTIS HC A02/MF A01

The toxicology of nickel compounds was investigated in rats and the metabolism of nickel was studied in humans. Lipid peroxidation is one of the molecular mechanisms of acute toxicity of NiCl2 in rats. The thymus is a target organ of acute nickel toxicity, as evidenced by the thymic involution that occurs within 24 hours after parenteral administration of NiCl2 to rats. The lung is the primary target organ of subacute nickel toxicity in rats, as manifested by marked bronchoalveolar proliferation and degenerative changes in the pulmonary vascular endothelium of rats after 3 to 6 weeks of daily injections of NiCl2. Electrothermal atomic absorption spectrophotometry with Zeeman background correction provides an accurate, sensitive, and practical routine method for analysis of nickel concentrations in body fluids and tissues of human subjects to monitor environmental, occupational, or iatrogenic exposures to nickel compounds. DOE

N88-12922* National Aeronautics and Space Administration, Washington, D.C.
AEROSPACE MEDICINE AND BIOLOGY: A CONTINUING BIBLIOGRAPHY WITH INDEXES
Dec. 1987 65 p
(NASA-SP-7011(304); NAS 1.21:7011(304)) Avail: NTIS HC A04; NTIS standing order as PB86-912300, $8.00 domestic, $16.00 foreign CSCL 06E

This bibliography lists 161 reports, articles, and other documents introduced into the NASA scientific and technical information system in November, 1987. Author

N88-12923# Advisory Group for Aerospace Research and Development, Neuilly-Sur-Seine (France). Aerospace Medical Panel.
HUMAN RESPIRATORY RESPONSES DURING HIGH PERFORMANCE FLIGHT
R. M. Harding (Institute of Aviation Medicine, Farnborough, England) Nov. 1987 93 p
(AGARD-AG-312; ISBN-92-835-1561-7) Copyright Avail: NTIS HC A05/MF A01

The respiratory responses of experienced pilots were studied during flight in a high performance jet aircraft. Over 38 hours of physiological monitoring was carried out involving over 47,000 breaths. The importance and relevance of information about these respiratory responses is reviewed, with particular emphasis on the difficulties of in-flight recording and the history of such experimentation in four specific areas of respiratory physiology: respiratory frequency and flow, added external resistance, hyperventilation, and the metabolic cost of flying. Author

N88-12510# Joint Publications Research Service, Arlington, Va.
MOTION AND SPACE SICKNESS
Naoki Isu *In its* JPRS Report: Science and Technology. Japan 24 Aug. 1987 p 28-30 Transl. into ENGLISH from Kogiken Nyusu (Tokyo, Japan), Nov. 1986 p 2-4 (For primary document see N88-12502 04-12)
Avail: NTIS HC A06/MF A01

N88-12525*# Naval Submarine Medical Research Lab., Groton, Conn.
FIRE-RELATED MEDICAL SCIENCE
Douglas R. Knight *In* NASA, Lewis Research Center, Spacecraft Fire Safety 1987 p 59-64 (For primary document see N88-12520 04-16)
Avail: NTIS HC A07/MF A01 CSCL 22B

53 BEHAVIORAL SCIENCES

Includes psychological factors; individual and group behavior; crew training and evaluation; and psychiatric research.

N88-12924*# National Aeronautics and Space Administration. Ames Research Center, Moffett Field, Calif.
RESEARCH PAPERS AND PUBLICATIONS (1981-1987): WORKLOAD RESEARCH PROGRAM
Sandra G. Hart, comp. Aug. 1987 124 p
(NASA-TM-100016; A-87196; NAS 1.15:100016) Avail: NTIS HC A06/MF A01 CSCL 05I

An annotated bibliography of the research reports written by participants in NASA's Workload Research Program since 1981 is presented, representing the results of theoretical and applied research conducted at Ames Research Center and at universities and industrial laboratories funded by the program. The major program elements included: 1) developing an understanding of the workload concept; 2) providing valid, reliable, and practical measures of workload; and 3) creating a computer model to predict workload. The goal is to provide workload-related design principles, measures, guidelines, and computational models. The research results are transferred to user groups by establishing close ties with manufacturers, civil and military operators of aerospace systems, and regulatory agencies; publishing scientific articles; participating in and sponsoring workshops and symposia; providing information, guidelines, and computer models; and contributing to the formulation of standards. In addition, the methods and theories developed have been applied to specific operational and design problems at the request of a number of industry and government agencies. Author

54 MAN/SYSTEM TECHNOLOGY AND LIFE SUPPORT

Includes human engineering; biotechnology; and space suits and protective clothing.

For related information see also *16 Space Transportation.*

N88-12925# Naval Submarine Medical Research Lab., Groton, Conn.

PERFORMANCE AND PREFERENCE WITH VARIOUS VDT (VIDEO DISPLAY TERMINAL) PHOSPHORS Interim Report

S. M. Luria, David F. Neri, and Christine Schlichting 24 Apr. 1987 20 p

(AD-A184085; NSMRL-1093) Avail: NTIS HC A02/MF A01 CSCL 07E

Subjects searched for target letters and symbols in VDT displays produced with phosphors of different colors: green, amber, yellow, red, blue, and white. There were no significant differences in search time, but there were significant differences in the number of errors made with different phosphors. Yellow produced the fewest errors and white the most. Speed and accuracy did not correlate with the preference ratings for the various phosphors. GRA

N88-12926*# Presearch, Inc., Houston, Tex.

AN ASSESSMENT OF CLINICAL CHEMICAL SENSING TECHNOLOGY FOR POTENTIAL USE IN SPACE STATION HEALTH MAINTENANCE FACILITY

31 Aug. 1987 308 p

(Contract NAS9-17594)

(NASA-CR-172013; NAS 1.26:172013) Avail: NTIS HC A14/MF A01 CSCL 06K

A Health Maintenance Facility is currently under development for space station application which will provide capabilities equivalent to those found on Earth. This final report addresses the study of alternate means of diagnosis and evaluation of impaired tissue perfusion in a microgravity environment. Chemical data variables related to the dysfunction and the sensors required to measure these variables are reviewed. A technology survey outlines the ability of existing systems to meet these requirements. How the candidate sensing system was subjected to rigorous testing is explored to determine its suitability. Recommendations for follow-on activities are included that would make the commercial system more appropriate for space station applications. Author

N88-12927*# National Aeronautics and Space Administration. Lyndon B. Johnson Space Center, Houston, Tex.

SPACE SUIT EXTRAVEHICULAR HAZARDS PROTECTION DEVELOPMENT

Joseph J. Kosmo Aug. 1987 29 p

(NASA-TM-100458; S-565; NAS 1.15:100458) Avail: NTIS HC A03/MF A01 CSCL 06K

Presented is an overview of the development of the integral thermal/micrometeoroid garment (ITMG) used for protection of a space-suited crewmember from hazards of various extravehicular environments. These hazard conditions can range from thermal extremes, meteoroid and debris particles, and radiation conditions in near-earth orbits and free space to sand and dust environments encountered on lunar and planetary surfaces. Representative ITMG materials cross-section layups are identified and described for various space suit configurations ranging from the Gemini program to planned protective requirements and considerations for anticipated Space Station EV operations. Author

55 SPACE BIOLOGY

Includes exobiology; planetary biology; and extraterrestrial life.

No abstracts in this category.

59 MATHEMATICAL AND COMPUTER SCIENCES (GENERAL)

N88-12928*# National Aeronautics and Space Administration. Langley Research Center, Hampton, Va.

APPLICATIONS OF THE HYBRID AUTOMATED RELIABILITY PREDICTOR

Salvatore J. Bavuso, Joanne Bechta Dugan, Kishor T. Trivedi, Beth Rothmann, and Mark Boyd (Duke Univ., Durham, N. C.) [1987] 31 p

(NASA-TP-2760; L-16304; NAS 1.60:2760) Avail: NTIS HC A03/MF A01 CSCL 12A

The Hybrid Automated Reliability Predictor (HARP) is a software package that implements advanced reliability modeling techniques. An overview is presented of some of the problems that arise in modeling highly reliable fault-tolerant systems, loosely divided into model construction and model solution problems. Then described is the HARP approach to these difficulties, which is facilitated by a technique called behavioral decomposition. The bulk of the paper presents examples of the evaluation of some typical fault tolerant systems, including a local area network, two fault-tolerant computer systems (Carnegie-Mellon University multiprocessor system C.mmp, and Software Implemented Fault Tolerance (SIFT)), and two examples of flight control systems. Author

60 COMPUTER OPERATIONS AND HARDWARE

Includes hardware for computer graphics, firmware, and data processing.

For components see *33 Electronics and Electrical Engineering.*

N88-12929# Oak Ridge National Lab., Tenn.

THE PROS AND CONS OF USING A CAI PACKAGE ON A CENTRAL COMPUTER AS OPPOSED TO A MICROPROCESSOR: WHAT'S YOUR CAI MO, MAINFRAME OR MICRO

B. H. Handler 1987 14 p Presented at the 29th International Conference of the Association for the Development of Computer-Based Instruction of Systems (ADCIS), Oakland, Calif., 9 Nov. 1987

(Contract DE-AC05-84OR-21400)

(DE87-011123; CONF-871136-1) Avail: NTIS HC A02/MF A01

When determining the compatibilities and differences between the use of the mainframe and microcomputer for use in computer aided instruction (CAI), each should be evaluated on its relative merits for the specific job to be done; authoring, presentation, or both. The alternatives must be evaluated regarding the content, subject matter and specific requirements of the course to be taught. The real issues are managing the CAI package correctly and being sure that the selected approach is educationally sound. DOE

N88-12930# Illinois Univ., Urbana. Center for Supercomputing Research and Development.

CENTER FOR SUPERCOMPUTING RESEARCH AND DEVELOPMENT (CEDAR) Progress Report, 25 Dec. 1986 - 24 Jan. 1988

D. J. Kuck, E. S. Davidson, D. H. Lawrie, and A. H. Sameh 1987 53 p

(Contract DE-FG02-85ER-25001)

(DE88-000807; DOE/ER-25001/31) Avail: NTIS HC A04/MF A01

The Center for Supercomputing Research and Development (CSRD) is pushing the frontiers of computational technology while building the Cedar System, a prototype multiprocessor. Clusters of 8 tightly-coupled processors are being bought from Alliant Computer Systems, which based its system design on earlier University of Illinois work by the CSRD group. CSRD efforts span the hardware, software, and applications areas. The hardware group is designing and building a global network and shared global

memory, as well as an Alliant interface. This will allow 4 clusters (of 8 processors) to operate together in 1988 and up to 8 clusters in the future. Synchronization and data sharing are allowed by powerful hardware primitives. The software group is developing a Unix-based multiprocessor operating system and a Parafrase (KAP)-based restructuring compiler. The compiler will transform serial as well as parallel Fortran constructs to exploit the system, dealing with vector as well as multiprocessing parallelism. The applications group is developing parallel algorithms and using them in a number of engineering and scientific applications. Thus, CSRD is working for a rapid architectural increase in speed across a number of applications. If Cedar can be exploited as planned on single jobs, speedup factors of one thousand per decade will be possible in future implementations. DOE

N88-12931# National Aeronautical Lab., Bangalore (India). Fluid Mechanics Div.
NCSU CODE: VALIDATION AND EXTENSION ON NAL'S UNIVAC 1100/60 SYSTEM
P. Ramamoorthy and K. Dhanalakshmi May 1987 28 p
(PD-FM-8716) Avail: NTIS HC A03/MF A01

An existing computer program for obtaining the pressures on an airfoil (called here NCSU CODE) is validated on the UNIVAC 1100/60 at Canada's National Aeronautical Laboratory. A graphic routine to plot the results is added to the program to enhance its utility. The code is tried on a large number of airfoils including the modern general aviation and natural laminar airfoils. Results agree quite well with experiment; one should realize, however, that such a comparison is between the calculation in a free jet with experiments in tunnels of different blockage ratios and free stream turbulence. Author

N88-12932*# National Aeronautics and Space Administration. Ames Research Center, Moffett Field, Calif.
CGI DELAY COMPENSATION
Richard E. McFarland Jan. 1986 30 p Previously announced in IAA as A86-37194
(NASA-TM-86703; Rept-85168; NAS 1.15:86703) Avail: NTIS HC A03/MF A01 CSCL 09B

Computer-generated graphics in real-time helicopter simulation produces objectionable scene-presentation time delays. In the flight simulation laboratory at Ames Research Center, it has been determined that these delays have an adverse influence on pilot performance during aggressive tasks such as nap-of-the-earth (NOE) maneuvers. Using contemporary equipment, computer-generated image (CGI) time delays are an unavoidable consequence of the operations required for scene generation. However, providing that magnitide distortions at higher frequencies are tolerable, delay compensation is possible over a restricted frequency range. This range, assumed to have an upper limit of perhaps 10 or 15 rad/sec, conforms approximately to the bandwidth associated with helicopter handling qualities research. A compensation algorithm is introduced here and evaluated in terms of tradeoffs in frequency responses. The algorithm has a discrete basis and accommodates both a large, constant transport delay interval and a periodic delay interval, as associated with asynchronous operations. Author

N88-12933# Du Pont de Nemours (E. I.) and Co., Aiken, S.C. Savannah River Plant.
INPUT/OUTPUT TECHNOLOGIES: AN OVERVIEW OF IMAGE SCANNING, STORAGE, AND DISPLAY
B. J. Hudson 1987 14 p Presented at the Department of Energy Automated Office Support System Conference, Denver, Colo, 7 Oct. 1987
(Contract DE-AC09-76SR-00001)
(DE87-014837; DP-MS-87-108; CONF-8710132-5) Avail: NTIS HC A03/MF A01

In recent years, price reductions and advances in technology have increased the availability of digital image scanners for personal minicomputers. Optical disk technology, which is known for its high capacity storage, has accompanied the advent of image scanning. Limitations still exist in the resolution and display capabilities of scanned images. This paper presents a brief introduction to the concepts and considerations of image scanning, storage, and display. DOE

N88-12511# Joint Publications Research Service, Arlington, Va.
NUMERICAL SIMULATION SYSTEM
In its JPRS Report: Science and Technology. Japan 24 Aug. 1987 p 30-33 Transl. into ENGLISH from Kogiken Nyusu (Tokyo, Japan), Nov. 1986 p 4-5 (For primary document see N88-12502 04-12)
Avail: NTIS HC A06/MF A01

61 COMPUTER PROGRAMMING AND SOFTWARE

Includes computer programs, routines, alogorithms, and specific applications, e.g., CAD/CAM.

N88-12934*# National Aeronautics and Space Administration. Langley Research Center, Hampton, Va.
COMPARING BARRIER ALGORITHMS Final Report
Norbert S. Arenstorf and Harry F. Jordan Sep. 1987 40 p
(Contract NAS1-18107)
(NASA-CR-178377; ICASE-87-65; NAS 1.26:178377) Avail: NTIS HC A03/MF A01 CSCL 09B

A barrier is a method for synchronizing a large number of concurrent computer processes. After considering some basic synchronization mechanisms, a collection of barrier algorithms with either linear or logarithmic depth are presented. A graphical model is described that profiles the execution of the barriers and other parallel programming constructs. This model shows how the interaction between the barrier algorithms and the work that they synchronize can impact their performance. One result is that logarithmic tree structured barriers show good performance when synchronizing fixed length work, while linear self-scheduled barriers show better performance when synchronizing fixed length work with an imbedded critical section. The linear barriers are better able to exploit the process skew associated with critical sections. Timing experiments, performed on an eighteen processor Flex/32 shared memory multiprocessor, that support these conclusions are detailed. Author

N88-12935*# National Aeronautics and Space Administration. Langley Research Center, Hampton, Va.
PRINCIPLES FOR PROBLEM AGGREGATION AND ASSIGNMENT IN MEDIUM SCALE MULTIPROCESSORS Final Report
David M. Nicol and Joel H. Saltz Sep. 1987 40 p Proposed for presentation to the IEEE Trans. Comput.
(Contract NAS1-18107)
(NASA-CR-178379; ICASE-87-39; NAS 1.26:178379) Avail: NTIS HC A03/MF A01 CSCL 09B

One of the most important issues in parallel processing is the mapping of workload to processors. This paper considers a large class of problems having a high degree of potential fine grained parallelism, and execution requirements that are either not predictable, or are too costly to predict. The main issues in mapping such a problem onto medium scale multiprocessors are those of aggregation and assignment. We study a method of parameterized aggregation that makes few assumptions about the workload. The mapping of aggregate units of work onto processors is uniform, and exploits locality of workload intensity to balance the unknown workload. In general, a finer aggregate granularity leads to a better balance at the price of increased communication/synchronization costs; the aggregation parameters can be adjusted to find a reasonable granularity. The effectiveness of this scheme is demonstrated on three model problems: an adaptive one-dimensional fluid dynamics problem with message passing, a sparse triangular linear system solver on both a shared memory and a message-passing machine, and a two-dimensional time-driven battlefield simulation employing message passing. Using

the model problems, the tradeoffs are studied between balanced workload and the communication/synchronization costs. Finally, an analytical model is used to explain why the method balances workload and minimizes the variance in system behavior. Author

N88-12936# Sandia National Labs., Albuquerque, N. Mex. Thermophysical Properties Div.
A DATA ANALYSIS ENVIRONMENT FOR HP (HEWLETT-PACKARD) 1000 COMPUTERS
W. D. Drotning 1987 10 p Presented at the Interex HP 1000 and HP 9000 User's Technical Conference, San Jose, Calif., 18 Oct. 1987
(Contract DE-AC04-76DP-00789)
(DE87-010511; SAND-87-0454C; CONF-8710149-1) Avail: NTIS HC A02/MF A01

An examination of data analysis programs used on our Hewlett-Packard (2) 1000 system showed that many programs used a large fraction of code and programming effort to accomplish common tasks, such as file access and creation, data retrieval and storage, and the like. A clear need existed for a comprehensive, well-structured environment which would consolidate many previously-separated functions in a consistent, robust, easy-to-use format. Program DATA was written to accomplish a wide variety of tasks related to analysis of data stored in File Manager files on Hewlett-Packard HP 1000 minicomputer systems. As a data analysis tool, DATA provides a number of mathematical analysis and data manipulation functions. Flexible file structures, on both input and output, are allowed. An editor is included which allows DATA to serve as a binary file editor for data; search routines based on numeric, rather than string, values are incorporated. Also included are graphical plotting of data and functions, cursor selection of specific data regions, and other graphics features. DATA also serves as a shell operating system, with direct interface to the RTE operating system. Commonly-used file management functions are incorporated or enhanced for operator convenience. DATA is both command- and softkey-driven, with on-line help facilities and extensive error-checking. Finally, DATA serves as a common framework for future expansion with additional libraries or user-defined functions. DOE

N88-12937# Naval Postgraduate School, Monterey, Calif.
A SURVEY OF OBJECT ORIENTED LANGUAGES IN PROGRAMMING ENVIRONMENTS M.S. Thesis
Harald Haakonsen Jun. 1987 105 p
(AD-A184127) Avail: NTIS HC A06/MF A01 CSCL 09B

This thesis addresses object oriented programming languages; and a restrictive definition of object oriented programming languages is presented and defended. Differences between programming languages are discussed and related to interactive integrated programming environments. Topics related to user friendly interface to the computer system and modern programming practice are discussed. The thesis especially addresses features in object oriented programming languages that are important when a user friendly interactive integrated programming environment is designed. Some future research areas are suggested. GRA

N88-12938# Naval Postgraduate School, Monterey, Calif.
AN INTERACTIVE COMPUTER GRAPHICS NETWORK MONITOR FOR A TACTICAL COMMUNICATIONS NETWORK M.S. Thesis
Laurence W. Griggs Jun. 1987 89 p
(AD-A184131) Avail: NTIS HC A05/MF A01 CSCL 09B

To apply modern networking technology, either circuit- or packet-switched, to tactical communications networks, network designers must develop (1) robust link level protocols to handle broadcast media and node mobility and (2) distributed, adaptive routing protocols to handle the rapid reconfigurations required by node mobility and mortality. In addition, from the network manager's point of view, combat imposes electronic order of battle constraints that can affect network performance and limit the available network configurations. Optimizing message throughput under such design and operational constraints is extremely difficult. Intended as an aid to both network designers and managers, this study describes a network monitor that uses modern high-speed graphics hardware and a responsive multi-window user interface to depict, in real time, the state of a packet- or circuit-switched tactical communications network. The network state is modeled as a set of overlays to an existing well-known tactical display format, namely that of Naval Tactical Data System (NTDS). In this implementation, tactical and network displays are decoupled to allow the network monitor's use with other graphical information systems. GRA

N88-12939# Maryland Univ., College Park. Center for Automation Research.
A TIGHT UPPER BOUND FOR THE SPEED-UP OF PARALLEL BEST-FIRST BRANCH-AND-BOUND ALGORITHMS
Shie-Rei Huang and Larry S. Davis May 1987 26 p
(Contract DACA76-84-C-0004)
(AD-A184246; CAR-TR-290; CS-TR-1852; ETL-0462) Avail: NTIS HC A03/MF A01 CSCL 12A

Most previous studies of the speedup of parallel branch-and-bound algorithms are based on the amount of work done in the parallel case and in the sequential case. Any evaluation of a parallel algorithm should include both the execution time and the synchronization delay. In this paper, a finite population queueing model is used to capture the synchronization delay in parallel branch-and-bound algorithms and to quantitatively predict the behavior of their speedup. A program to solve the Traveling Salesman Problem was written on a BBN Butterfly multiprocessor to empirically demonstrate the credibility of this theoretical analysis. Finally, we note that similar analyses can be applied to evaluate parallel AI systems in which processes communicate through a shared global database. GRA

N88-12940# California Univ., Berkeley. Computer Graphics Lab.
AN ADAPTIVE SUBDIVISION METHOD WITH CRACK PREVENTION FOR RENDERING BETA-SPLINE OBJECTS Technical Report, 7 Aug. 1984 - 6 Aug. 1987
Brian A. Barsky, Tony D. DeRose, and Mark D. Dippe 6 Aug. 1987 47 p
(Contracts N00039-84-C-0089; N00039-82-C-0235)
(AD-A184249) Avail: NTIS HC A03/MF A01 CSCL 20K

Adaptive subdivision is a method of creating polygonal approximations to spline surfaces. An adaptive subdivision algorithm takes as an input a spline surface and a tolerance epsilon, and outputs a piecewise planar approximation to the surface guaranteed to differ from the actual surface by a distance no greater than epsilon. These algorithms proceed by recursively splitting the surface into smaller subsurfaces, ultimately approximating subsurfaces with planar polyhedra. These algorithms are therefore characterized by the mathematics behind the splitting of a surface, the test that is used to determine when to stop the recursion, and the method by which a subsurface is approximated by polyhedra. Algorithms of this type are currently known for spline techniques such as Bezier and B-splines. This paper describes the Beta-spline curve and surface technique and derives the equations governing the splitting of Beta-spline curves and surfaces. It presents a very general adaptive subdivision algorithm that can be used with a variety of surface techniques. It incorporates splitting criteria based on flatness and prevents cracks from occurring between approximating polyhedra. The tolerance controlling the splitting process may itself be adaptive, so that as an object moves farther away the tolerance is automatically increased. GRA

N88-12941# Illinois Univ., Urbana. Applied Computation Theory Group.
A CHARACTERIZATION OF SEPARATING PAIRS AND TRIPLETS IN A GRAPH
Arkady Kanevsky and Vijaya Ramachandran Jul. 1987 16 p
(Contract N00014-84-C-0149; Grant NSF ECS-84-04866)
(AD-A184278; ACT-79; UILU-ENG-87-2242) Avail: NTIS HC A02/MF A01 CSCL 09B

Connectivity is an important graph property and there has been a considerable amount of work on algorithms for determining

connectivity of graphs. An undirected graph G =(V,E) is k-connected if for any subset V-prime of k-1 vertices of G the subgraph induced by V-V-prime is connected. A subset V-prime of k vertices is a separating k-set if the subgraph induced by V-V-prime is not connected. For k=1 the set V-prime becomes a single vertex which is called an articulation point, and for k=2,3 the set V-prime is called a separating pair and separating triplet, respectively. Efficient algorithms are available for finding all separating k-sets in k-connected undirected graphs for k less than or = 3. The authors address the following question: what is the maximum number of separating pairs and triplets in biconnected and triconnected undirected graphs, respectively? GRA

N88-12942# Illinois Univ., Urbana. Applied Computation Theory Group.
ON THE NUMBER OF MINIMUM SIZE SEPARATING VERTEX SETS IN A GRAPH
Arkady Kanevsky Jul. 1987 16 p
(Contract N00014-84-C-0149; Grant NSF ECS-84-04866)
(AD-A184279; ACT-80; UILU-ENG-87-2243) Avail: NTIS HC A02/MF A01 CSCL 09B

Connectivity is an important graph property and there has been a considerable amount of work on vertex connectivity of graphs. An undirected graph G = (V,E) is k-connected if for any subset V-prime of k-1 vertices of G the subgraph induced by V-V-prime is connected. A subset V-prime of k vertices is a separating k-set if the subgraph induced by V-V-prime is not connected. For k-1 the set V-prime becomes a single vertex which is called an articulation point, and for k=2,3 the sets V-prime are called a separating pair and separating triplet, respectively. Efficient algorithms are available for finding all separating k-sets in k-connected undirected graphs for k less than or = 3. The author addresses the following question: what is the maximum number of separating k-sets in a k-connected undirected graph? GRA

N88-12943# Aerospace Corp., El Segundo, Calif. Lab. Operations.
SDVS (STATE DELTA VERIFICATION SYSTEM) 5 USERS' MANUAL
Leo G. Marcus 1 Jul. 1987 101 p
(Contract F04701-85-C-0086)
(AD-A184339; TR-0086(6778)-2; SD-TR-87-37) Avail: NTIS HC A06/MF A01 CSCL 09B

This manual is meant for users of the State Delta Verification System (SDVS), version 5. This version of the manual supersedes the previous manual which described SDVS 4.1, although much of the text is common to both. SDVS 5 is implemented on the Symbolics Lisp Machine, and it is assumed that the reader of this manual is acquainted with that machine. No general Symbolics information is included here. The introduction will be sufficient to let the user get started on the system. Other sections go in more detail into various aspects of the theory and operation. The manual covers all facets of the verification system: (1) the internal language (state deltas); (2) the proof language; (3) the user interface; (4) actual system use; (5) the translation from the hardware description language ISPS to state deltas; (6) the capabilities of the static solvers; and (7) example proofs. GRA

N88-12944# University of Southern California, Marina del Rey. Information Sciences Inst.
THE ISI (INFORMATION SCIENCES INSTITUTE) GRAPHER: A PORTABLE TOOL FOR DISPLAYING GRAPHS PICTORIALLY
Gabriel Robins Sep. 1987 22 p
(Contract MDA903-81-C-0335)
(AD-A184354; ISI/RS-87-196) Avail: NTIS HC A03/MF A01 CSCL 09B

The advent of inexpensive personal workstations with high-resolution displays has helped to drastically increase end-user productivity. However, the same technology has also served to highlight the deficiencies inherent in current pieces of software and existing user-interfaces. A small set of concepts (e.g., windows, menus, icons, etc.) has established itself as a good model for user-interface design. We propose an important addition to this collection, namely the concept of a grapher; that is, the ability to interactively display and manipulate arbitrary directed graphs. We illustrate the usefulness of this idea, develop a practical linear-time algorithm for laying-out graphs, and describe our implementation of a prototype, the ISI Grapher. Author (GRA)

N88-12945# Massachusetts Inst. of Tech., Cambridge. Artificial Intelligence Lab.
ON THE RECOGNITION OF CURVED OBJECTS
W. E. Grimson Jul. 1987 34 p
(Contracts N00014-86-K-0685; N00014-85-K-0124)
(AD-A184441; AI-M-983) Avail: NTIS HC A03/MF A01 CSCL 09B

Determining the identity and pose of occluded objects from noisy data is a critical part of a system's intelligent interaction with an unstructured environment. Previous work has shown that local measurements of the position and surface orientation of small patches of an object's surface may be used in a constrained search process to solve this problem, for the case of rigid polygonal objects using two-dimensional sensory data, or rigid polyhedral objects using three-dimensional data. This note extends the recognition system to deal with the problem of recognizing and locating curved objects. The extension is done in two dimensions, and applies to the recognition of two-dimensional objects from two-dimensional data, or to the recognition of three-dimensional objects in stable positions from two-dimensional data. GRA

N88-12946# Scientific Research Associates, Inc., Glastonbury, Conn.
NUMERICAL STUDIES OF THE DUAL HEMT/ALGORITHM DEVELOPMENT AND NUMERICAL STUDIES OF SCHRODINGER'S EQUATION Final Report, 15 Apr. 1986 - 14 Apr. 1987
H. L. Grubin, M. Meyyappan, J. P. Kreskovsky, and S. M. Pincus 3 Aug. 1987 19 p
(Contract DAAL03-86-C-0013)
(AD-A184471; SRA-R930012F; ARO-23398.1-EL-5) Avail: NTIS HC A03/MF A01 CSCL 09A

Two studies were initiated under this Contract. It is anticipated that both studies will be included in broader programs under development. One study was concerned with establishing a set of design procedures for the dual High Electron Mobility Transitors (HEMT). The second was to develop algorithms and examine transport in quantum based electronic devices. The results of the latter study are currently being incorporated into other programs underway at SRA. Insofar as both studies are in their early stages, they will be only briefly described. The dual HEMT is considered first. GRA

N88-12947# Oak Ridge National Lab., Tenn.
A PORTABLE HYPERCUBE SIMULATOR
T. H. Dunigan Jul. 1987 26 p
(Contract DE-AC05-84OR-21400)
(DE87-013369; ORNL/TM-10410) Avail: NTIS HC A03

The structure and use of a hypercube simulator that runs on most UNIX systems is described. The simulator uses a library of message-passing routines and multiple user processes, written in either C or FORTRAN, to provide an environment for the development and testing of algorithms for hypercube parallel processors. The simulator produces a trace file that can be used for debugging, performance analysis, or graphical display. A version of the simulator that uses the shared memory of a Sequent multiprocessor is also described. DOE

N88-12948# Oak Ridge National Lab., Tenn.
STATISTICAL INFERENCE: COMPUTER ORIENTED ALGORITHMIC APPROACH
K. O. Bowman and L. R. Shenton 1987 11 p Presented at the 1st International Association for Statistical Computing World Conference, Shizuoka, Japan, 17 Sep. 1987 Prepared in cooperation with Georgia Univ., Athens
(Contract DE-AC05-84OR-21400)

(DE87-013874; CONF-8709128-1) Avail: NTIS HC A03/MF A01

Series for the moments of estimators and statistical functions often rely on a Taylor expansion, which is ultimately subject to modification by an expectation operator. These two phases are not of the same order of difficulty for, in general, it is the expectation of components of the series which quickly defy analytical development. The evolution of the subject in recent decades has been significantly affected by numerical analysis which is computer oriented. General characteristics are hard to define, and this paper illustrates the situations that can arise by briefly describing a few typical cases. Sign patterns and modulus patterns in components of series become discernible through extended computer methods, and this aspect poses many new developments and unsolved problems. DOE

N88-12949# Oak Ridge National Lab., Tenn.
IMPLEMENTATION OF A 3-D NONLINEAR MHD CALCULATION ON THE INTEL HYPERCUBE
J. B. Drake, W. F. Lawkins, B. A. Carreras, and H. R. Hicks Aug. 1987 20 p
(Contract DE-AC05-84OR-21400)
(DE87-014637; ORNL-6335) Avail: NTIS HC A03/MF A01

As part of an exploratory study of the suitability of hypercube multiprocessors for scientific computations, the non-linear magnetohydrodynamics (MHD) code RSF was parallelized for use on an Intel iPSC hypercube. This report presents the numerical algorithm of RSF and the techniques used to obtain parallelism without sacrificing the numerical properties of the serial algorithm. Timing results are presented for a sample problem. DOE

N88-12950# Argonne National Lab., Ill.
THE SUPRENUM COMMUNICATIONS SUBROUTINE LIBRARY FOR GRID-ORIENTED PROBLEMS
Rolf Hempel Jun. 1987 52 p
(Contract W-31-109-eng-38)
(DE88-000137; ANL-87-23) Avail: NTIS HC A04/MF A01

In the application software development of the SUPRENUM project (German supercomputer) many parallel grid-oriented algorithms are being programmed, especially multigrid and computational fluid dynamics codes. As the communication tasks are similar, a central SUPRENUM communications library with subroutines covering all communication requirements of the applications programs has been created. By implementing versions of the library for the Intel iPSC hypercube and the planned SUPRENUM machine, full portability of the applications software has been achieved. DOE

N88-12951# Lawrence Livermore National Lab., Calif.
PROVER: A FIRST-ORDER LOGIC SYSTEM IN Ada
R. Burback Sep. 1987 26 p Presented at the 3rd Annual Conference on Artificial Intelligence and Ada, Fairfax, Va., 14 Oct. 1987
(Contract W-7405-eng-48)
(DE88-000220; UCRL-96632; CONF-8710163-1) Avail: NTIS HC A03/MF A01

PROVER is a complete first-order-predicate logic system written in Ada. The system takes advantage of Ada strong typing to improve the run time performance of the unification algorithm. In addition, two new techniques of unification indexes and goal directed deductions are introduced and implemented. PROVER is based on the logic tableau method of Manna and Waldinger. A generalized resolution method combined with a polarity strategy is used to compute the goal-directed first-order logic deductions. The heart of the system is a most general unifier with support for variable renaming, string substitution, and complex list structures. Universal and existential skolemization is based on the force of quantifier method. Rules for true-false simplification, negation, splitting, and rewrites are supported. This paper describes the algorithms used in PROVER as well as implementation details of the Ada code. DOE

N88-12952*# Old Dominion Univ., Norfolk, Va. Dept. of Computer Science.
SOFTWARE RELIABILITY PERSPECTIVES Final Report, period ending 31 Mar. 1988
Larry Wilson and Wenhui Shen Dec. 1987 11 p
(Grant NAG1-750)
(NASA-CR-181523; NAS 1.26:181523) Avail: NTIS HC A03/MF A01 CSCL 09B

Software which is used in life critical functions must be known to be highly reliable before installation. This requires a strong testing program to estimate the reliability, since neither formal methods, software engineering nor fault tolerant methods can guarantee perfection. Prior to the final testing software goes through a debugging period and many models have been developed to try to estimate reliability from the debugging data. However, the existing models are poorly validated and often give poor performance. This paper emphasizes the fact that part of their failures can be attributed to the random nature of the debugging data given to these models as input, and it poses the problem of correcting this defect as an area of future research. Author

N88-12953*# Virginia Univ., Charlottesville. Dept. of Computer Science.
METHODS FOR DESIGN AND EVALUATION OF INTEGRATED HARDWARE/SOFTWARE SYSTEMS FOR CONCURRENT COMPUTATION Final Technical Report, 15 Mar. 1984 - 30 Sep. 1987
Terrence W. Pratt Dec. 1987 8 p
(Grant NAG1-467)
(NASA-CR-181522; NAS 1.26:181522) Avail: NTIS HC A02/MF A01 CSCL 09B

Two testbed programming environments to support the evaluation of a large range of parallel architectures have been implemented under the program Parallel Implementation of Scientific Computing Environments (PISCES). The PISCES 1 environment was applied to two areas of aerospace interest: a sparse matrix iterative equation solver and a dynamic scene analysis system. Currently, the NICE/SPAR testbed system for structural analysis is being modified for parallel operation under PISCES 2; the PISCES 1 applications are also being adapted for PISCES 2. A new formal model of concurrent computation has been developed, based on the mathematical system known as H graph semantics together with a timed Petri net model of the parallel aspects of a system. J.P.B.

N88-12954*# Sterling Software, Palo Alto, Calif.
SOFTWARE MAINTENANCE IN SCIENTIFIC AND ENGINEERING ENVIRONMENTS: AN INTRODUCTION AND GUIDE
David Wright Feb. 1986 27 p
(Contract NAS2-11555)
(NASA-CR-177409; NAS 1.26:177409; USAAVSCOM-TR-85-A-5)
Avail: NTIS HC A03/MF A01 CSCL 09B

The purpose of software maintenance techniques is addressed. The aims of perfective, adaptive and corrective software maintenance are defined and discussed, especially in the NASA research environment. Areas requiring maintenance, and tools available for this, and suggestions for their use are made. Stress is placed on the organizational aspect of maintenance at both the individual and group level. Particular emphasis is placed on the use of various forms of documentation as the basis around which to organize. Finally, suggestions are given on how to proceed in the partial or complete absence of such documentation. Author

N88-12955# Argonne National Lab., Ill.
A REVIEW AND ANALYSIS OF FORTRAN 8X
B. T. Smith, ed. Oct. 1987 51 p
(Contract W-31-109-eng-38)
(DE88-001320; ANL-87-40) Avail: NTIS HC A04/MF A01

The ANSI Standards Subcommittee X3J3 on Fortran has recently completed a draft proposed standard for the Fortran programming language. The draft proposed standard, known informally as Fortran 8x, is a revision of the current standard X3.9-1978, known informally as Fortran 77. This report is a review

of Fortran 8x and consists of a series of six articles. The first article gives a general overview of Fortran 8x. The next three articles give brief discussions of the array facilities; the enhanced numeric facilities; and user-defined data types, procedure interfaces, and the new program unit called a module. The fifth article provides a brief analysis of the controversial issues discussed by X3J3 (including both the accepted and rejected facilities for Fortran 8x). The sixth article gives a brief comparison with Ada. The report concludes with a summary giving information on how and where to express opinions of the draft proposed standard. DOE

N88-12956# Oak Ridge National Lab., Tenn.
QR FACTORIZATION OF A DENSE MATRIX ON A SHARED-MEMORY MULTIPROCESSOR
E. Chu and A. George Oct. 1987 34 p
(Contract DE-AC05-84OR-21400)
(DE88-001506; ORNL/TM-10581) Avail: NTIS HC A03/MF A01

A new algorithm for computing an orthogonal decomposition of a rectangular m x n matrix A on a shared-memory parallel computer is described. The algorithm uses Givens rotations, and has the feature that its synchronization cost is low. In particular, for a multiprocessor having p processors, an analysis of the algorithm shows that this cost is O (n2/p) if m/p greater than or equal to n, and O (mn/p2) if m/p less than n. Note that in the latter case, the synchronization cost is smaller than O (n2/p). Therefore, the synchronization cost of the algorithm proposed in this article is bounded by O (n2/p) when m greater than or equal to n. This is important for machines where synchronization cost is high, and when m is much greater than n. Analysis and experiments show that the algorithm is effective in balancing the load and producing high efficiency (speed-up). DOE

N88-12957# Michigan Technological Univ., Houghton.
PARALLELIZATION OF HYDROCODES ON THE INTEL HYPERCUBE, PART 2
D. L. Hicks, L. M. Liebrock, V. A. Mousseau, and G. A. Mortensen Aug. 1987 38 p Prepared in cooperation with Edgerton, Germeshausen and Grier, Inc., Idaho Falls, Idaho
(Contract DE-AC07-76ID-01570)
(DE88-001591; EGG-SPAG-7818-Pt-2) Avail: NTIS HC A03/MF A01

In a previous report, the first results of a computational experiments on the Intel iPSC-286 (a 32 node hypercube with nodes based on the 80286/80287 chip) with certain algorithms for concurrent computational continuum dynamics are described. The first results were disappointing: the best speedup factors were less than 4 out of a possible 32. Modifications of the earlier algorithms to better fit the iPSC architecture led to significant improvement: the best speedup factors on these improved algorithms are now in excess of 24 out of 32. The earlier parallel algorithms had speedup efficiences of 90 percent or better on several other parallel processors, namely the HEP, ELXSI/10, and Cray X-MP/4. These machines handled the global communications required by the earlier parallel algorithms more efficiently than the iPSC. The algorithmic modifications yielding the greatest speedup factor improvements reduced the amount of communications relative to the amount of computations. Author

N88-12958 Cornell Univ., Ithaca, N.Y.
LARGE CHANGE-OF-CURVATURE EFFECTS IN QUADRATIC FINITE ELEMENTS FOR CAD OF MEMBRANE STRUCTURES Ph.D. Thesis
David Charles Salmon 1987 179 p
Avail: Univ. Microfilms Order No. DA8715598

Within the context of computer aided design of fabric structures, the large displacement behavior of curved membrane finite elements was investigated. Included is a description of a locking phenomenon which produces parasitic strain errors. This phenomenon is inherent in all discrete numerical methods that explicitly model changes in a surface curvature in shells or membranes. A number of finite element formulations are examined for their performance in large displacement, large change of curvature finite element analysis. These formulations include: (1) reduced integration; (2) assumed strain methods; (3) a framework analogy method; (4) bubble mode methods; and (5) mixed methods. Of these, reduced integration is the most effective for pure membrane analysis. Large displacement patch tests are proposed which identify the severity of the strain errors generated through locking for arbitrary mesh configurations using a given finite element formulation. Other tests show the relationship between the expected strain in the analysis, as measured by a stress factor, and the stress error in the analysis results. Dissert. Abstr.

N88-12959*# Jet Propulsion Lab., California Inst. of Tech., Pasadena.
GUIDELINES FOR PREPARING SOFTWARE USER DOCUMENTATION
Diane F. Miller 1 Oct. 1987 81 p
(Contract NAS7-918)
(NASA-CR-181550; JPL-Pub-87-22; NAS 1.26:181550) Avail: NTIS HC A05/MF A01 CSCL 09B

Clear, easy-to-use software user's manuals make strong demands on special technical communication techniques. Principles and guidelines are given for analyzing the audience and dealing with wide-ranging backgrounds of potential users. Types of information to be included in a complete manual are suggested, with a technique for creating a user-oriented rather than process-oriented organization. Accuracy verification is emphasized. Simple tips are gievn for formatting for quick comprehension and reference, for deciding on packaging, for creating helpful illustrations and examples, and for setting up clear and consistent conventions. Simple guidelines are offered for writing clearly and concisely and for editing. Author

N88-12960# Los Alamos National Lab., N. Mex.
PARALLEL SUPERCONVERGENT MULTIGRID
Paul O. Frederickson and Oliver A. McBryan (Cornell Univ., Ithaca, N.Y.) 1987 21 p Presented at the 3rd Conference on Multigrid Methods, Copper Mountain, Colo., 6 Apr. 1987 Submitted for publication
(Contracts DE-AC02-76ER03077; W-7405-eng-36; Grant NSF DMS-83-12229)
(DE87-013153; LA-UR-87-2329; CONF-8704205-1) Avail: NTIS HC A03/MF A01

A class of multiscale algorithms is described for the solution of large sparse linear systems that are particularly well adapted to massively parallel supercomputers. While standard multigrid algorithms are unable to effectively use all processors when computing on coarse grids, the new algorithms utilize the same number of processors at all times. The basic idea is to solve many coarse scale problems simultaneously, combining the results in an optimal way to provide an improved fine scale solution. As a result, convergence rates are much faster than for standard multigrid methods - we have obtained V-cycle convergence rates as good as .0046 with one smoothing application per cycle, and .0013 with two smoothings. On massively parallel machines the improved convergence rate is attained at no extra computational cost since processors that would otherwise be sitting idle are utilized to provide the better convergence. On serial machines the algorithm is slower because of the extra time spent on multiple coarse scales, though in certain cases the improved convergence rate may justify this - particularly in cases where other methods do not converge. In constant coefficient situations the algorithm is easily analyzed theoretically using Fourier methods on a single grid. The fact that only one grid is involved substantially simplifies convergence proofs. A feature of the algorithms is the use of a matched pair of operators: an approximate inverse for smoothing and a superinterpolation operator to move the correction from coarse to fine scales, chosen to optimize the rate of convergence. DOE

N88-12961# Pacific Northwest Labs., Richland, Wash.
ON COMPUTING ENVIRONMENTS IN DATA ANALYSIS
W. L. Nicholson and D. B. Carr Aug. 1987 15 p Presented at

the 46th Session of the International Statistical Inst., Tokyo, Japan, 8 Sep. 1987
(Contract DE-AC06-76RL-01830)
(DE88-000078; PNL-SA-15189; CONF-870984-4) Avail: NTIS HC A03/MF A01

The paper presents the perspective of two data analysts on computing environments. The perspective focuses attention on general functional capabilities, computing interfaces and the evolution of computing environments. The paper notes the lack of involvement of data analysts in the evolution of general computing environments. Rather data analysts have been primarily relegated to adapting general-purpose tools. The suggestion is made that data analyst/computer-scientist teams work with those engaged in state-of-the-art research and participate on standards committees so that emerging general computing environments include tools well suited to data analysis. DOE

N88-12962# California Univ., Berkeley. Lawrence Berkeley Lab.
A NETWORK DEFINITION AND SOLUTION OF SIMULATION PROBLEMS
J. L. Anderson Sep. 1987 38 p
(Contract DE-AC03-76SF-00098)
(DE88-000675; LBL-21522) Avail: NTIS HC A03/MF A01

Most software tools currently used to solve simulation problems are monolithic FORTRAN programs. Such programs retard advances in modeling by being inflexible, hard to modify, and hard to use. Simulation programs can be defined in terms of a network of physical objects and links. The network concept allows modeling algorithms to be defined as abstract data types called objects. Objects separate the details of a model from the interface needed to use it in a simulation. This allows a network simulation program to be more flexible and more easily modified than traditional simulation programs. A network simulation program kernel that provides basic tools for simulations is described. The kernel provides a language designed to define simulation networks and a solution technique for simulation problems that works well with network definitions. This method is analyzed and shown to be faster than traditional solution methods by a significant factor. A network simulation problem kernel providing data abstraction should accelerate advances in modeling by providing facilities to create flexible, easily modified simulation programs. DOE

N88-12963# Lawrence Livermore National Lab., Calif.
COLA2: A COMPUTER PROGRAM FOR THE STRUCTURAL SYNTHESIS OF TWO COMPONENTS USING GENERAL MODAL COORDINATES
S. Bumpus 14 Aug. 1987 59 p
(Contract W-7405-eng-48)
(DE88-001457; UCID-21193) Avail: NTIS HC A04/MF A01

The COLA2 computer program was developed as part of the Mechanical Engineering Research Project Structural Control Technology Research to perform substructured modeling within the research project. COLA2 performs a component mode synthesis for two linear elastic components using modes that are more general than the structural eigenmodes; that is, Lanczos coordinates eigenmodes, static vectors, or other vectors for mode reduction can be used. Data for COLA2 is calculated using the GEMINI linear elastic finite element computer code. Besides the synthesis capability, COLA2 also has a dynamic response simulation capability that may be executed concurrently with the component mode synthesis or with a restart execution. COLA2 can be executed on the CRAY-1 computers at the Livermore Computer Center. An example showing the component model synthesis for a two-dimensional problem is presented along with the associated modal time history simulation. Another example, which is performed using the GEMINI code but which is capable of being performed with COLA2 given a two-component modal representation, is also presented to show simulation capabilities using constant gain control forces. DOE

N88-12964# California Univ., Berkeley. Lawrence Berkeley Lab.
DEVELOPMENT OF THE NON-EQUILIBRIUM REACTIVE CHEMICAL TRANSPORT CODE CHMTRNS
J. Noorishad, C. L. Carnahan, and L. V. Benson Sep. 1987 230 p Prepared in cooperation with Geological Survey, Denver, Colo.
(Contract DE-AC03-76SF-00098)
(DE88-000682; LBL-22361) Avail: NTIS HC A11/MF A01

A temperature-dependent nonequilibrium reactive chemical transport code has been developed on the basis of earlier work at Lawrence Berkeley Laboratory. The code is capable of simulating kinetic calcite and silica dissolution, irreversible glass dissolution, oxidation and reduction, and stable carbon isotope fractionation during transport. In the main part of the report necessary fundamentals and related algorithms are presented. Appendices 1 to 10 provide samples of inputs and outputs of solved problems. Appendices 11 and 12 include, respectively, the input preparation guide and the Fortran IV listing of the developed code CHMTRNS. DOE

N88-12965# Edgerton, Germeshausen and Grier, Inc., Los Angeles, Calif.
COMPUTER-AIDED X-RAY IMAGE SYSTEM DESIGN AND EVALUATION
C. A. Ciarcia and T. D. Rupp 1987 55 p Presented at the Symposium on Fusion Engineering, Monterey, Calif., 12 Oct. 1987
(Contract DE-AC08-83NV-10282)
(DE88-000997; CONF-871007-9) Avail: NTIS HC A04/MF A01

A comprehensive, integrated computer code structured to provide assistance during the design, optimization, fielding, and data reduction stages of an x-ray image test diagnostic will be presented. This three-dimensional x-ray transport and imaging model is designed to simulate the spatial distribution, resolution and radiance profile of a two-dimensional x-ray image displayed at the scintillation plane or the optical imaging plane of a coupled transfer system. Direct ray-trace and fast Fourier transform techniques are used to incorporate the response functions of each system component into the model. DOE

N88-12684*# Jet Propulsion Lab., California Inst. of Tech., Pasadena
NONLINEARITY IN MEASUREMENT SYSTEMS: EVALUATION METHOD AND APPLICATION TO MICROWAVE RADIOMETERS
C. T. Stelzried *In its* The Telecommunications and Data Acquisition Report 15 Nov. 1987 p 57-66 (For primary document see N88-12679 04-32)
Avail: NTIS HC A15/MF A01 CSCL 09B

62 COMPUTER SYSTEMS

Includes computer networks and special application computer systems.

N88-12966# California Univ., Berkeley. Lawrence Berkeley Lab.
MANAGING DISTRIBUTED DERIVED DATA: A PRELIMINARY PROPOSAL
M. C. Murphy Aug. 1987 15 p Prepared in cooperation with San Francisco State Univ., Calif.
(Contract DE-AC03-76SF-00098)
(DE88-000714; LBL-23861) Avail: NTIS HC A03/MF A01

This paper introduces a new class of distributed data: derived data. Derived data is information which is generated from and/or describes source data and algorithms. Derived data differs from source data in that typically it can be regenerated whenever it is needed, or generated then stored for later use. Stored derived data may become outdated as a result of update activity to the underlying source data, however it may still be accurate enough for its intended application. In this preliminary proposal we describe

several major classes of derived data, then develop a general framework for maintenance in a distributed environment. DOE

N88-12967# University of Northern Illinois, De Kalb.
AN APPROACH TO IMPLEMENTING STATE SPACE SEARCHES ON HETEROGENEOUS SYSTEMS OF MULTIPROCESSORS
B. Glickfeld and R. Overbeek Sep. 1987 62 p Prepared in cooperation with Argonne National Lab., Ill.
(Contract W-31-109-eng-38)
(DE88-001321; ANL-87-36) Avail: NTIS HC A04/MF A01

We report on experiments run on a set of shared-memory multiprocessors. Our goal was to demonstrate that one could conveniently utilize a set of shared-memory multiprocessors cooperatively working on typical state-space searches. We utilized a technology for writing portable code for multiprocessors, coded three depth-first state-space searches, and ran them on a set of multiprocessors. The final problem used substantial resources (over 65 hours on a single processor) and was successfully distributed over four distinct shared memory multiprocessors (2 Sequents and 2 Encores), reducing the time to perform the computation to slightly over 2 hours. DOE

N88-12968# Oak Ridge National Lab., Tenn.
USER INTERFACE FOR A PARTIALLY INCOMPATIBLE SYSTEM SOFTWARE ENVIRONMENT WITH NON-ADP USERS
R. S. Loffman Aug. 1987 223 p
(Contract DE-AC05-84OR-21400)
(DE88-001518; ORNL/TM-10486) Avail: NTIS HC A10/MF A01

Good user interfaces to computer systems and software applications are the result of combining an analysis of user needs with knowledge of interface design principles and techniques. Described is an interface for an environment: (a) that consists of users who are not computer science or data processing professionals; and (b) which is bound by predetermined software and hardware. Current literature was investigated to establish a baseline of knowledge about user interface design. There are many techniques which can be used to implement a user interface, but all should have the same basic goal, which is to assist the user in the performance of a task. This can be accomplished by providing consistent, well-structured interfaces which also provide flexibility to adapt to differences among users. The interface produced used menu selection and command language techniques to make two different operating system environments appear similar. The original goal was also to make the transition between the two systems transparent. This was not fully accomplished due to software and hardware limitations. features helped to address the needs of different users. The original goal was also to make the transition between the two systems transparent. This was not fully accomplished due to software and hardware limitations. DOE

63 CYBERNETICS

Includes feedback and control theory, artificial intelligence, robotics and expert systems.

For related information see also *54 Man/System Technology and Life Support.*

N88-12969*# Information and Control Systems, Inc., Hampton, Va.
INVESTIGATION, DEVELOPMENT AND APPLICATION OF OPTIMAL OUTPUT FEEDBACK THEORY. VOL. 4: MEASURES OF EIGENVALUE/EIGENVECTOR SENSITIVITY TO SYSTEM PARAMETERS AND UNMODELED DYNAMICS Final Report, Mar. 1985 - Jun. 1987
Nesim Halyo Dec. 1987 59 p
(Contract NAS1-15759)
(NASA-CR-4108; NAS 1.26:4108; FR-687103) Avail: NTIS HC A04/MF A01 CSCL 09B

Some measures of eigenvalue and eigenvector sensitivity applicable to both continuous and discrete linear systems are developed and investigated. An infinite series representation is developed for the eigenvalues and eigenvectors of a system. The coefficients of the series are coupled, but can be obtained recursively using a nonlinear coupled vector difference equation. A new sensitivity measure is developed by considering the effects of unmodeled dynamics. It is shown that the sensitivity is high when any unmodeled eigenvalue is near a modeled eigenvalue. Using a simple example where the sensor dynamics have been neglected, it is shown that high feedback gains produce high eigenvalue/eigenvector sensitivity. The smallest singular value of the return difference is shown not to reflect eigenvalue sensitivity since it increases with the feedback gains. Using an upper bound obtained from the infinite series, a procedure to evaluate whether the sensitivity to parameter variations is within given acceptable bounds is developed and demonstrated by an example. Author

N88-12970# Eurocontrol Experimental Centre, Bretigny (France).
EXPERIMENTAL USE OF ARTIFICIAL INTELLIGENCE FOR (FUTURE) ATC SYSTEMS
F. Krella 15 Sep. 1986 52 p
(PB87-106449; EEC/NOTE-15/86) Avail: NTIS HC E04/MF E04 CSCL 09B

An expert system shell and an expert system were implemented on an IBM compatible mainframe computer. The expert system represents a planning position of an air traffic controller suite, where aircraft conflicts are resolved prior to entry in a control zone by height separation. The expert system's findings are represented on a graphical screen. The planning position corresponds to an implementation made for a real time simulation, CAPE, the computer aided planning experiment. GRA

N88-12971# Carnegie-Mellon Univ., Pittsburgh, Pa. Robotics Inst.
IMPLEMENTATION AND PERFORMANCE OF A COMPLEX VISION SYSTEM ON A SYSTOLIC ARRAY MACHINE
Ed Clune, Jill D. Crisman, Gudrun J. Klinker, and Jon A. Webb Jun. 1987 26 p
(Contracts DACA76-85-C-0002; F33615-84-K-1520; N00039-85-C-0134; N00014-80-C-0236; N00014-85-K-0152)
(AD-A184331; CMU-RI-TR-87-16) Avail: NTIS HC A03/MF A01 CSCL 09B

Complex vision systems are usually quite slow, requiring tens of seconds or minutes of computer time for each image. As the complexity and experimental nature of the system increases, the speed is especially low, since all components of the system must be optimized if the system is to show good performance. The FIDO system, a stereo vision system for controlling a robot vehicle, has existed for a number of years and has been implemented on a number of different computers. These computers have ranged from a DEC KL10 to the current implementation on the Warp machine, a 100 Million Floating-point Operations Per Seconds (MFLOPS) systolic array machine. FIDO has shown an enormous range in speed; its ancestor took 15 minutes per step, while the Warp implementation takes less than 5 seconds per step. Moreover, while early versions of FIDO moved in slow, start-to-stop steps, FIDO now runs continuously at 100 mm/second. We review the history of the FIDO system, discuss its implementation on different computers, and concentrate on its current Warp implementation. GRA

N88-12972# Massachusetts Inst. of Tech., Cambridge. Artificial Intelligence Lab.
AN APPROACH TO OBJECT RECOGNITION: ALIGNING PICTORIAL DESCRIPTIONS
Shimon Ullman Dec. 1986 60 p
(Contract N00014-85-K-0214; Grant NSF IST-83-12240)
(AD-A184462; AI-M-931) Avail: NTIS HC A04/MF A01 CSCL 09B

This paper examines the problem of shape-based object recognition, and proposes a new approach, the alignment of pictorial descriptions. The first part of the paper reviews general approaches to visual object recognition, and divides these approaches into three broad classes; invariant properties methods,

object decomposition methods, and alignment methods. The second part presents the alignment method. In this approach the recognition process is divided into two stages. The first determines the transformation in space that is necessary to bring the viewed object into alignment with possible object-models. This stage can proceed on the basis of minimal information, such as the object's dominant orientation, or a small number of corresponding feature points in the object and model. The second stage determines the model that best matches the viewed object. At this stage, the search is over all the possible object-models, but not over their possible views, since the transformation has already been determined uniquely in the alignment stage. The proposed alignment method also uses abstract description, but unlike structural description methods, it uses them pictorially, rather than in symbolic structural descriptions. Author (GRA)

N88-12973# Pacific Northwest Labs., Richland, Wash.
THE CHARACTERIZATION OF DIAGNOSTIC TASKS FOR ENGINEERING SYSTEMS
S. C. Laufmann, M. A. Whiting, and R. B. Melton Feb. 1987 17 p Presented at the American Association for Artificial Intelligence Meeting, Seattle, Wash., 13 Jul. 1987
(Contract DE-AC06-76RL-01830)
(DE88-000093; PNL-SA-14674; CONF-870734-3) Avail: NTIS HC A03/MF A01

Knowledge-based systems (KBS) technology is rapidly gaining acceptance in the engineering community, due largely to the success of systems that are able to accurately diagnose faults in industrial or engineering applications. However, before diagnostic KBS problem-solving technology can become fully functional in the world of software engineering, we must gain a better understanding of the characterization of diagnostic tasks and the means by which such characterizations may be translated into solutions. In building upon previous task characterization work, we propose a framework for diagnostic task characterization. This framework provides the basis for a new methodology for mapping diagnostic task characterization into solution characteristics. DOE

N88-12974# California Univ., Berkeley. Lawrence Berkeley Lab.
AN EXPERT SYSTEM FOR MATERIALS DESIGN Ph.D. Thesis
D. E. Marinaro May 1987 48 p
(Contract DE-AC03-76SF-00098)
(DE88-000191; LBL-23852) Avail: NTIS HC A03/MF A01

As part of research to develop an expert system for materials design, an analysis of the knowledge and methods used by an expert was undertaken. The implications of this analysis led to the design and computer implementation of a unified, knowledge-based system consisting of a task-independent knowledge representation and a simple, but general, planning algorithm. The programs support the initial design formulation task of the evolutionary design approach: given an alloy system and a property that needs to be improved, the system will reason to a suggestion for improving the alloy. The particular example performed by the system is the addition of a micro-alloying element to improve the yield strength of an austenitic Fe-Ni based superalloy by increasing the lattice mismatch of the coherent hardening precipitate. DOE

N88-12975# California Univ., Berkeley.
A MODEL OF FUNCTIONAL KNOWLEDGE AND INSIGHT
James G. Greeno and Daniel Berger 21 Dec. 1987 55 p
(Contract N00014-85-K-0095; RR0-4206)
(AD-A184113; GK-1) Avail: NTIS HC A04/MF A01 CSCL 09B

We distinguish between routine, semiroutine, and nonroutine problems based on the problem solver's knowledge. Routine problems are solved by applying a known procedure, semiroutine problems require planning that uses functional knowledge, and nonroutine problems require generation of new functional knowledge. We have simulated nonroutine problem solving in which functional knowledge is derived from properties of objects that are available in the situation. In an experiment, we provided knowledge about functional relations of components of a device and found that this facilitated inference of operating procedures, in contrast to knowledge about the states of the individual components, which was ineffective. Author

N88-12976# Los Alamos National Lab., N. Mex.
GOLD: INTEGRATION OF MODEL-BASED CONTROL SYSTEMS WITH ARTIFICIAL INTELLIGENCE AND WORKSTATIONS
M. Lee and S. Clearwater Aug. 1987 10 p Presented at the Workshop on Model Based Accelerator Controls, Upton, N.Y., 16 Aug. 1987 Prepared in cooperation with Stanford Linear Accelerator Center, Menlo Park, Calif.
(Contract W-7405-eng-36)
(DE88-000506; LA-UR-87-2980; CONF-8708145-1) Avail: NTIS HC A02/MF A01

Our experience with model based accelerator control started at SPEAR. Since that time nearly all accelerator beam lines have been controlled using model-based application programs, for example, PEP and SLC at SLAC. In order to take advantage of state-of-the-art hardware and software technology, the design and implementation of the accelerator control programs have undergone radical change with time. Consequently, SPEAR, PEP, and SLC all use different control programs. Since many of these application programs are imbedded deep into the control system, they had to be rewritten each time. Each time this rewriting has occurred a great deal of time and effort has been spent on training physicists and programmers to do the job. Now, we have developed these application programs for a fourth time. This time, however, the programs we are developing are generic so that we will not have to do it again. We have developed an integrated system called GOLD (Generic Orbit and Lattice Debugger) for debugging and correcting trajectory errors in accelerator lattices. The system consists of a lattice modeling program (COMFORT), a beam simulator (PLUS), a graphical workstation environment (micro-VAX) and an expert system (ABLE). This paper will describe some of the features and applications of our integrated system with emphasis on the automation offered by expert systems. DOE

N88-12977# Stanford Linear Accelerator Center, Calif.
GOLD: INTEGRATION OF MODEL-BASED CONTROL SYSTEMS WITH ARTIFICIAL INTELLIGENCE AND WORKSTATIONS
M. Lee and S. Clearwater Aug. 1987 5 p Presented at the Workshop on Model Based Accelerator Controls, Upton, N.Y., 16 Aug. 1987 Prepared in cooperation with Los Alamos National Lab., N. Mex.
(Contract DE-AC03-76SF-00515)
(DE88-000706; SLAC-PUB-4396; CONF-8708145-2) Avail: NTIS HC A02/MF A01

Our experience with model-based accelerator control started at SPEAR. Since that time nearly all accelerator beamlines have been controlled using model-based application programs, for example, PEP and SLC at SLAC. In order to take advantage of state-of-the-art hardware and software technology, the design and implementation of the accelerator control programs have undergone radical changes with time. Consequently, SPEAR, PEP and SLC all use different control programs. Since many of these application programs are embedded deep into the control system, they had to be rewritten each time. Each time this rewriting has occurred a great deal of time and effort has been spent on training physicists and programmers to do the job. Now, we have developed an integrated system called GOLD (Genetic Orbit and Lattice Debugger) for debugging and correcting trajectory errors in accelerator lattices. The system consists of a lattice modeling program (COMFORT), a beam simulator (PLUS), a graphical workstation environment (micro-VAX) and an expert system (ABLE). This paper will describe some of the features and applications of our integrated system with emphasis on the automation offered by expert systems. DOE

N88-12978 Texas Univ., Austin.
CLOSED-LOOP SYSTEM ANALYSIS USING LYAPUNOV STABILITY THEORY Ph.D. Thesis

Paul Louis Vergez 1987 254 p
Avail: Univ. Microfilms Order No. DA8717559

A special class of closed-loop systems composed of a controller and observer in cascade are analyzed. The emphasis is on deriving and analyzing general Lyapunov functions which indicate system stability or a measure of system performance under parameter variations. The first Lyapunov function is developed by combining the separate controller and observer Lyapunov functions, both of which are quadratic. A second Lyapunov function is derived to account for the system where the controller is a function of the estimated states. A third function is derived to directly account for parameter uncertainties in the system model. All three functions are valid for linear, time-varying, and certain classes of nonlinear systems. A new control law is developed to improve the performance of the pseudomeasurement observer in the guidance loop. The control law is developed from linear quadratic Gaussian theory to minimize the final relative position states and to improve the pseudomeasurement observer's performance by reducing the observability Grammian matrix. Because of the linear quadratic nature of the problem, a closed-form solution is obtained. The performance gain is measured by the Lyapunov function.
Dissert. Abstr.

64 NUMERICAL ANALYSIS

Includes iteration, difference equations, and numerical approximation.

N88-12979*# National Aeronautics and Space Administration. Langley Research Center, Hampton, Va.
HIGH RESOLUTION FINITE VOLUME METHODS ON ARBITRARY GRIDS VIA WAVE PROPAGATION Final Report
Randall J. LeVeque Oct. 1987 30 p Submitted for publication
(Contract NAS1-18107)
(NASA-CR-178397; ICASE-87-68; NAS 1.26:178397) Avail: NTIS HC A03/MF A01 CSCL 12A

A generalization of Godunov's method for systems of conservation laws has been developed and analyzed that can be applied with arbitrary time steps on arbitrary grids in one space dimension. Stability for arbitrary time steps is achieved by allowing waves to propagate through more than one mesh cell in a time step. The method is extended here to second order accuracy and to a finite volume method in two space dimensions. This latter method is based on solving one dimensional normal and tangential Riemann problems at cell interfaces and again propagating waves through one or more mesh cells. By avoiding the usual time step restriction of explicit methods, it is possible to use reasonable time steps on irregular grids where the minimum cell area is much smaller than the average cell. Boundary conditions for the Euler equations are discussed and special attention is given to the case of a Cartesian grid cut by an irregular boundary. In this case small grid cells arise only near the boundary, and it is desirable to use a time step appropriate for the regular interior cells. Numerical results in two dimensions show that this can be achieved.
Author

N88-12980# California Univ., Berkeley.
BACK-OF-THE-ENVELOPE PROBLEMS
Joyce L. Moore Jul. 1987 63 p
(Contract N00014-85-K-0095; RR0-4206)
(AD-A184105; GK-3) Avail: NTIS HC A04/MF A01 CSCL 12A

Back-of-the-envelope problems call for approximate calculations of quantities that can be related to information in a person's knowledge but are not solved precisely. They therefore provide an opportunity for study of processes and role of general knowledge in ill-defined problem solving. Subjects with advanced and intermediate knowledge in different domains provided protocols solving back-of-the-envelope problems within and outside their fields of special knowledge. Their protocols were interpreted using a set of distinctions provided by Schoenfeld (1985). A model that simulates important aspects of the observed performance was developed by extending FERMI, a model of general problem-solving methods. An important feature of expert performance was the ability to use domain-specific knowledge in the service of general problem-solving methods. General methods of problem solving were similar across subjects who differed in knowledge. At the same time, expert knowledge probably provided guidance in solutions.
GRA

N88-12981# Ballistic Research Labs., Aberdeen Proving Ground, Md.
ON OPERATOR SPLITTING FOR UNSTEADY BOUNDARY VALUE PROBLEMS Final Report
Charlie H. Cooke Jun. 1987 20 p
(AD-A184281; BRL-MR-3605) Avail: NTIS HC A02/MF A01 CSCL 20D

A frozen Jacobian (locally linearized) analysis and again matrix approach is used to argue that a certain operator splitting of the two-dimensional, conservation form, Navier-Stokes equations is second-order accurate. MacCormack's intuitive result, which through the above approach can rigorously be shown valid only for linear systems, is also true in the presence of nonlinearity. Additional second-order splittings are obtained for the case in which derivative-free source terms are present in the fluid dynamics equations. Some discussion of operator optimality is given.
GRA

N88-12982# Stanford Univ., Calif. Dept. of Statistics.
ESTIMATION OF A MULTIVARIATE CONTINUOUS VARIABLE PANEL MODEL
Lawrence S. Mayer and Kun M. Chen Jun. 1987 45 p
(Contract DAAG29-85-K-0239)
(AD-A184472; TR-19; ARO-22729.4-MA) Avail: NTIS HC A03/MF A01 CSCL 12A

Continuous-variable panel models are widely used in social and business research to assess the effects of exogenous (and lagged endogenous variables) on endogenous variables over time given a large number of independent replications on variables measured at each of a small number of times. We consider the problem of estimating the parameters for a model in which the error includes a random individual component. The univariate version of this component of variance model has been widely studied in econometrics. Results in the mathematical statistics literature are used to characterize and study the maximum-likelihood estimators. The results are applied to a panel study of patients' attitudes and perceptions toward health maintenance organizations.
GRA

N88-12983# Argonne National Lab., Ill.
OSCILLATION THEORY FOR LINEAR SECOND-ORDER DIFFERENTIAL SYSTEMS
H. G. Kaper and Man Kam Kwong 1987 11 p Presented at the Oscillation, Bifurcation and Chaos Conference, Toronto, Ontario, 14 Jul. 1987
(Contract W-31-109-eng-38)
(DE87-011393; CONF-8707114-1) Avail: NTIS HC A03/MF A01

This article is concerned with the oscillatory behavior at infinity of the solution y:(a,infinity) yields R/sup n/ of a system of second-order differential equations, y double prime (t) + Q(t)y(t) = 0, t epsilon(a,infinity); Q is a continuous function on (a,infinity), whose values are real symmetric matrices of order n. It is shown that the solution is oscillatory at infinity if the largest eigenvalue of the matrix integral a Q(t) dt is sufficiently large on a sufficiently large set of t-values.
DOE

N88-12984# Oak Ridge National Lab., Tenn.
THE LINEAR CHARACTERISTIC METHOD IN XYZ GEOMETRY
R. L. Childs and W. A. Rhoades 1987 8 p Presented at the Joint Meeting of the American Nuclear Society and the Atomic Industrial Forum, Los Angeles, Calif., 15 Nov. 1987
(Contract DE-AC05-84OR-21400)
(DE87-011668; CONF-871101-34) Avail: NTIS HC A02/MF A01

The linear characteristic method (LC) has been previously investigated in XY geometry. In this paper, the implementation of the LC method in the three-dimensional discrete ordinates code TORT is described, and a comparison is made between LC and the other methods used in TORT, namely weighted difference and linear nodal (LN). DOE

N88-12985# Paraiba Univ., Joao Pessoa (Brazil). Dept. de Fisica.
CANONICAL TRANSFORMATIONS AND EXACT INVARIANTS FOR DISSIPATIVE SYSTEMS
I. A. Pedrosa 1986 7 p
(DE87-703663; UFPB-DF-14/86) Avail: NTIS (US Sales Only) HC A02/MF A01

A simple treatment to the problem of finding exact invariants and related auxiliary equations for time-dependent oscillators with friction is presented. The treatment is based on the use of a time-dependent canonical transformation and an auxiliary transformation. DOE

N88-12986# Oak Ridge National Lab., Tenn.
FOUNDATIONS OF O-THEORY 2: MEASUREMENTS AND RELATION TO FUZZY SET THEORY
E. M. Oblow Jul. 1987 38 p
(Contract DE-AC05-84OR-21400)
(DE88-000013; ORNL/TM-10493; CESAR-87/24) Avail: NTIS HC A03/MF A01

A conceptual experimental framework for O-theory and the possibility form of fuzzy set theory is presented. The framework is probabilistic and derived from experimental measurements of evidential support. It is used to quantify the probabilistic masses needed in O-theory and the membership functions used in fuzzy set theory. Instances in which these two different representations of the same experimental data are equivalent are then explored. The relationships between general operators in both theories are then discussed, along with their connection to Dempster-Shafer theory. Finally, several illustrative examples of deductive inferencing under uncertainty are solved. The equivalence of the representations of the results in both uncertainty theories is demonstrated. DOE

N88-12987# Illinois Univ., Urbana. Dept. of Computer Science.
A COMPARISON OF ADAPTIVE REFINEMENT TECHNIQUES FOR ELLIPTIC PROBLEMS
W. F. Mitchell Sep. 1987 49 p
(Contract DE-FG02-87ER-25026)
(DE88-000805; DOE/ER-25026/12; UIUCDCS-R-87-1375; UILU-ENG-87-1763) Avail: NTIS HC A03/MF A01

Adaptive refinement has proved to be a useful tool for reducing the size of the linear system of equations obtained by discretizing partial differential equations. We consider techniques for the adaptive refinement of triangulations used with the finite element method with piecewise linear functions. Several such techniques have been developed differing mainly in the method for dividing triangles and the method for estimating errors. We describe four methods for dividing triangles and eight methods for estimating errors. Angle bounds for the triangle division methods are compared. All combinations of triangle divisions and error estimates are compared in a numerical experiment using a population of eight test problems with a variety of difficulties (peaks, boundary layers, singularities, etc.). The comparison is based on the L/sub proportional to/ norm of the error vs. the number of vertices. It is found that most, but not all, of the methods produce asymptotically optimal grids and that the number of vertices needed for a given error rarely differs by more than a factor of two. DOE

N88-12988# Sandia National Labs., Albuquerque, N. Mex.
TWO CLASSES OF PRECONDITIONERS COMPUTED USING BLOCK MATRIX FACTORIZATION TECHNIQUES
L. S. Baca and D. E. Salane Jul. 1987 25 p
(Contract DE-AC04-76DP-00789)
(DE88-001313; SAND-87-0903) Avail: NTIS HC A03/MF A01

Two methods for computing preconditioners for nonsymmetric block tridiagonal systems of linear equations are investigated. Adaptable general purpose implementations are given for both methods. DOE

N88-12989# Cornell Univ., Ithaca, N.Y. Lab. of Atomic and Solid State Physics.
THE FINITE ELEMENT METHOD FOR ELECTRONIC STRUCTURE
S. R. White, J. W. Wilkins, and M. P. Tetor 31 Aug. 1987 53 p
Prepared in cooperation with Corning Glass Works, N.Y.
(Contract DE-FG02-86ER-45282)
(DE88-001708; DOE/ER-45282/7) Avail: NTIS HC A04/MF A01

We discuss the use of the finite element method in electronic structure calculations. Products of orthogonal or nonorthogonal 1-D finite element shape functions are used to form 3-D basis functions on a cubic grid. The strict locality of these functions means that the matrix for any local operator is very sparse, making calculation times proportional to the number of basis functions N possible. The completeness of the basis can be increased globally by decreasing the grid spacing and locally by increasing the number of basis functions per site. We discuss algorithms, including the highly efficient multigrid method, for solving the Poisson equation and for the ground state of the single particle Schroedinger equation in O(N) time. Results are presented for test calculations of H, H2(+), He, and H2 using as many as 500,000 basis functions. DOE

N88-12990# National Aeronautical Lab., Bangalore (India). Fluid Mechanics Div.
A QUADRATURE FORMULA FOR A DOUBLE-POLE SINGULAR INTEGRAL
Rajendra K. Bera Oct. 1987 14 p
(PD-FM-8725) Avail: NTIS HC A03/MF A01

Stark's quadrature formula for Cauchy integrals has been extended in a simple manner to evaluate double-pole singular integrals which occur in linear airfoil and wing theory. Author

N88-12991*# National Aeronautics and Space Administration. Ames Research Center, Moffett Field, Calif.
INS3D: AN INCOMPRESSIBLE NAVIER-STOKES CODE IN GENERALIZED THREE-DIMENSIONAL COORDINATES
S. E. Rogers, D. Kwak, and J. L. C. Chang (Rockwell International Corp., Cedar Rapids, Iowa.) Nov. 1987 43 p
(NASA-TM-100012; A-87293; NAS 1.15:100012) Avail: NTIS HC A03/MF A01 CSCL 12A

The operation of the INS3D code, which computes steady-state solutions to the incompressible Navier-Stokes equations, is described. The flow solver utilizes a pseudocompressibility approach combined with an approximate factorization scheme. This manual describes key operating features to orient new users. This includes the organization of the code, description of the input parameters, description of each subroutine, and sample problems. Details for more extended operations, including possible code modifications, are given in the appendix. Author

N88-12992# Aeronautical Research Labs., Melbourne (Australia).
A FINITE ELEMENT PROCEDURE FOR INTERFERENCE-FIT AND COLD-WORKING PROBLEMS WITH LIMITED YIELDING
R. P. Carey and B. C. Hoskin Dec. 1986 37 p
(AR-004-517; ARL-STRUC-R-425) Copyright Avail: NTIS HC A03/MF A01

A procedure is described for performing finite element analysis on an annular plate containing an interference-fit pin or a cold-worked hole by prescribing interface displacements. Strain-hardening is permitted but unloading beyond reverse yielding is not allowed. The procedure is verified against a comparable internal pressure case. An analytical solution for an infinite plate of a perfectly plastic material is also included for comparative purposes. Author

N88-12993 Texas Univ., Austin.
PROPAGATION OF RANDOM INITIAL CONDITIONS IN TIME Ph.D. Thesis
Ronald William Humble 1987 138 p
Avail: Univ. Microfilms Order No. DA8718437

A method for determining the effect of initial condition uncertainties on the system states at later times is presented. The method assumes that a probability measure of the initial states exists and that unique particular solutions to the set of system differential equations exist. Changes in the initial condition probability measure are evaluated using a form of the transformation Jacobian between the initial and final states. Several complexities in the evaluation are discussed, including multiple random initial conditions, implicit solutions, multi-valued mappings, and numerically integrated particular solutions. A large portion of the discussion considers the complicating effects of terminating an integration at some condition which is not a function of time alone. This, in general, requires that the independent variable, time, be considered random. In addition, a discussion on representing arbitrary probability distributions using Lagrange polynomials is given. A large number of implementation examples are presented. The majority of examples consider problems in celestial mechanics, specifically, the one dimensional two body problem, with and without drag terms. These examples include both determined and random final time integration termination conditions. Dissert. Abstr.

N88-12994# Illinois Univ., Urbana. Dept. of Computer Science.
THE SHIFTED ADAMS METHOD FOR ORDINARY DIFFERENTIAL EQUATIONS
Hon-Wah Tam Sep. 1987 31 p
(Contract DE-FG02-87ER-25026)
(DE88-000810; DOE/ER-25026/13; UIUCDCS-R-87-1376; UILU-ENG-87-1764) Avail: NTIS HC A03/MF A01

Exponential fitting is known to be effective for nonstiff ordinary differential equations, although there has been no way of systematically implementing it. This report extends the Adams method by incorporating exponential fitting. The user must supply either a real or a complex conjugate pair of shifting factors. DOE

N88-12995# Argonne National Lab., Ill. Mathematics and Computer Science Div.
AN EXACT PENALIZATION VIEWPOINT OF CONSTRAINED OPTIMIZATION
J. V. Burke Aug. 1987 48 p
(Contract W-31-109-eng-38)
(DE88-001477; ANL/MCS-TM-95) Avail: NTIS HC A03/MF A01

The published work on exact penalization is indeed vast. Recently this work has indicated an intimate relationship between exact penalization, Lagrange multipliers, and problem stability or calmness. In the present work we chronicle this development within a simple idealized problem framework, wherein we unify, extend, and refine much of the known theory. In particular, most of the foundations for constrained optimization are developed with the aid of exact penalization techniques. Our approach is highly geometric and is based upon the elementary subdifferential theory for distance functions. It is assumed that the reader is familiar with the theory of convex sets and functions. DOE

N88-12998*# Jet Propulsion Lab., California Inst. of Tech., Pasadena.
A SIMPLIFIED PROCEDURE FOR CORRECTING BOTH ERRORS AND ERASURES OF A REED-SOLOMON CODE USING THE EUCLIDEAN ALGORITHM
T. K. Truong, I. S. Hsu, W. L. Eastman, and I. S. Reed (University of Southern California, Los Angeles.) *In its* The Telecommunications and Data Acquisition Report 15 Nov. 1987 p 200-212 (For primary document see N88-12679 04-32)
Avail: NTIS HC A15/MF A01 CSCL 12A

N88-12999*# Jet Propulsion Lab., California Inst. of Tech., Pasadena.
MORE ON THE DECODER ERROR PROBABILITY FOR REED-SOLOMON CODES
K.-M. Cheung *In its* The Telecommunications and Data Acquisition Report 15 Nov. 1987 p 213-223 (For primary document see N88-12679 04-32)
Avail: NTIS HC A15/MF A01 CSCL 12A

65 STATISTICS AND PROBABILITY

Includes data sampling and smoothing; Monte Carlo method; and stochastic processes.

N88-12996# Georgia Univ., Athens. Dept. of Chemistry.
ON COLOR POLYNOMIALS OF FIBONACCI GRAPHS
Sherif El-Basil 11 Aug. 1987 14 p
(Contract N00014-84-K-0365)
(AD-A184133; TR-52) Avail: NTIS HC A03/MF A01 CSCL 12A

A recursion exists among the coefficients of the color polynomials of some of the families of graphs considered in recent work of Balasubramanian and Ramaraj. Such families of graphs have been called Fibonacci graphs. Application to king patterns of lattices is given. The method described here applies only to the so called Fibonacci graphs. GRA

N88-12997# American Society for Engineering Education, Washington, D. C.
LOWER BOUNDS ON BEARING ACCURACY FOR CLOSELY SPACED SOURCES Final Report
Miriam Hamilton 1 Sep. 1987 75 p
(Contract N00014-83-D-0689)
(AD-A184258) Avail: NTIS HC A04/MF A01 CSCL 12A

This report presents Cramer-Rao lower bounds on bearing estimation error for two closely spaced incoherent sources which radiate spectrally overlapping broadband Gaussian noise. The radiated signals are assumed to occupy the same frequency band which is taken to be lowpass and rectangular in shape. In the most general problem setting, when prior knowledge of signal levels or a single source bearing is unavailable, estimation accuracy is shown to degrade in proportion to the second power of the inverse angular spacing, resulting in large degradations when compared to the accuracy attainable in a single source setting. There is evidence that in certain situations, a form of apriori knowledge concerning signal power levels can be used to significant advantage in joint bearing estimation. Detectability of a second source from signal field containing two closely spaced sources that overlap in both time and frequency depends on the resolving power of the array and is expected to be poor at low signal-to-noise ratios and short observation times when the angular spacing is small. Results of a binary hypothesis test indicate that below a well defined threshold the probability of error in guessing the wrong hypothesis tends to one half. Reachability of the earlier computed Cramer-Rao lower bounds for this regime is questionable. GRA

N88-12998# California Univ., Berkeley. Operations Research Center.
AN URN MODEL FOR THE MULTI-SAMPLE CAPTURE/RECAPTURE SEQUENTIAL TAGGING PROCESS
Jose G. Leite and Carlos A. DeBragancaPereira Mar. 1987 10 p
(Contract DAAG29-85-K-0208)
(AD-A184470; ORC-87-10; ARO-22735.4-MA) Avail: NTIS HC A02/MF A01 CSCL 12A

The probability distribution associated with the multisample CMRR generalized sequential sampling process are obtained by using an analogy with a single urn model. Some statistical features are also discussed. The Capture/Marc/Release/Recapture (CMRR) sampling process is used whenever informative data must be obtained in order to estimate the unknown size, N, of a finite

(and closed) population. The sampling design for such a process is described in this document. Consider a population of finite size, N, such that during the study time it changes neither in size nor in form; that is, the population is closed during the study time. GRA

N88-12999# Centro Brasileiro de Pesquisas Fisicas, Rio de Janeiro.
CONSISTENCY QUESTION IN THE RENORMALIZATION GROUP ANALYSIS OF DEEP INELASTIC SCATTERING
S. A. Dias and J. A. Mignaco 1986 12 p
(DE87-703372; CBPF-NF-048/86) Avail: NTIS (US Sales Only) HC A03/MF A01

The application of renormalization group methods in perturbation theory results in a definite behavior for terms of higher orders under changes of renormalization prescription. Apparently, this fails to be true for the one-loop correction to the moments of the non-singlet structure functions, which is believed to be a renormalization group invariant. A possible explanation for this contradiction in the treatment of the terms taking into account non-pertubative effects is discussed. DOE

N88-12681*# Jet Propulsion Lab., California Inst. of Tech., Pasadena.
ROBUST STATISTICAL METHODS FOR AUTOMATED OUTLIER DETECTION
J. R. Jee *In its* The Telecommunications and Data Acquisition Report 15 Nov. 1987 p 23-28 (For primary document see N88-12679 04-32)
Avail: NTIS HC A15/MF A01 CSCL 12A

66 SYSTEMS ANALYSIS

Includes mathematical modeling; network analysis; and operations research.

N88-13000*# Draper (Charles Stark) Lab., Inc., Cambridge, Mass.
ON THE NEXT GENERATION OF RELIABILITY ANALYSIS TOOLS Contractor Report, Oct. 1985 - Feb. 1987
Philip S. Babcock, IV, Frank Leong, and Eli Gai Oct. 1987 38 p
(Contract NAS1-18061)
(NASA-CR-178380; NAS 1.26:178380) Avail: NTIS HC A03/MF A01 CSCL 12B

The current generation of reliability analysis tools concentrates on improving the efficiency of the description and solution of the fault-handling processes and providing a solution algorithm for the full system model. The tools have improved user efficiency in these areas to the extent that the problem of constructing the fault-occurrence model is now the major analysis bottleneck. For the next generation of reliability tools, it is proposed that techniques be developed to improve the efficiency of the fault-occurrence model generation and input. Further, the goal is to provide an environment permitting a user to provide a top-down design description of the system from which a Markov reliability model is automatically constructed. Thus, the user is relieved of the tedious and error-prone process of model construction, permitting an efficient exploration of the design space, and an independent validation of the system's operation is obtained. An additional benefit of automating the model construction process is the opportunity to reduce the specialized knowledge required. Hence, the user need only be an expert in the system he is analyzing; the expertise in reliability analysis techniques is supplied. Author

67 THEORETICAL MATHEMATICS

Includes topology and number theory.

No abstracts in this category.

70 PHYSICS (GENERAL)

For precision time and time interval (PTTI) see *35 Instrumentation and Photography;* for geophysics, astrophysics or solar physics see *46 Geophysics, 90 Astrophysics,* or *92 Solar Physics.*

N88-13001# Centro Brasileiro de Pesquisas Fisicas, Rio de Janeiro.
ON DEVIATIONS FROM NEWTON'S LAW AND THE PROPOSAL FOR A FIFTH FORCE
L. A. Ferreira and A. P. C. Malbouisson 1986 49 p
(DE87-703368; CBPF-NF-042/86; IFT-P-12/86) Avail: NTIS (US Sales Only) HC A03/MF A01

The results of geophysical and laboratory measurements of Newton's constant of gravitation, seem to disagree by one percent. Attempts to explain this have led to the revival of the proposal for a fifth interaction in Nature. The experimental results on measurements of G and tests of Newton's inverse square law are reviewed. The recent reanalysis of the Eoetvoes experiment and proposals for new experiments are discussed. DOE

71 ACOUSTICS

Includes sound generation, transmission and attenuation. For noise pollution see *45 Environmental Pollution.*

N88-13002*# National Aeronautics and Space Administration. Langley Research Center, Hampton, Va.
MEASUREMENT OF VELOCITY AND VORTICITY FIELDS IN THE WAKE OF AN AIRFOIL IN PERIODIC PITCHING MOTION
Earl R. Booth, Jr. Dec. 1987 31 p
(NASA-TP-2780; L-16339; NAS 1.60:2780) Avail: NTIS HC A03/MF A01 CSCL 20A

The velocity field created by the wake of an airfoil undergoing a prescribed pitching motion was sampled using hot wire anemometry. Data analysis methods concerning resolution of velocity components from cross wire data, computation of vorticity from velocity time history data, and calculation of vortex circulation from vorticity field data are discussed. These data analysis methods are applied to a flow field relevant to a two dimensional blade-vortex interaction study. Velocity time history data were differentiated to yield vorticity field data which are used to characterize the wake of the pitching airfoil. Measurement of vortex strength in sinusoidal and nonsinusoidal wakes show vortices in the sinusoidal wake have stronger circulation and more concentrated vorticity distributions than the tailored nonsinusoidal wake. Author

N88-13003*# National Aeronautics and Space Administration. Langley Research Center, Hampton, Va.
RESULTS OF THE 1986 NASA/FAA/DFVLR MAIN ROTOR TEST ENTRY IN THE GERMAN-DUTCH WIND TUNNEL (DNW)
Thomas F. Brooks and Ruth M. Martin Oct. 1987 24 p
(NASA-TM-100507; NAS 1.15:100507) Avail: NTIS HC A03/MF A01 CSCL 20A

An acoustics test of a 40%-scale MBB BO-105 helicopter main rotor was conducted in the Deutsch-Niederlandischer Windkanal (DNW). The research, directed by NASA Langley Research Center, concentrated on the generation and radiation of broadband noise and impulsive blade-vortex interaction (BVI) noise over ranges of pertinent rotor operational envelopes. Both the broadband and BVI experimental phases are reviewed, along with highlights of major technical results. For the broadband portion,

significant advancement is the demonstration of the accuracy of prediction methods being developed for broadband self noise, due to boundary layer turbulence. Another key result is the discovery of rotor blade-wake interaction (BWI) as an important contributor to mid frequency noise. Also the DNW data are used to determine for full scale helicopters the relative importance of the different discrete and broadband noise sources. For the BVI test portion, a comprehensive data base documents the BVI impulsive noise character and directionality as functions of rotor flight conditions. The directional mapping of BVI noise emitted from the advancing side as well as the retreating side of the rotor constitutes a major advancement in the understanding of this dominant discrete mechanism. Author

N88-13004# Tennessee Univ., Knoxville. Dept. of Physics.
NONLINEAR ACOUSTICS Final Report, 1 Dec. 1980 - 30 Jun. 1987
M. A. Breazeale 14 Aug. 1987 39 p
(Contract N00014-81-K-0229)
(AD-A184271; TR-27) Avail: NTIS HC A03/MF A01 CSCL 20A

The main objective was to define conditions under which nonlinear behavior of the propagating medium would be in evidence and to use quantitative evaluation of this nonlinearity to characterize the medium. This approach has taken us into the investigation of many phenomena. The description of some is adequate if one uses only the linear form of the equations. In some instances the nonlinearity was observable but could be ignored in the first approximation. In other instances the existence of nonlinearity forms the basis of the entire investigation. GRA

N88-13005*# Duke Univ., Durham, N. C. Dept. of Mechanical Engineering and Materials Science.
AIRCRAFT INTERIOR NOISE REDUCTION BY ALTERNATE RESONANCE TUNING Progress Report
James A. Gottwald and Donald B. Bliss Dec. 1987 14 p
(Grant NAG1-722)
(NASA-CR-181530; NAS 1.26:181530) Avail: NTIS HC A03/MF A01 CSCL 20A

Model problem development and analysis continues with the Alternate Resonance Tuning concept. Various topics are presently at different stages of completion and are described. These topics included optimization of panel mass ratios, panel computer code verification and agreement with experimental data, and flexible frame modeling. Author

N88-13006*# Astron Research and Engineering, Santa Monica, Calif.
AN ANALYSIS OF SOUND ABSORBING LININGS FOR THE INTERIOR OF THE NASA AMES 80 X 120-FOOT WIND TUNNEL
J. F. Wilby and P. H. White Nov. 1985 47 p
(NASA Order A-32501-C)
(NASA-CR-177396; NAS 1.26:177396; Rept-7066-01) Avail: NTIS HC A03/MF A01 CSCL 20A

It is desirable to achieve low frequency sound absorption in the tests section of the NASA Ames 80X120-ft wind tunnel. However, it is difficult to obtain information regarding sound absorption characteristics of potential treatments because of the restrictions placed on the dimensions of the test chambers. In the present case measurements were made in a large enclosure for aircraft ground run-up tests. The normal impedance of the acoustic treatment was measured using two microphones located close to the surface of the treatment. The data showed reasonably good agreement with analytical methods which were then used to design treatments for the wind tunnel test section. A sound-absorbing lining is proposed for the 80X120-ft wind tunnel. Author

N88-13007 Johns Hopkins Univ., Baltimore, Md.
BOUNDARY EFFECTS ON THE DRAG OF AN OSCILLATING SPHERE: APPLICATIONS TO THE MAGNETIC SPHERE RHEOMETER. ATTENUATION AND DISPERSION OF ACOUSTIC WAVES IN NEMATIC LIQUID CRYSTALS Ph.D Thesis
Howard Shaun Sellers 1987 86 p
Avail: Univ. Microfilms Order No. DA8716653

The effect of a closed, nearby boundary on the drag of a small, oscillating sphere in an incompressible, linearly viscoelastic medium is studied. Through a perturbation procedure the functional dependence of the drag on the complex oscillatory Reynolds number is determined and shown to differ from that of the unbounded case. There results account for the boundary effects in the determination of the complex viscosity using the magnetic sphere rheometer. Also studied was the propagation of forced infinitesimal harmonic plane waves in a nematic liquid crystal uniformly alighned by an external magnetic field. The complete linearized balance laws and constitutive relations of the Ericksen-Leslie continuum theory are used to solve for the attenuation and dispersion. Using data published in the literature for p-methoxy benzylidine p-n-butylaniline (MBBA), calculations show that the Ericksen-Leslie theory cannot account for the experimentally observed frequency dependence of the attenuation and velocity anisotropy and the orientation dependence of the velocity anisotropy. To account for possible induced conformational changes, the Ericksen-Leslie theory is generalized to a non-diffusive reacting binary mixture. The reaction rate is shown to be orientation dependent. The reaction contribution to the velocity and attenuation were determined. Several acoustic experiments are discussed with tend to support the presented theory. Also, some errors in the literature on data derived from acoustic experiments on MBBA are pointed out. Dissert. Abstr.

N88-13008# Oak Ridge Y-12 Plant, Tenn.
COMPUTERIZED CERTIFICATION OF DIGITAL ULTRASONIC INSTRUMENTATION
M. W. Moyer 30 Sep. 1987 19 p
(Contract DE-AC05-84OS-21400)
(DE88-000820; Y-2357) Avail: NTIS HC A03/MF A01

A computerized inspection system is being set up at the Oak Ridge Y-12 Plant to enable certification of the Krautkramer Branson ultrasonic instrumentation used extensively in Y-12 production operations. The system takes the data required to certify the linearity and frequency response of the receiver and to certify the correct operation of the pulsers, gates, and computer interface. A subset of the program will be able to verify correct instrumentation in the field by using the actual computer and instrumentation being used for production ultrasonic weld inspections. The system can reduce the certification time from approximately one week to less than an hour. DOE

72 ATOMIC AND MOLECULAR PHYSICS

Includes atomic structure, electron properties, and molecular spectra.

N88-13009# Brookhaven National Lab., Upton, N. Y.
SINGLE LEPTONS FROM HEAVY QUARK PRODUCTION
S. Dawson and S. Godfrey Aug. 1987 9 p Presented at the Workshop on Experiments, Detectors, and Experimental Areas for the Supercollider, Berkeley, Calif., 7 Jul. 1987
(Contract DE-AC02-76CH-00016)
(DE87-014917; BNL-40217; CONF-870739-2) Avail: NTIS HC A02/MF A01

We consider the single lepton decay mode of heavy quarks as a signature of heavy quark pair production at the SSC. We find that events with multijets (n/sub jet/ greater than or equal to 3) and a single high p/sub T/ lepton are a good signal for heavy quark production. DOE

N88-13010# Brookhaven National Lab., Upton, N. Y.
FEW BODY HYPERNUCLEAR SYSTEMS: WEAK DECAYS
C. B. Dover 1987 14 p Presented at the 11th European Conference on Few-Body Physics, Fontevraud, France, 31 Aug. 1987
(Contract DE-AC02-76CH-00016)

(DE87-014920; BNL-40210; CONF-8708143-1) Avail: NTIS HC A03/MF A01

The experimental and theoretical situation regarding mesonic and non-mesonic decays of light hypernuclei is reviewed. Although some models give reasonable results for pionic decays as well as the total weak decay rate, no existing approach explains, even qualitatively, the observed spin-isospin dependence of AN yields NN non-mesonic weak decays. DOE

N88-13011# Brookhaven National Lab., Upton, N. Y.
NUCLEAR BETA DECAY AFTER LES HOUCHES
E. K. Warburton 1987 9 p Presented at the Conference on Nuclear Interactions and Structures, Brighton, United Kingdom, 7 Sep. 1987
(Contract DE-AC02-76CH-00016)
(DE87-014921; BNL-40216; CONF-870909-2) Avail: NTIS HC A02/MF A01

Wilkinson's 1977 Les Houches lectures summarized in detail how nuclear beta decay can be used to investigate fundamental nuclear phenomena and the achievements of this utilization up to that time. In this short talk the subsequent activity is briefly summarized and one area of high activity, namely first-forbidden beta decay, is singled out for more lengthy discussion. Specifically, the subject of interest is the very large meson exchange contribution to the time-like component of the axial current and the efforts to isolate this enhancement by means of careful shell-model calculations. DOE

N88-13012# United Kingdom Atomic Energy Authority, Culham (England).
NEGATIVE ION BEAMS FOR HEATING AND CURRENT-DRIVE IN NET
M. Cox, T. S. Green, D. P. Hammond, and A. J. Holmes 1987 8 p
(AD-A184390; AD-F000100; CLM-P800) Avail: NTIS HC A02/MF A01 CSCL 20I

A study of the capabilities of beam injection into NET as determined by the plasma and beam characteristics has recently been undertaken; this paper summarises its findings. The report divides into two parts namely a study of the restrictions on beam parameters introduced by physics requirements and a review of the technical potential of negative ion based injection systems. Positive ion beam systems are excluded from consideration since their electrical efficiencies are too low to be practicable at the high energies needed to give acceptable beam penetration, optimum current drive efficiency and low divergence (to allow beam transport through narrow ducts in Tokamak blankets). GRA

N88-13013# Los Alamos National Lab., N. Mex.
FUTURE DIRECTIONS IN INTERPLAYS BETWEEN PARTICLE AND NUCLEAR PHYSICS: SUMMARY SESSION
G. T. Garvey 1987 31 p Presented at the 11th International Conference on Particles and Nuclei, Kyoto, Japan, 20 Apr. 1987
(Contract W-7405-eng-36)
(DE87-011791; LA-UR-87-1878; CONF-870413-2) Avail: NTIS HC A03/MF A01

This paper contains the summary comments on a session of the International Conference on Particles and Nuclei. The author discusses topics such as: rare decays forbidden in the Standard Model, various properties of the MEGA detector, broken symmetries in strongly interacting systems, and the need for a high-intensity high-energy facility in nuclear physics. DOE

N88-13014# Oak Ridge National Lab., Tenn.
MAGNETIC DIFFUSE SCATTERING
J. W. Cable 1987 14 p Presented at the Neutron Scattering Symposium on Advances and Applications, Sydney, Australia, 8 Aug. 1987
(Contract DE-AC05-84OR-21400)
(DE87-013539; CONF-8708117-4) Avail: NTIS HC A03/MF A01

The diffuse scattering of neutrons from magnetic materials provides unique and important information regarding the spatial correlations of the atoms and the spins. Such measurements have been extensively applied to magnetically ordered systems, such as the ferromagnetic binary alloys, for which the observed correlations describe the magnetic moment fluctuations associated with local environment effects. With the advent of polarization analysis, these techniques are increasingly being applied to study disordered paramagnetic systems such as the spin-glasses and the diluted magnetic semiconductors. The spin-pair correlations obtained are essential in understanding the exchange interactions of such systems. In this paper, we describe recent neutron diffuse scattering results on the atom-pair and spin-pair correlations in some of these disordered magnetic systems. DOE

N88-12645# Virginia Univ., Charlottesville.
COMPUTED NEUTRON TOMOGRAPHY AND CODED APERTURE HOLOGRAPHY FROM REAL TIME NEUTRON IMAGES
Mark F. Sulcoski *In* Army Materials Technology Lab., Work-in-Progress Presented at the Army Symposium on Solid Mechanics, 1986: Lightening of the Force Oct. 1986 p 1-2
(For primary document see N88-12644 04-31)
Avail: NTIS HC A04/MF A01 CSCL 20H

N88-12853# Joint Publications Research Service, Arlington, Va.
USE OF ELECTRON BEAM INSTRUMENTS TO DETERMINE FLUCTUATIONS IN VERTICAL REFRACTION PARTIAL ANGLE Abstract Only
A. S. Kolos *In its* USSR Report: Earth Sciences 22 Jul. 1986 p 55-56 Transl. into ENGLISH from Geodeziya i Kartografiya (Moscow, USSR), no. 2, Feb. 1986 p 21-23 (For primary document see N88-12831 04-42)
Avail: NTIS HC A05/MF A01

73 NUCLEAR AND HIGH-ENERGY PHYSICS

Includes elementary and nuclear particles; and reactor theory.

For space radiation see *93 Space Radiation.*

N88-13015*# National Aeronautics and Space Administration. Langley Research Center, Hampton, Va.
NUCLEAR TECHNIQUES IN STUDIES OF CONDENSED MATTER
Jag J. Singh Aug. 1987 22 p
(NASA-RP-1195; L-16361; NAS 1.61:1195) Avail: NTIS HC A03/MF A01 CSCL 20H

Nuclear techniques have played an important role in the studies of materials over the past several decades. For example, X-ray diffraction, neutron diffraction, neutron activation, and particle- or photon-induced X-ray emission techniques have been used extensively for the elucidation of structural and compositional details of materials. Several new techniques have been developed recently. Four such techniques are briefly reviewed which have great potential in the study and development of new materials. Of these four, Mossbauer spectroscopy, muon spin rotation, and positron annihilation spectroscopy techniques exploit their great sensitivity to the local atomic environments in the test materials. Interest in synchrotron radiation, on the other hand, stems from its special properties, such as high intensity, high degree of polarization, and high monochromaticity. It is hoped that this brief review will stimulate interest in the exploitation of these newer techniques for the development of improved materials. Author

74 OPTICS

Includes light phenomena; and optical devices.
For lasers see *36 Lasers and Masers.*

N88-13016*# National Aeronautics and Space Administration. Marshall Space Flight Center, Huntsville, Ala.
DEVELOPMENT OF OPTICAL MODULATORS FOR MEASUREMENTS OF SOLAR MAGNETIC FIELDS Final Report
E. A. West and J. E. Smith Oct. 1987 35 p
(NASA-TM-100315; NAS 1.15:100315) Avail: NTIS HC A03/MF A01 CSCL 20F

The measurement of polarized light allows solar astronomers to infer the magnetic field on the Sun. The accuracy of these measurements is dependent on the stable retardation characteristics of the polarization modulators used to minimize the atmospheric effects seen in ground-based observations. This report describes the work by the Space Science Laboratory at Marshall Space Flight Center to improve two types of polarization modulators. As a result, the timing characteristics for both electrooptic crystals (KD*Ps) and liquid crystal devices (LCDs) have been studied and will be used to enhance the capabilities of the MSFC Vector Magnetograph. Author

N88-13017# Ecole Centrale de Lyon (France). Lab. de Technologie des Surfaces.
CHARACTERIZATION OF THIN LAYERS FOR OPTICS [CARACTERISATION DE COUCHES MINCES POUR LOPTIQUE]
H. Montes, J. M. Martin, J. Brissot, J. L. Mansot, and M. Chuat Mar. 1987 62 p In FRENCH
(PB87-217949) Avail: NTIS HC E04/MF E04 CSCL 20F

This study correlates relationships between the microstructure of layers, their compositions, their formation conditions, and their optic properties. It is necessary to acquire the basic knowledge concerning the structure of thin layers, not only with purely optical methods (measurement of the refraction index or of the superficial roughness), but by using the following techniques: secondary ionic emission, X-ray analysis and microdiffraction for an analysis of its composition, and electron microscopy for visualization of the investigated surface. The objective of the study was to define as completely as possible a methodology for studying multilayered stratification and to determine the possibilities of each of these techniques. GRA

N88-13018# Environmental Research Inst. of Michigan, Ann Arbor. Advanced Concepts Div.
ALL-OPTICAL BEAM CONTROL BY FORCED RAYLEIGH SCATTERING Annual Report, 15 Feb. - 15 Sep. 1985
Lauren M. Peterson Dec. 1986 63 p
(Contracts F49620-84-C-0067; ARPA Order 4952)
(AD-A184315; ERIM-175900-11-T) Avail: NTIS HC A04/MF A01 CSCL 09E

An analysis is presented to support the experimental efforts directed toward the achievement of all-optical beam control based upon nonlinear optical effects of thermal origin. Although Stimulated Thermal Rayleigh Scattering (STRS) is the primary effect of interest, the analysis falls in the broader category of Forced Rayleigh Scattering (FRS) where the underlying principles are the same. The interference of two coherent beams of radiation is discussed quantitatively and serves as the driving mechanism for creating a thermally-induced phase grating in an absorbing liquid, which is also discussed quantitatively. The analysis shows that for our experimental conditions, an efficient thermal phase grating can be generated using laser pulses possessing a few microjoules of energy, and is being pursued experimentally using nanosecond laser pulses. A dye laser using a grazing incidence grating (Litterman design) which was purchased for its narrower spectral linewidth and longer coherence length compared to our previous dye laser is also described. GRA

N88-13019# Los Alamos National Lab., N. Mex.
INCREASED GAIN OF CHANNEL INTENSIFIER TUBES BY PULSED BIASING
B. W. Noel, M. R. Cates, and L. A. Franks Sep. 1987 16 p Presented at the 9th Symposium on Photoelectronic Imaging Devices, London, United Kingdom, 7 Sep. 1987 Prepared in cooperation with Oak Ridge Gaseous Diffusion Plant, Tenn. and Edgerton, Germeshausen and Grier, Inc., Goleta, Calif.
(Contract W-7405-eng-36)
(DE88-000512; LA-UR-87-2948; CONF-8709139-1) Avail: NTIS HC A03/MF A01

Although the most common use of proximity-focused channel intensifier tubes (CITs) is as optical image amplifiers, electrical gating allows them to be used as fast shutters. Except for gating, however, the effects of imposing transient or pulsed changes on CIT biases have received little attention in the literature. It would be desirable in many applications to attain the maximum possible gain, but not at the expense of reduced signal-to-noise ratio (SNR). In the experiments described here, pulsed biasing was used to increase gain; measurements show a marked increase in gain over the dc gain without the increase in electronic noise and risk of damage that higher dc potentials create. DOE

N88-13020# Brookhaven National Lab., Upton, N. Y.
NATIONAL SYNCHROTRON LIGHT SOURCE USERS MANUAL: GUIDE TO THE VUV AND X-RAY BEAM LINES
N. F. Gmuer, ed. and S. M. White-DePace, ed. Aug. 1987 102 p
(Contract DE-AC02-76CH-00016)
(DE88-001464; BNL-40156) Avail: NTIS HC A06/MF A01

The success of the National Synchrotron Light Source in the years to come will be based, in large part, on the size of the users community and the diversity of the scientific disciplines represented by these users. To promote this philosophy, this National Synchrotron Light Source (NSLS) Users Manual: Guide to the VUV and X-Ray Beam Lines, has been published, serving a number of purposes. In an effort to attract new research, it presents to the scientific community-at-large the current and projected architecture and capabilities of the various VUV and x-ray beam lines and storage rings. It is anticipated that this publication will be updated periodically in order to keep pace with the constant changes at the NSLS. DOE

75 PLASMA PHYSICS

Includes magnetohydrodynamics and plasma fusion.
For ionospheric plasmas see *46 Geophysics.* For space plasmas see *90 Astrophysics.*

N88-13021# Naval Research Lab., Washington, D.C.
VARIABLE COLLISION FREQUENCY EFFECTS ON HOSE AND SAUSAGE INSTABILITIES IN RELATIVISTIC ELECTRON BEAMS
Steven P. Slinker, Richard F. Hubbard, and Martin Lampe
12 Aug. 1987 43 p
(ARPA Order 4395)
(AD-A184206; NRL-MR-6004) Avail: NTIS HC A03/MF A01 CSCL 20G

A relativistic electron beam propagating in a dense gas typically ionizes the gas weakly, and the resulting plasma conductivity evolution strongly influences beam stability properties. The electric field E and the plasma electron temperature T sub e usually decrease with the distance zeta behind the beam head; as a result, the plasma electron-neutral collision frequency Nu sub m decreases with zeta, which depresses the conductivity sigma in the front of the beam and increases sigma further back in the beam. This variation of nu sub m, which has generally been ignored in previous models, substantially modifies beam instability evolution. Hose instability growth tends to increase very rapidly in the beam head and taper off to an asymptotic value for large zeta in contrast to the pure power law growth seen when d(sigma)/d (zeta) are assumed to be constant. A second effect arises from local decreases in the perturbed conductivity sigma I produced by perturbed electric field-driven increases in the local collision frequency. This destabilizing effect causes the beam to behave

as if the monopole conductivity sigma sub 0 were replaced. Analytical models for the case of constant perturbation illustrate the pattern of rapid hose instability growth in the beam head followed by a plateu in hose amplitudes that is also observed in hose simulations with the VIPER model. GRA

N88-13022# United Kingdom Atomic Energy Authority, Abingdon (England).
BALLOONING MODES OR FOURIER MODES IN A TOROIDAL PLASMA?
J. W. Connor and J. B. Taylor Jan. 1987 26 p
(AD-A184299; CLM-P797) Avail: NTIS HC A03/MF A01 CSCL 20I

The relationship between two different descriptions of eigenmodes in a torus is investigated. In one the eigenmodes are similar to Fourier modes in a cylinder and are highly localized near a particular rational surface. In the other they are the ballooning modes which extend over many rational surfaces. A model which represents both drift waves and resistive interchanges is used to investigate the transition from one of these structures to the other. In this simplified model the transition depends on a single parameter which embodies the competition between toroidal coupling of Fourier modes (which enhances ballooning) and another (which diminishes ballooning). As the coupling is increased each Fourier mode acquires a sideband on an adjacent rational surface and these sidebands then expand across the radius to form the extended mode described by the conventional ballooning mode approximation. This analysis shows the ballooning approximation is appropriate for drift waves in a tokamak but not for resistive interchanges in a pinch. In the latter the conventional ballooning effect is negligible but they may nevertheless show a ballooning feature. This is localized near the same rational surface as the primary Fourier mode and so does not lead to a radially extended structure. GRA

N88-13023# United Kingdom Atomic Energy Authority, Culham (England).
NUMERICAL SIMULATION OF THE REVERSED FIELD PINCH
P. Kirby 1987 18 p
(AD-A184353; CLM-P803) Avail: NTIS HC A03/MF A01 CSCL 20I

This paper describes a series of numerical simulations of field reversal in the Reversed Field Pinch, using an incompressible MHD model and a reference set of plasma conditions. Field reversal and maintenance are observed although at values of the pinch parameter theta larger than in experiment. This discrepancy is shown to arise largely from the unrealistic resistivity profile in the reference conditions and may not be fundamental. Qualitative agreement with experiment is demonstrated in several areas. The view that field reversal is due to a simple MHD dynamo is therefore given support. GRA

N88-13024*# National Aeronautics and Space Administration. Lyndon B. Johnson Space Center, Houston, Tex.
THE VISTA SPACECRAFT: ADVANTAGES OF ICF (INERTIAL CONFINEMENT FUSION) FOR INTERPLANETARY FUSIONS PROPULSION APPLICATIONS
Charles D. Orth, Gail Klein, Joel Sercel, Nate Hoffman, Kathy Murray, and Franklin Chang-Diaz 2 Oct. 1987 5 p Presented at the Symposium on Fusion Engineering, Monterey, Calif., 12 Oct. 1987 Prepared in cooperation with Lawrence Livermore National Lab., Calif., JPL, Pasadena, Calif. and Rockwell International Corp., Canoga Park, Calif.
(Contract W-7405-eng-48)
(NASA-CR-181549; NAS 1.26:181549; DE88-000417; UCRL-96676; CONF-871007-2) Avail: NTIS HC A02 CSCL 20I

Inertial Confinement Fusion (ICF) is an attractive engine power source for interplanetary manned spacecraft, especially for near-term missions requiring minimum flight duration, because ICF has inherent high power-to-mass ratios and high specific impulses. We have developed a new vehicle concept called VISTA that uses ICF and is capable of round-trip manned missions to Mars in 100 days using A.D. 2020 technology. We describe VISTA's engine operation, discuss associated plasma issues, and describe the advantages of DT fuel for near-term applications. Although ICF is potentially superior to non-fusion technologies for near-term interplanetary transport, the performance capabilities of VISTA cannot be meaningfully compared with those of magnetic-fusion systems because of the lack of a comparable study of the magnetic-fusion systems. We urge that such a study be conducted. DOE

N88-13025# Oak Ridge National Lab., Tenn.
THE ROLE OF STELLARATORS IN THE ADVANCED TOROIDAL PROGRAM
J. Sheffield 1987 4 p Presented at the Fusion Power Development: Breakeven and Beyond, Princeton, N.J., 27 Aug. 1987
(Contract DE-AC05-84OR-21400)
(DE87-014815; CONF-870883-1) Avail: NTIS HC A02/MF A01

The goals of this Program as discussed in the DOE-Magnetic Fusion Program Plan and in the Technical Program Activity, have two parts: development of a better understanding of the underlying physics of toroidal devices and the development of the stellarator as a candidate reactor, and as a source of building blocks for other toroidal reactors, such as the tokamak-stellarator hybrid. This paper briefly discusses these concepts. DOE

N88-13026# Oak Ridge National Lab., Tenn.
A THREE-BARREL REPEATING PNEUMATIC PELLET INJECTOR FOR PLASMA FUELING OF THE JOINT EUROPEAN TORUS
S. K. Combs, S. L. Milora, L. R. Baylor, C. R. Foust, F. E. Gethers, and D. O. Sparks 1987 17 p Presented at the 34th National Vacuum Symposium and Topical Conference, Anaheim, Calif., 2 Nov. 1987
(Contract DE-AC05-84OR-21400)
(DE88-000330; CONF-871125-1) Avail: NTIS HC A03/MF A01

A three barrel repeating pneumatic pellet injector was developed for plasma fueling of the Joint European Torus (JET) tokamak. The versatile device consists of three independent machine gun-like mechanisms that operate at cryogenic temperature (10 to 20 K). Individual extruders provide a continuous supply of solid hydrogen isotope to each gun assembly, where a reciprocating breech side cutter forms and chambers cylindrical pellets from the extrusion; the deuterium pellets are then accelerated in the gun barrels with compressed hydrogen gas (pressures up to 105 bar) to velocities less than or = to 1.5 km/s. The injector features three nominal pellet sizes and repetitive operation for quasi-steady-state conditions. The design allows the gun barrels to be mechanically aligned for accurate aiming. A remote, stand-alone control and data acquisition system is used for injector operation. The injector system was installed on JET. The design features, operation, and performance characteristics of the injector are described. DOE

N88-13027# Los Alamos National Lab., N. Mex.
TRANSPORT SIMULATIONS OF THE OSCILLATING FIELD CURRENT DRIVE EXPERIMENT IN THE ZT-40M REVERSED FIELD PINCH
R. A. Scardovelli, R. A. Nebel, K. A. Werley, and G. H. Miley 1987 10 p Presented at the Course and Workshop on Physics of Mirrors, Reversed Field Pinches and Compact Tori, Varenna, Italy, 1 Sep. 1987 Prepared in cooperation with Illinois Univ., Urbana
(Contract W-7405-eng-36)
(DE88-000538; LA-UR-87-3106; CONF-870908-7) Avail: NTIS HC A02/MF A01

Oscillating Field Current Drive (OFCD) is based on the premise that in order to sustain a relaxing Reversed Field Pinch (RFP) plasma, one needs only to supply magnetic helicity at the same rate it is consumed. The purpose of this work is to try to better understand the possible mechanisms underlying these relaxations within the context of different kinds of resistive MHD instabilities. DOE

N88-13028# Wisconsin Univ., Madison. Fusion Technology Inst.
INERTIAL CONFINEMENT FUSION REACTOR CAVITY ANALYSIS Progress Report, 1 Jul. 1986 - 30 Jun. 1987
R. R. Peterson, J. J. MacFarlane, G. A. Moses, M. El-Afify, and M. L. Corradini Jul. 1987 79 p Prepared in cooperation with Lawrence Livermore National Lab., Calif.
(Contract W-7405-eng-48)
(DE88-000788; UCRL-15942; UWFDM-725) Avail: NTIS HC A05/MF A01

This is a process report for research performed from July 1, 1986 to June 30, 1987, for Lawrence Livermore National Laboratory under subcontract number 9265205 with the project title: Inertial Confinement Fusion Reactor Cavity Analysis. This research generally considers the problems of vaporization and condensation of liquid metal or solid first surface materials in high yield ICF facilities such as reactors or high yield target test experiments. The past year's research consisted of 1.2 man years of effort on three tasks. These tasks were: verify the current vaporization-condensation models in CONRAD through literature surveys of relevant published data, and evaluation and comparison of these data with predictions by CONRAD on condensation phenomena, and with predictions by CONRAD, ZPINCH, and/or MIXERG on radiation phenomena, design a small-scale vaporization experiment by evaluating existing experimental facilities, selecting a primary facility, and conceptually designing an experiment complete with facility parameters and measurables, and design a small-scale condensation experiment including experimental parameters, measurables, and dignostics. DOE

N88-13029# College of William and Mary, Williamsburg, Va.
THEORETICAL PLASMA PHYSICS Progress Report, 1 Jan. - 31 Dec. 1987
A. H. Boozer, G. Vahala, and E. R. Tracy Sep. 1987 6 p
(Contract DE-FG05-84ER-53176)
(DE88-001475; DOE/ER-53176/4) Avail: NTIS HC A02/MF A01

During the past year, research has been carried out on current drive in tokamaks and in spheromaks, fast integration techniques for magnetic field lines, alpha particle diagnostics that use CO2 laser scattering, and plasma turbulence. This paper discusses this research. DOE

N88-13030# Nagoya Univ. (Japan). Inst. of Plasma Physics.
FINAL (n,l) STATE-RESOLVED ELECTRON CAPTURE BY MULTIPLY CHARGED IONS FROM NEUTRAL ATOMS
N. Shimakura, N. Toshima, T. Watanabe (Institute of Physical and Chemical Research, Saitama, Japan), and H. Tawara Aug. 1987 66 p
(IPPJ-AM-54) Avail: NTIS HC A04/MF A01

Thanks to the recent development of experimental techniques, it has become possible to measure the cross sections of the final (n, l) state-resolved electron capture processes. As for the process of electron capture by incident multicharged ions from neutral atoms, many theoretical calculations were made using several different methods, for example, impact parameter methods using molecular basis wavefunctions, or using atomic basis wavefunctions, classical trajectory Monte Carlo method. A review on the theoretical calculations for the process is given. Particular attention is paid to the difference of the theoretical methods applied for the physics governed in the process, for the selective properties of the capture process and for the absolute values of cross sections from the practical point of view. Author

N88-13031# Nagoya Univ. (Japan). Inst. of Plasma Physics.
DATA BASE ON THE HIGH HEAT FLUX BEHAVIOUR OF METALS AND CARBON MATERIALS FOR PLASMA FACING COMPONENTS: EXPERIMENTS AT THE 10 MW NEUTRAL BEAM INJECTION TEST STAND OF THE IPP NAGOYA
H. Bolt, C. D. Croessmann (Sandia National Labs., Albuquerque, N. Mex.), A. Miyahara, T. Kuroda, and Y. Oka Aug. 1987 132 p
(IPPJ-AM-53) Avail: NTIS HC A07/MF A01

Disruption events in tokamak devices are regarded as one of the main issues governing material and design considerations for in-vessel components. During disruptions heat loads in the order of 100 to 5000 MW/sq m for durations of about 100 microseconds to severl tens of microseconds can cause severe damage to plasma facing components and may possibly lead to their failure. To determine the response of materials to high heat fluxes, an experimental program was carried out on metals and carbon materials using the 10 MW Neutral Beam Injection Test Stand of the IPP Nagoya. Stainless steel, aluminum, copper, and molybdenum samples, 13 grades of fine grain graphites, and pyrolytic carbon samples were subjected to hydrogen beam exposure with power densities of 15 to 120 MW/sq m and pulse durations of 50 to 950 ms. Resulting damage and threshold values for the occurrence of damage were determined and documented. Main damage observed on samples includes melting, erosion, and crack formation. The high heat flux resistance of each material tested is compared comprehensively with that of the others. Processes leading to material damage are discussed. in the case of damage on graphite, models of erosion and cracking processes are given. The implication of the experimental results for material selection and design of first wall components under the high heat flux aspect is discussed. Author

N88-13032# Nagoya Univ. (Japan). Inst. of Plasma Physics.
CONFINEMENT TIME OF ELECTRONS AND H(-)/D(-) IONS IN THE URAMOTO TYPE SHEET PLASMA
Joshin Uramoto Oct. 1987 38 p
(IPPJ-852; ISSN-0469-4732) Avail: NTIS HC A03/MF A01

Confinement times of electrons and H(-)/D(-) ions in the Uramoto type sheet plasma as a H(-)/D(-) ion source of volume production are determined from e-folding decay times of negative current to a Langmuir probe, after a discharge for the sheet plasma production is stopped through SCR connected between the anode and the cathode. The confinement times depend mainly on a bias potential of the metal vacuum chamber outside of the sheet plasma, which are ranging from about 40 microsec (for plus bias voltage with respect to the anode) to about 300 microsec (for minus bias voltage). Then, in order to extract a volume produced H(-)/D(-) ion current in high efficiency, it is shown that a long confinement time is an important necessary condition with the two necessary conditions (high electron density in low electron temperature and electron beam components) reported already. Author

N88-13033# Nagoya Univ. (Japan). Inst. of Plasma Physics.
MONTE CARLO ANALYSIS OF NEOCLASSICAL TRANSPORT FOR A COMPACT HELICAL SYSTEM
T. S. Chen Oct. 1987 41 p
(IPPJ-850; ISSN-0469-4732) Avail: NTIS HC A03/MF A01

Neoclassical confinement behavior in the realistic field configurations of a low aspect ratio compact helical system (CHS) is analyzed numerically by Monte Carlo simulation. Both diffusion coefficient and particle confinement time are used as parameters for transport behavior assessment. The results of Monte Carlo analysis indicate that in the CHS plasma, the dependence of transport on collisionality is distinctly different between ion and electron species. Results also show that the employment of different helical ripple modulations can lead to a 1.5 to 3 times difference of the ion confinement time and a 4 times difference of the ion diffusion coefficient at the typical plasma temperature (500 eV) and density. Thus it is possible to decrease the CHS ion diffusion coefficient level to approach that of the stellarators with rather high aspect ratios but without helical ripple modulations. Finally it is noted that a high helical ripple modulation would display its best action on the overall ion confinement performance under situations where a negative ambipolar potential exists. Author

N88-13034# Nagoya Univ. (Japan). Inst. of Plasma Physics.
MAGNETIC FLUCTUATION BEHAVIOUR OF CURRENT TERMINATION IN REVERSED FIELD PINCH
A. Nagata, H. Arimoto, S. Masamune, S. Yamada, K. I. Sato, and T. Tamaru (Hiroshima Univ., Japan) Sep. 1987 14 p
(IPPJ-849; ISSN-0469-4732) Avail: NTIS HC A03/MF A01

Growth of the magnetic fluctuations due to the m=1 and m=2 modes, where m is the poloidal mode number, and succeeding phase-lock of these modes were found as the precursor phenomena of the rapid destruction of the plasma column (current termination) in reversed field pinch (RFP). By deepening the field reversal at the wall, these precursors disappear, and the plasma current duration becomes much longer. Thus the current termination is loosely connected with the growth of MHD instabilities with the m=1 and m=2 modes. Author

N88-13035# Nagoya Univ. (Japan). Inst. of Plasma Physics.
MONOCRYSTAL SPUTTERING BY THE COMPUTER SIMULATION CODE ACOCT
Yasunori Yamamura and Wataru Takeuchi Sep. 1987 40 p
Sponsored by Japanese Ministry of Education, Science and Culture
(IPPJ-848; ISSN-0469-4732) Avail: NTIS HC A03/MF A01

A computer code ACOCT was developed in order to simulate the atomic collisions in the crystalline target within the binary collision approximation. The present code is more convenient as compared with the MARLOWE code, and takes the higher-order simultaneous collisions into account. To check the validity of the ACOCT program, sputtering yields were calculated for various ion-target combinations and compared with the MARLOWE results. It is found tht the calculated yields by the ACOCT program are in good agreement with those by the MARLOWE code. The ejection patterns of sputtered atoms were also calculated for the major surfaces of fcc, bcc, diamond, and hcp structures with reasonable agreement with experimental results. In order to know the effects of the simultaneous collision in the slowing down process the sputtering yields and the projected ranges are calculated, changing the parameter of the criterion for the simultaneous collision, and the effect of the simultaneous collision is found to depend on the crystal orientation. Author

N88-13036# Nagoya Univ. (Japan). Inst. of Plasma Physics.
MICROSTRUCTURAL CHANGE OF Al ON H IMPLANTATION
K. Kamada, A. Sagara, H. Kinoshita, and H. Takahashi (Hokkaido Univ., Sapporo, Japan) Sep. 1987 25 p
(IPPJ-847; ISSN-0469-4732) Avail: NTIS HC A03/MF A01

Modifications to the subsurface layer of Al on 25 KeV H2(+) ion implantation to fluences of 4 x 10 to the 17th power - 2 x 10 to the 18th power H(+)/sq cm at room temperature were investigated by transmission electron microscopy (TEM) and elastic recoil detection (ERD) with 1.5 MeV He(+). Numerous bubbles ranging in diameter from 50 to 1000 A were observed with a sharp peak at 120 A irrespective of ion fluence. Stereomicroscopic observations revealed the depth distribution of the bubbles. At fluences greater than 6 x 10 to the 17th power H(+)/sq cm, a lateral layer of lower density compared with matrix was observed and named Swiss cheese structure since its estimated structure is similar to Emmenthal cheese containing many holes. This Swiss cheese structure causes the formation of layers on a free surface, and plays a precursor role for blistering. Hydrogen depth profiling with ERD was performed on every specimen revealing the collapse of the implanted hydrogen profiling due to the formation of the Swiss cheese structure. Author

N88-13037# Nagoya Univ. (Japan). Inst. of Plasma Physics.
PROMPT SIMULTANEOUS ACCELERATION OF PROTONS AND ELECTRONS TO RELATIVISTIC ENERGIES BY SHOCK WAVES IN SOLAR FLARES
Yukiharu Ohsawa and Jun-ichi Sakai Oct. 1987 28 p
(IPPJ-851; ISSN-0469-4732) Avail: NTIS HC A03/MF A01

It is shown by theory and fully relativistic, electromagnetic particle simulation that a collisionless fast magnetosonic shock wave can promptly accelerate protons and electrons to relativistic energies; proton energies approximate or greater than 10 to the 9th eV and electron energies approximate to or greater than a million eV. The strong nonstochastic acceleration occurs in a rather strong magnetic field such that omega sub ce is approximate to or greater than omega sub pe, where omega sub ce is the electron cyclotron frequency, and omega sub pe is the electron plasma frequency. The time needed for the proton acceleration is of the order of the ion cyclotron period and is quite short (much less than 1 s for solar plasmas). The electron acceleration time is shorter than the ion cyclotron period. The present shock acceleration mechanism can explain important features of observed particle acceleration in the impulsive phase of solar flares: simultaneous and prompt acceleration of protons and electrons to relativistic energies. Author

N88-13038 California Univ., Berkeley.
MHD STABILITY AND CONTROL FOR MIRROR MACHINES Ph.D. Thesis
Bongkoo Kang 1986 122 p
Avail: Univ. Microfilms Order No. DA8718035

The Magnetohydrodynamic (MHD) stability properties of magnetic mirrors are examined theoretically. A second order differential equation, governing the relative ballooning mode instability for an arbitrary plasma beta, is derived from a set of fluid equations. The resistive effects on the Berkeley ten meter multiple Mirror Experiment (MMX) stabilized by a conducting wall, cusps, and quadrupoles are numerically examined and compared with the known experimental results. Numerical results show that the resistive effects play a dominant role on the low temperature MMX. The possibility of feedback stabilization of the m = 1 flute mode for axisymmetric mirror machines is also considered. A three region plasma model is developed and analyzed, consisting of a hot core surrounded by a warm transition annulus, which in turn is surrounded by a warm halo annulus that is in contact with the feedback plate at the two endwalls. By a proper choice of feedback function, the m = 1 flute mode on the core plasma is stabilized by feedback signals applied to segmented, ring shaped feedback plated. For the asixymmetric MMX, TMX-U, and MFTF-B, the required feedback power and its scaling with plasma parameters are calculated. The results show that stability can be achieved in the MMX and TMX-U devices with a modest feedback gain and power. The power requirement for MFTF-B is more severe, but can be reduced by a modified choice of plasma parameters.
Dissert. Abstr.

N88-13039 California Univ., Berkeley.
COHERENT EMISSION FROM RELATIVISTIC BEAM-PLASMA INTERACTIONS Ph.D. Thesis
Peter Ellis Latham 1986 172 p
Avail: Univ. Microfilms Order No. DA8718055

A theoretical model for the production of high power, high frequency electromagnetic radiation from unmagnetized, relativistic beam plasma interactions is studied. Emphasis is placed on the injected beam system, for which the dominant portion of the radiation is emitted near the point where the beam enters the plasma. In such systems, frequencies of magnitude above that predicted by single particle radiation were observed experimentally. A two step process is proposed to explain these observations: electrostatic bunching of the beam followed by coherent radiation by the bunches. The first step, beam bunching, produces large amplitude electrostatic waves. A Green's function analysis is employed to understand the convective growth of those waves near the plasma boundary; their saturation amplitude is found by applying conservation of energy to the beam plasma system. An azimuthally symmetric model is used to compute the saturated spectrum analytically, and a relatively simple expression is found. The second step, the interaction of the electron beam with the electrostatic spectrum, lead to the production of high power, high frequency electromagnetic radiation. Dissert. Abstr.

N88-13040# Los Alamos National Lab., N. Mex.
REFUELING AND DENSITY CONTROL IN THE ZT-40M REVERSED FIELD PINCH
G. A. Wurden, P. G. Weber, R. G. Watt, C. P. Munson, T. E. Cayton, and K. Buechl 1987 22 p Presented at the Course and Workshop on Physics of Mirrors, Reversed Field Pinches and Compact Tori, Varenna, Italy, 1 Sep. 1987
(Contract W-7405-eng-36)
(DE88-000504; LA-UR-87-2985; CONF-870908-8) Avail: NTIS HC A03/MF A01

The effects of pellet injection and gas puff refueling have been studied in the ZT-40M Reversed Field Pinch. Multiple deuterium pellets (less than or equal to 6 x 10 to the 19th D atoms/pellet) with velocities ranging from 300 to 700 m/sec have been injected into plasmas with n-bar(sub e) approx 1 to 5 X 10 to the 19th/cu m, I(sub phi) approx 100 to 250 kA, T(sub e)(0) approx 150 to 300 eV and discharge durations of less than or equal to 20 msec. Photographs and an array D(sub alpha) detectors show substantial deflection of the pellet trajectory in both the poloidal and toroidal planes, due to asymmetric ablation of the pellet by electrons streaming along field lines. To compensate for the poloidal deflection, the injector was moved up +14 cm off-axis, allowing the pellets to curve down to the midplane. In this fashion, central peaking of the pellet density deposition profile can be obtained. Both electron and ion temperatures fall in response to the density rise, such that Beta (sub theta)(Beta (sub theta) identical to n-bar(sub e)(T(sub e)(0) + T(sub i))/(B(sub theta)(a)) sup 2) remains roughly constant. Energy confinement is momentarily degraded, and typically a decrease in F (F identical to B(sub phi)(a)/(B(sub phi)) is seen as magnetic energy is converted to plasma energy when the pellet ablates. As a result of pellet injection at I(sub phi) = 150 kA we observe T(sub e)(0) alpha n-bar(sub e)(sup -.9 +/- .1), while the helicity based resistivity eta(sub k) transiently varies as n-bar(sub e)(sup .7 +/- .1). While the achievement of center-peaked density profiles is possible with pellet injection, gas puffing at rates strong enough to show a 50% increase in n-bar(sub e) over a period of 10 msec (approx 150 torr-litres/sec) leads to hollow density profiles. The refueling requirements for parameters expected in the next generation RFPs (ZTH, RFX) can be extrapolated from these data using modified tokamak pellet ablation codes. DOE

N88-13041# University of Northern Illinois, De Kalb. Public Opinion Lab.

THE ATTITUDES OF SCIENCE POLICY, ENVIRONMENTAL, AND UTILITY LEADERS ON US ENERGY ISSUES AND FUSION

J. D. Miller 1 Nov. 1986 27 p Prepared in cooperation with Lawrence Livermore National Lab., Calif.
(Contract W-7405-eng-48)
(DE88-000784; UCRL-15894) Avail: NTIS HC A03/MF A01

One example of basic and applied research at LLNL that has produced major, highly visible scientific and engineering advances has been the research related to controlled fusion energy. Continuing experimentation at LLNL and elsewhere is likely to demonstrate that fusion is a viable, inexhaustible alternative source of energy. Having conducted major fusion energy experiments for over 30 years at LLNL, it scientists and engineers recognized the enormous challenges that lay ahead in this important endeavor. To be successful, it was clear that collaborative efforts with universities, private industry, and other national laboratories would need to be greatly expanded. Along with invention and scientific discovery would come the challenge of transferring the myriad of new technologies from the laboratories to the private sector for commercialization of the fusion energy process and the application of related technologies to yet unimagined new industries and products. Therefore, using fusion energy research as the focus, the Laboratory's Technology Transfer Initiatives Program contracted with the Public Opinion Laboratory to conduct a survey designed to promote a better understanding of effective technology transfer. As one of the recognized authorities on scientific surveys, Dr. Jon Miller of the POL worked with Laboratory scientists to understand the objectives of the survey. He then formulated the questions, designed the survey, and derived his survey sample from a qualified list developed at the POL, which has formed the basis for other survey panels. This report, prepared by Dr. Miller, describes the basis and methodology of this survey process and then presents the survey findings and some conclusions. DOE

N88-13042# Nagoya Univ. (Japan). Inst. of Plasma Physics.

PROCEEDINGS OF THE JAPAN-US WORKSHOP P-92 ON PLASMA MATERIAL INTERACTION/HIGH HEAT FLUX DATA NEEDS FOR THE NEXT STEP IGNITION AND STEADY STATE DEVICES

Akira Miyahara, ed. and K. L. Wilson, ed. May 1987 515 p Workshop held in Nagoya, Japan, 26 Jan. 1987 Prepared in cooperation with DOE, Washington, D.C.
(DE87-013568; IPPJ-AM-50; CONF-870185) Avail: NTIS HC A22/MF A01

The Japan-US workshop on 'Plasma Material Interaction/High Heat Flux Data Needs for the Next Step Ignition and Steady State Devices,' was held at the Institute of Plasma Physics, Nagoya University, on January 26-30, 1987. The primary objective of this workshop was to answer the question, 'Are existing carbon materials (graphites and carbon-carbon composites) feasible for the CIT-experiment?' The approach to this question needs a definition of how reference materials for CIT are to be selected from existing materials. Most papers in this report deal with this question by testing different types of graphite as a first wall material for thermonuclear devices. Forty-two reports were cataloged individually. DOE

N88-13043# Lawrence Livermore National Lab., Calif.

REVIEW OF X-RAY SPECTROSCOPY FROM LASER-PRODUCED PLASMAS

R. L. Kauffman Sep. 1987 19 p Presented at the International Colloquium on UV and X-ray Spectroscopy, Beaulieu-Sur-Mer, France, 9 Sep. 1987
(Contract W-7405-eng-48)
(DE88-000755; UCRL-97336; CONF-8709143-3) Avail: NTIS HC A03/MF A01

Recent progress in x-ray spectroscopy from laser plasmas is reviewed. Advances in the use of K-shell spectra as a diagnostic tool is discussed. Much progress has been made in understanding complex spectra, especially from the Ne I and Ni I isoelectronic series. Much of this progress has been due to observation of amplification from n = O transitions from these configurations. The spectroscopy will be discussed and examples of spectra of the amplified lines will be shown. Finally, recent work on using x-ray spectroscopy to diagnose high density implosions will be discussed. DOE

N88-13044# California Univ., Los Angeles. Plasma Physics Group.

PISCES: PLASMA-SURFACE INTERACTIONS AND MATERIALS RESEARCH Progress Report

R. W. Conn, D. M. Goebel, Y. Hirooka, B. LaBombard, W. K. Leung, and R. Nygren Jul. 1987 21 p
(Contract DE-FG03-86ER-52134)
(DE88-001323; UCLA/PPG-1074) Avail: NTIS HC A03/MF A01

This report briefly summarizes the status of the current PISCES experiments and near term plans for research by the PISCES Group in the areas of enhanced pumping of neutral gases by graphite, hydrogen recycling from activated graphite surfaces, erosion of graphite, new diagnostics for in-situ monitoring of erosion yield, pump limiter experiments, spectroscopy and diagnostic development. Experimental equipment includes the existing PISCES facility, AES/SIMS surface analysis facility, PISCES-B, which is now under construction, and experimental probes being developed for use in the Continuous Current Tokamak (CCT). DOE

N88-13045# Oak Ridge National Lab., Tenn.

MODULAR PUMP LIMITER SYSTEMS FOR LARGE TOKAMAKS

T. Uckan, C. C. Klepper, P. K. Mioduszewski, and R. T. McGrath Sep. 1987 45 p
(Contract DE-AC05-84OR-21400)
(DE88-001487; ORNL/TM-10164) Avail: NTIS HC A03/MF A01

Long-pulse (greater than 10-s) operation of large tokamaks with high-power (greater than 10-MW) heating and extensive

external fueling will require correspondingly efficient particle exhaust for density control. A pump limiter can provide the needed exhaust capability by removing a small percentage of the particles, which would otherwise be recycled. Single pump limiter modules have been operated successfully on ISX-B, PDX, TEXTOR, and PLT. An axisymmetric pump limiter is now being installed and will be studied in TEXTOR. A third type of pump limiter is a system that consists of several modules and exhibits performance different from that of a single module. To take advantage of the flexibility of a modular pump limiter system in a high-power, long-pulse device, the power load must be distributed among a number of modules. Because each added module changes the performance of all the others, a set of design criteria must be defined for the overall limiter system. The design parameters for the modules are then determined from the system requirements for particle and power removal. Design criteria and parameters are presented, and the impact on module design of the state of the art in engineering technolgy is discussed. The relationship between modules is considered from the standpoint of flux coverage and shadowing effects. The results are applied to the Tore Supra tokamak. A preliminary conceptual design for the Tore Supra pump limiter system is discussed, and the design parameters of the limiter modules are presented. DOE

N88-13046# Wisconsin Univ., Madison. Dept. of Electrical and Computer Engineering.
ICRF LAUNCHER STUDIES Progress Report
J. E. Scharer Sep. 1987 19 p
(Contract DE-FG02-86ER-52133)
(DE88-001710; DOE/ER-52133/2) Avail: NTIS HC A03/MF A01

Research accomplished during the past year includes the topics of ICRF fast wave coupling to L- and H-mode edge profiles, measurements of simulated plasma loads on an 85 MHz launcher, coupling of ion Bernstein waves and a simulation of the folded waveguide launcher. We have also begun to examine coupling between launched fast waves and ion Bernstein waves driven by density gradients near the plasma edge and the effects of known edge turbulence and ponderomotive forces on the direct launching of ion Bernstein waves. We find that a TE sub 10 ICRF fast mode waveguide launcher has only a moderate increase in its reflection coefficient when coupling into a model H-mode plasma density profile. We find that linear coupling from fast modes to ion Bernstein modes can only occur with large density gradient scale lengths near the plasma edge. The current power level of ion Bernstein wave heating experiments is found to yield ponderomotive force effects which can substantially modify plasma edge density profiles. DOE

76 SOLID-STATE PHYSICS

Includes superconductivity.

For related information, see also *33 Electronics and Electrical Engineering* and *36 Lasers and Masers.*

N88-13047# Los Alamos National Lab., N. Mex.
SOLITON TWIN BOUNDARIES OF THE CUBIC-TETRAGONAL MARTENSITIC TRANSFORMATIONS IN FERROELASTIC MATERIALS
A. Mazor and A. R. Bishop 1987 12 p Presented at the Workshop on Competing Interactions and Microstructures: Statics and Dynamics, Los Alamos, N. Mex., 5 May 1987
(Contract W-7405-eng-36)
(DE87-014741; LA-UR-87-2611; CONF-8705168-2) Avail: NTIS HC A03/MF A01

Described here is one set of results from a comprehensive study of the cubic-tetragonal Martensitic transformations in ferroelastic materials. The model being used is the soliton model of Barsch and Krumhansl which exhibits a first-order cubic-tetragonal martensitic phase transition. This is a nonlinear and nonlocal three-dimensional continuum model, with a two-component strain order parameter. The structure and the energy of the static (or traveling) soliton strain boundaries, associated with the minimal total free energy, is calculated at all temperatures. Insight is also gained of the corresponding type of trajectories in the order parameter space. Approaching the first-order transition temperature from below, the tetragonal-tetragonal soliton wall splits gradually into two cubic-tetragonal solitons of finite width. Their separation, however, diverges at the transition temperature. This temperature is the border point between two topologically different classes of domain walls, which apparently have also different time-dependence. Below the transition point the kink-like solutions are of traveling type, but above the transition temperature the pulse-like walls are not. DOE

N88-13048# Los Alamos National Lab., N. Mex.
THE MOESSBAUER EFFECT OF SnI4 AT HIGH PRESSURE
R. D. Taylor, M. Pasternak, and J. N. Farrell 1987 5 p Presented at the International Conference on the Applications of the Mossbauer Effect, Melbourne, Australia, 17 Aug. 1987
(Contract W-7405-eng-36)
(DE87-014771; LA-UR-87-2774; CONF-870825-1) Avail: NTIS HC A02/MF A01

Tetravalent tin iodide is a molecular crystal composed of SnI4 tetrahedra loosely packed into a cubic configuration. Under pressure SnI4 becomes metallic at about 15 GPa. We report a Moessbauer effect study of Sn-119 and I-129 in SnI4 to pressures of 26 GPa. The spectra exhibit dramatic changes with pressure starting at about 10 GPa and show large pressure hysteresis effects upon reducing the pressure from 26 GPa. In the intermediate region tin exists in both Sn(+4) and Sn(+2) states, and iodine exists in two nonequivalent sites characterized by a different symmetry and different sign and magnitude of the electric field gradient. DOE

N88-13049# Georgia Univ., Athens. Dept. of Chemistry.
TOPOLOGICAL ASPECTS OF INFINITE METAL CLUSTERS AND SUPERCONDUCTORS
R. B. King 11 Aug. 1987 23 p
(Contract N00014-84-K-0365)
(AD-A184104; TR-44) Avail: NTIS HC A03/MF A01 CSCL 07B

This paper summarizes the chemical bonding topology of infinite metal clusters as well as superconductors constructed from metal octahedra or metal tetrahedra. The chemical bonding topologies of discrete octahedral metal clusters can be either edge-localized (e.g., Mo6x8L64+ derivatives), face-localized (e.g., Nb6x12L62+ derivatives), or globally delocalized (e.g., Zr6mu2-CL)12ECLn-12 derivatives where E=Be, B, C, N,). Infinite fusion of metal octahedra in one, two, and three dimensions leads to metal cluster chains (e.g., Gd2Cl3), metal cluster sheets (e.g., ZrCL), and bulk metals, respectively. Superconductors exhibiting relatively high critical temperatures and magnetic fields are constructed from edge-localized metal polyhedra such as the Mo6 octahedra in the ternary molybdenum chalcogenides (Chevrel phases) and Rh4 tetrahedra in the ternary lanthanide rhodium borides leading naturally to the concept of porous delocalization in such materials. GRA

N88-13050# Oakland Univ., Rochester, Mich. Dept. of Chemistry.
FAR-INFRARED SPECTRA OF LITHIUM DEPOSITED ON A GOLD ELECTRODE: INTERPRETATION USING A CLUSTER MODEL
Mark W. Severson, P. P. Schmidt, Stanley Pons, Jianguo Li, and J. J. Smith Jul. 1987 19 p
(Contract N00014-77-C-0239)
(AD-A184231; TR-28) Avail: NTIS HC A03/MF A01 CSCL 07D

A cluster model for the calculation of surface atom vibrations is described. The model assumes central forces between all the atoms of the cluster. Using a Morse function for the potential energy, the model is used to interpret the recently reported

far-infrared spectrum of lithium deposited on a gold electrode. GRA

N88-13051# Illinois Univ., Urbana. Gaseous Electronics Lab.
MEASUREMENT OF THE ELECTRON DENSITY AND THE ATTACHMENT RATE COEFFICIENT IN SILANE/HELIUM DISCHARGES Final Technical Report, 12 Jul. 1983 - 30 Mar. 1986
Charles B. Fledderman, J. H. Beberman, J. T. Verdeyen, G. Hebner, and L. J. Overzet Sep. 1986 84 p
(Contract F33615-83-K-2335)
(AD-A184268; AFWAL-TR-86-2031) Avail: NTIS HC A05/MF A01 CSCL 07D

Discharge processing of semiconductor materials, either as an etch process step in microelectronic fabrication, or as a deposition scheme for solar cell or copier applications, has become indispensable in modern technology. This report is focussed on discharges used for such applications. The thesis by Fleddermann was a basic study of the attachment rate of electrons in discharges involving mixtures of silane and a rare gas as represented by helium. It was found that the primary attaching species was not the silane modecule but some daughter product created by the discharge. These results are indicative of the problems encountered in an attempt to model discharges in such gases: the rates for the radicals may be larger than that of the donor gases. GRA

N88-13052# Pennsylvania Univ., Philadelphia. Dept. of Physics.
VALENCE BOND THEORY AND SUPERCONDUCTIVITY
Richard P. Messmer and Robert B. Murphy Jun. 1987 17 p
(Contract N00014-86-K-0304)
(AD-A184274; TR-7) Avail: NTIS HC A02/MF A01 CSCL 07D

Two necessary criteria for a theory of superconductivity are a phase coherence of the wave function and an attractive electron-electron interaction. We review how the BCS theory achieves these criteria and then show how a valence bond wave function can also meet these conditions. The energy scale of the latter approach has a larger range in principle than that possible via the electron-phonon interaction. GRA

N88-13053# Pennsylvania Univ., Philadelphia. Dept. of Physics.
THE CHEMICAL BOND AND SUPERCONDUCTIVITY
Richard P. Messmer Jul. 1987 23 p
(Contract N00014-86-K-0304)
(AD-A184275; TR-8) Avail: NTIS HC A02/MF A01 CSCL 07D

The search for understanding of the physical mechanisms operating in the recently discovered high Tc superconductors forces a re-examination of the basic concepts and physical assumptions of current theoretical approaches. The attractive interaction of a more general theory may be rather more complicated than the electron-phonon interaction usually assumed. In fact, it probably contains the critical chemical parameters of the material. This is the motivation for the present work in which the focus is two-fold: first, to call attention to some recent developments in our understanding of the chemical bond, and second, to propose that this new understanding is not only germane to the electronic structure of solids but also provides a new perspective on the relationship between the chemical bond and superconductivity. Studying the connection between chemical bonding and superconductivity would seem to be rather academic exercise if it were not for the high temperature superconductors. These materials have brought to our attention in a dramatic fashion the ignorance which exists in relating chemistry to the important physical parameters of a superconductor. Although this point was raised in numerous contributions by Matthias, its full import was never so apparent when the superconductors were traditional metals and alloys. GRA

N88-13054# Pennsylvania Univ., Philadelphia. Dept. of Physics.
VALENCE BOND CLUSTER STUDIES OF ALKALI METAL/SEMICONDUCTOR BONDING
Robert C. Tatar and Richard P. Messmer 1 Dec. 1986 2 p
(Contract N00014-86-K-0304)
(AD-A184276; TR-3) Avail: NTIS HC A02/MF A01 CSCL 07D

We present results of cluster studies of alkali metal/semiconductor bonding. Using the Generalized Valence Bond (GVB) method, we find a remarkable consistency in the behavoir of bonding orbitals for a variety of systems, including: LiH, CLi4, LiH4 and several hypervalent systems, such as SiH3Li2, SiH4Li2. Our results show that the metal-semiconductor bonding in these systems can be understood in terms of a pairing between McAdon-Goddard type metallic bonding orbitals and a set of equivalent orbitals of the non-metallic species. We propose that the results are relevant to the initial stages of alkali overlayer growth on semiconductor surfaces and lead to a simple picture of the bonding including the transition from a non-conducting to a conducting layer. We have considered numerous proposed hypervalent structures in light of the above results and find that they can be understood. GRA

N88-13055# Pennsylvania Univ., Philadelphia. Dept. of Physics.
TETRAHEDRAL CARBON AND INTERSTITIAL ELECTRONS IN LI CLUSTER: CLI4 AND (LICH3)4
Richard P. Messmer and Robert C. Tatar Jan. 1987 9 p
(Contract N00014-86-K-0304)
(AD-A184277; TR-4) Avail: NTIS HC A02/MF A01 CSCL 07B

The use of electronic structure calculations which include important electron correlation effects have yielded recently two quite significant findings. The first, is the discovery by McAdon and Goddard that bonding in alkali metal clusters and simple metals is via interstitial one-electron bonds. The second is that the carbon atom employs essentially tetrahedral hybrid orbitals not only for single bonds in saturated molecules, but also for double bonds, triple bonds and conjugated molecules such as benzene. The object of the present work is to illustrate how these two concepts about chemical bonding can be combined to provide a simple consistent physical picture of the bonding in CLi4 and (LiCH3)4. The basic principles illustrated by these two molecules provide the basis for understanding the structure and bonding of a wide class of organolithium compounds. GRA

N88-13056# Pennsylvania Univ., Philadelphia. Dept. of Physics.
K-CO ON TRANSITION METALS: A LOCAL IONIC INTERACTION
Charles H. Patterson, Peter A. Schultz, and Richard P. Messmer May 1987 4 p
(Contract N00014-86-K-0304)
(AD-A184342; TR-5) Avail: NTIS HC A02/MF A01 CSCL 07B

The nature of the K-CO interaction on a transition metal surface is addressed when the K:CO stoichiometry is approx. 1. The interaction proposed is transfer of the K 4s electron to CO. A BORN-Haber cycle for this process on a surface has been calculated. The reference state is K plus CO, bound separately to the surface (a). A key point in the cycle is that removal of the electron from K bound to a metal surface (b) is less costly in energy (approx. metal/K surface, i.e., approx. +2.0 eV) than from K in the gas phase (IP = +4.3 eV). This means that the complex is significantly stabilized on the surface. The removed K electron is then transported to the isolated adsorbed CO (c) at a cost of the electron affinity of CO (approx. = 1.5 eV). When the isolated ions are brought together (d) the net stabilization at the equilibrium geometry is approx. - 1.8 eV. GRA

N88-13057# Temple Univ., Philadelphia, Pa. Dept. of Chemistry.
GUEST-HOST INTERACTIONS IN THERMOTROPIC AND LYOTROPIC LIQUID CRYSTALS Final Report, 1 Apr. 1984 - 31 Mar. 1987
M. M. Labes May 1987 117 p
(Contract DAAG29-84-K-0036)
(AD-A184402; ARO-21003.5-CH) Avail: NTIS HC A06/MF A01 CSCL 07D

Three problems were examined under this program. Reaction kinetics were studied in nematic lyotropic media and it was demonstrated that there are dramatic changes in reaction rates as one goes through the phase transitions from lamellar to cylindrical to spherical micellar structures. Several model reactions were studied including the catalyzed hydrolysis of phosphinate esters, where more than three orders of magnitude difference was observed in the rate constants between phases. Orientational spectroscopic techniques were developed for studying guest and hosts in lyotropic liquid crystals. A pearlescent suspension display concept was developed and reduced to practice which might be useful in large size electrically operated shutters. GRA

N88-13058# Northwestern Univ., Evanston, Ill. Dept. of Chemistry.

EFFECT OF SIDECHAIN LENGTH AND CROSSLINKING ON IONIC CONDUCTIVITY IN POLYPHOSPHAZENE SOLID ELECTROLYTES Interim Technical Report

J. S. Tonge, P. L. Blonsky, D. F. Shriver, H. R. Allcock, and P. A. Austin 24 Aug. 1987 2 p Prepared in cooperation with Pennsylvania State Univ., University Park

(Contract N00014-80-C-0532)

(AD-A184419; Rept-016) Avail: NTIS HC A02/MF A01 CSCL 07D

A series of fully substituted poly(phosphazenes) with alkoxy sidechains, and/or dialkoxy crosslinks were synthesized and investigated as electrolyte host materials. All of the polymers readily formed complexes with LISO3CF3, LIDO3C4F9 and Li2(SO3)2C2F2. The polymer with seven ether oxygens in its sidechain gives the highest conducting polymer salt complex at 30C. The crosslinked polymers were found to be totally amorphous with comparable conductivity and increased resistance to flow at elevated temperatures. GRA

N88-13059# Sandia National Labs., Albuquerque, N. Mex.

REEVALUATING THE WORST-CASE RADIATION RESPONSE OF MOS TRANSISTORS

D. M. Fleetwood 1987 10 p Presented at the VHSIC/VLSI Qualification Reliability and Logistics Conference, Colorado Springs, Colo., 25 Aug. 1987

(Contract DE-AC04-76DP-00789)

(DE87-014157; SAND-87-1001C; CONF-8708137-1) Avail: NTIS HC A02/MF A01

Predicting worst-case response of a semiconductor device to ionizing radiation is a formidable challenge. As processes change and MOS gate insulators become thinner in advanced VLSI and VHSIC technologies, failure mechanisms must be constantly re-examined. Results are presented of a recent study in which more than 100 MOS transistors were monitored for up to 300 days after Co-60 exposure. Based on these results, a reevaluation of worst-case n-channel transistor response (most positive threshold voltage shift) in low-dose-rate and postirradiation environments is required in many cases. It is shown for Sandia hardened n-channel transistors with a 32 nm gate oxide, that switching from zero-volt bias, held during the entire radiation period, to positive bias during anneal clearly leads to a more positive threshold voltage shift (and thus the slowest circuit response) after Co-60 exposure than the standard case of maintaining positive bias during irradiation and anneal. It is concluded that irradiating these kinds of transistors with zero-volt bias, and annealing with positive bias, leads to worst-case postirradiation response. For commercial devices (with few interface states at doses of interest), on the other hand, device response only improves postirradiation, and worst-case response (in terms of device leakage) is for devices irradiated under positive bias and annealed with zero-volts bias. DOE

N88-13060*# National Aeronautics and Space Administration. Goddard Space Flight Center, Greenbelt, Md.

DESIGN CONCEPTS FOR THE ASTROMAG CRYOGENIC SYSTEM

M. A. Green and S. Castles Jun. 1987 9 p Presented at the Conference on Advances in Cryogenic Engineering, St. Charles, Ill., 14 Jun. 1987 Prepared in cooperation with California Univ., Berkeley, Lawrence Berkeley Lab.

(Contract DE-AC03-76SF-00098)

(NASA-CR-181505; NAS 1.26:181505; DE87-014683; LBL-23822; CONF-8706125-13) Avail: NTIS HC A02/MF A01 CSCL 20L

Described is a proposed cryogenic system used to cool the superconducting magnet for the Space Station based ASTROMAG Particle Astrophysics Facility. This 2-meter diameter superconducting magnet will be cooled using stored helium II. The paper presents a liquid helium storage concept which would permit cryogenic lifetimes of up to 3 years between refills. It is proposed that the superconducting coil be cooled using superfluid helium pumped by the thermomechanical effect. It is also proposed that the storage tank be resupplied with helium in orbit. A method for charging and discharging the magnet with minimum helium loss using split gas-cooled leads is discussed. A proposal to use a Stirling cycle cryocooler to extend the storage life of the cryostat will also be presented. DOE

N88-13061# Centro Brasileiro de Pesquisas Fisicas, Rio de Janeiro.

INFLUENCE OF BOND DILUTION ON THE FREE SURFACE AND INTERFACE POTTS FERROMAGNETISM

E. F. Sarmento, E. L. deAlbuquerque, and C. Tsallis 1986 29 p

(DE87-703360; CBPF-NF-029/86) Avail: NTIS (US Sales Only) HC A03/MF A01

Within a simple real space renormalization group framework, the phase diagram of a q-state Potts ferromagnetic system constituted by two semi-infinite bulks separated by a planar interface is discussed. Quenched bond dilution has been assumed in the bulks as well as in the interface. The system exhibits percolation-like phenomena which generalize the standard d=2 and d=3 ones. Also, competition between bulk dilution (which enhances surface magnetism) and interface dilution (which depresses surface magnetism) is observed. DOE

N88-13062# Argonne National Lab., Ill.

NON-LATTICE MATCHED METALLIC SUPERLATTICES

I. K. Schuller and M. Grimsditch Mar. 1987 11 p Presented at the American Institute of Metallurgical Engineers Annual Meeting: Light Metals Session, Denver, Colo., 22 Feb. 1987

(Contract W-31-109-eng-38)

(DE87-011512; CONF-870272-9) Avail: NTIS HC A03

High quality multilayers can be grown by sputtering and molecular beam epitaxy techniques. If the constituents are not lattice matched and do not form solid solutions, the reasons for the growth into superlattices is not understood. For some limited cases (Mo/Ni, Nb/Cu, V/Ni, Ag/Co) high quality superlattices can be grown quite easily, although the in plane structure is polycrystalline. If the constituents form solid solutions and are lattice matched the growth into single crystalline superlattices is possible, although more interdiffusion is likely. The physical properties in nonlattice matched superlattices exhibit anomalous elastic constants and a metal-nonmetal transition in their normal state properties. By changing the relative coupling across a normal material we have observed dimensional crossover in superconducting superlattices and the development of magnon bands in magnetic superlattices. DOE

N88-13063# California Univ., Berkeley. Lawrence Berkeley Lab.

MAGNETIC FIELD DEPENDENCE OF THE SPECIFIC HEAT OF SOME HIGH-T/SUB c/ SUPERCONDUCTORS

N. E. Phillips, R. A. Fisher, S. E. Lacy, C. Marcenat, J. A. Olsen, W. K. Ham, and A. M. Stacy May 1987 6 p Presented at the 18th Conference on Low Temperature Physics, Kyoto, Japan, 20 Aug. 1987

(Contract DE-AC03-76SF-00098)

(DE87-014078; LBL-23531-Rev; CONF-870873-8-Rev) Avail: NTIS HC A02

This paper investigates the effect of magnetic fields on the specific heat of some high-T sub c superconductors. Measurements

of specific heat, C, were made on samples of La2CuO4-y (La1), La1.85M0.15CuO4-y (Ca1, Sr1, Sr2, Ba1 and Ba2) and YBa2Cu3O9-y (Y1). Meissner effect measurements were made in 12.5G. The high-temperature onset of a change in magnetic susceptibility, chi, was taken as T sub c, and the transition width, T sub c, as the temperature interval of the 10 to 90% change in chi. Calculation of the fractional Meissner effect, -4 chi sub V, was based on the total sample volume, with chi sub V corrected for demagnetizing effects. DOE

N88-13064# Oak Ridge National Lab., Tenn.
RADIATION INDUCED COLLAPSE OF THE CRYSTALLINE STRUCTURE
D. F. Pedraza Aug. 1987 20 p Presented at the Conference on Solid State Amorphizing Transformation, Los Alamos, N. Mex., 10 Aug. 1987
(Contract DE-AC05-84OR-21400)
(DE87-014407; CONF-8708104-2) Avail: NTIS HC A03/MF A01

A theory of irradiation-induced amorphization of ordered intermetallic compounds, based on the destabilization of the crystalline structure by excess defect accumulation, has been developed recently. The theory is reviewed starting with its phenomenological basis, where the microstructural evolution of intermetallic compounds that are turned amorphous by irradiation is emphasized. Next, the analysis of defect buildup that suggests the formation of a stable complex defect consisting of a vacancy-interstitial pair, called a complex, is reviewed. The possibility of a radiation induced microstructure such as interstitial clusters, in addition to complexes, in intermetallics that undergo the crystalline-to-amorphous transition is incorporated into the theory. A comparison of radiation effects in NiTi and in Zr3Al is made using a rate theory approach. In the case of the aluminide, it is found that cluster development can hinder the amorphous transition when the material is irradiated with electrons. On the other hand, enhancement of complex production in the collision cascade, explains the occurrence of the transition during ion combardment. DOE

N88-13065# State Univ. of New York, Stony Brook. Research Foundation.
ATOMIC AND ELECTRONIC STRUCTURE OF SURFACES AND CHEMISORBED LAYERS Progress Report, 1 Mar. 1986 - 31 Mar. 1988
2 Sep. 1987 8 p
(Contract DE-FG02-86ER-45239)
(DE87-014987; DOE/ER-45239/2) Avail: NTIS HC A02/MF A01

Efforts were concentrated on studies of chemisorption on solid surfaces, namely, the formation of mixed layers (as opposed to overlayers) of atoms of metallic adsorbates with atoms of the substrate. These mixed layers are called surface alloys. The studies have involved low-energy electron diffraction (LEED) and ultraviolet photoemission spectroscopy (UPS). Results proved quantitatively the formation of a mixed layer, to determine the relative positions of the atoms in the surface and that the first two atomic layers of the Cu(001)c(2 x 2)-Au phase have essentially the same structure as the first two layers of the (001) surface of the bulk CuAu alloy. We could also show that after formation of the surface alloy there was no measurable ordered content of Au not only in the second, but also in the third atomic layer. UPS showed that the width of the d band of the surface alloy was noticeably narrower than that of the bulk alloy, correcting an earlier misinterpretation; changes were identified in the valence band of the Cu substrate upon formation of the surface alloy; and the Au-induced d bands and their dispersions were determined. The last run at the NSLS (in June 1987) constituted the UPS part of a research project on the formation of another surface alloy. The resulting phase, Cu(001)c(2 x 2)-Pd, was suspected possibly to consist of a mixed layer. DOE

N88-13066# California Univ., Berkeley. Lawrence Berkeley Lab.
RAMAN SCATTERING SPECTRUM ALONG A BEVEL ETCHED GaAs ON Si, TEM (TRANSMISSION ELECTRON MICROSCOPE) STUDY AND GaAs P-I-N PHOTODETECTOR ON Si
Y. H. Lo, M. N. Charasse, H. Lee, D. Vakhshoori, Y. Huang, P. Yu, Z. Liliental-Weber, M. Werner, and S. Wang May 1987 8 p Presented at the Spring Meeting of the Materials Research Society, Anaheim, Calif., 21 Apr. 1987 Prepared in cooperation with California Univ., Berkeley
(Contract DE-AC03-76SF-00098)
(DE88-000210; LBL-23742; CONF-870438-37) Avail: NTIS HC A02/MF A01

Raman scattering is measured along a bevel-etched GaAs epitaxial film grown on Si by molecular beam epitaxial (MBE). From the correlation length profile of Raman scattering, most dislocation lines are confined in the 2000 A regions close to the interface. The strain profile calculated from the Raman peak shift shows that about 0.6% compressive strain exists near the interface because of lattice mismatch. However, as one moves away from the interface, the compressive strain is gradually counterbalanced by thermal expansion. Transmission electron microscope (TEM) studies of the local dislocation image and properties show that an ultra clean Si surface is essential for dislocation confinement. From high resolution TEM, we find that the distance between dislocations at the interface is nonuniform, varying from 50 A to 125 A with an average distance at 81 A. Finally, a GaAs p-i-n photodetector on Si substrate is fabricated. Even though a normal photoresponse curve is obtained, the high dark current (50nA) and relatively low responsivity (0.01A/W) show that the material quality needs to be further improved to make a minority carrier vertical transition device. DOE

N88-13067# Lawrence Livermore National Lab., Calif.
WAVELENGTHS OF THE 3p-3d TRANSITIONS OF THE Co- AND Fe-LIKE IONS: THE EFFECTS OF ELECTRON CORRELATION
Mau Hsiung Chen 2 Sep. 1987 6 p Presented at the International Colloquium on UV and X-ray Spectroscopy, Beaulieu-Sur-Mer, France, 9 Sep. 1987
(Contract W-7405-eng-48)
(DE88-000219; UCRL-97325; CONF-8709143-2) Avail: NTIS HC A02/MF A01

The experimental observations of the 3p6 3d9 2D - 3p5 3d10 2p transitions of the Co-like ions and 3p6 3d8 4F4 - 3p5 3d9 3F3 of the Fe-like ions have recently been extended to highly charged ions of heavy elements up to uranium (Z = 92). A comparison between the observed energies and calculated values from the Dirac-Fock model indicated persistent discrepancies of 3 to 4 eV for all ions. Systematic multiconfiguration Dirac-Fock calculations for these transitions have been carried out with emphases on the effects of electron correlation. The previously found discrepancies theory and experiment have mostly removed after the inclusion of the electron-electron correlation effects in the theoretical calculations. DOE

N88-13068# California Univ., Berkeley. Lawrence Berkeley Lab.
EVALUATION OF THE MELLEN EDG FURNACE FOR GROWTH OF LARGE DIAMETER GaAs SINGLE CRYSTALS IN A HORIZONTAL CONFIGURATION
E. D. Bourret, J. B. Guitron, and E. E. Haller Jun. 1987 17 p Presented at the American Conference on Crystal Growth, Monterey, Calif., 13 Jul. 1987
(Contract DE-AC03-76SF-00098)
(DE88-000463; LBL-22903; CONF-870799-3) Avail: NTIS HC A03/MF A01

An extensive evaluation of the Mellen EDG furnace has been conducted in order to assess its performance for growth of large diameter (2 and 3 in.) GaAs crystals in the horizontal configuration. The axial and radial temperature gradients were found to influence strongly the crystal-melt interface shape and crystalline perfection of the crystals. When the axial thermal gradients are small relative to the radial thermal gradients, the shape of the crystal-melt

interface fluctuates in time as growth proceeds, indicating the presence of oscillatory convective flows in the melt. The crystal-melt interface becomes stable as the axial component of the thermal gradient over the solid is increased. The crystals produced with optimized gradient conditions have a low and uniform dislocation density. DOE

N88-13069# Los Alamos National Lab., N. Mex.
RESISTIVITY OF EuBa2(Cu/SUB 1-y/Zn/SUB Y/)3O/SUB X/ AS A FFUNCTION OF TEMPERATURE, MAGNETIC FIELD, PRESSURE AND Zn CONCENTRATION
H. A. Borges, G. L. Wells, S. W. Cheong, R. S. Kwok, J. D. Thompson, Z. Fisk, J. L. Smith, and S. B. Oseroff (San Diego State Univ., Calif.) 1987 11 p Presented at the 18th Conference on Superconductivity in Highly Correlated Fermion Systems, Sendai, Japan, 31 Aug. 1987 Prepared in cooperation with San Diego State Univ., Calif.
(Contract W-7405-eng-36)
(DE87-014740; LA-UR-87-2617; CONF-870881-3) Avail: NTIS HC A03/MF A01

We report electrical resistance and magnetoresistance measurements on EuBa2(Cu(sub 1-y)Zn(sub y) sub 3 O(sub x) under pressure to 17 kbar. With Zn substitution, T(sub c) is depressed rapidly (approx 19 K/at% Zn) and there are qualitative changes in the temperature and field response of the resistance. Pressure drives the Zn-substituted samples toward undoped EuBa2Cu3O(sub x) behavior. Analysis of the temperature dependent resistance for y = 0.05 and P = O, together with Hall effect and thermopower data, suggests that the suppression of superconductivity may arise from weak three-dimensional localization promoted by Coulomb interactions. DOE

N88-13070# Brown Univ., Providence, R. I. Div. of Engineering.
NOVEL DYNAMICAL INVESTIGATIONS OF EXCITONS AND THEIR STRUCTURE IN SEMICONDUCTORS Final Report, Jun. 1984 - Nov. 1986
A. V. Nurmikko Aug. 1987 24 p
(Contract DE-FG02-84ER-45067)
(DE87-014868; DOE/ER-45067/T1) Avail: NTIS HC A03/MF A01

Two spectroscopic investigations in the time dependent behavior of excitons in selected semiconductors are discussed. First, as a continuation of previous grant work, issues of energy dependent exciton-exciton scattering in a model bulk semiconductor Cu2O have been studied. Picosecond photomodulation methods have yielded for the first time direct kinetic information about scattering involving the 1S and 2P exciton states. Second, exciton formation and localization kinetics have been investigated through time-resolved photoluminescence in a new wide bandgap semiconductor quantum well structure, based on the ZnSe/(Zn,Mn)Se heterojunction. In this case exciton formation and recombination rates have been shown to also depend on an additional energy relaxation channel into the Mn-ion d-electron excitations. DOE

N88-13071# Los Alamos National Lab., N. Mex.
THEORY AND SIMULATIONS OF ZONE 2 MICROSTRUCTURES IN THIN FILMS
D. J. Srolovitz, A. Mazor, B. G. Bukiet, and P. S. Hagan 1987 7 p Presented at the 34th National Vacuum Symposium and Topical Conference, Anaheim, Calif., 2 Nov. 1987
(Contract W-7405-eng-36)
(DE87-014752; LA-UR-87-2869; CONF-871125-3) Avail: NTIS HC A02/MF A01

The nature of the microstructure of vapor-deposited films is known to depend sensitively on the substrate temperature during deposition. At intermediate temperatures (T approx .45 Tm where Tm is the melting point of the film) the film is made up of columnar-grains separated by metallurgical grain boundaries. Both an analytical and numerical analysis is presented in which the space-time evolution of the columnar microstructure (Zone II) is studied. DOE

N88-13072# California Univ., Berkeley. Lawrence Berkeley Lab.
FAR INFRARED FOURIER TRANSFORM SPECTROSCOPY OF SEMICONDUCTORS
E. E. Haller Jul. 1987 34 p Presented at the 6th International Conference on Fourier Transform Spectroscopy, Vienna, Austria, 24 Aug. 1987
(Contract DE-AC03-76SF-00098)
(DE88-000188; LBL-23244; CONF-870809-1) Avail: NTIS HC A03/MF A01

Fourier transform spectroscopy (FTS) is one of the most important tools in the study of shallow level donors and acceptors in semiconductors. When combined with a two-step photothermal ionization process detected photoconductively, FTS allows measurement of optical transitions of donor-bound electrons (and acceptor-bound holes) in ultra-pure germanium samples with impurity concentrations less than 10 cm (i.e., one electrically active impurity in 4 x 10^{13} host atoms). The experimental high resolution study of the hydrogen-like excited state series of shallow levels has yielded as many as 19 lines of width as small as 10 eV for some centers. These results have stimulated theoretical work which has led to the unambiguous assignment of quantum states to many bound excited states. Extensive studies of ultra-pure Ge crystals grown under different well-controlled conditions have led to the discovery of a large number of novel shallow impurity complexes. Study of the multiplicities and symmetries of the associated electronic states has led to a detailed understanding of the unusual static and dynamic structures of these novel centers. The chemical composition has been deduced from correlations between the concentration of a particular center and the materials involved in crystal growth. DOE

N88-13073# California Univ., Berkeley. Lawrence Berkeley Lab.
THE STRUCTURE OF ADSORBED SULFUR AND CARBON ON MOLYBDENUM AND RHENIUM SINGLE CRYSTAL SURFACES, AND THEIR INFLUENCE ON CARBON MONOXIDE AND HYDROCARBON CHEMISORPTION Ph.D. Thesis
D. G. Kelly Aug. 1987 285 p
(Contract DE-AC03-76SF-00098)
(DE88-001393; LBL-23937) Avail: NTIS HC A13/MF A01

An ultra-high vacuum study was performed on the chemisorption and structures of S and C adsorbates on Mo(100), Re(0001), and Re(1010) single crystal surfaces. Both S and C adsorb strongly on Mo(100), Re(0001), and Re(1010), with adsorption energies greater than 70 kcal/mol for coverages less than saturation. S was proposed to adsorb in the highest symmetry sites on all surfaces except for theta sub s greater than 0.75 on Mo(100), where studies suggest two different adsorption sites. C adsorbs in a 'carbidic' or active phase on Mo(100), where it is also proposed to adsorb in the highest symmetry sites. However, C adsorbs in a 'graphitic' or inactive phase on Re(0001) and Re(1010). CO chemisorption on the S and C overlayers was found to be blocked (except for C on Mo(100)), with S blocking adsorption more efficiently than C. Changes in adsorption energy were determined to be caused by local crowding of CO molecules by S or C, rather than a long-range electronic interaction. Unsaturated hydrocarbons decomposed completely on Mo(100), Re(0001), and Re(1010). Similar to the results for CO chemisorption, strong adsorption of unsaturated hydrocarbons (leading to decomposition) was blocked by pre-adsorbed S, allowing only physisorption to occur. DOE

77 THERMODYNAMICS AND STATISTICAL PHYSICS

Includes quantum mechanics; theoretical physics; and Bose and Fermi statistics.

For related information see also *25 Inorganic and Physical Chemistry* and *34 Fluid Mechanics and Heat Transfer.*

N88-13074# Texas A&M Univ., College Station. Research Foundation.
THERMODYNAMIC PROPERTIES FOR NATURAL GAS BINARIES Final Report, Jan. 1982 - Dec. 1986
K. R. Hall, P. T. Eubank, and J. C. Holste Apr. 1987 281 p
(Contract GRI-5082-260-0591)
(PB87-226833; GRI-87/0136) Avail: NTIS HC A13/MF A01 CSCL 20M

The objective of this project was to supply a set of data covering PVT, enthalpy and liquid/vapor equilibrium for binary systems composed of natural gas components. The authors assembled various apparatus to provide state-of-the-art measurements for these properties and have compiled a significant set of data. Much of the first three years of the project involved apparatus design and construction, while much of the final two years involved data collection. GRA

N88-13075# California Univ., Berkeley.
MENTAL MODELS IN EXPERT PHYSICS REASONING
Jeremy Roschelle and James G. Greeno Jul. 1987 39 p
(Contract N00014-85-K-0095; RR0-4206)
(AD-A184106; GK-2) Avail: NTIS HC A03/MF A01 CSCL 20C

A relational framework is proposed for characterizing experienced physicists' representations of physics problem situations and the process of constructing these representations. A representation includes a coherent set of relations among (1) a mental model of the objects in the situation, along with their relevant properties and relations, (2) a mental model of theoretical idealizations of objects, and (3) parameter histories based on mental simulations of both models. Evidence from protocols and a small experiment support a conclusion that experienced physicists' processes of representing problem situations (a) use informal, commonsense knowledge, including envisionment of objects in the situations, and (b) are interactive, with mutual influences between informal knowledge and their technical, theoretical knowledge. We also describe characteristics of the mental models that represent problem situations and the process of constructing them, drawing from work by AI researchers on qualitative process models, and specifying several categories of rulers that would be needed for an implementation of the system as a simulation program. GRA

N88-13076# Centro Brasileiro de Pesquisas Fisicas, Rio de Janeiro.
ANALYSIS OF ABSOLUTE SPACE-TIME LORENTZ THEORIES
A. K. A. Maciel and J. Tiomno 1986 22 p
(DE87-703371; CBPF-NF-046/86) Avail: NTIS (US Sales Only) HC A03/MF A01

Two particular forms of absolute space time theories are presented together with a derivation of their predictions for measurements that are within presented day detection limits. DOE

N88-13077# Sao Paulo Univ. (Brazil). Inst. de Fisica.
HOMOGENEOUS SPACE-TIME OF GOEDEL TYPE IN HIGHER-DERIVATE GRAVITY
A. J. Accioly and A. T. Goncalves Oct. 1986 13 p
(DE87-703690; IFUSP-P-604) Avail: NTIS (US Sales Only) HC A03/MF A01

A general theorem concerning any Goedel-type solution of higher-derivative gravity field equations, which may be produced by any reasonable physical source with a constant energy-momentum tensor, is analysed. The resulting class of metrics depends on two parameters, one of which is related to the vorticity. A general class of solutions of Goedel-type space-time-homogeneous universes in the context of the higher-derivative theory is exhibited. This is the most general higher-derivative solution of such type of metric and includes all known solutions of Einstein's equations related to these geometries as a special case. A number of completely causal rotating models is also obtained. Some of them present the interesting feature of having no analogous in the framework of general relativity. DOE

N88-13078# Texas Univ., Austin. Center for Particle Theory.
A SUPERSYMMETRIC LAGRANGIAN FOR POINCARE GAUGE THEORIES OF GRAVITY
C. Castro Oct. 1987 19 p
(Contract DE-FG05-85ER-40200)
(DE88-001670; DOE/ER-40200/118) Avail: NTIS HC A03/MF A01

A supersymmetric construction of the most general quadratic field Lagrangian for Poincare Gauge Field Theories of gravity, recently proposed by Kuhfuss-Nitsch to be devoid of ghosts and tachyons, is presented. DOE

N88-13079# Texas Univ., Austin. Center for Particle Theory.
GRAVITY FROM SYMMETRY BREAKDOWN OF A GAUGE AFFINE THEORY
Y. Neeman and D. Sijacki Sep. 1987 26 p Prepared in cooperation with Tel Aviv Univ., Israel and Belgrade Univ., Yugoslavia
(Contract DE-FG05-85ER-40200)
(DE88-001671; DOE/ER-40200/117; TAUP/N-183/87) Avail: NTIS HC A03/MF A01

We construct a gauge field theory based on bar GA(4,R) space-time symmetry, and provide the full Lagrangian containing spinorial and tensorial (infinite-component) matter manifields. We break the dilation symmetry and thus trigger a spontaneous breaking of the bar SL(4,R)/bar SO(1,3), also generating Newton's constant. The resulting space-time is of Riemann-Cartan type and in the flat limit we recover Special Relativity. DOE

80 SOCIAL SCIENCES (GENERAL)

Includes educational matters.

No abstracts in this category.

81 ADMINISTRATION AND MANAGEMENT

Includes management planning and research.

N88-13080# Naval Postgraduate School, Monterey, Calif.
A COMPARISON OF THE BASKET METHOD AND THE STRATIFIED RANDOM SAMPLING FOR CONTRACT CHANGE ORDER NEGOTIATIONS M.S. Thesis
Scott W. Fisher Jun. 1987 41 p
(AD-A184170) Avail: NTIS HC A03/MF A01 CSCL 05A

This study compares two methods of statistical sampling for application in a contracting context. The methods are compared with the intent of demonstrating the superiority of one method over the other in assisting price analysts and contract negotiators in expediting processing of proposals for change orders while maintaining acceptable levels of risk. The Basket Method and Stratified Random Sampling techniques are examined to determine which method allows a more accurate estimate of a proposal population to be made. The several populations used in the simulation have errors planted to represent both random honest mistakes and weighted dishonest mistakes. The author concludes that the Basket Method has a more desirable accuracy pattern than the Stratified Random Sampling Technique. GRA

82 DOCUMENTATION AND INFORMATION SCIENCE

Includes information management; information storage and retrieval technology; technical writing; graphic arts; and micrography.

For computer documentation see *61 Computer Programming and Software.*

N88-13081# California Univ., Davis.
A DATA TRANSLATION METHOD FOR HETEROGENEOUS DATABASE SYSTEMS Ph.D. Thesis
John Leland Clevenger 1986 132 p
Avail: Univ. Microfilms Order No. DA8710778

The general problem of translating data between heterogeneous systems is considered in the context of transferring relations between heterogeneous Relational Database Management Systems (RDBMSs). Discussed are formal models for the translation process, and a model developed for a Generalized Relation translator (GRT), capable of transferring relations between arbitrary RDBMSs. The GRT model is based on a novel type of grammar, the Control Grammar (CG). CGs are similar to the two-level grammars of van Wijngaarden, but include a set of control rules which define allowable values for control variables. During parsing, the current set of control variable values defines a current environment which can be used to condition the invocation of control actions. Control actions can be used to modify the environment, thus providing a mechanism for the efficient implementation of the parsers, in terms of both time and space. CGs are formally defined, their properties discussed, and their use in the design of the GRT presented. In the GRT, specific RDBMS details are described by a set of rules, and the CG permits the restriction of sentences recognized by the parser to those associated with the current source RDBMS. Diferences among RDBMS forms are isolated in the CG rules, making extension of the GRT to include new systems straightforward. A working implementation of the GRT is described, including an Extender which provides for the addition of new RDBMSs to the translator repertoire. Dissert. Abstr.

N88-13082# Lawrence Livermore National Lab., Calif.
TOWARDS AUTOMATED CONSULTING: DESIGN FEEDBACK FROM THE PERFORMANCE OF ONLINE DOCUMENTATION
T. R. Girill, C. H. Luk, and S. Norton Jul. 1987 8 p Presented at the 50th Annual Meeting of the American Society for Information Science, Boston, Mass., 4 Oct. 1986
(Contract W-7405-eng-48)
(DE87-012243; UCRL-96911; CONF-8610336-1) Avail: NTIS HC A03

Usage monitoring of online documentation at a supercomputer center strongly suggests the importance of three strategies in the design of an effective consulting system to deliver full-text answer passages to end users: (1) persistent on-demand printing as well as online viewing make a shared database economically vital; (2) a broad range of subject queries makes retrieval on diverse topics through a single user interface psychologically beneficial to readers, and (3) vocabulary mismatch errors demand an active response to faulty search terms, but not at the cost of increased interface complexity. DOE

N88-13083*# National Aeronautics and Space Administration. Marshall Space Flight Center, Huntsville, Ala.
FY 1985 SCIENTIFIC AND TECHNICAL REPORTS, ARTICLES, PAPERS AND PRESENTATIONS
Joyce E. Turner, comp. Nov. 1985 82 p
(NASA-TM-86521; NAS 1.15:86521) Avail: NTIS HC A05/MF A01 CSCL 05B

This document presents formal NASA technical reports, papers published in technical journals, and presentations by Marshal Space Flight Center (MSFC) personnel in FY 85. It also includes papers of MSFC contractors. After being announced in STAR, all of the NASA series reports may be obtained from the National Technical Information Service (NTIS), 5285 Port Royal Road, Springfield, Va. 22161. Author

N88-13084*# California Univ., Santa Cruz. Computer and Information Sciences.
INTELLIGENT SIGNAL ANALYSIS AND RECOGNITION Report, 1 Dec. 1986 - 30 Nov. 1987
Robert Levinson, Daniel Helman, and Edward Oswalt 30 Nov. 1987 25 p
(Contract NCC2-438)
(NASA-CR-181531; NAS 1.26:181531) Avail: NTIS HC A03/MF A01 CSCL 05B

Progress in the research and development of self-organizing database system that can support the identification and characterization of signals in an RF environment is described. As the radio frequency spectrum becomes more crowded, there are a number of situations that require a characterization of the RF environment. This database system is designed to be practical in applications where communications and other instruments encounter a time varying and complex RF environment. The primary application of this system is the guidance and control of NASA's SETI Microwave Observing Project. Other possible applications include selection of telemety bands for communication with spacecraft, and the scheduling of antenna for radio astronomy are two examples where characterization of the RF environment is required. In these applications, the RF environment is constantly changing, and even experienced operators cannot quickly identify the multitude of signals that can be encountered. Some of these signals are repetitive, others appear to occur sporadically. Author

N88-13085 California Univ., Berkeley.
SUBJECTIVE PROBABILITY, COMBINATION OF EXPERT OPINION AND PROBABILISTIC APPROACHES TO INFORMATION RETRIEVAL Ph.D. Thesis
Paul Thompson 1986 184 p
Avail: Univ. Microfilms Order No. DA8718181

Probability and its application to the problem of information retrieval were studied. A survey and examination of current work on probabilistic indexing, probabilistic queries, and rules for how these can be combined and used in order to rank output documents by computed values of probability of relevance are presented. In these current approaches to probabilitistic information retrieval (PIR), probability is interpreted as a relative frequency or as a person's estimate of a relative frequency. There are three major conceptual difficulties with current theories: independence/dependence of individual term probabilities; the small sample return; and the validity of probabilities used. The psychological literature on human probability assessment was studied. A computerized simulation study examines how errors in estimation of term probabilities propagate into the combined probability for each document and how this affects the ranked output of documents. A mathematical model was developed for PIR which uses a subjective interpretation of probability, probability distributions, and the technique of combination of expert opionions. Dissert. Abstr.

N88-13086# Defense Technical Information Center, Alexandria, Va.
SOURCE HEADER LIST. VOLUME 1: A THROUGH K Annual Report, period ending Jun. 1987
Sherry Hart, comp. Sep. 1987 630 p Supersedes DTIC/TR/86/14-Vol-1
(AD-A184000; DTIC/TR/87/14-Vol-1; DTIC/TR/86/14-Vol-1)
Avail: NTIS HC A99/MF A01 CSCL 05B

This publication is the first of two volumes of an alphabetically arranged compilation of corporate author names used by the Defense Technical Information Center in the DTIC database system. Each source name is assigned a 6-digit numeric code for computer input and retrieval purposes plus a 4-digit alphanumeric geopolitical code and an alphanumeric type code. Source names displayed are included as data elements in the Technical Report.

Work Unit Information System and Independent Research and Development databases are maintained by DTIC. GRA

83 ECONOMICS AND COST ANALYSIS

Includes cost effectiveness studies.

No abstracts in this category.

84 LAW, POLITICAL SCIENCE AND SPACE POLICY

Includes NASA appropriation hearings; aviation law; space law and policy; international law; international cooperation; and patent policy.

No abstracts in this category.

85 URBAN TECHNOLOGY AND TRANSPORTATION

Includes applications of space technology to urban problems; technology transfer; technology assessment; and surface and mass transportation.

For related information see also *03 Air Transportation and Safety, 16 Space Transportation,* and *44 Energy Production and Conversion.*

N88-13087# Office of Technology Assessment, Washington, D.C.
TECHNOLOGY TRANSFER TO CHINA
Jul. 1987 249 p
(PB87-223418; OTA-ISC-340; LC-87-619823) Avail: NTIS HC A11/MF A01 CSCL 05A

The Chinese context for technology transfer: The Economic Issues; The Chinese context for technology transfer: Strategies and Issues for technology imports; The role of the United States in technology transfer to China; Policies of other supplier countries: Japan, France, West Germany, and Britain; China's economic and political trends; Strategic implications of a modernizing China; and US policy choices are discussed. GRA

N88-13088# Naval Ocean Systems Center, San Diego, Calif.
GROUND VEHICLE CONVOYING
D. W. Gage and J. B. Pletta 1987 17 p Presented at the SPIE Cambridge Symposium on Intelligent Robots and Computer Vision, Cambridge, Mass., 1 Nov. 1987 Prepared in cooperation with Sandia National Labs., Albuquerque, N. Mex.
(Contract DE-AC04-76DP-00789)
(DE88-000360; SAND-87-2363C; CONF-871163-4) Avail: NTIS HC A03/MF A01

Initial investigations into two different approaches for applying autonomous ground vehicle technology to the ground vehicle convoying application are described. A minimal capability system that would maintain desired speed and vehicle spacing while a human driver provided steering control could improve convoy performance and provide positive control in nighttime and inclement weather, but would not reduce driver manpower requirements. Such a system could be implemented in a modular and relatively low cost manner. A more capable system would eliminate the human driver in following vehicles and reduce manpower requirements for the transportation of supplies. This technology could also be used to aid in the deployment of teleoperated vehicles in a battlefield environment. The needs, requirements, and several proposed solutions for such an Attachable Robotic Convoy Capability (ARCC) system will be discussed. Included are discussions of sensors, actuators, computers, communications, control systems and safety issues. This advanced robotic convoy system will provide a much greater capability, but will be more difficult and expensive to implement. DOE

N88-13089# Howard Univ., Washington, D. C.
A NATIONAL MODEL AT HOWARD UNIVERSITY DEMONSTRATING PRIVATE SECTOR INTERRELATIONSHIPS THAT FACILITATE RESEARCH IN PREDOMINANTLY BLACK COLLEGES AND UNIVERSITIES Quarterly Report, 1 Jan. -31 Mar. 1987
1987 23 p
(Contract DE-FG05-86OR-21702)
(DE88-000160; DOE/OR-21702/T1) Avail: NTIS HC A03/MF A01

Plans for the May 19-20, 1987, forum on fostering research alliances are discussed. Research administration at Howard University is discussed. Future plans are outlined. DOE

N88-13090# California Univ., Berkeley. Lawrence Berkeley Lab.
THE ROLE OF BASIC RESEARCH IN SOCIETY
G. T. Seaborg Aug. 1987 10 p Presented at the Conference on the Superconducting Super Collider, Berkeley, Calif., 30 Jul. 1987
(Contract DE-AC03-76SF-00098)
(DE88-000459; LBL-23833; CONF-8707116-1) Avail: NTIS HC A02/MF A01

This report contains general remarks on accelerators, especially the Superconducting Super Collider, and their role in the advancement of modern scientific knowledge. DOE

N88-13091# Public Service Co. of New Mexico, Albuquerque.
PERFORMANCE MONITORING AND ANALYSIS OF ELECTRIC VAN FLEET VEHICLES Final Technical Report
T. M. Lechner Sep. 1987 111 p
(DE88-900066; NMRDI-2-74-4610) Avail: NTIS HC A06/MF A01

This report documents efforts of various organizations, working in concert, to improve on, produce, demonstrate, and commercialize a viable electric vehicle (EV) for fleet applications. In addition, it compares current EV technology to its compressed natural gas and gasoline counterparts. The report also assesses the potential impact of wide-scale EV commercialization on the state. The concept of using electricity to power vehicles for commercial or private transportation needs is not new; in the early 1900s EVs enjoyed wide popularity. Vast oil discoveries, cheap gasoline, and improvements in internal combustion engine technologies undermined EV popularity over a relatively short period. A serious reconsideration of EV technology began in the late 1970s when it became apparent that the world, and the US in particular, was not assured an endless supply of cheap petroleum fuels. DOE

88 SPACE SCIENCES (GENERAL)

No abstracts in this category.

89 ASTRONOMY

Includes radio, gamma-ray, and infrared astronomy, and astrometry.

N88-13092# Colorado Univ., Boulder.
FIFTH CAMBRIDGE WORKSHOP ON COOL STARS, STELLAR SYSTEMS AND THE SUN Abstracts Only

Susan Barnes, ed. and Robert Stencel, ed. Jul. 1987 144 p Workshop held in Boulder, Colo., 8-11 Jul. 1987
Avail: NTIS HC A07/MF A01

Topics addressed include: red giant stars; supergiant stars; stellar magnetic fields; nonthermal phenomena in stellar coronae; heating of stellar chromospheres and coronae; angular momentum history of stars; reexamination of the corona/wind dividing line; IRAS observations; stellar envelopes; and activity in pre-main sequence stars. For individual titles, see N88-13093 through N88-13192.

N88-13093# Harvard-Smithsonian Center for Astrophysics, Cambridge, Mass. Center for Astrophysics.
MEASUREMENTS OF STELLAR MAGNETIC FIELDS Abstract Only c90
L. Hartmann *In* Colorado Univ., 5th Cambridge Workshop on Cool Stars, Stellar Systems and the Sun Jul. 1987 1 p (For primary document see N88-13092 04-89)
Avail: NTIS HC A07/MF A01

A number of measurements of magnetic fields on late-type stars were reported using the Zeeman broadening technique. Measurements using optical lines require high signal-to-noise spectra and careful analysis. Simple models are developed to investigate the sensitivity of Zeeman broadening results to parameters such as velocity fields, line damping constants, and blending. These models are used to estimate uncertainties in the understanding of stellar magnetic fields. Author

N88-13094# Joint Inst. for Lab. Astrophysics, Boulder, Colo.
THE PHOTOSPHERIC MAGNETIC FIELDS OF COOL STARS: RECENT RESULTS OF SURVEY AND TIME-VARIABILITY PROGRAMS Abstract Only c90
S. H. Saar *In* Colorado Univ., 5th Cambridge Workshop on Cool Stars, Stellar Systems and the Sun Jul. 1987 1 p (For primary document see N88-13092 04-89)
Avail: NTIS HC A07/MF A01

The past decade has seen considerable advances in the ability to measure magnetic fields on cool stars. New observational and analytical techniques were employed, producing a considerable body of data on the mean magnetic field strength in stellar active regions (B) and the fraction (filling factor) of the stellar surface covered by these fields (f) for G, K, and M dwarfs. Recent results of observational programs aimed at surveying magnetic parameters on a broad range of stars were examined and the time-variability of B and f was studied. Conclusions are outlined. Author

N88-13095# Naval Research Lab., Washington, D.C. Center for Space Research.
FLUX TUBE DYNAMICS AND SOLAR/STELLAR REDSHIFT MEASUREMENTS Abstract Only c92
J. T. Mariska *In* Colorado Univ., 5th Cambridge Workshop on Cool Stars, Stellar Systems and the Sun Jul. 1987 1 p (For primary document see N88-13092 04-89)
Avail: NTIS HC A07/MF A01

On the Sun, where high spatial and spectral resolution observations are possible, mass motions are common at transition region temperatures. Doppler shifts were observed suggesting both upflowing and downflowing plasma. The upflowing plasma is often impulsive in nature, while the downflows can persist at the same site for long periods of time and suggest a steady flow. There are several possible explanations for these downflows. The most plausible explanation is that of a steady flow of plasma in a magnetic loop. Recent theoretical studies suggest that such a model will reproduce many of the observed properties of the flows. This model appears to explain both the magnitude of the observed Doppler shifts and the fact that there is a maximum temperature above which redshifts are not observed. Numerical simulations also suggest that it may provide a partial explanation of the behavior of the nonthermal broadening as a function of temperature observed in the solar transition region and corona. Observations of Doppler shifts in the transition regions of cool stars other than the Sun are at the current limits of existing spacecraft experiments. Initial studies with IUE show that redshifts indicating downflows of roughly the same magnitude as those observed on the Sun may be a common feature of cool-star transition regions and coronae. Author

N88-13096# Colorado Univ., Boulder. Dept. of Astrophysical, Planetary and Atmospheric Sciences.
NONTHERMAL PHENOMENA IN STELLAR CORONAE: EVIDENCE FROM RADIO OBSERVATIONS Abstract Only c93
George A. Dulk *In its* 5th Cambridge Workshop on Cool Stars, Stellar Systems and the Sun Jul. 1987 1 p (For primary document see N88-13092 04-89)
Avail: NTIS HC A07/MF A01

In the past few years a number of different kinds of stars were detected at radio wavelengths, the majority of them cool stars. In most cases the radio emission is indicative of high energy, nonthermal processes: acceleration of electrons to some 10's of keV or, in some circumstances, several MeV or more. These electrons then emit radio waves by the incoherent processes of gyroresonance and gyrosynchrotron radiation, and the coherent processes of cyclotron maser and plasma radiation. The source of energy for the electron acceleration in single stars and some binaries is probably the generation of magnetic fields in the stellar interior, their emergence above the photospheres, and their subsequent dissipation. Whatever the basic energy source, some energy appears in the form of fast electrons that are capable of generating intense radio waves. If the energy of the electrons is greater than or approximately 1 keV they may emit gyroresonance radiation of brightness temperature T sub B greater than or approximately 10 to the 7th K, and if greater than or approximately 100 keV they may emit gyrosynchrotron radiation with T sub B greater than or approximately 10 to the 8th K. For the coherent radiation mechanisms of cyclotron maser and plasma radiation, the electrons need not be more energetic than approximately 10 keV, but they must have free energy, probably in the form of a loss cone distribution or a bump-in-the-tail distribution. Then the electrons are able to emit radiation with T sub B greater than the maximum so far recorded, approximately 10 to the 15th K.
Author

N88-13097# Helsinki Univ. (Finland). Observatory and Astrophysics Lab.
OBSERVATIONAL CONSTRAINTS AND EVIDENCE FOR SATURATION Abstract Only c90
Osmi Vilhu *In* Colorado Univ., 5th Cambridge Workshop on Cool Stars, Stellar Systems and the Sun Jul. 1987 1 p (For primary document see N88-13092 04-89)
Avail: NTIS HC A07/MF A01

Chromospheric-coronal emission has a clear observed (spectral type dependent) upper limit (saturation). This boundary is seen in the surface flux vs. color diagrams for different types of cool stars, excluding T Tau and some RSCVn and FK Com type stars. At a fixed photospheric color the upper boundary is occupied by rapid rotators; their surfaces are also totally filled with equipartition magnetic flux tubes. This might be one of the reasons for the saturation: super-active regions with B = 1-2 kG totally fill the stellar surface, and no more magnetic flux can get out. For saturated stars the observed fluxes (over the disc) could also represent the local surface fluxes, if the many filling factors involved are really close to unity; then a comparison with heating theories is possible. The mechanical flux of convective motions (just below the photosphere) is not very much larger than the estimated total radiative losses from the chromospheric-coronal plasma of saturated stars. Hence, this mechanical driver of coronal heating might set another natural constraint. To conclude, it is suggested that the combination of filling factors are less than or equal to 1, and the finite amount of convective kinetic energy available, is the simple reason behind the saturation observed. Author

N88-13098# Joint Inst. for Lab. Astrophysics, Boulder, Colo.
HEATING OF STELLAR CHROMOSPHERES AND CORONAE: EVIDENCE FOR NON-MAGNETIC BASAL HEATING Abstract Only c90
C. J. Schrijver *In* Colorado Univ., 5th Cambridge Workshop on

Cool Stars, Stellar Systems and the Sun Jul. 1987 1 p (For primary document see N88-13092 04-89)
Avail: NTIS HC A07/MF A01

A detailed analysis of radiative losses from the outer atmospheres of magnetically active stars suggests that two distinct components are present. These two components in the emission may be caused by two distinct mechanisms of non-radiative heating that operate in the outer atmospheres of cool stars. One of these mechanisms depends on the stellar effective temperature and possibly on the stellar radius, but not on rotation. The associated radiative energy loss, corresponding to the observed lower boundary in diagrams of flux density versus effective temperature, may be a result of heating by purely acoustic waves. The temperatures in the part of atmosphere heated by this mechanism fall below a few tens of thousands of degrees, hence the name basal chromosphere. The dependence of the basal fluxes on stellar effective temperature is discussed. Some examples demonstrate the relative importance of the basal flux in the study of stellar magnetic activity. Author

N88-13099# Dominion Astrophysical Observatory, Victoria (British Columbia).
ANGULAR MOMENTUM EVOLUTION OF YOUNG STARS Abstract Only c90
John R. Stauffer *In* Colorado Univ., 5th Cambridge Workshop on Cool Stars, Stellar Systems and the Sun Jul. 1987 1 p (For primary document see N88-13092 04-89)
Avail: NTIS HC A07/MF A01

Theoretical studies of the angular momentum evolution of young stars were essentially unconstrained by the necessity of fitting observational data until recently. It is only within the last decade that observers have succeeded in estimating, even roughly, the rotational velocity distribution of T Tauri stars. Because of the advent of new instrumentation, and software to take advantage of that instrumentation, there is now an abundance of data. The new results and the implications for understanding the angular momentum evolution of low mass stars are summarized. Author

N88-13100# National Solar Observatory, Tucson, Ariz.
POST-ZERO-AGE MAIN SEQUENCE ROTATION Abstract Only c90
Myron A. Smith *In* Colorado Univ., 5th Cambridge Workshop on Cool Stars, Stellar Systems and the Sun Jul. 1987 1 p (For primary document see N88-13092 04-89)
Avail: NTIS HC A07/MF A01

A large sample of rotational velocities (V) from photometric modulation periods is now becoming available to complement the Vsini's obtained by analysis of spectral line profiles. A comparison of V's with Vsini's for F8-G8 dwarfs so far shows little hint of the influence of the sini projection factor experienced in the spectroscopic measurements, either of the mean or of the distribution of the parameter (Vsini/V). A second interesting result is that for solar-type dwarfs of a given age and mass the V's show at most a total range of 40% around a mean value; it is not a Maxwellian distribution. As a typical intermediate mass star evolves across the H-R Gap, its surface rotation cannot be readily reconciled with any of the historical scenarios that require conservation and internal redistribution of angular momentum. Gray's work shows convincing evidence that a boundary exists from GO IV to G5 III along which rotational velocities exhibit a strong discontinuity. The interaction of the rapid rotation and the deepening zone causes a rapid spindown of the stellar outer layers through the onset of a strong dynamo. Thereafter, a rotostat regulates the rotation because of the opposing actions of entrainment of angular momentum from the core to the outer layers, and the still growing convection zone. It is concluded that the rotation of massive stars during late evolutionary phases seems to be explainable solely by any internal redistribution of angular momentum. Author

N88-13101# Oxford Univ. (England). Dept. of Theoretical Physics.
A RE-EXAMINATION OF THE CORONA-WIND DIVIDING LINE: DIAGNOSTICS OF NON-CORONAL ATMOSPHERES Abstract Only c90
P. G. Judge *In* Colorado Univ., 5th Cambridge Workshop on Cool Stars, Stellar Systems and the Sun Jul. 1987 1 p (For primary document see N88-13092 04-89)
Avail: NTIS HC A07/MF A01

Since the original proposal by Linsky and Haisch (1979) of a solar/non-solar dividing line in the HR diagram, separating stars whose outer atmospheres had solar-like EUV spectra and those which did not, many relevant observations were made at wavelengths between the radio and X-ray regions. The present reexamination of the corona-wind dividing line addressed observations and analyses of the outer atmospheres of single giants and supergiants later than spectral type KO. Except for the known hybrid stars, these non-solar stars have no detectable UV emission at transition region temperatures or X-ray emission. These stars are at the lower limits of stellar activity. Following a critical overview of the quantitative differences between coronal and non-coronal stars, the techniques available for constraining and modelling chromospheres and winds are discussed. By taking well-studied examples from the literature, the topics covered included empirical and semi-empirical methods and their limitations. The diagnostic information available from emission and absorption lines formed under different conditions and by different processes is reviewed, together with constraints available from continua and other diagnostics. Finally, possible directions for future works are discussed. Author

N88-13102*# National Aeronautics and Space Administration. Goddard Space Flight Center, Greenbelt, Md.
EXPLOITING THE IR: SOLAR AND STELLAR SPECTROSCOPY IN THE IR Abstract Only
Drake Deming *In* Colorado Univ., 5th Cambridge Workshop on Cool Stars, Stellar Systems and the Sun Jul. 1987 1 p (For primary document see N88-13092 04-89)
Avail: NTIS HC A07/MF A01 CSCL 03A

Recent instrumental advances have provided the capability to perform high resolution spectroscopy, in the thermal infrared region of the solar spectrum, with high sensitivity. The 8 to 12 micron region was extensively observed using Fourier transform (FTS) and laser heterodyne techniques. The continuous opacity of the solar atmosphere, due to H(-), increases with wavelength in the infrared region longward of 1.6 microns. Consequently thermal infrared observations probe the upper photosphere, and give an insight into the dynamics and structure of this region. The most notable spectral features in the 10 micron window include pure rotation lines of OH, and emission lines due to high-n states in MgI and AlI. The high-n lines due to MgI and AlI are important to solar and stellar physics because of their very large Zeeman sensitivity. The recent development of a cryogenic grating postdispenser for the FTS has allowed low-noise solar observations of these lines in 90 seconds. Limited mapping of the lines in a sunspot penumbra was performed, and gives information of the structure of the penumbral magnetic field. Although the MgI lines were detected in red giant spectra, instrumental sensitivity is not yet sufficient to see them in stars where significant magnetic fields are expected. Author

N88-13103# Fairborn Observatory, Mesa, Ariz.
AUTOMATIC PHOTOMETRIC MONITORING OF COOL STARS Abstract Only
R. M. Genet, L. J. Boyd, D. S. Hayes, S. L. Baliunas, D. L. Crawford, and D. S. Hall (Dyer Observatory, Nashville, Tenn.) *In* Colorado Univ., 5th Cambridge Workshop on Cool Stars, Stellar Systems and the Sun Jul. 1987 1 p (For primary document see N88-13092 04-89)
Avail: NTIS HC A07/MF A01

Automatic photometric monitoring of cool stars is the major activity at the Automatic Photoelectric Telescope (APT) Service, a joint undertaking by the Fairborn Observatory and the Smithsonian

Institute. The two largest observing programs are RS CVn binaries, and the solar-type stars that are also being observed in the K-line on the 1.5 meter telescope at Mt. Wilson. There are also observing programs for sixteen other institutions. Two 0.75 meter APTs are under construction. These APTs were specifically designed for automated photometry. Having no eyepieces, the photometers are permanently mounted, and are only 6 feet tall when pointed at the zenith. Work has begun on Remote-Access Automatic Photometry (RAAP), to make the APT Service more timely and versatile. Instead of mailing in requests for observations and waiting for data to be retrieved from the mountain, analyzed, and returned via mail, requests will be sent directly by the astronomers via modem to a computer on Mt. Hopkins, and observations will be similarly retrieved. Requests made one afternoon will result in retrieved observations the next morning. Author

N88-13104# National Solar Observatory, Sunspot, N. Mex.
ATMOSPHERES OF STARS IN THE LIMITS OF THIN AND THICK CONVECTION ZONES: THE M DWARFS Abstract Only c90
Mark S. Giampapa *In* Colorado Univ., 5th Cambridge Workshop on Cool Stars, Stellar Systems and the Sun Jul. 1987 1 p (For primary document see N88-13092 04-89)
Avail: NTIS HC A07/MF A01

The M dwarf stars impact a significant range of topics in contemporary astrophysics. Their sheer numbers inevitably influence galactic dynamics and structure. The eventual accurate determination of their mass function at faint magnitudes will provide a critical constraint on models of star formation. In the context of solar-stellar physics, studies of M dwarf stars can elucidate aspects of magnetic field-related atmospheric heating processes and the nature of dynamo field generation, each in the limit of very low turbulent velocities and thick convection zones. Most research has concentrated mainly on the so-called dMe stars, i.e., M dwarfs characterized by intense chromospheric hydrogen and Ca II line emission combined with coronal X-ray emission at levels of approximately 10 to 1000 times that of the quiet Sun. Frequent flare activity at visible wavelengths is especially prominent. However, recent research suggests that ordinary dwarf M stars may serve as important links in the understanding of the origin and nature of magnetic activity in dwarf stars with thick convection zones. The chromospheric and coronal properties of M dwarf stars are summarized. The relationship between these properties and the nature of the underlying magnetic dynamo mechanism and atmospheric heating processes are discussed. Author

N88-13105# National Center for Atmospheric Research, Boulder, Colo. High Altitude Observatory.
ATMOSPHERES OF STARS IN THE LIMITS OF THICK AND THIN CONVECTION ZONES: M GIANTS Abstract Only c90
K. B. MacGregor *In* Colorado Univ., 5th Cambridge Workshop on Cool Stars, Stellar Systems and the Sun Jul. 1987 1 p (For primary document see N88-13092 04-89)
Avail: NTIS HC A07/MF A01

The post main sequence evolution of stars having masses between 1 and 15 solar mass is characterized by (among other things) the development of an extensive convective envelope. In the course of their evolution, giants and supergiants with masses in this range traverse that portion of the HR diagram in which atmospheric thermal and dynamical properties are known to undergo significant changes. It is therefore of interest to consider how atmospheric structure might be influenced by evolution-induced changes in convection zone (or other stellar) properties. In the present brief review, this and other questions are examined in a rudimentary way by summarizing the observationally inferred properties of the chromospheres, coronae, and winds of cool, low-gravity stars, and comparing the results with what little is known theoretically concerning post main sequence convection zone structure, its relation to surface activity, and mechanisms for mass loss. Author

N88-13106# Colorado Univ., Boulder.
DISK ACCRETION DURING THE EARLY STAGES OF STELLAR EVOLUTION Abstract Only c90
Scott Kenyon *In its* 5th Cambridge Workshop on Cool Stars, Stellar Systems and the Sun Jul. 1987 1 p (For primary document see N88-13092 04-89)
Avail: NTIS HC A07/MF A01

This review concentrates on observational evidence for small solar system-sized disks surrounding low mass, pre-main sequence stars. High and low resolution spectroscopic data for the FU Orionis variables are consistent with the idea that the eruptions of these objects are powered by the onset of rapid accretion through a viscous disk. The large accretion rates inferred from the energy distributions of FU Ori and V1057 Cyg suggest that approximately 0.001 to 0.01 solar mass is added to the central pre-main sequence star during an FU Ori event. If historical observations of FU Ori systems fairly represent the frequency of such eruptions, each low mass star must undergo approximately 10 outbursts and accrete at least 0.1 solar mass through a disk before reaching the main sequence. Simple statistical arguments indicate that T Tauri stars with substantial infrared excesses are also surrounded by disks. However, it appears that accretion through the disk is responsible for the infrared luminosity of only a small percentage of T Tauri stars. The overall energy distributions of most T Tauri stars are consistent with the hypothesis that the disk produces the infrared excess by reprocessing photons originally emitted by the central star. If this proposal is correct, then the shape of the infrared continuum places constraints on the physical structure in the disk and thus the initial conditions for the eventual formation of planets. Author

N88-13107# Pennsylvania State Univ., University Park.
MICROWAVE OBSERVATIONS OF NONTHERMAL PHENOMENA IN PRE-MAIN SEQUENCE STARS Abstract Only c90
Eric D. Feigelson *In* Colorado Univ., 5th Cambridge Workshop on Cool Stars, Stellar Systems and the Sun Jul. 1987 1 p (For primary document see N88-13092 04-89)
Avail: NTIS HC A07/MF A01

A modest fraction of low mass pre-main sequence (PMS) stars in nearby star forming clouds exhibit radio continuum emission detectable at the Very Large Array. It is frequently difficult, however, to determine whether the emission is nonthermal due to particles in surface magnetic fields, or thermal due to T Tauri winds, bipolar flows, accretion flows, or compact HII regions. There is good reason to believe many PMS stars are magnetically very active, particularly in the X-ray emitting naked T Tauri stars. Nonthermal radio emission may be distinguished from thermal emission by the following characteristics: rapid radio variability; high amplitude variability without comparable change in bolometric luminosity; unusual radio spectra, rising steeply at high frequency or falling at both high and low frequencies; circular polarization; and emission from stars with no apparent circumstellar gas that could produce thermal emission. Data were reviewed on a dozen PMS stars possessing one or more of these characteristics. Several are seen in the Taurus-Auriga cloud. The rho Ophiuchi cloud has at least three such stars. A portion of the Orion nebula near the Trapezium contains over 20 compact radio sources, at least two of which appear to be nonthermal. The nature of these stars are being investigated. Author

N88-13108*# National Aeronautics and Space Administration. Marshall Space Flight Center, Huntsville, Ala.
MAGNETIC FLUX TUBES AS SOURCES OF WAVE GENERATION Abstract Only c90
Z. E. Musielak, R. Rosner, and P. Ulmschneider (Heidelberg Univ., West Germany) *In* Colorado Univ., 5th Cambridge Workshop on Cool Stars, Stellar Systems and the Sun Jul. 1987 1 p (For primary document see N88-13092 04-89)
Avail: NTIS HC A07/MF A01 CSCL 03B

The structure of solar, and very likely stellar, surface magnetic fields is highly inhomogeneous: at the photospheric level, the fields are locally strong, and show concentration into a flux tube structure. In this case, the wave energy generated in stellar convection zones may be largely carried away by flux tube waves, which can then become important sources for the heating of the outer atmospheric

layers. Such flux tube wave generation may help to explain the UV and X-ray fluxes observed by the IUE and Einstein observatories. The generation of longitudinal tube waves in magnetic flux tubes embedded in an otherwise magnetic field-free, turbulent, and stratified medium was considered. It is shown that compressible tube waves are generated by dipole emission and that the generation efficiency is a strong function of the magnetic field strength. Energy flux calculations are presented for different magnetic flux tubes, and show how the results depend on the magnetic field strength and the characteristics of the convective turbulence. Author

N88-13109*# National Aeronautics and Space Administration. Goddard Space Flight Center, Greenbelt, Md.
THE ACCELERATION OF WINDS BY MHD WAVES IN OPEN MAGNETIC STRUCTURES Abstract Only **c92**
Joseph M. Davila *In* Colorado Univ., 5th Cambridge Workshop on Cool Stars, Stellar Systems and the Sun Jul. 1987 1 p (For primary document see N88-13092 04-89)
Avail: NTIS HC A07/MF A01 CSCL 03B

It has become increasingly clear in recent years that the available models describing the acceleration of high speed streams in solar coronal holes are inadequate. Thermal models do not result in winds with the proper thermal speed and density. In addition models which assume acceleration by Alfven waves, though promising, are not self-consistent when applied low in coronal holes where the acceleration of the wind takes place. An Alfven wave in the corona with a period of a few hundred seconds will have a wavelength of the order of 10 cm. This is of the order of the diameter of a coronal hole in the low corona, and therefore it is expected that the MHD waves are guided in some sense by the coronal hole in which they propagate. This basic idea led to the development of a leaky waveguide theory to describe MHD wave propagation in coronal holes. Recent efforts were concentrated in two areas: the development of numerical codes to properly describe the hydrodynamics of the flow, and more realistic models of the coronal hole properties such as density gradients and spherical divergence of the flux tube. Some of the important aspects of the theory are discussed, including the effect of density inhomogeneities and smooth transverse density gradients. In addition it is hoped that some early results from the numerical models will be presented. The acceleration of cool winds is a problem of interest in cool supergiants also. Some work was done on the development of wind models for these stars as well. Author

N88-13110# Hamburger Sternwarte (West Germany).
THE CLOSEST SOLAR ANALOGS IN THE BRIGHT STAR CATALOGUE Abstract Only **c92**
H. Neckel *In* Colorado Univ., 5th Cambridge Workshop on Cool Stars, Stellar Systems and the Sun Jul. 1987 1 p (For primary document see N88-13092 04-89)
Avail: NTIS HC A07/MF A01

A detailed comparison of the absolute energy distributions of the solar analog 16 Cyg B and of the Sun, which concerned the 3300 to 8500 A spectral region, revealed for the magnitude differences a 1/wavelength-proportional gradient, on which is superimposed a wavy pattern with maximum amplitudes of about 2 percent. Since this pattern must be attributed to error waves in the absolute energy distributions of the Sun and Vega rather than to intrinsic differences, the gradient defines very precisely colors and apparent magnitude of the Sun in relation to the stellar waves. These colors harmonize perfectly with the standard spectral types and the spectroscopically determined effective temperatures of the three stars 16 Cyg A, 16 Cyg B, and van Bueren 64. Reliable values of the physical parameters are available only for Cyg 16 A and B. The physical parameters follow from the conditions that in a luminosity-T sub eff diagram both stars should lie on or near the same isochrone and the variations of position angle and apparent distance with time and the difference in radial velocity are the results of orbital motion. Author

N88-13111# Hamburger Sternwarte (West Germany).
ASYMMETRY AND VARIATIONS OF SOLAR LIMB DARKENING ALONG THE DIAMETER DEFINED BY DIURNAL MOTION IN APRIL 1981 Abstract Only **c92**
H. Neckel and D. Labs (Landessternwarte auf dem Koenigstuhl, Heidelberg, West Germany) *In* Colorado Univ., 5th Cambridge Workshop on Cool Stars, Stellar Systems and the Sun Jul. 1987 1 p (For primary document see N88-13092 04-89)
Avail: NTIS HC A07/MF A01

Stimulated by unexpected asymmetries and variations in limb darkening profiles observed in June 1986, near the present minimum of solar activity, the former limb darkening observations made in April 1981 were re-analyzed using the McMath Solar Telescope at Kitt Peak. The results indicate rather definitely that the intensity distribution across the disk varies at all observed wavelengths between 3300 and 6600 A with amplitudes in the order of 1 to 2 percent and time-scales from minutes to hours. Asymmetries in the intensity distribution with respect to the disk center are a frequent phenomenon. There can be no doubt, that also the absolute disk center intensity undergoes variations with comparable size and modulation, as they were in fact recently observed by Koutchmy and Lebecq. Presumably, the solar oscillations contribute a significant part to the observed effects. However, due to the 5 to 7 minutes periodicity of the observations no definite conclusions can be drawn. Author

N88-13112# Naval Research Lab., Washington, D.C. Center for Space Research.
STATISTICAL PROPERTIES OF SMALL HIGH-VELOCITY EVENTS IN THE SOLAR TRANSITION REGION Abstract Only **c92**
J. W. Cook, P. A. Lund, J.-D. F. Bartoe, G. E. Brueckner, K. P. Dere, and D. G. Socker *In* Colorado Univ., 5th Cambridge Workshop on Cool Stars, Stellar Systems and the Sun Jul. 1987 1 p (For primary document see N88-13092 04-89)
Avail: NTIS HC A07/MF A01

One of the most interesting discoveries of the High Resolution Telescope and Spectrograph (HRTS) program was the spectrographic observation of small transition region events, seen best in the strong C IV 1548 and 1550 A lines, which have profiles broadened to the blue, to the red, or both. For Spacelab 2 a special survey program was designed which was meant to cover in spectral rasters approximately 30 percent of the flat disk surface. Thirteen executions of the survey were accomplished during orbits 80 to 83 of the Spacelab 2 mission. A visual inspection of the photographic prints of the fine rasters in C IV were made to find small events showing velocity signatures of at least 50 km/s to blue, to red, or both. At least 549 such features were found, with 35 percent blue shifted, 25 percent red shifted, and 40 percent both red and blue shifted. The distribution of lifetime of events was studied from a sequence executed in a later orbit which repeatedly rastered a 27 arc sec wide area over 17 minutes with 1 minute temporal resolution. A number of plasma properties were calculated using a combination of parameter values from the observations. The result is that these events are not energetic enough to directly provide the basic energy input for heating the transition region and corona. The events seem instead to be the after-products of the extremely turbulent energy dissipation which results from the actual basic nonthermal heating process of the upper solar atmosphere. Author

N88-13113# Indian Inst. of Astrophysics, Bangalore.
CALIBRATION ON THE SUN FOR STELLAR MAGNETIC FIELDS Abstract Only **c92**
K. R. Sivaraman, S. P. Bagare, S. S. Gupta, and R. Kariyappa *In* Colorado Univ., 5th Cambridge Workshop on Cool Stars, Stellar Systems and the Sun Jul. 1987 1 p (For primary document see N88-13092 04-89)
Avail: NTIS HC A07/MF A01

The intimate association between the surface magnetic fields and the Ca II K-line emission known to exist on the Sun, holds a promise for using this property to detect the presence of global magnetic fields on Sun-like stars. A large number of K-line profiles

were obtained over a variety of plages on the Sun and related the 1A emission flux centered at the K sub 3 minimum for these profiles with the corresponding values of the longitudinal component of the magnetic field. This provides a calibration for detecting and estimating the surface magnetic fields on stars. Author

N88-13114# Colorado Univ., Boulder.
SIMULTANEOUS, COSPATIAL IMAGING OF THE SUN IN CYANOGEN AND SINGLY-IONIZED CALCIUM Abstract Only **c92**
Thomas R. Ayres and Laurence J. November (National Solar Observatory, Sunspot, N. Mex.) *In its* 5th Cambridge Workshop on Cool Stars, Stellar Systems and the Sun Jul. 1987 1 p (For primary document see N88-13092 04-89)
(Grant NSF AST-85-07029)
Avail: NTIS HC A07/MF A01

A program of multi-wavelength, narrow-band cinematography of the solar surface is described. In the initial run three separate filters were operated simultaneously: the UBF in a continuum window near 6000 A; a 0.6 A bandpass Lyot filter centered on the Ca II K-line emission core; and an 8 A bandpass interference filter centered near 3881 A in the absorption bandhead of the violet system of cyanogen (NC). Given the distinct process of formation, differential comparisons of the CN and Ca II can provide valuable clues concerning the detailed structure of the low chromosphere. For example, during periods of exceptional seeing the CN pictures are quite sharp, and display small-scale bright-points at the limit of angular resolution; whereas the Ca II pictures are considerably more diffuse, and display structures no smaller than about 1 arc sec. Two possible explanations are discussed for the larger apparent surface coverage of the Ca II emission: horizontal transfer of K-line photons from intrinsically small structures; and vertical spreading of the emitting regions.
Author

N88-13115# Kiepenheuer-Inst. fuer Sonnenphysik, Freiburg (West Germany).
VARIATIONS OF THE VERTICAL AND HORIZONTAL VELOCITIES OF THE SMALL-SCALE STRUCTURES AND THE PHYSICAL PROBLEMS RELATED TO OVERSHOOT LAYERS Abstract Only **c92**
Anastasios Nesis and Giuseppe Severino (Osservatorio Astronomico, Capodimonte, Naples, Italy) *In* Colorado Univ., 5th Cambridge Workshop on Cool Stars, Stellar Systems and the Sun Jul. 1987 1 p (For primary document see N88-13092 04-89)
Avail: NTIS HC A07/MF A01

One of the most important parameters in astrophysical research is the mixing length. Using high resolution spectrograms, the dynamics of the overshoot layers of the Sun were studied. Small-scale velocity variations with height in the photosphere were determined for the vertical as well as the horizontal velocity, showing a minimum at a height L sub M of about 200 km above the continuum. This was interpreted as the height up to which the granulation looses completely its convective memory, and in which the granular hydrodynamics changes its character. In these layers turbulence, pressure and gravity waves have their origin. The observational results were compared with the theoretical results of Nelson. It is thought that the parameter L sub N = 200 km which is, according to Nelson, similar to the mixing length 1, is related to the height L sub M of the minima of velocity. The dependence of the overshoot scale heights (penetration) of the horizontal and vertical velocity on the spatial horizontal scale, which is also discussed by Nelson, could be verified by the results.
Author

N88-13116# Joint Inst. for Lab. Astrophysics, Boulder, Colo.
CALIBRATION OF THE Ca II K LINE-CORE DENSITY AND THE MAGNETIC FLUX DENSITY IN STARS USING SOLAR DATA Abstract Only **c92**
C. J. Schrijver and J. Cote (Laboratorium voor Ruimteonderzoek, Utrecht, Netherlands) *In* Colorado Univ., 5th Cambridge Workshop on Cool Stars, Stellar Systems and the Sun Jul. 1987 1 p (For primary document see N88-13092 04-89)
Avail: NTIS HC A07/MF A01

Simultaneous observations of the Ca II K line-core intensity and the magnetic flux density in a solar active region complex, observed at disk center, are analyzed. The scatter about the relation between the Ca II K line-core intensity and the magnetic flux density is large at the spatial resolution of 2.4 x 2.4 inch. The correlation is markedly improved by binning the data into larger resolution elements. The relation between the Ca II K excess intensity (i.e., the intensity above an empirical lower-limit intensity) and the magnetic flux density can be described by a power law, with an index around 0.6. Limb-darkening curves are used to convert Ca II line-core intensities to line-core flux densities, allowing a direct comparison between stellar and solar data. Author

N88-13117# Yale Univ., New Haven, Conn. Center for Solar and Space Research.
LARGE SCALE SOLAR AND STELLAR MAGNETIC FIELDS Abstract Only **c90**
Peter A. Fox *In* Colorado Univ., 5th Cambridge Workshop on Cool Stars, Stellar Systems and the Sun Jul. 1987 1 p (For primary document see N88-13092 04-89)
Avail: NTIS HC A07/MF A01

With the recent advent of stellar evolution that includes the effect of rotation the prospect of correctly evaluating the influence of magnetic fields in a wide class of stars was greatly improved. Calculations of large scale (global) magnetic fields are presented that utilize sequences of models of a rotating star (the Sun) that take into account differential rotation and meridional circulation. The influence of various magnetic field configurations and strengths are considered as well as the possible effect of the Lorentz force on the equations of motion. Author

N88-13118# Heidelberg Univ. (West Germany). Inst. fuer Theoretische Astrophysik.
THE DYNAMICS OF SOLAR MAGNETIC FLUX TUBES SUBJECTED TO RESONANT FOOT POINT SHAKING Abstract Only **c92**
Peter Ulmschneider and Kurt Zaehringer *In* Colorado Univ., 5th Cambridge Workshop on Cool Stars, Stellar Systems and the Sun Jul. 1987 1 p (For primary document see N88-13092 04-89)
Avail: NTIS HC A07/MF A01

Using local correlation tracking techniques on data obtained with the SOUP instrument on Spacelab 2, correlated horizontal displacements of solar surface regions of much larger than granular size with a periodicity of the five minute oscillation were measured. The time dependent development of waves in the thin magnetic flux tubes generated by this purely transverse foot point shaking was investigated. The resulting magnetic field and velocity variations, the pressure and temperature variations generated by nonlinear coupling to the longitudinal wave mode, as well as the expected resonance effects are discussed. Author

N88-13119# Armagh Observatory (Northern Ireland).
ACTIVE PHASES ON II PEG Abstract Only **c92**
P. Panagi and J. G. Doyle *In* Colorado Univ., 5th Cambridge Workshop on Cool Stars, Stellar Systems and the Sun Jul. 1987 1 p (For primary document see N88-13092 04-89)
Avail: NTIS HC A07/MF A01

IUE observations of the RS CVn star II Peg in the upper chromospheric and transition regions lines Mg II h and k, C IV and He II in 1981, 1983, and 1985 shows evidence for increased activity at certain phases. The Mg II k line flux shows an above average value between phases 0.0 and 0.5. This is largely based on 1981 and 1983 data sets, although the 1985 data is consistent with a flux increase in this phase interval. The C IV and He II flux show quite clear evidence of an active hemisphere, although the 1985 data is less convincing than the combined 1981, 1983 and 1985 data sets. This is perhaps explained by the reduced number of observations in 1985. The above would therefore imply the presence of a long lived plage region. The optical spot migration rate from late 1981 to early 1986 was only 0.03 rotations per year. The increase in the ultraviolet emission level occurs at the

time of the minimum in the optical curve, therefore implying a hot plage region overlying one of the cool optical spots. Author

N88-13120# Armagh Observatory (Northern Ireland).
THE GIANT SPOT ON II PEG IN 1986 Abstract Only c90
P. B. Byrne *In* Colorado Univ., 5th Cambridge Workshop on Cool Stars, Stellar Systems and the Sun Jul. 1987 1 p (For primary document see N88-13092 04-89)
Avail: NTIS HC A07/MF A01

An optical/near-infrared radiation (IR) light curve for the RS CVn star II Peg is presented which shows an unprecedented large amplitude variation. Modeling this light curve in terms of the rotation of a spotted star indicates that, at the phase of the optical light minimum, at least 20 percent of the area of the hemisphere visible at the time must be covered by spots. This figure corresponds to approx. 40 percent of the projected area of the star and is calculated for a perfectly black spot of circular outline which exactly crosses the observer's line of sight. Using near-IR color curves, researchers demonstrate that the spot temperature cannot be cooler than about 0.75 times the photospheric temperature. This increases the size of the minimum geometry spot to an area of at least 28 percent of the hemisphere or approx. 56 percent of its projected area. It is demonstrated that such a large area almost certainly constrains the dominant spot to a single entity, rather than a preferred spotted longitude containing many smaller spots. Author

N88-13121# Laboratorium voor Ruimteonderzoek, Utrecht (Netherlands).
A LARGE X-RAY FLARE ON SQUARED SIGMA CORONAE BOREALIS OBSERVED WITH EXOSAT Abstract Only c93
G. H. J. vandenOord, R. Mewe, and A. C. Brinkman *In* Colorado Univ., 5th Cambridge Workshop on Cool Stars, Stellar Systems and the Sun Jul. 1987 1 p (For primary document see N88-13092 04-89)
Avail: NTIS HC A07/MF A01

The RS CVn binary sigma 2 Coronae Borealis was observed on 29 September 1983 for 26 hours with the medium energy and low-energy detectors and the transmission grating spectrometer aboard EXOSAT. A strong X-ray flare, rising within about 5 minutes and lasting more than two hours, was detected. Flare volume and density are estimated. The energy requirements for the flare are discussed. It is asserted that current-driven turbulence can produce such a fast heating. A global equivalent-circuit description of the flare predicts an energy release on a timescale in accordance with observations. Author

N88-13122# Science Applications International Corp., Albuquerque, N. Mex.
SPECTRAL ANALYSIS OF APT RS CVn BINARY LIGHT CURVES Abstract Only
Eric R. Nelson, Louis J. Boyd, Russell M. Genet, and Douglas S. Hall (Fairborn Observatory, Mesa, Ariz.) *In* Colorado Univ., 5th Cambridge Workshop on Cool Stars, Stellar Systems and the Sun Jul. 1987 1 p Prepared in cooperation with New Mexico Univ., Albuquerque (For primary document see N88-13092 04-89)
Avail: NTIS HC A07/MF A01

Preliminary analysis of U band RS CVn photometric data taken with the Automated Photoelectric Telescope (APT) from the last quarter of 1983 to the first quarter of 1985 are presented. Of the 31 sources analyzed, 14 show clear indications of multiple periodic structure, while 13 others showed at least one period. The remaining four sources did not show clear evidence of periodicity. The determined fundamental photometric periods are tabulated and the possible multiple periodic structures are discussed in terms of multiple spot groups on a differentially rotating star. Author

N88-13123# New Mexico Univ., Albuquerque. Center for Astrophysics.
STARSPOTS ON THE SHORT-PERIOD RS CVn SYSTEM SV CAM: 45 YEARS OF ACTIVITY Abstract Only
Michael Zeilik, Cecilia DeBlasi, Michael Rhodes, and Edwin Budding (Carter Observatory, Wellington, New Zealand) *In* Colorado Univ., 5th Cambridge Workshop on Cool Stars, Stellar Systems and the Sun Jul. 1987 1 p (For primary document see N88-13092 04-89)
Avail: NTIS HC A07/MF A01

The sunspot analysis of Zeilik and Budding (Cool Stars IV, 1986, p. 294) was applied to the modeling of the active regions as dark, circular areas on the primary star (G3 V). From an analysis of the 45 years spanned by the observations of SV Cam, researchers reached the following conclusions: (1) the photosphere contains only one active region; (2) the active region has preferred longitudes, one grouped around 110 degrees, the other around 270 degrees; (3) the active region appears at a high latitude (near 75 degrees) rather than a lower one; and (4) the area of the active region changes by about a factor of two. Author

N88-13124# Carter Observatory, Wellington (New Zealand).
THE SHORT-PERIOD RS CVn STARS: STARSPOTS AND FUNDAMENTAL PROPERTIES Abstract Only
Edwin Budding and Michael Zeilik (New Mexico Univ., Albuquerque.) *In* Colorado Univ., 5th Cambridge Workshop on Cool Stars, Stellar Systems and the Sun Jul. 1987 1 p (For primary document see N88-13092 04-89)
Avail: NTIS HC A07/MF A01

A computer analysis was performed of selected V-band light curves of systems in the short-period RS CVn group: UV Psc, XY UMa, RT And, SV Cam, BH Vir, ER Vul, WY Cnc, and CG Cyg. For each set of photometric data, researchers fitted a model of a light curve in order to find the maculation wave that arises from active regions on the photosphere. Then they fitted the maculation wave using sunspots that are dark and circular. This fitting allowed researchers to infer the sizes and longitudes of the spot groups, and, if the observations had a high enough precision (1 percent or better), to estimate the latitudes roughly. The original light curves were corrected to remove the effects of the starspots and the new model was fitted to the cleaned light curves. This process allowed researchers to evaluate the geometrical, orbital, and physical parameters of the system without the distorting influence of the maculation waves. Author

N88-13125# Toledo Univ., Ohio. Dept. of Physics and Astronomy.
DOPPLER SNAPSHOTS Abstract Only
Paul V. Noah, Bernard W. Bopp, and Francis Fekel, Jr. (Dyer Observatory, Nashville, Tenn.) *In* Colorado Univ., 5th Cambridge Workshop on Cool Stars, Stellar Systems and the Sun Jul. 1987 1 p (For primary document see N88-13092 04-89)
Avail: NTIS HC A07/MF A01

An adaptation of the formal Doppler imaging procedure that uses spectroscopic data of moderate resolution and S/N and then combines these data with concurrent broad band photometry is described. The technique produces snapshots of the stellar surface brightness distribution with somewhat reduced detail, but which are much more precise than maps derived from photometric data alone. The procedure is illustrated with spectroscopic and photometric data obtained for UX Ari in 1983. Author

N88-13126# Pennsylvania State Univ., University Park.
TITANIUM OXIDE ABSORPTION AND SPOT SIZES IN II PEG, HR 1099 AND UX ARI Abstract Only
David P. Huenemoerder *In* Colorado Univ., 5th Cambridge Workshop on Cool Stars, Stellar Systems and the Sun Jul. 1987 1 p (For primary document see N88-13092 04-89)
Avail: NTIS HC A07/MF A01

Excess titanium oxide absorption at 886 nm and 710 nm were detected in II Peg, HR 1099, and UX Ari in January 1987. This detection is indicative of extensive cool regions, or spots, on the stellar surfaces. Since no variations were seen, the dominate contribution comes from polar spot groups or an even distribution of spots in stellar longitude. These moderate resolution CCD-echelle spectra have been modeled by fitting the spectra of inactive standard stars having spectral types which match the RS CVn stars plus an M-star component for the spot contribution. Polar spot areas were estimated from the relative weights of each

spectral component fit. In the case of II Peg, the most consistent results were given for the two bands with an equivalent spot spectral type of M6; the spot size is about 35 degrees for an inclination of 30 degrees and about 50 degrees for an inclination of 60 degrees. Similar modeling for HR 1099 and UX Ari, but accounting for the composite nature of their spectra, yielded spot sizes of 30 and 40 degrees, respectively. Application of the model to hypothetical geometries and temperatures shows the depth of TiO features and amplitudes of possible variations expected in some typical systems. Author

N88-13127# Pennsylvania State Univ., University Park.
SPECTROSCOPIC MONITORING OF RS CVn STARS AT KITT PEAK USING THE PENN STATE FIBER OPTIC ECHELLE Abstract Only
Lawrence W. Ramsey, David P. Huenemoerder, Derek Buzasi, and Samuel C. Barden (Kitt Peak National Observatory, Tucson, Ariz.) *In* Colorado Univ., 5th Cambridge Workshop on Cool Stars, Stellar Systems and the Sun Jul. 1987 1 p (For primary document see N88-13092 04-89)
Avail: NTIS HC A07/MF A01

A versatile echelle spectrograph coupled with a 1.6 meter telescope via an optical fiber was employed in a monitoring program which yields moderate resolution (lambda/delta equals 12000) spectra with good spectral coverage from 400 to 900 nm using a 0.2 mm core fiber. A 200 mm f/2 camera focuses the prism cross-dispersed beam on a RCA charge coupled device. Observations show that the fiber optic echelle is about twice as efficient as the coude Camera No. 5 for similar bandpass at 600 nm and is comparable in throughput at 390 nm using the coude feed telescope. A program was instituted to monitor about 10 regular RS CVn systems and about 6 short period and W UMa systems for a two week period each observing semester. The most important feature of the program is the ability to obtain simultaneously spectra of chromospheric features as well as Balmer line, Ca II H and IRT lines and He D3 as well as temperature sensitive photospheric features such as TiO bands. Author

N88-13128# Pennsylvania State Univ., University Park.
H ALPHA AND Ca II EMISSION LINE VARIABILITY OF FK COMAE Abstract Only
Derek Buzasi *In* Colorado Univ., 5th Cambridge Workshop on Cool Stars, Stellar Systems and the Sun Jul. 1987 1 p (For primary document see N88-13092 04-89)
Avail: NTIS HC A07/MF A01

The rapidly rotating G III star FK Comae (HD177555, P equals 2.4 d) was monitored for 18 days. The Penn State fiber optic echelle spectrograph was used on both the KPNO coude feed and 2.1 meter telescopes. While on the coude feed, two spectra were typically taken each night. The resulting data gives excellent phase coverage on FK Comae over about seven rotational periods. A subset of the data, taken over 10 days solely on the coude feed telescope, also possesses essentially complete phase coverage. The preliminary analysis presented here emphasizes correlation of variations of the H alpha, Ca II IRT, and Ca II H lines. Author

N88-13129# European Space Agency. European Space Operations Center, Darmstadt (West Germany).
THE X-RAY ORBITAL LIGHTCURVES OF AR LAC AND TY PYX Abstract Only
N. E. White, R. Shafer, A. N. Parmar, and J. L. Culhane *In* Colorado Univ., 5th Cambridge Workshop on Cool Stars, Stellar Systems and the Sun Jul. 1987 1 p (For primary document see N88-13092 04-89)
Avail: NTIS HC A07/MF A01

Using the EXOSAT observatory, researchers obtained the X-ray orbital light curves of AR Lac and TY Pyx. In the low energy telescope, a large orbital modulation is seen in both cases. In AR Lac a deep minimum occurs centered on primary minimum and a shallow eclipse preceeds the secondary eclipse. A program was developed to model the light curves expected from three dimensional X-ray emitting structures on the two stars. This shows that there are two relatively compact regions on the G star at latitudes of 3 and 154 degrees, with scale heights of 0.1 solar radii. In addition, there is a large X-ray structure with a height of three solar radii on the K star between latitudes 190 and 280 degrees. There is no strong modulation of the medium energy (1 to 10 KeV) X-ray flux. This indicates that this must originate from a very large component, possibly one that envelops the whole system. Similar modeling will be discussed for TY Pyx. Author

N88-13130# Franklin and Marshall Coll., Lancaster, Pa.
DIFFERENTIAL B AND V LIGHT CURVES OF THE BRIGHT BY DRACONIS STAR HD80715 Abstract Only
Harold Nations *In* Colorado Univ., 5th Cambridge Workshop on Cool Stars, Stellar Systems and the Sun Jul. 1987 1 p (For primary document see N88-13092 04-89)
Avail: NTIS HC A07/MF A01

The star HD 80715 (SAO 42826, Lallande 18397) was shown to be a double-lined spectroscopic binary (SB2) and one of the brighter members of the BY Draconis class of variables by Barden and Nations (1985). These authors found the system to consist of two nearly identical K2-3 dwarfs with an orbital period of 3.8025 days. Light curves for these stars are presented and discussed with particular emphasis on their short period variability. The light curves changed from being very asymmetric during the first half of the observing period to having quite well defined double maxima during the second half, a time span of only roughly ten orbits. This behavior is compared to that of similar chromospherically active dwarfs with short periods. Author

N88-13131# Laboratorium voor Ruimteonderzoek, Utrecht (Netherlands). Sonnenborgh Observatory.
ASYNCHRONOUS ROTATION IN CLOSE BINARY SYSTEMS WITH CIRCULAR ORBITS Abstract Only **c90**
Guillaume M. H. J. Habets *In* Colorado Univ., 5th Cambridge Workshop on Cool Stars, Stellar Systems and the Sun Jul. 1987 1 p (For primary document see N88-13092 04-89)
Avail: NTIS HC A07/MF A01

Tidal theory (Zahn 1977) predicts the rotation of a binary component of a late-type close binary system is in synchronization with the orbital motion before the orbit becomes circular by tidal interaction, unless the spin and angular momenta are comparable in magnitude. As a result the (sub-) giant components of late-type close binaries with orbital periods less than 100 d should be rotating synchronously, since most of these systems have circular orbits. The binaries Lambda And, AY Cet, and TZ For are three exceptions to this prediction because they contain asynchronous rotating late-type subgiants, although the binary orbit is circular. In order to trace the origin of the present asynchronism and orbital circularity, the evolution of the rotation rate of the components and the orbital circularization rate of these systems is obtained from evolutionary calculations. The present asynchronous rotation of the subgiants is mainly explained by the evolutionary increase in the moment of inertia which induces spin-down of the star and, in the cases of Lambda And and AY Cet, even to angular rotation rates smaller than the synchronous value. Author

N88-13132# Arizona Univ., Tucson. Steward Observatory.
PG 0308 + 096: A SHORT-PERIOD WHITE DWARF + dM BINARY WITH STRONGLY MODULATED H-ALPHA EMISSION Abstract Only **c90**
Richard A. Wade and Rex A. Saffer *In* Colorado Univ., 5th Cambridge Workshop on Cool Stars, Stellar Systems and the Sun Jul. 1987 1 p (For primary document see N88-13092 04-89)
Avail: NTIS HC A07/MF A01

This seven hour spectroscopic binary consists of a 20,000 DA primary star and a secondary star of approximate spectral type dM3. The system is detached and non-eclipsing. A narrow H-alpha emission feature, ascribed to the dM3 star, was used to establish the orbital period. It shows a strong but smooth modulation of intensity (contrast greater than 3) with the orbital period. The EUV photon flux from the DA primary does not appear to be strong enough to account directly for the emission, which therefore may

be of some interest in studies of activity on rapidly rotating cool main sequence stars. Author

N88-13133# Armagh Observatory (Northern Ireland).
EVIDENCE FOR AN ADDITIONAL SOURCE OF OPACITY DURING THE IMPULSIVE PHASE OF STELLAR FLARES Abstract Only
C. J. Butler, J. G. Doyle, and P. B. Byrne *In* Colorado Univ., 5th Cambridge Workshop on Cool Stars, Stellar Systems and the Sun Jul. 1987 1 p (For primary document see N88-13092 04-89)
Avail: NTIS HC A07/MF A01

Spectroscopic data were obtained on the SAAO 1.9m with the Reticon Photon Counting System from 17:51 UT to 23:40 UT on 4 March 1985. The CA I feature at 4227 angstroms changed dramatically during a 1.2 mag. U-band flare. In the spectrum taken during the rise phase, the CA I feature is both narrower and weaker than that of either the prefiare spectrum or spectra taken later in the flare. Several atomic features longward of 4227 angstroms show no change in the flare spectrum. Researchers compared the flare rise spectrum with spectra of several F, K and M stars of luminosity classes III and V. This revealed that the impulsive phase spectrum resembles more the narrow Ca I line of a giant star. This would indicate that the photospheric flare continuum observed here is perhaps a combination of a normal dM4.5e continuum plus an overlying continuum with a temperature of less than 4000 to 5000 K and a pressure of at least an order of magnitude less than that of a dM4.5e star. Author

N88-13134# Laboratorium voor Ruimteonderzoek, Utrecht (Netherlands).
EVIDENCE FOR EXPANDING MAGNETIC LOOPS IN CORONAE OF COOL STARS Abstract Only **c90**
R. Mewe, J. R. Lemen, C. J. Schrijver, and A. Fludra (Wroclaw Univ., Poland) *In* Colorado Univ., 5th Cambridge Workshop on Cool Stars, Stellar Systems and the Sun Jul. 1987 1 p (For primary document see N88-13092 04-89)
Avail: NTIS HC A07/MF A01

The cool stars Capella, Sigma 2 CrB, and Procyon were observed with the EXOSAT Transmission Grating Spectrometer. A doubly peaked differential emission measure distribution is derived from the X-ray spectra (10 to 200 angstroms), suggesting a model corona with only two distinct ensembles of loops. Fits of theoretical to calculated spectra indicate that the low temperature component of the coronae of Capella and Sigma 2 CrB corresponds to loops expanding with height, thus including loops with constant cross section. The expanding loop geometry inferred from the spectral analysis is consistent with observations of solar active region loops. The results of the high temperature component on Capella admit loops of nearly constant cross section, while the results for Sigma 2 CrB suggest expanding loops. Author

N88-13135# New Mexico State Univ., Las Cruces.
X-RAYS, COLOR, AND THE VAUGHAN-PRESTON GAP Abstract Only
Andrea K. DobsonHockey *In* Colorado Univ., 5th Cambridge Workshop on Cool Stars, Stellar Systems and the Sun Jul. 1987 1 p (For primary document see N88-13092 04-89)
Avail: NTIS HC A07/MF A01

In plots of chromospheric Ca II emission vs. B-V color, there exists a region of lower star density which was first noted by Vaughan and Preston (1978). Various arguments have been put forward regarding the possible cause of this distribution. A similar region of lower star density occurs in a plot of coronal soft X-ray emission vs. B-V color. This is not surprising, since the same magnetic dynamo is ultimately responsible for both chromospheric and coronal activity. These low density regions are noted as gaps primarily because they are surrounded by regions of higher star density. The overall structure of such plots is examined here and compared with the nature of the color dependence present in stellar activity. Author

N88-13136# Lowell Observatory, Flagstaff, Ariz.
STELLAR CYCLE VARIABILITY OF SOLAR-LIKE STARS: A SNEAK PREVIEW Abstract Only
G. W. Lockwood and B. A. Skiff *In* Colorado Univ., 5th Cambridge Workshop on Cool Stars, Stellar Systems and the Sun Jul. 1987 1 p (For primary document see N88-13092 04-89)
Avail: NTIS HC A07/MF A01

Progress is reported on a continuing photometric program to determine the nature of stochastic, rotationally modulated, and cyclic luminosity variations of about 30 stars chosen from the sample of main sequence stars whose chromospheric activity was surveyed by Olin Wilson. The purpose of the program is to characterize the variability of Sun-like stars generally and, if possible, to validate by stellar analogy the putative relationship between solar activity and the post-1978 secular 0.1 percent decline of the solar constant measured by radiometers aboard the Solar Maximum Mission and Nimbus 7 satellites. Author

N88-13137# Louisville Univ., Ky. Dept. of Physics.
MAGNETIC FIELDS ON K AND M STARS Abstract Only **c90**
David H. Bruning, Richard E. Chenoweth, and Geoffrey W. Marcy *In* Colorado Univ., 5th Cambridge Workshop on Cool Stars, Stellar Systems and the Sun Jul. 1987 1 p (For primary document see N88-13092 04-89)
Avail: NTIS HC A07/MF A01

Nine late K- and early M-type stars were observed using the Mount Wilson 2.5 meter telescope for the purpose of detecting magnetic fields. Excess broadening was found in several stars, suggesting the presence of magnetic fields on these stars. However, additional analysis is required to determine whether line blends may be responsible for the observed excess broadening (Saar 1987). Author

N88-13138# Oxford Univ. (England). Dept. of Theoretical Physics.
RELATIONS BETWEEN CHROMOSPHERIC AND CORONAL STRUCTURE, FLUX-FLUX CORRELATIONS AND CONVECTIVE ZONE PROPERTIES Abstract Only
C. Jordan, B. Montesinos, and P. G. Judge *In* Colorado Univ., 5th Cambridge Workshop on Cool Stars, Stellar Systems and the Sun Jul. 1987 1 p (For primary document see N88-13092 04-89)
Avail: NTIS HC A07/MF A01

A recent study of five main-sequence stars (Jordan et al. 1987) used observations in the ultraviolet and X-ray regions to develop models of the atmospheres between the chromosphere and corona. The model coronal pressures and observed temperatures were found to scale according to the powers predicted by Hearn (1977). A new empirical correlation between an effective chromospheric pressure and the coronal pressure was found and its significance is discussed. Author

N88-13139# Sacramento Peak Observatory, Sunspot, N. Mex.
STELLAR ACTIVITY AND THE ROTATION OF HYADES STARS Abstract Only **c90**
Richard R. Radick and Sallie L. Baliunas (Harvard-Smithsonian Center for Astrophysics, Cambridge, Mass.) *In* Colorado Univ., 5th Cambridge Workshop on Cool Stars, Stellar Systems and the Sun Jul. 1987 1 p (For primary document see N88-13092 04-89)
Avail: NTIS HC A07/MF A01

New measurements of rotation periods for Hyades stars which were obtained from reanalysis of Mount Wilson Observatory Ca II H-K emission flux measurements are discussed. The existence of systematic, color dependent discrepancies between the measured rotation periods for Hyades stars and those predicted by the Rossby relation as originally calibrated by Noyes et al. (1984) led researchers to re-examine the form of the relationship between chromospheric emission, rotation, and color. Author

N88-13140# Joint Inst. for Lab. Astrophysics, Boulder, Colo.
BROADBAND LINEAR POLARIZATION AND CHROMOSPHERIC CaII H AND K LINE EMISSION IN LATE-TYPE MAIN SEQUENCE STARS Abstract Only
J. Huovelin, S. Saar, I. Tuominen, S. Linnaluoto, and H. Virtanen (Helsinki Univ., Finland) *In* Colorado Univ., 5th Cambridge Workshop on Cool Stars, Stellar Systems and the Sun Jul. 1987 1 p (For primary document see N88-13092 04-89)
Avail: NTIS HC A07/MF A01

Broadband UBV linear polarization observations of a sample of late type (F7-K5) dwarfs are studied in connection with CaII H and K line core emission observations. Different parameters representing the average degree of polarization are compared in terms of relations with activity. Results indicate that the weighted average of the largest values for the polarization degree is the best parameter for activity diagnostics if the rotational phase of each observation is not known. Linear polarization, being extremely sensitive to differences in surface distribution of active areas, shows remarkable scatter when plotted against other activity indicators, such as Ca-flux R' sub HK and Rossby number. However, an increase with activity (in U and V bands) is clearly seen. The study of (B-V)-color dependence indicates considerable increase of the average maximum polarization in the ultraviolet from late F to late G stars. The small polarization observed in even highly active F stars is probably due to lack of large surface inhomogeneities on these stars with relatively thin outer convective zones. Author

N88-13141# Commonwealth Scientific and Industrial Research Organization, Epping (Australia).
THE PARKES RADIO SURVEY OF ACTIVE CHROMOSPHERE STARS Abstract Only
R. T. Stewart, O. B. Slee, G. J. Nelson, and A. E. Wright *In* Colorado Univ., 5th Cambridge Workshop on Cool Stars, Stellar Systems and the Sun Jul. 1987 1 p (For primary document see N88-13092 04-89)
Avail: NTIS HC A07/MF A01

Over 150 active chromosphere stars were surveyed at 5.0 or 8.4 GHz with the Parkes 64 meter telescope from 1981 to 1987. Most of the stars were observed on at least 10 separate occasions. The sample included RS CVn and ALgol-type binaries, bright CaII emission stars, dMe flare stars and several AM-Her type cataclysmic variables. More than 70 radio stars were detected for the first time. Research growing out of these observations are noted. Author

N88-13142# Colorado Univ., Boulder.
ACTIVITY IN WARM STARS Abstract Only **c90**
F. M. Walter and C. J. Schrijver (Joint Inst. for Lab. Astrophysics, Boulder, Colo.) *In its* 5th Cambridge Workshop on Cool Stars, Stellar Systems and the Sun Jul. 1987 1 p (For primary document see N88-13092 04-89)
Avail: NTIS HC A07/MF A01

The behavior of F type stars in which the convection zone is very thin is studied. It is shown that the F type main sequence stars obey a rotation activity relation for stars as hot as B-V to 0.36 (F2), if the proper basal fluxes, which are much higher than in G or K type stars, are subtracted from the emissions from the magnetically active atmosphere. The fluxes from the magnetically active part of the atmosphere of the F type dwarfs are shown to follow the flux-flux relations defined by the late F through late K type stars. Author

N88-13143# Western Research Corp., Tucson, Ariz.
A SEARCH FOR X-RAY LUMINOUS LATE TYPE STARS IN NIPSS DATA Abstract Only
Eric R. Craine, Santiago Tapia, and Roger B. Culver (Colorado State Univ., Fort Collins.) *In* Colorado Univ., 5th Cambridge Workshop on Cool Stars, Stellar Systems and the Sun Jul. 1987 1 p (For primary document see N88-13092 04-89)
Avail: NTIS HC A07/MF A01

Optical identification is obtained of X-ray luminous late type stars previously unidentified. This is done by detecting position coincidences between unidentified X-ray sources and stars for which (V-I) is greater than 3 mag., as obtained from the Near Infrared Photographic Sky Survey (NIPSS) database. The NIPSS photographs, obtained in V and I bands, are well suited to the detection of very red, faint stars which are absent or very weak on the E plates of the Palomar Observatory Sky Survey. Objects with effective temperatures below 3000 K, corresponding to spectral types later than M4, are the most frequent counterparts found. It is also expected to find new identifications for symbiotic systems with accretion into compact objects, dwarf M stars with active coronae and possibly some AGNs. Presented is a derivation of the detection limits of the NIPSS relevant to the lower main sequence dwarf stars. Significantly, M8 or M9 stars with apparent V magnitudes below the detection limit may still appear on the NIPSS I band photographs, where the detection limit is extended to pre-main sequence objects for about 0.03 solar luminosity. In addition, preliminary results from the initial X-ray source search are presented. Author

N88-13144*# National Aeronautics and Space Administration. Goddard Space Flight Center, Greenbelt, Md.
THE ONSET OF CHROMOSPHERIC ACTIVITY AMONG THE A- AND F- TYPE STARS Abstract Only
Theodore Simon and Wayne Landsman (ST Systems Corp., Greenbelt, Md.) *In* Colorado Univ., 5th Cambridge Workshop on Cool Stars, Stellar Systems and the Sun Jul. 1987 1 p (For primary document see N88-13092 04-89)
Avail: NTIS HC A07/MF A01 CSCL 03B

IUE observations of C II lambda1335 and C IV lambda1549 and ground-based observations of He I lambda5876 have previously discovered intense levels of chromospheric activity among early F type stars. Virtually all F dwarfs show stronger chromospheric and transition region emission than do the cooler and more deeply convective dwarf stars like the Sun. The IUE spectra and those of He lambda5876 place the onset of stellar activity along the main sequence near a color B - V = 0.28, which corresponds approximately to spectral type FO and an effective temperature of 7300 K. However, existing X-ray observations of A and F stars suggest that coronal activity may reach a peak blueward of this high temperature boundary at B - V = 0.28 before vanishing among the early and mid A-type stars. Discussed are preliminary results of a new effort to refine the location of the high temperature boundary to chromospheric activity among A- and F- type stars, making use of low dispersion short-wavelength spectra from the IUE archives from which the strengths of C IV, C II, and Lyman alpha emission have been measured. Author

N88-13145# Joint Inst. for Lab. Astrophysics, Boulder, Colo.
EMPIRICAL RELATIONS BETWEEN PHOTOSPHERIC MAGNETIC FIELDS AND ATMOSPHERIC RADIATIVE LOSSES FOR COOL DWARF STARS Abstract Only **c90**
S. H. Saar and C. J. Schrijver *In* Colorado Univ., 5th Cambridge Workshop on Cool Stars, Stellar Systems and the Sun Jul. 1987 1 p (For primary document see N88-13092 04-89)
Avail: NTIS HC A07/MF A01

Hot outer atmospheres appear to be a common property of F-, G-, K-, and M-type stars. The dissipation of magnetohydrodynamic energy is probably the most important heating mechanism operating in these atmospheres, as has been clearly demonstrated in the case of the Sun. Since the measurement of magnetic fields on stars is difficult, fluxes in optical and ultraviolet emission lines, and the soft X-ray flux are often used to measure the level of stellar activity. Author

N88-13146# Armagh Observatory (Northern Ireland).
EXCESS EMISSION IN THE WINGS OF THE HYDROGEN BALMER LINES DURING A FLARE ON THE LATE-TYPE dMe STAR YZ CMi Abstract Only
J. G. Doyle and P. B. Byrne *In* Colorado Univ., 5th Cambridge Workshop on Cool Stars, Stellar Systems and the Sun Jul. 1987 1 p (For primary document see N88-13092 04-89)
Avail: NTIS HC A07/MF A01

Spectroscopic observations of YZ CMi covering the wavelength region from 3600 to 4600 A were made on 4 March 1985. Simultaneous photometric data showed a 1.2 mag. flare at 19:55 UT, during which the optical spectra showed excess emission in the wings of all the hydrogen Balmer lines. Interpretation in terms of mass flows would imply material moving at approx 300 km/sec simultaneously to the blue and red or alternatively random mass motions with a velocity of a similar magnitude. At flare maximum, all the Balmer lines show excess emission in the wings with H gamma and H delta showing symmetrically broadened lines while higher members of the series such as H zeta and H eta show predominately red shifted material. Assuming a single loop flare, an interpretation in terms of directed mass flows would imply a loop of approx 2 to 3 x 10 to the 9th power cm; this would place the material in the corona where it should be observed in X-rays. However, simultaneous X-ray observations showed no significant increase. An alternative explanation also assuming directed mass flows could involve several small flare kernels, which brighten successively, producing a broadened profile. A similar explanation has been suggested to explain the excess emission seen in the wings of H alpha during solar flares. The Balmer lines contribute approx 10% to the energy in the U-band during the flare. Author

N88-13147# Joint Inst. for Lab. Astrophysics, Boulder, Colo.
VLA OBSERVATIONS OF THE X-RAY BRIGHT HYADES M-DWARFS Abstract Only
J.-P. Caillault *In* Colorado Univ., 5th Cambridge Workshop on Cool Stars, Stellar Systems and the Sun Jul. 1987 1 p (For primary document see N88-13092 04-89)
Avail: NTIS HC A07/MF A01

The interpretation of the observed quiescent microwave fluxes from dMe stars is that they arise as the result of an emission process which is magnetic in character, either gyroresonant or synchrotron. It is argued that cool, dark regions, needed to explain color anomalies and low level photospheric variations, must necessarily exist on the latest-type Hyades dwarfs. Th existence of these starspots makes it likely that large magnetic fields cover significant fractions of their surfaces, consistent with their conjectured emission mechanisms. The nine M-dwarfs in the Hyades Cluster which were detected as X-ray sources by the Einstein Observatory have been observed with the VLA at 6 cm. Only upper limits to the microwave emission were obtained (approx .1 to .2 mJy); however, in light of a recent rotational velocity study of these stars using the MMT, these Hyades M-dwarfs can now be compared in a meaningful way to other radio and X-ray active M-dwarfs. In particular, the BY Draconis variable stars, for which rotational periods are known, have recently been studied in both X-rays and at 6 cm. Plots of L sub R versus P sub rot and L sub R versus L sub x are shown. Author

N88-13148*# National Aeronautics and Space Administration. Marshall Space Flight Center, Huntsville, Ala.
MHD ENERGY FLUXES FOR LATE TYPE DWARFS Abstract Only **c90**
R. Rosner and Z. E. Musielak (Harvard-Smithsonian Center for Astrophysics, Cambridge, Mass.) *In* Colorado Univ., 5th Cambridge Workshop on Cool Stars, Stellar Systems and the Sun Jul. 1987 1 p (For primary document see N88-13092 04-89)
Avail: NTIS HC A07/MF A01 CSCL 03B

The efficiency of MHD wave generation by turbulent motions in stratified stellar atmospheres with embedded uniform magnetic fields is calculated. In contradiction with previous results, it is shown that there is no significant increase in the efficiency of wave generation because of the presence of magnetic fields, at least within the theory's limits of applicability. It is shown that MHD energy fluxes for late-type stars are less than those obtained for acoustic waves in a magnetic-field-free atmosphere, and do not vary enough for a given spectral type in order to explain observed UV and X-ray fluxes. Thus, the results show that MHD energy fluxes obtained if stellar surface magnetic fields are uniform cannot explain the observed stellar coronal emissions. Author

N88-13149# Texas Univ., Austin.
A SPECTRAL SURVEY OF 26 G9-M6 FLARE STARS IN THE SOLAR NEIGHBORHOOD Abstract Only
Suzanne L. Hawley and Bjorn R. Pettersen (Oslo Univ., Norway) *In* Colorado Univ., 5th Cambridge Workshop on Cool Stars, Stellar Systems and the Sun Jul. 1987 1 p (For primary document see N88-13092 04-89)
Avail: NTIS HC A07/MF A01

As a result of a major observational effort at McDonald Observatory during the past four years, several hundred spectra of flare stars have been obtained during both flaring and quiescent conditions. The quiescent properties of these stars are examined here. The spectral energy distribution from 3500 to 9000 A is presented for seven of the stars, and the dependence of the colors and molecular band strengths compared for temperature, absolute magnitude, and other physical parameters. Copies of the Spectral Atlas (University of Oslo Publication Series No. 2) are available on request. Author

N88-13150# Imperial Coll. of Science and Technology, London (England). Blackett Lab.
A SEARCH FOR VERY LOW MASS (BROWN DWARF) STARS AS WIDE BINARIES USING A SEVEN ELEMENT INFRARED CAMERA-PHOTOMETER Abstract Only
I. D. Hepburn *In* Colorado Univ., 5th Cambridge Workshop on Cool Stars, Stellar Systems and the Sun Jul. 1987 1 p (For primary document see N88-13092 04-89)
Avail: NTIS HC A07/MF A01

A seven-element linear infrared camera-photometer has been constructed for the sole purpose of searching for very low mass infrared stars (Brown Dwarfs). These objects have been proposed as a possible solution to the local missing mass problem. Attempts have been made to answer this question from the form of the mass and luminosity functions. This has proved unsuccessful due to the rarity of information at the low mass end. It has become apparent that the best chance for solving this problem and proving the possible existence of such objects will come from direct infrared observations. With this in mind the camera-photometer was built. It consists of 7 independent InSb detectors in an array each having a spatial resolution of 14 arcseconds on a 1.5 m F13.8 telescope, permitting an area of 112 x 14 arcseconds to be imaged. Author

N88-13151# Colorado Univ., Boulder.
EXOSAT RESULTS ON THE dMe FLARE STAR WOLF 630AB AND ON VB 8 Abstract Only
G. Tagliaferri, N. E. White, and P. Giommi *In its* 5th Cambridge Workshop on Cool Stars, Stellar Systems and the Sun Jul. 1987 1 p (For primary document see N88-13092 04-89)
Avail: NTIS HC A07/MF A01

Results from three X-ray observations of Wolf 630AB obtained from the Exosat archive are reported. Two flares have been detected in both the LE and ME experiments. In one case the source flux is sufficiently high to allow a spectral analysis. The Raymond-Smith plasma model gives an acceptable fit to the rise and fall phase with temperatures of 4.3 and 2.5 keV, respectively. During the March 1985 observation a 15 minute flare was detected from the nearby star VB 8 (about 4 arcmin far from Wolf 630AB). Combining Exosat and Einstein HRI data constrains the temperature of the quiescent X-ray emission to be higher than .13 KeV. Author

N88-13152# California Inst. of Tech., Pasadena.
IUE/OPTICAL/VLA FLARES ON AD LEO Abstract Only
D. E. Gary, P. B. Byrne, and C. J. Butler (Armagh Observatory, Northern Ireland) *In* Colorado Univ., 5th Cambridge Workshop on Cool Stars, Stellar Systems and the Sun Jul. 1987 1 p (For primary document see N88-13092 04-89)
Avail: NTIS HC A07/MF A01

Several flares from the dMe flare star AD Leo were recorded simultaneously with the IUE spacecraft, at U band with ground based photometry, and at 20 and 6 cm with the Very Large Array (VLA), during a coordinated observation period in February 1983. One flare was particularly well observed with all three instruments,

others were detected at two but not all three wavelength regimes. The best observed flare, peaking on 2 February 1983 at 1137 UT in the optical U band, was sharply peaked and lasted a brief two minutes. At 6 cm of the radio frequency, the flare resulted in enhanced emission that peaked much later (about 1145 UT) and lasted for over one hour. With preliminary IUE data, there was no enhancement in C IV or C II in an SWP exposure starting about 1145 UT, but the He II flux reached its highest point in three days of monitoring at this time. Mg II was also elevated at the time of the flare, on an exposure ranging from 1131 to 1155 UT. The time coincidence of the three wavelength regimes is presented as a means to determine the relationships among the activities they represent. The lack of correspondence with other flares of this period is also discussed. Author

N88-13153# Maryland Univ., Baltimore. Astronomy Program.
MICROWAVE OBSERVATIONS OF RED DWARF FLARE STARS Abstract Only
M. R. Kundu, P. D. Jackson, and S. M. White *In* Colorado Univ., 5th Cambridge Workshop on Cool Stars, Stellar Systems and the Sun Jul. 1987 1 p (For primary document see N88-13092 04-89)
Avail: NTIS HC A07/MF A01

Presented are the results of VLA observations of six flare star systems on March 21 to 22, 1985 at 6 and 20 cm wavelengths, i.e., AD Leo, EQ Peg, UV Ceti, Wolf 630, YZ CMi, and YY Gem. All the systems were detected at both wavelengths to have either unpolarized quiescent or circularly polarized flaring emission. The latter occurs on a range of time scales from a minute to several hours. It is sometimes difficult to make a morphological distinction between completely unpolarized quiescent emission and slightly polarized, slowly varying flares. The distinction may also be affected by the signal-to-noise ratio of the data. Simultaneous flaring from both members of the binary system UV Ceti (L726-8AB) is seen at 6 and 20 cm. Simultaneous flaring from both components of EQ Peg, and AT Mic as well as from L726-8 have been reported elsewhere. The possibility of a physical coordination existing between the emission from the separate stars is discussed.
Author

N88-13154# Maryland Univ., Baltimore. Astronomy Program.
A VLA SURVEY OF dMe FLARE STARS Abstract Only
P. D. Jackson, M. R. Kundu, and S. M. White *In* Colorado Univ., 5th Cambridge Workshop on Cool Stars, Stellar Systems and the Sun Jul. 1987 1 p (For primary document see N88-13092 04-89)
Avail: NTIS HC A07/MF A01

A survey is under way using the VLA at wavelengths of 6 and 20 cm to search for radio emission from all the dMe flare stars within about 10 parsecs of the Sun, and which have not yet been widely observed at radio wavelengths. Results so far, based on a total observing time of about one hour each during July 1986 have yielded detections from 9 of the 30 stellar systems in the program. At 20 cm, two bands centered at 1415 and 1515 MHz are observed, and at 6 cm two bands centered at 4535 and 4985 MHz are observed. A table is presented which gives, for each of those stars, the mean total (Stokes I) flux, and the mean polarized (Stokes V) flux in mJy at each of 6 and 20 cm (averaged over the two frequency bands). Mean rms errors are 0.13 mJy in I and 0.10 mJy in V; upper limits are 3 sigma. Also given in the table are the mean brightness temperature at 20 and 6 cm assuming a source angular size equal to the size of the stellar photosphere.
Author

N88-13155# Kitt Peak National Observatory, Tucson, Ariz.
CONTEMPORANEOUS B,V,R,I PHOTOMETRY AND H ALPHA SPECTROSCOPY OF YY GEM Abstract Only
S. C. Barden *In* Colorado Univ., 5th Cambridge Workshop on Cool Stars, Stellar Systems and the Sun Jul. 1987 1 p (For primary document see N88-13092 04-89)
Avail: NTIS HC A07/MF A01

H alpha emission equivalent widths versus orbital phase and B,V,R,I light curves are presented for the eclipsing binary YY Gem. The light curves indicate maximum light of the spot distortion to occur at 0.3 theta past primary eclipse. A modulation of the H alpha emission equivalent width shows a minimum of emission at 0.4 theta past primary eclipse. Three major flares were observed at H alpha and at least two flaring events occurred during the photometry run. By coincidence, the spectroscopic and photometric observing runs overlapped the H beta and IUE observing runs conducted by Baliunas, Raymond and Loeser. One of the H alpha flares was simultaneously observed by BRL at H beta and both photometric flares were also simultaneously seen in their H beta spectra. Author

N88-13156# Consejo Superior Investigaciones Cientificas, Tenerife (Spain).
LIGHT CURVE BEHAVIOUR IN THE NEAR IR OF THE CG CYG SYSTEM Abstract Only
J. J. Fuensalida, M. J. Arevalo, and D. K. Bedford (Birmingham Univ., England) *In* Colorado Univ., 5th Cambridge Workshop on Cool Stars, Stellar Systems and the Sun Jul. 1987 1 p (For primary document see N88-13092 04-89)
Avail: NTIS HC A07/MF A01

Light curves of the eclipsing system CG Cyg, which belongs to the group of RSCVn type stars, were obtained in the near IR (J, H, K) over a period of several years. Levels in orbital quadrature show an apparent IR excess, although this could be explained by interstellar reddening. A comparative study between curves of different epochs shows variations with time of the average level outside eclipses and of the minimums. The latter indicate a shift in the orbital phase, which is studied based on measurements published previously. A least squares fit frequency analysis of the curves outside the eclipses shows signs of variations in the range of 1 to 2 hours. Author

N88-13157# University of Western Ontario, London. Dept. of Astronomy.
AN ANALYSIS OF THE PHOTOSPHERIC LINE PROFILES IN F, G, AND K SUPERGIANTS Abstract Only
C. G. Toner and David F. Gray *In* Colorado Univ., 5th Cambridge Workshop on Cool Stars, Stellar Systems and the Sun Jul. 1987 1 p (For primary document see N88-13092 04-89)
Avail: NTIS HC A07/MF A01

Spectral-line broadening for thirty F, G, and K Ib supergiants has been measured. Fourier analysis for macroturbulence and rotation shows: (1) macroturbulent velocities larger than but compatible with values found for lower luminosity stars, and (2) rotation results that cannot be fully explained. Three plausible scenarios are suggested, but the one in which angular momentum of the surface shell is conserved during the evolutionary changes experienced by these stars is favored. The unusual distribution of rotation velocities may result from a preferential alignment of rotation axes with the galactic poles. Author

N88-13158*# National Aeronautics and Space Administration. Goddard Space Flight Center, Greenbelt, Md.
A FLASH SPECTRUM OF Cl I, C I, N I, AND Ni II ABSORPTION IN 31 CYGNI: A DIRECT OBSERVATION OF THE REVERSING LAYER Abstract Only
Imad A. Ahmad *In* Colorado Univ., 5th Cambridge Workshop on Cool Stars, Stellar Systems and the Sun Jul. 1987 1 p Prepared in cooperation with Imad-ad-Dean, Inc., Bethesda, Md. (For primary document see N88-13092 04-89)
(Contract NAS5-29381)
Avail: NTIS HC A07/MF A01 CSCL 03A

In the process of surveying IUE observations of the zeta Aurigae binary system 31 Cygni for evidence of a shock, the presence of narrow low temperature lines Cl I, C I, N I, and Ni II has been discovered. These lines cannot be due to the local interstellar medium, since they appear only in one of the 16 high resolution, short wavelength observations made of this system. The phase of their appearance is theta = 0.017, approximately two months after egress of the blue dwarf component from eclipse behind the cool supergiant. Such lines might be produced by the shining of the hot dwarf companion's continuum through the edge of the

supergiant's reversing layer or through a condensation in the supergiant atmosphere. If the former is the case, then the height of the reversing layer may be estimated from this observation. The radial velocities and equivalent widths of ten of these lines have been measured and the former is found to be -8.2 +/- 0.5 km/sec, precisely equal to the radial velocity of the system center of mass. This places a strict upper limit on the rotational velocity of the supergiant: V sub rot less than 2 km/s to better than 3 sigma. Author

N88-13159# Indian Inst. of Astrophysics, Bangalore.
SENSITIVITY OF THE H ALPHA LINE TO EXPANSION, GEOMETRICAL EXTENT AND TEMPERATURE GRADIENT IN THE G AND K SUPERGIANT CHROMOSPHERES Abstract Only
Sushma V. Mallik *In* Colorado Univ., 5th Cambridge Workshop on Cool Stars, Stellar Systems and the Sun Jul. 1987 1 p (For primary document see N88-13092 04-89)
Avail: NTIS HC A07/MF A01

The H alpha line in late G and K supergiants is a very strong absorption feature with a distinct blue asymmetry. The line is of chromospheric origin and the blue asymmetry suggests that the chromospheres of these stars are expanding. Apart from this deep, blue shifted absorption core, the H alpha line is also observed to have small emission components lying above the continuum either to the red or blue or both sides of the absorption profile. A formulation is described for treating the transfer of H alpha in supergiants by using the comoving frame technique suitably modified for the present context. The chromosphere is modeled as a spherically symmetric expanding atmosphere with given density and temperature structures. It is further assumed that the Lyman lines and the continua are in radiative detailed balance and the n=1 and n=2 level populations are connected by the Boltzmann factor. Author

N88-13160# ST Systems Corp., Lanham, Md.
RADIO CONTINUUM EMISSION FROM THE IONIZED STELLAR WINDS OF THE COOL SUPERGIANTS IN ZETA AURIGAE-LIKE SYSTEMS Abstract Only **c93**
Stephen A. Drake, Alexander Brown, and Dieter Reimers (Hamburger Sternwarte, West Germany) *In* Colorado Univ., 5th Cambridge Workshop on Cool Stars, Stellar Systems and the Sun Jul. 1987 1 p (For primary document see N88-13092 04-89)
Avail: NTIS HC A07/MF A01

A 6 cm continuum survey is conducted using the VLA of 10 binary systems that have cool, evolved primaries (mostly supergiants of spectral type G and K) and hot main sequence secondaries with spectral types between B2 and A3, including the prototype of the zeta Aurigae class of atmospheric-eclipsing binaries. The results of this survey show that only 47 Cyg and 31 Cyg are definitely detected, with inferred 6 cm liminosities of 1.7 x 10 to the 17th and 3 x 10 to the 16th power erg/s/Hz, respectively, while pi Pup is possibly detected with an estimated 6 cm luminosity of 10 to the 16th power erg/s/Hz. It is evident that the spectral type of the secondary is the most significant factor correlating with detectable radio continuum emission, since the 3 detected systems have the 3 hottest secondaries (approximately B3), while the non-detected systems (which include zeta Aurigae, 58 Per, and gamma Per) have spectral types later than B4. The simplest interpretation of these data is that, due to the rapid increase in the number N sub L of Lyman-ionizing photons in a fairly narrow range of spectral type of the secondary star (log N sub L = 42.2 for B5V, but = 43.4 for B3V), the stellar wind of the primary star in these binaries goes from being mostly neutral to mostly ionized (and hence a copious emitter of radio bremsstrahlung) in this same range. Author

N88-13161# Harvard-Smithsonian Center for Astrophysics, Cambridge, Mass. Center for Astrophysics.
NEW RESULTS FROM HIGH ANGULAR RESOLUTION OBSERVATIONS OF ALPHA ORI Abstract Only
M. Karovska, P. Nisenson, and R. Noyes *In* Colorado Univ., 5th Cambridge Workshop on Cool Stars, Stellar Systems and the Sun Jul. 1987 1 p (For primary document see N88-13092 04-89)
Avail: NTIS HC A07/MF A01

Speckle observations of alpha Ori in the H alpha line (CTIO 4m telescope, Aug. 1985) revealed the presence of a bright feature on the surface of the star, having a scale of approximately 16 mas. A similar feature had been observed in December 1983. The strong resemblence between these two features suggests that they may be in fact the same long-lived photospheric or chromospheric structure. The observed change in the position angle may be related to the rotation of the star. The previous detections of two close companions to alpha Ori (one at 0.05 and another at 0.5 arcsec distance from the supergiant) have been confirmed by speckle observations carried out with the CTIO (Aug. 1985) and Kitt Peak (Dec. 1986) 4m telescopes. Measured position angles and distances for the inner companion are in close agreement with those predicted by the existing orbit. The autocorrelation and image of alpha Ori obtained at 450.0 nm (CTIO. Aug. 1985) produced evidence for the existence of an elongated structure of 305 deg with approximate scale of 200 mas. The origin of this structure may be light scattered in the alpha Ori envelope rendered asymmetric as a result of the orbital motion of the inner companion. Author

N88-13162# Arizona State Univ., Tempe. Dept. of Physics.
THE ANGULAR DIAMETER OF ALPHA SCORPII IN THE NEAR-INFRARED Ca II TRIPLET Abstract Only
Paul C. Schmidtke *In* Colorado Univ., 5th Cambridge Workshop on Cool Stars, Stellar Systems and the Sun Jul. 1987 1 p (For primary document see N88-13092 04-89)
Avail: NTIS HC A07/MF A01

Time-resolved (60 to 90 Hz) spectra of the Ca II near-infrared triplet (1 A resolution) of alpha Scorpii have been obtained during two lunar occultations. Fitting a uniform-disc model to the data, the angular diameter is approximately 36 milliarcsecond (mas) in the continuum and approximately 59, 75 and 69 mas in the cores of the lines at 8498, 8542, and 8662 A, respectively. There is little change in the relative sizes if full limb darkening is assumed. Unlike the angular-diameter measurements of alpha Orionis from speckle interferometry (3 A resolution at 8542 A), the apparent size variation of alpha Scorpii cannot be explained by simply changing the limb-darkening coefficient. Comparison with model atmosphere calculations is in progress. Author

N88-13163# Bentley Coll., Boston, Mass.
EMISSION FEATURES IN IRAS LRS SPECTRA OF MS, S AND CS STARS Abstract Only
Stephen J. Little, Irene R. Little-Marenin, and Stephan D. Price (Air Force Geophysics Lab., Hanscom AFB, Mass.) *In* Colorado Univ., 5th Cambridge Workshop on Cool Stars, Stellar Systems and the Sun Jul. 1987 1 p (For primary document see N88-13092 04-89)
Avail: NTIS HC A07/MF A01

Stellar evolution theory predicts that M stars evolve to MS- greater than S- greater than (SC)- greater than C stars during the late stages of AGB evolution when helium-burning products (primarily C-12 and s-process elements) are dredged up. Many AGB stars lose mass and develop extensive circumstellar dust shells (CDS) at this time. The changing photospheric composition should be reflected in the composition of the dust grains since the lost photospheric material passes through the CDS in a very short time. IRAS obtained low resolution spectra (LRS) of bright sources in the 8 to 22 micron region where the emission features of silicates (at 10 and 18 microns) and of SiC (at 11.2 microns) are found. Some 70 LRS spectra of MS, S and SC stars were analyzed in order to see if the changing photospheric composition produces unusual emission features in the 8 to 22 micron region. Author

N88-13164# Harvard-Smithsonian Center for Astrophysics, Cambridge, Mass.
WINDS AND SHELLS AROUND LOW-MASS SUPERGIANTS Abstract Only **c90**
A. K. Dupree and H. E. Bond (Space Telescope Science Inst.,

Baltimore, Md.) *In* Colorado Univ., 5th Cambridge Workshop on Cool Stars, Stellar Systems and the Sun Jul. 1987 1 p (For primary document see N88-13092 04-89)
Avail: NTIS HC A07/MF A01

A class of A- and F-type supergiants lying at high galactic latitudes (the 89 Herculis or UU Herculis stars) has been known for some years. Recent evidence suggests that these are not young Population I objects, but instead are much older low-mass stars evolving off the tip of the asymptotic giant branch toward the regime of central stars of planetary nebulae. It is possible that these stars are already surrounded by relatively neutral material which will become a planetary nebula, if they have experienced an extreme mass-ejection episode (perhaps a superwind) when they were at the tip of the asymptotic giant branch. Appropriate spectra should reveal mass outflow from the stellar atmosphere, and the presence of circumstellar material. Discovery of such material would provide support for the scenario of planetary nebula formation outlined above. Spectra and infrared observations of two high-latitude giants, HR 4912 and HD 161796 support the hypothesis that they have a circumstellar envelope which may become a planetary nebula as the central star becomes sufficiently hot. Author

N88-13165# Colorado Univ., Boulder.
FAR INFRARED CIRCUMSTELLAR DEBRIS SHELLS OF RED SUPERGIANT STARS Abstract Only **c90**
R. E. Stencel, J. E. Pesce, and W. HagenBauer (Wellesley Coll., Mass.) *In its* 5th Cambridge Workshop on Cool Stars, Stellar Systems and the Sun Jul. 1987 1 p (For primary document see N88-13092 04-89)
Avail: NTIS HC A07/MF A01

There is yet another transition line between chromospheres and dust, which lies above and to the right of corona-wind transitions in the HR diagram. The IRAS 60-micron data appears to indicate the existence of very cool material extending tens of thousands of stellar radii around red supergiant stars. These circumstellar debris shells may prove useful in the analysis of larger scale galactic trends, such as metallicity. Author

N88-13166# Colorado Univ., Boulder.
IRAS AND COOL STELLAR MASS LOSS Abstract Only
C. J. Skinner and B. Whitmore *In its* 5th Cambridge Workshop on Cool Stars, Stellar Systems and the Sun Jul. 1987 1 p (For primary document see N88-13092 04-89)
Avail: NTIS HC A07/MF A01

Low resolution spectra have been obtained from a variety of sources (IRAS LRS Catalog and the literature) for cool, luminous oxygen-rich stars whose mass-loss rates have been determined by CO measurements. The power radiated in the silicate dust feature at 9.7 microns can easily be calculated from these spectra provided either the distance or the luminosity of the star is known. Although there is only a small sample of such stars (given the uncertainties in both distance and mass-loss rates), it is found that the power radiated in the 9.7 micron feature is correlated with the observed gas mass-loss rate. This indicates that the gas-to-dust ratio is roughly constant in O-rich giant and supergiant stars, and that the 9.7 micron dust feature can be used to estimate mass-loss rates for these stars (vastly increasing the number of stars for which this can be done). This technique is applied to M-Supergiants and to Mira variables (Red Giants), and shows that, using data from the General Catalog of Variable Stars, the mass-loss rates do not correlate in any simple way with either the amplitude or the visual light curve, or the period of the variability in either case. Nor does the mass-loss rate appear to be correlated with the photospheric radial velocity of the stars (measured indirectly via the amplitude and period of the pulsations). It is argued that this implies that radial pulsations are not important in driving mass-loss from Red Giants. Author

N88-13167# Consejo Superior Investigaciones Cientificas, Tenerife (Spain).
CARBON ABUNDANCES AND C12/C13 RATIOS IN M GIANTS Abstract Only
C. Lazaro, A. E. Lynas-Gray, R. E. S. Clegg, M. Mountain, and A. Zadrowny (Imperial Coll. of Science and Technology, London, England) *In* Colorado Univ., 5th Cambridge Workshop on Cool Stars, Stellar Systems and the Sun Jul. 1987 1 p (For primary document see N88-13092 04-89)
Avail: NTIS HC A07/MF A01

The infrared first-overtone CO bands are observed at 2.3 microns with a medium resolution grating spectrometer in a sample of 78 bright M giants. The spectral scans were analyzed by spectrum synthesis of the CO bands and the adjacent continuum, using model atmospheres for cool, low-gravity stars. The carbon abundances obtained suggest a moderate general deficiency for the M type giants, with a normal distribution centered around (C) approximately = -0.5. A few stars show carbon depleted by a factor greater than or = 10 over the solar value, but none can be considered with confidence as extremely poor. In addition to carbon abundances, the isotopic ratio of C-12 to C-13 is deduced. For most of the stars in the sample these ratios are in the range 10 to 30, but some of them reach values as low as 3. The significance of these results in terms of nucleosynthesis and mixing processes is discussed. Author

N88-13168# Iowa State Univ. of Science and Technology, Ames. Dept. of Physics.
APPLICATION OF DYNAMIC ATMOSPHERE MODELS TO THE ANALYSIS OF ANGULAR DIAMETER OBSERVATIONS OF MIRA VARIABLES Abstract Only **c90**
T. E. Beach, G. H. Bowen, and L. A. Willson *In* Colorado Univ., 5th Cambridge Workshop on Cool Stars, Stellar Systems and the Sun Jul. 1987 1 p (For primary document see N88-13092 04-89)
Avail: NTIS HC A07/MF A01

Dynamic effects in the atmospheres of Mira variables must be considered in order to correctly analyze angular diameter measurements of these stars. The results presented apply to the direct measurement of Mira angular diameters by lunar occultation and speckle interferometric measurements where a limb function must be assumed to derive the stellar diameters from the observations. The standard corrections for limb darkening, which are based on static model atmospheres, can give erroneous results, and in some cases the correction is a change in the wrong direction. Dynamic models of Mira atmospheres were used to determine the limb darkening and/or brightening functions for a range of phases, and for two wavelength bands and opacities. The angular diameters that would be found from lunar occultation observations of Miras with these limb functions were calculated, and compared to the actual diameter of the model star to determine the diameter correction as a function of phase. The shock structure in the innermost regions of the model atmosphere is also examined as it has an effect on the limb functions, especially at wavelengths where postshock cooling radiation dominates the spectrum.
Author

N88-13169*# National Aeronautics and Space Administration. Goddard Space Flight Center, Greenbelt, Md.
VLA OBSERVATIONS OF RAPID 6 cm FLUX VARIATIONS IN ALPHA ORI Abstract Only
J. A. Bookbinder, R. E. Stencel, S. A. Drake, T. Simon, J. L. Linsky, and D. Florkowski (Colorado Univ., Boulder.) *In* Colorado Univ., 5th Cambridge Workshop on Cool Stars, Stellar Systems and the Sun Jul. 1987 1 p (For primary document see N88-13092 04-89)
Avail: NTIS HC A07/MF A01 CSCL 03A

The red supergiant star alpha Ori was monitored with the Very Large Array (VLA). Thirteen observations at 6 cm show stochastic variations, at the 30 to 40 percent level, with no long term trend. All data was clipped and tapered in AIPS to minimize differences between VLA arrays. The calibration source varied by less than 10 percent over the same interval. The VLA observations of alpha Ori were continued, as well as alpha Her and alpha Sco, at both 2 and 6 cm, to confirm this result and search for long term trends. The stochastic 6 cm flux behavior, with 30 to 40 percent changes on all timescales from the shortest interval of 10 days to the

longest, seems at odds with the 400 day periodic variations in U-band photometry and Mg II UV fluxes reported by Dupree, et al. The observed 6 cm flux was 25 percent below the 6 cm flux reported earlier this decade. Several models for the outer atmosphere of alpha Ori place the 6 cm optical depth unity location at several stellar radii above the optical photosphere. The rapid, stochastic variations reported are difficult to reconcile with almost any global process, such as pulsation, Alfen waves or periastron passage. Author

N88-13170# Oslo Univ. (Norway). Inst. of Theoretical Astrophysics.
THE WILSON-BAPPU RELATIONSHIP: A BAROMETRIC EFFECT Abstract Only
O. Engvold and O. Elgaroy *In* Colorado Univ., 5th Cambridge Workshop on Cool Stars, Stellar Systems and the Sun Jul. 1987 1 p (For primary document see N88-13092 04-89)
Avail: NTIS HC A07/MF A01

The Wilson-Bappu relationship may be expressed as M sub v = A log W sub o + B, where M sub v is absolute visual luminosity and W sub o is basically the FWHM width of the central line emission of the Ca II K. Most cool stars from dwarfs to supergiants closely obey the relation over about 15 magnitudes. The slope is A approximately = 15. Analogue relations are found for the Mg II h and k lines. The investigation is based on high resolution spectral observations undertaken with the IUE satellite of 17 target stars. It is found that there is a Wilson-Bappu type relation also in the EUV emission lines formed in stellar chromosphere and transition regions. The study was to determine whether the width luminosity relation depends on line opacity or on turbulent velocity. It appears that the slope of the width luminosity relationship depends on the optical thickness of the line. Optically thin chromospheric lines show no Wilson-Bappu relationship. This implies that there exists no systematic Doppler broadening with stellar luminosity. Hence, the Wilson-Bappu relationship is primarily a barometric effect. Author

N88-13171# Oxford Univ. (England). Dept. of Theoretical Physics.
IUE OBSERVATIONS OF THE HYBRID K3 II STAR IOTA AURIGAE AND CONSTRAINTS ON THE OUTER ATMOSPHERIC STRUCTURE Abstract Only
G. M. Harper and P. G. Judge *In* Colorado Univ., 5th Cambridge Workshop on Cool Stars, Stellar Systems and the Sun Jul. 1987 1 p (For primary document see N88-13092 04-89)
Avail: NTIS HC A07/MF A01

High and low resolution spectra of the hybrid K3 II star Iota Aurigae are presented. A relative wavelength scale was adopted for the long LWP images by measuring photospheric absorption lines and this gives a wavelength scale accurate to + or - 5/kms. This enabled the measurement of the two absorption components in the Mg II emission line profiles. The low velocity component is at 6/kms relative to the photosphere and the high velocity component is between 70 and 80/kms relative to the photosphere. The emission line fluxes are used to derive an emission measure distribution which leads to some simple models of the outer atmospheric structure. The line widths of some optically thin lines suggest that mass motions give an additional pressure term, thus reducing the effective gravity, and giving a greater extent to the outer atmosphere than in the static case. The similarity of Iota Aurigae with other hybrid stars lends support to idea that these stars do form a distinct class. Author

N88-13172# Kitt Peak National Observatory, Tucson, Ariz.
TIME SERIES INFRARED SPECTROSCOPY OF LONG PERIOD VARIABLES Abstract Only
Kenneth H. Hinkle *In* Colorado Univ., 5th Cambridge Workshop on Cool Stars, Stellar Systems and the Sun Jul. 1987 1 p Prepared in cooperation with National Optical Astronomy Labs., Tucson, Ariz. (For primary document see N88-13092 04-89)
Avail: NTIS HC A07/MF A01

Time series infrared spectra were obtained for 6 Miras and 5 SRa and SRb long period variables. The CO delta v = 3 bands at 1.6 micron were studied in these stars in detail. Because of the large Rayleigh scattering and line blanketing opacity in the visual, the photospheres of typical Miras are not observable in visual spectra. The CO delta v = 3 bands cross the opacity minimum, so the CO lines sample conditions deep in the photosphere. Using CO delta v = 3 lines, the velocity, CO excitation temperature, and CO column density were derived. These results are powerful monitors of the radial pulsations of the long period variables. The semiregular type variables were the target of this synoptic program. While these variables are far more numerous than the much larger amplitude Mira variables, little is known about the kinematics of the semiregular variable stars. The results from the semiregular and Mira variable are compared. Most of the Miras observed were bright, M-type, field Miras not previously studied. Results are presented for the peculiar Mira Z Oph. Z Oph appears on the Mira spectral type period relation with a period twice too large for its spectral type. Author

N88-13173# Indiana Univ., Bloomington.
SYNTHETIC SPECTRA FOR THE N-TYPE CARBON STAR TX Psc Abstract Only
D. G. Luttermoser, H. R. Johnson, and E. H. Avrett (Center for Analysis, Newport Beach, Calif.) *In* Colorado Univ., 5th Cambridge Workshop on Cool Stars, Stellar Systems and the Sun Jul. 1987 1 p (For primary document see N88-13092 04-89)
Avail: NTIS HC A07/MF A01

A low and high resolution LWP spectrum are used to constrain a chromospheric model of the bright, cool carbon star TX Psc. The presence of a chromosphere is indicated by the appearance of several emission lines in the LWR spectrum, the strongest being Mg II, C II, and Fe II. This spectrum also shows a photospheric continuum rising above the noise longward of 2900 A. The LWP spectrum shows only the Mg II and a few Fe II emission lines. The modeling of the chromosphere of TX Psc is done in a fashion similar to the semi-empirical method commonly used on G and K giants. Models are generated by using a radiative equilibrium photosphere and adjusting the temperature profile in the outer layers to simulate a chromospheric temperature rise. Synthetic spectra are then calculated assuming a static, homogeneous, plane parallel geometry, and the chromospheric temperature profile altered until the observed fluxes are reproduced. Two approaches are made in the calculation of the synthetic spectra: (1) LTE calculations for the continuum and the lines; and (2) non-LTE calculations for H, H(-), H2, Mg I and II, C I and II, Na I, Ca I. Author

N88-13174# Mankato State Coll., Minn.
INFRARED EXCESSES OF BARIUM STARS Abstract Only
Jon Hakkila *In* Colorado Univ., 5th Cambridge Workshop on Cool Stars, Stellar Systems and the Sun Jul. 1987 1 p (For primary document see N88-13092 04-89)
Avail: NTIS HC A07/MF A01

A sample of 31 barium stars was studied using JHKLMN photometry. Infrared excesses are found to occur in the H, M, and N bands. The H-excess appears to correlate with the barium intensity (defined by the abnormal strength of the 4554 A Ball line), whereas the excesses in M and N do not. Two mechanisms are suggested for the production of these excesses: (1) redistribution of energy from the Bond-Neff optical depression into the infrared, and (2) thermal emission from residual material associated with mass transfer in a binary system. The correlation of the H-excess with suppressed optical flux is suggestive of energy redistribution, but the M and N-excesses might indicate thermal energy from gas and dust. Author

N88-13175# Space Telescope Science Inst., Baltimore, Md.
JHK PHOTOMETRY OF CN-RICH FIELD GIANTS Abstract Only
Graeme H. Smith *In* Colorado Univ., 5th Cambridge Workshop on Cool Stars, Stellar Systems and the Sun Jul. 1987 1 p (For primary document see N88-13092 04-89)
Avail: NTIS HC A07/MF A01

Infrared JHK photometry was obtained for a sample of CN-rich Population I field giants. On average, the CN-rich giants show a modest color separation from more typical field giants of near solar abundance in the J-H, H-K two-color diagram. Many of the CN enhanced stars exhibit a redder H-K color than solar neighborhood giants of similar J-H, with delta(H-K) approximately 0.02 to 0.04. A possible origin of this color difference is discussed in terms of the abundance differences between the CN-rich giants and more typical solar neighborhood stars. The JHK colors of the CN-rich giants are compared with those of Galactic bulge giants. Author

N88-13176# Wellesley Coll., Mass. Whitin Observatory.
WATER MASERS ASSOCIATED WITH 2 CARBON STARS: EU ANDROMEDAE AND V778 CYGNI Abstract Only **c90**
Irene R. Little-Marenin, Priscilla J. Benson, and Stephen J. Little (Bentley Coll., Boston, Mass.) *In* Colorado Univ., 5th Cambridge Workshop on Cool Stars, Stellar Systems and the Sun Jul. 1987 1 p (For primary document see N88-13092 04-89)
Avail: NTIS HC A07/MF A01

Seven carbon stars are associated with oxygen rich circumstellar shells as deduced from the presence of strong 10 micron emission features in their IRAS low resolution spectra (LRS). Only 4 of these carbon stars are visible with the 37 m Haystack Observatory radio telescope and a search for the 6 sub 16 -5 sub 23 H2O maser emission line at 22,235.080 MHz has proven successful for EU And and V778 Cyg. EU And was detected with a flux of 8.2 Jy at V sub LRS = -29.4/kms. V778 Cyg was detected with a flux of 1.9 Jy at V sub LRS = -17/kms. Both sources have shown variations in the H2O flux of a factor of about 8 during the last several months and have shown weaker multiple components at various times. EU And and V778 Cyg were classified as carbon stars in the visible region and the latter shows the typical strong CN absorption features in the 0.8 to 1 micron region. No information on the near infrared spectrum of EU And is available. Both objects were interpreted as being in binary systems with a C star component and an M star component with a relatively thick circumstellar shell. The circumstellar shell of the M star produces the emission features seen at 10 and 18 micron as well as the H2O maser line. Author

N88-13177*# National Aeronautics and Space Administration. Goddard Space Flight Center, Greenbelt, Md.
THE DELTA UPSILON = 1 FUNDAMENTAL BANDS OF CARBON MONOXIDE IN LATE-TYPE STARS Abstract Only
G. Wiedemann, T. Ayres, S. Saar (Joint Inst. for Lab. Astrophysics, Boulder, Colo.), and D. Jennings *In* Colorado Univ., 5th Cambridge Workshop on Cool Stars, Stellar Systems and the Sun Jul. 1987 1 p (For primary document see N88-13092 04-89)
(Grant NSF AST-85-07029)
Avail: NTIS HC A07/MF A01 CSCL 03A

A program was begun to develop the fundamental vibration-rotation bands of CO near 4.7 micron, as a tool to investigate the properties of late type stellar atmospheres. The strong delta v = 1 lines are sensitive probes of the thermal structure of the outer layers, which can be strongly affected by the CO, itself: cooling in the fundamental lines can depress the surface temperature to low values that are in sharp contrast with those derived from chromospheric diagnostics like Ca II K and Mg II k. Cool atmospheric models are being constructed to reproduce observed high resolution CO spectra of several late-type stars. The sensitivity is illustrated of CO LTE spectra to variations in T sub eff, log g, (Fe/H), and isotopic abundances of C and O for a grid of such models. In parallel, the assumptions of LTE line formation are tested using newly available cross sections for translational-to-vibrational energy exchange in collisions of atomic H on CO. In addition, spectra of CO and Ca II K calculated from semi-empirical UV based hot chromospheric models are used to estimate geometrical filling factors for the CO dominated and chromospheric regions on the stellar surface, in the spirit of Ayres' thermal bifurcation scenario. Author

N88-13178# Osservatorio Astronomico, Turin (Italy).
NEUTRON CAPTURE NUCLEOSYNTHESIS IN LOW MASS AGB STARS Abstract Only **c90**
M. Busso, G. Picchio, and R. Gallino (Turin Univ., Italy) *In* Colorado Univ., 5th Cambridge Workshop on Cool Stars, Stellar Systems and the Sun Jul. 1987 1 p (For primary document see N88-13092 04-89)
Avail: NTIS HC A07/MF A01

The heavy element synthesis induced by the large neutron fluxes deriving from the reaction C-13 (alpha, n) O-16 in low mass planetary nebula progenitors experiencing thermal pulses is examined. The mechanism of semi-convection proposed by Iben and Renzini for the synthesis of the initial C-13 is assumed to be effective. A large reaction network was created, incorporating updated values for the cross sections of alpha-, p- and n-captures on about 350 nuclei. It includes 80 branching points along the neutron capture path and extends from He to Po. The thermal pulses are followed until asymptotic values for the nuclear abundances are reached, and for each pulse the physical parameters of the models by Iben and Iben and Renzini are adopted. The results of the computations show that the AGB evolution of low mass stars is extremely important for the formation of the heaviest nuclei. This is important in the light of the strong difficulties recently advanced against an efficient s-element synthesis in Intermediate Mass Stars. Author

N88-13179# Institut d'Astrophysique, Paris (France).
PRE-MAIN SEQUENCE ACTIVITY: HOW FAR IS MAGNETISM INVOLVED Abstract Only **c90**
J. Bouvier *In* Colorado Univ., 5th Cambridge Workshop on Cool Stars, Stellar Systems and the Sun Jul. 1987 1 p (For primary document see N88-13092 04-89)
Avail: NTIS HC A07/MF A01

The detection of periodicities in the light curves of 8 bona fide T Tauri stars (TTS) is reported. This periodic behavior is interpreted as being due to spots located on the stellar surface. A model is applied to 21 periodic light curves to deduce the geometrical and physical properties of the spots. It is shown that the X-ray surface flux of TTS decreases as the rotation period increases. This activity rotation relationship is much similar to the one obeyed by RS CVn systems which is regarded as the signature of the dynamo process in the nonradiative heating of the X-ray emitting regions. On the opposite, the radiative losses undergone by cooler atmospheric regions, as measured by the surface flux emitted in the H sub alpha, Ca II K or Mg II k lines, do not scale with the stellar rotation rate. Thus, an additional energy source seems to overcome the contribution of magnetic processes in the nonradiative heating of the atmospheric regions where these spectral lines form. Hence, the comparison of TTS properties with those of solar type active stars allows one to disentangle the various energy sources TTS have at their disposal. Author

N88-13180# Joint Inst. for Lab. Astrophysics, Boulder, Colo.
CHROMOSPHERIC VARIABILITY MECHANISMS AFFECTING PRE-MAIN SEQUENCE STARS Abstract Only **c90**
Alexander Brown *In* Colorado Univ., 5th Cambridge Workshop on Cool Stars, Stellar Systems and the Sun Jul. 1987 1 p (For primary document see N88-13092 04-89)
Avail: NTIS HC A07/MF A01

Results are presented from a number of studies of T Tauri and Herbig emission line stars made using the IUE satellite, with particular attention being given to the variability of the stars RY Tau, T Tau, DR Tau and HR5999. These studies have sought to determine the physical causes of the observed chromospheric and transition region emission line variability of these stars. Several variability mechanisms were positively identified including changes in surface area coverage of dark optical starspot/UV bright plane regions, both rapid and long term changes in circumstellar extinction and time variable heating due to infalling material. Changes in stellar wind properties are also discussed. The relative importance of these and other possible processes, such as flaring, will be evaluated. Author

N88-13181# Yale Univ., New Haven, Conn. Center for Solar and Space Research.
SPIN-UP AND SPIN-DOWN ON THE WAY TO THE MAIN SEQUENCE Abstract Only **c90**
Steven D. Kawaler *In* Colorado Univ., 5th Cambridge Workshop on Cool Stars, Stellar Systems and the Sun Jul. 1987 1 p (For primary document see N88-13092 04-89)
Avail: NTIS HC A07/MF A01

Theoretical evolutionary sequences were constructed for low mass stars from the fully convective Hayashi contraction phase through the main sequence. Using these nonrotating models, the angular momentum redistribution was approximated. The first limit, solid body rotation, corresponds to complete redistribution of angular momentum. In the second case, solid body rotation was limited to the convective envelope, and local conservation of angular momentum was assumed in radiative regions. Partial angular momentum redistribution in radiative regions results in surface rotation velocities that lie between these two limits; the results obtained are fully consistent with those for rotating models that include mechanisms for angular momentum redistribution. This simple approach allows the exploration of the parameters of various models of angular momentum loss by magnetic winds. The observed distribution of rotation velocities of stars in young galactic clusters was used to constrain the dependence of the angular momentum loss rate on total stellar mass, rotation velocity, and mass loss rate. This analysis also places limits on the total angular momentum of low mass stars. Author

N88-13182*# Columbia Univ., New York, N.Y.
THE EINSTEIN SURVEY OF THE YOUNG STARS IN THE ORION NEBULA Abstract Only **c90**
S. Zoonematkermani and J.-P. Caillault (Joint Inst. for Lab. Astrophysics, Boulder, Colo.) *In* Colorado Univ., 5th Cambridge Workshop on Cool Stars, Stellar Systems and the Sun Jul. 1987 1 p (For primary document see N88-13092 04-89)
(Grants NAG8-497; NAG8-582)
Avail: NTIS HC A07/MF A01 CSCL 03B

The Orion Nebula is the best studied site of recent star formation in the Galaxy. The complete Einstein Observatory survey of the Orion Nebula covering a 2 deg x 2 deg region centered on the Trapezium is reported. An X-ray mosaic is presented for the Nebula along with a complete X-ray catalogue for this very young cluster. Approximately 150 distinct sources were found in this 4 sq deg region; spectral types and colors were obtained for about 1/2 of the optical counterparts of these sources. Comparison of the variability of the Orion X-ray sources with those found in the Rho Ophiuchi cloud leads to the conclusion that the Orion sources' variability is also likely to result from continual flaring activities. Eleven new late B stars associated with X-ray emission far exceeding that expected from early type stars were discovered. The X-rays may originate from pre-main sequence companions to these stars; a T-Tauri star of the same age would have the correct L sub x. Comparison of the solar type stars in Orion with those in the Pleiades, the Hyades, and the field suggests that the decay of activity with age is most appropriately described by an exponential, rather than a power law fit. Author

N88-13183# Five-College Astronomy Dept., Amherst, Mass.
THE CONTRIBUTION OF ACCRETION LUMINOSITY TO THE INFRARED SPECTRA OF T TAURI STARS: A POSSIBLE TEST Abstract Only **c90**
K. M. Strom and S. E. Strom *In* Colorado Univ., 5th Cambridge Workshop on Cool Stars, Stellar Systems and the Sun Jul. 1987 1 p (For primary document see N88-13092 04-89)
Avail: NTIS HC A07/MF A01

Ultraviolet, optical and infrared continuum excesses are characteristic properties of T Tauri stars (TTS). Ultraviolet and optical excesses are usually ascribed to contributions from active chromospheric regions, while the infrared excess is most commonly thought to arise from reprocessed photospheric and chromospheric radiation absorbed by circumstellar dust grains and reemitted in the infrared. A test is proposed which appears to provide the basis for diagnosing the contributions of accretion luminosity to the mid and far infrared spectra TTS. The test depends on a comparison of the effective temperature derived from the optical spectral type and an independent estimate derived from the ratio of the reddening corrected bolometric luminosity and the reddening corrected monochromatic luminosity. It is concluded that accretion luminosity may account for a significant fraction of the infrared luminosity of many TTS; those TTS which appear to show the largest accretion luminosity are those which drive optical jets and/or molecular outflows or which have the strongest winds as measured by (OI) emission strength. Author

N88-13184# Joint Inst. for Lab. Astrophysics, Boulder, Colo.
CHROMOSPHERIC AND CORONAL HEATING IN A BIAS-FREE SAMPLE OF K DWARFS Abstract Only **c90**
D. H. Neff and J. A. Bookbinder *In* Colorado Univ., 5th Cambridge Workshop on Cool Stars, Stellar Systems and the Sun Jul. 1987 1 p (For primary document see N88-13092 04-89)
Avail: NTIS HC A07/MF A01

In order to investigate the relative energy losses from stellar chromospheres and coronae in a broad class of stars, it is important that a well-defined, bias-free sample be used. Previous observations show that for G stars the radiation losses from the chromosphere greatly exceed the radiation losses from the corona. For M stars, the opposite is true. Hence, it is important to study the relative chromospheric and coronal losses from stars in the spectral range KO to MO, where stellar atmospheres change from having radiation losses dominated by the chromosphere to having radiation losses dominated by the corona. The IUE satellite was used to observe a volume-limited set of single K dwarfs previously observed with the Einstein satellite and the Mg II h and k fluxes of the stars were carefully measured. The Mg II fluxes are considered as indicators of chromospheric emission and the X-ray fluxes as indicators of coronal emission. Preliminary results show that the normalized X-ray fluxes and the normalized Mg II fluxes are related by a power law. The Mg II and X-ray surface fluxes show more scatter than the normalized fluxes, but they still seem to be related by a power law. Author

N88-13185# Joint Inst. for Lab. Astrophysics, Boulder, Colo.
MEASUREMENTS OF STELLAR MAGNETIC FIELDS: EMPIRICAL CONSTRAINTS ON DYNAMO AND ROTATIONAL EVOLUTION THEORIES Abstract Only **c90**
Jeffrey L. Linsky and Steven H. Saar *In* Colorado Univ., 5th Cambridge Workshop on Cool Stars, Stellar Systems and the Sun Jul. 1987 1 p (For primary document see N88-13092 04-89)
Avail: NTIS HC A07/MF A01

Recent results are presented of an ongoing survey of the magnetic field properties of over 30 dwarf stars of spectral types F to M. The data was analyzed using a modification of the Robinson technique that includes line saturation, the full Zeeman patterns, and compensation for line blends. The derived magnetic parameters, the mean active region field strength (B) and area filling factor (f) occupied by these fields, refer to magnetic regions outside of spot umbrae. Attention is called to important trends emerging in the data that provide empirical constraints on acceptable dynamo theories: (1) B increases toward T sub eff and larger g such that B approximately = B sub eq = (8piP sub gas) sup 0.5. Thus in the photosphere B is determined by the balance of magnetic pressure and the gas pressure, largely independent of the nature of the dynamo; (2) B and f are uncorrelated and fB is not a constant; (3) f does not depend on T sub eff; and (4) B is independent of stellar age, but f varies as t sup -0.6 for stars older than the Pleiades. This result is consistent with theoretical predictions of the angular momentum history of dwarf stars. It is concluded that decrease in activity with stellar age is due to the decrease in f as a star evolves. Author

N88-13186# Osservatorio Astronomico, Turin (Italy).
IRAS AND NEAR IR OBSERVATIONS OF ACTIVE BINARIES Abstract Only
F. Scaltriti, M. Busso, P. Persi, L. Origlia, M. Robberto, and G. Silvestro (Turin Univ., Italy) *In* Colorado Univ., 5th Cambridge Workshop on Cool Stars, Stellar Systems and the Sun Jul.

1987 1 p (For primary document see N88-13092 04-89)
Avail: NTIS HC A07/MF A01

Recent optical and infrared observations revealed the presence of remarkable IR excesses around some RS CVn binaries, that were interpreted as due to the presence of thin shells of circumstellar material. In order to understand if such a phenomenology is a common feature of the active binaries in that class, a systematic search was undertaken for nonstellar contributions to the observed flux, based on new broad band photometry in the optical and near infrared regions of the spectrum integrated by the data of the IRAS Point Source Catalogue. It is found that several objects of the RS CVn type were actually observed by IRAS. On the basis of the resulting energy distributions and of the known parameters of the binary systems, the statistical relevance of IR excesses and some hypotheses about their nature are briefly discussed. Author

N88-13187# Consejo Superior Investigaciones Cientificas, Tenerife (Spain).
STROMGREN PHOTOMETRY OF RSCVn AND HD108102 Abstract Only
M. J. Arevalo, C. Lazaro, J. J. Fensalida, V. Reglero, and J. L. Ballester (Universidad de Palma de Mallorca, Spain) *In* Colorado Univ., 5th Cambridge Workshop on Cool Stars, Stellar Systems and the Sun Jul. 1987 1 p (For primary document see N88-13092 04-89)
Avail: NTIS HC A07/MF A01

UVBY beta Stromgren photometry is reported of two RSCVn Systems. The eclipsing system RSCVn, prototype of the class, has been extensively studied by many authors, and almost uninterrupted series of light curves for each season for 30 yrs are available. HD108102, is a double lined spectroscopy binary, commonly known as T111. This system belongs to the open cluster in the constellation Coma Berenices, and the possibility that it could be an RSCVn system was pointed out. Because this would be the first RSCVn which is a known cluster member, this star could help to determine the evolutionary status, luminosity and initial abundance of this class of stars. Light curves are analyzed for two stars and T111 is definitely variable. The Stromgren colors index are compared with standard calibration for normal late type stars. A metallicity deficiency was found for the secondary component of RSCVn, with an anomaly in the opposite sense for the primary component. Using these photometric colors, the spectral types were classified for both systems. The color obtained at primary minima give for the cooler component in RSCVn a K4 V spectral type. For the system HD108102 a spectral type F8 V is found. Author

N88-13188# Arizona Univ., Tucson.
M DWARFS FROM THE EINSTEIN MEDIUM SENSITIVITY SURVEY Abstract Only
T. A. Fleming, J. Liebert, I. M. Gioia, and T. Maccacaro (Harvard-Smithsonian Center for Astrophysics, Cambridge, Mass.) *In* Colorado Univ., 5th Cambridge Workshop on Cool Stars, Stellar Systems and the Sun Jul. 1987 1 p (For primary document see N88-13092 04-89)
Avail: NTIS HC A07/MF A01

A complete sample of X-ray selected M dwarfs are presented which were serendipitously detected in the extended Einstein Observatory Medium Sensitivity Survey (MSS). The MSS detected only early M dwarfs (type MO through M5), 84 percent of which were emission stars (i.e., type Me V). It was calculated that the X-ray luminosity function for early M dwarfs with a log Lx greater than 27.6 and, by comparison to optical luminosity functions, find that about 25 percent of all early M dwarfs emit X-rays at a level greater than log Lx = 27.6. This result is compared to luminosity function estimates from optically selected samples and discussed in light of the sample's kinematic and mean age. Also presented is H alpha and Ca II K line fluxes for each member of the sample and it is shown that the surface H alpha and Ca II K luminosities do indeed correlate with Lx. The significance of this effect to theories of chromospheric and coronal heating is explained. Author

N88-13189# Toledo Univ., Ohio. Dept. of Physics and Astronomy.
A HELIUM FLARE ON THE ACTIVE G5 DWARF KAPPA CETI Abstract Only **c90**
Craig R. Robinson and Bernard W. Bopp *In* Colorado Univ., 5th Cambridge Workshop on Cool Stars, Stellar Systems and the Sun Jul. 1987 1 p (For primary document see N88-13092 04-89)
Avail: NTIS HC A07/MF A01

A strong emission-line flare on the chromospherically active G5 dwarf Kappa Ceti was observed. Using the fiber-coupled echelle spectrograph and intensified Reticon detector, these observations come from an archive of 1000 high-resolution, high signal-to-noise scans in the program of synoptic monitoring of Be and chromospherically active stars. During an observation of Kappa Ceti from 01:10 to 01:40 UT, lambda5876 He I was found in emission; a subsequent scan at 02:19 UT showed normal He I absorption. Mt. Wilson Ca II flux measures obtained the night after this event, suggest enhanced Ca II emission was present for several hours following the detection of He I emission. This behavior, where the decay of helium emission is much faster than that of Ca II, is similar to what is viewed on the Sun and on UV Ceti flare stars. Both the flare energetics and quiescent photometric behavior or Kappa Ceti are discussed. Author

N88-13190# Fairborn Observatory, Mesa, Ariz.
AUTOMATIC TELESCOPE OPERATIONS Abstract Only
Russell M. Genet, Louis J. Boyd, and Sallie L. Baliunas (Harvard-Smithsonian Center for Astrophysics, Cambridge, Mass.) *In* Colorado Univ., 5th Cambridge Workshop on Cool Stars, Stellar Systems and the Sun Jul. 1987 1 p (For primary document see N88-13092 04-89)
Avail: NTIS HC A07/MF A01

Three automatic telescopes make photometric measurements each clear night of a large number of cool stars. The automatic operation includes not only the telescopes, but the observatory itself. Each night a site control computer checks weather sensors and a clock and if the weather and time are appropriate, opens up the roof. After time for temperature stabilization, the site control computer informs each of the automatic telescopes that they can begin their observations. Observations are made by selecting stars from a stored list via an algorithm. The stars are observed automatically and the data stored on diskettes. This continues until morning or bad weather. The site control computer then tells the telescopes to stop observing, closes the roof, and gives a summary report, via modem, to another computer located elsewhere. This morning report includes information on the number of observations made by each telescope and an indicator of their quality, reports from the weather sensors, activities at the site, and the remaining space on each diskette for observational data. Author

N88-13191# Colorado Univ., Boulder.
RADIO EMISSION FROM RS CVn BINARIES: A 5 GHz VLA SURVEY OF 93 SYSTEMS Abstract Only **c93**
D. H. Morris and R. L. Mutel *In its* 5th Cambridge Workshop on Cool Stars, Stellar Systems and the Sun Jul. 1987 1 p (For primary document see N88-13092 04-89)
Avail: NTIS HC A07/MF A01

A 5 GHz radio survey of 93 close, late type stellar binaries is presented. The survey consists of all cataloged sources north of -45 deg declination. Of the 93 candidate stars, 52 were detected above the 0.4 mJy detection threshold. A comparison of median observed radio luminosity with rotational period, color (B-V) and Rossby number is presented. There is evidence that the color index of the cooler component of the system is related to the radio luminosity whereas that of the hotter component is not. This supports the view of a single active (cooler) star being responsible for the radio emission. While the rotational period is not correlated with radio luminosity for the complete sample, there is a marginally significant correlation for sources with periods of less than 10 days. There is also evidence that in this period range some combination of both the rotational period and the color index of the cooler component may be a superior indicator of radio

luminosity than either alone. The Rossby number, while such a combination of rotational and convective stellar properties, is not an effective indicator of radio luminosity in these systems.
Author

N88-13192# Colorado Univ., Boulder.
CATALOGUE OF CHROMOSPHERICALLY ACTIVE BINARIES Abstract Only
Klaus Strassmeier, Douglas Hall, Michael Zeilik, Eric Nelson, Zeki Eker, and Francis Fekel *In its* 5th Cambridge Workshop on Cool Stars, Stellar Systems and the Sun Jul. 1987 1 p (For primary document see N88-13092 04-89)
Avail: NTIS HC A07/MF A01

A catalogue was prepared of properties of all known chromospherically active binary stars. It includes 168 definite binaries and a few dozen possible candidates. Most of these have been previously classified as RS CVn or BY Dra binaries. W UMa binaries are not included even though they in certain ways can be considered chromospherically active. The catalogue includes material from the never published review paper mentioned by Hall, the data bank announced by Zeilik and Nelson, the RS CVn catalogue of Eker, and the catalogue of northern RS CVn binaries of Strassmeier.
Author

N88-13193# Chalmers Univ. of Technology, Goeteborg (Sweden). Raaoe Rymdobservatorium.
EVN (EUROPEAN VLBI NETWORK) AND MERLIN OBSERVATIONS OF 5 SUPERLUMINAL RADIO SOURCES
G. Pilbratt, R. S. Booth, and R. W. Porcas 1986 20 p
(PB87-110730; Rept-86/42) Avail: NTIS HC E03/MF E01
CSCL 03A

The authors report observations of five superluminal sources with the European VLBI Network (EVN) at 1.66 and 5 GHz, and MERLIN observations at 5 GHz. The observations were performed in an attempt to fill in the resolution gap between the milliarcsecond and arcsecond scales of previous observations; the sources observed were NRA0140, 3C120, 3C179, 3C279, and 3C345.
GRA

N88-13194 Colorado Univ., Boulder.
A COMPREHENSIVE EXPLORATION OF LATE-TYPE STARS IN THE FAR-ULTRAVIOLET Ph.D. Thesis
Jeffrey Owen Bennett 1987 206 p
Avail: Univ. Microfilms Order No. DA8716238

An examination of far ultraviolet emissions as a function of stellar type was undertaken using a database of spectra from the International Ultraviolet Explorer (IUE) and the Solar Mesosphere Explorer (SME). The existence of the dividing line between coronal and noncoronal giants is confirmed, as is the observation that O I lambda 1304 emission is enhanced relative to other chromospheric diagnostics among giants and supergiants. Far-ultraviolet emissions are found to be separated into a chromospheric group and related transition-zone group. With respect to solar variability during the declining phase of cycle 21, good correlations are found among solar far-ultraviolet emissions and between these emissions and sunspot numbers, as a function of time. The functional relations for temporal changes on the Sun are generally the same as those for stars as a function of mean activity, with the exception of relations involving C II lambda 1335 which show significant differences in the solar and stellar cases. Finally, an examination of far-ultraviolet variability of several stars which have been frequently observed for the last ten years is presented.
Dissert. Abstr.

N88-13195 California Univ., Berkeley.
AN ASTROMETRIC SEARCH FOR A STELLAR COMPANION TO THE SUN Ph.D. Thesis
Saul Perlmutter 1987 71 p
Avail: Univ. Microfilms Order No. DA8718121

An astrometric search for a nearby red dwarf companion with a six-month peak-to-peak parallax of greater than or = 2.5 arcseconds is described. The parallax of 2,770 candidate stars is being measured. An automated 30-inch telescope and charge-coupled device (CCD) camera system collect digitized images of the candidate stars, along with a 13 minute by 16 minute surrounding field of background stars. Second-epoch images, taken a few months later, are registered to the first epoch images using the background stars as fiducials. The precision of apparent motion found is sufficient to detect the parallactic motion of a star at 0.8 pc with a two-month interval between the observation epochs. Images with fewer fiducial stars above background noise are observed with a longer interval between epochs. So far, on observations of 41 stars, none has been shown to be a nearby star.
Dissert. Abstr.

N88-13196 Colorado Univ., Boulder.
OBSERVATIONS AND ANALYSIS OF THE PHOTOSPHERIC MAGNETIC FIELDS ON DWARF G, K AND M STARS Ph.D. Thesis
Steven Herbert Saar 1987 240 p
Avail: Univ. Microfilms Order No. DA8716295

An improved technique was developed for the analysis of magnetic broadening in stellar absorption line profiles. The technique is based on a model that includes radiative transfer effects and the full Zeeman patterns. The technique was applied to two sets of high resolution, low noise spectra. The first set consists of 29 stars, spanning spectral types from GO to M4.5 and a broad range of rotational rates and ages. Several major trends are apparent from the results. The stellar magnetic field strength is in pressure equilibrium with the photospheric gas pressure and is thus a function of spectral type. The filling factor is a linear function of angular velocity. The total magnetic flux on a star is thus a function of the star rotation rate, in agreement with simple dynamo theories. The technique was also used to study the spatial and temporal behavior of magnetic regions (f) and mean field strength in these regions (B) on the active star Epsilon Eri. Eleven observations were made over two months with contemporaneous measurements of the chromospheric Ca II emission flux.
Dissert. Abstr.

90 ASTROPHYSICS

Includes cosmology; celestial mechanics; space plasmas; and interstellar and interplanetary gases and dust.
For related information see also *75 Plasma Physics*.

N88-13197# Brookhaven National Lab., Upton, N. Y.
CORE BOUNCE SUPERNOVAE
J. Cooperstein 1987 11 p Presented at the 194th American Chemical Society National Meeting, New Orleans, La., 30 Aug. 1987
(Contract DE-AC02-76CH-00016)
(DE87-014910; BNL-40211; CONF-870802-20) Avail: NTIS HC A03/MF A01

The gravitational collapse mechanism for Type II supernovae is considered, concentrating on the direct implosion - core bounce - hydrodynamic explosion picture. We examine the influence of the stiffness of the dense matter equation of state and discuss how the shock wave is formed. Its chances of success are determined by the equation of state, general relativistic effects, neutrino transport, and the size of presupernova iron core.
DOE

N88-13198# Centro Brasileiro de Pesquisas Fisicas, Rio de Janeiro.
NEW COSMOLOGICAL SCENARIO
M. Novello 1986 12 p
(DE87-703357; CBPF-NF-025/86) Avail: NTIS (US Sales Only) HC A03/MF A01

A proposal for an alternative model for the Universe called the Eternal Universe is presented as an alternative to the Big Bang theory. An attempt is made to devise solutions for some shortcomings of this model.
DOE

N88-13199# Centro Brasileiro de Pesquisas Fisicas, Rio de Janeiro.
MOESSBAUER STUDY OF SHOCK INDUCED EFFECTS IN THE Fe-Ni 50/50 ORDERED ALLOY IN METEORITES
R. B. Scorzelli, I. S. Azevedo, and J. Danon 1986 10 p
(DE87-703364; CBPF-NF-036/86) Avail: NTIS (US Sales Only) HC A02/MF A01

Using the flying plate technique we have investigated by Moessbauer Spectroscopy, the shock induced effects in the ordered iron-nickel alloy of meteorites. The degree of long-range order in the ordered alloy is reduced by shock event. DOE

N88-13200# Instituto de Pesquisas Espaciais, Sao Jose dos Campos (Brazil).
MEASUREMENTS OF IRIDIUM AND THE METEORIC IMPACT HYPOTHESIS AT CRETACEOUS END M.S. Thesis
F. SircilliNeto Dec. 1986 117 p In PORTUGUESE; ENGLISH summary
(DE87-703765; INPE-4070) Avail: NTIS (US Sales Only) HC A06/MF A01

Both instrumental and radiochemical neutron activation analysis methods were developed for trace-element determination, such as iridium and gold, for application in cosmochemistry. The magnitude of the determined concentrations is in the range of parts per billion. In the instrumental method 1.5 grams of sample were submitted to irradiation by 10 to the 13th power thermal neutrons/sq cm/s during 32 hours. The gamma spectrometry is carried out with 10 to 12 hours counting time after 40 days of decay. In the radiochemical analysis a method of radiochemical separation of noble metals based on tellurium coprecipitation is implanted for iridium and gold determinations. As an application of the instrumental neutron activation analysis, preliminary iridium concentrations are measured for the first time in sedimentary rocks collected on Brazilian territory. These techniques for the determination of iridium content will be useful to check the asteroid impact hypothesis, supposedly the cause of the great Cretaceous/Tertiary mass extinction, using samples collected in the Southern Hemisphere. DOE

N88-13201 Rice Univ., Houston, Tex.
THE VELOCITY STRUCTURE AND TURBULENCE AT THE CENTER OF THE ORION NEBULA Ph.D. Thesis
Hector Osvaldo Castaneda 1987 190 p
Avail: Univ. Microfilms Order No. DA8718699

Using the Coude Feed System of the Kitt Peak National Observatory at its highest possible dispersion and a CCD detector with wide dynamic range it was possible to examine in detail the radial and turbulent velocities of the Orion Nebula at the seeing limit. For the first time, multiple components of the spectral lines were resolved and the gaussian profiles fit to them. Using four different observing runs, two circular areas 2 minutes in diameter were observed, the first centered on the theta sup 1 Orionis and the second centered on theta sup 1 Orionis. The velocity resoluton of 1 km/s combined with the angular resolution of 2 seconds allowed observation in detail at line splitting as well as the location and measurement of high internal motions, about -50 km/s with respect to the bulk of ionized matter. Because over 900 different positions were measured, modern statistical techniques were used for the analysis of turbulence, so that the dispersion relation and the structure function could be calculated and compared with predictions of the Kolmogorov theory. The random motions showed correlation with spatial separation, as expected for turbulence; but comparison with predictions of the classical theory for nebular turbulence showed poor agreement. If Kolmogorov theory applies, then the energy must be input at many scales. Dissert. Abstr.

N88-13202 Texas Univ., Austin.
COSMOLOGICAL APPLICATIONS OF SINGULAR HYPERSURFACES IN GENERAL RELATIVITY Ph.D. Thesis
Pablo Laguna-Castillo 1987 200 p
Avail: Univ. Microfilms Order No. DA8717462

Three applications to cosmology of surface layers, based on Israel's formalism of singular hypersurfaces and thin shells in general relativity, are presented. Einstein's field equations are analyzed in the presence of a bubble nucleated in vacuum phase transitions within the context of the old inflationary universe scenario. The evolution of a bubble with vanishing surface energy density is studied. It is found that such bubbles lead to a worm-hole matching. Next, the observable four-dimensional universe is considered as a singular hypersurface of discontinuity embedded in a five-dimensional Kaluza-Klein cosmology. It is possible to rewrite the projected five-dimensional Einstein equations on the surface layer in a similar way to the four-dimensional Robertson-Walker cosmology equations. Next, a model is described for an infinite-length, straight U(1) cosmic string as a cylindrical, singular shell enclosing a region of false vacuum. A set of equations is introduced which are required to develop a three-dimensional computer code whose purpose is to study the process of intercommuting cosmic strings with the inclusion of gravitational effects. The outcome is evolution and constraint equations for the gravitational, scalar and gauge field of two initially separated, perpendicular, cosmic strings. Dissert. Abstr.

N88-13203 Baylor Univ., Houston, Tex.
CONDITIONS FOR GEOMAGNETICALLY TRAPPING SUB-MICRON LUNAR EJECTA BETWEEN L = 1.2 AND L = 3.1 Ph.D. Thesis
Lily Manou Lodhi 1987 151 p
Avail: Univ. Microfilms Order No. DA8718339

An extensive analysis of field emission effects on the electrostatic breakup potential of lunar impact ejecta particles was conducted. It is shown that the dominant factor in the determination of the equilibrium potential of micron size particles in space is field emission. The dynamics of particles reaching the magnetosphere was studied. The most interesting region was the zone on the sunward side of the earth between L values of 1.2 and 3.1. These minute particles may have residence times in that zone that are considerably greater than that represented by interplanetary dust flowing through the same region. The spatial densities of lunar ejecta in these zones can be one to two orders of magnitude more than that in interplanetary space for the same particle size regime. However, significant permanent trapping is not found for these particle regimes at this time. Dissert. Abstr.

N88-13204 Johns Hopkins Univ., Baltimore, Md.
HYDROGEN AND DEUTERIUM IN THE LOCAL INTERSTELLAR MEDIUM Ph.D. Thesis
Jayant Narasimha Murthy 1987 125 p
Avail: Univ. Microfilms Order No. DA8716635

International Ultraviolet Explorer (IUE) observations lead to the derivation of density, velocity dispersion, and bulk velocity of the neutral hydrogen along the line of sight to Alpha Centauri B, Epsilon Eridani, Procyon, Altair, Capella, and HR 1099. Lower limits are placed on the deuterium to hydrogen ratio towards the same stars. The HI absorption profile towards Altair shows a broad saturated core and steep line wings, consistent with a multicomponent interstellar medium in that direction. The bulk velocities towards the other stars are consistent with a bulk flow from the approximate direction of the galactic center but do show local variations from a uniform flow, possibly indicating a complicated velocity structure even in the solar neighborhood. Interstellar deuterium is detected towards every star except Altair. Values for D/H ratios confirm earlier findings. The lower D/H ratios found towards several hot stars may indicate real variations in the D/H ratio in the local interstellar medium. Finally, an apparent step in the cosmic background and several galactic emission lines found by Auriemma et al. are found to be artifacts. Dissert. Abstr.

N88-13205 Princeton Univ., N. J.
GALAXY FORMATION BY GRAVITATIONAL COLLAPSE IN A UNIVERSE DOMINATED BY COLD DARK MATTER Ph.D. Thesis
Barbara Sue Ryden 1987 196 p
Avail: Univ. Microfilms Order No. DA8716901

In a density field which is originally a randon phase Gaussian distribution, the densities, dispersions, and angular momenta of

collapsed density peaks can be calculated. If the density distribution has a power spectrum produced by cold dark matter (CDM) in an omega = 1 universe, then the density peaks develop into objects with properties typical of galaxies. In the absence of baryon dissipation, CDM halos form with densities of the form p alpha r(sup -1.8). The orbits of the dark matter are more radial around high peaks than around low peaks. The matter around a peak acquires a net angular momentum from the tidal torques impartedby neighboring peaks. For matter at a given initial radium from a peak, the net angular momentum in inversely proportional to the initial peak height. The ratio of the ordered angular momentum to random angular momentum increases with distance from a peak; the outer regions are cooler. The baryons in typical halos are able to cool effectively by Compton cooling, bremsstrahlung, and radiative recombination. If the baryons dissipate their energy until they form a rotationally supported disk, adiabatically compressing the dark halo, then the resulting rotation curves of the structure are flat. A simple calculation of the mass function of efficiently cooled objects gives a function of the form. The multiplicity function of collapsed groups of galaxies is proportional to M(sup -1.8) at masses less that a few times 10 to the 14th solar mass.

Dissert. Abstr.

N88-13206 Colorado Univ., Boulder.
GALACTIC INTERSTELLAR ABUNDANCE SURVEYS WITH IUE AND IRAS Ph.D. Thesis
Michael Earl VanSteenberg 1987 174 p
Avail: Univ. Microfilms Order No. DA8716312

A survey is presented of interstellar densities, abundances, and cloud structure in the Galaxy, using 2 NASA satellites, the International Ultraviolet Explorer (IUE) and Infrared Astronomical Satellite (IRAS). From IUE high resolution spectra were measured equivalent widths of 18 ultraviolet resonance transitions and derived column densities for Si(+), Mn (+), Fe(+), S(+), and Zn(+) toward 261 early type stars. From the IRAS all sky survey were also measured the infrared cirrus flux. The variations were examined of the measured parameters with spectral type, E(B-V), galactic longitude and latitude, distance from the Sun, and mean density. The hydrogen column densities, metal column densities, and gas to dust ratio are in good agreement with Copernicus surveys.

Dissert. Abstr.

N88-13207# Oak Ridge National Lab., Tenn.
SUPERTRACKS: THE BUILDING BLOCKS OF CHAOS
E. M. Oblow 25 Aug. 1987 30 p
(Contract DE-AC05-84OR-21400)
(DE88-001513; ORNL/TM-10550; CESAR-87/39) Avail: NTIS HC A03/MF A01

A theoretical conjecture is made about the nature of chaotic behavior in systems with simple maps. This conjecture gives rise to a computational scheme based on trajectories starting from the maximum in the system map. These trajectories are called supertracks and their loci in the parameter phase-space indexed by iteration number are called supertracks functions. The chaotic regimes of two nonlinear systems with a single maximum are studied using this scheme. It is found that the behavior in these regimes can be characterized recursively by supertrack functions. At low recursion order these functions analytically describe the gross features of the chaotic regime (i.e. bounding envelopes, stable cycles, star points, etc.). They can be iterated to higher orders to study higher order features. The methodology employed is general enough to be used to study other nonlinear systems. It also has potential for identifying chaotic behavior experimentally. Universality is the basis for theoretically understanding the results.

DOE

N88-13208# California Univ., Berkeley. Lawrence Berkeley Lab.
INFLUENCES OF THE ASTROPHYSICAL ENVIRONMENT ON NUCLEAR DECAY RATES
E. B. Norman Sep. 1987 11 p Presented at the 194th American Chemical Society National Meeting, New Orleans, La., 30 Aug. 1987
(Contract DE-AC03-76SF-00098)
(DE88-001461; LBL-23037; CONF-870802-23) Avail: NTIS HC A03/MF A01

In many astronomical environments, physical conditions are so extreme that nuclear decay rates can be significantly altered from their laboratory values. Such effects are relevant to a number of current problems in nuclear astrophysics. Experiments related to these problems are now being pursued, and will be described.

DOE

N88-13093# Harvard-Smithsonian Center for Astrophysics, Cambridge, Mass. Center for Astrophysics.
MEASUREMENTS OF STELLAR MAGNETIC FIELDS Abstract Only
L. Hartmann *In* Colorado Univ., 5th Cambridge Workshop on Cool Stars, Stellar Systems and the Sun Jul. 1987 1 p (For primary document see N88-13092 04-89)
Avail: NTIS HC A07/MF A01

N88-13094# Joint Inst. for Lab. Astrophysics, Boulder, Colo.
THE PHOTOSPHERIC MAGNETIC FIELDS OF COOL STARS: RECENT RESULTS OF SURVEY AND TIME-VARIABILITY PROGRAMS Abstract Only
S. H. Saar *In* Colorado Univ., 5th Cambridge Workshop on Cool Stars, Stellar Systems and the Sun Jul. 1987 1 p (For primary document see N88-13092 04-89)
Avail: NTIS HC A07/MF A01

N88-13097# Helsinki Univ. (Finland). Observatory and Astrophysics Lab.
OBSERVATIONAL CONSTRAINTS AND EVIDENCE FOR SATURATION Abstract Only
Osmi Vilhu *In* Colorado Univ., 5th Cambridge Workshop on Cool Stars, Stellar Systems and the Sun Jul. 1987 1 p (For primary document see N88-13092 04-89)
Avail: NTIS HC A07/MF A01

N88-13098# Joint Inst. for Lab. Astrophysics, Boulder, Colo.
HEATING OF STELLAR CHROMOSPHERES AND CORONAE: EVIDENCE FOR NON-MAGNETIC BASAL HEATING Abstract Only
C. J. Schrijver *In* Colorado Univ., 5th Cambridge Workshop on Cool Stars, Stellar Systems and the Sun Jul. 1987 1 p (For primary document see N88-13092 04-89)
Avail: NTIS HC A07/MF A01

N88-13099# Dominion Astrophysical Observatory, Victoria (British Columbia).
ANGULAR MOMENTUM EVOLUTION OF YOUNG STARS Abstract Only
John R. Stauffer *In* Colorado Univ., 5th Cambridge Workshop on Cool Stars, Stellar Systems and the Sun Jul. 1987 1 p (For primary document see N88-13092 04-89)
Avail: NTIS HC A07/MF A01

N88-13100# National Solar Observatory, Tucson, Ariz.
POST-ZERO-AGE MAIN SEQUENCE ROTATION Abstract Only
Myron A. Smith *In* Colorado Univ., 5th Cambridge Workshop on Cool Stars, Stellar Systems and the Sun Jul. 1987 1 p (For primary document see N88-13092 04-89)
Avail: NTIS HC A07/MF A01

N88-13101# Oxford Univ. (England). Dept. of Theoretical Physics.
A RE-EXAMINATION OF THE CORONA-WIND DIVIDING LINE: DIAGNOSTICS OF NON-CORONAL ATMOSPHERES Abstract Only
P. G. Judge *In* Colorado Univ., 5th Cambridge Workshop on Cool Stars, Stellar Systems and the Sun Jul. 1987 1 p (For primary document see N88-13092 04-89)
Avail: NTIS HC A07/MF A01

N88-13104# National Solar Observatory, Sunspot, N. Mex.
ATMOSPHERES OF STARS IN THE LIMITS OF THIN AND THICK CONVECTION ZONES: THE M DWARFS Abstract Only
Mark S. Giampapa *In* Colorado Univ., 5th Cambridge Workshop on Cool Stars, Stellar Systems and the Sun Jul. 1987 1 p (For primary document see N88-13092 04-89)
Avail: NTIS HC A07/MF A01

N88-13105# National Center for Atmospheric Research, Boulder, Colo. High Altitude Observatory.
ATMOSPHERES OF STARS IN THE LIMITS OF THICK AND THIN CONVECTION ZONES: M GIANTS Abstract Only
K. B. MacGregor *In* Colorado Univ., 5th Cambridge Workshop on Cool Stars, Stellar Systems and the Sun Jul. 1987 1 p (For primary document see N88-13092 04-89)
Avail: NTIS HC A07/MF A01

N88-13106# Colorado Univ., Boulder.
DISK ACCRETION DURING THE EARLY STAGES OF STELLAR EVOLUTION Abstract Only
Scott Kenyon *In its* 5th Cambridge Workshop on Cool Stars, Stellar Systems and the Sun Jul. 1987 1 p (For primary document see N88-13092 04-89)
Avail: NTIS HC AC7/MF A01

N88-13107# Pennsylvania State Univ., University Park.
MICROWAVE OBSERVATIONS OF NONTHERMAL PHENOMENA IN PRE-MAIN SEQUENCE STARS Abstract Only
Eric D. Feigelson *In* Colorado Univ., 5th Cambridge Workshop on Cool Stars, Stellar Systems and the Sun Jul. 1987 1 p (For primary document see N88-13092 04-89)
Avail: NTIS HC A07/MF A01

N88-13108*# National Aeronautics and Space Administration. Marshall Space Flight Center, Huntsville, Ala.
MAGNETIC FLUX TUBES AS SOURCES OF WAVE GENERATION Abstract Only
Z. E. Musielak, R. Rosner, and P. Ulmschneider (Heidelberg Univ., West Germany) *In* Colorado Univ., 5th Cambridge Workshop on Cool Stars, Stellar Systems and the Sun Jul. 1987 1 p (For primary document see N88-13092 04-89)
Avail: NTIS HC A07/MF A01 CSCL 03B

N88-13117# Yale Univ., New Haven, Conn. Center for Solar and Space Research.
LARGE SCALE SOLAR AND STELLAR MAGNETIC FIELDS Abstract Only
Peter A. Fox *In* Colorado Univ., 5th Cambridge Workshop on Cool Stars, Stellar Systems and the Sun Jul. 1987 1 p (For primary document see N88-13092 04-89)
Avail: NTIS HC A07/MF A01

N88-13120# Armagh Observatory (Northern Ireland).
THE GIANT SPOT ON II PEG IN 1986 Abstract Only
P. B. Byrne *In* Colorado Univ., 5th Cambridge Workshop on Cool Stars, Stellar Systems and the Sun Jul. 1987 1 p (For primary document see N88-13092 04-89)
Avail: NTIS HC A07/MF A01

N88-13131# Laboratorium voor Ruimteonderzoek, Utrecht (Netherlands). Sonnenborgh Observatory.
ASYNCHRONOUS ROTATION IN CLOSE BINARY SYSTEMS WITH CIRCULAR ORBITS Abstract Only
Guillaume M. H. J. Habets *In* Colorado Univ., 5th Cambridge Workshop on Cool Stars, Stellar Systems and the Sun Jul. 1987 1 p (For primary document see N88-13092 04-89)
Avail: NTIS HC A07/MF A01

N88-13132# Arizona Univ., Tucson. Steward Observatory.
PG 0308 + 096: A SHORT-PERIOD WHITE DWARF + dM BINARY WITH STRONGLY MODULATED H-ALPHA EMISSION Abstract Only
Richard A. Wade and Rex A. Saffer *In* Colorado Univ., 5th Cambridge Workshop on Cool Stars, Stellar Systems and the Sun Jul. 1987 1 p (For primary document see N88-13092 04-89)
Avail: NTIS HC A07/MF A01

N88-13134# Laboratorium voor Ruimteonderzoek, Utrecht (Netherlands).
EVIDENCE FOR EXPANDING MAGNETIC LOOPS IN CORONAE OF COOL STARS Abstract Only
R. Mewe, J. R. Lemen, C. J. Schrijver, and A. Fludra (Wroclaw Univ., Poland) *In* Colorado Univ., 5th Cambridge Workshop on Cool Stars, Stellar Systems and the Sun Jul. 1987 1 p (For primary document see N88-13092 04-89)
Avail: NTIS HC A07/MF A01

N88-13137# Louisville Univ., Ky. Dept. of Physics.
MAGNETIC FIELDS ON K AND M STARS Abstract Only
David H. Bruning, Richard E. Chenoweth, and Geoffrey W. Marcy *In* Colorado Univ., 5th Cambridge Workshop on Cool Stars, Stellar Systems and the Sun Jul. 1987 1 p (For primary document see N88-13092 04-89)
Avail: NTIS HC A07/MF A01

N88-13139# Sacramento Peak Observatory, Sunspot, N. Mex.
STELLAR ACTIVITY AND THE ROTATION OF HYADES STARS Abstract Only
Richard R. Radick and Sallie L. Baliunas (Harvard-Smithsonian Center for Astrophysics, Cambridge, Mass.) *In* Colorado Univ., 5th Cambridge Workshop on Cool Stars, Stellar Systems and the Sun Jul. 1987 1 p (For primary document see N88-13092 04-89)
Avail: NTIS HC A07/MF A01

N88-13142# Colorado Univ., Boulder.
ACTIVITY IN WARM STARS Abstract Only
F. M. Walter and C. J. Schrijver (Joint Inst. for Lab. Astrophysics, Boulder, Colo.) *In its* 5th Cambridge Workshop on Cool Stars, Stellar Systems and the Sun Jul. 1987 1 p (For primary document see N88-13092 04-89)
Avail: NTIS HC A07/MF A01

N88-13145# Joint Inst. for Lab. Astrophysics, Boulder, Colo.
EMPIRICAL RELATIONS BETWEEN PHOTOSPHERIC MAGNETIC FIELDS AND ATMOSPHERIC RADIATIVE LOSSES FOR COOL DWARF STARS Abstract Only
S. H. Saar and C. J. Schrijver *In* Colorado Univ., 5th Cambridge Workshop on Cool Stars, Stellar Systems and the Sun Jul. 1987 1 p (For primary document see N88-13092 04-89)
Avail: NTIS HC A07/MF A01

N88-13148*# National Aeronautics and Space Administration. Marshall Space Flight Center, Huntsville, Ala.
MHD ENERGY FLUXES FOR LATE TYPE DWARFS Abstract Only
R. Rosner and Z. E. Musielak (Harvard-Smithsonian Center for Astrophysics, Cambridge, Mass.) *In* Colorado Univ., 5th Cambridge Workshop on Cool Stars, Stellar Systems and the Sun Jul. 1987 1 p (For primary document see N88-13092 04-89)
Avail: NTIS HC A07/MF A01 CSCL 03B

N88-13164# Harvard-Smithsonian Center for Astrophysics, Cambridge, Mass.
WINDS AND SHELLS AROUND LOW-MASS SUPERGIANTS Abstract Only
A. K. Dupree and H. E. Bond (Space Telescope Science Inst., Baltimore, Md.) *In* Colorado Univ., 5th Cambridge Workshop on Cool Stars, Stellar Systems and the Sun Jul. 1987 1 p (For primary document see N88-13092 04-89)
Avail: NTIS HC A07/MF A01

N88-13165# Colorado Univ., Boulder.
FAR INFRARED CIRCUMSTELLAR DEBRIS SHELLS OF RED SUPERGIANT STARS Abstract Only
R. E. Stencel, J. E. Pesce, and W. HagenBauer (Wellesley Coll., Mass.) *In its* 5th Cambridge Workshop on Cool Stars, Stellar Systems and the Sun Jul. 1987 1 p (For primary document

see N88-13092 04-89)
Avail: NTIS HC A07/MF A01

N88-13168# Iowa State Univ. of Science and Technology, Ames. Dept. of Physics.
APPLICATION OF DYNAMIC ATMOSPHERE MODELS TO THE ANALYSIS OF ANGULAR DIAMETER OBSERVATIONS OF MIRA VARIABLES Abstract Only
T. E. Beech, G. H. Bowen, and L. A. Willson *In* Colorado Univ., 5th Cambridge Workshop on Cool Stars, Stellar Systems and the Sun Jul. 1987 1 p (For primary document see N88-13092 04-89)
Avail: NTIS HC A07/MF A01

N88-13176# Wellesley Coll., Mass. Whitin Observatory.
WATER MASERS ASSOCIATED WITH 2 CARBON STARS: EU ANDROMEDAE AND V778 CYGNI Abstract Only
Irene R. Little-Marenin, Priscilla J. Benson, and Stephen J. Little (Bentley Coll., Boston, Mass.) *In* Colorado Univ., 5th Cambridge Workshop on Cool Stars, Stellar Systems and the Sun Jul. 1987 1 p (For primary document see N88-13092 04-89)
Avail: NTIS HC A07/MF A01

N88-13178# Osservatorio Astronomico, Turin (Italy).
NEUTRON CAPTURE NUCLEOSYNTHESIS IN LOW MASS AGB STARS Abstract Only
M. Busso, G. Picchio, and R. Gallino (Turin Univ., Italy) *In* Colorado Univ., 5th Cambridge Workshop on Cool Stars, Stellar Systems and the Sun Jul. 1987 1 p (For primary document see N88-13092 04-89)
Avail: NTIS HC A07/MF A01

N88-13179# Institut d'Astrophysique, Paris (France).
PRE-MAIN SEQUENCE ACTIVITY: HOW FAR IS MAGNETISM INVOLVED Abstract Only
J. Bouvier *In* Colorado Univ., 5th Cambridge Workshop on Cool Stars, Stellar Systems and the Sun Jul. 1987 1 p (For primary document see N88-13092 04-89)
Avail: NTIS HC A07/MF A01

N88-13180# Joint Inst. for Lab. Astrophysics, Boulder, Colo.
CHROMOSPHERIC VARIABILITY MECHANISMS AFFECTING PRE-MAIN SEQUENCE STARS Abstract Only
Alexander Brown *In* Colorado Univ., 5th Cambridge Workshop on Cool Stars, Stellar Systems and the Sun Jul. 1987 1 p (For primary document see N88-13092 04-89)
Avail: NTIS HC A07/MF A01

N88-13181# Yale Univ., New Haven, Conn. Center for Solar and Space Research.
SPIN-UP AND SPIN-DOWN ON THE WAY TO THE MAIN SEQUENCE Abstract Only
Steven D. Kawaler *In* Colorado Univ., 5th Cambridge Workshop on Cool Stars, Stellar Systems and the Sun Jul. 1987 1 p (For primary document see N88-13092 04-89)
Avail: NTIS HC A07/MF A01

N88-13182*# Columbia Univ., New York, N.Y.
THE EINSTEIN SURVEY OF THE YOUNG STARS IN THE ORION NEBULA Abstract Only
S. Zoonematkermani and J.-P. Caillault (Joint Inst. for Lab. Astrophysics, Boulder, Colo.) *In* Colorado Univ., 5th Cambridge Workshop on Cool Stars, Stellar Systems and the Sun Jul. 1987 1 p (For primary document see N88-13092 04-89)
(Grants NAG8-497; NAG8-582)
Avail: NTIS HC A07/MF A01 CSCL 03B

N88-13183# Five-College Astronomy Dept., Amherst, Mass.
THE CONTRIBUTION OF ACCRETION LUMINOSITY TO THE INFRARED SPECTRA OF T TAURI STARS: A POSSIBLE TEST Abstract Only
K. M. Strom and S. E. Strom *In* Colorado Univ., 5th Cambridge Workshop on Cool Stars, Stellar Systems and the Sun Jul. 1987 1 p (For primary document see N88-13092 04-89)
Avail: NTIS HC A07/MF A01

1987 1 p (For primary document see N88-13092 04-89)
Avail: NTIS HC A07/MF A01

N88-13184# Joint Inst. for Lab. Astrophysics, Boulder, Colo.
CHROMOSPHERIC AND CORONAL HEATING IN A BIAS-FREE SAMPLE OF K DWARFS Abstract Only
D. H. Neff and J. A. Bookbinder *In* Colorado Univ., 5th Cambridge Workshop on Cool Stars, Stellar Systems and the Sun Jul. 1987 1 p (For primary document see N88-13092 04-89)
Avail: NTIS HC A07/MF A01

N88-13185# Joint Inst. for Lab. Astrophysics, Boulder, Colo.
MEASUREMENTS OF STELLAR MAGNETIC FIELDS: EMPIRICAL CONSTRAINTS ON DYNAMO AND ROTATIONAL EVOLUTION THEORIES Abstract Only
Jeffrey L. Linsky and Steven H. Saar *In* Colorado Univ., 5th Cambridge Workshop on Cool Stars, Stellar Systems and the Sun Jul. 1987 1 p (For primary document see N88-13092 04-89)
Avail: NTIS HC A07/MF A01

N88-13189# Toledo Univ., Ohio. Dept. of Physics and Astronomy.
A HELIUM FLARE ON THE ACTIVE G5 DWARF KAPPA CETI Abstract Only
Craig R. Robinson and Bernard W. Bopp *In* Colorado Univ., 5th Cambridge Workshop on Cool Stars, Stellar Systems and the Sun Jul. 1987 1 p (For primary document see N88-13092 04-89)
Avail: NTIS HC A07/MF A01

91 LUNAR AND PLANETARY EXPLORATION

Includes planetology; and manned and unmanned flights. For spacecraft design or space stations see *18 Spacecraft Design, Testing and Performance.*

N88-13209*# National Aeronautics and Space Administration. Lewis Research Center, Cleveland, Ohio.
SMALL REACTOR POWER SYSTEMS FOR MANNED PLANETARY SURFACE BASES
Harvey S. Bloomfield Dec. 1987 15 p
(NASA-TM-100223; E-3839; NAS 1.15:100223) Avail: NTIS HC A03/MF A01 CSCL 10B

A preliminary feasibility study of the potential application of small nuclear reactor space power systems to manned planetary surface base missions was conducted. The purpose of the study was to identify and assess the technology, performance, and safety issues associated with integration of reactor power systems with an evolutionary manned planetary surface exploration scenario. The requirements and characteristics of a variety of human-rated modular reactor power system configurations selected for a range of power levels from 25 kWe to hundreds of kilowatts is described. Trade-off analyses for reactor power systems utilizing both man-made and indigenous shielding materials are provided to examine performance, installation and operational safety feasibility issues. The results of this study have confirmed the preliminary feasibility of a wide variety of small reactor power plant configurations for growth oriented manned planetary surface exploration missions. The capability for power level growth with increasing manned presence, while maintaining safe radiation levels, was favorably assessed for nominal 25 to 100 kWe modular configurations. No feasibility limitations or technical barriers were identified and the use of both distance and indigenous planetary soil material for human rated radiation shielding were shown to be viable and attractive options. Author

N88-12692*# Jet Propulsion Lab., California Inst. of Tech., Pasadena.
THE ATMOSPHERE OF MARS AND OPTICAL COMMUNICATIONS
J. Annis *In its* The Telecommunications and Data Acquisition Report 15 Nov. 1987 p 124-132 (For primary document see

N88-12679 04-32)
Avail: NTIS HC A15/MF A01 CSCL 03B

92 SOLAR PHYSICS

Includes solar activity, solar flares, solar radiation and sunspots.

For related information see *93 Space Radiation.*

N88-13210*# Stanford Univ., Calif. Center for Space Science and Astrophysics.
THREE-HALVES LAW IN SUNSPOT CYCLE SHAPE
R. N. Bracewell Jul. 1987 15 p
(Grant NGL-05-020-272)
(NASA-CR-181520; NAS 1.26:181520; AD-A184352; CSSA-ASTRO-87-8) Avail: NTIS HC A03/MF A01 CSCL 03B

Annual mean sunspot numbers R(t) since 1700 show evidence of a nonlinear effect, first evidenced by the detection of third harmonic in R +/- (t), the alternating representation of the magnetic (22 year) cycle of solar activity. The form of the nonlinearity proves to be a three-halves law R(t) = 100(absolute value R sub lin (t)/83) to the 3/2 power, where R sub lin (t), also an alternating quantity, is a presumed underlying or linearized sunspot number. The nonlinearity is of such a nature as to cause strong semicycles to be sharper than sinusoidal and to produce the inflexion in R +/- (t) noted at sunspot minimum. A search for a physical explanation of a three-halves law reveals that just such a law results because large sunspot groups, such as occur around strong sunspot maxima, enter into the sunspot number, as conventionally defined, over more days than small groups, simply because large groups last longer. Semicycle asymmetry, which cannot result from a simple nonlinear law, is here ascribed to magnetic buoyancy acting preferentially on the antinodal layers of a traveling wave. Profiles for semicycles of different strengths have been constructed on the assumption that the underlying influence is sinusoidal. Each sinusoid is distorted by the three-halves law, and then made unsymmetrical by applying a buoyancy theory for magnetized plasma rising against viscous drag. The majority of past semicycles, including those of the 18th century, can be matched quite well by the artificial profiles, a conclusion that supports the idea of an underlying influence that is sinusoidal, and the hypothesis that sunspots result from an upward traveling wave from a submerged 22-year oscillator. GRA

N88-13211 Rice Univ., Houston, Tex.
MODEL OF SOLAR-WIND MAGNETOSPHERE COUPLING Ph.D. Thesis
Frank Rocco Toffoletto 1987 92 p
Avail: Univ. Microfilms Order No. DA8718773

The control of the strength and pattern of magnetospheric convection by the interplanetary magnetic field (IMF) is widely interpreted as evidence for magnetic interconnection between the IMF and the magnetosphere. A quantitative model of a magnetically interconnected magnetosphere is developed. The model is based on the perturbation of a closed magnetic field configuration with a given magnetopause geometry. The internal field is the results of a dipole field confined by Chapman Ferraro currents at the magnetopause and stretched on the nightside to produce a tail field. The external field is taken from a model based on gas dynamic supersonic flow around a blunt object with an embedded magnetic field. The normal component at the magnetopause must be time independent and it is derived from two different hypotheses of magnetopause merging. The interconnection field is derived as a solution to a Neuman boundary value problem consisting of Laplace's equation with the magnetopause normal component distribution as a boundary condition. The resulting open magnetospheric configuration is used to map magnetopause electric fields down to the ionosphere in the polar cap thus producing electrostatic potential contours. Dissert. Abstr.

N88-13212 Catholic Univ. of America, Washington, D.C.
OBSERVATIONS OF TURBULENCE AND FLUCTUATIONS IN THE SOLAR WIND Ph.D. Thesis
Laurence William Klein 1987 206 p
Avail: Univ. Microfilms Order No. DA8717096

The origin and evolution of the fluctuations in the heliosphere are examined using Voyager 1 and 2, and ISEE-3 measurements to study the evolution of solar wind plasma and magnetic field between heliocentric distances of 1 and 20 AU and to more than 25 deg in latitude above the ecliptic plane. Parker's 1958 solar wind model is found to be accurate within 5 percent in predicting the behavior of long term (solar rotation) averages in the interplanetary magnetic field when time dependencies in the bulk plasma speed are included. No evidence was found of flux loss in the outer heliosphere as reported recently in the literature. Methods of turbulence analysis are used to organize the observations and several predictions and expectations of ideal MHD turbulence theory are tested. Spectral indices expected for inertial range turbulence are present in much of spatial scales with increasing radial distance from the sun. Evidence for inverse cascade of magnetic helicity is observed in selected intervals, although, it was not found to be true in general in the solar wind. Dissert. Abstr.

N88-13095# Naval Research Lab., Washington, D.C. Center for Space Research.
FLUX TUBE DYNAMICS AND SOLAR/STELLAR REDSHIFT MEASUREMENTS Abstract Only
J. T. Mariska *In* Colorado Univ., 5th Cambridge Workshop on Cool Stars, Stellar Systems and the Sun Jul. 1987 1 p (For primary document see N88-13092 04-89)
Avail: NTIS HC A07/MF A01

N88-13109*# National Aeronautics and Space Administration. Goddard Space Flight Center, Greenbelt, Md.
THE ACCELERATION OF WINDS BY MHD WAVES IN OPEN MAGNETIC STRUCTURES Abstract Only
Joseph M. Davila *In* Colorado Univ., 5th Cambridge Workshop on Cool Stars, Stellar Systems and the Sun Jul. 1987 1 p (For primary document see N88-13092 04-89)
Avail: NTIS HC A07/MF A01 CSCL 03B

N88-13110# Hamburger Sternwarte (West Germany).
THE CLOSEST SOLAR ANALOGS IN THE BRIGHT STAR CATALOGUE Abstract Only
H. Neckel *In* Colorado Univ., 5th Cambridge Workshop on Cool Stars, Stellar Systems and the Sun Jul. 1987 1 p (For primary document see N88-13092 04-89)
Avail: NTIS HC A07/MF A01

N88-13111# Hamburger Sternwarte (West Germany).
ASYMMETRY AND VARIATIONS OF SOLAR LIMB DARKENING ALONG THE DIAMETER DEFINED BY DIURNAL MOTION IN APRIL 1981 Abstract Only
H. Neckel and D. Labs (Landessternwarte auf dem Koenigstuhl, Heidelberg, West Germany) *In* Colorado Univ., 5th Cambridge Workshop on Cool Stars, Stellar Systems and the Sun Jul. 1987 1 p (For primary document see N88-13092 04-89)
Avail: NTIS HC A07/MF A01

N88-13112# Naval Research Lab., Washington, D.C. Center for Space Research.
STATISTICAL PROPERTIES OF SMALL HIGH-VELOCITY EVENTS IN THE SOLAR TRANSITION REGION Abstract Only
J. W. Cook, P. A. Lund, J.-D. F. Bartoe, G. E. Brueckner, K. P. Dere, and D. G. Socker *In* Colorado Univ., 5th Cambridge Workshop on Cool Stars, Stellar Systems and the Sun Jul. 1987 1 p (For primary document see N88-13092 04-89)
Avail: NTIS HC A07/MF A01

N88-13113# Indian Inst. of Astrophysics, Bangalore.
CALIBRATION ON THE SUN FOR STELLAR MAGNETIC FIELDS Abstract Only
K. R. Sivaraman, S. P. Bagare, S. S. Gupta, and R. Kariyappa

In Colorado Univ., 5th Cambridge Workshop on Cool Stars, Stellar Systems and the Sun Jul. 1987 1 p (For primary document see N88-13092 04-89)
Avail: NTIS HC A07/MF A01

N88-13114# Colorado Univ., Boulder.
SIMULTANEOUS, COSPATIAL IMAGING OF THE SUN IN CYANOGEN AND SINGLY-IONIZED CALCIUM Abstract Only
Thomas R. Ayres and Laurence J. November (National Solar Observatory, Sunspot, N. Mex.) *In its* 5th Cambridge Workshop on Cool Stars, Stellar Systems and the Sun Jul. 1987 1 p (For primary document see N88-13092 04-89)
(Grant NSF AST-85-07029)
Avail: NTIS HC A07/MF A01

N88-13115# Kiepenheuer-Inst. fuer Sonnenphysik, Freiburg (West Germany).
VARIATIONS OF THE VERTICAL AND HORIZONTAL VELOCITIES OF THE SMALL-SCALE STRUCTURES AND THE PHYSICAL PROBLEMS RELATED TO OVERSHOOT LAYERS Abstract Only
Anastasios Nesis and Giuseppe Severino (Osservatorio Astronomico, Capodimonte, Naples, Italy) *In* Colorado Univ., 5th Cambridge Workshop on Cool Stars, Stellar Systems and the Sun Jul. 1987 1 p (For primary document see N88-13092 04-89)
Avail: NTIS HC A07/MF A01

N88-13116# Joint Inst. for Lab. Astrophysics, Boulder, Colo.
CALIBRATION OF THE Ca II K LINE-CORE DENSITY AND THE MAGNETIC FLUX DENSITY IN STARS USING SOLAR DATA Abstract Only
C. J. Schrijver and J. Cote (Laboratorium voor Ruimteonderzoek, Utrecht, Netherlands) *In* Colorado Univ., 5th Cambridge Workshop on Cool Stars, Stellar Systems and the Sun Jul. 1987 1 p (For primary document see N88-13092 04-89)
Avail: NTIS HC A07/MF A01

N88-13118# Heidelberg Univ. (West Germany). Inst. fuer Theoretische Astrophysik.
THE DYNAMICS OF SOLAR MAGNETIC FLUX TUBES SUBJECTED TO RESONANT FOOT POINT SHAKING Abstract Only
Peter Ulmschneider and Kurt Zaehringer *In* Colorado Univ., 5th Cambridge Workshop on Cool Stars, Stellar Systems and the Sun Jul. 1987 1 p (For primary document see N88-13092 04-89)
Avail: NTIS HC A07/MF A01

N88-13119# Armagh Observatory (Northern Ireland).
ACTIVE PHASES ON II PEG Abstract Only
P. Panagi and J. G. Doyle *In* Colorado Univ., 5th Cambridge Workshop on Cool Stars, Stellar Systems and the Sun Jul. 1987 1 p (For primary document see N88-13092 04-89)
Avail: NTIS HC A07/MF A01

93 SPACE RADIATION

Includes cosmic radiation; and inner and outer earth's radiation belts.

For biological effects of radiation see *52 Aerospace Medicine*. For theory see *73 Nuclear and High-Energy Physics*.

N88-13213# Centro Brasileiro de Pesquisas Fisicas, Rio de Janeiro.
COSMIC-RAY NUCLEAR EVENT WITH AN ANOMALOUSLY STRONG CONCENTRATION OF ENERGY AND PARTICLES IN THE CENTRAL REGION
N. M. Amato, N. Arata, and R. H. C. Maldonado 1986 20 p (DE87-703376; CBPF-NF-056/86) Avail: NTIS (US Sales Only) HC A03/MF A01

A cosmic-ray induced nuclear event detected in the emulsion chamber is described. The event consists of 217 shower cores with Sigma E sub gamma = 1,275 TeV. In log scale, energy and particles are emitted most densely at the small lateral distance corresponding to 0.5 mm; 77% of the total energy and 61% of the total multiplicity are inside the radius of 0.65 cm. The shower cores in the central region show exponential-type energy distribution and non-isotropic azimuthal distribution. This event indicates a possibility that phenomena of large transverse momentum could produce a strong concentration of energy and particles in the very forward direction. DOE

N88-13214 Rice Univ., Houston, Tex.
GAMMA RAY LINES FROM NOVAE Ph.D. Thesis
Mark D. Leising 1987 119 p
Avail: Univ. Microfilms Order No. DA8718741

The potential for observing gamma ray line emission from novae--a unique signature of thermonuclear runaway models--is investigated. Simple models of the expansion of the nova atmospheres are evolved. These models yield the physical conditions of the outer atmospheres which serve as input to investigations into the fate of the positrons and the transfer of the photons. The latter is accomplished with Monte Carlo simulations of the photon histories. The resulting estimates suggest that nearby fast novae could yield detectable fluxes of annihilation gamma rays from positrons produced by decay of N-13 and F-18. It seems less likely that detectable fluxes of de-excitation photons would escape the nova atmosphere at early times, though significant quantities of long-lived nuclei might be produced (i.e., Na-22 and Al-26) and yield characteristic gamma rays from the accumulation of the radioactive debris of many novae. Thus novae appear to be a prime target for the Oriented Scintillation Spectrometer Experiment on Gamma Ray Observatory and to offer a potential for the use of the Solar Maximum Mission Gamma Ray Spectrometer as an astronomical observatory.
Dissert. Abstr.

N88-13096# Colorado Univ., Boulder. Dept. of Astrophysical, Planetary and Atmospheric Sciences.
NONTHERMAL PHENOMENA IN STELLAR CORONAE: EVIDENCE FROM RADIO OBSERVATIONS Abstract Only
George A. Dulk *In its* 5th Cambridge Workshop on Cool Stars, Stellar Systems and the Sun Jul. 1987 1 p (For primary document see N88-13092 04-89)
Avail: NTIS HC A07/MF A01

N88-13121# Laboratorium voor Ruimteonderzoek, Utrecht (Netherlands).
A LARGE X-RAY FLARE ON SQUARED SIGMA CORONAE BOREALIS OBSERVED WITH EXOSAT Abstract Only
G. H. J. vandenOord, R. Mewe, and A. C. Brinkman *In* Colorado Univ., 5th Cambridge Workshop on Cool Stars, Stellar Systems and the Sun Jul. 1987 1 p (For primary document see N88-13092 04-89)
Avail: NTIS HC A07/MF A01

N88-13160# ST Systems Corp., Lanham, Md.
RADIO CONTINUUM EMISSION FROM THE IONIZED STELLAR WINDS OF THE COOL SUPERGIANTS IN ZETA AURIGAE-LIKE SYSTEMS Abstract Only
Stephen A. Drake, Alexander Brown, and Dieter Reimers (Hamburger Sternwarte, West Germany) *In* Colorado Univ., 5th Cambridge Workshop on Cool Stars, Stellar Systems and the Sun Jul. 1987 1 p (For primary document see N88-13092 04-89)
Avail: NTIS HC A07/MF A01

N88-13191# Colorado Univ., Boulder.
RADIO EMISSION FROM RS CVn BINARIES: A 5 GHz VLA SURVEY OF 93 SYSTEMS Abstract Only
D. H. Morris and R. L. Mutel *In its* 5th Cambridge Workshop on Cool Stars, Stellar Systems and the Sun Jul. 1987 1 p (For primary document see N88-13092 04-89)
Avail: NTIS HC A07/MF A01

99 GENERAL

No abstracts in this category.

Typical Subject Index Listing

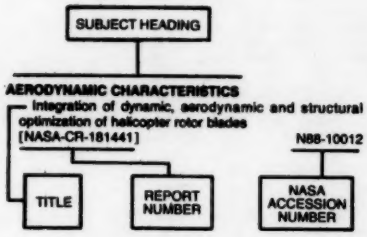

The subject heading is the key to the subject content of the document. Titles, report numbers, and accession numbers of pertinent documents are provided under each subject heading. When the title is insufficiently descriptive of the document content, a title extension has been added, separated from the title by three hyphens. The report number helps to indicate the type of document cited (e.g., NASA report, NASA translation, NASA contractor report). The NASA accession number is the number by which the document abstracts are arranged in this journal and by which the document is sold or requested. The titles, with title extensions if present, are arranged under each subject heading in ascending accession number order. The subject headings have been selected from the latest revision of the *NASA Thesaurus* (NASA SP-7053).

A

ABSORPTION COOLING
Technical evaluation of a solar-powered absorption cooling system (LiBr-H2O)
[PB87-108254] N88-12867
Design and development of absorption heat pumps
[DE88-000062] N88-12885

ABSORPTION SPECTRA
Far infrared Fourier transform spectroscopy of semiconductors
[DE88-000188] N88-13072
Titanium oxide absorption and spot sizes in II Peg, HR 1099 and UX Ari N88-13126
A flash spectrum of Cl I, C I, N I, and Ni II absorption in 31 Cygni: A direct observation of the reversing layer N88-13158
Sensitivity of the H alpha line to expansion, geometrical extent and temperature gradient in the G and K supergiant chromosphere N88-13159
IUE observations of the hybrid K3 II star Iota Aurigae and constraints on the outer atmospheric structure N88-13171

ABSORPTIVITY
Thermal stress in the edge cladding of Nova glass laser disks
[DE88-000425] N88-12780

ABSTRACTS
FY 1985 scientific and technical reports, articles, papers and presentations
[NASA-TM-88521] N88-13083

ABUNDANCE
Carbon abundances and C12/C13 ratios in M giants N88-13167
Infrared excesses of barium stars N88-13174
Galactic interstellar abundance surveys with IUE and IRAS N88-13206

ACCELERATION TOLERANCE
F-16 control stick response during +Gz-induced loss of consciousness
[AD-A184107] N88-12491

ACCELERATORS
GOLD: Integration of model-based control systems with artificial intelligence and workstations
[DE88-000506] N88-12976
GOLD: Integration of model-based control systems with artificial intelligence and workstations
[DE88-000706] N88-12977

ACCIDENTS
Structural analysis of a bolted joint concept for the space shuttle's solid rocket motor casing
[NASA-TM-89092] N88-12531

ACCRETION DISKS
Disk accretion during the early stages of stellar evolution N88-13106
The contribution of accretion luminosity to the infrared spectra of T Tauri stars: A possible test N88-13183

ACCURACY
Dynamic positioning at sea using the global positioning system
[AD-A184453] N88-12476
Optimization of dilatometer test procedures
[DE87-014998] N88-12769
Accuracy potential of non-metric cameras in close-range photogrammetry N88-12862
Lower bounds on bearing accuracy for closely spaced sources
[AD-A184258] N88-12997

ACETONE
Characterization of catalysts with metal-support effects and of the species adsorbed on their surfaces
[DE87-014836] N88-12584

ACIDS
Corrosion strength of niobium and its alloys
[DE87-703693] N88-12578

ACOUSTIC EMISSION
Development of an acoustic emission monitor and monitoring techniques for long-term monitoring of U-0.8Ti electron-beam weldments for postweld cracking
[DE88-000819] N88-12804

ACOUSTIC VELOCITY
Noncontact temperature measurements of hot steel bodies using an electromagnetic acoustic transducer (EMAT)
[DE88-000560] N88-12765
Coupled acoustic and ocean thermodynamic model
[AD-A184357] N88-12911

ACOUSTICS
Excitation of natural oscillations of a boundary layer by an external acoustic field N88-12634
Nonlinear acoustics
[AD-A184271] N88-13004

ACTUATORS
An evaluation plan of bus architectures and protocols using the NASA Ames intelligent redundant actuation system
[NASA-CR-177458] N88-12482

ADA (PROGRAMMING LANGUAGE)
PROVER: A first-order logic system in Ada
[DE88-000220] N88-12951
A review and analysis of Fortran 8x
[DE88-001320] N88-12955

ADDITIVES
Mechanical properties of an acicular ferrite steel microalloyed to niobium and vanadium
[DE87-703547] N88-12574
Partial substitution of vanadium by niobium in AISI H13 steel
[DE87-703548] N88-12575
Analysis of free cutting brass by A.C. polarography
[PD-MT-8728] N88-12587

ADHESION
Interfacial strength development in thermoplastic resins and fiber-reinforced thermoplastic composites
[NASA-CR-181525] N88-12549

ADMIXTURES
Structure of stably stratified atmospheric surface layer in presence of heat-releasing admixture N88-12856

ADSORPTION
Characterization of catalysts with metal-support effects and of the species adsorbed on their surfaces
[DE87-014836] N88-12564
The structure of adsorbed sulfur and carbon on molybdenum and rhenium single crystal surfaces, and their influence on carbon monoxide and hydrocarbon chemisorption
[DE88-001393] N88-13073

AERODYNAMIC CHARACTERISTICS
Planform effects on the supersonic aerodynamics of multibody configurations
[NASA-TP-2762] N88-12454
A method for the efficient calculation of elastic rotor blade dynamic response in forward flight N88-12460
An integrated study of structures, aerodynamics and controls on the forward swept wing X-29A and the oblique wing research aircraft
[NASA-CR-181548] N88-12486
Calculation of aerodynamic characteristics of three-dimensional finite span wings in potential incompressible flow N88-12631
Conical wing with maximum lift-to-drag ratio in supersonic gas flow N88-12633

AERODYNAMIC COEFFICIENTS
Semiempirical method for prediction of aerodynamic forces and moments on a steadily spinning light airplane
[NASA-TM-4009] N88-12456
Aerodynamic sensitivities from subsonic, sonic and supersonic unsteady, nonplanar lifting-surface theory
[NASA-TM-100502] N88-12459

AERODYNAMIC DRAG
Planform effects on the supersonic aerodynamics of multibody configurations
[NASA-TP-2762] N88-12454
Numerical study of supersonic flow around blunt bodies with extended needle nose N88-12635

AERODYNAMIC FORCES
Semiempirical method for prediction of aerodynamic forces and moments on a steadily spinning light airplane
[NASA-TM-4009] N88-12456

AERODYNAMIC HEATING
The aerodynamics of supersonic parachutes
[DE87-014846] N88-12464
Parachute materials
[DE87-014845] N88-12550

AERODYNAMIC INTERFERENCE
A 0.15-scale study of configuration effects on the aerodynamic interaction between main rotor and fuselage
[NASA-CR-166577] N88-12462

AERODYNAMIC STABILITY
Effects of jet exhaust yaw vane installation and operation on the longitudinal and lateral-directional characteristics of the F-14 airplane
[NASA-TP-2769] N88-12455

AERODYNAMIC STALLING
Measurements and calculations of aerodynamic torques for a vertical-axis wind turbine
[DE88-001783] N88-12878

AERODYNAMICS
Aeronautical engineering: A continuing bibliography with indexes (supplement 219)
[NASA-SP-7037(219)] N88-12470

AEROELASTICITY
The effect of mass, wind angle and erection technique on the aeroelastic behaviour of a cable-stayed bridge model
[NAE-AN-46] N88-12619

AERONAUTICAL ENGINEERING
Aeronautical engineering: A continuing bibliography with indexes (supplement 219)
[NASA-SP-7037(219)] N88-12470
JPRS report: Science and technology. Japan
[JPRS-JST-87-025] N88-12502
USSR report: Engineering and equipment
[JPRS-UEQ-87-006] N88-12621

AEROSOLS
Plume mechanics and aerosol growth processes
[AD-A184467] N88-12742
Thermophoresis of spherical aerosol particle at arbitrary Knudsen numbers N88-12850

Theory of heat and moisture exchange between finely disperse storm-generated spray and turbulent air flow N88-12851

Multiwave laser soundings of atmospheric aerosol: Experimental research (review) N88-12852

Structure of stably stratified atmospheric surface layer in presence of heat-releasing admixture N88-12856

AEROSPACE ENGINEERING

Numerical simulation system N88-12511

AEROSPACE MEDICINE

Motion and space sickness N88-12510

JPRS report: Science and technology. USSR: Life sciences
[JPRS-ULS-87-009] N88-12915

Study of certain biological characteristics of bacteria during the French-Soviet CYTOS-2 space experiment N88-12917

Aerospace medicine and biology: A continuing bibliography with indexes
[NASA-SP-7011(304)] N88-12922

Human respiratory responses during high performance flight
[AGARD-AG-312] N88-12923

AEROSPACE SYSTEMS

An approach to implementing state space searches on heterogeneous systems of multiprocessors
[DE88-001321] N88-12967

AGING (MATERIALS)

PRAAGE: An interactive IBM-PC code for unreliability/aging analysis
[DE87-012124] N88-12803

AGING (METALLURGY)

The aging behavior of types 308 and 308CRE stainless steels and its effect on mechanical properties
[DE87-012541] N88-12590

AGRICULTURE

JPRS report: Science and technology. USSR: Life sciences
[JPRS-ULS-87-009] N88-12915

AIR

The atomic weight and isotopic composition of oxygen and their variation in nature
[DE87-014307] N88-12558

AIR COOLING

National Aerospace Laboratory experiment N88-12509

AIR DROP OPERATIONS

Developmental airdrop testing techniques and devices
[AGARD-AG-300-VOL-6] N88-12481

AIR FLOW

National Aerospace Laboratory experiment N88-12509

AIR POLLUTION

Aircraft engine exhaust plume dynamics
[AD-A184238] N88-12488

Emerging environmental constraints on the use of gasoline and diesel fuel and tradeoffs associated with the use of alternative fuels
[DE87-011504] N88-12614

AIR QUALITY

Aircraft engine exhaust plume dynamics
[AD-A184238] N88-12488

AIR TRAFFIC CONTROL

Experimental use of artificial intelligence for (future) ATC systems
[PB87-106449] N88-12970

AIR WATER INTERACTIONS

Influence of stratification in near-surface water layer on intensity of gas exchange between atmosphere and water N88-12841

Studies of thin surface films aim at seeing deep ocean processes N88-12847

Theory of heat and moisture exchange between finely disperse storm-generated spray and turbulent air flow N88-12851

Interactions between the Asian monsoons, the tropical Pacific and the southern hemisphere extratropics N88-12907

AIRBORNE EQUIPMENT

Study of an airborne Doppler radar: Project Asterix
[BLL-MO-TRANS-1667-(9022.552)] N88-12675

AIRCRAFT ACCIDENTS

Aircraft fire safety research N88-12526

AIRCRAFT COMPARTMENTS

Aircraft fire safety research N88-12526

AIRCRAFT CONFIGURATIONS

Planform effects on the supersonic aerodynamics of multibody configurations
[NASA-TP-2782] N88-12454

A 0.15-scale study of configuration effects on the aerodynamic interaction between main rotor and fuselage
[NASA-CR-166577] N88-12462

AIRCRAFT CONTROL

Effects of jet exhaust yaw vane installation and operation on the longitudinal and lateral-directional characteristics of the F-14 airplane
[NASA-TP-2769] N88-12455

An integrated study of structures, aerodynamics and controls on the forward swept wing X-29A and the oblique wing research aircraft
[NASA-CR-181548] N88-12486

AIRCRAFT DESIGN

Flap-lag equations of motion of rigid, articulated rotor blades with three hinge sequences
[NASA-TM-100023] N88-12495

A reliability concept for optimizing aircraft design N88-12622

Renewed interest in airships for industry use discussed N88-12628

AIRCRAFT ENGINES

Aircraft engine exhaust plume dynamics
[AD-A184238] N88-12488

Aircraft classification by type of propulsive devices. Determination of type and number of carrying solutions N88-12626

Dynamics of reverse flows at pump inlet N88-12636

Calculation of the tribological properties of surfaces by semi-empirical methods
[AD-A184283] N88-12791

AIRCRAFT EQUIPMENT

NAVSIM 2: A computer program for simulating aided-inertial navigation for aircraft
[NASA-CR-177456] N88-12478

AIRCRAFT GUIDANCE

Some data processing requirements for precision Nap-Of-the-Earth (NOE) guidance and control of rotorcraft
[NASA-CR-177453] N88-12493

AIRCRAFT HAZARDS

Aircraft fire safety research N88-12526

AIRCRAFT MANEUVERS

Developmental airdrop testing techniques and devices
[AGARD-AG-300-VOL-6] N88-12481

AIRCRAFT NOISE

Results of the 1986 NASA/FAA/DFVLR main rotor test entry in the German-Dutch wind tunnel (DNW)
[NASA-TM-100507] N88-13003

Aircraft interior noise reduction by alternate resonance tuning
[NASA-CR-181550] N88-13005

AIRCRAFT PILOTS

Human respiratory responses during high performance flight
[AGARD-AG-312] N88-12923

AIRCRAFT SAFETY

Experimental evidence for modifying the current physical model for ice accretion on aircraft surfaces
[NASA-TM-87184] N88-12473

AIRCRAFT STABILITY

Local-optimal control in systems with delay N88-12627

AIRCRAFT STRUCTURES

A reliability concept for optimizing aircraft design N88-12622

Aircraft dynamic response calculation based on discrete-continual model N88-12624

Aircraft classification by type of propulsive devices. Determination of type and number of carrying solutions N88-12626

AIRFOILS

Investigation of low-speed turbulent separated flow around airfoils
[NASA-CR-177450] N88-12471

NCSU code: Validation and extension on NAL's UNIVAC 1100/60 system
[PD-FM-8716] N88-12931

Measurement of velocity and vorticity fields in the wake of an airfoil in periodic pitching motion
[NASA-TP-2780] N88-13002

AIRFRAMES

Reduced complexity structural modeling for automated airframe synthesis
[NASA-CR-177440] N88-12453

AIRSHIPS

Renewed interest in airships for industry use discussed N88-12628

ALDEHYDES

Characterization of catalysts with metal-support effects and of the species adsorbed on their surfaces
[DE87-014636] N88-12584

ALGORITHMS

Solution of the two-dimensional Euler equations on unstructured triangular meshes N88-12469

Two dimensional path planning with obstacles and shadows
[AD-A184075] N88-12474

Autonomous Land Vehicle (ALV) planning and navigation system
[AD-A184243] N88-12475

GPS vertical axis performance enhancement for helicopter precision landing approach
[NASA-CR-177443] N88-12477

New feedback design methodologies for large space structures: A multi-criterion optimization approach N88-12535

On M-ARY sequential hypotheses testing for the classification of radar signals
[AD-A184094] N88-12666

Design of source coders and joint source/channel coders for noisy channels
[NASA-CR-181547] N88-12678

A simplified procedure for correcting both errors and erasures of a Reed-Solomon code using the Euclidean algorithm N88-12698

On the VLSI design of a pipeline Reed-Solomon decoder using systolic arrays N88-12700

A modern control theory based algorithm for control of the NASA/JPL 70-meter antenna axis servos N88-12706

Programmable Logic Arrays (PLA's) design for testability
[PB87-102935] N88-12718

Studies of pressure-velocity coupling schemes for analysis of incompressible and compressible flows
[NASA-CR-181526] N88-12748

Optimization of explicit time-stepping algorithms and Stream-Function-Coordinate (SFC) concept for fluid dynamics problems N88-12762

Tracking through turbulence at the Tonopah Test Range
[DE88-001448] N88-12766

An algorithmic approach to crustal deformation analysis N88-12891

Coupled acoustic and ocean thermodynamic model
[AD-A184357] N88-12911

Comparing barrier algorithms
[NASA-CR-178377] N88-12934

A tight upper bound for the speed-up of parallel best-first branch-and-bound algorithms
[AD-A184246] N88-12939

A characterization of separating pairs and triplets in a graph
[AD-A184278] N88-12941

Numerical studies of the dual HEMT/algorithm development and numerical studies of Schrodinger's equation
[AD-A184471] N88-12948

Statistical inference: Computer oriented algorithmic approach
[DE87-013874] N88-12948

Methods for design and evaluation of integrated hardware/software systems for concurrent computation
[NASA-CR-181522] N88-12953

Parallelization of hydrocodes on the Intel Hypercube, part 2
[DE88-001591] N88-12957

Development of the non-equilibrium reactive chemical transport code CHMTRNS
[DE88-000882] N88-12964

On operator splitting for unsteady boundary value problems
[AD-A184281] N88-12981

A comparison of adaptive refinement techniques for elliptic problems
[DE88-000805] N88-12987

The finite element method for electronic structure
[DE88-001706] N88-12989

ALIGNMENT

Carbon-fiber reinforced plastics N88-12506

Optical alignment of Centaur's inertial guidance system
[NASA-TM-88844] N88-12515

ALKALI METALS

Valence bond cluster studies of alkali metal/semiconductor bonding
[AD-A184276] N88-13054

Tetrahedral carbon and interstitial electrons in Li cluster: CLi4 and (LiCH3)4
[AD-A184277] N88-13055

ALKALINITY

Corrosion strength of niobium and its alloys
[DE87-703693] N88-12578

ALKYL COMPOUNDS

Surface catalytic degradation study of two linear perfluoropolyalkylethers at 345 C
[NASA-TP-2774] N88-12543

ALLOYS

Progress in the development of niobium alloyed high speed steel
[DE87-703549] N88-12578

An expert system for materials design
[DE88-000191] N88-12974

ALPHA PARTICLES
Theoretical plasma physics
[DE88-001475] N88-13029
PG 0308 + 096: A short-period white dwarf + dM binary with strongly modulated H-alpha emission N88-13132
ALTERNATING CURRENT
Output power enhancement of AC Raman free-electron laser
[DE88-000503] N88-12786
ALTIMETRY
Considering refraction in leveling with laser plane N88-12857
ALTITUDE TESTS
Measured performance of the heat exchanger in the NASA icing research tunnel under severe icing and dry-air conditions
[NASA-TM-100116] N88-12796
ALUMINUM
Carbon-fiber reinforced aluminum N88-12507
Data base on the high heat flux behaviour of metals and carbon materials for plasma facing components: Experiments at the 10 MW neutral beam injection test stand of the IPP Nagoya
[IPPJ-AM-53] N88-13031
Microstructural change of Al on H implantation
[IPPJ-847] N88-13036
ALUMINUM ALLOYS
Corrosion behavior of P/M mechanically alloyed IN-9052.1: An electro-chemical investigation
[AD-A184191] N88-12567
Weldability of 2219-T851 and 2519-T87 aluminum armor alloys for use in Army vehicle systems
[AD-A184296] N88-12792
ALUMINUM CARBIDES
Research and development on high strength ceramic heaters discussed N88-12508
ALUMINUM GALLIUM ARSENIDES
Numerical studies of the dual HEMT/algorithm development and numerical studies of Schrodinger's equation
[AD-A184471] N88-12946
ALUMINUM OXIDES
Studies of alumina additions in zirconia - magnesia
[DE87-703500] N88-12602
AMMONIUM PERCHLORATES
Equilibrium calculations of ionization in tracer flames
[PB87-104154] N88-12555
AMMUNITION
Thermoplastic elastomers as LOVA (Low Vulnerability Ammunition) binders
[AD-A184350] N88-12599
AMPLIFICATION
Increased gain of channel intensifier tubes by pulsed biasing
[DE88-000512] N88-13019
AMPLIFIERS
Traveling-wave maser closed-cycle refrigerator data acquisition and display system N88-12708
Power density measurements in the near field of the DSS 13 26-meter antenna N88-12711
AMPLITUDE MODULATION
Fast autotuning of a hydrogen maser by cavity Q modulation N88-12707
AMPLITUDES
The giant spot on II Peg in 1986 N88-13120
ANECHOIC CHAMBERS
New main reflector, subreflector and dual chamber concepts for compact range applications
[NASA-CR-181506] N88-12498
ANGLE OF ATTACK
Optimum take-off run of aircraft on ground airfields N88-12623
ANGULAR MOMENTUM
Angular momentum evolution of young stars N88-13099
Post-zero-age main sequence rotation N88-13100
ANGULAR RESOLUTION
New results from high angular resolution observations of alpha Ori N88-13161
The angular diameter of alpha Scorpii in the near-infrared Ca II triplet N88-13162
ANGULAR VELOCITY
Spin-up and spin-down on the way to the main sequence N88-13181
ANISOTROPIC PLATES
A refined nonlinear analysis of laminated composite plates and shells
[AD-A184436] N88-12811
ANISOTROPIC SHELLS
A refined nonlinear analysis of laminated composite plates and shells
[AD-A184436] N88-12811
ANISOTROPY
Experimental perspectives on heavy electron metals
[DE87-014766] N88-12583
Structure of thermotropic polyesters with large substituents
[AD-A184086] N88-12595
ANNEALING
On the stressing of annealed NITINOL: The electrical resistance and calorimetric effects
[AD-A184465] N88-12569
ANNULAR PLATES
A finite element procedure for interference-fit and cold-working problems with limited yielding
[AR-004-517] N88-12992
ANODES
Impedance of passive lithium anodes in SOCl2 solutions under low-field polarization
[DE88-000922] N88-12728
Internal reforming development for solid oxide fuel cells
[DE87-006518] N88-12871
ANOMALIES
Failure control techniques for the SSME
[NASA-CR-179224] N88-12537
J = O Task Force
[DE88-001326] N88-12788
On the interannual variability of South American climate and the Southern Oscillation N88-12905
ANTENNA ARRAYS
Analysis of the ICE combiner for multiple antenna arraying N88-12704
ANTENNA DESIGN
New main reflector, subreflector and dual chamber concepts for compact range applications
[NASA-CR-181506] N88-12498
Band 2 VHF antenna for home construction
[BBC-RD-1987/13] N88-12677
ANTENNA RADIATION PATTERNS
New main reflector, subreflector and dual chamber concepts for compact range applications
[NASA-CR-181506] N88-12498
ANTIBIOTICS
Study of certain biological characteristics of bacteria during the French-Soviet CYTOS-2 space experiment N88-12917
ANTIFERROMAGNETISM
Experimental perspectives on heavy electron metals
[DE87-014766] N88-12583
APERTURES
An excitation-term modification for a certain class of electromagnetic aperture-coupling problems
[DE88-000260] N88-12713
APPLICATIONS PROGRAMS (COMPUTERS)
Solution of the two-dimensional Euler equations on unstructured triangular meshes N88-12469
An integrated study of structures, aerodynamics and controls on the forward swept wing X-29A and the oblique wing research aircraft
[NASA-CR-181548] N88-12486
Microgravity nucleation and particle coagulation experiments support
[NASA-CR-181540] N88-12618
Higher order theory analysis of a modified free-edge delamination specimen N88-12620
Applications of the hybrid automated reliability predictor
[NASA-TP-2760] N88-12928
The ISI (Information Sciences Institute) grapher: A portable tool for displaying graphs pictorially
[AD-A184354] N88-12944
Methods for design and evaluation of integrated hardware/software systems for concurrent computation
[NASA-CR-181522] N88-12953
Monocrystal sputtering by the computer simulation code ACOCT
[IPPJ-848] N88-13035
Cosmological applications of singular hypersurfaces in general relativity N88-13202
APPROACH
GPS vertical axis performance enhancement for helicopter precision landing approach
[NASA-CR-177443] N88-12477
Effect of motion cues during complex curved approach and landing tasks: A piloted simulation study
[NASA-TP-2773] N88-12480
APPROXIMATION
Finite deformations of shell with rigid inclusion N88-12639
Solution of three-dimensional inverse problem of gravimetry in contact surfaces class by local corrections method N88-12648
An adaptive subdivision method with crack prevention for rendering beta-spline objects
[AD-A184249] N88-12940
Back-of-the-envelope problems
[AD-A184105] N88-12980
ARC WELDING
The nature of metallurgical reactions in underwater welding
[AD-A184464] N88-12568
ARCHITECTURE (COMPUTERS)
Autonomous Land Vehicle (ALV) planning and navigation system
[AD-A184243] N88-12475
An evaluation plan of bus architectures and protocols using the NASA Ames intelligent redundant actuation system
[NASA-CR-177458] N88-12482
Programmable real-time digital video image processing
[PB87-104162] N88-12661
On the VLSI design of a pipeline Reed-Solomon decoder using systolic arrays N88-12700
Research in VLSI (Very Large Scale Integration) systems
[AD-A184089] N88-12721
Center for Supercomputing Research and Development (CEDAR)
[DE88-000807] N88-12930
Methods for design and evaluation of integrated hardware/software systems for concurrent computation
[NASA-CR-181522] N88-12953
Parallelization of hydrocodes on the Intel Hypercube, part 2
[DE88-001501] N88-12957
ARCTIC REGIONS
Huurre expedition to the North Pole in 1984
[PB87-220935] N88-12858
Disturbance and recovery of Arctic Alaskan tundra terrain. A review of recent investigations
[AD-A184442] N88-12867
ARMOR
Weldability of 2219-T851 and 2519-T87 aluminum armor alloys for use in Army vehicle systems
[AD-A184296] N88-12792
ARRAYS
Programmable Logic Arrays (PLA's) design for testability
[PB87-102935] N88-12718
Chemically modified microelectrode arrays. New kinds of electronic devices
[AD-A184389] N88-12724
ARTIFICIAL INTELLIGENCE
A tight upper bound for the speed-up of parallel best-first branch-and-bound algorithms
[AD-A184246] N88-12939
Experimental use of artificial intelligence for (future) ATC systems
[PB87-106449] N88-12970
An expert system for materials design
[DE88-000191] N88-12974
A model of functional knowledge and insight
[AD-A184113] N88-12975
GOLD: Integration of model-based control systems with artificial intelligence and workstations
[DE88-000506] N88-12976
GOLD: Integration of model-based control systems with artificial intelligence and workstations
[DE88-000706] N88-12977
ASTROMETRY
Phase-coherent astrometric interferometry
[AD-A184428] N88-12725
An astrometric search for a stellar companion to the sun N88-13195
ASTRONOMICAL CATALOGS
Catalogue of chromospherically active binaries N88-13192
ASTRONOMICAL MODELS
A re-examination of the corona-wind dividing line: Diagnostics of non-coronal atmospheres N88-13101
The acceleration of winds by MHD waves in open magnetic structures N88-13109
Large scale solar and stellar magnetic fields N88-13117
ASTRONOMICAL OBSERVATORIES
A near-earth optical communications terminal with a corevolving planetary sun shield N88-12693
Automatic telescope operations N88-13190
ASTRONOMICAL PHOTOGRAPHY
A search for X-ray luminous late type stars in NIPSS data N88-13143
ASTRONOMICAL PHOTOMETRY
Automatic telescope operations N88-13190
ASTRONOMICAL TELESCOPES
Automatic photometric monitoring of cool stars N88-13103
Statistical properties of small high-velocity events in the solar transition region N88-13112
Automatic telescope operations N88-13190
ASTROPHYSICS
Calibration on the Sun for stellar magnetic fields N88-13113

Variations of the vertical and horizontal velocities of the small-scale structures and the physical problems related to overshoot layers N88-13115
Influences of the astrophysical environment on nuclear decay rates
[DE88-001461] N88-13208
ASYMMETRY
Two classes of preconditioners computed using block matrix factorization techniques
[DE88-001313] N88-12988
Asymmetry and variations of solar limb darkening along the diameter defined by diurnal motion in April 1981 N88-13111
ASYMPTOTIC SERIES
Asymptotic form of stationary solutions of the Navier-Stokes equations for large Reynolds numbers N88-12838
ATLANTIC OCEAN
On the interannual variability of South American climate and the Southern Oscillation N88-12905
ATMOSPHERIC ATTENUATION
Absorption of far IR-radiation by H2O-N2 complexes under atmospheric conditions N88-12855
ATMOSPHERIC BOUNDARY LAYER
Heat and moisture transport in the atmospheric boundary layer
[AD-A184222] N88-12904
ATMOSPHERIC CHEMISTRY
The effects of minor trace gases on the transfer of thermal infrared radiation through the Earth's atmosphere N88-12893
ATMOSPHERIC CIRCULATION
Heat and moisture transport in the atmospheric boundary layer
[AD-A184222] N88-12904
ATMOSPHERIC COMPOSITION
Spacecraft Fire Safety
[NASA-CP-2478] N88-12520
Inerting and atmospheres N88-12524
Fire-related medical science N88-12525
Spacecraft material flammability testing and configurations N88-12529
ATMOSPHERIC EFFECTS
The atmosphere of Mars and optical communications N88-12692
Considering refraction in leveling with laser plane N88-12857
ATMOSPHERIC HEATING
Structure of stably stratified atmospheric surface layer in presence of heat-releasing admixture N88-12856
Flux tube dynamics and solar/stellar redshift measurements N88-13095
Observational constraints and evidence for saturation N88-13097
Heating of stellar chromospheres and coronae: Evidence for non-magnetic basal heating N88-13098
Atmospheres of stars in the limits of thin and thick convection zones: The M dwarfs N88-13104
Magnetic flux tubes as sources of wave generation N88-13108
Statistical properties of small high-velocity events in the solar transition region N88-13112
ATMOSPHERIC MODELS
Structure of stably stratified atmospheric surface layer in presence of heat-releasing admixture N88-12856
Banded ion morphology N88-12892
User's guide to NCAR (National Center for Atmospheric Research) CCM1
[PB87-224386] N88-12899
A review of parameterizations of microphysical processes in clouds for application in models of regional atmospheric deposition
[DE88-000451] N88-12909
Application of dynamic atmosphere models to the analysis of angular diameter observations of Mira variables N88-13168
ATMOSPHERIC MOISTURE
Lidar-radiometric method for determining liquid-water content of cirrus clouds N88-12854
ATMOSPHERIC PHYSICS
USSR report: Earth sciences
[JPRS-UES-88-006] N88-12831
ATMOSPHERIC PRESSURE
On the interannual variability of South American climate and the Southern Oscillation N88-12905
ATMOSPHERIC REFRACTION
Microwave refractive index structure function profiles (Cn2) measured from a small aircraft
[AD-A184343] N88-12670
Use of electron beam instruments to determine fluctuations in vertical refraction partial angle N88-12853
Considering refraction in leveling with laser plane N88-12857
ATMOSPHERIC SOUNDING
Multiwave laser soundings of atmospheric aerosol: Experimental research (review) N88-12852
ATMOSPHERIC STRATIFICATION
General theory of radio propagation through a stratified atmosphere
[PB87-226197] N88-12662
Structure of stably stratified atmospheric surface layer in presence of heat-releasing admixture N88-12856
ATMOSPHERIC TURBULENCE
The atmosphere of Mars and optical communications N88-12692
ATOMIC COLLISIONS
Final (n,l) state-resolved electron capture by multiply charged ions from neutral atoms
[IPPJ-AM-54] N88-13030
Monocrystal sputtering by the computer simulation code ACOCT
[IPPJ-848] N88-13035
ATOMIC ENERGY LEVELS
Wavelengths of the 3p-3d transitions of the Co- and Fe-like ions: The effects of electron correlation
[DE88-000219] N88-13067
The angular diameter of alpha Scorpii in the near-infrared Ca II triplet N88-13162
ATOMIC SPECTRA
Atomic frequency standards for ultra-high-frequency stability N88-12685
Hydrogen and deuterium in the local interstellar medium N88-13204
ATOMIC STRUCTURE
Experimental perspectives on heavy electron metals
[DE87-014766] N88-12583
The finite element method for electronic structure
[DE88-001708] N88-12989
Nuclear techniques in studies of condensed matter
[NASA-RP-1195] N88-13015
Tetrahedral carbon and interstitial electrons in Li cluster: CLi4 and (LiCH3)4
[AD-A184277] N88-13055
Atomic and electronic structure of surfaces and chemisorbed layers
[DE87-014987] N88-13065
Wavelengths of the 3p-3d transitions of the Co- and Fe-like ions: The effects of electron correlation
[DE88-000219] N88-13067
ATOMIC WEIGHTS
The atomic weight and isotopic composition of oxygen and their variation in nature
[DE87-014397] N88-12558
ATTENTION
Latency differences and effects of selective attention to gratings in the central and right visual fields: 2
[DE87-014730] N88-12918
AURIGA CONSTELLATION
A flash spectrum of Cl I, C I, N I, and Ni II absorption in 31 Cygni: A direct observation of the reversing layer N88-13158
AURORAS
Relativistic electron precipitations in a pulsating aurora N88-12894
AUSTENITIC STAINLESS STEELS
Influence of some parameters on the stress corrosion of a ABNT 304 stainless steel in MgCl/sub 2/
[DE87-703707] N88-12580
Method for the ultrasonic inspection of the soundness of the metal in weld joints in two-ply pipes
[BLL-CE-TRANS-8265-(9022.09)] N88-12805
Ultrasonic method of inspecting austenitic weld joints in nuclear power station equipment
[BLL-CE-TRANS-8281-(9022.09)] N88-12906
AUTOMATIC CONTROL
Some data processing requirements for precision Nap-Of-the-Earth (NOE) guidance and control of rotorcraft
[NASA-CR-177453] N88-12493
Failure control techniques for the SSME
[NASA-CR-179224] N88-12537
Robust statistical methods for automated outlier detection N88-12581
GOLD: Integration of model-based control systems with artificial intelligence and workstations
[DE88-000506] N88-12978
On the next generation of reliability analysis tools
[NASA-CR-178380] N88-13000
Ground vehicle convoying
[DE88-000360] N88-13088
Automatic telescope operations N88-13190
AUTOMATIC TEST EQUIPMENT
Automated microwave dielectric constant measurement
[AD-A184182] N88-12667
AUTONOMIC NERVOUS SYSTEM
Motion and space sickness N88-12510
AUTONOMOUS NAVIGATION
Autonomous Land Vehicle (ALV) planning and navigation system
[AD-A184243] N88-12475
Expert robots in nuclear plants
[DE87-014839] N88-12800
AUTOREGRESSIVE PROCESSES
Application of lattice filtering techniques to CW measured time domain data
[AD-A184351] N88-12671
AXIAL LOADS
Analysis and testing of predamaged shell structures N88-12653
AXISYMMETRIC BODIES
Numerical study of supersonic flow around blunt bodies with extended needle nose N88-12635
AZIMUTH
Optical alignment of Centaur's inertial guidance system
[NASA-TM-88844] N88-12515

B

B STARS
A helium flare on the active G5 dwarf Kappa Ceti N88-13189
B-70 AIRCRAFT
An experimental investigation of dynamic ground effect
[NASA-CR-4105] N88-12458
BACKSCATTERING
Measurement of cirrus cloud optical properties by high spectral resolution lidar N88-12906
BACTERIA
Study of certain biological characteristics of bacteria during the French-Soviet CYTOS-2 space experiment N88-12917
BACTERIOLOGY
Study of certain biological characteristics of bacteria during the French-Soviet CYTOS-2 space experiment N88-12917
BALANCE
Energy balance in laser-irradiated vaporizing droplets
[DE88-000525] N88-12782
BALLISTICS
High pressure strand burn rate tests of polyvinylnitrate/nitramine propellants
[AD-A184178] N88-12815
Composite materials applications program at the US Army Ballistic Research Laboratory: Work in progress N88-12951
BALLOONING MODES
Ballooning modes or Fourier modes in a toroidal plasma?
[AD-A184299] N88-13022
BALMER SERIES
Excess emission in the wings of the Hydrogen Balmer lines during a flare on the late-type dMe star YZ CMi N88-13146
BANDWIDTH
Bandwidth efficient block codes for M-ary PSK modulation
[NASA-CR-181543] N88-12712
Performance optimization of electronic networks in the frequency domain
[PB87-123873] N88-12720
BARIUM COMPOUNDS
Resistivity of EuBa2(Cu/sub 1-y/Zn/sub y/)3O/sub x/ as a function of temperature, magnetic field, pressure and Zn concentration
[DE87-014740] N88-13069
BAROTROPIC FLOW
Mesoscale eddy dynamics by the method of point vortices N88-12963
BEAM INJECTION
Negative ion beams for heating and current-drive in NET
[AD-A184390] N88-13012
Coherent emission from relativistic beam-plasma interactions N88-13039
BEAM INTERACTIONS
Coherent emission from relativistic beam-plasma interactions N88-13039
BEARING (DIRECTION)
Lower bounds on bearing accuracy for closely spaced sources
[AD-A184258] N88-12997
BEHAVIOR
Supertracks: The building blocks of chaos
[DE88-001513] N88-13207
BENDING
Analysis and testing of predamaged shell structures N88-12653
Kinematic formulation of finite elements for plate bending N88-12821

BERNSTEIN ENERGY PRINCIPLE
ICRF launcher studies
[DE88-001710] N88-13046
BETA PARTICLES
Nuclear beta decay after Los Houches
[DE87-014921] N88-13011
BIAS
Increased gain of channel intensifier tubes by pulsed biasing
[DE88-000512] N88-13019
BIBLIOGRAPHIES
Aeronautical engineering: A continuing bibliography with indexes (supplement 219)
[NASA-SP-7037(219)] N88-12470
Internal reforming development for solid oxide fuel cells
[DE87-006518] N88-12671
Aerospace medicine and biology: A continuing bibliography with indexes
[NASA-SP-7011(304)] N88-12922
Research papers and publications (1981-1987): Workload research program
[NASA-TM-100016] N88-12924
BIDIRECTIONAL REFLECTANCE
Cloud cover determination in polar regions from satellite imagery
[NASA-CR-181544] N88-12908
BIG BANG COSMOLOGY
New cosmological scenario
[DE87-703357] N88-13198
BINARY CODES
Bandwidth efficient block codes for M-ary PSK modulation
[NASA-CR-181543] N88-12712
BINARY MIXTURES
Thermodynamic properties for natural gas binaries
[PB87-226833] N88-13074
BINARY STARS
Differential B and V light curves of the bright by Draconis star HD80715 N88-13130
Asynchronous rotation in close binary systems with circular orbits N88-13131
PG 0308 + 096: A short-period white dwarf + dM binary with strongly modulated H-alpha emission N88-13132
The Parkes radio survey of active chromosphere stars N88-13141
IRAS and near IR observations of active binaries N88-13186
Radio emission from RS CVn binaries: A 5 GHz VLA survey of 93 systems N88-13191
Catalogue of chromospherically active binaries N88-13192
BINARY SYSTEMS (MATERIALS)
Retention processes in supercritical fluid chromatography
[DE88-000079] N88-12559
Thermodynamic properties of supercritical mixtures
[DE88-000609] N88-12562
Boundary effects on the drag of an oscillating sphere: Applications to the magnetic sphere rheometer. Attenuation and dispersion of acoustic waves in nematic liquid crystals N88-13007
BINDERS (MATERIALS)
Thermoplastic elastomers as LOVA (Low Vulnerability Ammunition) binders
[AD-A184350] N88-12599
BIOCHEMISTRY
JPRS report: Science and technology. USSR: Life sciences
[JPRS-ULS-87-009] N88-12915
BIOLOGICAL EFFECTS
Aerospace medicine and biology: A continuing bibliography with indexes
[NASA-SP-7011(304)] N88-12922
BIOMEDICAL DATA
Human respiratory responses during high performance flight
[AGARD-AG-312] N88-12923
BLACKOUT (PHYSIOLOGY)
F-16 control stick response during +Gz-induced loss of consciousness
[AD-A184107] N88-12491
BLADE-VORTEX INTERACTION
Results of the 1986 NASA/FAA/DFVLR main rotor test entry in the German-Dutch wind tunnel (DNW)
[NASA-TM-100507] N88-13003
BLAST LOADS
Composite materials applications program at the US Army Ballistic Research Laboratory: Work in progress N88-12651
BLOCK DIAGRAMS
A new state space model for the NASA/JPL 70-meter antenna servo controls N88-12702
BLOOD
An assessment of clinical chemical sensing technology for potential use in space station health maintenance facility
[NASA-CR-172013] N88-12926
BLOWDOWN WIND TUNNELS
The design and preliminary calibration of a boundary-layer flow channel
[NASA-CR-178399] N88-12457
BLUNT BODIES
Numerical study of supersonic flow around blunt bodies with extended needle nose N88-12635
BODIES OF REVOLUTION
Solution of geometrically nonlinear problem for reinforced shell of revolution having arbitrary shape N88-12637
Similar solutions for viscous hypersonic flow over a slender three-fourths-power body of revolution
[NASA-TM-100205] N88-12752
BOEING 737 AIRCRAFT
Simulation of an enhanced TCAS 2 system in operation
[NASA-CR-181545] N88-12479
BOLTED JOINTS
Structural analysis of a bolted joint concept for the space shuttle's solid rocket motor casing
[NASA-TM-89092] N88-12531
Nonlinear axial stiffness characteristics of axisymmetric bolted joints N88-12799
BOUNDARY LAYER FLOW
The design and preliminary calibration of a boundary-layer flow channel
[NASA-CR-178399] N88-12457
Total linearisation method for solving viscous free boundary flow problems by the finite element method
[PB87-222337] N88-12737
BOUNDARY LAYER SEPARATION
Calculation of three-dimensional stationary turbulent boundary layer on root section of wing ignoring compressibility N88-12630
Numerical simulation of unsteady separated flows
[AD-A184132] N88-12741
BOUNDARY LAYER TRANSITION
Excitation of natural oscillations of a boundary layer by an external acoustic field N88-12634
BOUNDARY LAYERS
A flash spectrum of Cl I, C I, N I, and Ni II absorption in 31 Cygni: A direct observation of the reversing layer N88-13158
BOUNDARY VALUE PROBLEMS
Numerical prediction of propeller performance by vortex lattice method
[UTIAS-TN-265] N88-12489
Three-dimensional, free-Lagrange hydrodynamics
[DE88-000494] N88-12749
Analytical studies of axially symmetric motion of an incompressible viscous fluid between two concentric rotating spheres N88-12757
Higher order theory analysis of a modified free-edge delamination specimen N88-12820
On operator splitting for unsteady boundary value problems
[AD-A184281] N88-12981
BOW WAVES
Slow-mode shocks in the earth's magnetosphere
[DE88-000483] N88-12895
BRAIN
Latency differences and effects of selective attention to gratings in the central and right visual fields: 2
[DE87-014730] N88-12918
BRAIN CIRCULATION
Change in functional activity of cortical brain structures and their blood supply in alert rabbits in response to rocking N88-12916
BRANCHING (MATHEMATICS)
Fully developed turbulence via Feigenbaum's period-doubling bifurcations
[DE88-000242] N88-12739
BRASSES
Analysis of free cutting brass by A.C. polarography
[PD-MT-8728] N88-12567
BRAVAIS CRYSTALS
Equilibria, lattices and chaotic dynamics of point vortices N88-12758
BRIDGES (STRUCTURES)
The effect of mass, wind angle and erection technique on the aeroelastic behaviour of a cable-stayed bridge model
[NAE-AN-46] N88-12819
BRIGHTNESS
The closest solar analogs in the bright star catalogue N88-13110
BRIGHTNESS DISTRIBUTION
Doppler snapshots N88-13125
BRITTLENESS
Effects of stress-relieving on the mechanical properties and the structure of specimens of high-temperature fine-grained structural steels heat-treated to simulate welding
[BLL-CE-TRANS-8258-(9022.09)] N88-12586
BROADBAND
Band 2 VHF antenna for home construction
[BBC-RD-1987/13] N88-12677
Broadband linear polarization and chromospheric CaII H and K line emission in late-type main sequence stars N88-13140
BROADCASTING
Band 2 VHF antenna for home construction
[BBC-RD-1987/13] N88-12677
BROMIDES
Technical evaluation of a solar-powered absorption cooling system (LiBr-H2O)
[PB87-108254] N88-12867
BUBBLES
Cosmological applications of singular hypersurfaces in general relativity N88-13202
BURNING RATE
High pressure strand burn rate tests of polyvinylnitrate/nitramine propellants
[AD-A184178] N88-12615

C

CALCIUM
Simultaneous, cospatial imaging of the Sun in cyanogen and singly-ionized calcium N88-13114
The angular diameter of alpha Scorpii in the near-infrared Ca II triplet N88-13162
CALIBRATING
The design and preliminary calibration of a boundary-layer flow channel
[NASA-CR-178399] N88-12457
Performance optimization of electronic networks in the frequency domain
[PB87-123873] N88-12720
Evaluation of the sensidyne toxic gas sensor for HF (Hydrogen Fluoride) vapor
[DE88-000547] N88-12767
Accuracy potential of non-metric cameras in close-range photogrammetry N88-12862
Radiometric calibration of the Earth observing system's imaging sensors
[NASA-CR-181542] N88-12865
Calibration on the Sun for stellar magnetic fields N88-13113
CALORIMETERS
Simultaneous TG/DSC (thermogravimetry/Differential Scanning Calorimetry) and TG/MS (thermogravimetry/Mass Spectrometry) analyses of polymeric and energetic materials
[DE88-000727] N88-12561
CAMERAS
Accuracy potential of non-metric cameras in close-range photogrammetry N88-12862
CANONICAL FORMS
Canonical transformations and exact invariants for dissipative systems
[DE87-703663] N88-12985
CAPILLARY FLOW
Experimental study of thermocapillary flows in a thin liquid layer with heat fluxes imposed on the free surface
[NASA-TM-100252] N88-12763
CAPILLARY WAVES
Dispersion equation for plane capillary-gravity wave on free surface of viscous incompressible fluid N88-12842
Influence of surfactants on damping of gravity-capillary waves. 1: Frequency dependence N88-12843
CARBON
Carbon abundances and C12/C13 ratios in M giants N88-13167
CARBON DIOXIDE
Carbon dioxide treatment for scale removal and control in potable water systems
[AD-A184346] N88-12556
CARBON FIBER REINFORCED PLASTICS
Solar converging method N88-12504
Carbon-fiber reinforced plastics N88-12506
CARBON FIBERS
Carbon-fiber reinforced aluminum N88-12507
Carbon fiber reinforced glass matrix composites for space based applications
[AD-A184355] N88-12546
Study of zero CTE (Coefficients of Thermal Expansion) of graphite/epoxy composites
[DE87-013557] N88-12554
CARBON MONOXIDE
Characterization of catalysts with metal-support effects and of the species adsorbed on their surfaces
[DE87-014636] N88-12564

K-CO on transition metals: A local ionic interaction [AD-A184342] N88-13056
The structure of adsorbed sulfur and carbon on molybdenum and rhenium single crystal surfaces, and their influence on carbon monoxide and hydrocarbon chemisorption [DE88-001393] N88-13073
The delta upsilon = 1 fundamental bands of carbon monoxide in late-type stars N88-13177

CARBON STARS
Synthetic spectra for the N-type carbon star TX Psc N88-13173
Water masers associated with 2 carbon stars: EU Andromedae and V778 Cygni N88-13176

CARBON STEELS
Method for the ultrasonic inspection of the soundness of the metal in weld joints in two-ply pipes [BLL-CE-TRANS-8265-(9022.09)] N88-12805

CARBON 12
Carbon abundances and C12/C13 ratios in M giants N88-13167

CARBON 13
Solid state C-13 NMR characterization of textiles: Qualitative and quantitative analysis [AD-A184349] N88-12598
Carbon abundances and C12/C13 ratios in M giants N88-13167

CARGO
Developmental airdrop testing techniques and devices [AGARD-AG-300-VOL-6] N88-12481

CARRIER TO NOISE RATIOS
Optimized tracking of RF carriers with phase noise, including Pioneer 10 results N88-12694

CASCADE CONTROL
Closed-loop system analysis using Lyapunov stability theory N88-12978

CASTING
Activities at government research laboratories reported N88-12503
Development of advanced fiber reinforced ceramics [DE88-000779] N88-12604

CASTINGS
Studies on estimation of nickel in zinc base die casting by D.C. polarography [PD-MT-8729] N88-12586

CATACLYSMIC VARIABLES
The Parkes radio survey of active chromosphere stars N88-13141

CATALOGS (PUBLICATIONS)
Source header list. Volume 1: A through K [AD-A184000] N88-13086

CATALYSIS
Surface catalytic degradation study of two linear perfluoropolyalkylethers at 345 C [NASA-TP-2774] N8' 12543

CATALYSTS
Characterization of catalysts with metal-support effects and of the species adsorbed on their surfaces [DE87-014636] N88-12564

CATHODES
Plasma thruster development [AD-A184173] N88-12536
Raman scattering as a diagnostic technique for cathode characterization [AD-A184434] N88-12726

CATIONS
Impedance of passive lithium anodes in SOCl2 solutions under low-field polarization [DE88-000922] N88-12728

CAUCHY INTEGRAL FORMULA
A quadrature formula for a double-pole singular integral [PD-FM-8725] N88-12990

CAUCHY PROBLEM
Cauchy problem for linearized system of Navier-Stokes equations considering compressibility N88-12837

CAVITATION FLOW
Some stochastic aspects of intergranular creep cavitation [DE88-000065] N88-12581

CAVITIES
Inertial confinement fusion reactor cavity analysis [DE88-000786] N88-13028

CELESTIAL MECHANICS
Propagation of random initial conditions in time N88-12993

CEMENTS
Open-graded bases for airfield pavements [AD-A184461] N88-12500

CENTER OF GRAVITY
Effect of permissible variations of center-of-gravity locations of cargo airplane on its mass N88-12625

CERAMIC MATRIX COMPOSITES
Carbon fiber reinforced glass matrix composites for space based applications [AD-A184355] N88-12546

CERAMICS
JPRS report: Science and technology. Japan [JPRS-JST-87-025] N88-12502
Ceramics thin film N88-12505
Research and development on high strength ceramic heaters discussed N88-12508
Effect of time and temperature on transformation toughened zirconias [AD-A184356] N88-12600
Molecular engineering of ceramics [DE88-000174] N88-12603
Development of advanced fiber reinforced ceramics [DE88-000779] N88-12604
Ceramic technology for advanced heat engines project [DE88-001520] N88-12605
Real-time Raman detection of molecular changes in ceramics undergoing sliding friction [DE88-000558] N88-12609

CEREBRAL CORTEX
Change in functional activity of cortical brain structures and their blood supply in alert rabbits in response to rocking N88-12916
Large-scale neuronal circuits for selective storage and recognition of complex stimuli, a pilot study [AD-A184134] N88-12920

CERMETS
Internal reforming development for solid oxide fuel cells [DE87-006518] N88-12871

CERTIFICATION
Computerized certification of digital ultrasonic instrumentation [DE88-000820] N88-13008

CHALLENGER (ORBITER)
Structural analysis of a bolted joint concept for the space shuttle's solid rocket motor casing [NASA-TM-89092] N88-12531

CHANNEL FLOW
The design and preliminary calibration of a boundary-layer flow channel [NASA-CR-178399] N88-12457

CHANNELS (DATA TRANSMISSION)
An evaluation plan of bus architectures and protocols using the NASA Ames intelligent redundant actuation system [NASA-CR-177458] N88-12482
Design of source coders and joint source/channel coders for noisy channels [NASA-CR-181547] N88-12678
Increased gain of channel intensifier tubes by pulsed biasing [DE88-000512] N88-13019

CHAOS
Fully developed turbulence via Feigenbaum's period-doubling bifurcations [DE88-000242] N88-12739
Supertracks: The building blocks of chaos [DE88-001513] N88-13207

CHARACTERIZATION
The characterization of diagnostic tasks for engineering systems [DE88-000093] N88-12973

CHARGE TRANSFER
Synthesis, NMR characterization and electrical properties of siloxane-based polymer electrolytes [AD-A184184] N88-12596
Final (n,l) state-resolved electron capture by multiply charged ions from neutral atoms [IPPJ-AM-54] N88-13030

CHARGED PARTICLES
Future directions in interplays between particle and nuclear physics: Summary session [DE87-011791] N88-13013
Cosmic-ray nuclear event with an anomalously strong concentration of energy and particles in the central region [DE87-703376] N88-13213

CHASSIS
Corrosion control by composite material substitution with application to the M-939 5-ton truck N88-12554

CHECKOUT
Software reliability perspectives [NASA-CR-181523] N88-12952

CHEMICAL ANALYSIS
Simultaneous TG/DSC (thermogravimetry/Differential Scanning Calorimetry) and TG/MS (thermogravimetry/Mass Spectrometry) analyses of polymeric and energetic materials [DE88-000727] N88-12561
Analysis of free cutting brass by A.C. polarography [PD-MT-8728] N88-12587
An assessment of clinical chemical sensing technology for potential use in space station health maintenance facility [NASA-CR-172013] N88-12926

CHEMICAL BONDS
Topological aspects of infinite metal clusters and superconductors [AD-A184104] N88-13049
Measurement of the electron density and the attachment rate coefficient in silane/helium discharges [AD-A184268] N88-13051
Valence bond theory and superconductivity [AD-A184274] N88-13052
The chemical bond and superconductivity [AD-A184275] N88-13053
Valence bond cluster studies of alkali metal/semiconductor bonding [AD-A184276] N88-13054
Tetrahedral carbon and interstitial electrons in Li cluster: CLi4 and (LiCH3)4 [AD-A184277] N88-13055
Effect of sidechain length and crosslinking on ionic conductivity in polyphosphazene solid electrolytes [AD-A184419] N88-13058

CHEMICAL COMPOSITION
The nature of metallurgical reactions in underwater welding [AD-A184464] N88-12568
Polymer composition --- cable insulation [EP-PATENT-0-199-444-A1] N88-12594
Raman scattering as a diagnostic technique for cathode characterization [AD-A184434] N88-12726
Nuclear techniques in studies of condensed matter [NASA-RP-1195] N88-13015

CHEMICAL EQUILIBRIUM
Equilibrium calculations of ionization in tracer flames [PB87-104154] N88-12555

CHEMICAL REACTIONS
Development of the non-equilibrium reactive chemical transport code CHMTRNS [DE88-000682] N88-12964

CHEMISORPTION
Ro-vibrational laser spectroscopy of ESD neutrals from chemisorbed species [DE87-013011] N88-12770
Atomic and electronic structure of surfaces and chemisorbed layers [DE87-014987] N88-13065
The structure of adsorbed sulfur and carbon on molybdenum and rhenium single crystal surfaces, and their influence on carbon monoxide and hydrocarbon chemisorption [DE88-001393] N88-13073

CHINA
Technology transfer to China [PB87-223418] N88-13087

CHIPS (ELECTRONICS)
The design plan of a VLSI single chip (255, 223) Reed-Solomon decoder N88-12697
Research in VLSI (Very Large Scale Integration) systems [AD-A184089] N88-12721

CHLORIDES
Corrosion susceptibility study of candidate pin materials for ALTC (Active Lithium/Thionyl Chloride) batteries [DE88-001449] N88-12734

CHOKES (RESTRICTIONS)
Geometric analysis of ensemble of solutions in two-phase flow and complete resolution of problem of choking [DE88-001687] N88-12764

CHROMATOGRAPHY
Retention processes in supercritical fluid chromatography [DE88-000079] N88-12559

CHROMIUM ALLOYS
A comparison of high damping shape memory alloys with Cu-Mn-based and Fe-Cr-based alloys [AD-A184110] N88-12566
Model for ultrasonic attenuation and elastic constant in chromium and its alloys [DE87-703478] N88-12570

CHROMOSPHERE
Simultaneous, cospatial imaging of the Sun in cyanogen and singly-ionized calcium N88-13114
Spectroscopic monitoring of RS CVn stars at Kitt Peak using the Penn State fiber optic echelle N88-13127
X-rays, color, and the Vaughan-Preston gap N88-13135
Relations between chromospheric and coronal structure, flux-flux correlations and convective zone properties N88-13138
Broadband linear polarization and chromospheric CaII H and K line emission in late-type main sequence stars N88-13140
The onset of chromospheric activity among the A- and F- type stars N88-13144

Sensitivity of the H alpha line to expansion, geometrical extent and temperature gradient in the G and K supergiant chromospheres N88-13159
The Wilson-Bappu relationship: A barometric effect N88-13170
Synthetic spectra for the N-type carbon star TX Psc N88-13173
Chromospheric variability mechanisms affecting pre-main sequence stars N88-13180
Chromospheric and coronal heating in a bias-free sample of K dwarfs N88-13184
Catalogue of chromospherically active binaries N88-13192
A comprehensive exploration of late-type stars in the far-ultraviolet N88-13194
Hydrogen and deuterium in the local interstellar medium N88-13204

CIRCUIT PROTECTION
The 8.4-GHz low-noise maser pump source assembly N88-12705

CIRCUITS
The Pierce diode with an external circuit. Part 1: Simulations in the linear regime
[DE88-000413] N88-12731
Radiation performance of AlGaAs concentrator cells and expected performance of cascade structures
[NASA-TM-100145] N88-12878

CIRCULAR PLATES
On the instability of thin circular shear layers N88-12467
Vibration and parametric excitation in rotating asymmetric circular plates N88-12823

CIRRUS CLOUDS
Lidar-radiometric method for determining liquid-water content of cirrus clouds N88-12854
Measurement of cirrus cloud optical properties by high spectral resolution lidar N88-12906
Galactic interstellar abundance surveys with IUE and IRAS N88-13206

CLADDING
Thermal stress in the edge cladding of Nova glass laser disks
[DE88-000425] N88-12780

CLASSICAL MECHANICS
Composite mechanics for engine structures
[NASA-TM-100176] N88-12552

CLASSIFICATIONS
Aircraft classification by type of propulsive devices. Determination of type and number of carrying solutions N88-12626
Cloud cover determination in polar regions from satellite imagery
[NASA-CR-181544] N88-12908

CLIMATE
On the interannual variability of South American climate and the Southern Oscillation N88-12905

CLINICAL MEDICINE
JPRS report: Science and technology. USSR: Life sciences
[JPRS-ULS-87-009] N88-12915
An assessment of clinical chemical sensing technology for potential use in space station health maintenance facility
[NASA-CR-172013] N88-12926

CLOSED CYCLES
A cold ejector for closed-cycle helium refrigerators N88-12690
Traveling-wave maser closed-cycle refrigerator data acquisition and display system N88-12706

CLOUD CHAMBERS
Microgravity nucleation and particle coagulation experiments support
[NASA-CR-181540] N88-12618

CLOUD COVER
Cloud cover determination in polar regions from satellite imagery
[NASA-CR-181544] N88-12908

CLOUD PHYSICS
Computer modeling aids studies of precipitation formation N88-12832

CLOUDS
A review of parameterizations of microphysical processes in clouds for application in models of regional atmospheric deposition
[DE88-000451] N88-12909

CLOUDS (METEOROLOGY)
Measurements of vapor flux, liquid water contents, precipitation rates and riming in a Utah mountain cloud system
[PB87-224945] N88-12900
Cloud cover determination in polar regions from satellite imagery
[NASA-CR-181544] N88-12908

CLUMPS
Simulation studies for surfaces and materials strength
[NASA-CR-181535] N88-12557

CN EMISSION
JHK photometry of CN-rich field giants N88-13175

COATINGS
Long-range pulselength scaling of 351nm laser damage thresholds
[DE87-014754] N88-12777
Thermomechanical cracking in coated media due to high speed asperity excitation
[AD-A184176] N88-12809

COCKPITS
Effects of combining vertical and horizontal information into a primary flight display
[NASA-TP-2783] N88-12487

CODERS
Design of source coders and joint source/channel coders for noisy channels
[NASA-CR-181547] N88-12678

CODING
Tau ranging revisited N88-12710
INS3D: An incompressible Navier-Stokes code in generalized three-dimensional coordinates
[NASA-TM-100012] N88-12991

COHERENT RADIATION
Center for X-Ray Optics, 1986
[DE88-000715] N88-12783
Coherent emission from relativistic beam-plasma interactions N88-13039

COLD WEATHER TESTS
Huurre expedition to the North Pole in 1984
[PB87-220935] N88-12858

COLD WORKING
A finite element procedure for interference-fit and cold-working problems with limited yielding
[AR-004-517] N88-12992

COLLAPSE
Radiation induced collapse of the crystalline structure
[DE87-014407] N88-13064

COLLISION AVOIDANCE
Simulation of an enhanced TCAS 2 system in operation
[NASA-CR-181545] N88-12479

COLLISIONAL PLASMAS
Variable collision frequency effects on hose and sausage instabilities in relativistic electron beams
[AD-A184206] N88-13021

COLLISIONLESS PLASMAS
Particle injection and cosmic ray acceleration at collisionless parallel shocks
[DE88-000507] N88-12665

COLOR
Performance and preference with various VDT (Video Display Terminal) phosphors
[AD-A184085] N88-12925
On color polynomials of Fibonacci graphs
[AD-A184133] N88-12996
X-rays, color, and the Vaughan-Preston gap N88-13135

COMBUSTION
Techniques for fire detection N88-12521
Fire-related standards and testing N88-12522
Fire-related medical science N88-12525
Space station internal environmental and safety concerns N88-12527
Microgravity combustion fundamentals N88-12528
Ignition and combustion of metals in oxygen N88-12530

COMBUSTION CHAMBERS
SCRAM JET (Supersonic Combustion Ramjet) combustion experiments N88-12512

COMBUSTION EFFICIENCY
Performance and combustion characteristics of direct-injection stratified-charge rotary engines
[NASA-TM-100134] N88-12490

COMBUSTION PHYSICS
Spacecraft Fire Safety
[NASA-CP-2476] N88-12520
Microgravity combustion fundamentals N88-12528
Spacecraft material flammability testing and configurations N88-12529

COMET TAILS
Analysis of the ICE combiner for multiple antenna arraying N88-12704

COMMAND MODULES
Optimization techniques applied to passive measures for in-orbit spacecraft survivability
[NASA-CR-179216] N88-12532

COMMUNICATION
Meteor-burst communications: Is this what the Navy needs?
[AD-A184433] N88-12672
The SUPRENUM communications subroutine library for grid-oriented problems
[DE88-000137] N88-12950

COMMUNICATION NETWORKS
Multicast gateway design considerations
[PB87-219960] N88-12663
Heterogeneous multi-trunking queueing systems
[AD-A184255] N88-12668
An interactive computer graphics network monitor for a tactical communications network
[AD-A184131] N88-12938

COMPANION STARS
Stellar cycle variability of solar-like stars: A sneak preview N88-13136

COMPATIBILITY
Compatability of dispersion-strengthened platinum with resistojet propellants
[NASA-TP-2765] N88-12536

COMPLEX COMPOUNDS
Topological aspects of infinite metal clusters and superconductors
[AD-A184104] N88-13049

COMPLEX SYSTEMS
Implementation and performance of a complex vision system on a systolic array machine
[AD-A184331] N88-12971

COMPONENT RELIABILITY
PRAAGE: An interactive IBM-PC code for unreliability/aging analysis
[DE87-012124] N88-12803
Extremum methods of structural analysis for system reliability assessment N88-12824

COMPOSITE MATERIALS
Fabrication and testing of fire resistant graphite composite panels
[NASA-CR-177397] N88-12472
JPRS report: Science and technology. Japan
[JPRS-JST-87-025] N88-12502
Activities at government research laboratories reported N88-12503
Carbon-fiber reinforced aluminum N88-12507
Failure analysis of composite structure materials
[AD-A184468] N88-12548
Composite mechanics for engine structures
[NASA-TM-100176] N88-12552
A creep measurement of unidirectional epoxy-fiberglass rod
[DE87-014812] N88-12553
Thermoplastic elastomers as LOVA (Low Vulnerability Ammunition) binders
[AD-A184350] N88-12599
Work-in-progress presented at the Army Symposium on Solid Mechanics, 1986: Lightening of the Force
[AD-A184791] N88-12844
Composite materials applications program at the US Army Ballistic Research Laboratory: Work in progress N88-12851
Damping characteristics of a composite-reinforced stainless-steel plate
[DE88-000303] N88-12828

COMPOSITE STRUCTURES
Failure analysis of composite structure materials
[AD-A184468] N88-12548
Composite mechanics for engine structures
[NASA-TM-100176] N88-12552
Corrosion control by composite material substitution with application to the M-939 5-ton truck N88-12654
Characterization of thin layers for optics
[PB87-217949] N88-13017

COMPRESSIBLE FLOW
A free-Lagrange method for 2-D compressible flows
[DE88-000216] N88-12745
Studies of pressure-velocity coupling schemes for analysis of incompressible and compressible flows
[NASA-CR-181526] N88-12748
TOPAZ: The transient one-dimensional pipe flow analyzer: An update on code improvements and increased capabilities
[DE88-001781] N88-12751
Cauchy problem for linearized system of Navier-Stokes equations considering compressibility N88-12837

COMPRESSIBLE FLUIDS
Dispersion equation for plane capillary-gravity wave on free surface of viscous incompressible fluid N88-12842

COMPRESSING
Design of source coders and joint source/channel coders for noisy channels
[NASA-CR-181547] N88-12678

COMPRESSION LOADS
Analysis and testing of predamaged shell structures N88-12853

COMPUTATION
Aircraft dynamic response calculation based on discrete-continual model N88-12824
Calculation of three-dimensional stationary turbulent boundary layer on root section of wing ignoring compressibility N88-12830
Back-of-the-envelope problems
[AD-A184105] N88-12980

COMPUTATIONAL FLUID DYNAMICS
Solution of the two-dimensional Euler equations on unstructured triangular meshes N88-12469

Experimental aerothermodynamic research of hypersonic aircraft
[NASA-CR-181533] N88-12483
USSR report: Engineering and equipment
[JPRS-UEQ-87-008] N88-12621
Some asymptotic modes of transonic vortex flow N88-12632
Numerical study of supersonic flow around blunt bodies with extended needle nose N88-12635
Studies of pressure-velocity coupling schemes for analysis of incompressible and compressible flows
[NASA-CR-181526] N88-12748
Optimization of explicit time-stepping algorithms and Stream-Function-Coordinate (SFC) concept for fluid dynamics problems N88-12762
Cauchy problem for linearized system of Navier-Stokes equations considering compressibility N88-12837
Asymptotic form of stationary solutions of the Navier-Stokes equations for large Reynolds numbers N88-12838

COMPUTATIONAL GRIDS
Solution of the two-dimensional Euler equations on unstructured triangular meshes N88-12469
Generating meshes for finite-difference analysis using a solid modeler
[DE88-001458] N88-12729
Parallel superconvergent multigrid
[DE87-013153] N88-12960
High resolution finite volume methods on arbitrary grids via wave propagation
[NASA-CR-178397] N88-12979
The finite element method for electronic structure
[DE88-001708] N88-12989

COMPUTER AIDED DESIGN
Digital-flight-control-system software written in automated-engineering-design language: A user's guide of verification and validation tools
[NASA-TM-88313] N88-12494
Numerical simulation system N88-12511
New feedback design methodologies for large space structures: A multi-criterion optimization approach N88-12535
Interactions between science and precision engineering
[DE87-010873] N88-12643
Input devices for tasks using interactive video
[PB87-220018] N88-12664
A procedural method for the efficient implementation of full-custom VLSI designs N88-12701
A new state space model for the NASA/JPL 70-meter antenna servo controls N88-12702
Large change-of-curvature effects in quadratic finite elements for CAD of membrane structures N88-12958
Computer-aided X-ray image system design and evaluation
[DE88-000997] N88-12965

COMPUTER AIDED MANUFACTURING
Interactions between science and precision engineering
[DE87-010873] N88-12643

COMPUTER AIDED TOMOGRAPHY
Computed neutron tomography and coded aperture holography from real time neutron images N88-12645

COMPUTER ASSISTED INSTRUCTION
The pros and cons of using a CAI package on a central computer as opposed to a microprocessor: What's your CAI MO, mainframe or micro
[DE87-011123] N88-12929

COMPUTER GRAPHICS
An inexpensive real-time interactive three-dimensional flight simulation system
[AD-A184340] N88-12499
NACHOS 2: A finite element computer program for incompressible flow problems. Part 2: User's manual
[DE88-001451] N88-12750
CGI delay compensation
[NASA-TM-86703] N88-12932
An interactive computer graphics network monitor for a tactical communications network
[AD-A184131] N88-12938
The ISI (Information Sciences Institute) grapher: A portable tool for displaying graphs pictorially
[AD-A184354] N88-12944
Implementation and performance of a complex vision system on a systolic array machine
[AD-A184331] N88-12971
GOLD: Integration of model-based control systems with artificial intelligence and workstations
[DE88-000506] N88-12976
GOLD: Integration of model-based control systems with artificial intelligence and workstations
[DE88-000706] N88-12977

COMPUTER NETWORKS
Center for Supercomputing Research and Development (CEDAR)
[DE88-000807] N88-12930
A data analysis environment for HP (Hewlett-Packard) 1000 computers
[DE87-010511] N88-12936
A survey of object oriented languages in programming environments
[AD-A184127] N88-12937
A network definition and solution of simulation problems
[DE88-000675] N88-12962
Managing distributed derived data: A preliminary proposal
[DE88-000714] N88-12966
An approach to implementing state space searches on heterogeneous systems of multiprocessors
[DE88-001321] N88-12967

COMPUTER PROGRAMMING
A survey of object oriented languages in programming environments
[AD-A184127] N88-12937
Guidelines for preparing software user documentation
[NASA-CR-181550] N88-12959
COLA2: A computer program for the structural synthesis of two components using general modal coordinates
[DE88-001457] N88-12963

COMPUTER PROGRAMS
NAVSIM 2: A computer program for simulating aided-inertial navigation for aircraft
[NASA-CR-177436] N88-12478
Aircraft dynamic response calculation based on discrete-continual model N88-12624
Automated microwave dielectric constant measurement
[AD-A184182] N88-12667
A simplified procedure for correcting both errors and erasures of a Reed-Solomon code using the Euclidean algorithm N88-12698
Departmental report on program EMTP-machine windings surge transients: Travelling wave method
[PB87-123733] N88-12719
TOPAZ: The transient one-dimensional pipe flow analyzer: An update on code improvements and increased capabilities
[DE88-001781] N88-12751
NCSU code: Validation and extension on NAL's UNIVAC 1100/60 system
[PD-FM-8716] N88-12931
A data analysis environment for HP (Hewlett-Packard) 1000 computers
[DE87-010511] N88-12936
Software reliability perspectives
[NASA-CR-181523] N88-12952
INS3D: An incompressible Navier-Stokes code in generalized three-dimensional coordinates
[NASA-TM-100012] N88-12991

COMPUTER STORAGE DEVICES
Storing photomicrographs on optical laser disks
[DE87-013747] N88-12785
Center for Supercomputing Research and Development (CEDAR)
[DE88-000807] N88-12930

COMPUTER SYSTEMS DESIGN
Methods for design and evaluation of integrated hardware/software systems for concurrent computation
[NASA-CR-181522] N88-12953
User interface for a partially incompatible system software environment with non-ADP users
[DE88-001518] N88-12968

COMPUTER SYSTEMS PERFORMANCE
Applications of the hybrid automated reliability predictor
[NASA-TP-2760] N88-12928
Parallelization of hydrocodes on the Intel Hypercube, part 2
[DE88-001591] N88-12957
Towards automated consulting: Design feedback from the performance of online documentation
[DE87-012243] N88-13082

COMPUTER TECHNIQUES
Band 2 VHF antenna for home construction
[BBC-RD-1987/13] N88-12677
Statistical inference: Computer oriented algorithmic approach
[DE87-013874] N88-12948
Automatic telescope operations N88-13190

COMPUTER VISION
On the recognition of curved objects
[AD-A184441] N88-12945
Implementation and performance of a complex vision system on a systolic array machine
[AD-A184331] N88-12971

COMPUTERIZED SIMULATION
NAVSIM 2: A computer program for simulating aided-inertial navigation for aircraft
[NASA-CR-177436] N88-12478
Simulation of an enhanced TCAS 2 system in operation
[NASA-CR-181545] N88-12479
An inexpensive real-time interactive three-dimensional flight simulation system
[AD-A184340] N88-12499
Numerical simulation system N88-12511
Analytical investigation of the dynamics of tethered constellations in Earth orbit (phase 2)
[NASA-CR-179218] N88-12533
Simulation studies for surfaces and materials strength
[NASA-CR-181535] N88-12557
The Pierce diode with an external circuit. Part 1: Simulations in the linear regime
[DE88-000413] N88-12731
PRAAGE: An interactive IBM-PC code for unreliability/aging analysis
[DE87-012124] N88-12803
A portable hypercube simulator
[DE87-013369] N88-12947
A network definition and solution of simulation problems
[DE88-000675] N88-12962
Development of the non-equilibrium reactive chemical transport code CHMTRNS
[DE88-000682] N88-12964
Computer-aided X-ray image system design and evaluation
[DE88-000997] N88-12965
GOLD: Integration of model-based control systems with artificial intelligence and workstations
[DE88-000506] N88-12976
GOLD: Integration of model-based control systems with artificial intelligence and workstations
[DE88-000706] N88-12977
Monocrystal sputtering by the computer simulation code ACOCT
[IPPJ-848] N88-13035
Theory and simulations of Zone 2 microstructures in thin films
[DE87-014752] N88-13071
Subjective probability, combination of expert opinion and probabilistic approaches to information retrieval N88-13085

COMPUTERS
On computing environments in data analysis
[DE88-000078] N88-12961

CONCATENATED CODES
The design plan of a VLSI single chip (255, 223) Reed-Solomon decoder N88-12897

CONCENTRATION (COMPOSITION)
Inerting and atmospheres N88-12524

CONCENTRATORS
Solar converging method N88-12504
Radiation performance of AlGaAs concentrator cells and expected performance of cascade structures
[NASA-TM-100145] N88-12878

CONCRETES
Open-graded bases for airfield pavements
[AD-A184461] N88-12500

CONCURRENT PROCESSING
Comparing barrier algorithms
[NASA-CR-178377] N88-12934
Methods for design and evaluation of integrated hardware/software systems for concurrent computation
[NASA-CR-181522] N88-12953

CONDENSING
Experimental and theoretical study of condensation in multicomponent mixtures
[DE88-000897] N88-12563
Inertial confinement fusion reactor cavity analysis
[DE88-000788] N88-13028

CONDUCTIVE HEAT TRANSFER
Microgravity nucleation and particle coagulation experiments support
[NASA-CR-181540] N88-12618
Microgravity nucleation and particle coagulation experiments support
[NASA-CR-181541] N88-12619

CONFERENCES
Spacecraft Fire Safety
[NASA-CP-2476] N88-12520
Proceedings of the Fifth Symposium on Energy Engineering Sciences: Instrumentation, Diagnostics, and Material Behavior
[DE88-001479] N88-12680
Proceedings: SDIO/DARPA Workshop on Laser Propulsion. Volume 3: Viewgraphs
[DE88-000964] N88-12790
Proceedings of the Eleventh DOE Solar Photochemistry Research Conference
[DE88-000678] N88-12883
Research papers and publications (1981-1987): Workload research program
[NASA-TM-100016] N88-12924

Proceedings of the Japan-US Workshop P-92 on Plasma Material Interaction/High Heat Flux Data Needs for the Next Step Ignition and Steady State Devices [DE87-013568] N88-13042
Fifth Cambridge Workshop on Cool Stars, Stellar Systems and the Sun N88-13092

CONICAL BODIES
Conical wing with maximum lift-to-drag ratio in supersonic gas flow N88-12633

CONICAL SHELLS
Effective treatment of membrane and shear locking phenomena in curved shear-deformable axisymmetric shell element N88-12652
Analysis and testing of predamaged shell structures N88-12653

CONJUGATE GRADIENT METHOD
Solution of geometrically nonlinear problem for reinforced shell of revolution having arbitrary shape N88-12637

CONSCIOUSNESS
F-16 control stick response during +Gz-induced loss of consciousness [AD-A184107] N88-12491

CONSERVATION LAWS
High resolution finite volume methods on arbitrary grids via wave propagation [NASA-CR-178397] N88-12979

CONSISTENCY
Consistency question in the renormalization group analysis of deep inelastic scattering [DE87-703372] N88-12999

CONSOLIDATION
Effects of combining vertical and horizontal information into a primary flight display [NASA-TP-2783] N88-12487

CONSTITUTIVE EQUATIONS
A direct method to obtain constitutive model constants from cylinder impact test results N88-12647

CONSTRAINTS
An exact penalization viewpoint of constrained optimization [DE88-001477] N88-12995

CONSULTING
Towards automated consulting: Design feedback from the performance of online documentation [DE87-012243] N88-13082

CONTAMINANTS
Influence of surfactants on damping of gravity-capillary waves. 1: Frequency dependence N88-12843

CONTINUOUS RADIATION
Application of lattice filtering techniques to CW measured time domain data [AD-A184351] N88-12671

CONTINUUMS
Radio continuum emission from the ionized stellar winds of the cool supergiants in zeta Aurigae-like systems N88-13160

CONTRACT MANAGEMENT
A comparison of the basket method and the stratified random sampling for contract change order negotiations [AD-A184170] N88-13080

CONTRACT NEGOTIATION
A comparison of the basket method and the stratified random sampling for contract change order negotiations [AD-A184170] N88-13080

CONTRACTS
A comparison of the basket method and the stratified random sampling for contract change order negotiations [AD-A184170] N88-13080

CONTROL STICKS
F-16 control stick response during +Gz-induced loss of consciousness [AD-A184107] N88-12491

CONTROL SURFACES
Experimental aerothermodynamic research of hypersonic aircraft [NASA-CR-181533] N88-12483

CONTROL SYSTEMS DESIGN
Space station resistojet system requirements and interface definition study [NASA-CR-180632] N88-12541

CONTROL THEORY
Analytical investigation of the dynamics of tethered constellations in Earth orbit (phase 2) [NASA-CR-179218] N88-12533
Natural control of flexible space structures N88-12534
A modern control theory based algorithm for control of the NASA/JPL 70-meter antenna axis servos N88-12706

CONTROLLED ATMOSPHERES
Fire-related medical science N88-12525

CONTROLLERS
Local-optimal control in systems with delay N88-12627
A modern control theory based algorithm for control of the NASA/JPL 70-meter antenna axis servos N88-12706

CONVECTION
Banded ion morphology N88-12892
Relations between chromospheric and coronal structure, flux-flux correlations and convective zone properties N88-13138

CONVECTIVE FLOW
High latitude F-region drift studies [AD-A184466] N88-12889

CONVERGENCE
Concepts for radically increasing the numerical convergence rate of the Euler equations [NASA-CR-177456] N88-12483
Parallel superconvergent multigrid [DE87-013153] N88-12960

COOL STARS
Fifth Cambridge Workshop on Cool Stars, Stellar Systems and the Sun N88-13092
The photospheric magnetic fields of cool stars: Recent results of survey and time-variability programs N88-13094
Flux tube dynamics and solar/stellar redshift measurements N88-13095
Nonthermal phenomena in stellar coronae: Evidence from radio observations N88-13096
Observational constraints and evidence for saturation N88-13097
Heating of stellar chromospheres and coronae: Evidence for non-magnetic basal heating N88-13098
Automatic photometric monitoring of cool stars N88-13103
Evidence for expanding magnetic loops in coronae of cool stars N88-13134
Empirical relations between photospheric magnetic fields and atmospheric radiative losses for cool dwarf stars N88-13145
Radio continuum emission from the ionized stellar winds of the cool supergiants in zeta Aurigae-like systems N88-13160
IRAS and cool stellar mass loss N88-13166
The Wilson-Bappu relationship: A barometric effect N88-13170
IUE observations of the hybrid K3 II star iota Aurigae and constraints on the outer atmospheric structure N88-13171
Synthetic spectra for the N-type carbon star TX Psc N88-13173

COOLING FINS
Advanced radiator concepts utilizing honeycomb panel heat pipes [NASA-CR-172017] N88-12747

COPOLYMERIZATION
Conducting hybrid polymeric systems [DE88-000527] N88-12611

COPOLYMERS
Polymer composition — cable insulation [EP-PATENT-0-199-444-A1] N88-12594
Synthesis, NMR characterization and electrical properties of siloxane-based polymer electrolytes [AD-A184184] N88-12596
Conductive polymers via reactive oligomer [AD-A184270] N88-12597
Advances in inherently conducting polymers [DE88-000501] N88-12610
Conducting hybrid polymeric systems [DE88-000527] N88-12611
Effect of sidechain length and crosslinking on ionic conductivity in polyphosphazene solid electrolytes [AD-A184419] N88-13058

COPPER
The effect of organic inhibitors on the atmospheric corrosion and solderability of copper [DE88-000261] N88-12585
Studies on high-speed electroforming [DE88-001395] N88-12656
Data base on the high heat flux behaviour of metals and carbon materials for plasma facing components: Experiments at the 10 MW neutral beam injection test stand of the IPP Nagoya [IPPJ-AM-53] N88-13031

COPPER ALLOYS
A comparison of high damping shape memory alloys with Cu-Mn-based and Fe-Cr-based alloys [AD-A184110] N88-12566

CORONA BOREALIS CONSTELLATION
A large X-ray flare on squared Sigma coronae borealis observed with exosat N88-13121

CORONAL LOOPS
Evidence for expanding magnetic loops in coronae of cool stars N88-13134

CORONAS
Chromospheric and coronal heating in a bias-free sample of K dwarfs N88-13184

CORRELATION
Using a new characterization of turbulent wind for accurate correlation of wind turbine response with wind speed [DE88-001453] N88-12881

CORROSION
The effect of organic inhibitors on the atmospheric corrosion and solderability of copper [DE88-000261] N88-12585
Corrosion strength of niobium and its alloys [DE87-703693] N88-12578
Corrosion of ferritic steels by molten lithium: Influence of competing thermal gradient mass transfer and surface product reactions [DE88-000334] N88-12585
Ceramic technology for advanced heat engines project [DE88-001520] N88-12605

CORROSION RESISTANCE
Corrosion behavior of P/M mechanically alloyed IN-9052.1: An electro-chemical investigation [AD-A184191] N88-12567
Work-in-progress presented at the Army Symposium on Solid Mechanics, 1986: Lightening of the Force [AD-A184791] N88-12644
Composite materials applications program at the US Army Ballistic Research Laboratory: Work in progress N88-12651
Corrosion control by composite material substitution with application to the M-939 5-ton truck N88-12654
Corrosion susceptibility study of candidate pin materials for ALTC (Active Lithium/Thionyl Chloride) batteries [DE88-001449] N88-12734
Reliability of LI/SO2 cells for long-life applications [DE88-001380] N88-12735

COSMIC RAY SHOWERS
Cosmic-ray nuclear event with an anomalously strong concentration of energy and particles in the central region [DE87-703376] N88-13213

COSMIC RAYS
Particle injection and cosmic ray acceleration at collisionless parallel shocks [DE88-000507] N88-12665

COSMIC X RAYS
Center for X-Ray Optics, 1986 [DE88-000715] N88-12783

COSMOLOGY
Homogeneous space-time of Goedel type in higher-derivate gravity [DE87-703690] N88-13077
Cosmological applications of singular hypersurfaces in general relativity N88-13202
Galaxy formation by gravitational collapse in a universe dominated by cold dark matter N88-13205

COSTS
A comparison of the basket method and the stratified random sampling for contract change order negotiations [AD-A184170] N88-13080

CRACK INITIATION
Creep life prediction based on stochastic model of microstructurally short crack growth [NASA-TM-100245] N88-12825
Data base on the high heat flux behaviour of metals and carbon materials for plasma facing components: Experiments at the 10 MW neutral beam injection test stand of the IPP Nagoya [IPPJ-AM-53] N88-13031

CRACK PROPAGATION
Mechanical behavior of a controlled rolled high-strength low alloy steel plate, microalloyed with Nb and V [DE87-703507] N88-12571
Effects of stress-relieving on the mechanical properties and the structure of specimens of high-temperature fine-grained structural steels heat-treated to simulate welding [BLL-CE-TRANS-8258-(9022.09)] N88-12586
Development of advanced fiber reinforced ceramics [DE88-000779] N88-12604
Plastic strain localization between voids in shear deformation fields N88-12648
Method for the ultrasonic inspection of the soundness of the metal in weld joints in two-ply pipes [BLL-CE-TRANS-8265-(9022.09)] N88-12805
Creep life prediction based on stochastic model of microstructurally short crack growth [NASA-TM-100245] N88-12825

CRACK TIPS
A study of the crack tip parameters that govern environmentally assisted cracking by use of the rising displacement test N88-12649

CRACKING (FRACTURING)
A study of the crack tip parameters that govern environmentally assisted cracking by use of the rising displacement test N88-12649

CRACKS
Welding and weldability of ductile intermetallic alloys [DE87-014061] N88-12582
Development of an acoustic emission monitor and monitoring techniques for long-term monitoring of U-0.8Ti electron-beam weldments for postweld cracking [DE88-000819] N88-12804
An adaptive subdivision method with crack prevention for rendering beta-spline objects [AD-A184249] N88-12940
CRANES
Renewed interest in airships for industry use discussed N88-12628
CREEP ANALYSIS
A creep measurement of unidirectional epoxy-fiberglass rod [DE87-014812] N88-12553
CREEP PROPERTIES
Some stochastic aspects of intergranular creep cavitation [DE88-000085] N88-12581
Influence of creep on the precipitate structure under conditions of long-term creep. 4: Experiments on 10 CrMo 9 10 steel [BLL-CE-TRANS-8256-(9022.09)] N88-12589
Creep life prediction based on stochastic model of microstructurally short crack growth [NASA-TM-100245] N88-12625
CRITICAL TEMPERATURE
Welding and weldability of ductile intermetallic alloys [DE87-014061] N88-12582
Magnetic field dependence of the specific heat of some high-T/sub c/ superconductors [DE87-014078] N88-13083
CROSS FLOW
Theory of one and two-pass cross-flow heat exchanger [PB87-225157] N88-12736
Comparative studies in the near-field of turbulent transports of heated and unheated jets normal to a cross stream N88-12756
CROSSLINKING
Effect of sidechain length and crosslinking on ionic conductivity in polyphosphazene solid electrolytes [AD-A184419] N88-13058
CRUSTAL FRACTURES
An algorithmic approach to crustal deformation analysis N88-12891
CRYOGENIC COOLING
Measurement and analysis of cryogenic sapphire dielectric resonators and DROs N88-12686
Low-noise cryogenic transmission line N88-12688
A 2.3-GHz cryogenically cooled HEMT amplifier for DSS 13 N88-12689
CRYOGENIC EQUIPMENT
A cold ejector for closed-cycle helium refrigerators N88-12690
CRYOGENICS
Design concepts for the ASTROMAG cryogenic system [NASA-CR-181505] N88-13060
CRYSTAL DEFECTS
Impedance of passive lithium anodes in SOCl2 solutions under low-field polarization [DE88-000922] N88-12728
CRYSTAL DISLOCATIONS
Raman scattering spectrum along a bevel etched GaAs on Si, TEM (Transmission Electron Microscope) study and GaAs P-I-N photodetector on Si [DE88-000210] N88-13066
CRYSTAL GROWTH
Evaluation of the Mellen EDG furnace for growth of large diameter GaAs single crystals in a horizontal configuration [DE88-000483] N88-13068
CRYSTAL LATTICES
A study of mechanisms of hydrogen diffusion in separation devices [DE88-000328] N88-12584
Radiation induced collapse of the crystalline structure [DE87-014407] N88-13064
Raman scattering spectrum along a bevel etched GaAs on Si, TEM (Transmission Electron Microscope) study and GaAs P-I-N photodetector on Si [DE88-000210] N88-13066
CRYSTAL OPTICS
Gamma-ray optics of multi-beam Borrmann modes with possible applications to nuclear lasing N88-12784
CRYSTAL STRUCTURE
Equilibria, lattices and chaotic dynamics of point vortices N88-12756
CRYSTAL SURFACES
The structure of adsorbed sulfur and carbon on molybdenum and rhenium single crystal surfaces, and their influence on carbon monoxide and hydrocarbon chemisorption [DE88-001393] N88-13073
CRYSTALLINITY
Gamma-ray optics of multi-beam Borrmann modes with possible applications to nuclear lasing N88-12784
Radiation induced collapse of the crystalline structure [DE87-014407] N88-13064
CRYSTALLITES
Characterization of catalysts with metal-support effects and of the species adsorbed on their surfaces [DE87-014636] N88-12564
CRYSTALLIZATION
Studies on some Ge-Se-Te glasses [PD-MT-8721] N88-12607
CRYSTALS
Research and development on high strength ceramic heaters discussed N88-12508
Far infrared Fourier transform spectroscopy of semiconductors [DE88-000188] N88-13072
CUES
Effect of motion cues during complex curved approach and landing tasks: A piloted simulation study [NASA-TP-2773] N88-12480
CURRENT DENSITY
Magnetic fluctuation behaviour of current termination in reversed field pinch [IPPJ-849] N88-13034
CURRENT DISTRIBUTION
Efficiency aspects of short, low velocity railguns [AR-004-847] N88-12517
CURVED PANELS
Vibration and buckling of geometrically imperfect laminated cylindrical shells N88-12822
CYANOGEN
Simultaneous, cospatial imaging of the Sun in cyanogen and singly-ionized calcium N88-13114
CYCLIC COMPOUNDS
Thermoplastic elastomers as LOVA (Low Vulnerability Ammunition) binders [AD-A184350] N88-12599
CYCLIC LOADS
Composite materials applications program at the US Army Ballistic Research Laboratory: Work in progress N88-12651
CYCLONES
Annual tropical cyclone report, 1986 [AD-A184082] N88-12903
CYCLOTRON RADIATION
Nonthermal phenomena in stellar coronae: Evidence from radio observations N88-13096
CYCLOTRON RESONANCE
Nonthermal phenomena in stellar coronae: Evidence from radio observations N88-13096
CYLINDRICAL SHELLS
Rational reinforcement of cylindrical shells with variable stiffness frames subjected to external pressure N88-12638
A direct method to obtain constitutive model constants from cylinder impact test results N88-12647
Analysis and testing of predamaged shell structures N88-12653
Vibration and buckling of geometrically imperfect laminated cylindrical shells N88-12822

D

DAMAGE
Analysis and testing of predamaged shell structures N88-12653
Data base on the high heat flux behaviour of metals and carbon materials for plasma facing components: Experiments at the 10 MW neutral beam injection test stand of the IPP Nagoya [IPPJ-AM-53] N88-13031
DAMAGE ASSESSMENT
Failure control techniques for the SSME [NASA-CR-179224] N88-12537
Low-cost teleoperator-controlled vehicle for damage assessment and dose measurement [DE88-000713] N88-12794
DAMPING
A comparison of high damping shape memory alloys with Cu-Mn-based and Fe-Cr-based alloys [AD-A184110] N88-12566
Damping characteristics of a composite-reinforced stainless-steel plate [DE88-000303] N88-12828
Influence of surfactants on damping of gravity-capillary waves. 1: Frequency dependence N88-12643
An analysis of sound absorbing linings for the interior of the NASA Ames 80 x 120-foot wind tunnel [NASA-CR-177396] N88-13006
DARK MATTER
Galaxy formation by gravitational collapse in a universe dominated by cold dark matter N88-13205
DATA ACQUISITION
Automated microwave dielectric constant measurement [AD-A184182] N88-12667
The Telecommunications and Data Acquisition Report [NASA-CR-181546] N88-12679
Traveling-wave maser closed-cycle refrigerator data acquisition and display system N88-12708
Tau ranging revisited N88-12710
Computerized certification of digital ultrasonic instrumentation [DE88-000820] N88-13008
Automatic photometric monitoring of cool stars N88-13103
DATA BASE MANAGEMENT SYSTEMS
User's guide to NCAR (National Center for Atmospheric Research) CCM1 [PB87-224386] N88-12699
Managing distributed derived data: A preliminary proposal [DE88-000714] N88-12966
A data translation method for heterogeneous database systems N88-13081
Towards automated consulting: Design feedback from the performance of online documentation [DE87-012243] N88-13082
DATA BASES
Statistical distribution of solar radiation (hourly sums): Cumulative frequency curves preparation of a European data set and direction for use [PB87-107454] N88-12886
Cloud cover determination in polar regions from satellite imagery [NASA-CR-181544] N88-12908
A tight upper bound for the speed-up of parallel best-first branch-and-bound algorithms [AD-A184246] N88-12939
Data base on the high heat flux behaviour of metals and carbon materials for plasma facing components: Experiments at the 10 MW neutral beam injection test stand of the IPP Nagoya [IPPJ-AM-53] N88-13031
DATA LINKS
The atmosphere of Mars and optical communications N88-12692
DATA PROCESSING
Experimental and theoretical study of condensation in multicomponent mixtures [DE88-000897] N88-12563
Interferometry theory for the block 2 processor [NASA-CR-181551] N88-12730
Complex for ocean study from space and hydroacoustic stations N88-12836
A data analysis environment for HP (Hewlett-Packard) 1000 computers [DE87-010511] N88-12936
On computing environments in data analysis [DE88-000078] N88-12961
DATA PROCESSING TERMINALS
Performance and preference with various VDT (Video Display Terminal) phosphors [AD-A184085] N88-12925
DATA STORAGE
Complex for ocean study from space and hydroacoustic stations N88-12836
DATA TRANSMISSION
Design of source coders and joint source/channel coders for noisy channels [NASA-CR-181547] N88-12678
DEBRIS
Far infrared circumstellar debris shells of red supergiant stars N88-13165
DECAY RATES
Influences of the astrophysical environment on nuclear decay rates [DE88-001461] N88-13208
DECISION MAKING
The pros and cons of using a CAI package on a central computer as opposed to a microprocessor: What's your CAI MO, mainframe or micro [DE87-011123] N88-12929
DECODERS
More on the decoder error probability for Reed-Solomon codes N88-12699
On the VLSI design of a pipeline Reed-Solomon decoder using systolic arrays N88-12700
DECOMPOSITION
Performance analysis of advanced spacecraft TPS [NASA-CR-181532] N88-12484

DEEP SPACE NETWORK
The Telecommunications and Data Acquisition Report [NASA-CR-181546] N88-12679
Low-noise cryogenic transmission line N88-12688
A 2.3-GHz cryogenically cooled HEMT amplifier for DSS 13 N88-12689
Frequency doubling conversion efficiencies for deep space optical communications N88-12691
The 8.4-GHz low-noise maser pump source assembly N88-12705
A modern control theory based algorithm for control of the NASA/JPL 70-meter antenna axis servos N88-12706
Power density measurements in the near field of the DSS 13 26-meter antenna N88-12711
DEFECTS
Detection of defects on structures [EP-PATENT-0-210-794-A2] N88-12807
Vibration and buckling of geometrically imperfect laminated cylindrical shells N88-12822
DEFENSE PROGRAM
Source header list. Volume 1: A through K [AD-A184000] N88-13066
DEFORMATION
Finite deformations of shell with rigid inclusion N88-12639
Fatigue failure of thin porous strips N88-12640
Explicit and implicit soil modelling for dynamic soil-structure interaction problems N88-12650
Effective treatment of membrane and shear locking phenomena in curved shear-deformable axisymmetric shell element N88-12652
A refined nonlinear analysis of laminated composite plates and shells [AD-A184436] N88-12811
An algorithmic approach to crustal deformation analysis N88-12891
DEGRADATION
Surface catalytic degradation study of two linear perfluoropolyalkylethers at 345 C [NASA-TP-2774] N88-12543
DELAMINATING
Free-edge delamination: Laminate width and loading conditions effects [NASA-TM-100236] N88-12551
Higher order theory analysis of a modified free-edge delamination specimen N88-12820
DELAY
Design of efficient FIR filters with minimal delay [PB87-100434] N88-12717
DELIVERY
Developmental airdrop testing techniques and devices [AGARD-AG-300-VOL-6] N88-12481
DELTA WINGS
An experimental investigation of dynamic ground effect [NASA-CR-4105] N88-12458
DENSE PLASMAS
Variable collision frequency effects on hose and sausage instabilities in relativistic electron beams [AD-A184206] N88-13021
DENSITY (MASS/VOLUME)
Studies on some Ge-Se-Te glasses [PD-MT-8721] N88-12607
Hydrogen and deuterium in the local interstellar medium N88-13204
DENSITY (NUMBER/VOLUME)
Refueling and density control in the ZT-40M reversed field pinch [DE88-000504] N88-13040
X-rays, color, and the Vaughan-Preston gap N88-13135
DEPOSITION
Tribological properties of rf-sputtered MoS2 coatings [DE88-000266] N88-12802
A review of parameterizations of microphysical processes in clouds for application in models of regional atmospheric deposition [DE88-000451] N88-12909
Far-infrared spectra of lithium deposited on a gold electrode: Interpretation using a cluster model [AD-A184231] N88-13050
DEPOSITS
Raman scattering as a diagnostic technique for cathode characterization [AD-A184434] N88-12726
DESIGN ANALYSIS
The design and preliminary calibration of a boundary-layer flow channel [NASA-CR-178399] N88-12457
Structural analysis of a bolted joint concept for the space shuttle's solid rocket motor casing [NASA-TM-89092] N88-12531
Optimization techniques applied to passive measures for in-orbit spacecraft survivability [NASA-CR-179216] N88-12532
New feedback design methodologies for large space structures: A multi-criterion optimization approach N88-12535
Multicast gateway design considerations [PB87-219960] N88-12663
On the VLSI design of a pipeline Reed-Solomon decoder using systolic arrays N88-12700
A procedural method for the efficient implementation of full-custom VLSI designs N88-12701
On dynamic loads in parallel shaft transmissions. 1: Modelling and analysis [NASA-TM-100180] N88-12797
On dynamic loads in parallel shaft transmissions. 2: Parameter study [NASA-TM-100181] N88-12798
Nonlinear axial stiffness characteristics of axisymmetric bolted joints N88-12799
Design and development of absorption heat pumps [DE88-900082] N88-12885
An expert system for materials design [DE88-000191] N88-12974
Design concepts for the ASTROMAG cryogenic system [NASA-CR-181505] N88-13060
Thermodynamic properties for natural gas binaries [PB87-226833] N88-13074
DESORPTION
Ro-vibrational laser spectroscopy of ESD neutrals from chemisorbed species [DE87-013011] N88-12770
DETECTION
Techniques for fire detection N88-12521
DEUTERIUM
Refueling and density control in the ZT-40M reversed field pinch [DE88-000504] N88-13040
Hydrogen and deuterium in the local interstellar medium N88-13204
DIAGNOSIS
The characterization of diagnostic tasks for engineering systems [DE88-000093] N88-12973
DIAMETERS
The angular diameter of alpha Scorpii in the near-infrared Ca II triplet N88-13162
DIELECTRICS
Automated microwave dielectric constant measurement [AD-A184182] N88-12687
Measurement and analysis of cryogenic sapphire dielectric resonators and DROs N88-12686
DIES
Studies on estimation of nickel in zinc base die casting by D.C. polarography [PD-MT-8729] N88-12588
DIESEL ENGINES
Ceramic technology for advanced heat engines project [DE88-001520] N88-12605
DIFFERENCES
GPS vertical axis performance enhancement for helicopter precision landing approach [NASA-CR-177443] N88-12477
DIFFERENTIAL EQUATIONS
Oscillation theory for linear second-order differential systems [DE87-011393] N88-12983
The shifted Adams method for ordinary differential equations [DE88-000810] N88-12994
DIFFUSE RADIATION
Magnetic diffuse scattering [DE87-013539] N88-13014
DIFFUSION
Thermal analysis of electromagnetic launcher rails [DE88-000166] N88-12514
A study of mechanisms of hydrogen diffusion in separation devices [DE88-000328] N88-12584
Thermophoresis of spherical aerosol particle at arbitrary Knudsen numbers N88-12850
DIGITAL FILTERS
Design of digital filters for electronic instrumentation [PB87-100418] N88-12716
DIGITAL SIMULATION
Numerical simulation of unsteady separated flows [AD-A184132] N88-12741
Computer modeling aids studies of precipitation formation N88-12832
Numerical simulation of the Reversed Field Pinch [AD-A184353] N88-13023
DIGITAL SYSTEMS
Digital-flight-control-system software written in automated-engineering-design language: A user's guide of verification and validation tools [NASA-TM-88313] N88-12494
DIGITAL TECHNIQUES
Input/output technologies: An overview of image scanning, storage, and display [DE87-014837] N88-12933
DIGITAL TELEVISION
Accommodating the residue of processed or computed digital video signals within the 8 bit CCIR recommendation 601 [BBC-RD-1987/12] N88-12876
DILUTION
Influence of bond dilution on the free surface and interface Potts ferromagnetism [DE87-703360] N88-13061
DIMENSIONAL STABILITY
Carbon-fiber reinforced plastics N88-12506
DIMENSIONS
A two-dimensional finite difference program for thermal analysis of rocket thrust chambers [NASA-TM-100191] N88-12539
INS3D: An incompressible Navier-Stokes code in generalized three-dimensional coordinates [NASA-TM-100012] N88-12991
DIODES
Fast autotuning of a hydrogen maser by cavity Q modulation N88-12707
The Pierce diode with an external circuit. Part 1: Simulations in the linear regime [DE88-000413] N88-12791
DIRECTIONAL STABILITY
Effects of jet exhaust yaw vane installation and operation on the longitudinal and lateral-directional characteristics of the F-14 airplane [NASA-TP-2769] N88-12455
DISCHARGE COEFFICIENT
Measurement of the electron density and the attachment rate coefficient in silane/helium discharges [AD-A184268] N88-13051
DISCRETE FUNCTIONS
Solution of the two-dimensional Euler equations on unstructured triangular meshes N88-12469
DISPERSING
Aircraft engine exhaust plume dynamics [AD-A184238] N88-12488
Activities at government research laboratories reported N88-12503
Compatability of dispersion-strengthened platinum with resistojet propellants [NASA-TP-2765] N88-12538
DISPLACEMENT
A study of the crack tip parameters that govern environmentally assisted cracking by use of the rising displacement test N88-12649
The dynamics of solar magnetic flux tubes subjected to resonant foot point shaking N88-13116
DISPLAY DEVICES
Effects of combining vertical and horizontal information into a primary flight display [NASA-TP-2783] N88-12487
Input devices for tasks using interactive video [PB87-220018] N88-12684
Traveling-wave maser closed-cycle refrigerator data acquisition and display system N88-12708
Input/output technologies: An overview of image scanning, storage, and display [DE87-014837] N88-12933
An interactive computer graphics network monitor for a tactical communications network [AD-A184131] N88-12938
DISSIPATION
A dissipation principle and its consequences for structured shock waves in thermoelastic materials [DE87-013723] N88-12813
Canonical transformations and exact invariants for dissipative systems [DE87-703663] N88-12985
DISTRIBUTED PROCESSING
Managing distributed derived data: A preliminary proposal [DE88-000714] N88-12966
DISTRIBUTION FUNCTIONS
Monte Carlo analysis of neoclassical transport for a compact helical system [IPPJ-850] N88-13033
DIURNAL VARIATIONS
Asymmetry and variations of solar limb darkening along the diameter defined by diurnal motion in April 1981 N88-13111
DOPPLER EFFECT
Flux tube dynamics and solar/stellar redshift measurements N88-13095
Doppler snapshots N88-13125
DOPPLER RADAR
Study of an airborne Doppler radar: Project Asterix [BLL-MO-TRANS-1667-(9022.552)] N88-12675

DOWNLINKING
Analysis of the ICE combiner for multiple antenna arraying N88-12704
DRAG
Boundary effects on the drag of an oscillating sphere: Applications to the magnetic sphere rheometer. Attenuation and dispersion of acoustic waves in nematic liquid crystals N88-13007
DRAINAGE
Open-graded bases for airfield pavements [AD-A184461] N88-12500
DROPS (LIQUIDS)
Experimental evidence for modifying the current physical model for ice accretion on aircraft surfaces [NASA-TM-87184] N88-12473
The TAB method for numerical calculation of spray droplet breakup [DE87-011756] N88-12743
Energy balance in laser-irradiated vaporizing droplets [DE88-000525] N88-12782
DROUGHT
Drought, solar activity link established by Leningrad geophysicists N88-12635
DUCTILITY
Welding and weldability of ductile intermetallic alloys [DE87-014061] N88-12582
DURABILITY
Work-in-progress presented at the Army Symposium on Solid Mechanics, 1986: Lightening of the Force [AD-A184791] N88-12644
Durability of powdered aluminum structures N88-12655
DWARF STARS
The photospheric magnetic fields of cool stars: Recent results of survey and time-variability programs N88-13094
Angular momentum evolution of young stars N88-13099
Post-zero-age main sequence rotation N88-13100
Atmospheres of stars in the limits of thin and thick convection zones: The M dwarfs N88-13104
Differential B and V light curves of the bright by Draconis star HD60715 N88-13130
Broadband linear polarization and chromospheric CaII H and K line emission in late-type main sequence stars N88-13140
The onset of chromospheric activity among the A- and F- type stars N88-13144
Empirical relations between photospheric magnetic fields and atmospheric radiative losses for cool dwarf stars N88-13145
VLA observations of the X-ray bright Hyades M-dwarfs N88-13147
MHD energy fluxes for late type dwarfs N88-13148
A search for very low mass (brown dwarf) stars as wide binaries using a seven element infrared camera-photometer N88-13150
Chromospheric and coronal heating in a bias-free sample of K dwarfs N88-13184
Measurements of stellar magnetic fields: Empirical constraints on dynamo and rotational evolution theories N88-13185
M dwarfs from the Einstein medium sensitivity survey N88-13188
DYE LASERS
Laser induced fluorescent study of relativistic electron beams [AD-A184456] N88-12774
All-optical beam control by forced Rayleigh scattering [AD-A184315] N88-13018
DYNAMIC CHARACTERISTICS
Hovering helicopter flight dynamics: A study of vertical motion [AR-004-526] N88-12485
DYNAMIC LOADS
Free-edge delamination: Laminate width and loading conditions effects [NASA-TM-100238] N88-12551
Static standing and dynamic walking of a practical biped robot [DE88-001367] N88-12795
On dynamic loads in parallel shaft transmissions. 1: Modelling and analysis [NASA-TM-100180] N88-12797
On dynamic loads in parallel shaft transmissions. 2: Parameter study [NASA-TM-100181] N88-12798
Input turbulence features at a megawatt-size wind turbine, Medicine Bow, Wyoming [DE88-000098] N88-12873
Measurements and calculations of aerodynamic torques for a vertical-axis wind turbine [DE88-001783] N88-12876
DYNAMIC RESPONSE
An experimental investigation of dynamic ground effect [NASA-CR-4105] N88-12458
A method for the efficient calculation of elastic rotor blade dynamic response in forward flight N88-12460
Aircraft dynamic response calculation based on discrete-continual model N88-12624
A comparison of structural frequency response functions measured with forces from 500 to 250,000 lb [DE88-000868] N88-12829
Using a new characterization of turbulent wind for accurate correlation of wind turbine response with wind speed [DE88-001453] N88-12881
DYNAMIC STRUCTURAL ANALYSIS
A comparison of structural frequency response functions measured with forces from 500 to 250,000 lb [DE88-000868] N88-12829
Aircraft interior noise reduction by alternate resonance tuning [NASA-CR-181530] N88-13005
DYNAMICAL SYSTEMS
Measurements of vapor flux, liquid water contents, precipitation rates and riming in a Utah mountain cloud system [PB87-224945] N88-12900
Propagation of random initial conditions in time N88-12993
Novel dynamical investigations of excitons and their structure in semiconductors [DE87-014868] N88-13070
DYNAMO THEORY
Atmospheres of stars in the limits of thin and thick convection zones: The M dwarfs N88-13104

E

EARLY STARS
Magnetic fields on K and M stars N88-13137
The Einstein survey of the young stars in the Orion Nebula N88-13182
Galactic interstellar abundance surveys with IUE and IRAS N88-13206
EARTH (PLANET)
Steady distortion of shape of geoid and normal gravity field under influence of tidal potential N88-12839
EARTH ATMOSPHERE
The effects of minor trace gases on the transfer of thermal infrared radiation through the Earth's atmosphere N88-12893
National Center for Atmospheric Research [PB87-226391] N88-12901
A review of parameterizations of microphysical processes in clouds for application in models of regional atmospheric deposition [DE88-000451] N88-12909
EARTH CRUST
A new approach to modeling and interpreting electromagnetic sounding data [DE88-000460] N88-12715
An algorithmic approach to crustal deformation analysis N88-12891
EARTH OBSERVING SYSTEM (EOS)
Radiometric calibration of the Earth observing system's imaging sensors [NASA-CR-181542] N88-12865
EARTH ORBITS
Precise near-earth navigation with GPS: A survey of techniques N88-12682
EARTH TIDES
Steady distortion of shape of geoid and normal gravity field under influence of tidal potential N88-12839
ECLIPSING BINARY STARS
Contemporaneous B,V,R,I photometry and H alpha spectroscopy of YY Gem N88-13155
Light curve behaviour in the near IR of the CG Cyg system N88-13156
A flash spectrum of CI I, C I, N I, and Ni II absorption in 31 Cygni: A direct observation of the reversing layer N88-13158
New results from high angular resolution observations of alpha Ori N88-13161
Stromgren photometry of RSCVn and HD108102 N88-13187
ECONOMICS
Technology transfer to China [PB87-223416] N88-13067
The role of basic research in society [DE88-000459] N88-13090
ECOSYSTEMS
Disturbance and recovery of Arctic Alaskan tundra terrain. A review of recent investigations [AD-A184442] N88-12887
EDDY CURRENTS
Pulsed eddy-current inspection of thin-walled stainless steel tubing [DE88-001492] N88-12830
EDGES
Free-edge delamination: Laminate width and loading conditions effects [NASA-TM-100238] N88-12551
EDUCATION
The pros and cons of using a CAI package on a central computer as opposed to a microprocessor: What's your CAI MO, mainframe or micro [DE87-011123] N88-12929
EFFICIENCY
High power ion thruster performance [NASA-TM-100127] N88-12542
MHD energy fluxes for late type dwarfs N88-13148
EIGENVALUES
Investigation, development and application of optimal output feedback theory. Vol. 4: Measures of eigenvalue/eigenvector sensitivity to system parameters and unmodeled dynamics [NASA-CR-4106] N88-12989
Ballooning modes or Fourier modes in a toroidal plasma? [AD-A184299] N88-13022
EIGENVECTORS
New feedback design methodologies for large space structures: A multi-criterion optimization approach N88-12535
Investigation, development and application of optimal output feedback theory. Vol. 4: Measures of eigenvalue/eigenvector sensitivity to system parameters and unmodeled dynamics [NASA-CR-4106] N88-12989
EINSTEIN EQUATIONS
Cosmological applications of singular hypersurfaces in general relativity N88-13202
EJECTA
Conditions for geomagnetically trapping sub-micron lunar ejecta between L = 1.2 and L = 3.1 N88-13203
EJECTORS
A cold ejector for closed-cycle helium refrigerators N88-12690
EL NINO
On the interannual variability of South American climate and the Southern Oscillation N88-12905
ELASTIC BUCKLING
Vibration and buckling of geometrically imperfect laminated cylindrical shells N88-12822
ELASTIC PROPERTIES
A method for the efficient calculation of elastic rotor blade dynamic response in forward flight N88-12460
Carbon-fiber reinforced plastics N88-12506
Natural control of flexible space structures N88-12534
Model for ultrasonic attenuation and elastic constant in chromium and its alloys [DE87-703478] N88-12570
Nonlinear acoustics [AD-A184271] N88-13004
Soliton twin boundaries of the cubic-tetragonal martensitic transformations in ferroelastic materials [DE87-014741] N88-13047
ELASTOMERS
Thermoplastic elastomer compositions — cable jackets [EP-PATENT-0-204-453-A1] N88-12593
Thermoplastic elastomers as LOVA (Low Vulnerability Ammunition) binders [AD-A184350] N88-12599
ELECTRIC BATTERIES
Applications of multivalent ionic conductors to polymeric electrolyte batteries [AD-A184252] N88-12722
Corrosion susceptibility study of candidate pin materials for ALTC (Active Lithium/Thionyl Chloride) batteries [DE88-001449] N88-12734
Reliability of Li/SO2 cells for long-life applications [DE88-001360] N88-12735
A hydrogen/nickel oxide battery for remote applications [DE87-009048] N88-12872
ELECTRIC COILS
Departmental report on program EMTP-machine windings surge transients: Travelling wave method [PB87-123733] N88-12719
ELECTRIC CONDUCTORS
Advances in inherently conducting polymers [DE88-000501] N88-12610
Departmental report on program EMTP-machine windings surge transients: Travelling wave method [PB87-123733] N88-12719
ELECTRIC DISCHARGES
Nitrogen energy transfer study [AD-A184457] N88-12689

ELECTRIC ENERGY STORAGE
Technology Base Research Project for electrochemical energy storage
[DE88-000649] N88-12868
ELECTRIC FIELDS
Thermal analysis of electromagnetic launcher rails
[DE88-000166] N88-12514
ELECTRIC GENERATORS
Solar energy: European research and development
[PB87-107645] N88-12866
Design description report for a photovoltaic power system for a remote satellite earth terminal
[NASA-CR-179586] N88-12875
ELECTRIC MOTOR VEHICLES
Performance monitoring and analysis of electric van fleet vehicles
[DE88-900066] N88-13091
ELECTRIC NETWORKS
Performance optimization of electronic networks in the frequency domain
[PB87-123873] N88-12720
ELECTRIC POTENTIAL
Departmental report on program EMTP-machine windings surge transients: Travelling wave method
[PB87-123733] N88-12719
Conditions for geomagnetically trapping sub-micron lunar ejecta between L = 1.2 and L = 3.1 N88-13203
ELECTRIC POWER PLANTS
USSR report: Engineering and equipment
[JPRS-UEQ-87-008] N88-12621
Solar energy: European research and development
[PB87-107645] N88-12866
ELECTRIC PROPULSION
High power ion thruster performance
[NASA-TM-100127] N88-12542
ELECTRIC PULSES
On M-ARY sequential hypotheses testing for the classification of radar signals
[AD-A184094] N88-12666
ELECTRICAL INSULATION
Polymer composition — cable insulation
[EP-PATENT-0-199-444-A1] N88-12594
ELECTRICAL MEASUREMENT
Analysis of free cutting brass by A.C. polarography
[PD-MT-8728] N88-12587
ELECTRICAL PROPERTIES
Research and development on high strength ceramic heaters discussed N88-12508
Synthesis, NMR characterization and electrical properties of siloxane-based polymer electrolytes
[AD-A184184] N88-12596
ELECTRICAL RESISTANCE
On the stressing of annealed NITINOL: The electrical resistance and calorimetric effects
[AD-A184465] N88-12569
Studies of alumina additions in zirconia - magnesia
[DE87-703500] N88-12602
ELECTRICAL RESISTIVITY
Research and development on high strength ceramic heaters discussed N88-12508
Ultimate velocities for induction launchers
[DE87-012360] N88-12513
Studies on some Ge-Se-Te glasses
[PD-MT-8721] N88-12607
Proton abstraction as a route to conductive polymers
[AD-A184019] N88-12612
Resistivity of EuBa2(Cu/sub 1-y/Zn/sub y/)3O/sub x/ as a function of temperature, magnetic field, pressure and Zn concentration
[DE87-014740] N88-13069
ELECTRO-OPTICS
Development of optical modulators for measurements of solar magnetic fields
[NASA-TM-100315] N88-13016
ELECTROACOUSTIC TRANSDUCERS
Noncontact temperature measurements of hot steel bodies using an electromagnetic acoustic transducer (EMAT)
[DE88-000560] N88-12765
ELECTROCATALYSTS
Internal reforming development for solid oxide fuel cells
[DE87-006518] N88-12871
ELECTROCHEMICAL CELLS
Reliability of Li/SO2 cells for long-life applications
[DE88-001360] N88-12735
Technology Base Research Project for electrochemical energy storage
[DE88-000649] N88-12868
ELECTROCHEMICAL CORROSION
Corrosion behavior of P/M mechanically alloyed IN-9052.1: An electro-chemical investigation
[AD-A184191] N88-12567
ELECTROCHEMISTRY
Advances in inherently conducting polymers
[DE88-000501] N88-12610
Chemically modified microelectrode arrays. New kinds of electronic devices
[AD-A184389] N88-12724
ELECTRODEPOSITION
Studies on high-speed electroforming
[DE88-001395] N88-12656
ELECTRODES
Chemically modified microelectrode arrays. New kinds of electronic devices
[AD-A184389] N88-12724
Far-infrared spectra of lithium deposited on a gold electrode: Interpretation using a cluster model
[AD-A184231] N88-13050
ELECTROENCEPHALOGRAPHY
Change in functional activity of cortical brain structures and their blood supply in alert rabbits in response to rocking N88-12916
ELECTROFORMING
Studies on high-speed electroforming
[DE88-001395] N88-12656
ELECTROLYTES
Applications of multivalent ionic conductors to polymeric electrolyte batteries
[AD-A184252] N88-12722
ELECTROMAGNETIC FIELDS
A new approach to modeling and interpreting electromagnetic sounding data
[DE88-000480] N88-12715
ELECTROMAGNETIC INTERFERENCE
Experimental and analytic studies of the triggered lightning environment of the F106B
[NASA-CR-4104] N88-12897
ELECTROMAGNETIC NOISE
On a circular correlation technique for filtering randomly noisy data
[AD-A184317] N88-12669
ELECTROMAGNETIC PROPULSION
Analysis of a series of electromagnetic launcher firings
[AR-005-131] N88-12516
ELECTROMAGNETIC PULSES
Ultimate velocities for induction launchers
[DE87-012360] N88-12513
Nitrogen energy transfer study
[AD-A184457] N88-12669
All-optical beam control by forced Rayleigh scattering
[AD-A184315] N88-13018
ELECTROMAGNETIC SCATTERING
New main reflector, subreflector and dual chamber concepts for compact range applications
[NASA-CR-181506] N88-12496
A study of scattering from E-plane circuit elements
[AD-A184473] N88-12673
ELECTROMAGNETS
An excitation-term modification for a certain class of electromagnetic aperture-coupling problems
[DE88-000260] N88-12713
ELECTRON ACCELERATION
Nonthermal phenomena in stellar coronae: Evidence from radio observations N88-13096
ELECTRON AFFINITY
K-CO on transition metals: A local ionic interaction
[AD-A184342] N88-13056
ELECTRON BEAM WELDING
Development of an acoustic emission monitor and monitoring techniques for long-term monitoring of U-0.8Ti electron-beam weldments for postweld cracking
[DE88-000819] N88-12804
ELECTRON BEAMS
The lasertron RF generator for FEL (Free-Electron Laser) applications
[DE88-000515] N88-12776
Development of an acoustic emission monitor and monitoring techniques for long-term monitoring of U-0.8Ti electron-beam weldments for postweld cracking
[DE88-000819] N88-12804
Use of electron beam instruments to determine fluctuations in vertical refraction partial angle N88-12853
ELECTRON CAPTURE
Final (n,l) state-resolved electron capture by multiply charged ions from neutral atoms
[IPPJ-AM-54] N88-13030
ELECTRON DENSITY (CONCENTRATION)
Equilibrium calculations of ionization in tracer flames
[PB87-104154] N88-12555
J = O Task Force
[DE88-001326] N88-12788
Measurement of the electron density and the attachment rate coefficient in silane/helium discharges
[AD-A184268] N88-13051
ELECTRON PRECIPITATION
Relativistic electron precipitations in a pulsating aurora N88-12894
ELECTRON STATES
Nitrogen energy transfer study
[AD-A184457] N88-12669
ELECTRON TRANSFER
K-CO on transition metals: A local ionic interaction
[AD-A184342] N88-13056
ELECTRON TRANSITIONS
XUV emission features from the Livermore soft X-ray laser experiments
[DE88-000420] N88-12779
J = O Task Force
[DE88-001326] N88-12788
Wavelengths of the 3p-3d transitions of the Co- and Fe-like ions: The effects of electron correlation
[DE88-000219] N88-13067
ELECTRONIC CONTROL
Engine/airframe response evaluation of the HH-60A helicopter equipped with the T700-GE-701 transient droop improvement electronic control unit
[AD-A184443] N88-12492
ELECTRONIC EQUIPMENT
Design of digital filters for electronic instrumentation
[PB87-100418] N88-12716
Alternating current circuit theory and pulsed NMR (Nuclear Magnetic Resonance)
[DE88-000641] N88-12732
ELECTRONS
Confinement time of electrons and H(-)/D(-) ions in the Uramoto type sheet plasma
[IPPJ-852] N88-13032
Prompt simultaneous acceleration of protons and electrons to relativistic energies by shock waves in solar flares
[IPPJ-851] N88-13037
Tetrahedral carbon and interstitial electrons in Li cluster: CLi4 and (LiCH3)4
[AD-A184277] N88-13055
ELECTROSTATIC CHARGE
Conditions for geomagnetically trapping sub-micron lunar ejecta between L = 1.2 and L = 3.1 N88-13203
ELECTROSTATICS
Some new ideas in liquid detectors
[DE88-000732] N88-12768
ELEVATORS (LIFTS)
Analytical investigation of the dynamics of tethered constellations in Earth orbit (phase 2)
[NASA-CR-179218] N88-12533
ELLIPTIC FUNCTIONS
A comparison of adaptive refinement techniques for elliptic problems
[DE88-000805] N88-12987
EMISSION
Emerging environmental constraints on the use of gasoline and diesel fuel and tradeoffs associated with the use of alternative fuels
[DE87-011504] N88-12614
EMISSION SPECTRA
Excess emission in the wings of the Hydrogen Balmer lines during a flare on the late-type dMe star YZ CMi N88-13146
Emission features in IRAS LRS spectra of MS, S and CS stars N88-13163
The Wilson-Bappu relationship: A barometric effect N88-13170
JHK photometry of CN-rich field giants N88-13175
Water masers associated with 2 carbon stars: EU Andromedae and V778 Cygni N88-13176
Chromospheric variability mechanisms affecting pre-main sequence stars N88-13180
The Einstein survey of the young stars in the Orion Nebula N88-13182
M dwarfs from the Einstein medium sensitivity survey N88-13188
A helium flare on the active G5 dwarf Kappa Ceti N88-13189
EMISSIVITY
Lidar-radiometric method for determining liquid-water content of cirrus clouds N88-12954
ENERGY BANDS
Banded ion morphology N88-12892
ENERGY BUDGETS
Energy balance in laser-irradiated vaporizing droplets
[DE88-000525] N88-12782
ENERGY CONSUMPTION
Optimized ground coupled heat pump mechanical package
[DE87-014899] N88-12738
ENERGY CONVERSION EFFICIENCY
Performance analysis of solar thermal power systems
[DE88-000563] N88-12874
International Energy Agency (IEA) Small Solar Power Systems (SSPS) sodium cavity and external receiver performance comparison
[DE88-001310] N88-12879
ENERGY DISSIPATION
Resistor cooling in a vacuum
[DE88-000666] N88-12733
Heating of stellar chromospheres and coronae: Evidence for non-magnetic basal heating N88-13098

Chromospheric and coronal heating in a bias-free sample of K dwarfs N88-13184

ENERGY DISTRIBUTION

The closest solar analogs in the bright star catalogue N88-13110

Statistical properties of small high-velocity events in the solar transition region N88-13112

ENERGY LEVELS

J = O Task Force
[DE88-001326] N88-12788

ENERGY POLICY

Emerging environmental constraints on the use of gasoline and diesel fuel and tradeoffs associated with the use of alternative fuels
[DE87-011504] N88-12614

ENERGY REQUIREMENTS

A large X-ray flare on squared Sigma coronae borealis observed with exosat N88-13121

ENERGY SPECTRA

A multiple-time-scale turbulence model based on variable partitioning of turbulent kinetic energy spectrum
[NASA-CR-179222] N88-12754

Spectral evolution equation for the sideband instability in a free-electron laser oscillator
[DE88-000510] N88-12771

Simultaneous, cospatial imaging of the Sun in cyancgen and singly-ionized calcium N88-13114

ENERGY STORAGE

A study of the optimal transition temperatue of PCM (Phase Change Material) wallboard for solar energy storage
[DE88-001522] N88-12882

ENERGY TECHNOLOGY

Proceedings of the Fifth Symposium on Energy Engineering Sciences: Instrumentation, Diagnostics, and Material Behavior
[DE88-001479] N88-12660

ENERGY TRANSFER

Theory of heat and moisture exchange between finely disperse storm-generated spray and turbulent air flow N88-12851

Nitrogen energy transfer study
[AD-A184457] N88-12869

Variable collision frequency effects on hose and sausage instabilities in relativistic electron beams
[AD-A184206] N88-13021

ENGINE CONTROL

Engine/airframe response evaluation of the HH-60A helicopter equipped with the T700-GE-701 transient droop improvement electronic control unit
[AD-A184443] N88-12492

ENGINE PARTS

Composite mechanics for engine structures
[NASA-TM-100176] N88-12552

ENGINE TESTS

Performance and combustion characteristics of direct-injection stratified-charge rotary engines
[NASA-TM-100134] N88-12490

ENGINEERING MANAGEMENT

Proceedings of the Fifth Symposium on Energy Engineering Sciences: Instrumentation, Diagnostics, and Material Behavior
[DE88-001479] N88-12660

The characterization of diagnostic tasks for engineering systems
[DE88-000053] N88-12973

ENTRAINMENT

Turbulent mixing in a rotating, stratified fluid N88-12759

ENTROPY

A dissipation principle and its consequences for structured shock waves in thermoelastic materials
[DE87-013723] N88-12813

ENVIRONMENT EFFECTS

Emerging environmental constraints on the use of gasoline and diesel fuel and tradeoffs associated with the use of alternative fuels
[DE87-011504] N88-12614

Disturbance and recovery of Arctic Alaskan tundra terrain. A review of recent investigations
[AD-A184442] N88-12887

ENVIRONMENTAL MONITORING

Evaluation of the sensidyne toxic gas sensor for HF (Hydrogen Fluoride) vapor
[DE88-000647] N88-12767

ENVIRONMENTS

On computing environments in data analysis
[DE88-000078] N88-12961

User interface for a partially incompatible system software environment with non-ADP users
[DE88-001518] N88-12968

EPHEMERIDES

Dynamic positioning at sea using the global positioning system
[AD-A184483] N88-12476

EPIDEMIOLOGY

JPRS report: Science and technology. USSR: Life sciences
[JPRS-ULS-87-009] N88-12915

EPOXY MATRIX COMPOSITES

A creep measurement of unidirectional epoxy-fiberglass rod
[DE87-014812] N88-12553

EQUATIONS OF MOTION

A method for the efficient calculation of elastic rotor blade dynamic response in forward flight N88-12480

Natural control of flexible space structures N88-12534

Aircraft dynamic response calculation based on discrete-continual model N88-12624

Local-optimal control in systems with delay N88-12627

Analytical studies of axially symmetric motion of an incompressible viscous fluid between two concentric rotating spheres N88-12757

EQUATIONS OF STATE

The LLNL 150-mm equation-of-state gun system
[DE88-000423] N88-12519

Studies of pressure-velocity coupling schemes for analysis of incompressible and compressible flows
[NASA-CR-181526] N88-12748

Core bounce supernovae
[DE87-014910] N88-13197

EQUILIBRIUM FLOW

Continuation finite element analysis of viscoelastic fluids N88-12761

EQUIVALENT CIRCUITS

A study of scattering from E-plane circuit elements
[AD-A184473] N88-12673

EROSION

Pipe and bend erosion by pneumatic transport of solids at high temperature
[DE88-001345] N88-12658

Data base on the high heat flux behaviour of metals and carbon materials for plasma facing components: Experiments at the 10 MW neutral beam injection test stand of the IPP Nagoya
[IPPJ-AM-53] N88-13031

PISCES: Plasma-surface interactions and materials research
[DE88-001323] N88-13044

ERROR ANALYSIS

Accommodating the residue of processed or computed digital video signals within the 8 bit CCIR recommendation 601
[BBC-RD-1987/12] N88-12676

More on the decoder error probability for Reed-Solomon codes N88-12699

Kinematic formulation of finite elements for plate bending N88-12821

ERROR CORRECTING CODES

A simplified procedure for correcting both errors and erasures of a Reed-Solomon code using the Euclidean algorithm N88-12686

More on the decoder error probability for Reed-Solomon codes N88-12699

ERROR CORRECTING DEVICES

Design of source coders and joint source/channel coders for noisy channels
[NASA-CR-181547] N88-12678

ERRORS

Optical alignment of Centaur's inertial guidance system
[NASA-TM-88844] N88-12515

Calibration of a laser-pumped, thermographic phosphor remote thermometry system
[DE88-000452] N88-12781

Radial orbit error reduction and sea surface topography determination using satellite altimetry N88-12861

GOLD: Integration of model-based control systems with artificial intelligence and workstations
[DE88-000706] N88-12977

ESCHERICHIA

Study of certain biological characteristics of bacteria during the French-Soviet CYTOS-2 space experiment N88-12917

ESTIMATES

Studies on estimation of nickel in zinc base die casting by D.C. polarography
[PD-MT-8729] N88-12588

ETCHING

Metallography of maraging 350 steel
[DE87-013746] N88-12591

ETHERS

Surface catalytic degradation study of two linear perfluoropolyalkylethers at 345 C
[NASA-TP-2774] N88-12543

EULER EQUATIONS OF MOTION

Application of Runge Kutta time marching scheme for the computation of transonic flows in turbomachines
[NASA-TM-88997] N88-12481

Concepts for radically increasing the numerical convergence rate of the Euler equations
[NASA-CR-177456] N88-12483

Solution of the two-dimensional Euler equations on unstructured triangular meshes N88-12489

A free-Lagrange method for 2-D compressible flows
[DE88-000216] N88-12745

EULER-LAGRANGE EQUATION

A free-Lagrange method for 2-D compressible flows
[DE88-000216] N88-12745

Three-dimensional, free-Lagrange hydrodynamics
[DE88-000494] N88-12749

EUROPE

Solar energy: European research and development
[PB87-107645] N88-12866

EUROPIUM COMPOUNDS

Resistivity of EuBa2(Cu/sub 1-y/Zn/sub y/)3O/sub x/ as a function of temperature, magnetic field, pressure and Zn concentration
[DE87-014740] N88-13089

EVALUATION

An evaluation plan of bus architectures and protocols using the NASA Ames intelligent redundant actuation system
[NASA-CR-177458] N88-12482

Non-linearity in measurement systems: Evaluation method and application to microwave radiometers N88-12884

Standard fatigue test specimens for fastener evaluation
[AGARD-AG-304] N88-12818

Methods for design and evaluation of integrated hardware/software systems for concurrent computation
[NASA-CR-181522] N88-12953

EVAPORATION

Ceramics thin film N88-12505

Effects of rainfall on the seasonal thermocline
[AD-A184432] N88-12912

EVAPORATIVE COOLING

Advanced radiator concepts utilizing honeycomb panel heat pipes
[NASA-CR-172017] N88-12747

EVOKED RESPONSE (PSYCHOPHYSIOLOGY)

Visual evoked responses to sinusoidal gratings presented in central and right visual fields: 1
[DE87-014731] N88-12919

EVOLUTION (DEVELOPMENT)

Cosmological applications of singular hypersurfaces in general relativity N88-13202

EXCITATION

Excitation of natural oscillations of a boundary layer by an external acoustic field N88-12634

An excitation-term modification for a certain class of electromagnetic aperture-coupling problems
[DE88-000260] N88-12713

Alternating current circuit theory and pulsed NMR (Nuclear Magnetic Resonance)
[DE88-000641] N88-12732

J = O Task Force
[DE88-001326] N88-12788

Thermomechanical cracking in coated media due to high speed asperity excitation
[AD-A184176] N88-12809

Mechanical shock test specification using nonstationary random excitation models
[DE87-013650] N88-12812

Vibration and parametric excitation in rotating asymmetric circular plates N88-12823

Implementation of a new shock testing procedure using nonstationary random excitation
[DE87-014643] N88-12827

Nitrogen energy transfer study
[AD-A184457] N88-12869

EXCITONS

Novel dynamical investigations of excitons and their structure in semiconductors
[DE87-014868] N88-13070

EXOBIOLOGY

Aerospace medicine and biology: A continuing bibliography with indexes
[NASA-SP-7011(304)] N88-12922

EXOSAT SATELLITE

The X-ray orbital lightcurves of AR Lac and TY Pyx N88-13129

Evidence for expanding magnetic loops in coronae of cool stars N88-13134

Exosat results on the dMe flare Star Wolf 630AB and on VB 8 N88-13151

EXPANSION

Pulse-mode expansions and refractive indices in plane-wave propagation
[DE88-001328] N88-12714

EXPEDITIONS

Huurre expedition to the North Pole in 1984
[PB87-220935] N88-12858

EXPERIMENT DESIGN
Access to microgravity: A technical description of the NAE T-33 microgravity facility
[NAE-AN-47] N88-12518
Experimental use of artificial intelligence for (future) ATC systems
[PB87-106449] N88-12970
EXPERT SYSTEMS
An evaluation plan of bus architectures and protocols using the NASA Ames Intelligent redundant actuation system
[NASA-CR-177458] N88-12482
Expert robots in nuclear plants
[DE87-014839] N88-12800
Experimental use of artificial intelligence for (future) ATC systems
[PB87-106449] N88-12970
The characterization of diagnostic tasks for engineering systems
[DE88-000093] N88-12973
An expert system for materials design
[DE88-000191] N88-12974
GOLD: Integration of model-based control systems with artificial intelligence and workstations
[DE88-000508] N88-12976
GOLD: Integration of model-based control systems with artificial intelligence and workstations
[DE88-000706] N88-12977
Intelligent signal analysis and recognition
[NASA-CR-181531] N88-13084
EXPLOSIONS
Aircraft fire safety research N88-12526
EXPLOSIVES
The LLNL 150-mm equation-of-state gun system
[DE88-000423] N88-12519
DOE explosives safety manual
[DE88-000831] N88-12616
EXTENSOMETERS
Optimization of dilatometer test procedures
[DE87-014998] N88-12769
Small-diameter wire tensile testing
[DE88-000835] N88-12815
EXTINCTION
Measurements of iridium and the meteoric impact hypothesis at cretaceous end
[DE87-703765] N88-13200
EXTRATERRESTRIAL INTELLIGENCE
The Telecommunications and Data Acquisition Report
[NASA-CR-181548] N88-12679
Intelligent signal analysis and recognition
[NASA-CR-181531] N88-13084
EXTRAVEHICULAR ACTIVITY
Space suit extravehicular hazards protection development
[NASA-TM-100458] N88-12927
EXTREME ULTRAVIOLET RADIATION
XUV emission features from the Livermore soft X-ray laser experiments
[DE88-000420] N88-12779
EXTRUDING
Activities at government research laboratories reported N88-12503
Continuation finite element analysis of viscoelastic fluids N88-12761
EYE (ANATOMY)
Motion and space sickness N88-12510

F

F REGION
High latitude F-region drift studies
[AD-A184466] N88-12889
F-14 AIRCRAFT
Effects of jet exhaust yaw vane installation and operation on the longitudinal and lateral-directional characteristics of the F-14 airplane
[NASA-TP-2769] N88-12455
F-106 AIRCRAFT
An experimental investigation of dynamic ground effect
[NASA-CR-4105] N88-12458
Experimental and analytic studies of the triggered lightning environment of the F106B
[NASA-CR-4104] N88-12897
FABRICATION
Development of advanced fiber reinforced ceramics
[DE88-000779] N88-12604
Raman scattering spectrum along a bevel etched GaAs on Si, TEM (Transmission Electron Microscope) study and GaAs P-I-N photodetector on Si
[DE88-000210] N88-13066
Performance monitoring and analysis of electric van fleet vehicles
[DE88-900066] N88-13091
FACTORIZATION
QR factorization of a dense matrix on a shared-memory multiprocessor
[DE88-001506] N88-12956
Two classes of preconditioners computed using block matrix factorization techniques
[DE88-001313] N88-12988
FAILURE
Fatigue failure of thin porous strips N88-12640
Programmable Logic Arrays (PLA's) design for testability
[PB87-102935] N88-12718
FAILURE ANALYSIS
Analysis of 7- X 10-foot high speed wind tunnel shaft loads in support of fan blade failure investigation
[NASA-TM-100504] N88-12496
Failure analysis of composite structure materials
[AD-A184468] N88-12548
FAINT OBJECT CAMERA
A search for very low mass (brown dwarf) stars as wide binaries using a seven element infrared camera-photometer N88-13150
FAN BLADES
Analysis of 7- X 10-foot high speed wind tunnel shaft loads in support of fan blade failure investigation
[NASA-TM-100504] N88-12496
FAR INFRARED RADIATION
Absorption of far IR-radiation by H2O-N2 complexes under atmospheric conditions N88-12855
Far-infrared spectra of lithium deposited on a gold electrode: Interpretation using a cluster model
[AD-A184231] N88-13050
Far infrared Fourier transform spectroscopy of semiconductors
[DE88-000188] N88-13072
Far infrared circumstellar debris shells of red supergiant stars N88-13165
FAR ULTRAVIOLET RADIATION
A comprehensive exploration of late-type stars in the far-ultraviolet N88-13194
FARADAY EFFECT
Laser induced fluorescent study of relativistic electron beams
[AD-A184456] N88-12774
FASTENERS
Standard fatigue test specimens for fastener evaluation
[AGARD-AG-304] N88-12818
FATIGUE (MATERIALS)
Mechanical behavior of a controlled rolled high-strength low alloy steel plate, microalloyed with Nb and V
[DE87-703507] N88-12571
Work-in-progress presented at the Army Symposium on Solid Mechanics, 1986: Lightening of the Force
[AD-A184791] N88-12644
FATIGUE LIFE
Durability of powdered aluminum structures N88-12655
Input turbulence features at a megawatt-size wind turbine, Medicine Bow, Wyoming
[DE88-000098] N88-12873
FATIGUE TESTS
Standard fatigue test specimens for fastener evaluation
[AGARD-AG-304] N88-12818
FEASIBILITY ANALYSIS
Repulsive force support system feasibility study
[NASA-CR-178400] N88-12497
Light funnel concentrator panel for solar power
[NASA-CR-179223] N88-12870
The VISTA spacecraft: Advantages of ICF (Inertial Confinement Fusion) for interplanetary fusions propulsion applications
[NASA-CR-181549] N88-13024
Ground vehicle convoying
[DE88-000360] N88-13088
Performance monitoring and analysis of electric van fleet vehicles
[DE88-900066] N88-13091
FEEDBACK
New feedback design methodologies for large space structures: A multi-criterion optimization approach N88-12535
Investigation, development and application of optimal output feedback theory. Vol. 4: Measures of eigenvalue/eigenvector sensitivity to system parameters and unmodeled dynamics
[NASA-CR-4106] N88-12969
FEEDBACK CONTROL
A modern control theory based algorithm for control of the NASA/JPL 70-meter antenna axis servos N88-12706
Fast autotuning of a hydrogen maser by cavity Q modulation N88-12707
FERRITIC STAINLESS STEELS
Mechanical properties of an acicular ferrite steel microalloyed to niobium and vanadium
[DE87-703547] N88-12574
FERROMAGNETIC MATERIALS
Influence of bond dilution on the free surface and interface Potts ferromagnetism
[DE87-703360] N88-13061
FERROMAGNETISM
Influence of bond dilution on the free surface and interface Potts ferromagnetism
[DE87-703360] N88-13061
FIBER COMPOSITES
Optimal ribbing of long plate made of composite material N88-12641
FIBER OPTICS
An inexpensive real-time interactive three-dimensional flight simulation system
[AD-A184340] N88-12499
Spectroscopic monitoring of RS CVn stars at Kitt Peak using the Penn State fiber optic echelle N88-13127
FIBER REINFORCED COMPOSITES
Carbon fiber reinforced glass matrix composites for space based applications
[AD-A184355] N88-12548
Molecular composites: Processing, post-treatment and mechanics
[AD-A184458] N88-12547
Interfacial strength development in thermoplastic resins and fiber-reinforced thermoplastic composites
[NASA-CR-181525] N88-12549
Development of advanced fiber reinforced ceramics
[DE88-000779] N88-12604
FIBER STRENGTH
Carbon-fiber reinforced aluminum N88-12507
FIBONACCI NUMBERS
On color polynomials of Fibonacci graphs
[AD-A184133] N88-12996
FIELD EMISSION
Conditions for geomagnetically trapping sub-micron lunar ejecta between L = 1.2 and L = 3.1 N88-13203
FIELD OF VIEW
Two dimensional path planning with obstacles and shadows
[AD-A184075] N88-12474
FIELD STRENGTH
Magnetic flux tubes as sources of wave generation N88-13106
Measurements of stellar magnetic fields: Empirical constraints on dynamo and rotational evolution theories N88-13185
Observations and analysis of the photospheric magnetic fields on dwarf G, K and M stars N88-13196
FIELD THEORY (PHYSICS)
Gravity from symmetry breakdown of a gauge affine theory
[DE88-001671] N88-13079
FILM COOLING
National Aerospace Laboratory experiment N88-12509
FILTRATION
Plume mechanics and aerosol growth processes
[AD-A184467] N88-12742
FINENESS RATIO
Planform effects on the supersonic aerodynamics of multibody configurations
[NASA-TP-2762] N88-12454
FINITE DIFFERENCE THEORY
A two-dimensional finite difference program for thermal analysis of rocket thrust chambers
[NASA-TM-100191] N88-12539
Calculation of three-dimensional stationary turbulent boundary layer on root section of wing ignoring compressibility N88-12630
Generating meshes for finite-difference analysis using a solid modeler
[DE88-001458] N88-12729
FINITE ELEMENT METHOD
Total linearisation method for solving viscous free boundary flow problems by the finite element method
[PB87-222337] N88-12737
NACHOS 2: A finite element computer program for incompressible flow problems. Part 2: User's manual
[DE88-001451] N88-12750
TOPAZ: The transient one-dimensional pipe flow analyzer: An update on code improvements and increased capabilities
[DE88-001781] N88-12751
Continuation finite element analysis of viscoelastic fluids N88-12761
Nonlinear axial stiffness characteristics of axisymmetric bolted joints N88-12799
A refined nonlinear analysis of laminated composite plates and shells
[AD-A184436] N88-12811

Kinematic formulation of finite elements for plate bending N88-12821
Large change-of-curvature effects in quadratic finite elements for CAD of membrane structures N88-12958
A comparison of adaptive refinement techniques for elliptic problems
[DE88-000805] N88-12987
The finite element method for electronic structure
[DE88-001708] N88-12989
A finite element procedure for interference-fit and cold-working problems with limited yielding
[AR-004-517] N88-12992

FINITE VOLUME METHOD
High resolution finite volume methods on arbitrary grids via wave propagation
[NASA-CR-178397] N88-12979

FINLAND
Huurre expedition to the North Pole in 1984
[PB87-220935] N88-12858

FIR FILTERS
Design of efficient FIR filters with minimal delay
[PB87-100434] N88-12717

FIRE EXTINGUISHERS
Spacecraft Fire Safety
[NASA-CP-2476] N88-12520
Fire extinguishment and inhibition in spacecraft environments N88-12523
Inerting and atmospheres N88-12524
Aircraft fire safety research N88-12526
Space station internal environmental and safety concerns N88-12527

FIRES
Spacecraft Fire Safety
[NASA-CP-2476] N88-12520
Techniques for fire detection N88-12521
Fire-related standards and testing N88-12522
Fire extinguishment and inhibition in spacecraft environments N88-12523
Inerting and atmospheres N88-12524
Fire-related medical science N88-12525
Aircraft fire safety research N88-12526
Space station internal environmental and safety concerns N88-12527
Microgravity combustion fundamentals N88-12528
Spacecraft material flammability testing and configurations N88-12529

FLAME PROPAGATION
Fire-related standards and testing N88-12522
Space station internal environmental and safety concerns N88-12527
Microgravity combustion fundamentals N88-12528

FLAME RETARDANTS
Thermoplastic elastomer compositions — cable jackets
[EP-PATENT-0-204-453-A1] N88-12593

FLAMES
Equilibrium calculations of ionization in tracer flames
[PB87-104154] N88-12555

FLAMMABILITY
Fabrication and testing of fire resistant graphite composite panels
[NASA-CR-177397] N88-12472
Spacecraft Fire Safety
[NASA-CP-2476] N88-12520
Fire-related standards and testing N88-12522
Spacecraft material flammability testing and configurations N88-12529

FLAPPING HINGES
Flap-lag equations of motion of rigid, articulated rotor blades with three hinge sequences
[NASA-TM-100023] N88-12495

FLAPS (CONTROL SURFACES)
Flap-lag equations of motion of rigid, articulated rotor blades with three hinge sequences
[NASA-TM-100023] N88-12495

FLARE STARS
A spectral survey of 26 G9-M6 flare stars in the solar neighborhood N88-13149
Exosat results on the dMe flare Star Wolf 630AB and on VB 8 N88-13151
IUE/Optical/VLA flares on AD Leo N88-13152
Microwave observations of red dwarf flare stars N88-13153
A VLA survey of dMe flare stars N88-13154

FLAT PLATES
Kinematic formulation of finite elements for plate bending N88-12821

FLEXIBLE BODIES
Finite deformations of shell with rigid inclusion N88-12639

FLEXIBLE SPACECRAFT
Natural control of flexible space structures N88-12534

FLIGHT CHARACTERISTICS
Development and application of computational aerothermodynamics flowfield computer codes
[NASA-CR-181534] N88-12465
Hovering helicopter flight dynamics: A study of vertical motion
[AR-004-526] N88-12485

FLIGHT CONTROL
An evaluation plan of bus architectures and protocols using the NASA Ames intelligent redundant actuation system
[NASA-CR-177458] N88-12482
Digital-flight-control-system software written in automated-engineering-design language: A user's guide of verification and validation tools
[NASA-TM-88313] N88-12494
Applications of the hybrid automated reliability predictor
[NASA-TP-2760] N88-12928

FLIGHT SIMULATION
An inexpensive real-time interactive three-dimensional flight simulation system
[AD-A184340] N88-12499
CGI delay compensation
[NASA-TM-86703] N88-12932

FLIGHT SIMULATORS
An inexpensive real-time interactive three-dimensional flight simulation system
[AD-A184340] N88-12499

FLIGHT TESTS
Developmental airdrop testing techniques and devices
[AGARD-AG-300-VOL-6] N88-12481
Human respiratory responses during high performance flight
[AGARD-AG-312] N88-12923

FLOATING POINT ARITHMETIC
Implementation and performance of a complex vision system on a systolic array machine
[AD-A184331] N88-12971

FLOOD PREDICTIONS
NWS (National Weather Service) watch/warning verification flash flood, winter storm and high wind, January 1986 - June 1986
[PB87-223053] N88-12898

FLOW DISTRIBUTION
Development and application of computational aerothermodynamics flowfield computer codes
[NASA-CR-181534] N88-12465
Three-dimensional unsteady flow elicited by finite wings and complex configurations N88-12468
A study of two-phase flow in a reduced gravity environment
[NASA-CR-172035] N88-12617
Ideal-viscoplastic extrusion model with application to deforming pistons in light-gas guns
[UTIAS-TN-266] N88-12657
Equilibria, lattices and chaotic dynamics of point vortices N88-12758
Optimization of explicit time-stepping algorithms and Stream-Function-Coordinate (SFC) concept for fluid dynamics problems N88-12762

FLOW EQUATIONS
Use of a thermodynamic analog for pneumatic transport in horizontal pipes
[AD-A184076] N88-12740

FLOW STABILITY
On the instability of thin circular shear layers N88-12467

FLOW THEORY
Steady shearing in a viscoplastic solid
[AD-A184341] N88-12810

FLOW VELOCITY
Geometric analysis of ensemble of solutions in two-phase flow and complete resolution of problem of choking
[DE88-001667] N88-12764
Variations of the vertical and horizontal velocities of the small-scale structures and the physical problems related to overshoot layers N88-13115

FLOW VISUALIZATION
Experimental aerothermodynamic research of hypersonic aircraft
[NASA-CR-181533] N88-12483
Observations on the hydrodynamic flow visualization at ONERA
[PD-FM-8718] N88-12753

FLUENCE
Microstructural change of Al on H implantation
[IPPJ-847] N88-13036

FLUID DYNAMICS
Dynamics of reverse flows at pump inlet N88-12636

FLUID FILMS
Studies of thin surface films aim at seeing deep ocean processes N88-12847

FLUID FLOW
Theory of one and two-pass cross-flow heat exchanger
[PB87-225157] N88-12736
Studies of pressure-velocity coupling schemes for analysis of incompressible and compressible flows
[NASA-CR-181526] N88-12748
Three-dimensional, free-Lagrange hydrodynamics
[DE88-000494] N88-12749
The modelling of orientation in planar polymer welding flows
[AD-A184404] N88-12793

FLUID MANAGEMENT
Space station resistojet system requirements and interface definition study
[NASA-CR-180832] N88-12541

FLUID MECHANICS
Some experiences with the viscous-inviscid interaction approach
[NASA-TM-100015] N88-12466
Low gravity fluid-thermal experiments
[DE88-000553] N88-12620
Proceedings of the Fifth Symposium on Energy Engineering Sciences: Instrumentation, Diagnostics, and Material Behavior
[DE88-001479] N88-12660
NACHOS 2: A finite element computer program for incompressible flow problems. Part 2: User's manual
[DE88-001451] N88-12750

FLUX (RATE)
A comprehensive exploration of late-type stars in the far-ultraviolet N88-13194
Gamma ray lines from novae N88-13214

FLUX DENSITY
Power density measurements in the near field of the DSS 13 26-meter antenna N88-12711
Measurements of vapor flux, liquid water contents, precipitation rates and riming in a Utah mountain cloud system
[PB87-224945] N88-12900
Calibration of the Ca II K line-core density and the magnetic flux density in stars using solar data N88-13118
VLA observations of the X-ray bright Hyades M-dwarfs N88-13147
MHD energy fluxes for late type dwarfs N88-13148

FORCE
Repulsive force support system feasibility study
[NASA-CR-178400] N88-12497

FORTRAN
Generating meshes for finite-difference analysis using a solid modeler
[DE88-001458] N88-12729
A review and analysis of Fortran 8x
[DE88-001320] N88-12955

FOUNDATIONS
Open-graded bases for airfield pavements
[AD-A184461] N88-12500

FOURIER ANALYSIS
Ballooning modes or Fourier modes in a toroidal plasma?
[AD-A184299] N88-13022

FOURIER TRANSFORMATION
Mutual admittance between slots in cylinders of arbitrary shape
[AD-A184254] N88-12723
Far infrared Fourier transform spectroscopy of semiconductors
[DE88-000188] N88-13072
Exploiting the IR: Solar and stellar spectroscopy in the IR N88-13102

FRACTOGRAPHY
Failure analysis of composite structure materials
[AD-A184468] N88-12548

FRACTURE MECHANICS
Ceramic technology for advanced heat engine project
[DE88-001520] N88-12605
Work-in-progress presented at the Army Symposium on Solid Mechanics, 1986: Lightening of the Force
[AD-A184791] N88-12644
Method for the ultrasonic inspection of the soundness of the metal in weld joints in two-ply pipes
[BLL-CE-TRANS-8265-(9022.09)] N88-12805

FRACTURE STRENGTH
Interfacial strength development in thermoplastic resins and fiber-reinforced thermoplastic composites
[NASA-CR-181525] N88-12549
Plastic strain localization between voids in shear deformation fields N88-12648

FRACTURING
Small-diameter wire tensile testing
[DE88-000835] N88-12815

FREE BOUNDARIES
Total linearisation method for solving viscous free boundary flow problems by the finite element method
[PB87-222337] N88-12737
FREE ELECTRON LASERS
Spectral evolution equation for the sideband instability in a free-electron laser oscillator
[DE88-000510] N88-12771
The free electron laser sideband instability reconsidered
[AD-A184269] N88-12773
High-power RF-pulsed modulators for the Los Alamos free-electron laser
[DE88-000514] N88-12775
The lasertron RF generator for FEL (Free-Electron Laser) applications
[DE88-000515] N88-12776
Analysis of sideband spectra from untapered undulator using analytical technique
[DE87-014763] N88-12778
Output power enhancement of AC Raman free-electron laser
[DE88-000503] N88-12786
The generation and suppression of synchrotron sidebands
[DE88-000532] N88-12787
Comparison of sideband spectra obtained from analytical formula and from numerical simulation in free-electron laser
[DE88-000521] N88-12789
FREE ENERGY
Soliton twin boundaries of the cubic-tetragonal martensitic transformations in ferroelastic materials
[DE87-014741] N88-13047
FREEZING
Experimental evidence for modifying the current physical model for ice accretion on aircraft surfaces
[NASA-TM-87164] N88-12473
FREQUENCIES
Lower bounds on bearing accuracy for closely spaced sources
[AD-A184258] N88-12997
FREQUENCY DISTRIBUTION
Statistical distribution of solar radiation (hourly sums): Cumulative frequency curves preparation of a European data set and direction for use
[PB87-107454] N88-12886
FREQUENCY MODULATION
Fast autotuning of a hydrogen maser by cavity Q modulation N88-12707
FREQUENCY MULTIPLIERS
Frequency doubling conversion efficiencies for deep space optical communications N88-12691
FREQUENCY STABILITY
X-band uplink ground systems development: Part 2 N88-12703
FRICTION
Ignition and combustion of metals in oxygen N88-12530
Canonical transformations and exact invariants for dissipative systems
[DE87-703663] N88-12985
FRICTION REDUCTION
Multipath gear-friction planetary transmissions N88-12629
FRONTS (METEOROLOGY)
Interactions between the Asian monsoons, the tropical Pacific and the southern hemisphere extratropics N88-12907
FROST
Measurements of vapor flux, liquid water contents, precipitation rates and riming in a Utah mountain cloud system
[PB87-224945] N88-12900
FUEL CELLS
Internal reforming development for solid oxide fuel cells
[DE87-006518] N88-12871
FUEL COMBUSTION
SCRAM JET (Supersonic Combustion Ramjet) combustion experiments N88-12512
FUEL FLOW
SCRAM JET (Supersonic Combustion Ramjet) combustion experiments N88-12512
FUEL INJECTION
Performance and combustion characteristics of direct-injection stratified-charge rotary engines
[NASA-TM-100134] N88-12490
SCRAM JET (Supersonic Combustion Ramjet) combustion experiments N88-12512
A three-barrel repeating pneumatic pellet injector for plasma fueling of the Joint European Torus
[DE88-000330] N88-13026
FUEL SPRAYS
SCRAM JET (Supersonic Combustion Ramjet) combustion experiments N88-12512
FUEL SYSTEMS
Aircraft fire safety research N88-12526
FUEL TANKS
Performance analysis of advanced spacecraft TPS
[NASA-CR-181532] N88-12484
FUNCTIONAL DESIGN SPECIFICATIONS
Study of an airborne Doppler radar: Project Asterix
[BLL-MO-TRANS-1667-(9022.552)] N88-12575
FURNACES
Evaluation of the Mellen EDG furnace for growth of large diameter GaAs single crystals in a horizontal configuration
[DE88-000463] N88-13068
FUSELAGES
A 0.15-scale study of configuration effects on the aerodynamic interaction between main rotor and fuselage
[NASA-CR-166577] N88-12462
FUSION REACTORS
Inertial confinement fusion reactor cavity analysis
[DE88-000788] N88-13028
Refueling and density control in the ZT-40M reversed field pinch
[DE88-000504] N88-13040
PISCES: Plasma-surface interactions and materials research
[DE88-001323] N88-13044
ICRF launcher studies
[DE88-001710] N88-13046
FUZZY SETS
Foundations of O-theory 2: Measurements and relation to fuzzy set theory
[DE88-000013] N88-12986
FUZZY SYSTEMS
Foundations of O-theory 2: Measurements and relation to fuzzy set theory
[DE88-000013] N88-12986

G

GALACTIC EVOLUTION
New cosmological scenario
[DE87-703357] N88-13198
Galaxy formation by gravitational collapse in a universe dominated by cold dark matter N88-13205
GALACTIC RADIATION
Galactic interstellar abundance surveys with IUE and IRAS N88-13206
GALLIUM ARSENIDES
Performance of GaAs and silicon concentrator cells under 37 MeV proton irradiation
[NASA-TM-100144] N88-12877
Radiation performance of AlGaAs concentrator cells and expected performance of cascade structures
[NASA-TM-100145] N88-12878
Evaluation of the Mellen EDG furnace for growth of large diameter GaAs single crystals in a horizontal configuration
[DE88-000463] N88-13068
GAMMA RAY ABSORPTION
Gamma-ray optics of multi-beam Borrmann modes with possible applications to nuclear lasing N88-12784
GAMMA RAY ASTRONOMY
Gamma ray lines from novae N88-13214
GAMMA RAY LASERS
Gamma-ray optics of multi-beam Borrmann modes with possible applications to nuclear lasing N88-12784
GAMMA RAY SPECTRA
Gamma ray lines from novae N88-13214
GAS DISCHARGES
Measurement of the electron density and the attachment rate coefficient in silane/helium discharges
[AD-A184268] N88-13051
GAS DYNAMICS
Some asymptotic modes of transonic vortex flow N88-12632
Model of solar-wind magnetosphere coupling N88-13211
GAS EXCHANGE
Influence of stratification in near-surface water layer on intensity of gas exchange between atmosphere and water N88-12841
GAS FLOW
Conical wing with maximum lift-to-drag ratio in supersonic gas flow N88-12633
GAS MIXTURES
TOPAZ: The transient one-dimensional pipe flow analyzer: An update on code improvements and increased capabilities
[DE88-001781] N88-12751
GAS TRANSPORT
TOPAZ: The transient one-dimensional pipe flow analyzer: An update on code improvements and increased capabilities
[DE88-001781] N88-12751
GAS TURBINE ENGINES
Composite mechanics for engine structures
[NASA-TM-100178] N88-12552
GASEOUS DIFFUSION
Microgravity nucleation and particle coagulation experiments support
[NASA-CR-181540] N88-12618
Microgravity nucleation and particle coagulation experiments support
[NASA-CR-181541] N88-12619
GAUGE THEORY
A supersymmetric Lagrangian for Poincare gauge theories of gravity
[DE88-001670] N88-13078
Gravity from symmetry breakdown of a gauge affine theory
[DE88-001671] N88-13079
GEARS
Multipath gear-friction planetary transmissions N88-12629
On dynamic loads in parallel shaft transmissions. 1: Modelling and analysis
[NASA-TM-100180] N88-12797
On dynamic loads in parallel shaft transmissions. 2: Parameter study
[NASA-TM-100181] N88-12798
GELATION
Molecular engineering of ceramics
[DE88-000174] N88-12603
GELS
Molecular engineering of ceramics
[DE88-000174] N88-12603
GENERAL AVIATION AIRCRAFT
Semiempirical method for prediction of aerodynamic forces and moments on a steadily spinning light airplane
[NASA-TM-4009] N88-12456
GENETICS
JPRS report: Science and technology. USSR: Life sciences
[JPRS-ULS-87-009] N88-12915
GEOCHEMISTRY
A mineral reconnaissance sampling manual for Costa Rica: Central American energy and resource project
[DE87-014997] N88-12859
Summaries of physical research in the geosciences
[DE88-000833] N88-12896
RRS DISCOVERY cruise 160, 30 June-25 July, 1986. Geochemical sampling over the Madeira and Porcupine Abyssal Plains
[PB87-222030] N88-12910
GEOCHRONOLOGY
Measurements of iridium and the meteoric impact hypothesis at cretaceous end
[DE87-703765] N88-13200
GEODETIC ACCURACY
A demonstration of high precision GPS orbit determination for geodetic applications N88-12680
GEODETIC SURVEYS
Considering refraction in leveling with laser plane N88-12857
GEODYNAMICS
The Telecommunications and Data Acquisition Report
[NASA-CR-181546] N88-12879
GEOLOGY
Summaries of physical research in the geosciences
[DE88-000833] N88-12896
GEOMAGNETISM
Statistics of the geomagnetic secular variation for the past 5Ma
[NASA-CR-181558] N88-12890
GEOMETRIC DILUTION OF PRECISION
GPS vertical axis performance enhancement for helicopter precision landing approach
[NASA-CR-177443] N88-12477
GEOMETRY
Observations on the hydrodynamic flow visualization at ONERA
[PD-FM-8718] N88-12753
The linear characteristic method in XYZ geometry
[DE87-011668] N88-12984
GEOPHYSICS
USSR report: Earth sciences
[JPRS-UES-86-006] N88-12831
Summaries of physical research in the geosciences
[DE88-000833] N88-12896
GERMANIUM
Thermal expansion of some Ge-Se-Te glasses
[PD-MT-8722] N88-12606
Studies on some Ge-Se-Te glasses
[PD-MT-8721] N88-12607
GIACOBINI-ZINNER COMET
Analysis of the ICE combiner for multiple antenna arraying N88-12704
GIANT STARS
A re-examination of the corona-wind dividing line: Diagnostics of non-coronal atmospheres N88-13101

Atmospheres of stars in the limits of thick and thin convection zones: M giants N88-13105
Carbon abundances and C12/C13 ratios in M giants N88-13167
JHK photometry of CN-rich field giants N88-13175
A comprehensive exploration of late-type stars in the far-ultraviolet N88-13194

GLASS
Carbon fiber reinforced glass matrix composites for space based applications
[AD-A184355] N88-12548
Thermal expansion of some Ge-Se-Te glasses
[PB-MT-8722] N88-12606
Reliability of Li/SO2 cells for long-life applications
[DE88-001360] N88-12735

GLASS FIBER REINFORCED PLASTICS
Determination of through-plane shear moduli for glass-reinforced plastics
[PB87-106274] N88-12592

GLASS FIBERS
A creep measurement of unidirectional epoxy-fiberglass rod
[DE87-014812] N88-12553

GLASS LASERS
Thermal stress in the edge cladding of Nova glass laser disks
[DE88-000425] N88-12780

GLASS TRANSITION TEMPERATURE
Studies on some Ge-Se-Te glasses
[PB-MT-8721] N88-12607

GLOBAL POSITIONING SYSTEM
Dynamic positioning at sea using the global positioning system
[AD-A184453] N88-12478
GPS vertical axis performance enhancement for helicopter precision landing approach
[NASA-CR-177443] N88-12477
A demonstration of high precision GPS orbit determination for geodetic applications N88-12680
Precise near-earth navigation with GPS: A survey of techniques N88-12682

GOLD
Far-infrared spectra of lithium deposited on a gold electrode: Interpretation using a cluster model
[AD-A184231] N88-13050

GRAIN BOUNDARIES
Some stochastic aspects of intergranular creep cavitation
[DE88-000065] N88-12581
Welding and weldability of ductile intermetallic alloys
[DE87-014061] N88-12582

GRAIN SIZE
Characterization of catalysts with metal-support effects and of the species adsorbed on their surfaces
[DE87-014636] N88-12564

GRANTS
Materials sciences programs: Fiscal Year 1987
[DE88-000672] N88-12659

GRAPH THEORY
A characterization of separating pairs and triplets in a graph
[AD-A184278] N88-12941
On the number of minimum size separating vertex sets in a graph
[AD-A184279] N88-12942
On color polynomials of Fibonacci graphs
[AD-A184133] N88-12996

GRAPHITE
Fabrication and testing of fire resistant graphite composite panels
[NASA-CR-177397] N88-12472
Data base on the high heat flux behaviour of metals and carbon materials for plasma facing components: Experiments at the 10 MW neutral beam injection test stand of the IPP Nagoya
[IPPJ-AM-53] N88-13031
Proceedings of the Japan-US Workshop P-92 on Plasma Material Interaction/High Heat Flux Data Needs for the Next Step Ignition and Steady State Devices
[DE87-013568] N88-13042
PISCES: Plasma-surface interactions and materials research
[DE88-001323] N88-13044

GRAPHITE-EPOXY COMPOSITES
Study of zero CTE (Coefficients of Thermal Expansion) of graphite/epoxy composites
[DE87-013557] N88-12554
Corrosion control by composite material substitution with application to the M-939 5-ton truck N88-12654

GRAPHITE-POLYIMIDE COMPOSITES
Effect of long-term thermal aging on coated Celion/LARC-160 composites
[NASA-TM-100495] N88-12544

GRAPHS (CHARTS)
The ISI (Information Sciences Institute) grapher: A portable tool for displaying graphs pictorially
[AD-A184354] N88-12944

GRATINGS (SPECTRA)
All-optical beam control by forced Rayleigh scattering
[AD-A184315] N88-13018

GRAVIMETRY
Solution of three-dimensional inverse problem of gravimetry in contact surfaces class by local corrections method N88-12848
On deviations from Newton's law and the proposal for a Fifth Force
[DE87-703368] N88-13001

GRAVITATION
Steady distortion of shape of geoid and normal gravity field under influence of tidal potential N88-12839
On deviations from Newton's law and the proposal for a Fifth Force
[DE87-703368] N88-13001
Homogeneous space-time of Goedel type in higher-derivate gravity
[DE87-703690] N88-13077
A supersymmetric Lagrangian for Poincare gauge theories of gravity
[DE88-001670] N88-13078

GRAVITATION THEORY
Gravity from symmetry breakdown of a gauge affine theory
[DE88-001671] N88-13079

GRAVITATIONAL COLLAPSE
Core bounce supernovae
[DE87-014910] N88-13197
Galaxy formation by gravitational collapse in a universe dominated by cold dark matter N88-13205

GRAVITATIONAL CONSTANT
On deviations from Newton's law and the proposal for a Fifth Force
[DE87-703368] N88-13001

GRAVITATIONAL EFFECTS
Steady distortion of shape of geoid and normal gravity field under influence of tidal potential N88-12839
Two-layer stratified flow analysis of gravity currents and turbidity currents in lakes, reservoirs and the ocean N88-12864

GRAVITY WAVES
Dispersion equation for plane capillary-gravity wave on free surface of viscous incompressible fluid N88-12842
Influence of surfactants on damping of gravity-capillary waves. 1: Frequency dependence N88-12843

GRAZING
All-optical beam control by forced Rayleigh scattering
[AD-A184315] N88-13018

GREENHOUSE EFFECT
The effects of minor trace gases on the transfer of thermal infrared radiation through the Earth's atmosphere N88-12893

GROUND EFFECT (AERODYNAMICS)
An experimental investigation of dynamic ground effect
[NASA-CR-4105] N88-12458

GROUND STATIONS
The Telecommunications and Data Acquisition Report
[NASA-CR-181546] N88-12679
A hydrogen/nickel oxide battery for remote applications
[DE87-009048] N88-12872
Design description report for a photovoltaic power system for a remote satellite earth terminal
[NASA-CR-179586] N88-12875

GROUP THEORY
Group analysis of equations arising in ocean acoustics N88-12914

GUN PROPELLANTS
Thermoplastic elastomers as LOVA (Low Vulnerability Ammunition) binders
[AD-A184350] N88-12599
High pressure strand burn rate tests of polyvinylnitrate/nitramine propellants
[AD-A184178] N88-12615

GUNFIRE
Analysis of a series of electromagnetic launcher firings
[AR-005-131] N88-12516
Efficiency aspects of short, low velocity railguns
[AR-004-847] N88-12517

GUNS (ORDNANCE)
The LLNL 150-mm equation-of-state gun system
[DE88-000423] N88-12519

GUY WIRES
The effect of mass, wind angle and erection technique on the aeroelastic behaviour of a cable-stayed bridge model
[NAE-AN-46] N88-12819

H

H ALPHA LINE
Contemporaneous B,V,R,I photometry and H alpha spectroscopy of YY Gem N88-13155
Sensitivity of the H alpha line to expansion, geometrical extent and temperature gradient in the G and K supergiant chromospheres N88-13159

HABITABILITY
Disturbance and recovery of Arctic Alaskan tundra terrain. A review of recent investigations
[AD-A184442] N88-12887

HAMILTONIAN FUNCTIONS
Equilibria, lattices and chaotic dynamics of point vortices N88-12758

HARDENING (MATERIALS)
An expert system for materials design
[DE88-000191] N88-12974

HARDNESS
Weldability of 2219-T851 and 2519-T87 aluminum armor alloys for use in Army vehicle systems
[AD-A184296] N88-12792

HARTREE APPROXIMATION
The finite element method for electronic structure
[DE88-001708] N88-12989

HEALTH
An assessment of clinical chemical sensing technology for potential use in space station health maintenance facility
[NASA-CR-172013] N88-12926

HEAO 2
Exosat results on the dMe flare Star Wolf 630AB and on VB 8 N88-13151

HEAT AFFECTED ZONE
Effects of stress-relieving on the mechanical properties and the structure of specimens of high-temperature fine-grained structural steels heat-treated to simulate welding
[BLL-CE-TRANS-8258-(9022.09)] N88-12586

HEAT EXCHANGERS
Two-watt, 4-Kelvin closed cycle refrigerator performance N88-12709
Theory of one and two-pass cross-flow heat exchanger
[PB87-225157] N88-12736
Measured performance of the heat exchanger in the NASA icing research tunnel under severe icing and dry-air conditions
[NASA-TM-100116] N88-12796
Design and development of absorption heat pumps
[DE88-000062] N88-12885

HEAT FLUX
Experimental study of thermocapillary flows in a thin liquid layer with heat fluxes imposed on the free surface
[NASA-TM-100252] N88-12783
Data base on the high heat flux behaviour of metals and carbon materials for plasma facing components: Experiments at the 10 MW neutral beam injection test stand of the IPP Nagoya
[IPPJ-AM-53] N88-13031
Proceedings of the Japan-US Workshop P-92 on Plasma Material Interaction/High Heat Flux Data Needs for the Next Step Ignition and Steady State Devices
[DE87-013568] N88-13042

HEAT MEASUREMENT
On the stressing of annealed NITINOL: The electrical resistance and calorimetric effects
[AD-A184465] N88-12569

HEAT PIPES
Advanced radiator concepts utilizing honeycomb panel heat pipes
[NASA-CR-172017] N88-12747

HEAT PUMPS
Optimized ground coupled heat pump mechanical package
[DE87-014899] N88-12738
Design and development of absorption heat pumps
[DE88-000062] N88-12885

HEAT RADIATORS
Advanced radiator concepts utilizing honeycomb panel heat pipes
[NASA-CR-172017] N88-12747

HEAT TRANSFER
Performance analysis of advanced spacecraft TPS
[NASA-CR-181532] N88-12484
Thermal analysis of electromagnetic launcher rails
[DE88-000166] N88-12514
Ceramic technology for advanced heat engines project
[DE88-001520] N88-12605
Resistor cooling in a vacuum
[DE88-000896] N88-12733
NACHOS 2: A finite element computer program for incompressible flow problems. Part 2: User's manual
[DE88-001451] N88-12750

Steady shearing in a viscoplastic solid
[AD-A184341] N88-12810
Theory of heat and moisture exchange between finely disperse storm-generated spray and turbulent air flow N88-12851
Structure of stably stratified atmospheric surface layer in presence of heat-releasing admixture N88-12856
Influence of bond dilution on the free surface and interface Potts ferromagnetism
[DE87-703360] N88-13061

HEAT TREATMENT
Effect of long-term thermal aging on coated Celion/LARC-160 composites
[NASA-TM-100495] N88-12544
Effect of time and temperature on transformation toughened zirconias
[AD-A184956] N88-12600

HEATERS
Research and development on high strength ceramic heaters discussed N88-12508

HEATING
A large X-ray flare on squared Sigma coronae borealis observed with exosat N88-13121
Chromospheric and coronal heating in a bias-free sample of K dwarfs N88-13184

HEATING EQUIPMENT
SCRAM JET (Supersonic Combustion Ramjet) combustion experiments N88-12512

HEAVY IONS
Wavelengths of the 3p-3d transitions of the Co- and Fe-like ions: The effects of electron correlation
[DE88-000219] N88-13067

HEAVY NUCLEI
Neutron capture nucleosynthesis in low mass AGB stars N88-13178

HEISENBERG THEORY
A study of mechanisms of hydrogen diffusion in separation devices
[DE88-000328] N88-12584

HELICOPTER CONTROL
Engine/airframe response evaluation of the HH-60A helicopter equipped with the T700-GE-701 transient droop improvement electronic control unit
[AD-A184443] N88-12492

HELICOPTER DESIGN
Results of the 1986 NASA/FAA/DFVLR main rotor test entry in the German-Dutch wind tunnel (DNW)
[NASA-TM-100507] N88-13003

HELICOPTER PERFORMANCE
Engine/airframe response evaluation of the HH-60A helicopter equipped with the T700-GE-701 transient droop improvement electronic control unit
[AD-A184443] N88-12492

HELICOPTERS
A full potential flow analysis with realistic wake influence for helicopter rotor airload prediction
[NASA-CR-4007] N88-12452
A 0.15-scale study of configuration effects on the aerodynamic interaction between main rotor and fuselage
[NASA-CR-166577] N88-12462
GPS vertical axis performance enhancement for helicopter precision landing approach
[NASA-CR-177443] N88-12477
Hovering helicopter flight dynamics: A study of vertical motion
[AR-004-526] N88-12485
Some data processing requirements for precision Nap-Of-the-Earth (NOE) guidance and control of rotorcraft
[NASA-CR-177453] N88-12493
Flap-lag equations of motion of rigid, articulated rotor blades with three hinge sequences
[NASA-TM-100023] N88-12495

HELIOSPHERE
Observations of turbulence and fluctuations in the solar wind N88-13212

HELIUM
A cold ejector for closed-cycle helium refrigerators N88-12890
Design concepts for the ASTROMAG cryogenic system
[NASA-CR-181505] N88-13060
A helium flare on the active G5 dwarf Kappa Ceti N88-13189

HELMHOLTZ VORTICITY EQUATION
Group analysis of equations arising in ocean acoustics N88-12914

HERTZSPRUNG-RUSSELL DIAGRAM
A re-examination of the corona-wind dividing line: Diagnostics of non-coronal atmospheres N88-13101

HETERODYNING
Exploiting the IR: Solar and stellar spectroscopy in the IR N88-13102

HETEROGENEITY
Heterogeneous multi-trunking queueing systems
[AD-A184255] N88-12668
A data translation method for heterogeneous database systems N88-13081

HEURISTIC METHODS
Autonomous Land Vehicle (ALV) planning and navigation system
[AD-A184243] N88-12475

HEWLETT-PACKARD COMPUTERS
A data analysis environment for HP (Hewlett-Packard) 1000 computers
[DE87-010511] N88-12936

HIGH ELECTRON MOBILITY TRANSISTORS
A 2.3-GHz cryogenically cooled HEMT amplifier for DSS 13 N88-12689
Numerical studies of the dual HEMT/algorithm development and numerical studies of Schrodinger's equation
[AD-A184471] N88-12946

HIGH LEVEL LANGUAGES
A survey of object oriented languages in programming environments
[AD-A184127] N88-12937

HIGH POWER LASERS
High-power RF-pulsed modulators for the Los Alamos free-electron laser
[DE88-000514] N88-12775

HIGH PRESSURE
High pressure strand burn rate tests of polyvinylnitrate/nitramine propellants
[AD-A184178] N88-12615

HIGH RESOLUTION
Implementation and performance of a complex vision system on a systolic array machine
[AD-A184331] N88-12971
High resolution finite volume methods on arbitrary grids via wave propagation
[NASA-CR-178397] N88-12979
Exosat results on the dMe flare Star Wolf 630AB and on VB 8 N88-13151
New results from high angular resolution observations of alpha Ori N88-13161

HIGH REYNOLDS NUMBER
Asymptotic form of stationary solutions of the Navier-Stokes equations for large Reynolds numbers N88-12838

HIGH SPEED
Analysis of 7- X 10-foot high speed wind tunnel shaft loads in support of fan blade failure investigation
[NASA-TM-100504] N88-12496
Progress in the development of niobium alloyed high speed steel
[DE87-703549] N88-12578
Thermomechanical cracking in coated media due to high speed asperity excitation
[AD-A184176] N88-12809

HIGH STRENGTH STEELS
Mechanical behavior of a controlled rolled high-strength low alloy steel plate, microalloyed with Nb and V
[DE87-703507] N88-12571

HIGH TEMPERATURE
Research and development on high strength ceramic heaters discussed N88-12508
Pipe and bend erosion by pneumatic transport of solids at high temperature
[DE88-001345] N88-12658

HIGH TEMPERATURE AIR
SCRAM JET (Supersonic Combustion Ramjet) combustion experiments N88-12512

HIGH TEMPERATURE ENVIRONMENTS
Calculation of the tribological properties of surfaces by semi-empirical methods
[AD-A184283] N88-12791

HIGH TEMPERATURE SUPERCONDUCTORS
The chemical bond and superconductivity
[AD-A184275] N88-13053

HMX
High pressure strand burn rate tests of polyvinylnitrate/nitramine propellants
[AD-A184178] N88-12615

HOLOGRAPHY
Computed neutron tomography and coded aperture holography from real time neutron images N88-12645

HONEYCOMB STRUCTURES
Solar converging method N88-12504
Advanced radiator concepts utilizing honeycomb panel heat pipes
[NASA-CR-172017] N88-12747

HORIZONTAL ORIENTATION
Effects of combining vertical and horizontal information into a primary flight display
[NASA-TP-2783] N88-12487
Aircraft engine exhaust plume dynamics
[AD-A184238] N88-12488

HOSES
Variable collision frequency effects on hose and sausage instabilities in relativistic electron beams
[AD-A184206] N88-13021

HOVERING
Hovering helicopter flight dynamics: A study of vertical motion
[AR-004-526] N88-12485

HUMAN FACTORS ENGINEERING
Research papers and publications (1981-1987): Workload research program
[NASA-TM-100016] N88-12924

HUMAN PERFORMANCE
Research papers and publications (1981-1987): Workload research program
[NASA-TM-100016] N88-12924

HUMIDITY
The effect of organic inhibitors on the atmospheric corrosion and solderability of copper
[DE88-000261] N88-12565

HUMIDITY MEASUREMENT
Lidar-radiometric method for determining liquid-water content of cirrus clouds N88-12854

HYBRID STRUCTURES
Design description report for a photovoltaic power system for a remote satellite earth terminal
[NASA-CR-179586] N88-12875

HYDROCARBONS
The structure of adsorbed sulfur and carbon on molybdenum and rhenium single crystal surfaces, and their influence on carbon monoxide and hydrocarbon chemisorption
[DE88-001393] N88-13073

HYDRODYNAMICS
Three-dimensional, free-Lagrange hydrodynamics
[DE88-000494] N88-12749
Observations on the hydrodynamic flow visualization at ONERA
[PD-FM-8718] N88-12753
Dynamics of isolated intrathermocline eddy N88-12845
Variations of the vertical and horizontal velocities of the small-scale structures and the physical problems related to overshoot layers N88-13115

HYDROFLUORIC ACID
Evaluation of the sensidyne toxic gas sensor for HF (Hydrogen Fluoride) vapor
[DE88-000647] N88-12767

HYDROGEN
Characterization of catalysts with metal-support effects and of the species adsorbed on their surfaces
[DE87-014636] N88-12564
A hydrogen/nickel oxide battery for remote applications
[DE87-009048] N88-12872
Excess emission in the wings of the Hydrogen Balmer lines during a flare on the late-type dMe star YZ CMi N88-13146
Hydrogen and deuterium in the local interstellar medium N88-13204

HYDROGEN ATOMS
A study of mechanisms of hydrogen diffusion in separation devices
[DE88-000328] N88-12584

HYDROGEN BONDS
High pressure strand burn rate tests of polyvinylnitrate/nitramine propellants
[AD-A184178] N88-12615

HYDROGEN MASERS
Fast autotuning of a hydrogen maser by cavity Q modulation N88-12707

HYDROGEN PRODUCTION
The developmental status of solar thermochemical hydrogen production
[DE88-001778] N88-12884

HYDROGENATION
Characterization of catalysts with metal-support effects and of the species adsorbed on their surfaces
[DE87-014636] N88-12564

HYDROXYL COMPOUNDS
High pressure strand burn rate tests of polyvinylnitrate/nitramine propellants
[AD-A184178] N88-12615

HYPERBARIC CHAMBERS
Space station internal environmental and safety concerns N88-12527

HYPERCUBE MULTIPROCESSORS
A portable hypercube simulator
[DE87-013369] N88-12947
Implementation of a 3-D nonlinear MHD calculation on the Intel hypercube
[DE87-014637] N88-12949
Parallelization of hydrocodes on the Intel Hypercube, part 2
[DE88-001591] N88-12957

HYPERNUCLEI
Few body hypernuclear systems: Weak decays
[DE87-014920] N88-13010
HYPERSONIC AIRCRAFT
Experimental aerothermodynamic research of hypersonic aircraft
[NASA-CR-181533] N88-12483
HYPERSONIC FLOW
Similar solutions for viscous hypersonic flow over a slender three-fourths-power body of revolution
[NASA-TM-100205] N88-12752
HYPERSONIC SPEED
SCRAM JET (Supersonic Combustion Ramjet) combustion experiments N88-12512
HYPERVELOCITY IMPACT
Measurements of iridium and the meteoric impact hypothesis at cretaceous end
[DE87-703765] N88-13200
Conditions for geomagnetically trapping sub-micron lunar ejecta between L = 1.2 and L = 3.1 N88-13203
HYPERVELOCITY LAUNCHERS
Ultimate velocities for induction launchers
[DE87-012360] N88-12513
Analysis of a series of electromagnetic launcher firings
[AR-005-131] N88-12516
HYPERVELOCITY PROJECTILES
Efficiency aspects of short, low velocity railguns
[AR-004-847] N88-12517
HYPOTHESES
Lower bounds on bearing accuracy for closely spaced sources
[AD-A184258] N88-12997
Measurements of iridium and the meteoric impact hypothesis at cretaceous end
[DE87-703765] N88-13200

I

ICE FORMATION
Experimental evidence for modifying the current physical model for ice accretion on aircraft surfaces
[NASA-TM-87184] N88-12473
Measured performance of the heat exchanger in the NASA icing research tunnel under severe icing and dry-air conditions
[NASA-TM-100116] N88-12796
IDENTIFYING
A search for X-ray luminous late type stars in NIPSS data N88-13143
IGNITION
Ignition and combustion of metals in oxygen N88-12530
Proceedings of the Japan-US Workshop P-92 on Plasma Material Interaction/High Heat Flux Data Needs for the Next Step Ignition and Steady State Devices
[DE87-013568] N88-13042
IMAGE ANALYSIS
Input/output technologies: An overview of image scanning, storage, and display
[DE87-014837] N88-12933
On the recognition of curved objects
[AD-A184441] N88-12945
IMAGE INTENSIFIERS
Increased gain of channel intensifier tubes by pulsed biasing
[DE88-000512] N88-13019
IMAGE PROCESSING
Programmable real-time digital video image processing
[PB87-104162] N88-12661
Design of source coders and joint source/channel coders for noisy channels
[NASA-CR-181547] N88-12678
Tracking through turbulence at the Tonopah Test Range
[DE88-001448] N88-12766
Cloud cover determination in polar regions from satellite imagery
[NASA-CR-181544] N88-12908
Input/output technologies: An overview of image scanning, storage, and display
[DE87-014837] N88-12933
Computer-aided X-ray image system design and evaluation
[DE88-000997] N88-12965
IMAGE RESOLUTION
Input/output technologies: An overview of image scanning, storage, and display
[DE87-014837] N88-12933
IMAGES
Design of source coders and joint source/channel coders for noisy channels
[NASA-CR-181547] N88-12678
IMAGING SPECTROMETERS
Radiometric calibration of the Earth observing system's imaging sensors
[NASA-CR-181542] N88-12965
IMAGING TECHNIQUES
Some new ideas in liquid detectors
[DE88-000732] N88-12768
Simultaneous, coaxial imaging of the Sun in cyanogen and singly-ionized calcium N88-13114
Doppler snapshots N88-13125
IMMUNOLOGY
JPRS report: Science and technology. USSR: Life sciences
[JPRS-ULS-87-009] N88-12915
IMPACT TESTS
A direct method to obtain constitutive model constants from cylinder impact test results N88-12647
IMPEDANCE
Impedance of passive lithium anodes in SOCl2 solutions under low-field polarization
[DE88-000922] N88-12728
IMPURITIES
Far infrared Fourier transform spectroscopy of semiconductors
[DE88-000188] N88-13072
INCOHERENT SCATTERING
Lower bounds on bearing accuracy for closely spaced sources
[AD-A184258] N88-12997
INCOMPRESSIBLE FLOW
On the instability of thin circular shear layers N88-12467
Calculation of aerodynamic characteristics of three-dimensional finite span wings in potential incompressible flow N88-12631
Studies of pressure-velocity coupling schemes for analysis of incompressible and compressible flows
[NASA-CR-181526] N88-12748
NACHOS 2: A finite element computer program for incompressible flow problems. Part 2: User's manual
[DE88-001451] N88-12750
Analytical studies of axially symmetric motion of an incompressible viscous fluid between two concentric rotating spheres N88-12757
INS3D: An incompressible Navier-Stokes code in generalized three-dimensional coordinates
[NASA-TM-100012] N88-12991
INDEPENDENT VARIABLES
Group analysis of equations arising in ocean acoustics N88-12914
Investigation, development and application of optimal output feedback theory. Vol. 4: Measures of eigenvalue/eigenvector sensitivity to system parameters and unmodeled dynamics
[NASA-CR-4106] N88-12969
INDEXES (DOCUMENTATION)
Source header list. Volume 1: A through K
[AD-A184000] N88-13086
INDIAN OCEAN
Interactions between the Asian monsoons, the tropical Pacific and the southern hemisphere extratropics N88-12907
INDUCTANCE
Inductance effects in the high-power transmitter crowbar system N88-12687
INDUSTRIES
A national model at Howard University demonstrating private sector interrelationships that facilitate research in predominantly Black colleges and universities
[DE88-000160] N88-13089
INELASTIC SCATTERING
Consistency question in the renormalization group analysis of deep inelastic scattering
[DE87-703372] N88-12999
INERT ATMOSPHERE
Spacecraft Fire Safety
[NASA-CP-2476] N88-12520
Fire extinguishment and inhibition in spacecraft environments N88-12523
Inerting and atmospheres N88-12524
INERTIAL CONFINEMENT FUSION
Interplanetary propulsion using inertial fusion
[NASA-TM-89661] N88-12540
The VISTA spacecraft: Advantages of ICF (Inertial Confinement Fusion) for interplanetary fusions propulsion applications
[NASA-CR-181549] N88-13024
Inertial confinement fusion reactor cavity analysis
[DE88-000788] N88-13026
ICRF launcher studies
[DE88-001710] N88-13046
INERTIAL FUSION (REACTOR)
Interplanetary propulsion using inertial fusion
[NASA-TM-89661] N88-12540
INERTIAL GUIDANCE
Optical alignment of Centaur's inertial guidance system
[NASA-TM-88844] N88-12515
INERTIAL NAVIGATION
NAVSIM 2: A computer program for simulating aided-inertial navigation for aircraft
[NASA-CR-177436] N88-12478
INFERENCE
Statistical inference: Computer oriented algorithmic approach
[DE87-013874] N88-12948
INFORMATION ADAPTIVE SYSTEM
An interactive computer graphics network monitor for a tactical communications network
[AD-A184131] N88-12938
INFORMATION DISSEMINATION
Automatic photometric monitoring of cool stars N88-13103
INFORMATION RETRIEVAL
Towards automated consulting: Design feedback from the performance of online documentation
[DE87-012243] N88-13082
Subjective probability, combination of expert opinion and probabilistic approaches to information retrieval N88-13085
INFORMATION SYSTEMS
Materials sciences programs: Fiscal Year 1987
[DE88-000672] N88-12659
INFORMATION THEORY
Bandwidth efficient block codes for M-ary PSK modulation
[NASA-CR-181543] N88-12712
INFRARED ABSORPTION
Absorption of far IR-radiation by H2O-N2 complexes under atmospheric conditions N88-12855
INFRARED ASTRONOMY SATELLITE
Emission features in IRAS LRS spectra of MS, S and CS stars N88-13163
IRAS and cool stellar mass loss N88-13166
INFRARED DETECTORS
Exosat results on the dMe flare Star Wolf 630AB and on VB 8 N88-13151
INFRARED IMAGERY
Aircraft engine exhaust plume dynamics
[AD-A184238] N88-12488
INFRARED PHOTOMETRY
A search for very low mass (brown dwarf) stars as wide binaries using a seven element infrared camera-photometer N88-13150
IRAS and near IR observations of active binaries N88-13186
INFRARED RADIATION
The effects of minor trace gases on the transfer of thermal infrared radiation through the Earth's atmosphere N88-12893
The giant spot on II Peg in 1986 N88-13120
INFRARED SPECTRA
Far-infrared spectra of lithium deposited on a gold electrode: Interpretation using a cluster model
[AD-A184231] N88-13060
Infrared excesses of barium stars N88-13174
The contribution of accretion luminosity to the infrared spectra of T Tauri stars: A possible test N88-13183
IRAS and near IR observations of active binaries N88-13186
INFRARED SPECTROSCOPY
Far infrared Fourier transform spectroscopy of semiconductors
[DE88-000188] N88-13072
Time series infrared spectroscopy of long period variables N88-13172
INFRARED STARS
A search for very low mass (brown dwarf) stars as wide binaries using a seven element infrared camera-photometer N88-13150
INJECTION LOCKING
An analytical and experimental study of injection-locked two-port oscillators
[NASA-TM-100119] N88-12727
INJECTORS
A three-barrel repeating pneumatic pellet injector for plasma fueling of the Joint European Torus
[DE88-000330] N88-13026
INSERTS
A low volume insert for solid state magic angle spinning NMR of small samples
[AD-A184359] N88-12601
INSPECTION
Ultrasonic method of inspecting austenitic weld joints in nuclear power station equipment
[BLL-CE-TRANS-8281-(9022.09)] N88-12806
Pulsed eddy-current inspection of thin-walled stainless steel tubing
[DE88-001492] N88-12830

Computerized certification of digital ultrasonic instrumentation
[DE88-000820] N88-13008
INSTRUMENT COMPENSATION
CGI delay compensation
[NASA-TM-88703] N88-12932
INTAKE SYSTEMS
Dynamics of reverse flows at pump inlet N88-12636
INTEGRAL EQUATIONS
Mutual admittance between slots in cylinders of arbitrary shape
[AD-A184254] N88-12723
INTEGRAL TRANSFORMATIONS
Thermomechanical cracking in coated media due to high speed asperity excitation
[AD-A184176] N88-12809
INTEGRATED CIRCUITS
A procedural method for the efficient implementation of full-custom VLSI designs N88-12701
Programmable Logic Arrays (PLA's) design for testability
[PB87-102935] N88-12718
INTERFACES
Materials sciences programs: Fiscal Year 1987
[DE88-000672] N88-12659
On computing environments in data analysis
[DE88-000078] N88-12961
Influence of bond dilution on the free surface and interface Potts ferromagnetism
[DE87-703360] N88-13061
Non-lattice matched metallic superlattices
[DE87-011512] N88-13062
INTERFACIAL TENSION
Interfacial strength development in thermoplastic resins and fiber-reinforced thermoplastic composites
[NASA-CR-181525] N88-12549
INTERFERENCE FIT
A finite element procedure for interference-fit and cold-working problems with limited yielding
[AR-004-517] N88-12992
INTERFEROMETRY
Short baseline phase delay interferometry N88-12683
Interferometry theory for the block 2 processor
[NASA-CR-181551] N88-12730
INTERMETALLICS
Welding and weldability of ductile intermetallic alloys
[DE87-014061] N88-12582
Experimental perspectives on heavy electron metals
[DE87-014766] N88-12583
INTERNATIONAL COOPERATION
Solar energy: European research and development
[PB87-107645] N88-12886
Technology transfer to China
[PB87-223418] N88-13087
INTERPLANETARY MAGNETIC FIELDS
Model of solar-wind magnetosphere coupling N88-13211
Observations of turbulence and fluctuations in the solar wind N88-13212
INTERPLANETARY SPACECRAFT
The VISTA spacecraft: Advantages of ICF (Inertial Confinement Fusion) for interplanetary fusions propulsion applications
[NASA-CR-181549] N88-13024
INTERSTELLAR MATTER
Hydrogen and deuterium in the local interstellar medium N88-13204
Galactic interstellar abundance surveys with IUE and IRAS N88-13206
INVARIANCE
Carbon-fiber reinforced plastics N88-12506
INVERSIONS
Review of inversion techniques for spaceborne lidar systems
[AD-A184164] N88-12772
Lower bounds on bearing accuracy for closely spaced sources
[AD-A184258] N88-12997
INVESTIGATION
Analysis of 7- X 10-foot high speed wind tunnel shaft loads in support of fan blade failure investigation
[NASA-TM-100504] N88-12496
The effect of mass, wind angle and erection technique on the aeroelastic behaviour of a cable-stayed bridge model
[NAE-AN-46] N88-12819
INVISCID FLOW
Some experiences with the viscous-inviscid interaction approach
[NASA-TM-100015] N88-12466
Solution of the two-dimensional Euler equations on unstructured triangular meshes N88-12469
Optimization of explicit time-stepping algorithms and Stream-Function-Coordinate (SFC) concept for fluid dynamics problems N88-12762
Mesoscale eddy dynamics by the method of point vortices N88-12863
IODINE ISOTOPES
The Moessbauer effect of SnI4 at high pressure
[DE87-014771] N88-13048
ION BEAMS
Negative ion beams for heating and current-drive in NET
[AD-A184390] N88-13012
PISCES: Plasma-surface interactions and materials research
[DE88-001323] N88-13044
ICRF launcher studies
[DE88-001710] N88-13048
ION CURRENTS
Applications of multivalent ionic conductors to polymeric electrolyte batteries
[AD-A184252] N88-12722
Effect of sidechain length and crosslinking on ionic conductivity in polyphosphazene solid electrolytes
[AD-A184419] N88-13058
ION IMPLANTATION
Microstructural change of Al on H implantation
[IPPJ-847] N88-13036
ION INJECTION
Particle injection and cosmic ray acceleration at collisionless parallel shocks
[DE88-000507] N88-12665
ION PROPULSION
High power ion thruster performance
[NASA-TM-100127] N88-12542
IONIC COLLISIONS
Radiation induced collapse of the crystalline structure
[DE87-014407] N88-13064
IONIZATION
Equilibrium calculations of ionization in tracer flames
[PB87-104154] N88-12555
High efficiency generation of 130-nm radiation from sum-frequency mixing in Hg
[DE87-013714] N88-12674
Radio continuum emission from the ionized stellar winds of the cool supergiants in zeta Aurigae-like systems N88-13160
IONIZATION CHAMBERS
High efficiency generation of 130-nm radiation from sum-frequency mixing in Hg
[DE87-013714] N88-12674
IONIZING RADIATION
Reevaluating the worst-case radiation response of MOS transistors
[DE87-014157] N88-13059
IONOSPHERIC DISTURBANCES
High latitude F-region drift studies
[AD-A184466] N88-12889
IONOSPHERIC DRIFT
High latitude F-region drift studies
[AD-A184466] N88-12889
IRIDIUM
Measurements of iridium and the meteoric impact hypothesis at cretaceous end
[DE87-703765] N88-13200
IRON ALLOYS
A comparison of high damping shape memory alloys with Cu-Mn-based and Fe-Cr-based alloys
[AD-A184110] N88-12566
IRON METEORITES
Moessbauer study of shock induced effects in the Fe-Ni 50/50 ordered alloy in meteorites
[DE87-703364] N88-13199
IRRADIANCE
Radiometric calibration of the Earth observing system's imaging sensors
[NASA-CR-181542] N88-12665
Statistical distribution of solar radiation (hourly sums): Cumulative frequency curves preparation of a European data set and direction for use
[PB87-107454] N88-12886
IRRADIATION
Performance of GaAs and silicon concentrator cells under 37 MeV proton irradiation
[NASA-TM-100144] N88-12877
PISCES: Plasma-surface interactions and materials research
[DE88-001323] N88-13044
Reevaluating the worst-case radiation response of MOS transistors
[DE87-014157] N88-13059
ISOPROPYL ALCOHOL
Characterization of catalysts with metal-support effects and of the species adsorbed on their surfaces
[DE87-014636] N88-12564
ISOTOPE SEPARATION
A study of mechanisms of hydrogen diffusion in separation devices
[DE88-000328] N88-12584
ISOTOPIC SPIN
Few body hypernuclear systems: Weak decays
[DE87-014920] N88-13010
IUE
Active phases on II Peg N88-13119
The onset of chromospheric activity among the A- and F- type stars N88-13144
IUE/Optical/VLA flares on AD Leo N88-13152
A flash spectrum of CI I, C I, N I, and Ni II absorption in 31 Cygni: A direct observation of the reversing layer N88-13158
Hydrogen and deuterium in the local interstellar medium N88-13204

J

JAPAN
JPRS report: Science and technology. Japan
[JPRS-JST-87-025] N88-12502
JET AIRCRAFT
Aircraft engine exhaust plume dynamics
[AD-A184238] N88-12488
JET EXHAUST
Aircraft engine exhaust plume dynamics
[AD-A184238] N88-12488
JET FLOW
On the instability of thin circular shear layers N88-12467
Comparative studies in the near-field of turbulent transports of heated and unheated jets normal to a cross stream N88-12756
Mesoscale eddy dynamics by the method of point vortices N88-12863
JET THRUST
Aircraft engine exhaust plume dynamics
[AD-A184238] N88-12488
JET VANES
Effects of jet exhaust yaw vane installation and operation on the longitudinal and lateral-directional characteristics of the F-14 airplane
[NASA-TP-2769] N88-12455
JOINT EUROPEAN TORUS
A three-barrel repeating pneumatic pellet injector for plasma fueling of the Joint European Torus
[DE88-000330] N88-13026
JOINTS (JUNCTIONS)
Reduced complexity structural modeling for automated airframe synthesis
[NASA-CR-177440] N88-12453
Influence of bond dilution on the free surface and interface Potts ferromagnetism
[DE87-703360] N88-13061

K

K LINES
Simultaneous, cospatial imaging of the Sun in cyanogen and singly-ionized calcium N88-13114
KALMAN FILTERS
GPS vertical axis performance enhancement for helicopter precision landing approach
[NASA-CR-177443] N88-12477
KINEMATICS
Static standing and dynamic walking of a practical biped robot
[DE88-001367] N88-12705
Kinematic formulation of finite elements for plate bending N88-12821
Extremum methods of structural analysis for system reliability assessment N88-12824
KINETIC ENERGY
A multiple-time-scale turbulence model based on variable partitioning of turbulent kinetic energy spectrum
[NASA-CR-179222] N88-12754
KINETICS
Molecular engineering of ceramics
[DE88-000174] N88-12603
KLYSTRONS
Inductance effects in the high-power transmitter crowbar system N88-12687
KNOWLEDGE REPRESENTATION
The characterization of diagnostic tasks for engineering systems
[DE88-000093] N88-12973
KOLMOGOROFF THEORY
The velocity structure and turbulence at the center of the Orion Nebula N88-13201

L

LABORATORIES
Materials sciences programs: Fiscal Year 1987
[DE88-000672] N88-12659

LABORATORY EQUIPMENT
A low volume insert for solid state magic angle spinning NMR of small samples
[AD-A184359] N88-12601
LAMINAR BOUNDARY LAYER
Excitation of natural oscillations of a boundary layer by an external acoustic field N88-12634
LAMINAR FLOW
Experiments on densely-loaded non-Newtonian slurries in laminar and turbulent pipe flows
[DE88-000719] N88-12746
Studies of pressure-velocity coupling schemes for analysis of incompressible and compressible flows
[NASA-CR-181526] N88-12748
LAMINATES
Carbon-fiber reinforced plastics N88-12506
Thixotropic surface composition for phenolaldehyde resin laminates
[GB-PATENT-2-180-251-A] N88-12545
Study of zero CTE (Coefficients of Thermal Expansion) of graphite/epoxy composites
[DE87-013557] N88-12554
Spatial strength variation and statistical size effect of laminated orthotropic composite materials N88-12645
A refined nonlinear analysis of laminated composite plates and shells
[AD-A184436] N88-12811
Vibration and buckling of geometrically imperfect laminated cylindrical shells N88-12822
LANDING
Effect of motion cues during complex curved approach and landing tasks: A piloted simulation study
[NASA-TP-2773] N88-12480
LARGE SPACE STRUCTURES
New feedback design methodologies for large space structures: A multi-criterion optimization approach N88-12535
LASER ALTIMETERS
Considering refraction in leveling with laser plane N88-12857
LASER APPLICATIONS
High efficiency generation of 130-nm radiation from sum-frequency mixing in Hg
[DE87-013714] N88-12674
Lasers measure atmosphere N88-12849
Multiwave laser soundings of atmospheric aerosol: Experimental research (review) N88-12852
JPRS report: Science and technology. USSR: Life sciences
[JPRS-ULS-87-009] N88-12915
Theoretical plasma physics
[DE88-001475] N88-13029
LASER DAMAGE
Long-range pulselength scaling of 351nm laser damage thresholds
[DE87-014754] N88-12777
LASER FUSION
Interplanetary propulsion using inertial fusion
[NASA-TM-89961] N88-12540
Thermal stress in the edge cladding of Nova glass laser disks
[DE88-000425] N88-12780
Inertial confinement fusion reactor cavity analysis
[DE88-000788] N88-13028
LASER INDUCED FLUORESCENCE
Laser induced fluorescent study of relativistic electron beams
[AD-A184456] N88-12774
Calibration of a laser-pumped, thermographic phosphor remote thermometry system
[DE88-000452] N88-12781
Nitrogen energy transfer study
[AD-A184457] N88-12869
LASER INTERFEROMETRY
Phase-coherent astrometric interferometry
[AD-A184428] N88-12725
LASER OUTPUTS
Plume mechanics and aerosol growth processes
[AD-A184467] N88-12742
The lasertron RF generator for FEL (Free-Electron Laser) applications
[DE88-000515] N88-12776
LASER PLASMAS
Review of X-ray spectroscopy from laser-produced plasmas
[DE88-000755] N88-13043
LASER PROPULSION
Proceedings: SDIO/DARPA Workshop on Laser Propulsion. Volume 3: Viewgraphs
[DE88-000964] N88-12790
LASER SPECTROSCOPY
Ro-vibrational laser spectroscopy of ESD neutrals from chemisorbed species
[DE87-013011] N88-12770
LASERS
Storing photomicrographs on optical laser disks
[DE87-013747] N88-12785
Lasers measure atmosphere N88-12849
LATE STARS
Measurements of stellar magnetic fields N88-13093
Magnetic fields on K and M stars N88-13137
Broadband linear polarization and chromospheric CaII H and K line emission in late-type main sequence stars N88-13140
A search for X-ray luminous late type stars in NIPSS data N88-13143
Excess emission in the wings of the Hydrogen Balmer lines during a flare on the late-type dMe star YZ CMi N88-13146
MHD energy fluxes for late type dwarfs N88-13148
Sensitivity of the H alpha line to expansion, geometrical extent and temperature gradient in the G and K supergiant chromospheres N88-13159
The delta upsilon = 1 fundamental bands of carbon monoxide in late-type stars N88-13177
A comprehensive exploration of late-type stars in the far-ultraviolet N88-13194
Hydrogen and deuterium in the local interstellar medium N88-13204
LATERAL STABILITY
Effects of jet exhaust yaw vane installation and operation on the longitudinal and lateral-directional characteristics of the F-14 airplane
[NASA-TP-2769] N88-12455
LATTICES (MATHEMATICS)
Application of lattice filtering techniques to CW measured time domain data
[AD-A184351] N88-12671
LAUNCHERS
Thermal analysis of electromagnetic launcher rails
[DE88-000166] N88-12514
ICRF launcher studies
[DE88-001710] N88-13046
LAWS
Three-halves law in sunspot cycle shape
[NASA-CR-181520] N88-13210
LAYOUTS
A procedural method for the efficient implementation of full-custom VLSI designs N88-12701
LEAD (METAL)
Analysis of free cutting brass by A.C. polarography
[PD-MT-8728] N88-12587
LIAPUNOV FUNCTIONS
Closed-loop system analysis using Lyapunov stability theory N88-12978
LIBRARIES
The SUPRENUM communications subroutine library for grid-oriented problems
[DE88-000137] N88-12950
LIFE (DURABILITY)
Reliability of LI/SO2 cells for long-life applications
[DE88-001360] N88-12735
LIFE CYCLE COSTS
Optimized ground coupled heat pump mechanical package
[DE87-014899] N88-12738
Technology Base Research Project for electrochemical energy storage
[DE88-000649] N88-12868
LIFE SCIENCES
JPRS report: Science and technology. USSR: Life sciences
[JPRS-ULS-87-009] N88-12915
LIFT
Aerodynamic sensitivities from subsonic, sonic and supersonic unsteady, nonplanar lifting-surface theory
[NASA-TM-100502] N88-12459
LIFT DEVICES
Aircraft dynamic response calculation based on discrete-continual model N88-12824
LIFT DRAG RATIO
Conical wing with maximum lift-to-drag ratio in supersonic gas flow N88-12833
LIGHT CURVE
The giant spot on II Peg in 1986 N88-13120
The short-period RS CVn stars: Starspots and fundamental properties N88-13124
The X-ray orbital lightcurves of AR Lac and TY Pyx N88-13129
Differential B and V light curves of the bright by Draconis star HD80715 N88-13130
Light curve behaviour in the near IR of the CG Cyg system N88-13156
Stromgren photometry of RSCVn and HD106102 N88-13187
LIGHT EMISSION
IUE/Optical/VLA flares on AD Leo N88-13152
LIGHT GAS GUNS
Ideal-viscoplastic extrusion model with application to deforming pistons in light-gas guns
[UTIAS-TN-266] N88-12857
LIGHT MODULATION
Development of optical modulators for measurements of solar magnetic fields
[NASA-TM-100315] N88-13016
LIGHT SCATTERING
All-optical beam control by forced Rayleigh scattering
[AD-A184315] N88-13018
LIGHT SOURCES
National Synchrotron Light Source users manual: Guide to the VUV and X-ray beam lines
[DE88-001484] N88-13020
LIGHTNING
Experimental and analytic studies of the triggered lightning environment of the F106B
[NASA-CR-4104] N88-12897
LIMB DARKENING
Asymmetry and variations of solar limb darkening along the diameter defined by diurnal motion in April 1981 N88-13111
Calibration of the Ca II K line-core density and the magnetic flux density in stars using solar data N88-13118
LIMITERS (FUSION REACTORS)
Modular pump limiter systems for large tokamaks
[DE88-001487] N88-13045
LINE SPECTRA
Active phases on II Peg N88-13119
H alpha and Ca II emission line variability of FK comae N88-13126
Magnetic fields on K and M stars N88-13137
Broadband linear polarization and chromospheric CaII H and K line emission in late-type main sequence stars N88-13140
An analysis of the photospheric line profiles in F, G, and K supergiants N88-13157
The Wilson-Bappu relationship: A barometric effect N88-13170
Synthetic spectra for the N-type carbon star TX Psc N88-13173
Infrared excesses of barium stars N88-13174
The delta upsilon = 1 fundamental bands of carbon monoxide in late-type stars N88-13177
A helium flare on the active G5 dwarf Kappa Ceti N88-13189
LINEAR ACCELERATORS
Proceedings: SDIO/DARPA Workshop on Laser Propulsion. Volume 3: Viewgraphs
[DE88-000964] N88-12790
LINEAR PROGRAMMING
Methods for design and evaluation of integrated hardware/software systems for concurrent computation
[NASA-CR-181522] N88-12953
Parallel superconvergent multigrid
[DE87-013153] N88-12960
LINEAR QUADRATIC GAUSSIAN CONTROL
New feedback design methodologies for large space structures: A multi-criterion optimization approach N88-12535
Closed-loop system analysis using Lyapunov stability theory N88-12978
LINEAR SYSTEMS
A new state space model for the NASA/JPL 70-meter antenna servo controls N88-12702
Parallel superconvergent multigrid
[DE87-013153] N88-12960
Closed-loop system analysis using Lyapunov stability theory N88-12978
Oscillation theory for linear second-order differential systems
[DE87-011393] N88-12983
The linear characteristic method in XYZ geometry
[DE87-011668] N88-12984
LINEAR VIBRATION
Vibration and buckling of geometrically imperfect laminated cylindrical shells N88-12822
LINEARITY
Total linearisation method for solving viscous free boundary flow problems by the finite element method
[PB87-222337] N88-12737
LININGS
An analysis of sound absorbing linings for the interior of the NASA Ames 80 x 120-foot wind tunnel
[NASA-CR-177396] N88-13006
LIQUID CRYSTALS
Boundary effects on the drag of an oscillating sphere: Applications to the magnetic sphere rheometer. Attenuation and dispersion of acoustic waves in nematic liquid crystals N88-13007
Guest-host interactions in thermotropic and lyotropic liquid crystals
[AD-A184402] N88-13057

LIQUID LITHIUM
Corrosion of ferritic steels by molten lithium: Influence of competing thermal gradient mass transfer and surface product reactions
[DE88-000334] N88-12585
LIQUID METALS
Corrosion strength of niobium and its alloys
[DE87-703693] N88-12578
Inertial confinement fusion reactor cavity analysis
[DE88-000788] N88-13029
LIQUID PROPELLANT ROCKET ENGINES
Space station resistojet system requirements and interface definition study
[NASA-CR-180832] N88-12541
LIQUID ROCKET PROPELLANTS
Performance analysis of advanced spacecraft TPS
[NASA-CR-181532] N88-12484
Space station resistojet system requirements and interface definition study
[NASA-CR-180832] N88-12541
LIQUID WASTES
Space station resistojet system requirements and interface definition study
[NASA-CR-180832] N88-12541
LIQUID-GAS MIXTURES
Thermodynamic properties for natural gas binaries
[PB87-226833] N88-13074
LIQUIDS
Novel macrocyclic carriers for proton-coupled liquid membrane transport
[DE88-000636] N88-12560
Experimental study of thermocapillary flows in a thin liquid layer with heat fluxes imposed on the free surface
[NASA-TM-100252] N88-12763
Some new ideas in liquid detectors
[DE88-000732] N88-12768
LITHIUM
Corrosion susceptibility study of candidate pin materials for ALTC (Active Lithium/Thionyl Chloride) batteries
[DE88-001449] N88-12734
Technical evaluation of a solar-powered absorption cooling system (LiBr-H2O)
[PB87-106254] N88-12667
Far-infrared spectra of lithium deposited on a gold electrode: Interpretation using a cluster model
[AD-A184231] N88-13050
LITHIUM SULFUR BATTERIES
Impedance of passive lithium anodes in SOCl2 solutions under low-field polarization
[DE88-000922] N88-12728
Reliability of Li/SO2 cells for long-life applications
[DE88-001360] N88-12735
LOAD TESTS
A study of the crack tip parameters that govern environmentally assisted cracking by use of the rising displacement test N88-12649
Durability of powdered aluminum structures N88-12655
LOADING RATE
Composite materials applications program at the US Army Ballistic Research Laboratory: Work in progress N88-12651
LOADS (FORCES)
Ideal-viscoplastic extrusion model with application to deforming pistons in light-gas guns
[UTIAS-TN-266] N88-12657
The effect of mass, wind angle and erection technique on the aeroelastic behaviour of a cable-stayed bridge model
[NAE-AN-46] N88-12819
A comparison of structural frequency response functions measured with forces from 500 to 250,000 lb
[DE88-000668] N88-12829
LOCAL AREA NETWORKS
Applications of the hybrid automated reliability predictor
[NASA-TP-2760] N88-12928
LOGIC CIRCUITS
Programmable Logic Arrays (PLA's) design for testability
[PB87-102935] N88-12718
Mental models in expert physics reasoning
[AD-A184106] N88-13075
LOGIC DESIGN
Mental models in expert physics reasoning
[AD-A184106] N88-13075
LOGIC PROGRAMMING
Programmable Logic Arrays (PLA's) design for testability
[PB87-102935] N88-12718
PROVER: A first-order logic system in Ada
[DE88-000220] N88-12951
LONG TERM EFFECTS
Effect of long-term thermal aging on coated Celion/LARC-160 composites
[NASA-TM-100495] N88-12544
Influence of creep on the precipitate structure under conditions of long-term creep. 4: Experiments on 10 CrMo 9 10 steel
[BLL-CE-TRANS-8256-(9022.09)] N88-12589
LONGITUDINAL STABILITY
Effects of jet exhaust yaw vane installation and operation on the longitudinal and lateral-directional characteristics of the F-14 airplane
[NASA-TP-2769] N88-12455
LORENTZ CONTRACTION
Analysis of absolute space-time Lorentz theories
[DE87-703371] N88-13076
LOSSES
Empirical relations between photospheric magnetic fields and atmospheric radiative losses for cool dwarf stars N88-13145
IRAS and cool stellar mass loss N88-13166
LOW NOISE
Low-noise cryogenic transmission line N88-12688
The 8.4-GHz low-noise maser pump source assembly N88-12705
LOW PASS FILTERS
On a circular correlation technique for filtering randomly noisy data
[AD-A184317] N88-12669
LOW SPEED
Investigation of low-speed turbulent separated flow around airfoils
[NASA-CR-177450] N88-12471
LUMINOSITY
Stellar cycle variability of solar-like stars: A sneak preview N88-13136
A search for X-ray luminous late type stars in NIPSS data N88-13143
LUNAR CRATERS
Conditions for geomagnetically trapping sub-micron lunar ejecta between L = 1.2 and L = 3.1 N88-13203
LYMAN ALPHA RADIATION
Hydrogen and deuterium in the local interstellar medium N88-13204

M

M STARS
Evidence for an additional source of opacity during the impulsive phase of stellar flares N88-13133
Magnetic fields on K and M stars N88-13137
Carbon abundances and C12/C13 ratios in M giants N88-13167
M dwarfs from the Einstein medium sensitivity survey N88-13188
MACHINING
Interactions between science and precision engineering
[DE87-010873] N88-12643
MAGNESIUM CHLORIDES
Influence of some parameters on the stress corrosion of a ABNT 304 stainless steel in MgCl/sub 2/
[DE87-703707] N88-12580
MAGNETIC DISTURBANCES
New results from high angular resolution observations of alpha Ori N88-13161
MAGNETIC EFFECTS
Magnetic field dependence of the specific heat of some high-T/sub c/ superconductors
[DE87-014078] N88-13063
MAGNETIC FIELD CONFIGURATIONS
Laser induced fluorescent study of relativistic electron beams
[AD-A184456] N88-12774
Large scale solar and stellar magnetic fields N88-13117
Model of solar-wind magnetosphere coupling N88-13211
MAGNETIC FIELD RECONNECTION
Numerical modeling of slow shocks
[DE87-014768] N88-12808
Model of solar-wind magnetosphere coupling N88-13211
MAGNETIC FIELDS
Relativistic electron precipitations in a pulsating aurora N88-12894
Magnetic field dependence of the specific heat of some high-T/sub c/ superconductors
[DE87-014078] N88-13063
Resistivity of EuBa2(Cu/sub 1-y/Zn/sub y/)3O/sub x/ as a function of temperature, magnetic field, pressure and Zn concentration
[DE87-014740] N88-13069
The dynamics of solar magnetic flux tubes subjected to resonant foot point shaking N88-13118
MAGNETIC FLUX
Observational constraints and evidence for saturation N88-13097
Magnetic flux tubes as sources of wave generation N88-13108
Calibration of the Ca II K line-core density and the magnetic flux density in stars using solar data N88-13116
The dynamics of solar magnetic flux tubes subjected to resonant foot point shaking N88-13118
MAGNETIC LEVITATION VEHICLES
Repulsive force support system feasibility study
[NASA-CR-178400] N88-12497
MAGNETIC MATERIALS
Magnetic diffuse scattering
[DE87-013539] N88-13014
MAGNETIC MEASUREMENT
Measurements of stellar magnetic fields N88-13093
The photospheric magnetic fields of cool stars: Recent results of survey and time-variability programs N88-13094
MAGNETIC MIRRORS
MHD stability and control for mirror machines N88-13038
MAGNETIC SUSPENSION
Repulsive force support system feasibility study
[NASA-CR-178400] N88-12497
MAGNETICALLY TRAPPED PARTICLES
Conditions for geomagnetically trapping sub-micron lunar ejecta between L = 1.2 and L = 3.1 N88-13203
MAGNETOHYDRODYNAMIC FLOW
Flux tube dynamics and solar/stellar redshift measurements N88-13095
MAGNETOHYDRODYNAMIC STABILITY
The role of stellarators in the advanced toroidal program
[DE87-014815] N88-13025
Transport simulations of the oscillating field current drive experiment in the ZT-40M reversed field pinch
[DE88-000538] N88-13027
Magnetic fluctuation behaviour of current termination in reversed field pinch
[IPPJ-849] N88-13034
MHD stability and control for mirror machines N88-13038
MAGNETOHYDRODYNAMIC WAVES
The acceleration of winds by MHD waves in open magnetic structures N88-13109
MHD energy fluxes for late type dwarfs N88-13148
MAGNETOHYDRODYNAMICS
Numerical modeling of slow shocks
[DE87-014768] N88-12808
Implementation of a 3-D nonlinear MHD calculation on the Intel hypercube
[DE87-014637] N88-12949
Numerical simulation of the Reversed Field Pinch
[AD-A184353] N88-13023
MAGNETOPLASMADYNAMICS
Plasma thruster development
[AD-A184173] N88-12536
MAGNETOSPHERE
Slow-mode shocks in the earth's magnetosphere
[DE88-000483] N88-12695
Conditions for geomagnetically trapping sub-micron lunar ejecta between L = 1.2 and L = 3.1 N88-13203
MAGNETOSPHERE-IONOSPHERE COUPLING
Model of solar-wind magnetosphere coupling N88-13211
MAGNONS
Non-lattice matched metallic superlattices
[DE87-011512] N88-13062
MAIN SEQUENCE STARS
PG 0308 + 096: A short-period white dwarf + dM binary with strongly modulated H-alpha emission N88-13132
Stellar cycle variability of solar-like stars: A sneak preview N88-13136
Relations between chromospheric and coronal structure, flux-flux correlations and convective zone properties N88-13138
Broadband linear polarization and chromospheric CaII H and K line emission in late-type main sequence stars N88-13140
Activity in warm stars N88-13142
Emission features in IRAS LRS spectra of MS, S and CS stars N88-13163
Spin-up and spin-down on the way to the main sequence N88-13181
MAINTENANCE
Software maintenance in scientific and engineering environments: An introduction and guide
[NASA-CR-177409] N88-12954
MAN ENVIRONMENT INTERACTIONS
Disturbance and recovery of Arctic Alaskan tundra terrain. A review of recent investigations
[AD-A184442] N88-12887
MAN MACHINE SYSTEMS
Ground vehicle convoying
[DE88-000360] N88-13088

MAN-COMPUTER INTERFACE
SDVS (State Delta Verification System) 5 users' manual
[AD-A184339] N88-12943
The ISI (Information Sciences Institute) grapher: A portable tool for displaying graphs pictorially
[AD-A184354] N88-12944
User interface for a partially incompatible system software environment with non-ADP users
[DE88-001518] N88-12968
MANAGEMENT PLANNING
Experimental use of artificial intelligence for (future) ATC systems
[PB87-106449] N88-12970
MANEUVERS
Analytical investigation of the dynamics of tethered constellations in Earth orbit (phase 2)
[NASA-CR-179218] N88-12533
Combined problem of slew maneuver control and vibration suppression
[NASA-CR-181537] N88-12817
MANGANESE
Sintered steels of high resistance alloyed to Nb, Mo, Mn and Si
[DE87-703546] N88-12573
MANGANESE ALLOYS
A comparison of high damping shape memory alloys with Cu-Mn-based and Fe-Cr-based alloys
[AD-A184110] N88-12566
MANNED SPACECRAFT
Techniques for fire detection N88-12521
MANUALS
DOE explosives safety manual
[DE88-000631] N88-12616
A portable hypercube simulator
[DE87-013369] N88-12947
National Synchrotron Light Source users manual: Guide to the VUV and X-ray beam lines
[DE89-001464] N88-13020
MANUFACTURING
Activities at government research laboratories reported N88-12503
Research and development on high strength ceramic heaters discussed N88-12508
Thixotropic surface composition for phenolaldehyde resin laminates
[GB-PATENT-2-180-251-A] N88-12545
MAPPING
Principles for problem aggregation and assignment in medium scale multiprocessors
[NASA-CR-178379] N88-12935
Foundations of O-theory 2: Measurements and relation to fuzzy set theory
[DE88-000013] N88-12966
MAPS
X-rays, color, and the Vaughan-Preston gap N88-13135
MARAGING STEELS
Metallography of maraging 350 steel
[DE87-013746] N88-12591
MARINE METEOROLOGY
New precipitation map of world ocean N88-12634
MARS (PLANET)
A near-earth optical communications terminal with a corevolving planetary sun shield N88-12693
MARS ATMOSPHERE
The atmosphere of Mars and optical communications N88-12692
MARTENSITE
A comparison of high damping shape memory alloys with Cu-Mn-based and Fe-Cr-based alloys
[AD-A184110] N88-12566
MARTENSITIC TRANSFORMATION
Soliton twin boundaries of the cubic-tetragonal martensitic transformations in ferroelastic materials
[DE87-014741] N88-13047
MASERS
The 8.4-GHz low-noise maser pump source assembly N88-12705
Traveling-wave maser closed-cycle refrigerator data acquisition and display system N88-12708
Two-watt, 4-Kelvin closed cycle refrigerator performance N88-12709
Nonthermal phenomena in stellar coronae: Evidence from radio observations N88-13096
MASS
Effect of permissible variations of center-of-gravity locations of cargo airplane on its mass N88-12825
A search for very low mass (brown dwarf) stars as wide binaries using a seven element infrared camera-photometer N88-13150
MASS FLOW
IRAS and cool stellar mass loss N88-13166
MASS SPECTROSCOPY
Simultaneous TG/DSC (thermogravimetry/Differential Scanning Calorimetry) and TG/MS (thermogravimetry/Mass Spectrometry) analyses of polymeric and energetic materials
[DE88-000727] N88-12561
MASS TRANSFER
Novel macrocyclic carriers for proton-coupled liquid membrane transport
[DE88-000636] N88-12560
Corrosion of ferritic steels by molten lithium: influence of competing thermal gradient mass transfer and surface product reactions
[DE88-000334] N88-12585
Heat and moisture transport in the atmospheric boundary layer
[AD-A184222] N88-12904
MATCHED FILTERS
Detection of signals by the digital integrate-and-dump filter with offset sampling N88-12695
Detection of signals by weighted integrate-and-dump filter N88-12696
MATERIALS HANDLING
DOE explosives safety manual
[DE88-000631] N88-12616
Nuclear techniques in studies of condensed matter
[NASA-RP-1195] N88-13015
MATHEMATICAL LOGIC
An exact penalization viewpoint of constrained optimization
[DE88-001477] N88-12995
MATHEMATICAL MODELS
Hovering helicopter flight dynamics: A study of vertical motion
[AR-004-526] N88-12485
An integrated study of structures, aerodynamics and controls on the forward swept wing X-29A and the oblique wing research aircraft
[NASA-CR-181548] N88-12486
Aircraft engine exhaust plume dynamics
[AD-A184238] N88-12488
Efficiency aspects of short, low velocity railguns
[AR-004-847] N88-12517
Analytical investigation of the dynamics of tethered constellations in Earth orbit (phase 2)
[NASA-CR-179218] N88-12533
A study of mechanisms of hydrogen diffusion in separation devices
[DE88-000326] N88-12584
Microgravity nucleation and particle coagulation experiments support
[NASA-CR-181540] N88-12618
Microgravity nucleation and particle coagulation experiments support
[NASA-CR-181541] N88-12619
Aircraft dynamic response calculation based on discrete-continual model N88-12624
A direct method to obtain constitutive model constants from cylinder impact test results N88-12647
Ideal-viscoplastic extrusion model with application to deforming pistons in light-gas guns
[UTIAS-TN-266] N88-12657
Heterogeneous multi-trunking queueing systems
[AD-A184255] N88-12668
Programmable Logic Arrays (PLA's) design for testability
[PB87-102935] N88-12718
An analytical and experimental study of injection-locked two-port oscillators
[NASA-TM-100119] N88-12727
The Pierce diode with an external circuit. Part 1: Simulations in the linear regime
[DE88-000413] N88-12731
Fully developed turbulence via Feigenbaum's period-doubling bifurcations
[DE88-000242] N88-12739
Numerical simulation of unsteady separated flows
[AD-A184132] N88-12741
Tracking through turbulence at the Tonopah Test Range
[DE88-001448] N88-12766
Analysis of sideband spectra from untapered undulator using analytical technique
[DE87-014783] N88-12778
The modelling of orientation in planar polymer welding flows
[AD-A184404] N88-12793
Nonlinear axial stiffness characteristics of axisymmetric bolted joints N88-12799
Creep life prediction based on stochastic model of microstructurally short crack growth
[NASA-TM-100245] N88-12825
Two-layer stratified flow analysis of gravity currents and turbidity currents in lakes, reservoirs and the ocean N88-12864
Statistics of the geomagnetic secular variation for the past 5Ma
[NASA-CR-181558] N88-12890
An algorithmic approach to crustal deformation analysis N88-12891
The effects of minor trace gases on the transfer of thermal infrared radiation through the Earth's atmosphere N88-12893
Experimental and analytic studies of the triggered lightning environment of the F106B
[NASA-CR-4104] N88-12897
Estimation of a multivariate continuous variable panel model
[AD-A184472] N88-12982
The shifted Adams method for ordinary differential equations
[DE88-000810] N88-12994
Radiation induced collapse of the crystalline structure
[DE87-014407] N88-13064
Subjective probability, combination of expert opinion and probabilistic approaches to information retrieval N88-13085
The acceleration of winds by MHD waves in open magnetic structures N88-13109
Cosmological applications of singular hypersurfaces in general relativity N88-13202
Gamma ray lines from novae N88-13214
MATRICES (MATHEMATICS)
QR factorization of a dense matrix on a shared-memory multiprocessor
[DE88-001506] N88-12958
Two classes of preconditioners computed using block matrix factorization techniques
[DE89-001313] N88-12988
MATRIX MATERIALS
Carbon fiber reinforced glass matrix composites for space based applications
[AD-A184355] N88-12546
MAXIMUM LIKELIHOOD ESTIMATES
Tau ranging revisited N88-12710
Estimation of a multivariate continuous variable panel model
[AD-A184472] N88-12982
An urn model for the multi-sample capture/recapture sequential tagging process
[AD-A184470] N88-12998
MAXWELL EQUATION
Spectral evolution equation for the sideband instability in a free-electron laser oscillator
[DE88-000510] N88-12771
MEASURING INSTRUMENTS
Proceedings of the Fifth Symposium on Energy Engineering Sciences: Instrumentation, Diagnostics, and Material Behavior
[DE88-001479] N88-12880
Non-linearity in measurement systems: Evaluation method and application to microwave radiometers N88-12884
Evaluation of the sensidyne toxic gas sensor for HF (Hydrogen Fluoride) vapor
[DE88-000647] N88-12787
Optimization of dilatometer test procedures
[DE87-014998] N88-12789
Use of electron beam instruments to determine fluctuations in vertical refraction partial angle N88-12853
Computerized certification of digital ultrasonic instrumentation
[DE88-000820] N88-13008
MECHANICAL ENGINEERING
Interactions between science and precision engineering
[DE87-010873] N88-12643
COLA2: A computer program for the structural synthesis of two components using general modal coordinates
[DE88-001457] N88-12963
MECHANICAL PROPERTIES
Research and development on high strength ceramic heaters discussed N88-12508
Parachute materials
[DE87-014845] N88-12550
Mechanical properties of a microalloyed steel with high niobium content
[DE87-703545] N88-12572
Mechanical properties of an acicular ferrite steel microalloyed to niobium and vanadium
[DE87-703547] N88-12574
Mechanical strength and niobium and niobium-base alloys substructures
[DE87-703692] N88-12577
Effects of stress-relieving on the mechanical properties and the structure of specimens of high-temperature fine-grained structural steels heat-treated to simulate welding
[BLL-CE-TRANS-8258-(9022.09)] N88-12586

The aging behavior of types 308 and 308CRE stainless steels and its effect on mechanical properties
[DE87-012541] N88-12590
Development of advanced fiber reinforced ceramics
[DE88-000779] N88-12604
Thermomechanical cracking in coated media due to high speed asperity excitation
[AD-A184176] N88-12809
MECHANICAL SHOCK
Mechanical shock test specification using nonstationary random excitation models
[DE87-013650] N88-12812
MELTING
Data base on the high heat flux behaviour of metals and carbon materials for plasma facing components: Experiments at the 10 MW neutral beam injection test stand of the IPP Nagoya
[IPPJ-AM-53] N88-13031
MEMBRANE STRUCTURES
Large change-of-curvature effects in quadratic finite elements for CAD of membrane structures N88-12958
MEMBRANES
Novel macrocyclic carriers for proton-coupled liquid membrane transport
[DE88-000636] N88-12560
MEMORY (COMPUTERS)
An approach to implementing state space searches on heterogeneous systems of multiprocessors
[DE88-001321] N88-12967
MENTAL PERFORMANCE
Mental models in expert physics reasoning
[AD-A184106] N88-13075
MERCURY VAPOR
High efficiency generation of 130-nm radiation from sum-frequency mixing in Hg
[DE87-013714] N88-12674
MESOSCALE PHENOMENA
Mesoscale eddy dynamics by the method of point vortices N88-12863
MESSAGE PROCESSING
An interactive computer graphics network monitor for a tactical communications network
[AD-A184131] N88-12938
METABOLISM
The toxicology and metabolism of nickel compounds
[DE87-014801] N88-12921
METAL BONDING
Valence bond cluster studies of alkali metal/semiconductor bonding
[AD-A184276] N88-13054
METAL CUTTING
Analysis of free cutting brass by A.C. polarography
[PD-MT-8728] N88-12587
METAL FATIGUE
Fatigue failure of thin porous strips N88-12640
METAL HYDRIDES
Performance analysis of advanced spacecraft TPS
[NASA-CR-181532] N88-12484
METAL MATRIX COMPOSITES
Damping characteristics of a composite-reinforced stainless-steel plate
[DE88-000303] N88-12828
METAL OXIDE SEMICONDUCTORS
Reevaluating the worst-case radiation response of MOS transistors
[DE87-014157] N88-13059
METAL PLATES
Fatigue failure of thin porous strips N88-12640
METAL POWDER
Fatigue failure of thin porous strips N88-12640
METAL SHEETS
Fatigue failure of thin porous strips N88-12640
METAL SURFACES
The structure of adsorbed sulfur and carbon on molybdenum and rhenium single crystal surfaces, and their influence on carbon monoxide and hydrocarbon chemisorption
[DE88-001393] N88-13073
METAL VAPORS
Microgravity nucleation and particle coagulation experiments support
[NASA-CR-181541] N88-12619
METALLIC GLASSES
Studies on some Ge-Se-Te glasses
[PD-MT-8721] N88-12607
METALLOGRAPHY
Metallography of maraging 350 steel
[DE87-013746] N88-12591
METALS
Activities at government research laboratories reported N88-12503
Ignition and combustion of metals in oxygen N88-12530
Topological aspects of infinite metal clusters and superconductors
[AD-A184104] N88-13049
METEOR TRAILS
Meteor-burst communications: Is this what the Navy needs?
[AD-A184433] N88-12672
METEORITE COLLISIONS
Measurements of iridium and the meteoric impact hypothesis at cretaceous end
[DE87-703765] N88-13200
Conditions for geomagnetically trapping sub-micron lunar ejecta between L = 1.2 and L = 3.1 N88-13203
METEORITES
Moessbauer study of shock induced effects in the Fe-Ni 50/50 ordered alloy in meteorites
[DE87-703364] N88-13199
METEOROID PROTECTION
Optimization techniques applied to passive measures for in-orbit spacecraft survivability
[NASA-CR-179216] N88-12532
Space suit extravehicular hazards protection development
[NASA-TM-100458] N88-12927
METEOROID SHOWERS
Meteor-burst communications: Is this what the Navy needs?
[AD-A184433] N88-12672
METEOROLOGICAL CHARTS
New precipitation map of world ocean N88-12834
METEOROLOGY
Study of an airborne Doppler radar: Project Asterix
[BLL-MO-TRANS-1667-(9022.552)] N88-12675
USSR report: Earth sciences
[JPRS-UES-86-006] N88-12831
METHOD OF CHARACTERISTICS
The linear characteristic method in XYZ geometry
[DE87-011668] N88-12984
METRIC PHOTOGRAPHY
Accuracy potential of non-metric cameras in close-range photogrammetry N88-12862
MICHELSON INTERFEROMETERS
Phase-coherent astrometric interferometry
[AD-A184428] N88-12725
MICROBIOLOGY
JPRS report: Science and technology. USSR: Life sciences
[JPRS-ULS-87-009] N88-12915
MICROELECTRONICS
Chemically modified microelectrode arrays. New kinds of electronic devices
[AD-A184389] N88-12724
MICROHARDNESS
Welding and weldability of ductile intermetallic alloys
[DE87-014061] N88-12582
MICROPROCESSORS
The pros and cons of using a CAI package on a central computer as opposed to a microprocessor: What's your CAI MO, mainframe or micro
[DE87-011123] N88-12929
MICROSTRUCTURE
Corrosion behavior of P/M mechanically alloyed IN-9052.1: An electro-chemical investigation
[AD-A184191] N88-12567
The nature of metallurgical reactions in underwater welding
[AD-A184464] N88-12568
Mechanical properties of a microalloyed steel with high niobium content
[DE87-703545] N88-12572
Mechanical strength and niobium and niobium-base alloys substructures
[DE87-703692] N88-12577
Welding and weldability of ductile intermetallic alloys
[DE87-014061] N88-12582
The accommodation of precipitate plates modelled as a tensile test
[DE88-000207] N88-12814
Characterization of thin layers for optics
[PB87-217949] N88-13017
Microstructural change of Al on H implantation
[IPPJ-847] N88-13036
Theory and simulations of Zone 2 microstructures in thin films
[DE87-014752] N88-13071
MICROWAVE ANTENNAS
The 8.4-GHz low-noise maser pump source assembly N88-12705
MICROWAVE EMISSION
VLA observations of the X-ray bright Hyades M-dwarfs N88-13147
Microwave observations of red dwarf flare stars N88-13153
MICROWAVE EQUIPMENT
Microwave refractive index structure function profiles (Cn2) measured from a small aircraft
[AD-A184343] N88-12670
The lasertron RF generator for FEL (Free-Electron Laser) applications
[DE88-000515] N88-12776
MICROWAVE LANDING SYSTEMS
Effect of motion cues during complex curved approach and landing tasks: A piloted simulation study
[NASA-TP-2773] N88-12480
MICROWAVE RADIOMETERS
Non-linearity in measurement systems: Evaluation method and application to microwave radiometers N88-12684
A multibody dynamic analysis of the N-ROSS (Navy Remote Ocean Sensing System) satellite rotating flexible reflector using Kane's method
[AD-A184452] N88-12880
Cloud cover determination in polar regions from satellite imagery
[NASA-CR-181544] N88-12908
MICROWAVE SPECTRA
Microwave observations of nonthermal phenomena in pre-main sequence stars N88-13107
MICROWAVES
Automated microwave dielectric constant measurement
[AD-A184182] N88-12667
MINERAL DEPOSITS
A mineral reconnaissance sampling manual for Costa Rica: Central American energy and resource project
[DE87-014997] N88-12859
MINERAL EXPLORATION
A mineral reconnaissance sampling manual for Costa Rica: Central American energy and resource project
[DE87-014997] N88-12859
MINICOMPUTERS
A data analysis environment for HP (Hewlett-Packard) 1000 computers
[DE87-010511] N88-12936
MINORITIES
A national model at Howard University demonstrating private sector interrelationships that facilitate research in predominantly Black colleges and universities
[DE88-000160] N88-13069
MIRA VARIABLES
Application of dynamic atmosphere models to the analysis of angular diameter observations of Mira variables N88-13166
MIRRORS
Solar converging method N88-12504
Long-range pulselength scaling of 351nm laser damage thresholds
[DE87-014754] N88-12777
MISSION PLANNING
High power ion thruster performance
[NASA-TM-100127] N88-12542
MIXING
Activities at government research laboratories reported N88-12503
Atomic and electronic structure of surfaces and chemisorbed layers
[DE87-014987] N88-13065
MIXTURES
Thermodynamic properties of supercritical mixtures
[DE88-000809] N88-12562
MODELS
Reduced complexity structural modeling for automated airframe synthesis
[NASA-CR-177440] N88-12453
Experimental evidence for modifying the current physical model for ice accretion on aircraft surfaces
[NASA-TM-87184] N88-12473
A multiple-time-scale turbulence model based on variable partitioning of turbulent kinetic energy spectrum
[NASA-CR-179222] N88-12754
On dynamic loads in parallel shaft transmissions. 1: Modelling and analysis
[NASA-TM-100180] N88-12797
On dynamic loads in parallel shaft transmissions. 2: Parameter study
[NASA-TM-100181] N88-12798
User's guide to NCAR (National Center for Atmospheric Research) CCM1
[PB87-224366] N88-12899
A tight upper bound for the speed-up of parallel best-first branch-and-bound algorithms
[AD-A184246] N88-12939
Mental models in expert physics reasoning
[AD-A184106] N88-13075
MODULATION
High-power RF-pulsed modulators for the Los Alamos free-electron laser
[DE88-000514] N88-12775
MODULATORS
The 8.4-GHz low-noise maser pump source assembly N88-12705

MODULES
Modular pump limiter systems for large tokamaks
[DE88-001487] N88-13045
MODULUS OF ELASTICITY
Carbon fiber reinforced glass matrix composites for space based applications
[AD-A184355] N88-12546
Determination of through-plane shear moduli for glass-reinforced plastics
[PB87-106274] N88-12592
MOISTURE
Theory of heat and moisture exchange between finely disperse storm-generated spray and turbulent air flow N88-12851
MOISTURE CONTENT
Lidar-radiometric method for determining liquid-water content of cirrus clouds N88-12854
MOLDS
Process for producing sandwich mouldings
[EP-PATENT-0-191-623-A2] N88-12642
MOLECULAR BEAM EPITAXY
Raman scattering spectrum along a bevel etched GaAs on Si, TEM (Transmission Electron Microscope) study and GaAs P-I-N photodetector on Si
[DE88-000210] N88-13066
MOLECULAR BEAMS
Ceramics thin film N88-12505
MOLECULAR DIFFUSION
The modelling of orientation in planar polymer welding flows
[AD-A184404] N88-12793
MOLECULAR EXCITATION
Ro-vibrational laser spectroscopy of ESD neutrals from chemisorbed species
[DE87-013011] N88-12770
MOLECULAR ROTATION
Ro-vibrational laser spectroscopy of ESD neutrals from chemisorbed species
[DE87-013011] N88-12770
MOLECULAR STRUCTURE
Molecular engineering of ceramics
[DE88-000174] N88-12603
Advances in inherently conducting polymers
[DE88-000501] N88-12610
The Moessbauer effect of SnI4 at high pressure
[DE87-014771] N88-13048
MOLECULES
Tetrahedral carbon and interstitial electrons in Li cluster: CLi4 and (LiCH3)4
[AD-A184277] N88-13055
MOLYBDENUM
Sintered steels of high resistance alloyed to Nb, Mo, Mn and Si
[DE87-703546] N88-12573
Data base on the high heat flux behaviour of metals and carbon materials for plasma facing components: Experiments at the 10 MW neutral beam injection test stand of the IPP Nagoya
[IPPJ-AM-53] N88-13031
MOMENTS
Semiempirical method for prediction of aerodynamic forces and moments on a steadily spinning light airplane
[NASA-TM-4009] N88-12456
MOMENTUM TRANSFER
Variable collision frequency effects on hose and sausage instabilities in relativistic electron beams
[AD-A184206] N88-13021
Spin-up and spin-down on the way to the main sequence N88-13181
MONITORS
Development of an acoustic emission monitor and monitoring technique for long-term monitoring of U-0.8Ti electron-beam weldments for postweld cracking
[DE88-000819] N88-12804
An interactive computer graphics network monitor for a tactical communications network
[AD-A184131] N88-12938
MONOMOLECULAR FILMS
Ceramics thin film N88-12505
MONSOONS
Interactions between the Asian monsoons, the tropical Pacific and the southern hemisphere extratropics N88-12907
MONTE CARLO METHOD
Creep life prediction based on stochastic model of microstructurally short crack growth
[NASA-TM-100245] N88-12825
Final (n,l) state-resolved electron capture by multiply charged ions from neutral atoms
[IPPJ-AM-54] N88-13030
Monte Carlo analysis of neoclassical transport for a compact helical system
[IPPJ-850] N88-13033
MORPHOLOGY
Corrosion behavior of P/M mechanically alloyed IN-9052.1: An electro-chemical investigation
[AD-A184191] N88-12567
Steady shearing in a viscoplastic solid
[AD-A184341] N88-12810
Banded ion morphology N88-12992
Study of certain biological characteristics of bacteria during the French-Soviet CYTOS-2 space experiment N88-12917
MOSSBAUER EFFECT
The Moessbauer effect of SnI4 at high pressure
[DE87-014771] N88-13048
Moessbauer study of shock induced effects in the Fe-Ni 50/50 ordered alloy in meteorites
[DE87-703364] N88-13199
MOTION
Effect of motion cues during complex curved approach and landing tasks: A piloted simulation study
[NASA-TP-2773] N88-12480
MOTION SICKNESS
Motion and space sickness N88-12510
Change in functional activity of cortical brain structures and their blood supply in alert rabbits in response to rocking N88-12916
MOTOR VEHICLES
Ground vehicle convoying
[DE88-000360] N88-13088
MOUNTAINS
Measurements of vapor flux, liquid water contents, precipitation rates and riming in a Utah mountain cloud system
[PB87-224945] N88-12900
MULTIPROCESSING (COMPUTERS)
Comparing barrier algorithms
[NASA-CR-178377] N88-12934
Principles for problem aggregation and assignment in medium scale multiprocessors
[NASA-CR-178379] N88-12935
An approach to implementing state space searches on heterogeneous systems of multiprocessors
[DE88-001321] N88-12967
MULTISPECTRAL BAND SCANNERS
Cloud cover determination in polar regions from satellite imagery
[NASA-CR-181544] N88-12908
MULTIVARIATE STATISTICAL ANALYSIS
Estimation of a multivariate continuous variable panel model
[AD-A184472] N88-12982
MUSCLES
Motion and space sickness N88-12510

N

NAP-OF-THE-EARTH NAVIGATION
Some data processing requirements for precision Nap-Of-the-Earth (NOE) guidance and control of rotorcraft
[NASA-CR-177453] N88-12493
NASA PROGRAMS
FY 1985 scientific and technical reports, articles, papers and presentations
[NASA-TM-86521] N88-13083
NASA SPACE PROGRAMS
The Telecommunications and Data Acquisition Report
[NASA-CR-181546] N88-12679
NATURAL GAS
Thermodynamic properties for natural gas binaries
[PB87-226833] N88-13074
NAVIER-STOKES EQUATION
Development and application of computational aerothermodynamics flowfield computer codes
[NASA-CR-181534] N88-12485
Blowup for a nonlinear evolution equation and self-reproducing strained shear layers N88-12755
Cauchy problem for linearized system of Navier-Stokes equations considering compressibility N88-12837
Asymptotic form of stationary solutions of the Navier-Stokes equations for large Reynolds numbers N88-12838
On operator splitting for unsteady boundary value problems
[AD-A184281] N88-12981
INS3D: An incompressible Navier-Stokes code in generalized three-dimensional coordinates
[NASA-TM-100012] N88-12991
NAVIGATION SATELLITES
Dynamic positioning at sea using the global positioning system
[AD-A184453] N88-12476
NEAR FIELDS
Power density measurements in the near field of the DSS 13 26-meter antenna N88-12711
NEAR INFRARED RADIATION
A search for X-ray luminous late type stars in NIPSS data N88-13143
Light curve behaviour in the near IR of the CG Cyg system N88-13156
The angular diameter of alpha Scorpii in the near-infrared Ca II triplet N88-13162
NECK (ANATOMY)
Motion and space sickness N88-12510
NEGATIVE IONS
Negative ion beams for heating and current-drive in NET
[AD-A184390] N88-13012
NERVES
Motion and space sickness N88-12510
NETWORK CONTROL
Multicast gateway design considerations
[PB87-219960] N88-12663
NEURAL NETS
Large-scale neuronal circuits for selective storage and recognition of complex stimuli, a pilot study
[AD-A184134] N88-12920
NEUROPHYSIOLOGY
Visual evoked responses to sinusoidal gratings presented in central and right visual fields: 1
[DE87-014731] N88-12919
Large-scale neuronal circuits for selective storage and recognition of complex stimuli, a pilot study
[AD-A184134] N88-12920
NEUROTRANSMITTERS
Large-scale neuronal circuits for selective storage and recognition of complex stimuli, a pilot study
[AD-A184134] N88-12920
NEUTRAL ATOMS
Ro-vibrational laser spectroscopy of ESD neutrals from chemisorbed species
[DE87-013011] N88-12770
NEUTRON IRRADIATION
Computed neutron tomography and coded aperture holography from real time neutron images N88-12645
NEUTRON RADIOGRAPHY
Computed neutron tomography and coded aperture holography from real time neutron images N88-12645
NEUTRON STARS
Core bounce supernovae
[DE87-014910] N88-13197
NICKEL
Studies on estimation of nickel in zinc base die casting by D.C. polarography
[PD-MT-8729] N88-12588
Moessbauer study of shock induced effects in the Fe-Ni 50/50 ordered alloy in meteorites
[DE87-703364] N88-13199
NICKEL COMPOUNDS
The toxicology and metabolism of nickel compounds
[DE87-014801] N88-12921
NICKEL OXIDES
A hydrogen/nickel oxide battery for remote applications
[DE87-009048] N88-12872
NIOBIUM
Mechanical properties of a microalloyed steel with high niobium content
[DE87-703545] N88-12572
Sintered steels of high resistance alloyed to Nb, Mo, Mn and Si
[DE87-703546] N88-12573
Mechanical properties of an acicular ferrite steel microalloyed to niobium and vanadium
[DE87-703547] N88-12574
Partial substitution of vanadium by niobium in AISI H13 steel
[DE87-703548] N88-12575
Progress in the development of niobium alloyed high speed steel
[DE87-703549] N88-12576
Hadfield steels with Nb and Ti carbides
[DE87-703706] N88-12579
NIOBIUM ALLOYS
Mechanical strength and niobium and niobium-base alloys substructures
[DE87-703692] N88-12577
Corrosion strength of niobium and its alloys
[DE87-703693] N88-12578
NITINOL ALLOYS
On the stressing of annealed NITINOL: The electrical resistance and calorimetric effects
[AD-A184465] N88-12569
NITRAMINE PROPELLANTS
High pressure strand burn rate tests of polyvinylnitrate/nitramine propellants
[AD-A184178] N88-12615
NITRATES
High pressure strand burn rate tests of polyvinylnitrate/nitramine propellants
[AD-A184178] N88-12615

NITROGEN
Absorption of far IR-radiation by H2O-N2 complexes under atmospheric conditions N88-12855
Nitrogen energy transfer study [AD-A184457] N88-12869
NOISE REDUCTION
On a circular correlation technique for filtering randomly noisy data [AD-A184317] N88-12669
Design of source coders and joint source/channel coders for noisy channels [NASA-CR-181547] N88-12678
Aircraft interior noise reduction by alternate resonance tuning [NASA-CR-181530] N88-13005
NONDESTRUCTIVE TESTS
Failure analysis of composite structure materials [AD-A184468] N88-12548
Detection of defects on structures [EP-PATENT-0-210-794-A2] N88-12807
NONEQUILIBRIUM CONDITIONS
Development of the non-equilibrium reactive chemical transport code CHMTRNS [DE88-000682] N88-12964
NONLINEAR EQUATIONS
Blowup for a nonlinear evolution equation and self-reproducing strained shear layers N88-12755
Solution of three-dimensional inverse problem of gravimetry in contact surfaces class by local corrections method N88-12848
NONLINEAR SYSTEMS
A refined nonlinear analysis of laminated composite plates and shells [AD-A184436] N88-12811
Nonlinear acoustics [AD-A184271] N88-13004
Supertracks: The building blocks of chaos [DE88-001513] N88-13207
NONLINEARITY
Non-linearity in measurement systems: Evaluation method and application to microwave radiometers N88-12684
Implementation of a 3-D nonlinear MHD calculation on the Intel hypercube [DE87-014637] N88-12949
NORMAL DENSITY FUNCTIONS
Statistics of the geomagnetic secular variation for the past 5Ma [NASA-CR-181558] N88-12890
NORMALIZING (STATISTICS)
Consistency question in the renormalization group analysis of deep inelastic scattering [DE87-703372] N88-12999
NOSE CONES
Numerical study of supersonic flow around blunt bodies with extended needle nose N88-12635
NOTCH STRENGTH
Influence of strain rate and notch depth on tensile properties of HITCO 6250 [DE88-001324] N88-12816
NOTCHES
Influence of strain rate and notch depth on tensile properties of HITCO 6250 [DE88-001324] N88-12816
NOVA LASER SYSTEM
Thermal stress in the edge cladding of Nova glass laser disks [DE88-000425] N88-12780
NOVAE
Gamma ray lines from novae N88-13214
NOZZLE GEOMETRY
Development and application of computational aerothermodynamics flowfield computer codes [NASA-CR-181534] N88-12465
NUCLEAR CAPTURE
Neutron capture nucleosynthesis in low mass AGB stars N88-13178
NUCLEAR ENERGY
USSR report: Engineering and equipment [JPRS-UEQ-87-008] N88-12621
NUCLEAR FUSION
The attitudes of science policy, environmental, and utility leaders on US energy issues and fusion [DE88-000784] N88-13041
Neutron capture nucleosynthesis in low mass AGB stars N88-13178
NUCLEAR INTERACTIONS
Cosmic-ray nuclear event with an anomalously strong concentration of energy and particles in the central region [DE87-703376] N88-13213
NUCLEAR MAGNETIC RESONANCE
Synthesis, NMR characterization and electrical properties of siloxane-based polymer electrolytes [AD-A184184] N88-12596
Solid state C-13 NMR characterization of textiles: Qualitative and quantitative analysis [AD-A184349] N88-12598
A low volume insert for solid state magic angle spinning NMR of small samples [AD-A184359] N88-12601
Alternating current circuit theory and pulsed NMR (Nuclear Magnetic Resonance) [DE88-000641] N88-12732
NUCLEAR PHYSICS
Future directions in interplays between particle and nuclear physics: Summary session [DE87-011791] N88-13013
Nuclear techniques in studies of condensed matter [NASA-RP-1195] N88-13015
NUCLEAR POWER PLANTS
Expert robots in nuclear plants [DE87-014839] N88-12800
Ultrasonic method of inspecting austenitic weld joints in nuclear power station equipment [BLL-CE-TRANS-8281-(9022.09)] N88-12806
NUCLEAR POWER REACTORS
Small reactor power systems for manned planetary surface bases [NASA-TM-100223] N88-13209
NUCLEAR WEAPONS
An excitation-term modification for a certain class of electromagnetic aperture-coupling problems [DE88-000260] N88-12713
NUCLEATION
Experimental and theoretical study of condensation in multicomponent mixtures [DE88-000697] N88-12563
Microgravity nucleation and particle coagulation experiments support [NASA-CR-181540] N88-12618
Microgravity nucleation and particle coagulation experiments support [NASA-CR-181541] N88-12619
Plume mechanics and aerosol growth processes [AD-A184467] N88-12742
NUMERICAL ANALYSIS
Concepts for radically increasing the numerical convergence rate of the Euler equations [NASA-CR-177456] N88-12463
Natural control of flexible space structures N88-12534
An analytical and experimental study of injection-locked two-port oscillators [NASA-TM-100119] N88-12727
Numerical simulation of unsteady separated flows [AD-A184132] N88-12741
Methods for design and evaluation of integrated hardware/software systems for concurrent computation [NASA-CR-181522] N88-12953
Flux tube dynamics and solar/stellar redshift measurements N88-13095
NUMERICAL INTEGRATION
Propagation of random initial conditions in time N88-12993

O

OBLIQUE WINGS
An integrated study of structures, aerodynamics and controls on the forward swept wing X-29A and the oblique wing research aircraft [NASA-CR-181548] N88-12486
OBSERVABILITY (SYSTEMS)
Closed-loop system analysis using Lyapunov stability theory N88-12978
OCEAN BOTTOM
RRS DISCOVERY cruise 160, 30 June-25 July, 1986. Geochemical sampling over the Madeira and Porcupine Abyssal Plains [PB87-222030] N88-12910
OCEAN CURRENTS
Experimental study of turbulent diffusion parameters in ocean N88-12840
Intensive synoptic eddies and quasigeostrophic approximation N88-12844
Dynamics of isolated intrathermocline eddy N88-12845
Influence of secondary eddy currents on scattering of admixture in zonal flow N88-12846
OCEAN DATA ACQUISITIONS SYSTEMS
Complex for ocean study from space and hydroacoustic stations N88-12836
A multibody dynamic analysis of the N-ROSS (Navy Remote Ocean Sensing System) satellite rotating flexible reflector using Kane's method [AD-A184452] N88-12860
OCEAN DYNAMICS
Dynamics of isolated intrathermocline eddy N88-12845
Influence of secondary eddy currents on scattering of admixture in zonal flow N88-12846
Studies of thin surface films aim at seeing deep ocean processes N88-12847
OCEAN MODELS
Intensive synoptic eddies and quasigeostrophic approximation N88-12844
Coupled acoustic and ocean thermodynamic model [AD-A184357] N88-12911
OCEAN SURFACE
Studies of thin surface films aim at seeing deep ocean processes N88-12847
Theory of heat and moisture exchange between finely disperse storm-generated spray and turbulent air flow N88-12851
Radial orbit error reduction and sea surface topography determination using satellite altimetry N88-12861
Sea level changes [DE87-014357] N88-12913
OCEANOGRAPHY
USSR report: Earth sciences [JPRS-UES-88-006] N88-12831
Experimental study of turbulent diffusion parameters in ocean N88-12840
Effects of rainfall on the seasonal thermocline [AD-A184432] N88-12912
ON-LINE SYSTEMS
Towards automated consulting: Design feedback from the performance of online documentation [DE87-012243] N88-13062
ONBOARD EQUIPMENT
An assessment of clinical chemical sensing technology for potential use in space station health maintenance facility [NASA-CR-172013] N88-12926
OPACITY
Evidence for an additional source of opacity during the impulsive phase of stellar flares N88-13133
OPERATORS (MATHEMATICS)
On operator splitting for unsteady boundary value problems [AD-A184281] N88-12981
OPERATORS (PERSONNEL)
Input devices for tasks using interactive video [PB87-220018] N88-12664
OPTICAL COMMUNICATION
Frequency doubling conversion efficiencies for deep space optical communications N88-12691
The atmosphere of Mars and optical communications N88-12692
A near-earth optical communications terminal with a corevolving planetary sun shield N88-12693
OPTICAL DISKS
Storing photomicrographs on optical laser disks [DE87-013747] N88-12785
OPTICAL EQUIPMENT
Storing photomicrographs on optical laser disks [DE87-013747] N88-12785
Development of optical modulators for measurements of solar magnetic fields [NASA-TM-100315] N88-13016
OPTICAL MEASUREMENT
Lidar-radiometric method for determining liquid-water content of cirrus clouds N88-12854
OPTICAL MEASURING INSTRUMENTS
Optical instrumentation and study of gas-solid suspension flows [DE88-000147] N88-12744
OPTICAL PATHS
All-optical beam control by forced Rayleigh scattering [AD-A184315] N88-13018
OPTICAL PROPERTIES
Advances in inherently conducting polymers [DE88-000501] N88-12610
Conducting hybrid polymeric systems [DE88-000527] N88-12611
Measurement of cirrus cloud optical properties by high spectral resolution lidar N88-12906
Characterization of thin layers for optics [PB87-217949] N88-13017
OPTICAL RADAR
Review of inversion techniques for spaceborne lidar systems [AD-A184164] N88-12772
Multiwave laser soundings of atmospheric aerosol: Experimental research (review) N88-12852
Lidar-radiometric method for determining liquid-water content of cirrus clouds N88-12854
Measurement of cirrus cloud optical properties by high spectral resolution lidar N88-12906
OPTIMAL CONTROL
Local-optimal control in systems with delay N88-12627

OPTIMIZATION
Reduced complexity structural modeling for automated airframe synthesis
[NASA-CR-177440] N88-12453
New feedback design methodologies for large space structures: A multi-criterion optimization approach N88-12535
Performance optimization of electronic networks in the frequency domain
[PB87-123873] N88-12720
Optimization of explicit time-stepping algorithms and Stream-Function-Coordinate (SFC) concept for fluid dynamics problems N88-12762
Optimization of dilatometer test procedures
[DE87-014998] N88-12769
Parallel superconvergent multigrid
[DE87-013153] N88-12960
Investigation, development and application of optimal output feedback theory. Vol. 4: Measures of eigenvalue/eigenvector sensitivity to system parameters and unmodeled dynamics
[NASA-CR-4108] N88-12969
An exact penalization viewpoint of constrained optimization
[DE88-001477] N88-12995

ORBIT CALCULATION
A demonstration of high precision GPS orbit determination for geodetic applications N88-12680

ORBITAL MANEUVERS
Study of Plasma Motor Generator (PMG) tether system for orbit reboost
[NASA-CR-172015] N88-12501

ORBITAL MECHANICS
Radial orbit error reduction and sea surface topography determination using satellite altimetry N88-12861

ORBITAL POSITION ESTIMATION
Precise near-earth navigation with GPS: A survey of techniques N88-12682
Short baseline phase delay interferometry N88-12683

ORBITAL SERVICING
Space station resistojet system requirements and interface definition study
[NASA-CR-180832] N88-12541

ORGANIC LITHIUM COMPOUNDS
Tetrahedral carbon and interstitial electrons in Li cluster: CLi4 and (LiCH3)4
[AD-A184277] N88-13055

ORGANIC MATERIALS
Proton abstraction as a route to conductive polymers
[AD-A184019] N88-12612

ORGANIZATIONS
National Center for Atmospheric Research
[PB87-226391] N88-12901
Source header list. Volume 1: A through K
[AD-A184000] N88-13086

ORION NEBULA
The Einstein survey of the young stars in the Orion Nebula N88-13182
The velocity structure and turbulence at the center of the Orion Nebula N88-13201

ORTHOTROPIC PLATES
Spatial strength variation and statistical size effect of laminated orthotropic composite materials N88-12646

OSCILLATIONS
Excitation of natural oscillations of a boundary layer by an external acoustic field N88-12634
Dynamics of reverse flows at pump inlet N88-12636
On the interannual variability of South American climate and the Southern Oscillation N88-12905
Oscillation theory for linear second-order differential systems
[DE87-011393] N88-12983
Boundary effects on the drag of an oscillating sphere: Applications to the magnetic sphere rheometer. Attenuation and dispersion of acoustic waves in nematic liquid crystals N88-13007
The dynamics of solar magnetic flux tubes subjected to resonant foot point shaking N88-13118

OSCILLATORS
Measurement and analysis of cryogenic sapphire dielectric resonators and DROs N88-12666
The 8.4-GHz low-noise maser pump source assembly N88-12705
An analytical and experimental study of injection-locked two-port oscillators
[NASA-TM-100119] N88-12727
Spectral evolution equation for the sideband instability in a free-electron laser oscillator
[DE88-000510] N88-12771

OUTLIERS (STATISTICS)
Robust statistical methods for automated outlier detection N88-12681

OUTPUT
Output power enhancement of AC Raman free-electron laser
[DE88-000503] N88-12786

OXIDATION
The effect of organic inhibitors on the atmospheric corrosion and solderability of copper
[DE88-000261] N88-12565

OXIDATION RESISTANCE
Research and development on high strength ceramic heaters discussed N88-12508

OXYGEN
Inerting and atmospheres N88-12524
Fire-related medical science N88-12525
Ignition and combustion of metals in oxygen N88-12530
High efficiency generation of 130-nm radiation from sum-frequency mixing in Hg
[DE87-013714] N88-12674

OXYGEN ISOTOPES
The atomic weight and isotopic composition of oxygen and their variation in nature
[DE87-014397] N88-12558

P

P WAVES
Multichannel deconvolution of P waves at seismic arrays and three component stations
[AD-A184450] N88-12888

PACIFIC OCEAN
On the interannual variability of South American climate and the Southern Oscillation N88-12905
Interactions between the Asian monsoons, the tropical Pacific and the southern hemisphere extratropics N88-12907

PAIR PRODUCTION
Single leptons from heavy quark production
[DE87-014917] N88-13009

PALEOMAGNETISM
Statistics of the geomagnetic secular variation for the past 5Ma
[NASA-CR-181558] N88-12890

PALLADIUM
Characterization of catalysts with metal-support effects and of the species adsorbed on their surfaces
[DE87-014636] N88-12564

PANELS
Fabrication and testing of fire resistant graphite composite panels
[NASA-CR-177397] N88-12472

PAPERS
FY 1985 scientific and technical reports, articles, papers and presentations
[NASA-TM-86521] N88-13083

PARABOLIC ANTENNAS
New main reflector, subreflector and dual chamber concepts for compact range applications
[NASA-CR-181506] N88-12498

PARABOLIC FLIGHT
Access to microgravity: A technical description of the NAE T-33 microgravity facility
[NAE-AN-47] N88-12518

PARABOLIC REFLECTORS
New main reflector, subreflector and dual chamber concepts for compact range applications
[NASA-CR-181506] N88-12498

PARACHUTE FABRICS
Parachute materials
[DE87-014845] N88-12550

PARACHUTES
Developmental airdrop testing techniques and devices
[AGARD-AG-300-VOL-6] N88-12481
Parachute materials
[DE87-014845] N88-12550

PARALLEL FLOW
Some asymptotic modes of transonic vortex flow N88-12632

PARALLEL PROCESSING (COMPUTERS)
Programmable real-time digital video image processing
[PB87-104162] N88-12661
Center for Supercomputing Research and Development (CEDAR)
[DE88-000807] N88-12930
Principles for problem aggregation and assignment in medium scale multiprocessors
[NASA-CR-178379] N88-12935
A tight upper bound for the speed-up of parallel best-first branch-and-bound algorithms
[AD-A184248] N88-12939
Methods for design and evaluation of integrated hardware/software systems for concurrent computation
[NASA-CR-181522] N88-12953
A review and analysis of Fortran 8x
[DE88-001320] N88-12955
QR factorization of a dense matrix on a shared-memory multiprocessor
[DE88-001506] N88-12956
Parallel superconvergent multigrid
[DE87-013153] N88-12960
An approach to implementing state space searches on heterogeneous systems of multiprocessors
[DE88-001321] N88-12967

PARAMETERIZATION
Simulation studies for surfaces and materials strength
[NASA-CR-181535] N88-12557
Local-optimal control in systems with delay N88-12627
A review of parameterizations of microphysical processes in clouds for application in models of regional atmospheric deposition
[DE88-000451] N88-12909
Estimation of a multivariate continuous variable panel model
[AD-A184472] N88-12982

PARTIAL DIFFERENTIAL EQUATIONS
Optimization of explicit time-stepping algorithms and Stream-Function-Coordinate (SFC) concept for fluid dynamics problems N88-12762
A comparison of adaptive refinement techniques for elliptic problems
[DE88-000805] N88-12967
Two classes of preconditioners computed using block matrix factorization techniques
[DE88-001313] N88-12968

PARTIAL PRESSURE
Inerting and atmospheres N88-12524

PARTICLE ACCELERATION
Particle injection and cosmic ray acceleration at collisionless parallel shocks
[DE88-000507] N88-12665
Prompt simultaneous acceleration of protons and electrons to relativistic energies by shock waves in solar flares
[IPPJ-851] N88-13037

PARTICLE ACCELERATORS
The role of basic research in society
[DE88-000459] N88-13090

PARTICLE EMISSION
Single leptons from heavy quark production
[DE87-014917] N88-13009

PARTICLE ENERGY
Cosmic-ray nuclear event with an anomalously strong concentration of energy and particles in the central region
[DE87-703376] N88-13213

PARTICLE INTERACTIONS
Future directions in interplays between particle and nuclear physics: Summary session
[DE87-011791] N88-13013

PARTICLE SIZE DISTRIBUTION
Experimental and theoretical study of condensation in multicomponent mixtures
[DE88-000697] N88-12583
Experiments on density-loaded non-Newtonian slurries in laminar and turbulent pipe flows
[DE88-000719] N88-12748

PARTICLE TRACKS
Some new ideas in liquid detectors
[DE88-000732] N88-12768

PARTICLES
Activities at government research laboratories reported N88-12503
Use of a thermodynamic analog for pneumatic transport in horizontal pipes
[AD-A184076] N88-12740
Plume mechanics and aerosol growth processes
[AD-A184487] N88-12742
Experimental and analytic studies of the triggered lightning environment of the F106B
[NASA-CR-4104] N88-12897

PARTITIONS (MATHEMATICS)
A multiple-time-scale turbulence model based on variable partitioning of turbulent kinetic energy spectrum
[NASA-CR-179222] N88-12754

PATENT POLICY
Thixotropic surface composition for phenolaldehyde resin laminates
[GB-PATENT-2-180-251-A] N88-12545
Thermoplastic elastomer compositions — cable jackets
[EP-PATENT-0-204-453-A1] N88-12593
Detection of defects on structures
[EP-PATENT-0-210-794-A2] N88-12807

PATHS
Two dimensional path planning with obstacles and shadows
[AD-A184075] N88-12474

PATTERN RECOGNITION
On the recognition of curved objects
[AD-A184441] N88-12945

An approach to object recognition: Aligning pictorial descriptions
[AD-A184462] N88-12972
Intelligent signal analysis and recognition
[NASA-CR-181531] N88-13084
PAVEMENTS
Open-graded bases for airfield pavements
[AD-A184461] N88-12500
PEEK
Molecular composites: Processing, post-treatment and mechanics
[AD-A184458] N88-12547
PENALTY FUNCTION
An exact penalization viewpoint of constrained optimization
[DE88-001477] N88-12995
PENUMBRAS
Exploiting the IR: Solar and stellar spectroscopy in the IR N88-13102
PERFLUORO COMPOUNDS
Surface catalytic degradation study of two linear perfluoropolyalkylethers at 345 C
[NASA-TP-2774] N88-12543
PERFORMANCE PREDICTION
Numerical prediction of propeller performance by vortex lattice method
[UTIAS-TN-265] N88-12489
Applications of the hybrid automated reliability predictor
[NASA-TP-2760] N88-12928
PERFORMANCE TESTS
The aerodynamics of supersonic parachutes
[DE87-014846] N88-12484
Performance and combustion characteristics of direct-injection stratified-charge rotary engines
[NASA-TM-100134] N88-12490
Programmable Logic Arrays (PLA's) design for testability
[PB87-102935] N88-12718
Long-range pulselength scaling of 351nm laser damage thresholds
[DE87-014754] N88-12777
Calculation of the tribological properties of surfaces by semi-empirical methods
[AD-A184283] N88-12791
Performance analysis of solar thermal power systems
[DE88-000583] N88-12874
Performance monitoring and analysis of electric van fleet vehicles
[DE88-900066] N88-13091
PERIOD DOUBLING
Fully developed turbulence via Feigenbaum's period-doubling bifurcations
[DE88-000242] N88-12739
PERIODIC VARIATIONS
On the interannual variability of South American climate and the Southern Oscillation N88-12905
PERMEABILITY
Novel macrocyclic carriers for proton-coupled liquid membrane transport
[DE88-000636] N88-12560
A study of mechanisms of hydrogen diffusion in separation devices
[DE88-000328] N88-12584
PERMITTIVITY
Automated microwave dielectric constant measurement
[AD-A184182] N88-12667
PERSONNEL
On computing environments in data analysis
[DE88-000078] N88-12961
PERTURBATION THEORY
Analytical studies of axially symmetric motion of an incompressible viscous fluid between two concentric rotating spheres N88-12757
The free electron laser sideband instability reconsidered
[AD-A184289] N88-12773
Vibration and parametric excitation in rotating asymmetric circular plates N88-12823
Model of solar-wind magnetosphere coupling N88-13211
PHARMACOLOGY
JPRS report: Science and technology. USSR: Life sciences
[JPRS-ULS-87-009] N88-12915
PHASE CHANGE MATERIALS
Performance analysis of advanced spacecraft TPS
[NASA-CR-181532] N88-12484
A study of the optimal transition temperatue of PCM (Phase Change Material) wallboard for solar energy storage
[DE88-001522] N88-12882
PHASE COHERENCE
Optimized tracking of RF carriers with phase noise, including Pioneer 10 results N88-12694
PHASE LOCKED SYSTEMS
Detection of signals by weighted integrate-and-dump filter N88-12696
PHASE MATCHING
Frequency doubling conversion efficiencies for deep space optical communications N88-12691
PHASE SHIFT
Short baseline phase delay interferometry N88-12683
PHASE SHIFT KEYING
Bandwidth efficient block codes for M-ary PSK modulation
[NASA-CR-181543] N88-12712
PHASE TRANSFORMATIONS
Experimental perspectives on heavy electron metals
[DE87-014786] N88-12583
Syntheses of the monoclinic yttria by thermal plasma processing
[DE88-000496] N88-12608
Nonlinear acoustics
[AD-A184271] N88-13004
The Moessbauer effect of SnI4 at high pressure
[DE87-014771] N88-13048
Guest-host interactions in thermotropic and lyotropic liquid crystals
[AD-A184402] N88-13057
Radiation induced collapse of the crystalline structure
[DE87-014407] N88-13064
PHASED ARRAYS
Multichannel deconvolution of P waves at seismic arrays and three component stations
[AD-A184450] N88-12688
PHENOLIC RESINS
Thixotropic surface compoeition for phenolaldehyde resin laminates
[GB-PATENT-2-180-251-A] N88-12545
PHOSPHAZENE
Effect of sidechain length and crosslinking on ionic conductivity in polyphosphazene solid electrolytes
[AD-A184419] N88-13058
PHOSPHORS
Calibration of a laser-pumped, thermographic phosphor remote thermometry system
[DE88-000452] N88-12781
Performance and preference with various VDT (Video Display Terminal) phosphors
[AD-A184065] N88-12925
PHOTOCHEMICAL REACTIONS
Proceedings of the Eleventh DOE Solar Photochemistry Research Conference
[DE88-000678] N88-12883
PHOTOELECTRIC EMISSION
Atomic and electronic structure of surfaces and chemisorbed layers
[DE87-014987] N88-13065
PHOTOGRAMMETRY
Accuracy potential of non-metric cameras in close-range photogrammetry N88-12662
PHOTOGRAPHY
Tracking through turbulence at the Tonopah Test Range
[DE88-001448] N88-12766
PHOTOMETRY
Spectral analysis of APT RS CVn binary light curves N88-13122
Starspots on the short-period RS CVn system SV Cam: 45 years of activity N88-13123
The short-period RS CVn stars: Starspots and fundamental properties N88-13124
Doppler snapshots N88-13125
Titanium oxide absorption and spot sizes in II Peg, HR 1099 and UX Ari N88-13126
Stellar cycle variability of solar-like stars: A sneak preview N88-13136
Contemporaneous B,V,R,I photometry and H alpha spectroscopy of YY Gem N88-13155
PHOTOMICROGRAPHS
Storing photomicrographs on optical laser disks
[DE87-013747] N88-12785
PHOTON BEAMS
National Synchrotron Light Source users manual: Guide to the VUV and X-ray beam lines
[DE88-001464] N88-13020
PHOTONS
Gamma ray lines from novae N88-13214
PHOTOSPHERE
Empirical relations between photospheric magnetic fields and atmospheric radiative losses for cool dwarf stars N88-13145
An analysis of the photospheric line profiles in F, G, and K supergiants N88-13157
New results from high angular resolution observations of alpha Ori N88-13161
Emission features in IRAS LRS spectra of MS, S and CS stars N88-13163
IUE observations of the hybrid K3 II star Iota Aurigae and constraints on the outer atmospheric structure N88-13171
PHOTOVOLTAIC CELLS
Light funnel concentrator panel for solar power
[NASA-CR-179223] N88-12870
Design description report for a photovoltaic power system for a remote satellite earth terminal
[NASA-CR-179586] N88-12875
Radiation performance of AlGaAs concentrator cells and expected performance of cascade structures
[NASA-TM-100145] N88-12878
PHYSIOLOGICAL EFFECTS
Change in functional activity of cortical brain structures and their blood supply in alert rabbits in response to rocking N88-12916
Human respiratory responses during high performance flight
[AGARD-AG-312] N88-12923
PHYSIOLOGY
JPRS report: Science and technology. USSR: Life sciences
[JPRS-ULS-87-009] N88-12915
PILOT PERFORMANCE
Effect of motion cues during complex curved approach and landing tasks: A piloted simulation study
[NASA-TP-2773] N88-12480
Some data processing requirements for precision Nap-Of-the-Earth (NOE) guidance and control of rotorcraft
[NASA-CR-177453] N88-12493
CGI delay compensation
[NASA-TM-86703] N88-12932
PIPE FLOW
Carbon dioxide treatment for scale removal and control in potable water systems
[AD-A184346] N88-12556
Dynamics of reverse flows at pump inlet N88-12636
Use of a thermodynamic analog for pneumatic transport in horizontal pipes
[AD-A184076] N88-12740
Experiments on densely-loaded non-Newtonian slurries in laminar and turbulent pipe flows
[DE88-000719] N88-12748
PIPELINING (COMPUTERS)
On the VLSI design of a pipeline Reed-Solomon decoder using systolic arrays N88-12700
PIPES (TUBES)
Dynamics of reverse flows at pump inlet N88-12636
Pipe and bend erosion by pneumatic transport of solids at high temperature
[DE88-001345] N88-12658
Pulsed eddy-current inspection of thin-walled stainless steel tubing
[DE88-001492] N88-12830
PISTONS
Ideal-viscoplastic extrusion model with application to deforming pistons in light-gas guns
[UTIAS-TN-266] N88-12657
PITCH (INCLINATION)
Measurement of velocity and vorticity fields in the wake of an airfoil in periodic pitching motion
[NASA-TP-2780] N88-13002
PLANAR STRUCTURES
A study of scattering from E-plane circuit elements
[AD-A184473] N88-12673
An adaptive subdivision method with crack prevention for rendering beta-spline objects
[AD-A184249] N88-12940
PLANE WAVES
New main reflector, subreflector and dual chamber concepts for compact range applications
[NASA-CR-181506] N88-12496
Pulse-mode expansions and refractive indices in plane-wave propagation
[DE88-001328] N88-12714
Dispersion equation for plane capillary-gravity wave on free surface of viscous incompressible fluid N88-12842
Boundary effects on the drag of an oscillating sphere: Applications to the magnetic sphere rheometer. Attenuation and dispersion of acoustic waves in nematic liquid crystals N88-13007
PLANETARY BOUNDARY LAYER
Effects of rainfall on the seasonal thermocline
[AD-A184432] N88-12912
PLANETARY IONOSPHERES
Relativistic electron precipitations in a pulsating aurora N88-12894
PLANETARY NEBULAE
Winds and shells around low-mass supergiants N88-13164
PLANETARY SURFACES
Small reactor power systems for manned planetary surface bases
[NASA-TM-100223] N88-13209

PLANETARY WAVES
Dynamics of isolated intrathermocline eddy
N88-12845
PLANFORMS
Planform effects on the supersonic aerodynamics of multibody configurations
[NASA-TP-2762] N88-12454
PLASMA ACCELERATION
Particle injection and cosmic ray acceleration at collisionless parallel shocks
[DE88-000507] N88-12665
PLASMA CONTROL
The role of stellarators in the advanced toroidal program
[DE87-014815] N88-13025
Data base on the high heat flux behaviour of metals and carbon materials for plasma facing components: Experiments at the 10 MW neutral beam injection test stand of the IPP Nagoya
[IPPJ-AM-53] N88-13031
Confinement time of electrons and H(-)/D(-) ions in the Uramoto type sheet plasma
[IPPJ-852] N88-13032
Monte Carlo analysis of neoclassical transport for a compact helical system
[IPPJ-850] N88-13033
MHD stability and control for mirror machines
N88-13038
PLASMA CURRENTS
Magnetic fluctuation behaviour of current termination in reversed field pinch
[IPPJ-849] N88-13034
PLASMA DIAGNOSTICS
Review of X-ray spectroscopy from laser-produced plasmas
[DE88-000755] N88-13043
PLASMA ENGINES
Study of Plasma Motor Generator (PMG) tether system for orbit reboost
[NASA-CR-172015] N88-12501
PLASMA FLUX MEASUREMENT
MHD energy fluxes for late type dwarfs N88-13148
PLASMA GENERATORS
Analysis of a series of electromagnetic launcher firings
[AR-005-131] N88-12516
ICRF launcher studies
[DE88-001710] N88-13046
PLASMA HEATING
Negative ion beams for heating and current-drive in NET
[AD-A184390] N88-13012
PLASMA INTERACTIONS
Coherent emission from relativistic beam-plasma interactions N88-13036
PLASMA PHYSICS
Theoretical plasma physics
[DE88-001475] N88-13029
PLASMA PINCH
Numerical simulation of the Reversed Field Pinch
[AD-A184353] N88-13023
PLASMA POTENTIALS
Confinement time of electrons and H(-)/D(-) ions in the Uramoto type sheet plasma
[IPPJ-852] N88-13032
PLASMA PROPULSION
Study of Plasma Motor Generator (PMG) tether system for orbit reboost
[NASA-CR-172015] N88-12501
Plasma thruster development
[AD-A184173] N88-12536
Interplanetary propulsion using inertial fusion
[NASA-TM-89861] N88-12540
PLASMA TURBULENCE
Theoretical plasma physics
[DE88-001475] N88-13029
Observations of turbulence and fluctuations in the solar wind N88-13212
PLASMA WAVES
Output power enhancement of AC Raman free-electron laser
[DE88-000503] N88-12788
Ballooning modes or Fourier modes in a toroidal plasma?
[AD-A184299] N88-13022
PLASMAS (PHYSICS)
Confinement time of electrons and H(-)/D(-) ions in the Uramoto type sheet plasma
[IPPJ-852] N88-13032
Monte Carlo analysis of neoclassical transport for a compact helical system
[IPPJ-850] N88-13033
Proceedings of the Japan-US Workshop P-92 on Plasma Material Interaction/High Heat Flux Data Needs for the Next Step Ignition and Steady State Devices
[DE87-013568] N88-13042
Review of X-ray spectroscopy from laser-produced plasmas
[DE88-000755] N88-13043
PISCES: Plasma-surface interactions and materials research
[DE88-001323] N88-13044
Radio continuum emission from the ionized stellar winds of the cool supergiants in zeta Aurigae-like systems
N88-13160
PLASTIC DEFORMATION
Plastic strain localization between voids in shear deformation fields N88-12648
PLATES
Damping characteristics of a composite-reinforced stainless-steel plate
[DE88-000303] N88-12828
PLATINUM
Compatability of dispersion-strengthened platinum with resistojet propellants
[NASA-TP-2785] N88-12538
Characterization of catalysts with metal-support effects and of the species adsorbed on their surfaces
[DE87-014836] N88-12584
PLUMES
Development and application of computational aerothermodynamics flowfield computer codes
[NASA-CR-181534] N88-12465
Aircraft engine exhaust plume dynamics
[AD-A184238] N88-12488
Plume mechanics and aerosol growth processes
[AD-A184467] N88-12742
PNEUMATIC CONTROL
Space station resistojet system requirements and interface definition study
[NASA-CR-180832] N88-12541
Use of a thermodynamic analog for pneumatic transport in horizontal pipes
[AD-A184076] N88-12740
PNEUMATIC EQUIPMENT
A three-barrel repeating pneumatic pellet injector for plasma fueling of the Joint European Torus
[DE88-000330] N88-13026
PNEUMATICS
Pipe and bend erosion by pneumatic transport of solids at high temperature
[DE88-001345] N88-12658
POINTING CONTROL SYSTEMS
A new state space model for the NASA/JPL 70-meter antenna servo controls N88-12702
A modern control theory based algorithm for control of the NASA/JPL 70-meter antenna axis servos
N88-12706
POISSON EQUATION
The finite element method for electronic structure
[DE88-001708] N88-12989
POLAR REGIONS
USSR report: Earth sciences
[JPRS-UES-88-006] N88-12831
Huurre expedition to the North Pole in 1984
[PB87-220935] N88-12858
Cloud cover determination in polar regions from satellite imagery
[NASA-CR-181544] N88-12908
POLARIZATION
Broadband linear polarization and chromospheric CaII H and K line emission in late-type main sequence stars
N88-13140
POLARIZATION (WAVES)
Development of optical modulators for measurements of solar magnetic fields
[NASA-TM-100315] N88-13016
POLICIES
The attitudes of science policy, environmental, and utility leaders on US energy issues and fusion
[DE88-000784] N88-13041
POLITICS
Technology transfer to China
[PB87-223418] N88-13087
POLLUTION CONTROL
Emerging environmental constraints on the use of gasoline and diesel fuel and tradeoffs associated with the use of alternative fuels
[DE87-011504] N88-12614
POLLUTION MONITORING
Influence of surfactants on damping of gravity-capillary waves. 1: Frequency dependence N88-12843
POLYESTERS
Structure of thermotropic polyesters with large substituents
[AD-A184066] N88-12595
POLYETHYLENES
Polymer composition --- cable insulation
[EP-PATENT-0-199-444-A1] N88-12594
POLYMER CHEMISTRY
Simultaneous TG/DSC (thermogravimetry/Differential Scanning Calorimetry) and TG/MS (thermogravimetry/Mass Spectrometry) analyses of polymeric and energetic materials
[DE88-000727] N88-12561
Effect of sidechain length and crosslinking on ionic conductivity in polyphosphazene solid electrolytes
[AD-A184419] N88-13058
POLYMERIC FILMS
Molecular composites: Processing, post-treatment and mechanics
[AD-A184458] N88-12547
POLYMERIZATION
Conductive polymers via reactive oligomer
[AD-A184270] N88-12597
Conducting hybrid polymeric systems
[DE88-000527] N88-12611
Proton abstraction as a route to conductive polymers
[AD-A184019] N88-12612
POLYNOMIALS
A simplified procedure for correcting both errors and erasures of a Reed-Solomon code using the Euclidean algorithm N88-12998
On color polynomials of Fibonacci graphs
[AD-A184133] N88-12996
POPULATION THEORY
A tight upper bound for the speed-up of parallel best-first branch-and-bound algorithms
[AD-A184246] N88-12939
An urn model for the multi-sample capture/recapture sequential tagging process
[AD-A184470] N88-12998
A comparison of the basket method and the stratified random sampling for contract change order negotiations
[AD-A184170] N88-13080
POROUS PLATES
Fatigue failure of thin porous strips N88-12640
PORTABLE EQUIPMENT
A portable hypercube simulator
[DE87-013369] N88-12947
PORTS (OPENINGS)
An analytical and experimental study of injection-locked two-port oscillators
[NASA-TM-100119] N88-12727
POSITION (LOCATION)
GPS vertical axis performance enhancement for helicopter precision landing approach
[NASA-CR-177443] N88-12477
Effect of permissible variations of center-of-gravity locations of cargo airplane on its mass N88-12625
POSITION INDICATORS
Effects of combining vertical and horizontal information into a primary flight display
[NASA-TP-2783] N88-12487
POTABLE WATER
Carbon dioxide treatment for scale removal and control in potable water systems
[AD-A184346] N88-12556
POTASSIUM
K-CO on transition metals: A local ionic interaction
[AD-A184342] N88-13056
POTENTIAL ENERGY
Simulation studies for surfaces and materials strength
[NASA-CR-181535] N88-12557
POTENTIAL FLOW
A full potential flow analysis with realistic wake influence for helicopter rotor airload prediction
[NASA-CR-4007] N88-12452
Calculation of aerodynamic characteristics of three-dimensional finite span wings in potential incompressible flow N88-12631
POWDER METALLURGY
Durability of powdered aluminum structures
N88-12655
POWDERED ALUMINUM
Durability of powdered aluminum structures
N88-12655
POWER LINES
Thermoplastic elastomer compositions --- cable jackets
[EP-PATENT-0-204-453-A1] N88-12593
POWER SPECTRA
Multichannel deconvolution of P waves at seismic arrays and three component stations
[AD-A184450] N88-12888
PRE-MAIN SEQUENCE STARS
Fifth Cambridge Workshop on Cool Stars, Stellar Systems and the Sun N88-13092
Disk accretion during the early stages of stellar evolution N88-13106
Microwave observations of nonthermal phenomena in pre-main sequence stars N88-13107
Pre-main sequence activity: How far is magnetism involved N88-13179

Chromospheric variability mechanisms affecting pre-main sequence stars N88-13180
PRECIPITATES
The accommodation of precipitate plates modelled as a tensile test
[DE88-000207] N88-12814
PRECIPITATION (CHEMISTRY)
Influence of creep on the precipitate structure under conditions of long-term creep. 4: Experiments on 10 CrMo 9 10 steel
[BLL-CE-TRANS-8256-(9022.09)] N88-12589
PRECIPITATION (METEOROLOGY)
Computer modeling aids studies of precipitation formation N88-12832
New precipitation map of world ocean N88-12834
Measurements of vapor flux, liquid water contents, precipitation rates and riming in a Utah mountain cloud system
[PB87-224945] N88-12900
PRECIPITATION HARDENING
Compatability of dispersion-strengthened platinum with resistojet propellants
[NASA-TP-2765] N88-12538
PRECISION
GPS vertical axis performance enhancement for helicopter precision landing approach
[NASA-CR-177443] N88-12477
Interactions between science and precision engineering
[DE87-010873] N88-12643
A demonstration of high precision GPS orbit determination for geodetic applications N88-12680
Precise near-earth navigation with GPS: A survey of techniques N88-12682
Short baseline phase delay interferometry N88-12683
PREDICTION ANALYSIS TECHNIQUES
Numerical prediction of propeller performance by vortex lattice method
[UTIAS-TN-265] N88-12489
A study of two-phase flow in a reduced gravity environment
[NASA-CR-172035] N88-12617
Creep life prediction based on stochastic model of microstructurally short crack growth
[NASA-TM-100245] N88-12825
Results of the 1986 NASA/FAA/DFVLR main rotor test entry in the German-Dutch wind tunnel (DNW)
[NASA-TM-100507] N88-13003
PREDICTIONS
Vibration and parametric excitation in rotating asymmetric circular plates N88-12823
Reevaluating the worst-case radiation response of MOS transistors
[DE87-014157] N88-13059
The velocity structure and turbulence at the center of the Orion Nebula N88-13201
PREPOLYMERS
Conductive polymers via reactive oligomer
[AD-A184270] N88-12597
PRESSURE
Studies of pressure-velocity coupling schemes for analysis of incompressible and compressible flows
[NASA-CR-181526] N88-12748
PRESSURE DEPENDENCE
Ignition and combustion of metals in oxygen N88-12530
Retention processes in supercritical fluid chromatography
[DE88-000079] N88-12559
Experimental perspectives on heavy electron metals
[DE87-014766] N88-12583
PRESSURE DISTRIBUTION
An experimental investigation of unsteadiness in swept shock wave/turbulent boundary layer interactions N88-12760
PRESSURE EFFECTS
The Moessbauer effect of SnI4 at high pressure
[DE87-014771] N88-13048
PRESSURE GRADIENTS
NCSU code: Validation and extension on NAL's UNIVAC 1100/60 system
[PD-FM-8716] N88-12931
PRESSURE REDUCTION
A study of two-phase flow in a reduced gravity environment
[NASA-CR-172035] N88-12617
PREVENTION
An adaptive subdivision method with crack prevention for rendering beta-spline objects
[AD-A184249] N88-12940
PRINTED CIRCUITS
The 8.4-GHz low-noise maser pump source assembly N88-12705
PRISMS
Optical alignment of Centaur's inertial guidance system
[NASA-TM-88844] N88-12515
PROBABILITY DISTRIBUTION FUNCTIONS
Propagation of random initial conditions in time N88-12993
An urn model for the multi-sample capture/recapture sequential tagging process
[AD-A184470] N88-12998
PROBABILITY THEORY
More on the decoder error probability for Reed-Solomon codes N88-12699
Foundations of O-theory 2: Measurements and relation to fuzzy set theory
[DE88-000013] N88-12986
Lower bounds on bearing accuracy for closely spaced sources
[AD-A184258] N88-12997
Subjective probability, combination of expert opinion and probabilistic approaches to information retrieval N88-13085
PROBLEM SOLVING
Design of digital filters for electronic instrumentation
[PB87-100418] N88-12716
Principles for problem aggregation and assignment in medium scale multiprocessors
[NASA-CR-178379] N88-12935
A model of functional knowledge and insight
[AD-A184113] N88-12975
Back-of-the-envelope problems
[AD-A184105] N88-12980
PROCEDURES
Implementation of a new shock testing procedure using nonstationary random excitation
[DE87-014643] N88-12827
PROGRAM VERIFICATION (COMPUTERS)
Experimental aerothermodynamic research of hypersonic aircraft
[NASA-CR-181533] N88-12483
Digital-flight-control-system software written in automated-engineering-design language: A user's guide of verification and validation tools
[NASA-TM-88313] N88-12494
SDVS (State Delta Verification System) 5 users' manual
[AD-A184339] N88-12943
Aircraft interior noise reduction by alternate resonance tuning
[NASA-CR-181530] N88-13005
PROGRAMMERS
On computing environments in data analysis
[DE88-000078] N88-12961
PROGRAMMING LANGUAGES
A network definition and solution of simulation problems
[DE88-000675] N88-12962
PROGRESS
Progress in the development of niobium alloyed high speed steel
[DE87-703549] N88-12576
PROJECT SETI
Intelligent signal analysis and recognition
[NASA-CR-181531] N88-13084
PROJECTILES
The LLNL 150-mm equation-of-state gun system
[DE88-000423] N88-12519
PROPAGATION
Propagation of random initial conditions in time N88-12993
PROPELLANT BINDERS
High pressure strand burn rate tests of polyvinylnitrate/nitramine propellants
[AD-A184178] N88-12615
PROPELLANT COMBUSTION
High pressure strand burn rate tests of polyvinylnitrate/nitramine propellants
[AD-A184178] N88-12615
PROPELLANT STORAGE
DOE explosives safety manual
[DE88-000831] N88-12616
PROPELLER BLADES
Numerical prediction of propeller performance by vortex lattice method
[UTIAS-TN-265] N88-12489
PROPORTIONAL LIMIT
Carbon fiber reinforced glass matrix composites for space based applications
[AD-A184355] N88-12548
PROTECTIVE COATINGS
Carbon-fiber reinforced aluminum N88-12507
Effect of long-term thermal aging on coated Celion/LARC-160 composites
[NASA-TM-100495] N88-12544
Ceramic technology for advanced heat engines project
[DE88-001520] N88-12605
Tribological properties of rf-sputtered MoS2 coatings
[DE88-000266] N88-12802
PROTOCOL (COMPUTERS)
An evaluation plan of bus architectures and protocols using the NASA Ames intelligent redundant actuation system
[NASA-CR-177458] N88-12482
PROTON BEAMS
Performance of GaAs and silicon concentrator cells under 37 MeV proton irradiation
[NASA-TM-100144] N88-12677
PROTONS
Proton abstraction as a route to conductive polymers
[AD-A184019] N88-12612
Prompt simultaneous acceleration of protons and electrons to relativistic energies by shock waves in solar flares
[IPPJ-851] N88-13037
PROTOTYPES
Renewed interest in airships for industry use discussed N88-12628
Light funnel concentrator panel for solar power
[NASA-CR-179223] N88-12870
PSEUDOMONAS
Study of certain biological characteristics of bacteria during the French-Soviet CYTOS-2 space experiment N88-12917
PSYCHOLOGY
The attitudes of science policy, environmental, and utility leaders on US energy issues and fusion
[DE88-000784] N88-13041
PUBLIC HEALTH
JPRS report: Science and technology. USSR: Life sciences
[JPRS-ULS-87-009] N88-12915
PULSE DURATION
Long-range pulselength scaling of 351nm laser damage thresholds
[DE87-014754] N88-12777
PULSED LASERS
The generation and suppression of synchrotron sidebands
[DE88-000532] N88-12767
All-optical beam control by forced Rayleigh scattering
[AD-A184315] N88-13018
PULSES
Alternating current circuit theory and pulsed NMR (Nuclear Magnetic Resonance)
[DE88-000641] N88-12732
High-power RF-pulsed modulators for the Los Alamos free-electron laser
[DE88-000514] N88-12775
Increased gain of channel intensifier tubes by pulsed biasing
[DE88-000512] N88-13019
PUMPS
Dynamics of reverse flows at pump inlet N88-12636
The 8.4-GHz low-noise maser pump source assembly N88-12705
Modular pump limiter systems for large tokamaks
[DE88-001487] N88-13045
PURITY
Conductive polymers via reactive oligomer
[AD-A184270] N88-12597
PYROLYTIC GRAPHITE
Data base on the high heat flux behaviour of metals and carbon materials for plasma facing components: Experiments at the 10 MW neutral beam injection test stand of the IPP Nagoya
[IPPJ-AM-53] N88-13031
PYROMETALLURGY
The nature of metallurgical reactions in underwater welding
[AD-A184464] N88-12568

Q

QUADRATURES
A quadrature formula for a double-pole singular integral
[PD-FM-8725] N88-12990
QUALITATIVE ANALYSIS
Solid state C-13 NMR characterization of textiles: Qualitative and quantitative analysis
[AD-A184349] N88-12598
A low volume insert for solid state magic angle spinning NMR of small samples
[AD-A184359] N88-12601
QUALITY CONTROL
Software maintenance in scientific and engineering environments: An introduction and guide
[NASA-CR-177409] N88-12954

QUANTITATIVE ANALYSIS
Studies on estimation of nickel in zinc base die casting by D.C. polarography
[PD-MT-8729] N88-12588
Solid state C-13 NMR characterization of textiles: Qualitative and quantitative analysis
[AD-A184349] N88-12598
QUANTUM ELECTRONICS
Numerical studies of the dual HEMT/algorithm development and numerical studies of Schrodinger's equation
[AD-A184471] N88-12946
QUANTUM MECHANICS
A study of mechanisms of hydrogen diffusion in separation devices
[DE88-000328] N88-12584
Final (n,l) state-resolved electron capture by multiply charged ions from neutral atoms
[IPPJ-AM-54] N88-13030
QUARKS
Single leptons from heavy quark production
[DE87-014917] N88-13009
QUEUEING THEORY
Heterogeneous multi-trunking queueing systems
[AD-A184255] N88-12668

R

RACE FACTORS
A national model at Howard University demonstrating private sector interrelationships that facilitate research in predominantly Black colleges and universities
[DE88-000160] N88-13089
RADAR
On M-ARY sequential hypotheses testing for the classification of radar signals
[AD-A184094] N88-12666
RADAR SCATTERING
New main reflector, subreflector and dual chamber concepts for compact range applications
[NASA-CR-181506] N88-12498
RADAR TARGETS
New main reflector, subreflector and dual chamber concepts for compact range applications
[NASA-CR-181506] N88-12498
RADIAL FLOW
Continuation finite element analysis of viscoelastic fluids N88-12761
RADIATION DAMAGE
Performance of GaAs and silicon concentrator cells under 37 MeV proton irradiation
[NASA-TM-100144] N88-12877
Radiation performance of AlGaAs concentrator cells and expected performance of cascade structures
[NASA-TM-100145] N88-12878
Reevaluating the worst-case radiation response of MOS transistors
[DE87-014157] N88-13059
RADIATION DETECTORS
Design of source coders and joint source/channel coders for noisy channels
[NASA-CR-181547] N88-12678
Low-cost teleoperator-controlled vehicle for damage assessment and dose measurement
[DE88-000713] N88-12794
RADIATION DISTRIBUTION
Gamma-ray optics of multi-beam Borrmann modes with possible applications to nuclear lasing N88-12784
Statistical distribution of solar radiation (hourly sums): Cumulative frequency curves preparation of a European data set and direction for use
[PB87-107454] N88-12686
RADIATION EFFECTS
Microgravity nucleation and particle coagulation experiments support
[NASA-CR-181540] N88-12618
JPRS report: Science and technology. USSR: Life sciences
[JPRS-ULS-87-009] N88-12915
Radiation induced collapse of the crystalline structure
[DE87-014407] N88-13064
RADIATION MEASUREMENT
Empirical relations between photospheric magnetic fields and atmospheric radiative losses for cool dwarf stars N88-13145
RADIATION SOURCES
Center for X-Ray Optics, 1986
[DE88-000715] N88-12783
RADIATION SPECTRA
Cloud cover determination in polar regions from satellite imagery
[NASA-CR-181544] N88-12908
RADIATIVE HEAT TRANSFER
The effects of minor trace gases on the transfer of thermal infrared radiation through the Earth's atmosphere N88-12693
Heating of stellar chromospheres and coronae: Evidence for non-magnetic basal heating N88-13096
RADIATIVE TRANSFER
Observations and analysis of the photospheric magnetic fields on dwarf G, K and M stars N88-13196
RADIO ANTENNAS
A new state space model for the NASA/JPL 70-meter antenna servo controls N88-12702
Analysis of the ICE combiner for multiple antenna arraying N88-12704
A modern control theory based algorithm for control of the NASA/JPL 70-meter antenna axis servos N88-12706
Power density measurements in the near field of the DSS 13 26-meter antenna N88-12711
RADIO ASTRONOMY
The Telecommunications and Data Acquisition Report
[NASA-CR-181546] N88-12679
Intelligent signal analysis and recognition
[NASA-CR-181531] N88-13084
Nonthermal phenomena in stellar coronae: Evidence from radio observations N88-13096
A re-examination of the corona-wind dividing line: Diagnostics of non-coronal atmospheres N88-13101
EVN (European VLBI network) and MERLIN observations of 5 superluminal radio sources
[PB87-110730] N88-13193
RADIO EMISSION
A VLA survey of dMe flare stars N88-13154
Radio continuum emission from the ionized stellar winds of the cool supergiants in zeta Aurigae-like systems N88-13160
Radio emission from RS CVn binaries: A 5 GHz VLA survey of 93 systems N88-13191
RADIO EQUIPMENT
X-band uplink ground systems development: Part 2 N88-12703
RADIO FREQUENCIES
High-power RF-pulsed modulators for the Los Alamos free-electron laser
[DE88-000514] N88-12775
Tribological properties of rf-sputtered MoS2 coatings
[DE88-000266] N88-12802
RADIO NAVIGATION
The Telecommunications and Data Acquisition Report
[NASA-CR-181546] N88-12679
RADIO RECEIVERS
X-band uplink ground systems development: Part 2 N88-12703
RADIO SIGNALS
Meteor-burst communications: Is this what the Navy needs?
[AD-A184433] N88-12672
RADIO SOURCES (ASTRONOMY)
Microwave observations of nonthermal phenomena in pre-main sequence stars N88-13107
EVN (European VLBI network) and MERLIN observations of 5 superluminal radio sources
[PB87-110730] N88-13193
RADIO STARS
The Parkes radio survey of active chromosphere stars N88-13141
RADIO TRANSMISSION
Meteor-burst communications: Is this what the Navy needs?
[AD-A184433] N88-12672
RADIO TRANSMITTERS
Analysis of the ICE combiner for multiple antenna arraying N88-12704
Power density measurements in the near field of the DSS 13 26-meter antenna N88-12711
RADIO WAVES
General theory of radio propagation through a stratified atmosphere
[PB87-226197] N88-12662
RADIOACTIVE DECAY
Few body hypernuclear systems: Weak decays
[DE87-014920] N88-13010
Nuclear beta decay after Los Houches
[DE87-014921] N88-13011
Influences of the astrophysical environment on nuclear decay rates
[DE88-001461] N88-13208
RADIOMETERS
Lidar-radiometric method for determining liquid-water content of cirrus clouds N88-12854
Radiometric calibration of the Earth observing system's imaging sensors
[NASA-CR-181542] N88-12665
Cloud cover determination in polar regions from satellite imagery
[NASA-CR-181544] N88-12908
RAILGUN ACCELERATORS
Ultimate velocities for induction launchers
[DE87-012360] N88-12513
Thermal analysis of electromagnetic launcher rails
[DE88-000166] N88-12514
Analysis of a series of electromagnetic launcher firings
[AR-005-131] N88-12516
Efficiency aspects of short, low velocity railguns
[AR-004-847] N88-12517
RAIN
On the interannual variability of South American climate and the Southern Oscillation N88-12905
Effects of rainfall on the seasonal thermocline
[AD-A184432] N88-12912
RAINSTORMS
Interactions between the Asian monsoons, the tropical Pacific and the southern hemisphere extratropics N88-12907
RAMAN LASERS
Output power enhancement of AC Raman free-electron laser
[DE88-000503] N88-12786
RAMAN SPECTRA
Raman scattering spectrum along a bevel etched GaAs on Si, TEM (Transmission Electron Microscope) study and GaAs P-I-N photodetector on Si
[DE88-000210] N88-13066
RAMAN SPECTROSCOPY
Real-time Raman detection of molecular changes in ceramics undergoing sliding friction
[DE88-000558] N88-12609
Raman scattering as a diagnostic technique for cathode characterization
[AD-A184434] N88-12726
RANDOM PROCESSES
Mechanical shock test specification using nonstationary random excitation models
[DE87-013650] N88-12812
Implementation of a new shock testing procedure using nonstationary random excitation
[DE87-014643] N88-12827
Propagation of random initial conditions in time N88-12993
RANGEFINDING
GPS vertical axis performance enhancement for helicopter precision landing approach
[NASA-CR-177443] N88-12477
Tau ranging revisited N88-12710
RARE GASES
Microgravity nucleation and particle coagulation experiments support
[NASA-CR-181541] N88-12619
RATES (PER TIME)
Asynchronous rotation in close binary systems with circular orbits N88-13131
RATIOS
Microgravity nucleation and particle coagulation experiments support
[NASA-CR-181541] N88-12619
Carbon abundances and C12/C13 ratios in M giants N88-13167
Hydrogen and deuterium in the local interstellar medium N88-13204
RATS
The toxicology and metabolism of nickel compounds
[DE87-014801] N88-12921
RAY TRACING
Coupled acoustic and ocean thermodynamic model
[AD-A184357] N88-12911
RAYLEIGH SCATTERING
All-optical beam control by forced Rayleigh scattering
[AD-A184315] N88-13018
RAYLEIGH-BENARD CONVECTION
A dissipation principle and its consequences for structured shock waves in thermoelastic materials
[DE87-013723] N88-12813
RDX
High pressure strand burn rate tests of polyvinylnitrate/nitramine propellants
[AD-A184178] N88-12615
REACTION KINETICS
Development of the non-equilibrium reactive chemical transport code CHMTRNS
[DE88-000682] N88-12984
Guest-host interactions in thermotropic and lyotropic liquid crystals
[AD-A184402] N88-13057
REACTIVITY
Conductive polymers via reactive oligomer
[AD-A184270] N88-12587
REACTOR DESIGN
Modular pump limiter systems for large tokamaks
[DE88-001487] N88-13045

REACTOR MATERIALS
Data base on the high heat flux behaviour of metals and carbon materials for plasma facing components: Experiments at the 10 MW neutral beam injection test stand of the IPP Nagoya
[IPPJ-AM-53] N88-13031
REAL TIME OPERATION
An inexpensive real-time interactive three-dimensional flight simulation system
[AD-A184340] N88-12499
Real-time Raman detection of molecular changes in ceramics undergoing sliding friction
[DE88-000558] N88-12609
RECEIVERS
Tau ranging revisited N88-12710
RECTANGULAR PANELS
Advanced radiator concepts utilizing honeycomb panel heat pipes
[NASA-CR-172017] N88-12747
RECURSIVE FUNCTIONS
Design of digital filters for electronic instrumentation
[PB87-100418] N88-12716
RED DWARF STARS
Microwave observations of red dwarf flare stars N88-13153
An astrometric search for a stellar companion to the sun N88-13195
RED GIANT STARS
Fifth Cambridge Workshop on Cool Stars, Stellar Systems and the Sun N88-13092
Exploiting the IR: Solar and stellar spectroscopy in the IR N88-13102
VLA observations of rapid 6 cm flux variations in alpha Ori N88-13169
Infrared excesses of barium stars N88-13174
RED SHIFT
Flux tube dynamics and solar/stellar redshift measurements N88-13095
REDUCED GRAVITY
Access to microgravity: A technical description of the NAE T-33 microgravity facility
[NAE-AN-47] N88-12518
Microgravity combustion fundamentals N88-12528
A study of two-phase flow in a reduced gravity environment
[NASA-CR-172035] N88-12617
Microgravity nucleation and particle coagulation experiments support
[NASA-CR-181540] N88-12618
Microgravity nucleation and particle coagulation experiments support
[NASA-CR-181541] N88-12619
Low gravity fluid-thermal experiments
[DE88-000553] N88-12620
REDUNDANCY
An evaluation plan of bus architectures and protocols using the NASA Ames intelligent redundant actuation system
[NASA-CR-177458] N88-12482
REDUNDANT COMPONENTS
PRAAGE: An interactive IBM-PC code for unreliability/aging analysis
[DE87-012124] N88-12803
REENTRY VEHICLES
Proceedings: SDIO/DARPA Workshop on Laser Propulsion. Volume 3: Viewgraphs
[DE88-000964] N88-12790
REFLECTION
A new approach to modeling and interpreting electromagnetic sounding data
[DE88-000460] N88-12715
REFLECTORS
A multibody dynamic analysis of the N-ROSS (Navy Remote Ocean Sensing System) satellite rotating flexible reflector using Kane's method
[AD-A184452] N88-12860
REFRACTIVITY
Microwave refractive index structure function profiles (Cn2) measured from a small aircraft
[AD-A184343] N88-12670
Pulse-mode expansions and refractive indices in plane-wave propagation
[DE88-001328] N88-12714
REFRIGERANTS
Optimized ground coupled heat pump mechanical package
[DE87-014899] N88-12738
REFRIGERATORS
A 2.3-GHz cryogenically cooled HEMT amplifier for DSS 13 N88-12689
A cold ejector for closed-cycle helium refrigerators N88-12690
Traveling-wave maser closed-cycle refrigerator data acquisition and display system N88-12706
Two-watt, 4-Kelvin closed cycle refrigerator performance N88-12709
REFUELING
Refueling and density control in the ZT-40M reversed field pinch
[DE88-000504] N88-13040
REGRESSION COEFFICIENTS
Estimation of a multivariate continuous variable panel model
[AD-A184472] N88-12982
REGULATIONS
DOE explosives safety manual
[DE88-000831] N88-12616
REINFORCED PLATES
Optimal ribbing of long plate made of composite material N88-12641
REINFORCED SHELLS
Solution of geometrically nonlinear problem for reinforced shell of revolution having arbitrary shape N88-12637
Rational reinforcement of cylindrical shells with variable stiffness frames subjected to external pressure N88-12638
REINFORCEMENT (STRUCTURES)
Optimal ribbing of long plate made of composite material N88-12641
RELATIVISTIC ELECTRON BEAMS
Laser induced fluorescent study of relativistic electron beams
[AD-A184456] N88-12774
Relativistic electron precipitations in a pulsating aurora N88-12894
Variable collision frequency effects on hose and sausage instabilities in relativistic electron beams
[AD-A184206] N88-13021
Coherent emission from relativistic beam-plasma interactions N88-13039
RELATIVITY
Analysis of absolute space-time Lorentz theories
[DE87-703371] N88-13076
Homogeneous space-time of Goedel type in higher-derivate gravity
[DE87-703690] N88-13077
Gravity from symmetry breakdown of a gauge affine theory
[DE88-001671] N88-13079
Cosmological applications of singular hypersurfaces in general relativity N88-13202
RELIABILITY
Programmable Logic Arrays (PLA's) design for testability
[PB87-102935] N88-12718
Reliability of Li/SO2 cells for long-life applications
[DE88-001360] N88-12735
Software reliability perspectives
[NASA-CR-181523] N88-12952
RELIABILITY ANALYSIS
A reliability concept for optimizing aircraft design N88-12822
Applications of the hybrid automated reliability predictor
[NASA-TP-2760] N88-12928
On the next generation of reliability analysis tools
[NASA-CR-178360] N88-13000
REMOTE CONTROL
Low-cost teleoperator-controlled vehicle for damage assessment and dose measurement
[DE88-000713] N88-12794
REMOTE HANDLING
A hydrogen/nickel oxide battery for remote applications
[DE87-009048] N88-12872
REMOTE SENSING
Calibration of a laser-pumped, thermographic phosphor remote thermometry system
[DE88-000452] N88-12781
REMOTE SENSORS
A multibody dynamic analysis of the N-ROSS (Navy Remote Ocean Sensing System) satellite rotating flexible reflector using Kane's method
[AD-A184452] N88-12860
REPORTS
National Center for Atmospheric Research
[PB87-228391] N88-12901
FY 1985 scientific and technical reports, articles, papers and presentations
[NASA-TM-86521] N88-13083
REQUIREMENTS
Fire-related standards and testing N88-12522
MHD stability and control for mirror machines N88-13038
RESEARCH AIRCRAFT
An integrated study of structures, aerodynamics and controls on the forward swept wing X-29A and the oblique wing research aircraft
[NASA-CR-181548] N88-12486
RESEARCH AND DEVELOPMENT
Solar energy: European research and development
[PB87-107645] N88-12866
RESEARCH FACILITIES
FY 1985 scientific and technical reports, articles, papers and presentations
[NASA-TM-86521] N88-13083
RESEARCH MANAGEMENT
Materials sciences programs: Fiscal Year 1987
[DE88-000672] N88-12659
National Center for Atmospheric Research
[PB87-228391] N88-12901
COLA2: A computer program for the structural synthesis of two components using general modal coordinates
[DE88-001457] N88-12963
Nuclear techniques in studies of condensed matter
[NASA-RP-1195] N88-13015
A national model at Howard University demonstrating private sector interrelationships that facilitate research in predominantly Black colleges and universities
[DE88-000160] N88-13089
The role of basic research in society
[DE88-000459] N88-13090
RESIDUAL STRESS
On the stressing of annealed NITINOL: The electrical resistance and calorimetric effects
[AD-A184465] N88-12569
RESISTOJET ENGINES
Compatability of dispersion-strengthened platinum with resistojet propellants
[NASA-TP-2765] N88-12538
Space station resistojet system requirements and interface definition study
[NASA-CR-180832] N88-12541
RESISTORS
Resistor cooling in a vacuum
[DE88-000696] N88-12733
RESOLUTION
Geometric analysis of ensemble of solutions in two-phase flow and complete resolution of problem of choking
[DE88-001687] N88-12764
RESONANCE
The dynamics of solar magnetic flux tubes subjected to resonant foot point shaking N88-13118
RESONATORS
Measurement and analysis of cryogenic sapphire dielectric resonators and DROs N88-12686
RESPIRATION
Human respiratory responses during high performance flight
[AGARD-AG-312] N88-12923
RESPONSES
Engine/airframe response evaluation of the HH-60A helicopter equipped with the T700-GE-701 transient droop improvement electronic control unit
[AD-A184443] N88-12492
RETARDING
The generation and suppression of synchrotron sidebands
[DE88-000532] N88-12787
REVERSE FIELD PINCH
Numerical simulation of the Reversed Field Pinch
[AD-A184353] N88-13023
Transport simulations of the oscillating field current drive experiment in the ZT-40M reversed field pinch
[DE88-000538] N88-13027
Magnetic fluctuation behaviour of current termination in reversed field pinch
[IPPJ-849] N88-13034
Refueling and density control in the ZT-40M reversed field pinch
[DE88-000504] N88-13040
REVERSED FLOW
Dynamics of reverse flows at pump inlet N88-12636
REVERSING
A flash spectrum of CI I, C I, N I, and Ni II absorption in 31 Cygni: A direct observation of the reversing layer N88-13158
RHEOLOGY
Experiments on densely-loaded non-Newtonian slurries in laminar and turbulent pipe flows
[DE88-000719] N88-12748
RIBBON PARACHUTES
The aerodynamics of supersonic parachutes
[DE87-014846] N88-12464
RIBS (SUPPORTS)
Optimal ribbing of long plate made of composite material N88-12641
RICCATI EQUATION
Oscillation theory for linear second-order differential systems
[DE87-011393] N88-12963

RIGID STRUCTURES
Flap-lag equations of motion of rigid, articulated rotor blades with three hinge sequences
[NASA-TM-100023] N88-12495
ROBOTICS
Two dimensional path planning with obstacles and shadows
[AD-A184075] N88-12474
Autonomous Land Vehicle (ALV) planning and navigation system
[AD-A184243] N88-12475
ROBOTS
Low-cost teleoperator-controlled vehicle for damage assessment and dose measurement
[DE88-000713] N88-12794
Static standing and dynamic walking of a practical biped robot
[DE88-001387] N88-12795
Expert robots in nuclear plants
[DE87-014839] N88-12800
Controlling robots with spoken commands
[DE88-000537] N88-12801
Ground vehicle convoying
[DE88-000360] N88-13088
ROBUSTNESS (MATHEMATICS)
New feedback design methodologies for large space structures: A multi-criterion optimization approach N88-12535
Robust statistical methods for automated outlier detection N88-12681
ROCKET ENGINES
Plasma thruster development
[AD-A184173] N88-12536
A two-dimensional finite difference program for thermal analysis of rocket thrust chambers
[NASA-TM-100191] N88-12539
The VISTA spacecraft: Advantages of ICF (Inertial Confinement Fusion) for interplanetary fusions propulsion applications
[NASA-CR-181549] N88-13024
ROCKET PROPELLANTS
Compatability of dispersion-strengthened platinum with resistojet propellants
[NASA-TP-2765] N88-12538
ROCKET THRUST
A two-dimensional finite difference program for thermal analysis of rocket thrust chambers
[NASA-TM-100191] N88-12539
ROCKS
A mineral reconnaissance sampling manual for Costa Rica: Central American energy and resource project
[DE87-014997] N88-12859
RODS
A creep measurement of unidirectional epoxy-fiberglass rod
[DE87-014812] N88-12553
ROOT-MEAN-SQUARE ERRORS
Detection of signals by weighted integrate-and-dump filter N88-12696
ROSSBY REGIMES
Radio emission from RS CVn binaries: A 5 GHz VLA survey of 93 systems N88-13191
ROTARY ENGINES
Performance and combustion characteristics of direct-injection stratified-charge rotary engines
[NASA-TM-100134] N88-12490
ROTATING BODIES
Semiempirical method for prediction of aerodynamic forces and moments on a steadily spinning light airplane
[NASA-TM-4009] N88-12456
ROTATING FLUIDS
Turbulent mixing in a rotating, stratified fluid N88-12759
ROTATING SPHERES
Analytical studies of axially symmetric motion of an incompressible viscous fluid between two concentric rotating spheres N88-12757
ROTOR AERODYNAMICS
A full potential flow analysis with realistic wake influence for helicopter rotor airload prediction
[NASA-CR-4007] N88-12452
ROTOR BLADES (TURBOMACHINERY)
A method for the efficient calculation of elastic rotor blade dynamic response in forward flight N88-12460
Measurements and calculations of aerodynamic torques for a vertical-axis wind turbine
[DE88-001783] N88-12876
Results of the 1986 NASA/FAA/DFVLR main rotor test entry in the German-Dutch wind tunnel (DNW)
[NASA-TM-100607] N88-13003
ROTOR BODY INTERACTIONS
A 0.15-scale study of configuration effects on the aerodynamic interaction between main rotor and fuselage
[NASA-CR-166577] N88-12462
ROTORS
A full potential flow analysis with realistic wake influence for helicopter rotor airload prediction
[NASA-CR-4007] N88-12452
Flap-lag equations of motion of rigid, articulated rotor blades with three hinge sequences
[NASA-TM-100023] N88-12495
ROUGHNESS
Studies on high-speed electroforming
[DE88-001395] N88-12656
ROUTES
Two dimensional path planning with obstacles and shadows
[AD-A184075] N88-12474
RUBY LASERS
Noncontact temperature measurements of hot steel bodies using an electromagnetic acoustic transducer (EMAT)
[DE88-000560] N88-12765
RUNGE-KUTTA METHOD
Application of Runge Kutta time marching scheme for the computation of transonic flows in turbomachines
[NASA-TM-86997] N88-12461
RUNWAYS
Optimum take-off run of aircraft on ground airfields N88-12623

S

S STARS
Emission features in IRAS LRS spectra of MS, S and CS stars N88-13163
SAFETY
DOE explosives safety manual
[DE88-000631] N88-12616
SALINITY
Effects of rainfall on the seasonal thermocline
[AD-A184432] N88-12912
SAMPLING
A mineral reconnaissance sampling manual for Costa Rica: Central American energy and resource project
[DE87-014997] N88-12859
RRS DISCOVERY cruise 160, 30 June-25 July, 1986. Geochemical sampling over the Madeira and Porcupine Abyssal Plains
[PB87-222030] N88-12910
An urn model for the multi-sample capture/recapture sequential tagging process
[AD-A184470] N88-12998
SANDWICH STRUCTURES
Process for producing sandwich mouldings
[EP-PATENT-0-191-623-A2] N88-12642
SAPPHIRE
Measurement and analysis of cryogenic sapphire dielectric resonators and DROs N88-12686
SATELLITE ALTIMETRY
Radial orbit error reduction and sea surface topography determination using satellite altimetry N88-12861
SATELLITE COMMUNICATION
Design description report for a photovoltaic power system for a remote satellite earth terminal
[NASA-CR-179586] N88-12875
SATELLITE IMAGERY
Cloud cover determination in polar regions from satellite imagery
[NASA-CR-181544] N88-12908
SATELLITE NAVIGATION SYSTEMS
GPS vertical axis performance enhancement for helicopter precision landing approach
[NASA-CR-177443] N88-12477
A demonstration of high precision GPS orbit determination for geodetic applications N88-12680
Precise near-earth navigation with GPS: A survey of techniques N88-12682
SATELLITE OBSERVATION
IRAS and near IR observations of active binaries N88-13186
SATELLITE ROTATION
A multibody dynamic analysis of the N-ROSS (Navy Remote Ocean Sensing System) satellite rotating flexible reflector using Kane's method
[AD-A184452] N88-12980
SATELLITE TRACKING
Optimized tracking of RF carriers with phase noise, including Pioneer 10 results N88-12694
SATELLITE-BORNE RADAR
Review of inversion techniques for spaceborne lidar systems
[AD-A184184] N88-12772
SCALE (CORROSION)
Carbon dioxide treatment for scale removal and control in potable water systems
[AD-A184348] N88-12556
SCALE MODELS
A 0.15-scale study of configuration effects on the aerodynamic interaction between main rotor and fuselage
[NASA-CR-166577] N88-12462
Analytical investigation of the dynamics of tethered constellations in Earth orbit (phase 2)
[NASA-CR-179218] N88-12533
SCALING
A multiple-time-scale turbulence model based on variable partitioning of turbulent kinetic energy spectrum
[NASA-CR-179222] N88-12754
SCALING LAWS
An experimental investigation of unsteadiness in swept shock wave/turbulent boundary layer interactions N88-12760
SCATTERING CROSS SECTIONS
Magnetic diffuse scattering
[DE87-013539] N88-13014
SCENE ANALYSIS
Methods for design and evaluation of integrated hardware/software systems for concurrent computation
[NASA-CR-181522] N88-12953
SCHROEDINGER EQUATION
Numerical studies of the dual HEMT/algorithm development and numerical studies of Schrodinger's equation
[AD-A184471] N88-12948
SCIENTISTS
National Center for Atmospheric Research
[PB87-228391] N88-12901
SCORPIUS CONSTELLATION
The angular diameter of alpha Scorpii in the near-infrared Ca II triplet N88-13162
SEA LEVEL
Sea level changes
[DE87-014357] N88-12913
SEA ROUGHNESS
Studies of thin surface films aim at seeing deep ocean processes N88-12847
SEA SURFACE TEMPERATURE
A multibody dynamic analysis of the N-ROSS (Navy Remote Ocean Sensing System) satellite rotating flexible reflector using Kane's method
[AD-A184452] N88-12980
On the interannual variability of South American climate and the Southern Oscillation N88-12905
SEARCHING
An astrometric search for a stellar companion to the sun N88-13195
SECULAR VARIATIONS
Statistics of the geomagnetic secular variation for the past 5Ma
[NASA-CR-181558] N88-12890
SEDIMENTS
A mineral reconnaissance sampling manual for Costa Rica: Central American energy and resource project
[DE87-014997] N88-12859
Two-layer stratified flow analysis of gravity currents and turbidity currents in lakes, reservoirs and the ocean N88-12864
RRS DISCOVERY cruise 160, 30 June-25 July, 1986. Geochemical sampling over the Madeira and Porcupine Abyssal Plains
[PB87-222030] N88-12910
SEISMIC WAVES
A new approach to modeling and interpreting electromagnetic sounding data
[DE88-000460] N88-12715
Multichannel deconvolution of P waves at seismic arrays and three component stations
[AD-A184450] N88-12888
SELENIUM
Thermal expansion of some Ge-Se-Te glasses
[PD-MT-8722] N88-12606
Studies on some Ge-Se-Te glasses
[PD-MT-8721] N88-12607
J = O Task Force
[DE88-001326] N88-12788
SELF EXCITATION
Dynamics of reverse flows at pump inlet N88-12636
SELF TESTS
Programmable Logic Arrays (PLA's) design for testability
[PB87-102935] N88-12718
SEMICONDUCTORS (MATERIALS)
Measurement of the electron density and the attachment rate coefficient in silane/helium discharges
[AD-A184268] N88-13051
Valence bond cluster studies of alkali metal/semiconductor bonding
[AD-A184276] N88-13054
Novel dynamical investigations of excitons and their structure in semiconductors
[DE87-014868] N88-13070

Far infrared Fourier transform spectroscopy of semiconductors
[DE88-000188] N88-13072

SENSITIVITY
Aerodynamic sensitivities from subsonic, sonic and supersonic unsteady, nonplanar lifting-surface theory
[NASA-TM-100502] N88-12459
Investigation, development and application of optimal output feedback theory. Vol. 4: Measures of eigenvalue/eigenvector sensitivity to system parameters and unmodeled dynamics
[NASA-CR-4108] N88-12969
Sensitivity of the H alpha line to expansion, geometrical extent and temperature gradient in the G and K supergiant chromospheres N88-13159

SEPARATED FLOW
Three-dimensional unsteady flow elicited by finite wings and complex configurations N88-12468
Investigation of low-speed turbulent separated flow around airfoils
[NASA-CR-177450] N88-12471
Numerical simulation of unsteady separated flows
[AD-A184132] N88-12741

SERIES EXPANSION
Asymptotic form of stationary solutions of the Navier-Stokes equations for large Reynolds numbers N88-12838
The shifted Adams method for ordinary differential equations
[DE88-000810] N88-12994

SERVOCONTROL
A new state space model for the NASA/JPL 70-meter antenna servo controls N88-12702
A modern control theory based algorithm for control of the NASA/JPL 70-meter antenna axis servos N88-12706

SET THEORY
A characterization of separating pairs and triplets in a graph
[AD-A184278] N88-12941
On the number of minimum size separating vertex sets in a graph
[AD-A184279] N88-12942
Foundations of O-theory 2: Measurements and relation to fuzzy set theory
[DE88-000013] N88-12986

SHAFTS (MACHINE ELEMENTS)
Analysis of 7- X 10-foot high speed wind tunnel shaft loads in support of fan blade failure investigation
[NASA-TM-100504] N88-12496

SHALLOW SHELL EQUATIONS
Effective treatment of membrane and shear locking phenomena in curved shear-deformable axisymmetric shell element N88-12652

SHAPE MEMORY ALLOYS
A comparison of high damping shape memory alloys with Cu-Mn-based and Fe-Cr-based alloys
[AD-A184110] N88-12566

SHAPES
Observations on the hydrodynamic flow visualization at ONERA
[PD-FM-8718] N88-12753
An approach to object recognition: Aligning pictorial descriptions
[AD-A184462] N88-12972

SHEAR FLOW
Heat and moisture transport in the atmospheric boundary layer
[AD-A184222] N88-12904

SHEAR LAYERS
On the instability of thin circular shear layers N88-12467
Blowup for a nonlinear evolution equation and self-reproducing strained shear layers N88-12755

SHEAR PROPERTIES
Determination of through-plane shear moduli for glass-reinforced plastics
[PB87-106274] N88-12592
Steady shearing in a viscoplastic solid
[AD-A184341] N88-12810
The evolution of plastic strain in steady, plastic shock waves
[DE87-013812] N88-12826

SHEAR STRAIN
Plastic strain localization between voids in shear deformation fields N88-12648
Effective treatment of membrane and shear locking phenomena in curved shear-deformable axisymmetric shell element N88-12652
Vibration and buckling of geometrically imperfect laminated cylindrical shells N88-12822

SHEAR STRENGTH
Spatial strength variation and statistical size effect of laminated orthotropic composite materials N88-12646

SHEAR STRESS
Free-edge delamination: Laminate width and loading conditions effects
[NASA-TM-100238] N88-12551
A refined nonlinear analysis of laminated composite plates and shells
[AD-A184436] N88-12811

SHEARING
Steady shearing in a viscoplastic solid
[AD-A184341] N88-12810

SHELL THEORY
Solution of geometrically nonlinear problem for reinforced shell of revolution having arbitrary shape N88-12637
Rational reinforcement of cylindrical shells with variable stiffness frames subjected to external pressure N88-12638
Finite deformations of shell with rigid inclusion N88-12639
Effective treatment of membrane and shear locking phenomena in curved shear-deformable axisymmetric shell element N88-12652

SHELLS (STRUCTURAL FORMS)
USSR report: Engineering and equipment
[JPRS-UEQ-87-006] N88-12621
Finite deformations of shell with rigid inclusion N88-12639

SHOCK TESTS
Mechanical shock test specification using nonstationary random excitation models
[DE87-013650] N88-12812
Implementation of a new shock testing procedure using nonstationary random excitation
[DE87-014643] N88-12827

SHOCK WAVE PROPAGATION
Explicit and implicit soil modelling for dynamic soil-structure interaction problems N88-12650

SHOCK WAVES
Particle injection and cosmic ray acceleration at collisionless parallel shocks
[DE88-000507] N88-12685
Three-dimensional, free-Lagrange hydrodynamics
[DE88-000494] N88-12749
An experimental investigation of unsteadiness in swept shock wave/turbulent boundary layer interactions N88-12760
Numerical modeling of slow shocks
[DE87-014768] N88-12808
A dissipation principle and its consequences for structured shock waves in thermoelastic materials
[DE87-013723] N88-12813
The evolution of plastic strain in steady, plastic shock waves
[DE87-013812] N88-12826
Slow-mode shocks in the earth's magnetosphere
[DE88-000483] N88-12895
Prompt simultaneous acceleration of protons and electrons to relativistic energies by shock waves in solar flares
[IPPJ-851] N88-13037
Core bounce supernovae
[DE87-014910] N88-13197

SHORT WAVE RADIO TRANSMISSION
Meteor-burst communications: Is this what the Navy needs?
[AD-A184433] N88-12672

SHRINKAGE
Process for producing sandwich mouldings
[EP-PATENT-0-191-823-A2] N88-12642

SHUTDOWNS
Failure control techniques for the SSME
[NASA-CR-179224] N88-12537

SIDEBANDS
Spectral evolution equation for the sideband instability in a free-electron laser oscillator
[DE88-000510] N88-12771
The free electron laser sideband instability reconsidered
[AD-A184269] N88-12773
Analysis of sideband spectra from untapered undulator using analytical technique
[DE87-014763] N88-12778
The generation and suppression of synchrotron sidebands
[DE88-000532] N88-12787
Comparison of sideband spectra obtained from analytical formula and from numerical simulation in free-electron laser
[DE88-000521] N88-12789

SIGNAL ANALYSIS
Intelligent signal analysis and recognition
[NASA-CR-181531] N88-13084

SIGNAL ANALYZERS
Lower bounds on bearing accuracy for closely spaced sources
[AD-A184258] N88-12997

SIGNAL DETECTION
Detection of signals by the digital integrate-and-dump filter with offset sampling N88-12695
Detection of signals by weighted integrate-and-dump filter N88-12696

SIGNAL ENCODING
Bandwidth efficient block codes for M-ary PSK modulation
[NASA-CR-181543] N88-12712

SIGNAL PROCESSING
Optical alignment of Centaur's inertial guidance system
[NASA-TM-88844] N88-12515
On a circular correlation technique for filtering randomly noisy data
[AD-A184317] N88-12669
Application of lattice filtering techniques to CW measured time domain data
[AD-A184351] N88-12671
Accommodating the residue of processed or computed digital video signals within the 8 bit CCIR recommendation 601
[BBC-RD-1987/12] N88-12676
Robust statistical methods for automated outlier detection N88-12681
Frequency doubling conversion efficiencies for deep space optical communications N88-12691
Design of digital filters for electronic instrumentation
[PB87-100418] N88-12716
Interferometry theory for the block 2 processor
[NASA-CR-181551] N88-12730

SIGNAL RECEPTION
Optimized tracking of RF carriers with phase noise, including Pioneer 10 results N88-12694

SIGNAL STABILIZATION
Optimized tracking of RF carriers with phase noise, including Pioneer 10 results N88-12694
X-band uplink ground systems development: Part 2 N88-12703

SIGNAL TO NOISE RATIOS
Optimized tracking of RF carriers with phase noise, including Pioneer 10 results N88-12694
Detection of signals by the digital integrate-and-dump filter with offset sampling N88-12695
Detection of signals by weighted integrate-and-dump filter N88-12696
Lower bounds on bearing accuracy for closely spaced sources
[AD-A184258] N88-12997

SIGNAL TRANSMISSION
Design of digital filters for electronic instrumentation
[PB87-100418] N88-12716

SILANES
Measurement of the electron density and the attachment rate coefficient in silane/helium discharges
[AD-A184268] N88-13051

SILICON
Performance of GaAs and silicon concentrator cells under 37 MeV proton irradiation
[NASA-TM-100144] N88-12877

SILICON CARBIDES
Carbon-fiber reinforced aluminum N88-12507

SILOXANES
Synthesis, NMR characterization and electrical properties of siloxane-based polymer electrolytes
[AD-A184184] N88-12596

SIMILARITY THEOREM
Similar solutions for viscous hypersonic flow over a slender three-fourths-power body of revolution
[NASA-TM-100205] N88-12752

SIMULATION
Some experiences with the viscous-inviscid interaction approach
[NASA-TM-100015] N88-12466
Analysis of sideband spectra from untapered undulator using analytical technique
[DE87-014763] N88-12778
A network definition and solution of simulation problems
[DE88-000675] N88-12962
Transport simulations of the oscillating field current drive experiment in the ZT-40M reversed field pinch
[DE88-000538] N88-13027
A comparison of the basket method and the stratified random sampling for contract change order negotiations
[AD-A184170] N88-13060

SIMULATORS
New main reflector, subreflector and dual chamber concepts for compact range applications
[NASA-CR-181506] N88-12498
SCRAM JET (Supersonic Combustion Ramjet) combustion experiments N88-12512

SINGLE CRYSTALS
Monocrystal sputtering by the computer simulation code ACOCT
[IPPJ-848] N88-13035

Evaluation of the Mellen EDG furnace for growth of large diameter GaAs single crystals in a horizontal configuration
[DE88-000463] N88-13068
The structure of adsorbed sulfur and carbon on molybdenum and rhenium single crystal surfaces, and their influence on carbon monoxide and hydrocarbon chemisorption
[DE88-001393] N88-13073
SINGULAR INTEGRAL EQUATIONS
A quadrature formula for a double-pole singular integral
[PD-FM-8725] N88-12990
SINTERING
Research and development on high strength ceramic heaters discussed N88-12508
Sintered steels of high resistance alloyed to Nb, Mo, Mn and Si
[DE87-703546] N88-12573
Studies of alumina additions in zirconia - magnesia
[DE87-703500] N88-12602
Fatigue failure of thin porous strips N88-12640
SITE SELECTION
Variability of wind power near Oklahoma City and implications for siting of wind turbines
[DE88-000444] N88-12902
SIZE (DIMENSIONS)
Titanium oxide absorption and spot sizes in II Peg, HR 1099 and UX Ari N88-13126
SKY SURVEYS (ASTRONOMY)
A search for X-ray luminous late type stars in NIPSS data N88-13143
A search for very low mass (brown dwarf) stars as wide binaries using a seven element infrared camera-photometer N88-13150
A VLA survey of dMe flare stars N88-13154
SLEWING
Combined problem of slew maneuver control and vibration suppression
[NASA-CR-181537] N88-12617
SLIDING FRICTION
Real-time Raman detection of molecular changes in ceramics undergoing sliding friction
[DE88-000558] N88-12609
SLOT ANTENNAS
Mutual admittance between slots in cylinders of arbitrary shape
[AD-A184254] N88-12723
SLOTS
Mutual admittance between slots in cylinders of arbitrary shape
[AD-A184254] N88-12723
SLURRIES
Experiments on densely-loaded non-Newtonian slurries in laminar and turbulent pipe flows
[DE88-000719] N88-12746
SOCIAL FACTORS
The role of basic research in society
[DE88-000459] N88-13090
SOFTWARE ENGINEERING
Programmable real-time digital video image processing
[PB87-104162] N88-12661
Software reliability perspectives
[NASA-CR-181523] N88-12952
Software maintenance in scientific and engineering environments: An introduction and guide
[NASA-CR-177409] N88-12954
Managing distributed derived data: A preliminary proposal
[DE88-000714] N88-12966
Intelligent signal analysis and recognition
[NASA-CR-181531] N88-13084
SOFTWARE TOOLS
Guidelines for preparing software user documentation
[NASA-CR-181550] N88-12959
A network definition and solution of simulation problems
[DE88-000675] N88-12962
On the next generation of reliability analysis tools
[NASA-CR-178380] N88-13000
SOIL MECHANICS
Explicit and implicit soil modelling for dynamic soil-structure interaction problems N88-12650
SOLAR ACTIVITY
Asymmetry and variations of solar limb darkening along the diameter defined by diurnal motion in April 1961 N88-13111
Calibration of the Ca II K line-core density and the magnetic flux density in stars using solar data N88-13116
Three-halves law in sunspot cycle shape
[NASA-CR-181520] N88-13210
SOLAR ARRAYS
Characteristics of current solar central receiver projects
[DE88-001314] N88-12880
SOLAR CELLS
Performance of GaAs and silicon concentrator cells under 37 MeV proton irradiation
[NASA-TM-100144] N88-12877
Radiation performance of AlGaAs concentrator cells and expected performance of cascade structures
[NASA-TM-100145] N88-12878
Characteristics of current solar central receiver projects
[DE88-001314] N88-12880
SOLAR COLLECTORS
Light funnel concentrator panel for solar power
[NASA-CR-179223] N88-12870
Performance of GaAs and silicon concentrator cells under 37 MeV proton irradiation
[NASA-TM-100144] N88-12877
International Energy Agency (IEA) Small Solar Power Systems (SSPS) sodium cavity and external receiver performance comparison
[DE88-001310] N88-12879
Characteristics of current solar central receiver projects
[DE88-001314] N88-12880
SOLAR CORONA
Statistical properties of small high-velocity events in the solar transition region N88-13112
SOLAR CYCLES
Drought, solar activity link established by Leningrad geophysicists N88-12835
Spectral analysis of APT RS CVn binary light curves N88-13122
Starspots on the short-period RS CVn system SV Cam: 45 years of activity N88-13123
Stellar cycle variability of solar-like stars: A sneak preview N88-13136
A comprehensive exploration of late-type stars in the far-ultraviolet N88-13194
SOLAR ENERGY
Solar energy: European research and development
[PB87-107645] N88-12866
Technical evaluation of a solar-powered absorption cooling system (LiBr-H2O)
[PB87-106254] N88-12867
International Energy Agency (IEA) Small Solar Power Systems (SSPS) sodium cavity and external receiver performance comparison
[DE88-001310] N88-12879
A study of the optimal transition temperatue of PCM (Phase Change Material) wallboard for solar energy storage
[DE88-001522] N88-12882
Proceedings of the Eleventh DOE Solar Photochemistry Research Conference
[DE88-000678] N88-12883
The developmental status of solar thermochemical hydrogen production
[DE88-001778] N88-12884
SOLAR FLARES
Prompt simultaneous acceleration of protons and electrons to relativistic energies by shock waves in solar flares
[IPPJ-851] N88-13037
A large X-ray flare on squared Sigma coronae borealis observed with exosat N88-13121
Excess emission in the wings of the Hydrogen Balmer lines during a flare on the late-type dMe star YZ CMi N88-13146
SOLAR FLUX
VLA observations of rapid 6 cm flux variations in alpha Ori N88-13169
SOLAR GENERATORS
Solar converging method N88-12504
Design description report for a photovoltaic power system for a remote satellite earth terminal
[NASA-CR-179586] N88-12875
International Energy Agency (IEA) Small Solar Power Systems (SSPS) sodium cavity and external receiver performance comparison
[DE88-001310] N88-12879
SOLAR HEATING
Statistical distribution of solar radiation (hourly sums): Cumulative frequency curves preparation of a European data set and direction for use
[PB87-107454] N88-12886
SOLAR MAGNETIC FIELD
Development of optical modulators for measurements of solar magnetic fields
[NASA-TM-100315] N88-13016
Large scale solar and stellar magnetic fields N88-13117
SOLAR NEIGHBORHOOD
A spectral survey of 26 G9-M6 flare stars in the solar neighborhood N88-13149
A VLA survey of dMe flare stars N88-13154
An astrometric search for a stellar companion to the sun N88-13195
Hydrogen and deuterium in the local interstellar medium N88-13204
SOLAR PHYSICS
Exploiting the IR: Solar and stellar spectroscopy in the IR N88-13102
Three-halves law in sunspot cycle shape
[NASA-CR-181520] N88-13210
SOLAR RADIATION
Statistical distribution of solar radiation (hourly sums): Cumulative frequency curves preparation of a European data set and direction for use
[PB87-107454] N88-12886
A comprehensive exploration of late-type stars in the far-ultraviolet N88-13194
SOLAR RADIATION SHIELDING
A near-earth optical communications terminal with a corevolving planetary sun shield N88-12693
SOLAR REFLECTORS
Solar converging method N88-12504
SOLAR TERRESTRIAL INTERACTIONS
Drought, solar activity link established by Leningrad geophysicists N88-12835
SOLAR THERMAL ELECTRIC POWER PLANTS
Performance analysis of solar thermal power systems
[DE88-000563] N88-12874
SOLAR WIND
High latitude F-region drift studies
[AD-A184466] N88-12889
Model of solar-wind magnetosphere coupling N88-13211
Observations of turbulence and fluctuations in the solar wind N88-13212
SOLAR X-RAYS
A large X-ray flare on squared Sigma coronae borealis observed with exosat N88-13121
SOLDERING
The effect of organic inhibitors on the atmospheric corrosion and solderability of copper
[DE88-000261] N88-12565
SOLID ELECTROLYTES
Studies of alumina additions in zirconia - magnesia
[DE87-703500] N88-12602
Effect of sidechain length and crosslinking on ionic conductivity in polyphosphazene solid electrolytes
[AD-A184419] N88-13058
SOLID LUBRICANTS
Calculation of the tribological properties of surfaces by semi-empirical methods
[AD-A184283] N88-12791
SOLID PROPELLANT ROCKET ENGINES
Structural analysis of a bolted joint concept for the space shuttle's solid rocket motor casing
[NASA-TM-89092] N88-12531
SOLID PROPELLANTS
High pressure strand burn rate tests of polyvinylnitrate/nitramine propellants
[AD-A184178] N88-12615
SOLID ROCKET PROPELLANTS
Test number 2 of propellant for rocket motor MK52
[PB87-226155] N88-12613
SOLID SOLUTIONS
Non-lattice matched metallic superlattices
[DE87-011512] N88-13062
SOLID STATE DEVICES
Chemically modified microelectrode arrays. New kinds of electronic devices
[AD-A184389] N88-12724
SOLIDS
Optical instrumentation and study of gas-solid suspension flows
[DE88-000147] N88-12744
Monocrystal sputtering by the computer simulation code ACOCT
[IPPJ-848] N88-13035
SOLITARY WAVES
Intensive synoptic eddies and quasigeostrophic approximation N88-12844
Dynamics of isolated intrathermocline eddy N88-12845
Soliton twin boundaries of the cubic-tetragonal martensitic transformations in ferroelastic materials
[DE87-014741] N88-13047
SOLUBILITY
Conducting hybrid polymeric systems
[DE88-000527] N88-12611
SOUND FIELDS
Excitation of natural oscillations of a boundary layer by an external acoustic field N88-12634
SOUND TRANSDUCERS
Noncontact temperature measurements of hot steel bodies using an electromagnetic acoustic transducer (EMAT)
[DE88-000580] N88-12765
SOUND TRANSMISSION
Nonlinear acoustics
[AD-A184271] N88-13004

Aircraft interior noise reduction by alternate resonance tuning
[NASA-CR-181530] N88-13005
An analysis of sound absorbing linings for the interior of the NASA Ames 80 x 120-foot wind tunnel
[NASA-CR-177396] N88-13006
SOUND WAVES
Boundary effects on the drag of an oscillating sphere: Applications to the magnetic sphere rheometer. Attenuation and dispersion of acoustic waves in nematic liquid crystals N88-13007
SOUNDING
A new approach to modeling and interpreting electromagnetic sounding data
[DE88-000460] N88-12715
SOUTH AMERICA
On the interannual variability of South American climate and the Southern Oscillation N88-12905
SPACE BASES
Small reactor power systems for manned planetary surface bases
[NASA-TM-100223] N88-13209
SPACE COMMUNICATION
The Telecommunications and Data Acquisition Report
[NASA-CR-181546] N88-12679
SPACE DENSITY
Galactic interstellar abundance surveys with IUE and IRAS N88-13206
SPACE EXPLORATION
Small reactor power systems for manned planetary surface bases
[NASA-TM-100223] N88-13209
SPACE MANUFACTURING
Microgravity nucleation and particle coagulation experiments support
[NASA-CR-181540] N88-12618
SPACE PERCEPTION
Latency differences and effects of selective attention to gratings in the central and right visual fields: 2
[DE87-014730] N88-12918
SPACE PLASMAS
Flux tube dynamics and solar/stellar redshift measurements N88-13095
Nonthermal phenomena in stellar coronae: Evidence from radio observations N88-13096
Observational constraints and evidence for saturation N88-13097
Observations of turbulence and fluctuations in the solar wind N88-13212
SPACE POWER REACTORS
Low gravity fluid-thermal experiments
[DE88-000553] N88-12620
SPACE SHUTTLE MAIN ENGINE
Failure control techniques for the SSME
[NASA-CR-179224] N88-12537
SPACE SHUTTLE PAYLOADS
High power ion thruster performance
[NASA-TM-100127] N88-12542
SPACE SHUTTLES
Spacecraft material flammability testing and configurations N88-12529
Structural analysis of a bolted joint concept for the space shuttle's solid rocket motor casing
[NASA-TM-89092] N88-12531
Proceedings: SDIO/DARPA Workshop on Laser Propulsion. Volume 3: Viewgraphs
[DE88-000964] N88-12790
SPACE STATION POWER SUPPLIES
Solar converging method N88-12504
SPACE STATION STRUCTURES
Space station resistojet system requirements and interface definition study
[NASA-CR-180832] N88-12541
Advanced radiator concepts utilizing honeycomb panel heat pipes
[NASA-CR-172017] N88-12747
SPACE STATIONS
Spacecraft Fire Safety
[NASA-CP-2476] N88-12520
Space station internal environmental and safety concerns N88-12527
Optimization techniques applied to passive measures for in-orbit spacecraft survivability
[NASA-CR-179216] N88-12532
An assessment of clinical chemical sensing technology for potential use in space station health maintenance facility
[NASA-CR-172013] N88-12926
Space suit extravehicular hazards protection development
[NASA-TM-100458] N88-12927
SPACE SUITS
Space suit extravehicular hazards protection development
[NASA-TM-100458] N88-12927
SPACE-TIME FUNCTIONS
Analysis of absolute space-time Lorentz theories
[DE87-703371] N88-13076
Homogeneous space-time of Goedel type in higher-derivate gravity
[DE87-703690] N88-13077
SPACEBORNE EXPERIMENTS
Microgravity nucleation and particle coagulation experiments support
[NASA-CR-181540] N88-12618
Microgravity nucleation and particle coagulation experiments support
[NASA-CR-181541] N88-12619
Study of certain biological characteristics of bacteria during the French-Soviet CYTOS-2 space experiment N88-12917
SPACECRAFT COMPONENTS
Fire-related standards and testing N88-12522
Fire extinguishment and inhibition in spacecraft environments N88-12523
SPACECRAFT CONSTRUCTION MATERIALS
Fire-related standards and testing N88-12522
Spacecraft material flammability testing and configurations N88-12529
Carbon fiber reinforced glass matrix composites for space based applications
[AD-A184355] N88-12546
SPACECRAFT CONTROL
New feedback design methodologies for large space structures: A multi-criterion optimization approach N88-12535
Combined problem of slew maneuver control and vibration suppression
[NASA-CR-181537] N88-12617
SPACECRAFT DESIGN
New feedback design methodologies for large space structures: A multi-criterion optimization approach N88-12535
SPACECRAFT ENVIRONMENTS
Spacecraft Fire Safety
[NASA-CP-2476] N88-12520
Fire extinguishment and inhibition in spacecraft environments N88-12523
Inerting and atmospheres N88-12524
Fire-related medical science N88-12525
Aircraft fire safety research N88-12526
Space station internal environmental and safety concerns N88-12527
Microgravity combustion fundamentals N88-12528
Spacecraft material flammability testing and configurations N88-12529
SPACECRAFT EQUIPMENT
Microgravity nucleation and particle coagulation experiments support
[NASA-CR-181540] N88-12618
Microgravity nucleation and particle coagulation experiments support
[NASA-CR-181541] N88-12619
SPACECRAFT MODULES
Space station internal environmental and safety concerns N88-12527
SPACECRAFT POWER SUPPLIES
Study of Plasma Motor Generator (PMG) tether system for orbit reboost
[NASA-CR-172015] N88-12501
Space station resistojet system requirements and interface definition study
[NASA-CR-180832] N88-12541
Low gravity fluid-thermal experiments
[DE88-000553] N88-12620
SPACECRAFT PROPULSION
Interplanetary propulsion using inertial fusion
[NASA-TM-89661] N88-12540
The VISTA spacecraft: Advantages of ICF (Inertial Confinement Fusion) for interplanetary fusions propulsion applications
[NASA-CR-181549] N88-13024
SPACECRAFT SHIELDING
Optimization techniques applied to passive measures for in-orbit spacecraft survivability
[NASA-CR-179216] N88-12532
SPACECREWS
An assessment of clinical chemical sensing technology for potential use in space station health maintenance facility
[NASA-CR-172013] N88-12926
SPATIAL DEPENDENCIES
Spatial strength variation and statistical size effect of laminated orthotropic composite materials N88-12646
SPATIAL DISTRIBUTION
Cloud cover determination in polar regions from satellite imagery
[NASA-CR-181544] N88-12908
The giant spot on II Peg in 1986 N88-13120
SPATIAL RESOLUTION
Visual evoked responses to sinusoidal gratings presented in central and right visual fields: 1
[DE87-014731] N88-12919
SPECIFIC HEAT
Magnetic field dependence of the specific heat of some high-T/sub c/ superconductors
[DE87-014078] N88-13083
SPECIFICATIONS
The aerodynamics of supersonic parachutes
[DE87-014846] N88-12464
Mechanical shock test specification using nonstationary random excitation models
[DE87-013650] N88-12812
SPECKLE INTERFEROMETRY
New results from high angular resolution observations of alpha Ori N88-13161
SPECTRA
Comparison of sideband spectra obtained from analytical formula and from numerical simulation in free-electron laser
[DE88-000521] N88-12789
SPECTRAL EMISSION
PG 0308 + 096: A short-period white dwarf + dM binary with strongly modulated H-alpha emission N88-13132
Evidence for expanding magnetic loops in coronae of cool stars N88-13134
X-rays, color, and the Vaughan-Preston gap N88-13135
SPECTRAL ENERGY DISTRIBUTION
A spectral survey of 26 G9-M6 flare stars in the solar neighborhood N88-13149
SPECTROGRAMS
Variations of the vertical and horizontal velocities of the small-scale structures and the physical problems related to overshoot layers N88-13115
SPECTROMETERS
Evidence for expanding magnetic loops in coronae of cool stars N88-13134
SPECTROSCOPY
Doppler snapshots N88-13125
Spectroscopic monitoring of RS CVn stars at Kitt Peak using the Penn State fiber optic echelle N88-13127
H alpha and Ca II emission line variability of FK comae N88-13128
Evidence for an additional source of opacity during the impulsive phase of stellar flares N88-13133
Contemporaneous B,V,R,I photometry and H alpha spectroscopy of YY Gem N88-13155
SPECTRUM ANALYSIS
Analysis of sideband spectra from untapered undulator using analytical technique
[DE87-014763] N88-12778
Evidence for expanding magnetic loops in coronae of cool stars N88-13134
Magnetic fields on K and M stars N88-13137
A spectral survey of 26 G9-M6 flare stars in the solar neighborhood N88-13149
SPEECH RECOGNITION
Controlling robots with spoken commands
[DE88-000537] N88-12801
SPEED REGULATORS
Engine/airframe response evaluation of the HH-60A helicopter equipped with the T700-GE-701 transient droop improvement electronic control unit
[AD-A184443] N88-12492
SPHERICAL HARMONICS
Statistics of the geomagnetic secular variation for the past 5Ma
[NASA-CR-181558] N88-12890
SPHERICAL SHELLS
Microgravity nucleation and particle coagulation experiments support
[NASA-CR-181541] N88-12619
SPLINE FUNCTIONS
An adaptive subdivision method with crack prevention for rendering beta-spline objects
[AD-A184249] N88-12940
SPRAYERS
The TAB method for numerical calculation of spray droplet breakup
[DE87-011756] N88-12743
SPRAYING
Ceramics thin film N88-12505
Fire extinguishment and inhibition in spacecraft environments N88-12523
SPUTTERING
Tribological properties of rf-sputtered MoS2 coatings
[DE88-000266] N88-12602
Monocrystal sputtering by the computer simulation code ACOCT
[IPPJ-848] N88-13095
Non-lattice matched metallic superlattices
[DE87-011512] N88-13062

STABILITY
Atomic frequency standards for ultra-high-frequency stability N88-12685
The shifted Adams method for ordinary differential equations
[DE88-000610] N88-12994
Variable collision frequency effects on hose and sausage instabilities in relativistic electron beams
[AD-A184206] N88-13021
STAINLESS STEELS
Mechanical properties of a microalloyed steel with high niobium content
[DE87-703545] N88-12572
Partial substitution of vanadium by niobium in AISI H13 steel
[DE87-703548] N88-12575
The aging behavior of types 308 and 308CRE stainless steels and its effect on mechanical properties
[DE87-012541] N88-12590
Creep life prediction based on stochastic model of microstructurally short crack growth
[NASA-TM-100245] N88-12825
Damping characteristics of a composite-reinforced stainless-steel plate
[DE88-000303] N88-12828
Pulsed eddy-current inspection of thin-walled stainless steel tubing
[DE88-001492] N88-12830
Data base on the high heat flux behaviour of metals and carbon materials for plasma facing components: Experiments at the 10 MW neutral beam injection test stand of the IPP Nagoya
[IPPJ-AM-53] N88-13031
STANDARDS
Fire-related standards and testing N88-12522
The atomic weight and isotopic composition of oxygen and their variation in nature
[DE87-014397] N88-12558
Atomic frequency standards for ultra-high-frequency stability N88-12685
Optimization of dilatometer test procedures
[DE87-014998] N88-12769
Standard fatigue test specimens for fastener evaluation
[AGARD-AG-304] N88-12818
STAPHYLOCOCCUS
Study of certain biological characteristics of bacteria during the French-Soviet CYTOS-2 space experiment N88-12917
STAR FORMATION
The Einstein survey of the young stars in the Orion Nebula N88-13182
STARS
Calibration of the Ca II K line-core density and the magnetic flux density in stars using solar data N88-13116
Active phases on II Peg N88-13119
The giant spot on II Peg in 1966 N88-13120
Spectral analysis of APT RS CVn binary light curves N88-13122
Starspots on the short-period RS CVn system SV Cam: 45 years of activity N88-13123
The short-period RS CVn stars: Starspots and fundamental properties N88-13124
Doppler snapshots N88-13125
Titanium oxide absorption and spot sizes in II Peg, HR 1099 and UX Ari N88-13126
Spectroscopic monitoring of RS CVn stars at Kitt Peak using the Penn State fiber optic echelle N88-13127
The X-ray orbital lightcurves of AR Lac and TY Pyx N88-13129
X-rays, color, and the Vaughan-Preston gap N88-13135
Stellar activity and the rotation of Hyades stars N88-13139
STATIC LOADS
Static standing and dynamic walking of a practical biped robot
[DE88-001367] N88-12795
STATISTICAL ANALYSIS
Spatial strength variation and statistical size effect of laminated orthotropic composite materials N88-12646
Robust statistical methods for automated outlier detection N88-12681
Statistics of the geomagnetic secular variation for the past 5Ma
[NASA-CR-181558] N88-12890
Statistical inference: Computer oriented algorithmic approach
[DE87-013874] N88-12948
An urn model for the multi-sample capture/recapture sequential tagging process
[AD-A184470] N88-12998
Statistical properties of small high-velocity events in the solar transition region N88-13112
STATISTICAL CORRELATION
The velocity structure and turbulence at the center of the Orion Nebula N88-13201
STEADY STATE
Proceedings of the Japan-US Workshop P-92 on Plasma Material Interaction/High Heat Flux Data Needs for the Next Step Ignition and Steady State Devices
[DE87-013568] N88-13042
PISCES: Plasma-surface interactions and materials research
[DE88-001323] N88-13044
STEAM
National Aerospace Laboratory experiment N88-12509
STEAM FLOW
National Aerospace Laboratory experiment N88-12509
STEELS
Sintered steels of high resistance alloyed to Nb, Mo, Mn and Si
[DE87-703546] N88-12573
Progress in the development of niobium alloyed high speed steel
[DE87-703549] N88-12576
Hadfield steels with Nb and Ti carbides
[DE87-703706] N88-12579
Corrosion of ferritic steels by molten lithium: Influence of competing thermal gradient mass transfer and surface product reactions
[DE88-000334] N88-12585
Effects of stress-relieving on the mechanical properties and the structure of specimens of high-temperature fine-grained structural steels heat-treated to simulate welding
[BLL-CE-TRANS-8258-(9022.09)] N88-12586
Influence of creep on the precipitate structure under conditions of long-term creep. 4: Experiments on 10 CrMo 9 10 steel
[BLL-CE-TRANS-8258-(9022.09)] N88-12589
STEERING
GPS vertical axis performance enhancement for helicopter precision landing approach
[NASA-CR-177443] N88-12477
STELLAR ACTIVITY
Fifth Cambridge Workshop on Cool Stars, Stellar Systems and the Sun N88-13092
The photospheric magnetic fields of cool stars: Recent results of survey and time-variability programs N88-13094
Observational constraints and evidence for saturation N88-13097
Heating of stellar chromospheres and coronae: Evidence for non-magnetic basal heating N88-13098
Active phases on II Peg N88-13119
Stellar activity and the rotation of Hyades stars N88-13139
Activity in warm stars N88-13142
Measurements of stellar magnetic fields: Empirical constraints on dynamo and rotational evolution theories N88-13185
STELLAR ATMOSPHERES
Atmospheres of stars in the limits of thin and thick convection zones: The M dwarfs N88-13104
Atmospheres of stars in the limits of thick and thin convection zones: M giants N88-13105
Spectroscopic monitoring of RS CVn stars at Kitt Peak using the Penn State fiber optic echelle N88-13127
Magnetic fields on K and M stars N88-13137
Activity in warm stars N88-13142
Empirical relations between photospheric magnetic fields and atmospheric radiative losses for cool dwarf stars N88-13145
A flash spectrum of Cl I, C I, N I, and Ni II absorption in 31 Cygni: A direct observation of the reversing layer N88-13158
Application of dynamic atmosphere models to the analysis of angular diameter observations of Mira variables N88-13168
IUE observations of the hybrid K3 II star Iota Aurigae and constraints on the outer atmospheric structure N88-13171
Time series infrared spectroscopy of long period variables N88-13172
Water masers associated with 2 carbon stars: EU Andromedae and V778 Cygni N88-13176
Gamma ray lines from novae N88-13214
STELLAR COLOR
Stellar activity and the rotation of Hyades stars N88-13139
JHK photometry of CN-rich field giants N88-13175
Radio emission from RS CVn binaries: A 5 GHz VLA survey of 93 systems N88-13191
STELLAR CORONAS
A re-examination of the corona-wind dividing line: Diagnostics of non-coronal atmospheres N88-13101
X-rays, color, and the Vaughan-Preston gap N88-13135
Relations between chromospheric and coronal structure, flux-flux correlations and convective zone properties N88-13138
STELLAR ENVELOPES
Emission features in IRAS LRS spectra of MS, S and CS stars N88-13163
Winds and shells around low-mass supergiants N88-13164
Far infrared circumstellar debris shells of red supergiant stars N88-13165
STELLAR EVOLUTION
Angular momentum evolution of young stars N88-13099
Post-zero-age main sequence rotation N88-13100
Atmospheres of stars in the limits of thick and thin convection zones: M giants N88-13105
Disk accretion during the early stages of stellar evolution N88-13106
The onset of chromospheric activity among the A- and F- type stars N88-13144
Neutron capture nucleosynthesis in low mass AGB stars N88-13178
Spin-up and spin-down on the way to the main sequence N88-13181
The Einstein survey of the young stars in the Orion Nebula N88-13182
Measurements of stellar magnetic fields: Empirical constraints on dynamo and rotational evolution theories N88-13185
Stromgren photometry of RSCVn and HD108102 N88-13187
Influences of the astrophysical environment on nuclear decay rates
[DE88-001461] N88-13208
STELLAR FLARES
Atmospheres of stars in the limits of thin and thick convection zones: The M dwarfs N88-13104
Evidence for an additional source of opacity during the impulsive phase of stellar flares N88-13133
The Parkes radio survey of active chromosphere stars N88-13141
Exosat results on the dMe flare Star Wolf 630AB and on VB 8 N88-13151
IUE/Optical/VLA flares on AD Leo N88-13152
A helium flare on the active G5 dwarf Kappa Ceti N88-13189
STELLAR LUMINOSITY
The closest solar analogs in the bright star catalogue N88-13110
The Wilson-Bappu relationship: A barometric effect N88-13170
Pre-main sequence activity: How far is magnetism involved N88-13179
The contribution of accretion luminosity to the infrared spectra of T Tauri stars: A possible test N88-13183
M dwarfs from the Einstein medium sensitivity survey N88-13188
Radio emission from RS CVn binaries: A 5 GHz VLA survey of 93 systems N88-13191
STELLAR MAGNETIC FIELDS
Fifth Cambridge Workshop on Cool Stars, Stellar Systems and the Sun N88-13092
Measurements of stellar magnetic fields N88-13093
The photospheric magnetic fields of cool stars: Recent results of survey and time-variability programs N88-13094
Nonthermal phenomena in stellar coronae: Evidence from radio observations N88-13096
Calibration on the Sun for stellar magnetic fields N88-13113
Large scale solar and stellar magnetic fields N88-13117
The short-period RS CVn stars: Starspots and fundamental properties N88-13124
Evidence for expanding magnetic loops in coronae of cool stars N88-13134
Magnetic fields on K and M stars N88-13137
Activity in warm stars N88-13142
Empirical relations between photospheric magnetic fields and atmospheric radiative losses for cool dwarf stars N88-13145
Pre-main sequence activity: How far is magnetism involved N88-13179
Measurements of stellar magnetic fields: Empirical constraints on dynamo and rotational evolution theories N88-13185
Observations and analysis of the photospheric magnetic fields on dwarf G, K and M stars N88-13198
STELLAR MAGNITUDE
The closest solar analogs in the bright star catalogue N88-13110
STELLAR MASS
Flux tube dynamics and solar/stellar redshift measurements N88-13095

Atmospheres of stars in the limits of thick and thin convection zones: M giants N88-13105
Disk accretion during the early stages of stellar evolution N88-13106
Microwave observations of nonthermal phenomena in pre-main sequence stars N88-13107
The closest solar analogs in the bright star catalogue N88-13110
Application of dynamic atmosphere models to the analysis of angular diameter observations of Mira variables N88-13168
Neutron capture nucleosynthesis in low mass AGB stars N88-13178

STELLAR MASS ACCRETION
The contribution of accretion luminosity to the infrared spectra of T Tauri stars: A possible test N88-13183

STELLAR MASS EJECTION
IRAS and cool stellar mass loss N88-13166

STELLAR MODELS
Relations between chromospheric and coronal structure, flux-flux correlations and convective zone properties N88-13138

STELLAR ORBITS
Asynchronous rotation in close binary systems with circular orbits N88-13131

STELLAR PHYSICS
Active phases on II Peg N88-13119
The short-period RS CVn stars: Starspots and fundamental properties N88-13124

STELLAR RADIATION
A comprehensive exploration of late-type stars in the far-ultraviolet N88-13194

STELLAR ROTATION
Angular momentum evolution of young stars N88-13099
Post-zero-age main sequence rotation N88-13100
Large scale solar and stellar magnetic fields N88-13117
Asynchronous rotation in close binary systems with circular orbits N88-13131
Relations between chromospheric and coronal structure, flux-flux correlations and convective zone properties N88-13138
Stellar activity and the rotation of Hyades stars N88-13139
Broadband linear polarization and chromospheric CaII H and K line emission in late-type main sequence stars N88-13140
The delta upsilon = 1 fundamental bands of carbon monoxide in late-type stars N88-13177
Spin-up and spin-down on the way to the main sequence N88-13181
Observations and analysis of the photospheric magnetic fields on dwarf G, K and M stars N88-13196

STELLAR SPECTRA
A large X-ray flare on squared Sigma coronae borealis observed with exosat N88-13121
Spectroscopic monitoring of RS CVn stars at Kitt Peak using the Penn State fiber optic echelle N88-13127
H alpha and Ca II emission line variability of FK comae N88-13128
PG 0308 + 096: A short-period white dwarf + dM binary with strongly modulated H-alpha emission N88-13132
Evidence for an additional source of opacity during the impulsive phase of stellar flares N88-13133
Magnetic fields on K and M stars N88-13137
The Wilson-Bappu relationship: A barometric effect N88-13170
IUE observations of the hybrid K3 II star Iota Aurigae and constraints on the outer atmospheric structure N88-13171
Time series infrared spectroscopy of long period variables N88-13172
Synthetic spectra for the N-type carbon star TX Psc N88-13173
Water masers associated with 2 carbon stars: EU Andromedae and V778 Cygni N88-13176
The delta upsilon = 1 fundamental bands of carbon monoxide in late-type stars N88-13177
Pre-main sequence activity: How far is magnetism involved N88-13179
Chromospheric variability mechanisms affecting pre-main sequence stars N88-13180
Measurements of stellar magnetic fields: Empirical constraints on dynamo and rotational evolution theories N88-13185
IRAS and near IR obeservations of active binaries N88-13186
M dwarfs from the Einstein medium sensitivity survey N88-13188
A helium flare on the active G5 dwarf Kappa Ceti N88-13189
A comprehensive exploration of late-type stars in the far-ultraviolet N88-13194

STELLAR SPECTROPHOTOMETRY
VLA observations of rapid 6 cm flux variations in alpha Ori N88-13169
Infrared excesses of barium stars N88-13174
JHK photometry of CN-rich field giants N88-13175
Stromgren photometry of RSCVn and HD106102 N88-13187

STELLAR STRUCTURE
The onset of chromospheric activity among the A- and F- type stars N88-13144

STELLAR SYSTEMS
Fifth Cambridge Workshop on Cool Stars, Stellar Systems and the Sun N88-13092

STELLAR TEMPERATURE
Application of dynamic atmosphere models to the analysis of angular diameter observations of Mira variables N88-13168
Pre-main sequence activity: How far is magnetism involved N88-13179

STELLAR WINDS
A re-examination of the corona-wind dividing line: Diagnostics of non-coronal atmospheres N88-13101
The acceleration of winds by MHD waves in open magnetic structures N88-13109
Radio continuum emission from the ionized stellar winds of the cool supergiants in zeta Aurigae-like systems N88-13160
Winds and shells around low-mass supergiants N88-13184

STELLARATORS
The role of stellarators in the advanced toroidal program [DE87-014815] N88-13025

STIFFENING
Vibration and buckling of geometrically imperfect laminated cylindrical shells N88-12622

STIRLING CYCLE
Design concepts for the ASTROMAG cryogenic system [NASA-CR-181505] N88-13060

STOCHASTIC PROCESSES
Some stochastic aspects of intergranular creep cavitation [DE88-000065] N88-12581
The TAB method for numerical calculation of spray droplet breakup [DE87-011756] N88-12743

STORMS
NWS (National Weather Service) watch/warning verification flash flood, winter storm and high wind, January 1980 - June 1986 [PB87-223053] N88-12898

STORMS (METEOROLOGY)
Theory of heat and moisture exchange between finely disperse storm-generated spray and turbulent air flow N88-12851

STRAIN HARDENING
Hadfield steels with Nb and Ti carbides [DE87-703706] N88-12579

STRAIN RATE
Work-in-progress presented at the Army Symposium on Solid Mechanics, 1986: Lightening of the Force [AD-A184791] N88-12644
A direct method to obtain constitutive model constants from cylinder impact test results N88-12647
Influence of strain rate and notch depth on tensile properties of HITCO 6250 [DE88-001324] N88-12816
The evolution of plastic strain in steady, plastic shock waves [DE87-013812] N88-12826

STRAPDOWN INERTIAL GUIDANCE
NAVSIM 2: A computer program for simulating aided-inertial navigation for aircraft [NASA-CR-177438] N88-12478

STRATEGY
Technology transfer to China [PB87-223418] N88-13067

STRATIFICATION
Influence of stratification in near-surface water layer on intensity of gas exchange between atmosphere and water N88-12841

STREAM FUNCTIONS (FLUIDS)
Optimization of explicit time-stepping algorithms and Stream-Function-Coordinate (SFC) concept for fluid dynamics problems N88-12762

STREAMLINING
Observations on the hydrodynamic flow visualization at ONERA [PD-FM-8718] N88-12753

STRESS ANALYSIS
Failure analysis of composite structure materials [AD-A184468] N88-12548
On the stressing of annealed NITINOL: The electrical resistance and calorimetric effects [AD-A184465] N88-12569
Effects of stress-relieving on the mechanical properties and the structure of specimens of high-temperature fine-grained structural steels heat-treated to simulate welding [BLL-CE-TRANS-8258-(9022.09)] N88-12586
Influence of creep on the precipitate structure under conditions of long-term creep. 4: Experiments on 10 CrMo 9 10 steel [BLL-CE-TRANS-8256-(9022.09)] N88-12589
Influence of strain rate and notch depth on tensile properties of HITCO 6250 [DE88-001324] N88-12816
Higher order theory analysis of a modified free-edge delamination specimen N88-12820
The evolution of plastic strain in steady, plastic shock waves [DE87-013812] N88-12826
A comparison of structural frequency response functions measured with forces from 500 to 250,000 lb [DE88-000668] N88-12829
Large change-of-curvature effects in quadratic finite elements for CAD of membrane structures N88-12958

STRESS CORROSION
Influence of some parameters on the stress corrosion of a ABNT 304 stainless steel in MgCl/sub 2/ [DE87-703707] N88-12580

STRESS CORROSION CRACKING
Effects of stress-relieving on the mechanical properties and the structure of specimens of high-temperature fine-grained structural steels heat-treated to simulate welding [BLL-CE-TRANS-8258-(9022.09)] N88-12586

STRESS DISTRIBUTION
Free-edge delamination: Laminate width and loading conditions effects [NASA-TM-100236] N88-12551
Plastic strain localization between voids in shear deformation fields N88-12648

STRESS INTENSITY FACTORS
Large change-of-curvature effects in quadratic finite elements for CAD of membrane structures N88-12958

STRESS-STRAIN RELATIONSHIPS
A direct method to obtain constitutive model constants from cylinder impact test results N88-12647

STRING THEORY
Cosmological applications of singular hypersurfaces in general relativity N88-13202

STRUCTURAL ANALYSIS
Reduced complexity structural modeling for automated airframe synthesis [NASA-CR-177440] N88-12453
An integrated study of structures, aerodynamics and controls on the forward swept wing X-29A and the oblique wing research aircraft [NASA-CR-181548] N88-12486
USSR report: Engineering and equipment [JPRS-UEQ-87-008] N88-12621
Work-in-progress presented at the Army Symposium on Solid Mechanics, 1986: Lightening of the Force [AD-A184791] N88-12644
Explicit and implicit soil modelling for dynamic soil-structure interaction problems N88-12650
Corrosion control by composite material substitution with application to the M-939 5-ton truck N88-12654
Detection of defects on structures [EP-PATENT-0-210-794-A2] N88-12807
A refined nonlinear analysis of laminated composite plates and shells [AD-A184436] N88-12811
Extremum methods of structural analysis for system reliability assessment N88-12824
Light funnel concentrator panel for solar power [NASA-CR-179223] N88-12870
Methods for design and evaluation of integrated hardware/software systems for concurrent computation [NASA-CR-181522] N88-12953
Large change-of-curvature effects in quadratic finite elements for CAD of membrane structures N88-12958
COLA2: A computer program for the structural synthesis of two components using general modal coordinates [DE88-001457] N88-12963
Nuclear techniques in studies of condensed matter [NASA-RP-1195] N88-13015
Novel dynamical investigations of excitons and their structure in semiconductors [DE87-014868] N88-13070

STRUCTURAL DESIGN
Parachute materials [DE87-014845] N88-12550
Design of digital filters for electronic instrumentation [PB87-100418] N88-12716
Design of efficient FIR filters with minimal delay [PB87-100434] N88-12717

STRUCTURAL DESIGN CRITERIA
Rational reinforcement of cylindrical shells with variable stiffness frames subjected to external pressure N88-12638

STRUCTURAL RELIABILITY
A reliability concept for optimizing aircraft design N88-12622

STRUCTURAL STABILITY
Vibration and buckling of geometrically imperfect laminated cylindrical shells N88-12822

SUBDIVISIONS
An adaptive subdivision method with crack prevention for rendering beta-spline objects [AD-A184249] N88-12940

SUBGIANT STARS
Infrared excesses of barium stars N88-13174

SUBROUTINE LIBRARIES (COMPUTERS)
The SUPRENUM communications subroutine library for grid-oriented problems [DE88-000137] N88-12950

SUBSONIC FLOW
Solution of the two-dimensional Euler equations on unstructured triangular meshes N88-12469

SUBSONIC SPEED
Aerodynamic sensitivities from subsonic, sonic and supersonic unsteady, nonplanar lifting-surface theory [NASA-TM-100502] N88-12459

SUBSTRUCTURES
Mechanical strength and niobium and niobium-base alloys substructures [DE87-703692] N88-12577

SUMMARIES
Summaries of physical research in the geosciences [DE88-000833] N88-12896

SUN
Fifth Cambridge Workshop on Cool Stars, Stellar Systems and the Sun N88-13092
Calibration on the Sun for stellar magnetic fields N88-13113
Variations of the vertical and horizontal velocities of the small-scale structures and the physical problems related to overshoot layers N88-13115
The dynamics of solar magnetic flux tubes subjected to resonant foot point shaking N88-13118

SUNSPOT CYCLE
Three-halves law in sunspot cycle shape [NASA-CR-181520] N88-13210

SUNSPOTS
The giant spot on II Peg in 1986 N88-13120
Spectral analysis of APT RS CVn binary light curves N88-13122
Starspots on the short-period RS CVn system SV Cam: 45 years of activity N88-13123
The short-period RS CVn stars: Starspots and fundamental properties N88-13124
Titanium oxide absorption and spot sizes in II Peg, HR 1099 and UX Ari N88-13126

SUPERCOMPUTERS
Numerical simulation system N88-12511
Center for Supercomputing Research and Development (CEDAR) [DE88-000807] N88-12930
The SUPRENUM communications subroutine library for grid-oriented problems [DE88-000137] N88-12950

SUPERCONDUCTING MAGNETS
Design concepts for the ASTROMAG cryogenic system [NASA-CR-181505] N88-13060

SUPERCONDUCTIVITY
Experimental perspectives on heavy electron metals [DE87-014766] N88-12583
Valence bond theory and superconductivity [AD-A184274] N88-13052
The chemical bond and superconductivity [AD-A184275] N88-13053
Non-lattice matched metallic superlattices [DE87-011512] N88-13062

SUPERCONDUCTORS
Topological aspects of infinite metal clusters and superconductors [AD-A184104] N88-13049
Magnetic field dependence of the specific heat of some high-T/sub c/ superconductors [DE87-014078] N88-13063

SUPERCRITICAL FLUIDS
Retention processes in supercritical fluid chromatography [DE88-000079] N88-12559
Thermodynamic properties of supercritical mixtures [DE88-000809] N88-12562

SUPERFLUIDITY
Design concepts for the ASTROMAG cryogenic system [NASA-CR-181505] N88-13060

SUPERGIANT STARS
Fifth Cambridge Workshop on Cool Stars, Stellar Systems and the Sun N88-13092
The acceleration of winds by MHD waves in open magnetic structures N88-13109
An analysis of the photospheric line profiles in F, G, and K supergiants N88-13157
A flash spectrum of Cl I, C I, N I, and Ni II absorption in 31 Cygni: A direct observation of the reversing layer N88-13158
Sensitivity of the H alpha line to expansion, geometrical extent and temperature gradient in the G and K supergiant chromospheres N88-13159
Radio continuum emission from the ionized stellar winds of the cool supergiants in zeta Aurigae-like systems N88-13160
Winds and shells around low-mass supergiants N88-13164
Far infrared circumstellar debris shells of red supergiant stars N88-13165
A comprehensive exploration of late-type stars in the far-ultraviolet N88-13194

SUPERHIGH FREQUENCIES
X-band uplink ground systems development: Part 2 N88-12703

SUPERLATTICES
Non-lattice matched metallic superlattices [DE87-011512] N88-13062

SUPERNOVAE
Core bounce supernovae [DE87-014910] N88-13197

SUPERSATURATION
Microgravity nucleation and particle coagulation experiments support [NASA-CR-181540] N88-12618
Microgravity nucleation and particle coagulation experiments support [NASA-CR-181541] N88-12619

SUPERSONIC COMBUSTION RAMJET ENGINES
SCRAM JET (Supersonic Combustion Ramjet) combustion experiments N88-12512

SUPERSONIC FLOW
Experimental and theoretical study of condensation in multicomponent mixtures [DE88-000897] N88-12563
Conical wing with maximum lift-to-drag ratio in supersonic gas flow N88-12633
Numerical study of supersonic flow around blunt bodies with extended needle nose N88-12635

SUPERSONIC SPEED
Aerodynamic sensitivities from subsonic, sonic and supersonic unsteady, nonplanar lifting-surface theory [NASA-TM-100502] N88-12459
The aerodynamics of supersonic parachutes [DE87-014846] N88-12484

SUPERSONICS
Planform effects on the supersonic aerodynamics of multibody configurations [NASA-TP-2762] N88-12454

SUPERSYMMETRY
A supersymmetric Lagrangian for Poincare gauge theories of gravity [DE88-001670] N88-13078

SUPPORT SYSTEMS
Repulsive force support system feasibility study [NASA-CR-178400] N88-12497
The effect of mass, wind angle and erection technique on the aeroelastic behaviour of a cable-stayed bridge model [NAE-AN-46] N88-12819

SURFACE CRACKS
Thermomechanical cracking in coated media due to high speed asperity excitation [AD-A184176] N88-12809

SURFACE LAYERS
Far-infrared spectra of lithium deposited on a gold electrode: Interpretation using a cluster model [AD-A184231] N88-13050
Atomic and electronic structure of surfaces and chemisorbed layers [DE87-014987] N88-13065
Cosmological applications of singular hypersurfaces in general relativity N88-13202

SURFACE NAVIGATION
Autonomous Land Vehicle (ALV) planning and navigation system [AD-A184243] N88-12475

SURFACE PROPERTIES
Characterization of catalysts with metal-support effects and of the species adsorbed on their surfaces [DE87-014636] N88-12564
Characterization of thin layers for optics [PB87-217949] N88-13017
Calibration on the Sun for stellar magnetic fields N88-13113
The dynamics of solar magnetic flux tubes subjected to resonant foot point shaking N88-13118

SURFACE REACTIONS
Surface catalytic degradation study of two linear perfluoropolyalkylethers at 345 C [NASA-TP-2774] N88-12543
Simulation studies for surfaces and materials strength [NASA-CR-181535] N88-12557
Influence of stratification in near-surface water layer on intensity of gas exchange between atmosphere and water N88-12841

SURFACES
Aerodynamic sensitivities from subsonic, sonic and supersonic unsteady, nonplanar lifting-surface theory [NASA-TM-100502] N88-12459

SURFACTANTS
Influence of surfactants on damping of gravity-capillary waves. 1: Frequency dependence N88-12843

SURGES
Departmental report on program EMTP-machine windings surge transients: Travelling wave method [PB87-123733] N88-12719

SURVEYS
Subjective probability, combination of expert opinion and probabilistic approaches to information retrieval N88-13085
The Parkes radio survey of active chromosphere stars N88-13141

SUSPENDING (MIXING)
Optical instrumentation and study of gas-solid suspension flows [DE88-000147] N88-12744

SWEEP EFFECT
Three-dimensional unsteady flow elicited by finite wings and complex configurations N88-12468

SWEPT WINGS
Three-dimensional unsteady flow elicited by finite wings and complex configurations N88-12468
Calculation of three-dimensional stationary turbulent boundary layer on root section of wing ignoring compressibility N88-12630

SYMMETRY
The finite element method for electronic structure [DE88-001708] N88-12989

SYNAPSES
Large-scale neuronal circuits for selective storage and recognition of complex stimuli, a pilot study [AD-A184134] N88-12920

SYNCHRONISM
Comparing barrier algorithms [NASA-CR-178377] N88-12934
Asynchronous rotation in close binary systems with circular orbits N88-13131

SYNCHROTRON RADIATION
Resistor cooling in a vacuum [DE88-000696] N88-12733
Center for X-Ray Optics, 1986 [DE88-000715] N88-12783
The generation and suppression of synchrotron sidebands [DE88-000532] N88-12787

SYNCHROTRONS
National Synchrotron Light Source users manual: Guide to the VUV and X-ray beam lines [DE88-001464] N88-13020

SYNTHESIS
Reduced complexity structural modeling for automated airframe synthesis [NASA-CR-177440] N88-12453

SYNTHESIS (CHEMISTRY)
Ceramics thin film N88-12505
Synthesis, NMR characterization and electrical properties of siloxane-based polymer electrolytes [AD-A184184] N88-12596
Conductive polymers via reactive oligomer [AD-A184270] N88-12597
Thermoplastic elastomers as LOVA (Low Vulnerability Ammunition) binders [AD-A184350] N88-12599
Proton abstraction as a route to conductive polymers [AD-A184019] N88-12612

SYNTHETIC FIBERS
Molecular composites: Processing, post-treatment and mechanics [AD-A184458] N88-12547
Structure of thermotropic polyesters with large substituents [AD-A184086] N88-12595
Solid state C-13 NMR characterization of textiles: Qualitative and quantitative analysis [AD-A184349] N88-12598

SYNTHETIC FUELS
Emerging environmental constraints on the use of gasoline and diesel fuel and tradeoffs associated with the use of alternative fuels [DE87-011504] N88-12614

SYSTEMS ANALYSIS
An evaluation plan of bus architectures and protocols using the NASA Ames intelligent redundant actuation system
[NASA-CR-177458] N88-12482
On dynamic loads in parallel shaft transmissions. 1: Modelling and analysis
[NASA-TM-100180] N88-12797
PRAAGE: An interactive IBM-PC code for unreliability/aging analysis
[DE87-012124] N88-12803
Extremum methods of structural analysis for system reliability assessment N88-12824
Performance analysis of solar thermal power systems
[DE88-000563] N88-12874
Applications of the hybrid automated reliability predictor
[NASA-TP-2760] N88-12928
Software maintenance in scientific and engineering environments: An introduction and guide
[NASA-CR-177409] N88-12954
Investigation, development and application of optimal output feedback theory. Vol. 4: Measures of eigenvalue/eigenvector sensitivity to system parameters and unmodeled dynamics
[NASA-CR-4108] N88-12969
Propagation of random initial conditions in time N88-12993
SYSTEMS ENGINEERING
Multicast gateway design considerations
[PB87-219980] N88-12663
SYSTEMS INTEGRATION
Methods for design and evaluation of integrated hardware/software systems for concurrent computation
[NASA-CR-181522] N88-12953
GOLD: Integration of model-based control systems with artificial intelligence and workstations
[DE88-000706] N88-12977
SYSTEMS STABILITY
Closed-loop system analysis using Lyapunov stability theory N88-12978
SYSTOLIC ARRAYS
Implementation and performance of a complex vision system on a systolic array machine
[AD-A184331] N88-12971

T

T TAURI STARS
Angular momentum evolution of young stars N88-13099
Disk accretion during the early stages of stellar evolution N88-13106
The contribution of accretion luminosity to the infrared spectra of T Tauri stars: A possible test N88-13183
T-33 AIRCRAFT
Access to microgravity: A technical description of the NAE T-33 microgravity facility
[NAE-AN-47] N88-12518
TACTICS
An interactive computer graphics network monitor for a tactical communications network
[AD-A184131] N88-12938
TAIL ASSEMBLIES
Effect of permissible variations of center-of-gravity locations of cargo airplane on its mass N88-12625
TAIL SURFACES
Effect of permissible variations of center-of-gravity locations of cargo airplane on its mass N88-12625
TAKEOFF
Optimum take-off run of aircraft on ground airfields N88-12623
TANKS (COMBAT VEHICLES)
Weldability of 2219-T851 and 2519-T87 aluminum armor alloys for use in Army vehicle systems
[AD-A184296] N88-12792
TASKS
Some data processing requirements for precision Nap-Of-the-Earth (NOE) guidance and control of rotorcraft
[NASA-CR-177453] N88-12493
The characterization of diagnostic tasks for engineering systems
[DE88-000093] N88-12973
TECHNOLOGY ASSESSMENT
Progress in improving weather forecasting viewed N88-12833
The role of basic research in society
[DE88-000459] N88-13090
TECHNOLOGY TRANSFER
The attitudes of science policy, environmental, and utility leaders on US energy issues and fusion
[DE88-000784] N88-13041
Technology transfer to China
[PB87-223418] N88-13067
TECHNOLOGY UTILIZATION
Lasers measure atmosphere N88-12849
TELECOMMUNICATION
Heterogeneous multi-trunking queusing systems
[AD-A184255] N88-12668
The Telecommunications and Data Acquisition Report
[NASA-CR-181546] N88-12679
TELEMETRY
Detection of signals by weighted integrate-and-dump filter N88-12696
Analysis of the ICE combiner for multiple antenna arraying N88-12704
TELESCOPES
Spectral analysis of APT RS CVn binary light curves N88-13122
H alpha and Ca II emission line variability of FK comae N88-13128
TELLURIUM
Thermal expansion of some Ge-Se-Te glasses
[PD-MT-8722] N88-12606
Studies on some Ge-Se-Te glasses
[PD-MT-8721] N88-12607
TEMPERATURE
Studies of pressure-velocity coupling schemes for analysis of incompressible and compressible flows
[NASA-CR-181526] N88-12748
TEMPERATURE CONTROL
Traveling-wave maser closed-cycle refrigerator data acquisition and display system N88-12708
Two-watt, 4-Kelvin closed cycle refrigerator performance N88-12709
TEMPERATURE DEPENDENCE
Ignition and combustion of metals in oxygen N88-12530
Retention processes in supercritical fluid chromatography
[DE88-000079] N88-12559
Experimental perspectives on heavy electron metals
[DE87-014766] N88-12583
Magnetic field dependence of the specific heat of some high-T/sub c/ superconductors
[DE87-014078] N88-13063
TEMPERATURE DISTRIBUTION
Thermal analysis of electromagnetic launcher rails
[DE88-000166] N88-12514
Microgravity nucleation and particle coagulation experiments support
[NASA-CR-181540] N88-12618
Microgravity nucleation and particle coagulation experiments support
[NASA-CR-181541] N88-12619
Resistivity of EuBa2(Cu/sub 1-y/Zn/sub y/)3O/sub x/ as a ffunction of temperature, magnetic field, pressure and Zn concentration
[DE87-014740] N88-13069
Flux tube dynamics and solar/stellar redshift measurements N88-13095
TEMPERATURE EFFECTS
Structure of thermotropic polyesters with large substituents
[AD-A184086] N88-12595
Effect of time and temperature on transformation toughened zirconias
[AD-A184356] N88-12600
Pipe and bend erosion by pneumatic transport of solids at high temperature
[DE88-001345] N88-12658
TEMPERATURE GRADIENTS
Corrosion of ferritic steels by molten lithium: Influence of competing thermal gradient mass transfer and surface product reactions
[DE88-000334] N88-12585
Influence of stratification in near-surface water layer on intensity of gas exchange between atmosphere and water N88-12841
Thermophoresis of spherical aerosol particle at arbitrary Knudsen numbers N88-12850
Evaluation of the Mellen EDG furnace for growth of large diameter GaAs single crystals in a horizontal configuration
[DE88-000463] N88-13068
Sensitivity of the H alpha line to expansion, geometrical extent and temperature gradient in the G and K supergiant chromospheres N88-13159
TEMPERATURE MEASUREMENT
Resistor cooling in a vacuum
[DE88-000696] N88-12733
Noncontact temperature measurements of hot steel bodies using an electromagnetic acoustic transducer (EMAT)
[DE88-000560] N88-12765
Calibration of a laser-pumped, thermographic phosphor remote thermometry system
[DE88-000452] N88-12781
TEMPERING
Partial substitution of vanadium by niobium in AISI H13 steel
[DE87-703548] N88-12575
TEMPORAL DISTRIBUTION
Optimization of explicit time-stepping algorithms and Stream-Function-Coordinate (SFC) concept for fluid dynamics problems N88-12762
TEMPORAL RESOLUTION
Visual evoked responses to sinusoidal gratings presented in central and right visual fields: 1
[DE87-014731] N88-12919
TENSILE PROPERTIES
Carbon fiber reinforced glass matrix composites for space based applications
[AD-A184355] N88-12546
Molecular composites: Processing, post-treatment and mechanics
[AD-A184458] N88-12547
Mechanical behavior of a controlled rolled high-strength low alloy steel plate, microalloyed with Nb and V
[DE87-703507] N88-12571
Welding and weldability of ductile intermetallic alloys
[DE87-014061] N88-12582
The accommodation of precipitate plates modelled as a tensile test
[DE88-000207] N88-12814
Small-diameter wire tensile testing
[DE88-000635] N88-12815
Influence of strain rate and notch depth on tensile properties of HITCO 6250
[DE88-001324] N88-12816
TENSILE STRENGTH
Test number 2 of propellant for rocket motor MK52
[PB87-226155] N88-12613
Weldability of 2219-T851 and 2519-T87 aluminum armor alloys for use in Army vehicle systems
[AD-A184296] N88-12792
TENSILE TESTS
Test number 2 of propellant for rocket motor MK52
[PB87-226155] N88-12613
The accommodation of precipitate plates modelled as a tensile test
[DE88-000207] N88-12814
TERMINAL VELOCITY
Efficiency aspects of short, low velocity railguns
[AR-004-847] N88-12517
TERNARY SYSTEMS
Thermodynamic properties of supercritical mixtures
[DE88-000809] N88-12562
TERRAIN
Disturbance and recovery of Arctic Alaskan tundra terrain. A review of recent investigations
[AD-A184442] N88-12887
TEST FACILITIES
The LLNL 150-mm equation-of-state gun system
[DE88-000423] N88-12519
Measured performance of the heat exchanger in the NASA icing research tunnel under severe icing and dry-air conditions
[NASA-TM-100116] N88-12796
TEST FIRING
Failure control techniques for the SSME
[NASA-CR-179224] N88-12537
TEST PATTERN GENERATORS
Programmable Logic Arrays (PLA's) design for testability
[PB87-102935] N88-12718
TESTS
Fire-related standards and testing N88-12522
TETHERING
Analytical investigation of the dynamics of tethered constellations in Earth orbit (phase 2)
[NASA-CR-179218] N88-12533
TETHERLINES
Study of Plasma Motor Generator (PMG) tether system for orbit reboost
[NASA-CR-172015] N88-12501
TEXTILES
Solid state C-13 NMR characterization of textiles: Qualitative and quantitative analysis
[AD-A184349] N88-12598
TEXTURES
Cloud cover determination in polar regions from satellite imagery
[NASA-CR-181544] N88-12908
THEMATIC MAPPING
New precipitation map of world ocean N88-12834
THEODOLITES
Optical alignment of Centaur's inertial guidance system
[NASA-TM-88844] N88-12515
THEOREMS
Homogeneous space-time of Goedel type in higher-derivate gravity
[DE87-703690] N88-13077

THEORETICAL PHYSICS
Theoretical plasma physics
[DE88-001475] N88-13029
THERMAL ANALYSIS
Thermal analysis of electromagnetic launcher rails
[DE88-000186] N88-12514
A two-dimensional finite difference program for thermal analysis of rocket thrust chambers
[NASA-TM-100191] N88-12539
Synthesis of the monoclinic yttria by thermal plasma processing
[DE88-000496] N88-12608
Light funnel concentrator panel for solar power
[NASA-CR-179223] N88-12870
THERMAL CYCLING TESTS
Effect of long-term thermal aging on coated Celion/LARC-160 composites
[NASA-TM-100495] N88-12544
THERMAL EMISSION
Microwave observations of nonthermal phenomena in pre-main sequence stars N88-13107
THERMAL EXPANSION
Carbon-fiber reinforced plastics N88-12506
Study of zero CTE (Coefficients of Thermal Expansion) of graphite/epoxy composites
[DE87-013557] N88-12554
Thermal expansion of some Ge-Se-Te glasses
[PD-MT-8722] N88-12606
THERMAL PLASMAS
Synthesis of the monoclinic yttria by thermal plasma processing
[DE88-000496] N88-12608
THERMAL PROTECTION
Performance analysis of advanced spacecraft TPS
[NASA-CR-181532] N88-12484
Space suit extravehicular hazards protection development
[NASA-TM-100458] N88-12927
THERMAL RADIATION
The effects of minor trace gases on the transfer of thermal infrared radiation through the Earth's atmosphere N88-12893
THERMAL STRESSES
Welding and weldability of ductile intermetallic alloys
[DE87-014061] N88-12582
Thermal stress in the edge cladding of Nova glass laser disks
[DE88-000425] N88-12780
Thermomechanical cracking in coated media due to high speed asperity excitation
[AD-A184176] N88-12809
THERMOCHEMISTRY
The developmental status of solar thermochemical hydrogen production
[DE88-001778] N88-12884
THERMOCLINES
Dynamics of isolated intrathermocline eddy N88-12845
Effects of rainfall on the seasonal thermocline
[AD-A184432] N88-12912
THERMODYNAMIC CYCLES
Two-watt, 4-Kelvin closed cycle refrigerator performance N88-12709
THERMODYNAMIC PROPERTIES
Research and development on high strength ceramic heaters discussed N88-12508
Thermodynamic properties of supercritical mixtures
[DE88-000809] N88-12562
Experimental study of thermocapillary flows in a thin liquid layer with heat fluxes imposed on the free surface
[NASA-TM-100252] N88-12763
Thermodynamic properties for natural gas binaries
[PB87-226833] N88-13074
Atmospheres of stars in the limits of thick and thin convection zones: M giants N88-13105
THERMODYNAMICS
Retention processes in supercritical fluid chromatography
[DE88-000079] N88-12559
Model for ultrasonic attenuation and elastic constant in chromium and its alloys
[DE87-703476] N88-12570
Use of a thermodynamic analog for pneumatic transport in horizontal pipes
[AD-A184076] N88-12740
Coupled acoustic and ocean thermodynamic model
[AD-A184357] N88-12911
Non-lattice matched metallic superlattices
[DE87-011512] N88-13062
THERMOELASTICITY
A comparison of high damping shape memory alloys with Cu-Mn-based and Fe-Cr-based alloys
[AD-A184110] N88-12566
A dissipation principle and its consequences for structured shock waves in thermoelastic materials
[DE87-013723] N88-12813
THERMOGRAPHY
Calibration of a laser-pumped, thermographic phosphor remote thermometry system
[DE88-000452] N88-12781
THERMOGRAVIMETRY
Simultaneous TG/DSC (thermogravimetry/Differential Scanning Calorimetry) and TG/MS (thermogravimetry/Mass Spectrometry) analyses of polymeric and energetic materials
[DE88-000727] N88-12561
THERMOHYDRAULICS
Low gravity fluid-thermal experiments
[DE88-000553] N88-12620
THERMONUCLEAR POWER GENERATION
Study of Plasma Motor Generator (PMG) tether system for orbit reboost
[NASA-CR-172015] N88-12501
THERMOPHORESIS
Thermophoresis of spherical aerosol particle at arbitrary Knudsen numbers N88-12850
THERMOPLASTIC FILMS
Molecular composites: Processing, post-treatment and mechanics
[AD-A184458] N88-12547
THERMOPLASTIC RESINS
Interfacial strength development in thermoplastic resins and fiber-reinforced thermoplastic composites
[NASA-CR-181525] N88-12549
Thermoplastic elastomer compositions — cable jackets
[EP-PATENT-0-204-453-A1] N88-12593
Thermoplastic elastomers as LOVA (Low Vulnerability Ammunition) binders
[AD-A184350] N88-12599
THIN FILMS
Experimental study of thermocapillary flows in a thin liquid layer with heat fluxes imposed on the free surface
[NASA-TM-100252] N88-12763
Studies of thin surface films aim at seeing deep ocean processes N88-12847
Theory and simulations of Zone 2 microstructures in thin films
[DE87-014752] N88-13071
THIN PLATES
On the instability of thin circular shear layers N88-12467
Fatigue failure of thin porous strips N88-12640
The accommodation of precipitate plates modelled as a tensile test
[DE88-000207] N88-12814
THIN WALLS
Pulsed eddy-current inspection of thin-walled stainless steel tubing
[DE88-001492] N88-12830
THIXOTROPY
Thixotropic surface composition for phenolaldehyde resin laminates
[GB-PATENT-2-180-251-A] N88-12545
THREE DIMENSIONAL BODIES
On the recognition of curved objects
[AD-A184441] N88-12945
THREE DIMENSIONAL FLOW
Development and application of computational aerothermodynamics flowfield computer codes
[NASA-CR-181534] N88-12485
THRUST
High power ion thruster performance
[NASA-TM-100127] N88-12542
THRUST CHAMBERS
A two-dimensional finite difference program for thermal analysis of rocket thrust chambers
[NASA-TM-100191] N88-12539
THRUST VECTOR CONTROL
Effects of jet exhaust yaw vane installation and operation on the longitudinal and lateral-directional characteristics of the F-14 airplane
[NASA-TP-2769] N88-12455
THUNDERSTORMS
Experimental and analytic studies of the triggered lightning environment of the F106B
[NASA-CR-4104] N88-12897
TIME
A multiple-time-scale turbulence model based on variable partitioning of turbulent kinetic energy spectrum
[NASA-CR-179222] N88-12754
Propagation of random initial conditions in time N88-12993
TIME DEPENDENCE
Effect of time and temperature on transformation toughened zirconias
[AD-A184356] N88-12600
Alternating current circuit theory and pulsed NMR (Nuclear Magnetic Resonance)
[DE88-000641] N88-12732
Canonical transformations and exact invariants for dissipative systems
[DE87-703663] N88-12985
TIME LAG
Flap-lag equations of motion of rigid, articulated rotor blades with three hinge sequences
[NASA-TM-100023] N88-12495
CGI delay compensation
[NASA-TM-86703] N88-12932
TIME MARCHING
Application of Runge Kutta time marching scheme for the computation of transonic flows in turbomachines
[NASA-TM-86997] N88-12461
TIME SERIES ANALYSIS
Time series infrared spectroscopy of long period variables N88-13172
TIME TEMPERATURE PARAMETER
Effect of time and temperature on transformation toughened zirconias
[AD-A184356] N88-12600
TIN COMPOUNDS
The Moessbauer effect of SnI4 at high pressure
[DE87-014771] N88-13048
TITANIUM BORIDES
Carbon-fiber reinforced aluminum N88-12507
TITANIUM CARBIDES
Hadfield steels with Nb and Ti carbides
[DE87-703706] N88-12579
TITANIUM OXIDES
Characterization of catalysts with metal-support effects and of the species adsorbed on their surfaces
[DE87-014836] N88-12584
Titanium oxide absorption and spot sizes in II Peg, HR 1099 and UX Ari N88-13126
TOKAMAK DEVICES
Negative ion beams for heating and current-drive in NET
[AD-A184390] N88-13012
Data base on the high heat flux behaviour of metals and carbon materials for plasma facing components: Experiments at the 10 MW neutral beam injection test stand of the IPP Nagoya
[IPPJ-AM-53] N88-13031
Refueling and density control in the ZT-40M reversed field pinch
[DE88-000504] N88-13040
Modular pump limiter systems for large tokamaks
[DE88-001487] N88-13045
ICRF launcher studies
[DE88-001710] N88-13048
TOPOGRAPHY
Considering refraction in leveling with laser plane N88-12857
Radial orbit error reduction and sea surface topography determination using satellite altimetry N88-12861
TOPOLOGY
Topological aspects of infinite metal clusters and superconductors
[AD-A184104] N88-13049
TOROIDAL PLASMAS
Ballooning modes or Fourier modes in a toroidal plasma?
[AD-A184299] N88-13022
The role of stellarators in the advanced toroidal program
[DE87-014815] N88-13025
A three-barrel repeating pneumatic pellet injector for plasma fueling of the Joint European Torus
[DE88-000330] N88-13026
Transport simulations of the oscillating field current drive experiment in the ZT-40M reversed field pinch
[DE88-000538] N88-13027
TORQUE
Measurements and calculations of aerodynamic torques for a vertical-axis wind turbine
[DE88-001783] N88-12876
TORSION
Vibration and buckling of geometrically imperfect laminated cylindrical shells N88-12822
TOUGHNESS
Carbon fiber reinforced glass matrix composites for space based applications
[AD-A184355] N88-12546
Interfacial strength development in thermoplastic resins and fiber-reinforced thermoplastic composites
[NASA-CR-181525] N88-12549
TOXIC HAZARDS
Space station internal environmental and safety concerns N88-12527
TOXICITY
Aircraft fire safety research N88-12526
Evaluation of the sensidyne toxic gas sensor for HF (Hydrogen Fluoride) vapor
[DE88-000647] N88-12767
The toxicology and metabolism of nickel compounds
[DE87-014801] N88-12921

TRACE ELEMENTS
The effects of minor trace gases on the transfer of thermal infrared radiation through the Earth's atmosphere N88-12693
TRACKING (POSITION)
Effect of motion cues during complex curved approach and landing tasks: A piloted simulation study [NASA-TP-2773] N88-12480
A modern control theory based algorithm for control of the NASA/JPL 70-meter antenna axis servos N88-12706
Supertracks: The building blocks of chaos [DE88-001513] N88-13207
TRAFFIC CONTROL
Simulation of an enhanced TCAS 2 system in operation [NASA-CR-181545] N88-12479
TRAJECTORIES
A dissipation principle and its consequences for structured shock waves in thermoelastic materials [DE87-013723] N88-12813
Supertracks: The building blocks of chaos [DE88-001513] N88-13207
TRANSFORMATIONS (MATHEMATICS)
Group analysis of equations arising in ocean acoustics N88-12914
Canonical transformations and exact invariants for dissipative systems [DE87-703663] N88-12985
TRANSISTOR AMPLIFIERS
A 2.3-GHz cryogenically cooled HEMT amplifier for DSS 13 N88-12689
TRANSISTORS
Chemically modified microelectrode arrays. New kinds of electronic devices [AD-A184389] N88-12724
Reevaluating the worst-case radiation response of MOS transistors [DE87-014157] N88-13059
TRANSITION METALS
K-CO on transition metals: A local ionic interaction [AD-A184342] N88-13056
TRANSITION TEMPERATURE
Soliton twin boundaries of the cubic-tetragonal martensitic transformations in ferroelastic materials [DE87-014741] N88-13047
TRANSLATING
A data translation method for heterogeneous database systems N88-13081
TRANSMISSION LINES
Low-noise cryogenic transmission line N88-12688
Departmental report on program EMTP-machine windings surge transients: Travelling wave method [PB87-123733] N88-12719
TRANSMISSIONS (MACHINE ELEMENTS)
Multipath gear-friction planetary transmissions N88-12629
On dynamic loads in parallel shaft transmissions. 1: Modelling and analysis [NASA-TM-100180] N88-12797
On dynamic loads in parallel shaft transmissions. 2: Parameter study [NASA-TM-100181] N88-12798
TRANSMISSIVITY
National Aerospace Laboratory experiment N88-12509
TRANSMITTERS
Inductance effects in the high-power transmitter crowbar system N88-12687
TRANSONIC FLOW
Application of Runge Kutta time marching scheme for the computation of transonic flows in turbomachines [NASA-TM-86997] N88-12461
Concepts for radically increasing the numerical convergence rate of the Euler equations [NASA-CR-177456] N88-12463
Solution of the two-dimensional Euler equations on unstructured triangular meshes N88-12469
Some asymptotic modes of transonic vortex flow N88-12632
TRANSPORT AIRCRAFT
Effect of permissible variations of center-of-gravity locations of cargo airplane on its mass N88-12625
TRANSPORT PROPERTIES
Novel macrocyclic carriers for proton-coupled liquid membrane transport [DE88-000836] N88-12560
Heat and moisture transport in the atmospheric boundary layer [AD-A184222] N88-12904
TRANSPORT THEORY
Two-layer stratified flow analysis of gravity currents and turbidity currents in lakes, reservoirs and the ocean N88-12864
Development of the non-equilibrium reactive chemical transport code CHMTRNS [DE88-000682] N88-12964
Transport simulations of the oscillating field current drive experiment in the ZT-40M reversed field pinch [DE88-000538] N88-13027
TRAPPED PARTICLES
The free electron laser sideband instability reconsidered [AD-A184269] N88-12773
TRAPPING
Conditions for geomagnetically trapping sub-micron lunar ejecta between L = 1.2 and L = 3.1 N88-13203
TRAVELING WAVES
The 8.4-GHz low-noise maser pump source assembly N88-12705
Traveling-wave maser closed-cycle refrigerator data acquisition and display system N88-12708
Departmental report on program EMTP-machine windings surge transients: Travelling wave method [PB87-123733] N88-12719
TRENDS
Technology transfer to China [PB87-223418] N88-13087
TRIANGLES
Solution of the two-dimensional Euler equations on unstructured triangular meshes N88-12469
TRIBOLOGY
Calculation of the tribological properties of surfaces by semi-empirical methods [AD-A184283] N88-12791
Tribological properties of rf-sputtered MoS2 coatings [DE88-000266] N88-12802
TROPICAL METEOROLOGY
Annual tropical cyclone report, 1986 [AD-A184082] N88-12903
Interactions between the Asian monsoons, the tropical Pacific and the southern hemisphere extratropics N88-12907
TROPICAL REGIONS
On the interannual variability of South American climate and the Southern Oscillation N88-12905
TUNDRA
Disturbance and recovery of Arctic Alaskan tundra terrain. A review of recent investigations [AD-A184442] N88-12887
TUNING
Fast autotuning of a hydrogen maser by cavity Q modulation N88-12707
TURBIDITY
Two-layer stratified flow analysis of gravity currents and turbidity currents in lakes, reservoirs and the ocean N88-12864
TURBINE BLADES
National Aerospace Laboratory experiment N88-12509
TURBINE ENGINES
USSR report: Engineering and equipment [JPRS-UEQ-87-008] N88-12621
TURBOMACHINERY
Application of Runge Kutta time marching scheme for the computation of transonic flows in turbomachines [NASA-TM-86997] N88-12461
TURBULENCE
Investigation of low-speed turbulent separated flow around airfoils [NASA-CR-177450] N88-12471
Fully developed turbulence via Feigenbaum's period-doubling bifurcations [DE88-000242] N88-12739
Optical instrumentation and study of gas-solid suspension flows [DE88-000147] N88-12744
A multiple-time-scale turbulence model based on variable partitioning of turbulent kinetic energy spectrum [NASA-CR-179222] N88-12754
Tracking through turbulence at the Tonopah Test Range [DE88-001448] N88-12766
Input turbulence features at a megawatt-size wind turbine, Medicine Bow, Wyoming [DE88-000098] N88-12873
Using a new characterization of turbulent wind for accurate correlation of wind turbine response with wind speed [DE88-001453] N88-12881
The velocity structure and turbulence at the center of the Orion Nebula N88-13201
TURBULENT BOUNDARY LAYER
Calculation of three-dimensional stationary turbulent boundary layer on root section of wing ignoring compressibility N88-12630
An experimental investigation of unsteadiness in swept shock wave/turbulent boundary layer interactions N88-12760
Heat and moisture transport in the atmospheric boundary layer [AD-A184222] N88-12904
TURBULENT DIFFUSION
Experimental study of turbulent diffusion parameters in ocean N88-12840
TURBULENT FLOW
Optical instrumentation and study of gas-solid suspension flows [DE88-000147] N88-12744
Experiments on densely-loaded non-Newtonian slurries in laminar and turbulent pipe flows [DE88-000719] N88-12748
Theory of heat and moisture exchange between finely disperse storm-generated spray and turbulent air flow N88-12851
TURBULENT HEAT TRANSFER
Heat and moisture transport in the atmospheric boundary layer [AD-A184222] N88-12904
TURBULENT JETS
Comparative studies in the near-field of turbulent transports of heated and unheated jets normal to a cross stream N88-12756
TURBULENT MIXING
Blowup for a nonlinear evolution equation and self-reproducing strained shear layers N88-12755
Turbulent mixing in a rotating, stratified fluid N88-12759
TWO BODY PROBLEM
Propagation of random initial conditions in time N88-12993
TWO DIMENSIONAL BOUNDARY LAYER
Numerical simulation of unsteady separated flows [AD-A184132] N88-12741
TWO DIMENSIONAL FLOW
Solution of the two-dimensional Euler equations on unstructured triangular meshes N88-12469
A free-Lagrange method for 2-D compressible flows [DE88-000216] N88-12745
Continuation finite element analysis of viscoelastic fluids N88-12761
TWO PHASE FLOW
A study of two-phase flow in a reduced gravity environment [NASA-CR-172035] N88-12617
Geometric analysis of ensemble of solutions in two-phase flow and complete resolution of problem of choking [DE88-001687] N88-12764
TYPHOONS
Annual tropical cyclone report, 1986 [AD-A184082] N88-12903

U

U.S.S.R.
USSR report: Engineering and equipment [JPRS-UEQ-87-008] N88-12621
USSR report: Earth sciences [JPRS-UES-88-006] N88-12831
U.S.S.R. SPACE PROGRAM
JPRS report: Science and technology. USSR: Life sciences [JPRS-ULS-87-009] N88-12915
ULTRAHIGH FREQUENCIES
Atomic frequency standards for ultra-high-frequency stability N88-12685
ULTRAHIGH VACUUM
Ceramics thin film N88-12505
ULTRASONIC FLAW DETECTION
Method for the ultrasonic inspection of the soundness of the metal in weld joints in two-ply pipes [BLL-CE-TRANS-8265-(9022.09)] N88-12805
Ultrasonic method of inspecting austenitic weld joints in nuclear power station equipment [BLL-CE-TRANS-8281-(9022.09)] N88-12806
ULTRASONIC RADIATION
Model for ultrasonic attenuation and elastic constant in chromium and its alloys [DE87-703478] N88-12570
ULTRASONICS
Computerized certification of digital ultrasonic instrumentation [DE88-000820] N88-13008
ULTRAVIOLET ASTRONOMY
A comprehensive exploration of late-type stars in the far-ultraviolet N88-13194
ULTRAVIOLET RADIATION
The onset of chromospheric activity among the A- and F- type stars N88-13144
VLA observations of rapid 6 cm flux variations in alpha Ori N88-13189

ULTRAVIOLET SPECTRA
Relations between chromospheric and coronal structure, flux-flux correlations and convective zone properties
N88-13138
UMBRAS
A near-earth optical communications terminal with a corevolving planetary sun shield
[AD-A184484] N88-12693
UNDERWATER ACOUSTICS
Coupled acoustic and ocean thermodynamic model
[AD-A184357] N88-12911
UNDERWATER ENGINEERING
The nature of metallurgical reactions in underwater welding
[AD-A184484] N88-12568
UNDERWATER STRUCTURES
Detection of defects on structures
[EP-PATENT-0-210-794-A2] N88-12607
UNIFIED FIELD THEORY
A supersymmetric Lagrangian for Poincare gauge theories of gravity
[DE88-001670] N88-13078
UNIVERSE
New cosmological scenario
[DE87-703357] N88-13198
Cosmological applications of singular hypersurfaces in general relativity N88-13202
Galaxy formation by gravitational collapse in a universe dominated by cold dark matter N88-13205
UNIVERSITIES
National Center for Atmospheric Research
[PB87-228391] N88-12901
A national model at Howard University demonstrating private sector interrelationships that facilitate research in predominantly Black colleges and universities
[DE88-000160] N88-13089
UNSTEADY FLOW
Aerodynamic sensitivities from subsonic, sonic and supersonic unsteady, nonplanar lifting-surface theory
[NASA-TM-100502] N88-12459
Application of Runge Kutta time marching scheme for the computation of transonic flows in turbomachines
[NASA-TM-88997] N88-12481
Three-dimensional unsteady flow elicited by finite wings and complex configurations N88-12468
Numerical simulation of unsteady separated flows
[AD-A184132] N88-12741
An experimental investigation of unsteadiness in swept shock wave/turbulent boundary layer interactions
N88-12760
UPLINKING
X-band uplink ground systems development: Part 2
N88-12703
Tau ranging revisited N88-12710
USER MANUALS (COMPUTER PROGRAMS)
Digital-flight-control-system software written in automated-engineering-design language: A user's guide of verification and validation tools
[NASA-TM-88313] N88-12494
NACHOS 2: A finite element computer program for incompressible flow problems. Part 2: User's manual
[DE88-001451] N88-12750
User's guide to NCAR (National Center for Atmospheric Research) CCM1
[PB87-224366] N88-12899
SDVS (State Delta Verification System) 5 users' manual
[AD-A184339] N88-12943
PROVER: A first-order logic system in Ada
[DE88-000220] N88-12951
Guidelines for preparing software user documentation
[NASA-CR-181550] N88-12959
USER REQUIREMENTS
Guidelines for preparing software user documentation
[NASA-CR-181550] N88-12959
User interface for a partially incompatible system software environment with non-ADP users
[DE88-001518] N88-12968
On the next generation of reliability analysis tools
[NASA-CR-178380] N88-13000
Small reactor power systems for manned planetary surface bases
[NASA-TM-100223] N88-13209

V

VALENCE
Valence bond theory and superconductivity
[AD-A184274] N88-13052
Valence bond cluster studies of alkali metal/semiconductor bonding
[AD-A184278] N88-13054
Atomic and electronic structure of surfaces and chemisorbed layers
[DE87-014987] N88-13065
VANADIUM
Mechanical properties of an acicular ferrite steel microalloyed to niobium and vanadium
[DE87-703547] N88-12574
Partial substitution of vanadium by niobium in AISI H13 steel
[DE87-703548] N88-12575
VAPOR DEPOSITION
Inertial confinement fusion reactor cavity analysis
[DE88-000788] N88-13028
VAPORIZING
Energy balance in laser-irradiated vaporizing droplets
[DE88-000525] N88-12782
VAPORS
Experimental and theoretical study of condensation in multicomponent mixtures
[DE88-000697] N88-12563
VARIABILITY
A multiple-time-scale turbulence model based on variable partitioning of turbulent kinetic energy spectrum
[NASA-CR-179222] N88-12754
VARIABLE GEOMETRY STRUCTURES
Solution of geometrically nonlinear problem for reinforced shell of revolution having arbitrary shape
N88-12637
VARIABLE STARS
Differential B and V light curves of the bright by Draconis star HD80715 N88-13130
Time series infrared spectroscopy of long period variables N88-13172
A comprehensive exploration of late-type stars in the far-ultraviolet N88-13194
VARIATIONS
The atomic weight and isotopic composition of oxygen and their variation in nature
[DE87-014397] N88-12558
VEGETATION GROWTH
Disturbance and recovery of Arctic Alaskan tundra terrain. A review of recent investigations
[AD-A184442] N88-12687
VELOCITY
Ultimate velocities for induction launchers
[DE87-012360] N88-12513
Use of a thermodynamic analog for pneumatic transport in horizontal pipes
[AD-A184076] N88-12740
The velocity structure and turbulence at the center of the Orion Nebula N88-13201
Hydrogen and deuterium in the local interstellar medium N88-13204
VELOCITY DISTRIBUTION
Comparative studies in the near-field of turbulent transports of heated and unheated jets normal to a cross stream N88-12756
Hydrogen and deuterium in the local interstellar medium N88-13204
VELOCITY MEASUREMENT
Comparative studies in the near-field of turbulent transports of heated and unheated jets normal to a cross stream N88-12756
VERTICAL LANDING
GPS vertical axis performance enhancement for helicopter precision landing approach
[NASA-CR-177443] N88-12477
VERTICAL ORIENTATION
Effects of combining vertical and horizontal information into a primary flight display
[NASA-TP-2783] N88-12487
VERY LARGE ARRAY (VLA)
VLA observations of the X-ray bright Hyades M-dwarfs N88-13147
IUE/Optical/VLA flares on AD Leo N88-13152
Microwave observations of red dwarf flare stars N88-13153
A VLA survey of dMe flare stars N88-13154
VLA observations of rapid 6 cm flux variations in alpha Ori N88-13169
VERY LARGE SCALE INTEGRATION
The design plan of a VLSI single chip (255, 223) Reed-Solomon decoder N88-12697
A simplified procedure for correcting both errors and erasures of a Reed-Solomon code using the Euclidean algorithm N88-12698
On the VLSI design of a pipeline Reed-Solomon decoder using systolic arrays N88-12700
A procedural method for the efficient implementation of full-custom VLSI designs N88-12701
Research in VLSI (Very Large Scale Integration) systems
[AD-A184089] N88-12721
VERY LONG BASE INTERFEROMETRY
EVN (European VLBI network) and MERLIN observations of 5 superluminal radio sources
[PB87-210730] N88-13193
VESTIBULES
Motion and space sickness N88-12510
VIBRATION
Vibration and parametric excitation in rotating asymmetric circular plates N88-12823
VIBRATION DAMPING
Combined problem of slew maneuver control and vibration suppression
[NASA-CR-181537] N88-12817
VIBRATIONAL SPECTRA
Ro-vibrational laser spectroscopy of ESD neutrals from chemisorbed species
[DE87-013011] N88-12770
Absorption of far IR-radiation by H2O-N2 complexes under atmospheric conditions N88-12855
The delta upsilon = 1 fundamental bands of carbon monoxide in late-type stars N88-13177
VIDEO EQUIPMENT
Input devices for tasks using interactive video
[PB87-220018] N88-12864
VIDEO SIGNALS
Programmable real-time digital video image processing
[PB87-104162] N88-12861
Accommodating the residue of processed or computed digital video signals within the 8 bit CCIR recommendation 601
[BBC-RD-1987/12] N88-12878
VIEW EFFECTS
Cloud cover determination in polar regions from satellite imagery
[NASA-CR-181544] N88-12906
VISCOELASTICITY
Explicit and implicit soil modelling for dynamic soil-structure interaction problems N88-12850
Continuation finite element analysis of viscoelastic fluids N88-12761
VISCOPLASTICITY
Ideal-viscoplastic extrusion model with application to deforming pistons in light-gas guns
[UTIAS-TN-266] N88-12857
Steady shearing in a viscoplastic solid
[AD-A184341] N88-12810
VISCOUS FLOW
Some experiences with the viscous-inviscid interaction approach
[NASA-TM-100015] N88-12488
Total linearisation method for solving viscous free boundary flow problems by the finite element method
[PB87-222337] N88-12737
Similar solutions for viscous hypersonic flow over a slender three-fourths-power body of revolution
[NASA-TM-100205] N88-12752
Analytical studies of axially symmetric motion of an incompressible viscous fluid between two concentric rotating spheres N88-12757
VISCOUS FLUIDS
Dispersion equation for plane capillary-gravity wave on free surface of viscous incompressible fluid N88-12842
VISUAL DISCRIMINATION
Latency differences and effects of selective attention to gratings in the central and right visual fields: 2
[DE87-014730] N88-12918
Visual evoked responses to sinusoidal gratings presented in central and right visual fields: 1
[DE87-014731] N88-12919
VISUAL FIELDS
Latency differences and effects of selective attention to gratings in the central and right visual fields: 2
[DE87-014730] N88-12918
Visual evoked responses to sinusoidal gratings presented in central and right visual fields: 1
[DE87-014731] N88-12919
VISUAL PERCEPTION
An approach to object recognition: Aligning pictorial descriptions
[AD-A184462] N88-12972
VITERBI DECODERS
The design plan of a VLSI single chip (255, 223) Reed-Solomon decoder N88-12697
A simplified procedure for correcting both errors and erasures of a Reed-Solomon code using the Euclidean algorithm N88-12698
VOICE CONTROL
Controlling robots with spoken commands
[DE88-000537] N88-12801
VOIDS
Plastic strain localization between voids in shear deformation fields N88-12648
VORTICES
Numerical prediction of propeller performance by vortex lattice method
[UTIAS-TN-265] N88-12489
Activities at government research laboratories reported N88-12503
Some asymptotic modes of transonic vortex flow N88-12632

Optical instrumentation and study of gas-solid suspension flows
[DE88-000147] N88-12744
Blowup for a nonlinear evolution equation and self-reproducing strained shear layers N88-12755
Equilibria, lattices and chaotic dynamics of point vortices N88-12758
Turbulent mixing in a rotating, stratified fluid N88-12759
Intensive synoptic eddies and quasigeostrophic approximation N88-12844
Dynamics of isolated intrathermocline eddy N88-12845
Influence of secondary eddy currents on scattering of admixture in zonal flow N88-12846
Mesoscale eddy dynamics by the method of point vortices N88-12863
Measurement of velocity and vorticity fields in the wake of an airfoil in periodic pitching motion
[NASA-TP-2780] N88-13002

VORTICITY
Measurement of velocity and vorticity fields in the wake of an airfoil in periodic pitching motion
[NASA-TP-2780] N88-13002

W

WAKES
A full potential flow analysis with realistic wake influence for helicopter rotor airload prediction
[NASA-CR-4007] N88-12452
Measurement of velocity and vorticity fields in the wake of an airfoil in periodic pitching motion
[NASA-TP-2780] N88-13002

WALKING
Static standing and dynamic walking of a practical biped robot
[DE88-001367] N88-12795

WALL FLOW
SCRAM JET (Supersonic Combustion Ramjet) combustion experiments N88-12512

WALLS
A study of the optimal transition temperatue of PCM (Phase Change Material) wallboard for solar energy storage
[DE88-001522] N88-12882
Aircraft interior noise reduction by alternate resonance tuning
[NASA-CR-181530] N88-13005

WANKEL ENGINES
Performance and combustion characteristics of direct-injection stratified-charge rotary engines
[NASA-TM-100134] N88-12490

WARNING SYSTEMS
Techniques for fire detection N88-12521
Annual tropical cyclone report, 1986
[AD-A184082] N88-12903

WATER
Technical evaluation of a solar-powered absorption cooling system (LiBr-H2O)
[PB87-108254] N88-12867
RRS DISCOVERY cruise 160, 30 June-25 July, 1986. Geochemical sampling over the Madeira and Porcupine Abyssal Plains
[PB87-222030] N88-12910

WATER DEPTH
Sea level changes
[DE87-014357] N88-12913

WATER FLOW
Experimental evidence for modifying the current physical model for ice accretion on aircraft surfaces
[NASA-TM-87184] N88-12473

WATER MASERS
Water masers associated with 2 carbon stars: EU Andromedae and V778 Cygni N88-13176

WATER POLLUTION
Influence of surfactants on damping of gravity-capillary waves. 1: Frequency dependence N88-12843

WATER TEMPERATURE
Influence of stratification in near-surface water layer on intensity of gas exchange between atmosphere and water N88-12841

WATER TREATMENT
Carbon dioxide treatment for scale removal and control in potable water systems
[AD-A184346] N88-12556

WATER VAPOR
Absorption of far IR-radiation by H2O-N2 complexes under atmospheric conditions N88-12855
Measurements of vapor flux, liquid water contents, precipitation rates and riming in a Utah mountain cloud system
[PB87-224945] N88-12900

WATER WAVES
Studies of thin surface films aim at seeing deep ocean processes N88-12847

WAVE ATTENUATION
Influence of surfactants on damping of gravity-capillary waves. 1: Frequency dependence N88-12843

WAVE DISPERSION
Dispersion equation for plane capillary-gravity wave on free surface of viscous incompressible fluid N88-12842

WAVE EQUATIONS
Pulse-mode expansions and refractive indices in plane-wave propagation
[DE88-001328] N88-12714

WAVE FUNCTIONS
The finite element method for electronic structure
[DE88-001708] N88-12989
Final (n,l) state-resolved electron capture by multiply charged ions from neutral atoms
[IPPJ-AM-54] N88-13030

WAVE GENERATION
Magnetic flux tubes as sources of wave generation N88-13108

WAVE PROPAGATION
General theory of radio propagation through a stratified atmosphere
[PB87-226197] N88-12662
Pulse-mode expansions and refractive indices in plane-wave propagation
[DE88-001328] N88-12714
High resolution finite volume methods on arbitrary grids via wave propagation
[NASA-CR-178397] N88-12979
Boundary effects on the drag of an oscillating sphere: Applications to the magnetic sphere rheometer. Attenuation and dispersion of acoustic waves in nematic liquid crystals N88-13007
The acceleration of winds by MHD waves in open magnetic structures N88-13109
The dynamics of solar magnetic flux tubes subjected to resonant foot point shaking N88-13118

WAVE REFLECTION
Multichannel deconvolution of P waves at seismic arrays and three component stations
[AD-A184450] N88-12888

WAVEFORMS
Experimental and analytic studies of the triggered lightning environment of the F106B
[NASA-CR-4104] N88-12897

WAVEGUIDE FILTERS
A study of scattering from E-plane circuit elements
[AD-A184473] N88-12673

WEAK ENERGY INTERACTIONS
Few body hypernuclear systems: Weak decays
[DE87-014920] N88-13010

WEAR
Real-time Raman detection of molecular changes in ceramics undergoing sliding friction
[DE88-000558] N88-12609

WEAR RESISTANCE
Ceramic technology for advanced heat engines project
[DE88-001520] N88-12605
Corrosion control by composite material substitution with application to the M-939 5-ton truck N88-12654

WEATHER
Drought, solar activity link established by Leningrad geophysicists N88-12835

WEATHER FORECASTING
Progress in improving weather forecasting viewed N88-12833
NWS (National Weather Service) watch/warning verification flash flood, winter storm and high wind, January 1980 - June 1986
[PB87-223053] N88-12898
Annual tropical cyclone report, 1986
[AD-A184082] N88-12903

WEATHER MODIFICATION
Measurements of vapor flux, liquid water contents, precipitation rates and riming in a Utah mountain cloud system
[PB87-224945] N88-12900

WEIGHT REDUCTION
Rational reinforcement of cylindrical shells with variable stiffness frames subjected to external pressure N88-12638
Corrosion control by composite material substitution with application to the M-939 5-ton truck N88-12654

WEIGHTLESSNESS SIMULATION
Access to microgravity: A technical description of the NAE T-33 microgravity facility
[NAE-AN-47] N88-12518

WELD TESTS
Detection of defects on structures
[EP-PATENT-0-210-794-A2] N88-12807

WELDABILITY
Welding and weldability of ductile intermetallic alloys
[DE87-014061] N88-12582
Weldability of 2219-T851 and 2519-T87 aluminum armor alloys for use in Army vehicle systems
[AD-A184296] N88-12792

WELDED JOINTS
Welding and weldability of ductile intermetallic alloys
[DE87-014061] N88-12582
Development of an acoustic emission monitor and monitoring techniques for long-term monitoring of U-0.8Ti electron-beam weldments for postweld cracking
[DE88-000819] N88-12804
Method for the ultrasonic inspection of the soundness of the metal in weld joints in two-ply pipes
[BLL-CE-TRANS-8265-(9022.09)] N88-12805
Ultrasonic method of inspecting austenitic weld joints in nuclear power station equipment
[BLL-CE-TRANS-8281-(9022.09)] N88-12806

WELDED STRUCTURES
Advanced radiator concepts utilizing honeycomb panel heat pipes
[NASA-CR-172017] N88-12747

WELDING
Effects of stress-relieving on the mechanical properties and the structure of specimens of high-temperature fine-grained structural steels heat-treated to simulate welding
[BLL-CE-TRANS-8258-(9022.09)] N88-12586
The modelling of orientation in planar polymer welding flows
[AD-A184404] N88-12793

WHITE DWARF STARS
PG 0308 + 096: A short-period white dwarf + dM binary with strongly modulated H-alpha emission N88-13132

WHITE NOISE
Detection of signals by the digital integrate-and-dump filter with offset sampling N88-12695

WIGGLER MAGNETS
Center for X-Ray Optics, 1986
[DE86-000715] N88-12783

WIND (METEOROLOGY)
NWS (National Weather Service) watch/warning verification flash flood, winter storm and high wind, January 1980 - June 1986
[PB87-223053] N88-12898

WIND EFFECTS
The effect of mass, wind angle and erection technique on the aeroelastic behaviour of a cable-stayed bridge model
[NAE-AN-46] N88-12819
Theory of heat and moisture exchange between finely disperse storm-generated spray and turbulent air flow N88-12851

WIND TUNNEL DRIVES
Analysis of 7- X 10-foot high speed wind tunnel shaft loads in support of fan blade failure investigation
[NASA-TM-100504] N88-12496

WIND TUNNEL STABILITY TESTS
Effects of jet exhaust yaw vane installation and operation on the longitudinal and lateral-directional characteristics of the F-14 airplane
[NASA-TP-2769] N88-12455

WIND TUNNEL TESTS
Experimental aerothermodynamic research of hypersonic aircraft
[NASA-CR-181533] N88-12483
Results of the 1986 NASA/FAA/DFVLR main rotor test entry in the German-Dutch wind tunnel (DNW)
[NASA-TM-100507] N88-13003

WIND TUNNEL WALLS
An analysis of sound absorbing linings for the interior of the NASA Ames 80 x 120-foot wind tunnel
[NASA-CR-177396] N88-13006

WIND TUNNELS
Analysis of 7- X 10-foot high speed wind tunnel shaft loads in support of fan blade failure investigation
[NASA-TM-100504] N88-12496
Measured performance of the heat exchanger in the NASA icing research tunnel under severe icing and dry-air conditions
[NASA-TM-100116] N88-12798

WIND TURBINES
Input turbulence features at a megawatt-size wind turbine, Medicine Bow, Wyoming
[DE88-000098] N88-12873
Measurements and calculations of aerodynamic torques for a vertical-axis wind turbine
[DE88-001783] N88-12876
Using a new characterization of turbulent wind for accurate correlation of wind turbine response with wind speed
[DE88-001453] N88-12881
Variability of wind power near Oklahoma City and implications for siting of wind turbines
[DE88-000444] N88-12902

WIND VELOCITY
Using a new characterization of turbulent wind for accurate correlation of wind turbine response with wind speed
[DE88-001453] N88-12881
Variability of wind power near Oklahoma City and implications for siting of wind turbines
[DE88-000444] N88-12902
WINDING
Departmental report on program EMTP-machine windings surge transients: Travelling wave method
[PB87-123733] N88-12719
WINDPOWER UTILIZATION
Variability of wind power near Oklahoma City and implications for siting of wind turbines
[DE88-000444] N88-12902
WING PROFILES
Three-dimensional unsteady flow elicited by finite wings and complex configurations N88-12466
Conical wing with maximum lift-to-drag ratio in supersonic gas flow N88-12633
WINGS
Reduced complexity structural modeling for automated airframe synthesis
[NASA-CR-177440] N88-12453
Calculation of aerodynamic characteristics of three-dimensional finite span wings in potential incompressible flow N88-12631
WINTER
NWS (National Weather Service) watch/warning verification flash flood, winter storm and high wind, January 1980 - June 1986
[PB87-223053] N88-12898
WIRE
Carbon-fiber reinforced aluminum N88-12507
Small-diameter wire tensile testing
[DE88-000835] N88-12815
WORKLOADS (PSYCHOPHYSIOLOGY)
Effect of motion cues during complex curved approach and landing tasks: A piloted simulation study
[NASA-TP-2773] N88-12480
Research papers and publications (1981-1987): Workload research program
[NASA-TM-100016] N88-12924

X

X RAY ANALYSIS
The Einstein survey of the young stars in the Orion Nebula N88-13182
X RAY ASTRONOMY
A re-examination of the corona-wind dividing line: Diagnostics of non-coronal atmospheres N88-13101
X RAY IMAGERY
Computer-aided X-ray image system design and evaluation
[DE88-000997] N88-12965
X RAY LASERS
XUV emission features from the Livermore soft X-ray laser experiments
[DE88-000420] N88-12779
J = O Task Force
[DE88-001326] N88-12788
X RAY SOURCES
A search for X-ray luminous late type stars in NIPSS data N88-13143
X RAY SPECTRA
Relations between chromospheric and coronal structure, flux-flux correlations and convective zone properties N88-13138
VLA observations of the X-ray bright Hyades M-dwarfs N88-13147
Exosat results on the dMe flare Star Wolf 630AB and on VB 8 N88-13151
X RAY SPECTROSCOPY
Center for X-Ray Optics, 1986
[DE88-000715] N88-12783
Review of X-ray spectroscopy from laser-produced plasmas
[DE88-000755] N88-13043
X RAYS
The X-ray orbital lightcurves of AR Lac and TY Pyx N88-13129
X-29 AIRCRAFT
An integrated study of structures, aerodynamics and controls on the forward swept wing X-29A and the oblique wing research aircraft
[NASA-CR-181548] N88-12486

Y

YIELD POINT
Long-range pulselength scaling of 351nm laser damage thresholds
[DE87-014754] N88-12777
A finite element procedure for interference-fit and cold-working problems with limited yielding
[AR-004-517] N88-12992
YIELD STRENGTH
Small-diameter wire tensile testing
[DE88-000835] N88-12815
YTTRIUM OXIDES
Synthesis of the monoclinic yttria by thermal plasma processing
[DE88-000496] N88-12608

Z

ZEEMAN EFFECT
Laser induced fluorescent study of relativistic electron beams
[AD-A184456] N88-12774
Measurements of stellar magnetic fields N88-13093
Exploiting the IR: Solar and stellar spectroscopy in the IR N88-13102
Magnetic fields on K and M stars N88-13137
Observations and analysis of the photospheric magnetic fields on dwarf G, K and M stars N88-13196
ZERO LIFT
Planform effects on the supersonic aerodynamics of multibody configurations
[NASA-TP-2762] N88-12454
ZINC COMPOUNDS
Studies on estimation of nickel in zinc base die casting by D.C. polarography
[PD-MT-8729] N88-12588
Resistivity of EuBa2(Cu/sub 1-y/Zn/sub y/)3O/sub x/ as a ffunction of temperature, magnetic field, pressure and Zn concentration
[DE87-014740] N88-13069
ZIRCONIUM OXIDES
Effect of time and temperature on transformation toughened zirconias
[AD-A184356] N88-12600
Studies of alumina additions in zirconia - magnesia
[DE87-703500] N88-12602
Internal reforming development for solid oxide fuel cells
[DE87-006518] N88-12871

Typical Personal Author Index Listing

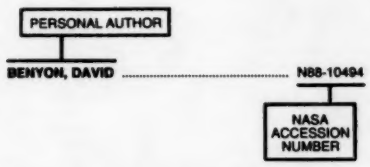

Listings in this index are arranged alphabetically by personal author. The NASA accession number denotes the number by which the citation is identified.

A

ABBOTT, TERENCE S. N88-12487
ABDELRAHMAN, M. H. N88-12719
ABDELSALAM, M. K. N88-12497
ACCIOLY, A. J. N88-13077
ACEITUNO, PATRICIO N88-12905
ADKINS, JAMES A. N88-12492
AEPPLI, G. N88-12583
AGNEW, S. N88-12611
AHMAD, IMAD A. N88-13158
AHMADI-MOGHADAM, AZAM N88-12467
AINE, C. J. N88-12918
N88-12919
AITKEN, J. F. N88-12518
AKINS, R. E. N88-12876
AKIYAMA, JUICHIRO N88-12864
ALDISSI, M. N88-12610
N88-12611
ALFORD, W. J. N88-12674
ALLAN, PETER STEWART N88-12642
ALLCOCK, H. R. N88-13058
ALLISON, S. W. N88-12781
ALONSO, N. N88-12578
AMATO, N. M. N88-13213
AMAYENC, P. N88-12675
AMSDEN, A. A. N88-12743
ANDERSON, D. F. N88-12768
ANDERSON, J. L. N88-12962
ANDRIULLI, J. B. N88-12826
ANGEL, E. C. N88-12767
ANIKIYEV, V. V. N88-12840
ANNIS, J. N88-12692
ANTONYUK, P. N. N88-12842
ANTSIFEROVA, N. G. N88-12917
ANTUFYEV, B. A. N88-12839
ANZINI, DAVID JOSEPH N88-12593
ARATA, N. N88-13213
ARENSTORF, NORBERT S. N88-12934
AREVALO, M. J. N88-13156
N88-13187
ARIMOTO, H. N88-13034
ARINCHEV, S. V. N88-12622
ARIYE, M. N88-12628
ARMSTRONG, R. L. N88-12782
ARNOLD, S. C. N88-12597
ARROYO, I. K. N88-12573
ARTLEY, MARGERY N88-12655
ASHWORTH, JEFFREY CLAYTON N88-12468
ATKINSON, D. P. N88-12643
AUSTIN, P. A. N88-13058
AUWETER-KURTZ, M. N88-12536
AVRETT, E. H. N88-13173
AYOUB, ALFRED N88-12483
AYRES, T. N88-13177
AYRES, THOMAS R. N88-13114
AZAROFF, L. V. N88-12595
AZEVEDO, I. S. N88-13199

B

BABCOCK, PHILIP S., IV N88-13000
BABRAUSKAS, VYTENIS N88-12522
BACA, L. S. N88-12988
BACA, T. J. N88-12612
N88-12827
BACON, L. D. N88-12713
BADYAGIN, A. A. N88-12623
BAGARE, S. P. N88-13113
BAKER, A. F. N88-12879
N88-12880
BALANCIN, O. N88-12575
BALIUNAS, S. L. N88-13103
BALIUNAS, SALLIE L. N88-13139
N88-13190
BALLESTER, J. L. N88-13187
BANDY, JOHN T. N88-12556
BANGA, R. N88-12586
BARDEN, S. C. N88-13155
BARDEN, SAMUEL C. N88-13127
BARKER, WALTER R. N88-12500
BARKEY, D. P. N88-12656
BARNES, SUSAN N88-13092
BARRETT, J. W. N88-12725
BARRY, R. G. N88-12908
BARSKY, BRIAN A. N88-12940
BARTOE, J.-D. F. N88-13112
BAST, R. N88-12519
BASU, BHARATHI BAI J N88-12587
BATEMAN, V. I. N88-12829
BATH, L. M. N88-12899
BAUDIN, F. N88-12675
BAVUSO, SALVATORE J. N88-12928
BAYLOR, L. R. N88-13026
BEACH, T. E. N88-13168
BEBERMAN, J. H. N88-13051
BEDFORD, D. K. N88-13156
BELK, P. N88-12701
BELUBEKYAN, E. V. N88-12641
BENDER, GARY L. N88-12492
BENNER, ROBERT E. N88-12726
BENNETT, JEFFREY OWEN N88-13194
BENSON, L. V. N88-12964
BENSON, PRISCILLA J. N88-13176
BENZ, FRANK J. N88-12530
BERA, RAJENDRA K. N88-12990
BERESNEV, S. A. N88-12850
BERG, D. E. N88-12876
BERGER, DANIEL N88-12975
BERRIER, BOBBY L. N88-12455
BERTRAM, W. N88-12586
BESER, JACQUES N88-12477
BEUGELSDIJK, T. N88-12801
BEVIS, MICHAEL JOHN N88-12642
BHANJI, A. N88-12687
BIBL, KLAUS N88-12889
BISHOP, A. R. N88-13047
BJORKMAN, WILLIAM S. N88-12478
BLISS, DONALD B. N88-13005
BLONSKY, P. I. N88-13058
BLOOMFIELD, HARVEY S. N88-13209
BOGDANOVA, E. G. N88-12834
BOGUE, R. K. N88-12481
BOLIVAR, S. N88-12859
BOLT, H. N88-13031
BOND, H. E. N88-13164
BOOKBINDER, J. A. N88-13169
N88-13184
BOOM, R. W. N88-12497
BOOTH, EARL R., JR. N88-13002
BOOTH, R. S. N88-13193
BOOZER, A. H. N88-13029
BOPP, BERNARD W. N88-13125
N88-13189
BORDER, J. S. N88-12680
BORGES, H. A. N88-13069
BORISENKOV, YE. P. N88-12851
BOSTICK, W. D. N88-12767
BOTTERI, BENITO P. N88-12526
BOURGES, B. N88-12886
BOURGET, C. N88-12657
BOURRET, E. D. N88-13068
BOUVIER, J. N88-13179
BOVARD, FRANCINE S. N88-12734
BOWEN, G. H. N88-13168
BOWMAN, K. O. N88-12948
BOYD, D. M. N88-12785
BOYD, L. J. N88-13103
BOYD, LOUIS J. N88-13122
N88-13190
BOYD, MARK N88-12928
BOZZOLA, R. N88-12461
BRACEWELL, R. N. N88-13210
BRADSHAW, J. W. N88-12560
BRAGINA, M. P. N88-12917
BRATKOV, V. I. N88-12841
BREAZEALE, M. A. N88-13004
BREKHOVSKIKH, V. F. N88-12641
BRIDGES, JAMES L. N88-12601
BRINKMAN, A. C. N88-13121
BRISSOT, J. N88-13017
BRITCLIFFE, M. N88-12706
N88-12709
BROCK, J. R. N88-12742
BROOKS, THOMAS F. N88-13003
BROWN, ALEXANDER N88-13160
N88-13180
BROWN, C. R. N88-12561
BROWN, D. H. N88-12694
BROWN, HOWARD WILLIAM, III N88-12820
BROWN, JERRY N88-12887
BRUECKNER, G. E. N88-13112
BRUNING, DAVID H. N88-13137
BRUNO, J. C. N88-12571
N88-12574
BUCHAU, JURGEN N88-12889
BUDDEMEIER, R. W. N88-12913
BUDDING, EDWIN N88-13123
N88-13124
BUECHL, K. N88-13040
BUKIET, B. G. N88-13071
BUKOWSKI, RICHARD W. N88-12521
BUMPUS, S. N88-12963
BURBACK, R. N88-12951
BURGREEN, GREGORY WAYNE N88-12748
BURKE, J. V. N88-12995
BURNS, A. R. N88-12770
BURNSIDE, W. D. N88-12479
N88-12498
BURTON, LARRY W. N88-12651
BUSH, D. M. N88-12872
BUSSO, M. N88-13178
N88-13186
BUTLER, C. J. N88-13133
N88-13152
BUZASI, DEREK N88-13127
N88-13128
BYRD, J. S. N88-12900
BYRNE, P. B. N88-13120
N88-13133
N88-13146
N88-13152
BYSTROV, V. V. N88-12622

C

CABLE, J. W. N88-13014
CABRAL, B. K. N88-12729
CAILLAULT, J.-P. N88-13147
N88-13182
CANDIDO, L. C. N88-12560
CARDENAS, R. N88-12705
CAREY, R. P. N88-12992
CARHART, HOMER W. N88-12524
CARNAHAN, C. L. N88-12964
CARR, D. B. N88-12961
CARRERAS, B. A. N88-12949
CARUSO, STEVEN C. N88-12463
CASTANEDA, HECTOR OSVALDO N88-13201
CASTLES, S. N88-13060
CASTRO, C. N88-13078
CASTRO, E. P. N88-12570
CATAN, M. A. N88-12736
CATE, DAVID N88-12887
CATES, M. R. N88-12781
N88-13019

LAWSON, W. S. N88-12731
LAZAREV, A. A. N88-12843
LAZARO, C. N88-13167
N88-13187
LECHNER, T. M. N88-13091
LEDOUX, PAUL W. N88-12529
LEE, A. L. N88-12671
LEE, H. N88-13066
LEE, I. Y. N88-12909
LEE, K. H. N88-12715
LEE, M. N88-12978
N88-12977
LEE, M. H. N88-12584
LEE, PAI HUNG N88-12458
LEES, A. C. N88-12888
LEIBOVICH, SIDNEY N88-12904
LEISING, MARK D. N88-13214
LEITE, JOSE G. N88-12998
LEMEN, J. R. N88-13134
LENZ, R. W. N88-12595
LEONG, FRANK N88-13000
LESUER, D. R. N88-12816
LEUNG, W. K. N88-13044
LEVENTIS, NICHOLAS N88-12724
LEVEQUE, RANDALL J. N88-12979
LEVINSON, ROBERT N88-13084
LEVY, SAMUEL C. N88-12735
LI, JIANGUO N88-13050
LICHTEN, S. M. N88-12680
LIEBERT, J. N88-13188
LIEBROCK, L. M. N88-12957
LIGTHART, M. M. N88-12718
LILIENTAL-WEBER, Z. N88-13066
LILJEGREN, T. N88-12555
LILLELEHT, L. U. N88-12618
N88-12619
LILLYA, C. P. N88-12599
LIN, CHIN-SHUN N88-12752
LIN, EDWARD HSIANG-HSI N88-12797
N88-12798
LIN, SHU N88-12712
LINDELL, MICHAEL C. N88-12531
LING, S. C. N88-12744
LINNALUOTO, S. N88-13140
LINSKY, J. L. N88-13169
LINSKY, JEFFREY L. N88-13185
LITTLE-MARENIN, IRENE R. N88-13163
N88-13176
LITTLE, STEPHEN J. N88-13163
N88-13176
LIU, JEW-CHY N88-12809
LO, Y. H. N88-13066
LOCKWOOD, G. W. N88-13136
LOCKWOOD, ROY A. N88-12492
LODHI, LILY MANOU N88-13203
LOFFMAN, R. S. N88-12968
LONDON, R. A. N88-12788
LONGLEY-COOK, ROBERT N88-12807
LOOS, ALFRED C. N88-12549
LORENZINI, ENRICO C. N88-12533
LUK, C. H. N88-13062
LUMLEY, JOHN L. N88-12904
LUND, P. A. N88-13112
LURIA, S. M. N88-12925
LUTTERMOSER, D. G. N88-13173
LUTZ, W. H. N88-12781
LYNAS-GRAY, A. E. N88-13167
LYNCH, M. T. N88-12775
LYONS, J. E. N88-12802

M

MACCACARO, T. N88-13188
MACFARLANE, J. J. N88-13028
MACGOWAN, B. J. N88-12788
MACGREGOR, K. B. N88-13105
MACIEL, A. K. A. N88-13076
MADANI, MOSTAFA SEYED N88-12862
MAGDELENO, RAYMOND E. N88-12493
MAHADEVAN, SUDHA N88-12606
N88-12607
MAKSIMIUK, V. F. N88-12916
MALBOUISSON, A. P. C. N88-13001
MALDONADO, R. H. C. N88-13213
MALEKI, L. N88-12685
MALLIK, SUSHMA V. N88-13159
MALONE, M. F. N88-12547
MANNHEIMER, R. J. N88-12746
MANSOT, J. L. N88-13017
MARCENAT, C. N88-13063
MARCUS, LEO G. N88-12943
MARCY, GEOFFREY W. N88-13137
MARGLE, JANICE M. N88-12520
MARIA, C. R. N88-12571
MARINA, M. N88-12704
MARINARO, D. E. N88-12974
MARISKA, J. T. N88-13095
MARQUES, G. E. N88-12570
MARSHALL, M. E. N88-12888
MARSHALL, N. A. N88-12875
MARTIN, J. E. N88-12603
MARTIN, J. M. N88-13017
MARTIN, RUTH M. N88-13003
MARTIN, T. P. N88-12800
MASAMUNE, S. N88-13034
MASLANIK, J. A. N88-12908
MASLOV, A. A. N88-12634
MATHIAS, LON J. N88-12598
N88-12601
MAVRIPLIS, DIMITRI JAMES N88-12469
MAYER, LAWRENCE S. N88-12982
MAYVILLE, R. N88-12649
MAZOR, A. N88-13047
N88-13071
MCBRYAN, OLIVER A. N88-12960
MCCLOSKEY, R. N88-12669
MCCLURE, E. R. N88-12643
MCDANIEL, J. A. N88-12561
MCELFRESH, T. W. N88-12668
MCFARLAND, RICHARD E. N88-12932
MCGHEE, ROBERT B. N88-12499
MCGRATH, R. T. N88-13045
MCINTOSH, G. E. N88-12497
MCINTYRE, J. F. N88-12567
MCMILLIN, NAOMI N88-12454
MCRUER, DUANE T. N88-12493
MEEHL, GERALD ALLEN N88-12907
MELTON, R. B. N88-12973
MERKE, W. D. N88-12538
MERTEN, C. W. N88-12591
MESSINA, NEALE A. N88-12615
MESSMER, RICHARD P. N88-13052
N88-13053
N88-13054
N88-13055
N88-13056
MEWE, R. N88-13121
N88-13134
MEYYAPPAN, M. N88-12946
MICHELS, ALAN N88-12678
MIGNACO, J. A. N88-12999
MILAN, S. N88-12664
MILEY, G. H. N88-13027
MILLER, DIANE F. N88-12959
MILLER, J. D. N88-13041
MILORA, S. L. N88-13026
MIODUSZEWSKI, P. K. N88-13045
MITCHELL, J. R. N88-12726
MITCHELL, J. S. N88-12475
MITCHELL, W. F. N88-12987
MITTRA, R. N88-12723
MIYAHARA, A. N88-13031
MIYAHARA, AKIRA N88-13042
MIZIK, P. M. N88-12815
MOG, ROBERT A. N88-12532
MONTEIRO, W. A. N88-12577
MONTES, H. N88-13017
MONTESINOS, B. N88-13138
MOOR, E. N88-12519
MOORE, JOYCE L. N88-12980
MORALES, WILFREDO N88-12543
MOROZ, A. F. N88-12917
MORRIS, D. H. N88-13191
MORRIS, GEORGE ROBERT N88-12821
MORRIS, J. N88-12714
MORRIS, V. R. N88-12873
MORRISSEY, JAMES F. N88-12670
MORROW, T. B. N88-12748
MORTENSEN, G. A. N88-12957
MORTON, MARK HARRISON N88-12534
MOSES, D. O. N88-12614
MOSES, G. A. N88-13028
MOSTAFA, SAMIR I. N88-12741
MOUNTAIN, M. N88-13167
MOUSSEAU, V. A. N88-12957
MOYER, M. W. N88-13008
MUCCILLO, R. N88-12602
MUELLER, I. L. N88-12580
MUIRHEAD, VINCENT U. N88-12458
MUNSHI, M. Z. N88-12722
MUNSHI, N. A. N88-12553
MUNSON, C. P. N88-13040
MURPHY, M. C. N88-12988
MURPHY, ROBERT B. N88-13052
MURRAY, K. N88-12540
MURRAY, KATHY N88-13024
MURRAY, RICHARD B. N88-12651
MURTHY, JAYANT NARASIMHA N88-13204
MURTHY, P. L. N. N88-12551
MUSIELAK, Z. E. N88-13108
N88-13148
MUTEL, R. L. N88-13191
MYLER, CRAIG A. N88-12740

N

NAFDAY, AVINASH MADHUKAR N88-12824
NAFF, G. J. N88-12875
NAGATA, A. N88-13034
NARAGHI, MOHAMMAD H. N88-12539
NATAUPSKY, MARK N88-12487
NATHAL, MICHAEL V. N88-12538
NATIONS, HAROLD N88-13130
NEBEL, R. A. N88-13027
NECKEL, H. N88-13110
N88-13111
NEEMAN, Y. N88-13079
NEFF, CHESTER H. N88-12556
NEFF, D. H. N88-13184
NEHME, O. A. N88-12547
NELSON, ERIC N88-13192
NELSON, ERIC R. N88-13122
NELSON, G. J. N88-13141
NELSON, JAMES B. N88-12544
NERI, DAVID F. N88-12925
NESIS, ANASTASIOS N88-13115
NEYELOV, I. A. N88-12848
NG, POH H. N88-12897
NGUYEN, HUNG LEE N88-12490
NICHOLSON, W. L. N88-12961
NICOL, DAVID M. N88-12933
NISENSON, P. N88-13161
NIXON, DAVID N88-12463
NOAH, PAUL V. N88-13125
NOEL, B. W. N88-13019
NOH, YIGH N88-12759
NOORISHAD, J. N88-12964
NORDLUND, O. P. N88-12858
NORMAN, E. B. N88-13208
NORRIS, D. N88-12686
NORTON, S. N88-13082
NOVELLO, M. N88-13198
NOVEMBER, LAURENCE J. N88-13114
NOYES, R. N88-13161
NURMIKKO, A. V. N88-13070
NUSSLE, R. N88-12796
NYGREN, R. N88-13044

O

OBLOW, E. M. N88-12986
N88-13207
OHSAWA, YUKIHARU N88-13037
OHTANI, RYUICHI N88-12825
OKA, Y. N88-13031
OLSEN, J. A. N88-13063
OLSEN, W. N88-12473
N88-12796
OLSON, D. L. N88-12568
ORIOLIA, L. N88-13186
OROURKE, P. J. N88-12743
ORTH, C. D. N88-12540
ORTH, CHARLES D. N88-13024
OSEROFF, S. B. N88-13069
OSWALT, EDWARD N88-13084
OTT, H. R. N88-12583
OVERBEEK, R. N88-12967
OVERZET, L. J. N88-13051
OWENS, BOONE B. N88-12722

P

PAEZ, T. L. N88-12812
N88-12827
PAISNER, J. A. N88-12714
PALAIS, ROBERT ANDREW N88-12755
PALERMO, M. R. N88-12574
PALZ, W. N88-12868
PAMADI, BANDU N. N88-12456
PANAGI, P. N88-13119
PANITZ, J. K. G. N88-12802
PAO, H. P. N88-12744
PARK, J. T. N88-12746
PARKER, R. L. N88-12890
PARKER, S. R. N88-12671
PARMAR, A. N. N88-13129
PASTERNAK, M. N88-13048
PATTERSON, CHARLES H. N88-13056
PATTERSON, MICHAEL J. N88-12542
PATTERSON, VERNON G. N88-12903
PATTON, EDWARD M. N88-12651
PAYTON, D. W. N88-12475
PECK, S. J. N88-12747
PEDRAZA, D. F. N88-13064
PEDROSA, I. A. N88-12985

PERALA, RODNEY A. N88-12897
PERFECT, S. N88-12519
PERLMUTTER, SAUL N88-13195
PERRONE, P. J. N88-12648
PERSI, P. N88-13186
PESCE, J. E. N88-13165
PETERSON, A. F. N88-12723
PETERSON, C. W. N88-12464
N88-12550
PETERSON, LAUREN M. N88-13018
PETERSON, R. R. N88-13028
PETTERSEN, BJORN R. N88-13149
PHELAN, P. N88-12601
PHILLIPS, N. E. N88-13063
PHILLIPS, T. W. N88-12788
PICCHIO, G. N88-13178
PICKETT, C. A. N88-12830
PILBRATT, G. N88-13193
PIN, TONG N88-12654
PINCUS, S. M. N88-12946
PISTORIUS, C. W. I. N88-12498
PITTS, J. H. N88-12780
PITTS, WILLIAM C. N88-12484
PLETTA, J. B. N88-13088
PLUMMER, JAMES N88-12721
POBEDINSKIY, G. G. N88-12857
POCHTMAN, YU. M. N88-12638
POKAZEYEV, K. V. N88-12843
PONS, STANLEY N88-13050
POOJARY, AITHU N88-12587
N88-12588
POPE, L. E. N88-12802
POPOV, V. L. N88-12917
PORCAS, R. W. N88-13193
POSNER, E. C. N88-12679
POULTER, G. A. N88-12565
POWELL, DOUGLAS G. N88-12601
PRAKASH, TEMKAR M. N88-12556
PRALNIKOV, ANDREY N88-12833
PRATT, TERRENCE W. N88-12953
PRESTAGE, J. D. N88-12685
PRETZEL, C. W. N88-12884
PREWO, KARL M. N88-12546
PRICE, D. MARVIN N88-12532
PRICE, STEPHAN D. N88-13163
PRUTKIN, I. L. N88-12848
PURI, SUNIL N88-12474

Q

QUEST, K. B. N88-12665

R

RACINE, CHARLES N88-12887
RADICK, RICHARD R. N88-13139
RADKO, V. I. N88-12805
RAJAGOPALAN, S. R. N88-12587
N88-12588
RAMACHANDRAN, VIJAYA N88-12941
RAMAMOORTHY, P. N88-12931
RAMSEY, LAWRENCE W. N88-13127
RANSICK, M. H. N88-12785
RAO, DHANVADA M. N88-12457
RAO, K. V. N88-12466
RAO, M. N88-12795
RAWLIN, VINCENT K. N88-12542
REDDY, J. N. N88-12811
REECE, ERIC N88-12653
REED, I. S. N88-12698
N88-12700
REGLERO, V. N88-13187
REIMERS, DIETER N88-13160
REINISCH, BODO W. N88-12889
REUBUSH, DAVID E. N88-12455
REW, DONG-WON N88-12535
RHOADES, W. A. N88-12984
RHODES, MICHAEL N88-13123
RICHARDS, PAMELA JANE CHILDS N88-12914
RICHEY, M. W. N88-12804
RIENECKER, F. N88-12519
RILEY, D. J. N88-12713
RITTER, R. C. N88-12781
RIYOPOULOS, S. N88-12773
ROBBERTO, M. N88-13186
ROBINS, GABRIEL N88-12944
ROBINSON, CRAIG R. N88-13189
ROBINSON, D. L. N88-12691
ROGERS, S. E. N88-12991
ROJAS, R. G. N88-12479
ROPER, W. D. N88-12472
ROSCHELLE, JEREMY N88-13075
ROSEN, M. D. N88-12788
ROSNER, R. N88-13106
N88-13148
ROST, MARTIN C. N88-12678
ROTHMANN, BETH N88-12928
ROZENTUR, L. I. N88-12640
RUDOLPH, TERENCE N88-12897
RUPP, T. D. N88-12965
RYAGUZOV, YE. A. N88-12631
RYDEN, BARBARA SUE N88-13205

S

SAAR, S. N88-13140
N88-13177
SAAR, S. H. N88-13094
N88-13145
SAAR, STEVEN H. N88-13185
SAAR, STEVEN HERBERT N88-13196
SAASTAMOINEN, J. N88-12736
SACH, C. I. N88-12517
SACKS, R. N88-12714
SACKSTEDER, KURT R. N88-12528
SADR, R. N88-12695
N88-12698
SAFFER, REX A. N88-13132
SAFONOV, A. S. N88-12624
SAGARA, A. N88-13036
SAITO, JIM N88-12494
SAITO, T. T. N88-12643
SAKAI, JUN-ICHI N88-13037
SAKHAROV, V. I. N88-12635
SALANE, D. E. N88-12988
SALCEDO, R. A. N88-12573
SALMON, DAVID CHARLES N88-12958
SALTZ, JOEL H. N88-12935
SAMARAS, ELIAS N88-12646
SAMEH, A. H. N88-12930
SANCHEZ, R. J. N88-12618
SANTELLA, M. L. N88-12582
SARICKS, C. L. N88-12614
SARMENTO, E. F. N88-13061
SATO, K. I. N88-13034
SAUTHOFF, GERHARD N88-12589
SAYOOD, KHALID N88-12678
SCALTRITI, F. N88-13186
SCANLON, CHARLES H. N88-12480
SCARDOVELLI, R. A. N88-13027
SCHARER, J. E. N88-13046
SCHAUER, DALE A. N88-12554
SCHIOLER, LISELOTTE J. N88-12600
SCHLICHTING, CHRISTINE N88-12925
SCHMIDT, P. P. N88-13050
SCHMIDTKE, PAUL C. N88-13162
SCHNURR, N. M. N88-12514
SCHOLZE, RICHARD J. N88-12556
SCHRADE, H. O. N88-12536
SCHRIJVER, C. J. N88-13098
N88-13116
N88-13134
N88-13142
N88-13145
SCHROEDER, R. M. N88-12580
SCHULLER, I. K. N88-13062
SCHULTZ, PETER A. N88-13056
SCHULZ, OTTO N88-12589
SCHWARTZ, A. N88-12613
SCOFIELD, J. H. N88-12779
SCORZELLI, R. B. N88-13199
SEABORG, G. T. N88-13090
SEGAL, A. N88-12737
SEITCHEK, GLENN D. N88-12488
SELLERS, HOWARD SHAUN N88-13007
SEMENOV, N. V. N88-12634
SERCEL, JOEL N88-13024
SEVERINO, GIUSEPPE N88-13115
SEVERSON, MARK W. N88-13050
SEVERYNA, KAREN N88-12655
SHAFER, R. N88-13129
SHAO, H. M. N88-12697
N88-12700
SHAPIRO, G. I. N88-12845
SHATOV, A. K. N88-12837
SHCHEDRIN, I. F. N88-12806
SHCHEKIN, G. A. N88-12630
SHEDD, CHARLES DAINS N88-12593
SHEFFIELD, J. N88-13025
SHELL, T. L. N88-12561
SHELTON, R. L. N88-12691
SHEN, WENHUI N88-12952
SHENTON, L. R. N88-12948
SHILOV, V. M. N88-12917
SHIMAKURA, N. N88-13030
SHINOZUKA, MASANOBU N88-12646
SHORE, B. W. N88-12714
SHRIVER, D. F. N88-12596
N88-13058
SHUMWAY, R. H. N88-12688
SIJACKI, D. N88-13079
SILVESTRO, G. N88-13186
SIMON, T. N88-13169
SIMON, THEODORE N88-13144
SINDORF, J. F. N88-12872
SINGH, A. K. N88-12606
N88-12607
SINGH, JAG J. N88-13015
SINGH, M. K. N88-12614
SIRCILLINETO, F. N88-13200
SIVARAMAN, K. R. N88-13113
SKIFF, B. A. N88-13136
SKINNER, C. J. N88-13166
SKINROOD, A. C. N88-12880
SKOROMNYY, N. A. N88-12916
SLATER, P. N. N88-12865
SLEE, O. B. N88-13141
SLEZIONA, P. C. N88-12536
SLINKER, STEVEN P. N88-13021
SMELYANSKIY, V. I. N88-12648
SMITH, A. V. N88-12674
SMITH, B. T. N88-12955
SMITH, BRIAN N88-12548
SMITH, DOUGLAS B. N88-12499
SMITH, EDGAR D. N88-12556
SMITH, GRAEME H. N88-13175
SMITH, I. E. N88-12685
SMITH, J. E. N88-13016
SMITH, J. J. N88-13050
SMITH, J. L. N88-13069
SMITH, M. D. N88-12592
SMITH, MYRON A. N88-13100
SMITH, R. D. N88-12559
SMYRL, W. H. N88-12722
SNIDER, J. B. N88-12900
SOCKER, D. G. N88-13112
SORENSEN, N. R. N88-12565
SPARKS, D. O. N88-13026
SPARKS, S. PATRICK N88-12452
SPERLINE, P. D. N88-12765
SPINDLER, R. N88-12596
SPIRIDIGLIOZZI, L. N88-12652
SREEPATHY, S. N88-12587
N88-12588
SROLOVITZ, D. J. N88-13071
STACY, A. M. N88-13063
STAELIN, DAVID H. N88-12725
STALEY, D. J. N88-12802
STALNAKER, WINIFRED A. N88-12531
STARR, T. L. N88-12604
STAUFFER, JOHN R. N88-13099
STECHEL, E. B. N88-12770
STEGER, J. L. N88-12466
STEINBRUCK, CHARLES G. N88-12903
STEINMETZ, GEORGE G. N88-12487
STELZRIED, C. T. N88-12684
STENCEL, R. E. N88-13165
N88-13169
STENCEL, ROBERT N88-13092
STEWART, JAMES J. N88-12791
STEWART, R. T. N88-13141
STONE, P. A. N88-12567
STRASSMEIER, KLAUS N88-13192
STREYLE, DALE G. N88-12499
STROM, K. M. N88-13183
STROM, S. E. N88-13183
SUBRAMANIAN, S. V. N88-12481
SULCOSKI, MARK F. N88-12645
SUMMERFIELD, MARTIN N88-12615
SUMMERSCALES, J. N88-12592
SUNDARAM, S. N88-12753
SUNDERMAN, F. W., JR. N88-12921
SWANSON, JON T. N88-12791
SWARTZ, CLIFFORD K. N88-12677
N88-12678

T

TAGLIAFERRI, G. N88-13151
TAI, RONALD C. N88-12488
TAKAHASHI, H. N88-13036
TAKANO, C. N88-12578
TAKEDA, H. N88-12778
N88-12789
TAKEUCHI, WATARU N88-13035
TALLERICO, P. J. N88-12775
N88-12776
TAM, HON-WAH N88-12994
TAMARU, T. N88-13034
TANG, C. M. N88-12773
TANIDA, L. N88-12689
TANIGUCHI, M. H. N88-12537
TANZER, H. J. N88-12747
TAPIA, SANTIAGO N88-13143
TATAR, ROBERT C. N88-13054
N88-13055

TAUSWORTHE, R. C. N88-12710
TAWARA, H. N88-13030
TAYLOR, C. D. N88-12669
TAYLOR, DANA JAMES N88-12460
TAYLOR, J. B. N88-13022
TAYLOR, J. H. N88-12803
TAYLOR, LAWRENCE W., JR. N88-12456
TAYLOR, R. D. N88-13048
TERENTYEV, S. A. N88-12627
TESSLER, A. N88-12652
TESTUD, JACQUES N88-12675
TETER, M. P. N88-12969
THOMAS, C. N88-12664
THOMAS, J. B. N88-12730
THOMAS, R. L. N88-12794
THOMPSON, J. D. N88-13069
THOMPSON, PAUL N88-13085
THOMSON, J. N88-12910
TIOMNO, J. N88-13076
TOFFOLETTO, FRANK ROCCO N88-13211
TONER, C. G. N88-13157
TONGE, J. S. N88-13058
TORTORELLI, P. F. N88-12585
TOSHIMA, H. N88-13030
TRACEY, D. H. N88-12648
TRACY, E. R. N88-13029
TRAN, TRIET THUONG N88-12760
TREASE, H. N88-12749
TREDWAY, WILLIAM K. N88-12546
TREPT, TED N88-12462
TRETYAKOV, P. V. N88-12633
TRIVEDI, KISHOR T. N88-12928
TRUONG, T. K. N88-12698
TSALLIS, C. N88-13061
TSENG, D. Y. N88-12475
TUCKER, T. K. N88-12707
TUOMINEN, I. N88-13140
TURNER, JOYCE E. N88-13083
TYREE, W. H. N88-12794
TZUOO, KEH-LIH N88-12463

U

UCKAN, T. N88-13045
ULLMAN, SHIMON N88-12972
ULMSCHNEIDER, P. N88-13106
ULMSCHNEIDER, PETER N88-13118
UMPLEBY, JEFFREY DAVID N88-12594
URAMOTO, JOSHIN N88-13032
UTTAL, T. N88-12900

V

VAHALA, G. N88-13029
VAKHITOV, M. B. N88-12624
VAKHSHOORI, D. N88-13066
VANDALSEM, W. R. N88-12466
VANDENOORD, G. H. J. N88-13121
VANDERZANDEN, J. N88-12737
VANFOSSEN, J. N88-12796
VANNICE, M. A. N88-12564
VANSCHIE, J. P. N88-12867
VANSTEENBERG, MICHAEL EARL N88-13208
VATAVUK, J. N88-12579
VENKATAPATHY, ETHIRAJ N88-12465
VERDEYEN, J. T. N88-13051
VERGEZ, PAUL LOUIS N88-12978
VIGASIN, A. A. N88-12855
VILHU, OSMI N88-13097
VILNROTTER, V. A. N88-12694
VIRTANEN, H. N88-13140
VITEK, J. M. N88-12590
VOGT, G. J. N88-12608

W

WADCOCK, ALAN J. N88-12471
WADE, RICHARD A. N88-13132
WAKELING, S. N88-12677
WAKER, D. A. N88-12769
WALDRON, R. N88-12519
WALKER, DONALD A. N88-12887
WALKER, E. N88-12473
WALTER, F. M. N88-13142
WANG, S. N88-13066
WARBURTON, E. K. N88-13011
WARREN, R. W. N88-12787
WARREN, T. N88-12649
WATANABE, T. N88-13030
WATERHOUSE, R. N88-12563
WATT, R. G. N88-13040
WEBB, JON A. N88-12971
WEBER, EDWARD J. N88-12669
WEBER, P. G. N88-13040
WEI, KUNG-HWA N88-12793
WEISS, J. D. N88-12766
WELLS, G. L. N88-13069
WERLEY, K. A. N88-13027
WERNER, M. N88-13066
WEST, E. A. N88-13016
WESTMACOTT, K. H. N88-12814
WESTON, M. N88-12678
WHALEN, MARGARET V. N88-12538
WHELEN, D. A. N88-12788
WHINNERY, JAMES E. N88-12491
WHITAKER, R. B. N88-12561
WHITE-DEPACE, S. M. N88-13020
WHITE, J. W. N88-12611
WHITE, N. E. N88-13129
N88-13151
WHITE, P. H. N88-13006
WHITE, S. M. N88-13153
N88-13154
WHITE, S. R. N88-12969
WHITE, W. T. N88-12729
WHITING, M. A. N88-12973
WHITMORE, B. N88-13166
WHITTAKER, J. W. N88-12804
WHITTEN, B. L. N88-12788
WIEDEMANN, G. N88-13177
WILBY, J. F. N88-13006
WILEMSKI, G. N88-12563
WILKINS, J. W. N88-12969
WILLIAMS, T. A. N88-12874
WILLIAMSON, D. L. N88-12899
WILLIAMSON, G. S. N88-12899
WILLSON, L. A. N88-13168
WILSON, K. L. N88-13042
WILSON, LARRY N88-12952
WINSKE, D. N88-12808
WINTER, H. H. N88-12599
WINTERS, W. S. N88-12751
WNEK, G. E. N88-12597
WOLFE, THOMAS D. N88-12792
WOLGAST, R. C. N88-12553
WOLSKI, R. J. N88-12899
WONG, V. S. N88-12475
WOOD, RICHARD M. N88-12454
WRIGHT, A. E. N88-13141
WRIGHT, DAVID N88-12954
WRIGHT, THOMAS W. N88-12810
WRIGHTON, MARK S. N88-12724
WU, J. N88-12682
WU, S. C. N88-12682
WURDEN, G. A. N88-13040

Y

YADLOWSKY, EDWARD J. N88-12774
YAMADA, S. N88-13034
YAMAMURA, YASUNORI N88-13035
YAN, Y. T. N88-12788
YANAGI, RYOJI N88-12509
YAROSH, V. V. N88-12840
YATES, E. CARSON, JR. N88-12459
YEREMEYEV, V. N. N88-12846
YERMOLENKO, S. D. N88-12631
YERSHOV, N. S. N88-12636
YONKER, C. R. N88-12559
YU, P. N88-13066
YU, RAY-CHUNG N88-12823
YUNCK, T. P. N88-12682

Z

ZABOTIN, A. N88-12847
ZADROWNY, A. N88-13167
ZAEHRINGER, KURT N88-13118
ZALOGUYEV, S. N. N88-12917
ZAN, S. J. N88-12819
ZARDECKI, A. N88-12782
ZAYTSEV, O. V. N88-12840
ZAYTSEVA, T. V. N88-12840
ZEILIK, MICHAEL N88-13123
N88-13124
N88-13192
ZETLEN, BRYAN A. N88-12488
ZHANG, QIU N88-12673
ZHENG, YUAN F. N88-12795
ZHU, S. N88-12530
ZHURAVLEVA, V. A. N88-12954
ZOONEMATKERMANI, S. N88-13182
ZYDA, MICHAEL J. N88-12499

Typical Corporate Source Index Listing

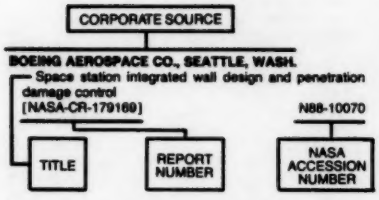

Listings in this index are arranged alphabetically by corporate source. The title of the document provides the user with a brief description of the subject matter. The report number helps to indicate the type of document cited (e.g., NASA report, translation, NASA contractor report). The NASA accession number denotes the number by which the citation is identified. The titles are arranged under each corporate source in ascending accession number order.

A

ADVISORY GROUP FOR AEROSPACE RESEARCH AND DEVELOPMENT, NEUILLY-SUR-SEINE (FRANCE).
Developmental airdrop testing techniques and devices
[AGARD-AG-300-VOL-6] N88-12481
Human respiratory responses during high performance flight
[AGARD-AG-312] N88-12923

ADVISORY GROUP FOR AEROSPACE RESEARCH AND DEVELOPMENT, PARIS (FRANCE).
Standard fatigue test specimens for fastener evaluation
[AGARD-AG-304] N88-12818

AERONAUTICAL RESEARCH LABS., MELBOURNE (AUSTRALIA).
Hovering helicopter flight dynamics: A study of vertical motion
[AR-004-526] N88-12485
A finite element procedure for interference-fit and cold-working problems with limited yielding
[AR-004-517] N88-12992

AEROSPACE CORP., EL SEGUNDO, CALIF.
SDVS (State Delta Verification System) 5 users' manual
[AD-A184339] N88-12943

AIR FORCE ACADEMY, COLO.
Calculation of the tribological properties of surfaces by semi-empirical methods
[AD-A184283] N88-12791

AIR FORCE GEOPHYSICS LAB., HANSCOM AFB, MASS.
Microwave refractive index structure function profiles (Cn2) measured from a small aircraft
[AD-A184343] N88-12670

AIR FORCE WRIGHT AERONAUTICAL LABS., WRIGHT-PATTERSON AFB, OHIO.
Aircraft fire safety research N88-12526
Durability of powdered aluminum structures N88-12655

ALABAMA UNIV., HUNTSVILLE.
Studies of pressure-velocity coupling schemes for analysis of incompressible and compressible flows
[NASA-CR-181526] N88-12748

ALLIED BENDIX AEROSPACE, KANSAS CITY, MO.
Small-diameter wire tensile testing
[DE88-000835] N88-12815

AMERICAN SOCIETY FOR ENGINEERING EDUCATION, WASHINGTON, D. C.
On a circular correlation technique for filtering randomly noisy data
[AD-A184317] N88-12669
Lower bounds on bearing accuracy for closely spaced sources
[AD-A184258] N88-12997

AMES LAB., IOWA.
Alternating current circuit theory and pulsed NMR (Nuclear Magnetic Resonance)
[DE88-000641] N88-12732

ANALYTICAL MECHANICS ASSOCIATES, INC., MOUNTAIN VIEW, CALIF.
NAVSIM 2: A computer program for simulating aided-inertial navigation for aircraft
[NASA-CR-177438] N88-12478

ANALYTICAL METHODS, INC., REDMOND, WASH.
Investigation of low-speed turbulent separated flow around airfoils
[NASA-CR-177450] N88-12471

ARGONNE NATIONAL LAB., ILL.
Emerging environmental constraints on the use of gasoline and diesel fuel and tradeoffs associated with the use of alternative fuels
[DE87-011504] N88-12614
Proceedings of the Fifth Symposium on Energy Engineering Sciences: Instrumentation, Diagnostics, and Material Behavior
[DE88-001479] N88-12660
A review of parameterizations of microphysical processes in clouds for application in models of regional atmospheric deposition
[DE88-000451] N88-12909
The SUPRENUM communications subroutine library for grid-oriented problems
[DE88-000137] N88-12950
A review and analysis of Fortran 8x
[DE88-001320] N88-12955
An approach to implementing state space searches on heterogeneous systems of multiprocessors
[DE88-001321] N88-12967
Oscillation theory for linear second-order differential systems
[DE87-011393] N88-12983
An exact penalization viewpoint of constrained optimization
[DE88-001477] N88-12995
Non-lattice matched metallic superlattices
[DE87-011512] N88-13082

ARIZONA STATE UNIV., TEMPE.
The angular diameter of alpha Scorpii in the near-infrared Ca II triplet N88-13162

ARIZONA UNIV., TUCSON.
Radiometric calibration of the Earth observing system's imaging sensors
[NASA-CR-181542] N88-12865
PG 0308 + 096: A short-period white dwarf + dM binary with strongly modulated H-alpha emission N88-13132
M dwarfs from the Einstein medium sensitivity survey N88-13188

ARMAGH OBSERVATORY (NORTHERN IRELAND).
Active phases on II Peg N88-13119
The giant spot on II Peg in 1986 N88-13120
Evidence for an additional source of opacity during the impulsive phase of stellar flares N88-13133
Excess emission in the wings of the Hydrogen Balmer lines during a flare on the late-type dMe star YZ CMi N88-13148

ARMY AVIATION ENGINEERING FLIGHT ACTIVITY, EDWARDS AFB, CALIF.
Engine/airframe response evaluation of the HH-60A helicopter equipped with the T700-GE-701 transient droop improvement electronic control unit
[AD-A184443] N88-12492

ARMY COLD REGIONS RESEARCH AND ENGINEERING LAB., HANOVER, N. H.
Disturbance and recovery of Arctic Alaskan tundra terrain. A review of recent investigations
[AD-A184442] N88-12887

ARMY CONSTRUCTION ENGINEERING RESEARCH LAB., CHAMPAIGN, ILL.
Carbon dioxide treatment for scale removal and control in potable water systems
[AD-A184346] N88-12556

ARMY ENGINEER WATERWAYS EXPERIMENT STATION, VICKSBURG, MISS.
Open-graded bases for airfield pavements
[AD-A184461] N88-12500

ARMY LAB. COMMAND, WATERTOWN, MASS.
Effect of time and temperature on transformation toughened zirconias
[AD-A184356] N88-12800
Weldability of 2219-T851 and 2519-T87 aluminum armor alloys for use in Army vehicle systems
[AD-A184296] N88-12792

ARMY MATERIALS TECHNOLOGY LAB., WATERTOWN, MASS.
Work-in-progress presented at the Army Symposium on Solid Mechanics, 1986: Lightening of the Force
[AD-A184791] N88-12644
Plastic strain localization between voids in shear deformation fields N88-12648
Explicit and implicit soil modelling for dynamic soil-structure interaction problems N88-12650
Effective treatment of membrane and shear locking phenomena in curved shear-deformable axisymmetric shell element N88-12652

ARMY MILITARY PERSONNEL CENTER, ALEXANDRIA, VA.
Use of a thermodynamic analog for pneumatic transport in horizontal pipes
[AD-A184076] N88-12740

ASTRON RESEARCH AND ENGINEERING, SANTA MONICA, CALIF.
An analysis of sound absorbing linings for the interior of the NASA Ames 80 x 120-foot wind tunnel
[NASA-CR-177396] N88-13008

AUSTRALIAN NATIONAL UNIV., CANBERRA.
Conducting hybrid polymeric systems
[DE88-000527] N88-12611

B

BALLISTIC RESEARCH LABS., ABERDEEN PROVING GROUND, MD.
Composite materials applications program at the US Army Ballistic Research Laboratory: Work in progress N88-12651
Steady shearing in a viscoplastic solid
[AD-A184341] N88-12810
On operator splitting for unsteady boundary value problems
[AD-A184281] N88-12981

BAYLOR UNIV., HOUSTON, TEX.
Conditions for geomagnetically trapping sub-micron lunar ejecta between L = 1.2 and L = 3.1 N88-13203

BELGRADE UNIV. (YUGOSLAVIA).
Gravity from symmetry breakdown of a gauge affine theory
[DE88-001671] N88-13079

BELL TELEPHONE LABS., INC., MURRAY HILL, N. J.
Experimental perspectives on heavy electron metals
[DE87-014766] N88-12583

BENTLEY COLL., BOSTON, MASS.
Emission features in IRAS LRS spectra of MS, S and CS stars N88-13163

BOEING AEROSPACE CO., SEATTLE, WASH.
Light funnel concentrator panel for solar power
[NASA-CR-179223] N88-12870

BOEING MILITARY AIRPLANE DEVELOPMENT, SEATTLE, WASH.
Failure analysis of composite structure materials
[AD-A184468] N88-12548

BRADFORD UNIV. (ENGLAND).
Performance optimization of electronic networks in the frequency domain
[PB87-123873] N88-12720

BRIGHAM YOUNG UNIV., PROVO, UTAH.
Novel macrocyclic carriers for proton-coupled liquid membrane transport
[DE88-000636] N88-12580
Thermodynamic properties of supercritical mixtures
[DE88-000609] N88-12562

BRITISH BROADCASTING CORP., KINGSWOOD (ENGLAND).
Accommodating the residue of processed or computed digital video signals within the 8 bit CCIR recommendation 601
[BBC-RD-1987/12] N88-12676

Band 2 VHF antenna for home construction
[BBC-RD-1987/13] N88-12677

BRITISH PETROLEUM CO. LTD., SUNBURY-ON-THAMES (ENGLAND).
Thixotropic surface composition for phenolaldehyde resin laminates
[GB-PATENT-2-180-251-A] N88-12545
Thermoplastic elastomer compositions
[EP-PATENT-0-204-453-A1] N88-12593
Polymer composition
[EP-PATENT-0-199-444-A1] N88-12594
Process for producing sandwich mouldings
[EP-PATENT-0-191-623-A2] N88-12642
Detection of defects on structures
[EP-PATENT-0-210-794-A2] N88-12807

BROOKHAVEN NATIONAL LAB., UPTON, N. Y.
The atomic weight and isotopic composition of oxygen and their variation in nature
[DE87-014397] N88-12558
Optimized ground coupled heat pump mechanical package
[DE87-014809] N88-12738
PRAAGE: An interactive IBM-PC code for unreliability/aging analysis
[DE87-012124] N88-12803
Single leptons from heavy quark production
[DE87-014917] N88-13009
Few body hypernuclear systems: Weak decays
[DE87-014920] N88-13010
Nuclear beta decay after Les Houches
[DE87-014921] N88-13011
National Synchrotron Light Source users manual: Guide to the VUV and X-ray beam lines
[DE88-001464] N88-13020
Core bounce supernovae
[DE87-014910] N88-13197

BROWN UNIV., PROVIDENCE, R. I.
Equilibria, lattices and chaotic dynamics of point vortices N88-12758
Geometric analysis of ensemble of solutions in two-phase flow and complete resolution of problem of choking
[DE88-001687] N88-12764
Novel dynamical investigations of excitons and their structure in semiconductors
[DE87-014866] N88-13070

C

CALIFORNIA INST. OF TECH., PASADENA.
IUE/Optical/VLA flares on AD Leo N88-13152

CALIFORNIA UNIV., BERKELEY.
The Pierce diode with an external circuit. Part 1: Simulations in the linear regime
[DE88-000413] N88-12731
Blowup for a nonlinear evolution equation and self-reproducing strained shear layers N88-12755
Kinematic formulation of finite elements for plate bending N88-12821
Vibration and parametric excitation in rotating asymmetric circular plates N88-12823
An adaptive subdivision method with crack prevention for rendering beta-spline objects
[AD-A184249] N88-12940
A model of functional knowledge and insight
[AD-A184113] N88-12975
Back-of-the-envelope problems
[AD-A184105] N88-12980
An urn model for the multi-sample capture/recapture sequential tagging process
[AD-A184470] N88-12998
MHD stability and control for mirror machines N88-13038
Coherent emission from relativistic beam-plasma interactions N88-13039
Raman scattering spectrum along a bevel etched GaAs on Si, TEM (Transmission Electron Microscope) study and GaAs P-I-N photodetector on Si
[DE88-000210] N88-13066
Mental models in expert physics reasoning
[AD-A184106] N88-13075
Subjective probability, combination of expert opinion and probabilistic approaches to information retrieval N88-13085
An astrometric search for a stellar companion to the sun N88-13195

CALIFORNIA UNIV., BERKELEY. LAWRENCE BERKELEY LAB.
A creep measurement of unidirectional epoxy-fiberglass rod
[DE87-014812] N88-12553
Studies on high-speed electroforming
[DE88-001395] N88-12656
A new approach to modeling and interpreting electromagnetic sounding data
[DE88-000480] N88-12715
Center for X-Ray Optics, 1986
[DE88-000715] N88-12783
The accommodation of precipitate plates modelled as a tensile test
[DE88-000207] N88-12814
Technology Base Research Project for electrochemical energy storage
[DE88-000649] N88-12868
Proceedings of the Eleventh DOE Solar Photochemistry Research Conference
[DE88-000678] N88-12883
Slow-mode shocks in the earth's magnetosphere
[DE88-000483] N88-12895
A network definition and solution of simulation problems
[DE88-000675] N88-12962
Development of the non-equilibrium reactive chemical transport code CHMTRNS
[DE88-000682] N88-12964
Managing distributed derived data: A preliminary proposal
[DE88-000714] N88-12966
An expert system for materials design
[DE88-000191] N88-12974
Design concepts for the ASTROMAG cryogenic system
[NASA-CR-181505] N88-13060
Magnetic field dependence of the specific heat of some high-T/sub c/ superconductors
[DE87-014078] N88-13063
Raman scattering spectrum along a bevel etched GaAs on Si, TEM (Transmission Electron Microscope) study and GaAs P-I-N photodetector on Si
[DE88-000210] N88-13066
Evaluation of the Mellen EDG furnace for growth of large diameter GaAs single crystals in a horizontal configuration
[DE88-000463] N88-13068
Far infrared Fourier transform spectroscopy of semiconductors
[DE88-000188] N88-13072
The structure of adsorbed sulfur and carbon on molybdenum and rhenium single crystal surfaces, and their influence on carbon monoxide and hydrocarbon chemisorption
[DE88-001393] N88-13073
The role of basic research in society
[DE88-000459] N88-13090
Influences of the astrophysical environment on nuclear decay rates
[DE88-001461] N88-13208

CALIFORNIA UNIV., DAVIS.
A data translation method for heterogeneous database systems N88-13081

CALIFORNIA UNIV., IRVINE.
Large-scale neuronal circuits for selective storage and recognition of complex stimuli, a pilot study
[AD-A184134] N88-12920

CALIFORNIA UNIV., LOS ANGELES.
PISCES: Plasma-surface interactions and materials research
[DE88-001323] N88-13044

CALIFORNIA UNIV., SANTA CRUZ.
Intelligent signal analysis and recognition
[NASA-CR-181531] N88-13084

CAMBRIDGE UNIV. (ENGLAND).
Departmental report on program EMTP-machine windings surge transients: Travelling wave method
[PB87-123733] N88-12719

CARNEGIE-MELLON UNIV., PITTSBURGH, PA.
Implementation and performance of a complex vision system on a systolic array machine
[AD-A184331] N88-12971

CARTER OBSERVATORY, WELLINGTON (NEW ZEALAND).
The short-period RS CVn stars: Starspots and fundamental properties N88-13124

CATHOLIC UNIV. OF AMERICA, WASHINGTON, D.C.
Optical instrumentation and study of gas-solid suspension flows
[DE88-000147] N88-12744
Observations of turbulence and fluctuations in the solar wind N88-13212

CENTRAL ELECTRICITY GENERATING BOARD, LONDON (ENGLAND).
Effects of stress-relieving on the mechanical properties and the structure of specimens of high-temperature fine-grained structural steels heat-treated to simulate welding
[BLL-CE-TRANS-8258-(9022.09)] N88-12586
Influence of creep on the precipitate structure under conditions of long-term creep. 4: Experiments on 10 CrMo 9 10 steel
[BLL-CE-TRANS-8256-(9022.09)] N88-12589
Method for the ultrasonic inspection of the soundness of the metal in weld joints in two-ply pipes
[BLL-CE-TRANS-8265-(9022.09)] N88-12805
Ultrasonic method of inspecting austenitic weld joints in nuclear power station equipment
[BLL-CE-TRANS-8261-(9022.09)] N88-12806

CENTRO BRASILEIRO DE PESQUISAS FISICAS, RIO DE JANEIRO.
Consistency question in the renormalization group analysis of deep inelastic scattering
[DE87-703372] N88-12999
On deviations from Newton's law and the proposal for a Fifth Force
[DE87-703368] N88-13001
Influence of bond dilution on the free surface and interface Potts ferromagnetism
[DE87-703360] N88-13061
Analysis of absolute space-time Lorentz theories
[DE87-703371] N88-13076
New cosmological scenario
[DE87-703357] N88-13198
Moessbauer study of shock induced effects in the Fe-Ni 50/50 ordered alloy in meteorites
[DE87-703364] N88-13199
Cosmic-ray nuclear event with an anomalously strong concentration of energy and particles in the central region
[DE87-703376] N88-13213

CHALMERS UNIV. OF TECHNOLOGY, GOETEBORG (SWEDEN).
EVN (European VLBI network) and MERLIN observations of 5 superluminal radio sources
[PB87-110730] N88-13193

CLEMSON UNIV., S.C.
Static standing and dynamic walking of a practical biped robot
[DE88-001367] N88-12795

COLLEGE OF WILLIAM AND MARY, WILLIAMSBURG, VA.
Theoretical plasma physics
[DE88-001475] N88-13029

COLORADO SCHOOL OF MINES, GOLDEN.
The nature of metallurgical reactions in underwater welding
[AD-A184464] N88-12568

COLORADO STATE UNIV., FORT COLLINS.
Continuation finite element analysis of viscoelastic fluids N88-12761

COLORADO UNIV., BOULDER.
Three-dimensional unsteady flow elicited by finite wings and complex configurations N88-12468
Interactions between the Asian monsoons, the tropical Pacific and the southern hemisphere extratropics N88-12907
Cloud cover determination in polar regions from satellite imagery
[NASA-CR-181544] N88-12908
Fifth Cambridge Workshop on Cool Stars, Stellar Systems and the Sun N88-13092
Nonthermal phenomena in stellar coronae: Evidence from radio observations N88-13096
Disk accretion during the early stages of stellar evolution N88-13106
Simultaneous, cospatial imaging of the Sun in cyanogen and singly-ionized calcium N88-13114
Activity in warm stars N88-13142
Exosat results on the dMe flare Star Wolf 630AB and on VB 8 N88-13151
Far infrared circumstellar debris shells of red supergiant stars N88-13165
IRAS and cool stellar mass loss N88-13166
Radio emission from RS CVn binaries: A 5 GHz VLA survey of 93 systems N88-13191
Catalogue of chromospherically active binaries N88-13192
A comprehensive exploration of late-type stars in the far-ultraviolet N88-13194
Observations and analysis of the photospheric magnetic fields on dwarf G, K and M stars N88-13196
Galactic interstellar abundance surveys with IUE and IRAS N88-13206

COLUMBIA UNIV., NEW YORK, N.Y.
Spatial strength variation and statistical size effect of laminated orthotropic composite materials N88-12646
The Einstein survey of the young stars in the Orion Nebula N88-13182

COMMISSION OF THE EUROPEAN COMMUNITIES (LUXEMBOURG).
Solar energy: European research and development
[PB87-107645] N88-12666

Statistical distribution of solar radiation (hourly sums): Cumulative frequency curves preparation of a European data set and direction for use
[PB87-107454] N88-12886

COMMONWEALTH SCIENTIFIC AND INDUSTRIAL RESEARCH ORGANIZATION, EPPING (AUSTRALIA).
The Perkes radio survey of active chromosphere stars N88-13141

CONNECTICUT UNIV., FARMINGTON.
The toxicology and metabolism of nickel compounds
[DE87-014801] N88-12921

CONNECTICUT UNIV., STORRS.
Structure of thermotropic polyesters with large substituents
[AD-A184066] N88-12595

CONSEJO SUPERIOR INVESTIGACIONES CIENTIFICAS, TENERIFE (SPAIN).
Light curve behaviour in the near IR of the CG Cyg system N88-13156
Carbon abundances and C12/C13 ratios in M giants N88-13167
Stromgren photometry of RSCVn and HD106102 N88-13187

CORNELL UNIV., ITHACA, N.Y.
Large change-of-curvature effects in quadratic finite elements for CAD of membrane structures N88-12958
The finite element method for electronic structure
[DE88-001706] N88-12969

CORNING GLASS WORKS, N.Y.
The finite element method for electronic structure
[DE88-001706] N88-12969

CRANFIELD INST. OF TECH., BEDFORD (ENGLAND).
Design and development of absorption heat pumps
[DE88-900062] N88-12885

D

DEFENSE TECHNICAL INFORMATION CENTER, ALEXANDRIA, VA.
Source header list. Volume 1: A through K
[AD-A184000] N88-13086

DENVER UNIV., COLO.
Relativistic electron precipitations in a pulsating aurora N88-12894

DEPARTMENT OF ENERGY, WASHINGTON, D. C.
DOE explosives safety manual
[DE88-000831] N88-12616
Materials sciences programs: Fiscal Year 1987
[DE88-000672] N88-12659
Summaries of physical research in the geosciences
[DE88-000833] N88-12896
Proceedings of the Japan-US Workshop P-92 on Plasma Material Interaction/High Heat Flux Data Needs for the Next Step Ignition and Steady State Devices
[DE87-013568] N88-13042

DOMINION ASTROPHYSICAL OBSERVATORY, VICTORIA (BRITISH COLUMBIA).
Angular momentum evolution of young stars N88-13099

DRAPER (CHARLES STARK) LAB., INC., CAMBRIDGE, MASS.
On the next generation of reliability analysis tools
[NASA-CR-178360] N88-13000

DU PONT DE NEMOURS (E. I.) AND CO., AIKEN, S.C.
Expert robots in nuclear plants
[DE87-014839] N88-12800
Input/output technologies: An overview of image scanning, storage, and display
[DE87-014837] N88-12933

DUKE UNIV., DURHAM, N. C.
Aircraft interior noise reduction by alternate resonance tuning
[NASA-CR-181530] N88-13005

E

ECOLE CENTRALE DE LYON (FRANCE).
Characterization of thin layers for optics
[PB87-217949] N88-13017

EDGERTON, GERMESHAUSEN AND GRIER, INC., GOLETA, CALIF.
Increased gain of channel intensifier tubes by pulsed biasing
[DE88-000512] N88-13019

EDGERTON, GERMESHAUSEN AND GRIER, INC., IDAHO FALLS, IDAHO.
Parallelization of hydrocodes on the Intel Hypercube, part 2
[DE88-001591] N88-12957

EDGERTON, GERMESHAUSEN AND GRIER, INC., LOS ANGELES, CALIF.
Computer-aided X-ray image system design and evaluation
[DE88-000997] N88-12965

EIDGENOESSISCHE TECHNISCHE HOCHSCHULE, ZURICH (SWITZERLAND).
Experimental perspectives on heavy electron metals
[DE87-014766] N88-12583

ELECTRO MAGNETIC APPLICATIONS, INC., DENVER, COLO.
Experimental and analytic studies of the triggered lightning environment of the F106B
[NASA-CR-4104] N88-12897

ELORET CORP., SUNNYVALE, CALIF.
Development and application of computational aerothermodynamics flowfield computer codes
[NASA-CR-181534] N88-12465
Experimental aerothermodynamic research of hypersonic aircraft
[NASA-CR-181533] N88-12483
Performance analysis of advanced spacecraft TPS
[NASA-CR-181532] N88-12484
Simulation studies for surfaces and materials strength
[NASA-CR-181535] N88-12557

ENVIRONMENTAL RESEARCH INST. OF MICHIGAN, ANN ARBOR.
All-optical beam control by forced Rayleigh scattering
[AD-A184315] N88-13018

EUROCONTROL EXPERIMENTAL CENTRE, BRETIGNY (FRANCE).
Experimental use of artificial intelligence for (future) ATC systems
[PB87-106449] N88-12970

EUROPEAN SPACE AGENCY. EUROPEAN SPACE OPERATIONS CENTER, DARMSTADT (WEST GERMANY).
The X-ray orbital lightcurves of AR Lac and TY Pyx N88-13129

F

FACTORY MUTUAL RESEARCH CORP., NORWOOD, MASS.
Fire extinguishment and inhibition in spacecraft environments N88-12523

FAIRBORN OBSERVATORY, MESA, ARIZ.
Automatic photometric monitoring of cool stars N88-13103
Automatic telescope operations N88-13190

FERMI NATIONAL ACCELERATOR LAB., BATAVIA, ILL.
Resistor cooling in a vacuum
[DE88-000696] N88-12733
Some new ideas in liquid detectors
[DE88-000732] N88-12768

FIVE-COLLEGE ASTRONOMY DEPT., AMHERST, MASS.
The contribution of accretion luminosity to the infrared spectra of T Tauri stars: A possible test N88-13183

FLORIDA UNIV., GAINESVILLE.
Reduced complexity structural modeling for automated airframe synthesis
[NASA-CR-177440] N88-12453

FLOW ANALYSIS ASSOCIATES, ITHACA, N.Y.
Heat and moisture transport in the atmospheric boundary layer
[AD-A184222] N88-12904

FOERSVARETS FORSKINGSANSALT, STOCKHOLM (SWEDEN).
Equilibrium calculations of ionization in tracer flames
[PB87-104154] N88-12555
Test number 2 of propellant for rocket motor MK52
[PB87-226155] N88-12613

FRANKLIN AND MARSHALL COLL., LANCASTER, PA.
Differential B and V light curves of the bright by Draconis star HD60715 N88-13130

G

GEOLOGICAL SURVEY, DENVER, COLO.
Development of the non-equilibrium reactive chemical transport code CHMTRNS
[DE88-000682] N88-12964

GEORGE MASON UNIV., FAIRFAX, VA.
Heterogeneous multi-trunking queueing systems
[AD-A184255] N88-12668

GEORGIA INST. OF TECH., ATLANTA.
A method for the efficient calculation of elastic rotor blade dynamic response in forward flight N88-12460
Development of advanced fiber reinforced ceramics
[DE88-000779] N88-12604
Group analysis of equations arising in ocean acoustics N88-12914

GEORGIA UNIV., ATHENS.
A study of mechanisms of hydrogen diffusion in separation devices
[DE88-000328] N88-12584
Statistical inference: Computer oriented algorithmic approach
[DE87-013874] N88-12948
On color polynomials of Fibonacci graphs
[AD-A184133] N88-12996
Topological aspects of infinite metal clusters and superconductors
[AD-A184104] N88-13049

H

HAMBURGER STERNWARTE (WEST GERMANY).
The closest solar analogs in the bright star catalogue N88-13110
Asymmetry and variations of solar limb darkening along the diameter defined by diurnal motion in April 1981 N88-13111

HARVARD-SMITHSONIAN CENTER FOR ASTROPHYSICS, CAMBRIDGE, MASS.
Measurements of stellar magnetic fields N88-13093
New results from high angular resolution observations of alpha Ori N88-13161
Winds and shells around low-mass supergiants N88-13184

HAWAII UNIV., HONOLULU.
Bandwidth efficient block codes for M-ary PSK modulation
[NASA-CR-181543] N88-12712

HEIDELBERG UNIV. (WEST GERMANY).
The dynamics of solar magnetic flux tubes subjected to resonant foot point shaking N88-13118

HELSINKI UNIV. (FINLAND).
Theory of one and two-pass cross-flow heat exchanger
[PB87-225157] N88-12736
Observational constraints and evidence for saturation N88-13097

HERCULES AEROSPACE CO., MAGNA, UTAH.
Fabrication and testing of fire resistant graphite composite panels
[NASA-CR-177397] N88-12472

HONEYWELL, INC., EDINA, MINN.
A direct method to obtain constitutive model constants from cylinder impact test results N88-12647

HOWARD UNIV., WASHINGTON, D. C.
A national model at Howard University demonstrating private sector interrelationships that facilitate research in predominantly Black colleges and universities
[DE88-000160] N88-13089

HUGHES AIRCRAFT CO., LONG BEACH, CALIF.
Design description report for a photovoltaic power system for a remote satellite earth terminal
[NASA-CR-179586] N88-12875

HUGHES AIRCRAFT CO., TORRANCE, CALIF.
Advanced radiator concepts utilizing honeycomb panel heat pipes
[NASA-CR-172017] N88-12747

HUGHES RESEARCH LABS., MALIBU, CALIF.
Autonomous Land Vehicle (ALV) planning and navigation system
[AD-A184243] N88-12475

HY-TECH RESEARCH CORP., RADFORD, VA.
Laser induced fluorescent study of relativistic electron beams
[AD-A184456] N88-12774

I

ILLINOIS INST. OF TECH., CHICAGO.
On the instability of thin circular shear layers N88-12457

ILLINOIS UNIV., URBANA.
Mutual admittance between slots in cylinders of arbitrary shape
[AD-A184254] N88-12723
Center for Supercomputing Research and Development (CEDAR)
[DE88-000807] N88-12930
A characterization of separating pairs and triplets in a graph
[AD-A184278] N88-12941
On the number of minimum size separating vertex sets in a graph
[AD-A184279] N88-12942
A comparison of adaptive refinement techniques for elliptic problems
[DE88-000905] N88-12987
The shifted Adams method for ordinary differential equations
[DE88-000810] N88-12994
Transport simulations of the oscillating field current drive experiment in the ZT-40M reversed field pinch
[DE88-000538] N88-13027
Measurement of the electron density and the attachment rate coefficient in silane/helium discharges
[AD-A184266] N88-13051

IMAD AD DEAN, INC., BETHESDA, MD.
A flash spectrum of Ca I, C I, N I, and Ni II absorption in 31 Cygni: A direct observation of the reversing layer N88-13158
IMPERIAL COLL. OF SCIENCE AND TECHNOLOGY, LONDON (ENGLAND).
A search for very low mass (brown dwarf) stars as wide binaries using a seven element infrared camera-photometer N88-13150
INDIAN INST. OF ASTROPHYSICS, BANGALORE.
Calibration on the Sun for stellar magnetic fields N88-13113
Sensitivity of the H alpha line to expansion, geometrical extent and temperature gradient in the G and K supergiant chromospheres N88-13159
INDIANA UNIV., BLOOMINGTON.
Synthetic spectra for the N-type carbon star TX Psc N88-13173
INFORMATION AND CONTROL SYSTEMS, INC., HAMPTON, VA.
Investigation, development and application of optimal output feedback theory. Vol. 4: Measures of eigenvalue/eigenvector sensitivity to system parameters and unmodeled dynamics [NASA-CR-4108] N88-12969
INSTITUT D'ASTROPHYSIQUE, PARIS (FRANCE).
Pre-main sequence activity: How far is magnetism involved N88-13179
INSTITUTE OF GAS TECHNOLOGY, CHICAGO, ILL.
Internal reforming development for solid oxide fuel cells [DE87-006518] N88-12871
INSTITUTE OF OCEANOGRAPHIC SCIENCES, WORMLEY (ENGLAND).
RRS DISCOVERY cruise 160, 30 June-25 July, 1986. Geochemical sampling over the Madeira and Porcupine Abyssal Plains [PB87-222030] N88-12910
INSTITUTO DE PESQUISAS ENERGETICAS E NUCLEARES, SAO PAULO (BRAZIL).
Mechanical strength and niobium and niobium-base alloys substructures [DE87-703692] N88-12577
Studies of alumina additions in zirconia - magnesia [DE87-703500] N88-12602
INSTITUTO DE PESQUISAS ESPACIAIS, SAO JOSE DOS CAMPOS (BRAZIL).
Measurements of iridium and the meteoric impact hypothesis at cretaceous end [DE87-703765] N88-13200
INSTITUTO DE PESQUISAS TECNOLOGICAS, SAO PAULO (BRAZIL).
Corrosion strength of niobium and its alloys [DE87-703693] N88-12578
IOWA STATE UNIV. OF SCIENCE AND TECHNOLOGY, AMES.
Application of dynamic atmosphere models to the analysis of angular diameter observations of Mira variables N88-13168

J

JET PROPULSION LAB., CALIFORNIA INST. OF TECH., PASADENA.
Interplanetary propulsion using inertial fusion [NASA-TM-89661] N88-12540
The Telecommunications and Data Acquisition Report [NASA-CR-181546] N88-12679
A demonstration of high precision GPS orbit determination for geodetic applications N88-12680
Robust statistical methods for automated outlier detection N88-12681
Precise near-earth navigation with GPS: A survey of techniques N88-12682
Short baseline phase delay interferometry N88-12683
Non-linearity in measurement systems: Evaluation method and application to microwave radiometers N88-12684
Atomic frequency standards for ultra-high-frequency stability N88-12685
Measurement and analysis of cryogenic sapphire dielectric resonators and DROs N88-12686
Inductance effects in the high-power transmitter crowbar system N88-12687
Low-noise cryogenic transmission line N88-12688
A 2.3-GHz cryogenically cooled HEMT amplifier for DSS 13 N88-12689
A cold ejector for closed-cycle helium refrigerators N88-12690
Frequency doubling conversion efficiencies for deep space optical communications N88-12691
The atmosphere of Mars and optical communications N88-12692
A near-earth optical communications terminal with a corevolving planetary sun shield N88-12693
Optimized tracking of RF carriers with phase noise, including Pioneer 10 results N88-12694
Detection of signals by the digital integrate-and-dump filter with offset sampling N88-12695
Detection of signals by weighted integrate-and-dump filter N88-12696
The design plan of a VLSI single chip (255, 223) Reed-Solomon decoder N88-12697
A simplified procedure for correcting both errors and erasures of a Reed-Solomon code using the Euclidean algorithm N88-12698
More on the decoder error probability for Reed-Solomon codes N88-12699
On the VLSI design of a pipeline Reed-Solomon decoder using systolic arrays N88-12700
A procedural method for the efficient implementation of full-custom VLSI designs N88-12701
A new state space model for the NASA/JPL 70-meter antenna servo controls N88-12702
X-band uplink ground systems development: Part 2 N88-12703
Analysis of the ICE combiner for multiple antenna arraying N88-12704
The 8.4-GHz low-noise maser pump source assembly N88-12705
A modern control theory based algorithm for control of the NASA/JPL 70-meter antenna axis servos N88-12706
Fast autotuning of a hydrogen maser by cavity Q modulation N88-12707
Traveling-wave maser closed-cycle refrigerator data acquisition and display system N88-12708
Two-watt, 4-Kelvin closed cycle refrigerator performance N88-12709
Tau ranging revisited N88-12710
Power density measurements in the near field of the DSS 13 26-meter antenna N88-12711
Interferometry theory for the block 2 processor [NASA-CR-181551] N88-12730
Guidelines for preparing software user documentation [NASA-CR-181550] N88-12959
The VISTA spacecraft: Advantages of ICF (Inertial Confinement Fusion) for interplanetary fusions propulsion applications [NASA-CR-181549] N88-13024
JOHNS HOPKINS UNIV., BALTIMORE, MD.
Turbulent mixing in a rotating, stratified fluid N88-12759
Extremum methods of structural analysis for system reliability assessment N88-12824
Boundary effects on the drag of an oscillating sphere: Applications to the magnetic sphere rheometer. Attenuation and dispersion of acoustic waves in nematic liquid crystals N88-13007
Hydrogen and deuterium in the local interstellar medium N88-13204
JOHNSON CONTROLS, INC., MILWAUKEE, WIS.
A hydrogen/nickel oxide battery for remote applications [DE87-009048] N88-12872
JOINT INST. FOR LAB. ASTROPHYSICS, BOULDER, COLO.
The photospheric magnetic fields of cool stars: Recent results of survey and time-variability programs N88-13094
Heating of stellar chromospheres and coronas: Evidence for non-magnetic basal heating N88-13098
Calibration of the Ca II K line-core density and the magnetic flux density in stars using solar data N88-13116
Broadband linear polarization and chromospheric CaII H and K line emission in late-type main sequence stars N88-13140
Empirical relations between photospheric magnetic fields and atmospheric radiative losses for cool dwarf stars N88-13145
VLA observations of the X-ray bright Hyades M-dwarfs N88-13147
Chromospheric variability mechanisms affecting pre-main sequence stars N88-13180
Chromospheric and coronal heating in a bias-free sample of K dwarfs N88-13184
Measurements of stellar magnetic fields: Empirical constraints on dynamo and rotational evolution theories N88-13185
JOINT PUBLICATIONS RESEARCH SERVICE, ARLINGTON, VA.
JPRS report: Science and technology. Japan [JPRS-JST-87-025] N88-12502
Activities at government research laboratories reported N88-12503
Solar converging method N88-12504
Ceramics thin film N88-12505
Carbon-fiber reinforced plastics N88-12506
Carbon-fiber reinforced aluminum N88-12507
Research and development on high strength ceramic heaters discussed N88-12508
National Aerospace Laboratory experiment N88-12509
Motion and space sickness N88-12510
Numerical simulation system N88-12511
SCRAM JET (Supersonic Combustion Ramjet) combustion experiments N88-12512
USSR report: Engineering and equipment [JPRS-UEQ-87-008] N88-12621
A reliability concept for optimizing aircraft design N88-12622
Optimum take-off run of aircraft on ground airfields N88-12623
Aircraft dynamic response calculation based on discrete-continual model N88-12624
Effect of permissible variations of center-of-gravity locations of cargo airplane on its mass N88-12625
Aircraft classification by type of propulsive devices. Determination of type and number of carrying solutions N88-12626
Local-optimal control in systems with delay N88-12627
Renewed interest in airships for industry use discussed N88-12628
Multipath gear-friction planetary transmissions N88-12629
Calculation of three-dimensional stationary turbulent boundary layer on root section of wing ignoring compressibility N88-12630
Calculation of aerodynamic characteristics of three-dimensional finite span wings in potential incompressible flow N88-12631
Some asymptotic modes of transonic vortex flow N88-12632
Conical wing with maximum lift-to-drag ratio in supersonic gas flow N88-12633
Excitation of natural oscillations of a boundary layer by an external acoustic field N88-12634
Numerical study of supersonic flow around blunt bodies with extended needle nose N88-12635
Dynamics of reverse flows at pump inlet N88-12636
Solution of geometrically nonlinear problem for reinforced shell of revolution having arbitrary shape N88-12637
Rational reinforcement of cylindrical shells with variable stiffness frames subjected to external pressure N88-12638
Finite deformations of shell with rigid inclusion N88-12639
Fatigue failure of thin porous stripe N88-12640
Optimal ribbing of long plate made of composite material N88-12641
USSR report: Earth sciences [JPRS-UES-86-006] N88-12831
Computer modeling aids studies of precipitation formation N88-12832
Progress in improving weather forecasting viewed N88-12833
New precipitation map of world ocean N88-12834
Drought, solar activity link established by Leningrad geophysicists N88-12835
Complex for ocean study from space and hydroacoustic stations N88-12836
Cauchy problem for linearized system of Navier-Stokes equations considering compressibility N88-12837
Asymptotic form of stationary solutions of the Navier-Stokes equations for large Reynolds numbers N88-12838
Steady distortion of shape of geoid and normal gravity field under influence of tidal potential N88-12839
Experimental study of turbulent diffusion parameters in ocean N88-12840
Influence of stratification in near-surface water layer on intensity of gas exchange between atmosphere and water N88-12841
Dispersion equation for plane capillary-gravity wave on free surface of viscous incompressible fluid N88-12842
Influence of surfactants on damping of gravity-capillary waves. 1: Frequency dependence N88-12843
Intensive synoptic eddies and quasigeostrophic approximation N88-12844
Dynamics of isolated intrathermocline eddy N88-12845
Influence of secondary eddy currents on scattering of admixture in zonal flow N88-12846
Studies of thin surface films aim at seeing deep ocean processes N88-12847
Solution of three-dimensional inverse problem of gravimetry in contact surfaces class by local corrections method N88-12848
Lasers measure atmosphere N88-12849
Thermophoresis of spherical aerosol particle at arbitrary Knudsen numbers N88-12850

Theory of heat and moisture exchange between finely disperse storm-generated spray and turbulent air flow N88-12851
Multiwave laser soundings of atmospheric aerosol: Experimental research (review) N88-12852
Use of electron beam instruments to determine fluctuations in vertical refraction partial angle N88-12853
Lidar-radiometric method for determining liquid-water content of cirrus clouds N88-12854
Absorption of far IR-radiation by H2O-N2 complexes under atmospheric conditions N88-12855
Structure of stably stratified atmospheric surface layer in presence of heat-releasing admixture N88-12856
Considering refraction in leveling with laser plane N88-12857
JPRS report: Science and technology. USSR: Life sciences
[JPRS-ULS-87-009] N88-12915
Change in functional activity of cortical brain structures and their blood supply in alert rabbits in response to rocking N88-12916
Study of certain biological characteristics of bacteria during the French-Soviet CYTOS-2 space experiment N88-12917

K

KAMAN SCIENCES CORP., COLORADO SPRINGS, COLO.
Analysis and testing of predamaged shell structures N88-12853
KANSAS UNIV. CENTER FOR RESEARCH, INC., LAWRENCE.
An experimental investigation of dynamic ground effect
[NASA-CR-4105] N88-12458
An integrated study of structures, aerodynamics and controls on the forward swept wing X-29A and the oblique wing research aircraft
[NASA-CR-181548] N88-12486
KIEPENHEUER-INST. FUER SONNENPHYSIK, FREIBURG (WEST GERMANY).
Variations of the vertical and horizontal velocities of the small-scale structures and the physical problems related to overshoot layers N88-13115
KITT PEAK NATIONAL OBSERVATORY, TUCSON, ARIZ.
Contemporaneous B,V,R,I photometry and H alpha spectroscopy of YY Gem N88-13155
Time series infrared spectroscopy of long period variables N88-13172

L

LABORATORIUM VOOR RUIMTEONDERZOEK, UTRECHT (NETHERLANDS).
A large X-ray flare on squared Sigma coronae borealis observed with exosat N88-13121
Asynchronous rotation in close binary systems with circular orbits N88-13131
Evidence for expanding magnetic loops in coronae of cool stars N88-13134
LAWRENCE LIVERMORE NATIONAL LAB., CALIF.
The LLNL 150-mm equation-of-state gun system
[DE88-000423] N88-12519
Interplanetary propulsion using inertial fusion
[NASA-TM-89881] N88-12540
Study of zero CTE (Coefficients of Thermal Expansion) of graphite/epoxy composites
[DE87-013557] N88-12554
Interactions between science and precision engineering
[DE87-010873] N88-12643
Application of lattice filtering techniques to CW measured time domain data
[AD-A184351] N88-12671
Pulse-mode expansions and refractive indices in plane-wave propagation
[DE88-001328] N88-12714
Generating meshes for finite-difference analysis using a solid modeler
[DE88-001458] N88-12729
Fully developed turbulence via Feigenbaum's period-doubling bifurcations
[DE88-000242] N88-12739
A free-Lagrange method for 2-D compressible flows
[DE88-000216] N88-12745
XUV emission features from the Livermore soft X-ray laser experiments
[DE88-000420] N88-12779
Thermal stress in the edge cladding of Nova glass laser disks
[DE88-000425] N88-12780
J = O Task Force
[DE88-001326] N88-12788
Proceedings: SDIO/DARPA Workshop on Laser Propulsion. Volume 3: Viewgraphs
[DE88-000964] N88-12790
Influence of strain rate and notch depth on tensile properties of HITCO 6250
[DE88-001324] N88-12816
Sea level changes
[DE87-014357] N88-12913
PROVER: A first-order logic system in Ada
[DE88-000220] N88-12951
COLA2: A computer program for the structural synthesis of two components using general modal coordinates
[DE88-001457] N88-12963
The VISTA spacecraft: Advantages of ICF (Inertial Confinement Fusion) for interplanetary fusions propulsion applications
[NASA-CR-181549] N88-13024
Inertial confinement fusion reactor cavity analysis
[DE88-000786] N88-13028
The attitudes of science policy, environmental, and utility leaders on US energy issues and fusion
[DE88-000784] N88-13041
Review of X-ray spectroscopy from laser-produced plasmas
[DE88-000755] N88-13043
Wavelengths of the 3p-3d transitions of the Co- and Fe-like ions: The effects of electron correlation
[DE88-000219] N88-13067
Towards automated consulting: Design feedback from the performance of online documentation
[DE87-012243] N88-13082
LEHIGH UNIV., BETHLEHEM, PA.
Some stochastic aspects of intergranular creep cavitation
[DE88-000085] N88-12581
LITTLE (ARTHUR D.), INC., CAMBRIDGE, MASS.
A study of the crack tip parameters that govern environmentally assisted cracking by use of the rising displacement test N88-12649
LOS ALAMOS NATIONAL LAB., N. MEX.
Thermal analysis of electromagnetic launcher rails
[DE88-000166] N88-12514
Experimental perspectives on heavy electron metals
[DE87-014766] N88-12583
Synthesis of the monoclinic yttria by thermal plasma processing
[DE88-000496] N88-12606
Advances in inherently conducting polymers
[DE88-000501] N88-12610
Conducting hybrid polymeric systems
[DE88-000527] N88-12611
Particle injection and cosmic ray acceleration at collisionless parallel shocks
[DE88-000507] N88-12665
The TAB method for numerical calculation of spray droplet breakup
[DE87-011756] N88-12743
Three-dimensional, free-Lagrange hydrodynamics
[DE88-000494] N88-12749
Spectral evolution equation for the sideband instability in a free-electron laser oscillator
[DE88-000510] N88-12771
High-power RF-pulsed modulators for the Los Alamos free-electron laser
[DE88-000514] N88-12775
The lasertron RF generator for FEL (Free-Electron Laser) applications
[DE88-000515] N88-12776
Long-range pulselength scaling of 351nm laser damage thresholds
[DE87-014754] N88-12777
Analysis of sideband spectra from untapered undulator using analytical technique
[DE87-014763] N88-12778
Energy balance in laser-irradiated vaporizing droplets
[DE88-000525] N88-12782
Output power enhancement of AC Raman free-electron laser
[DE88-000503] N88-12786
The generation and suppression of synchrotron sidebands
[DE88-000532] N88-12787
Comparison of sideband spectra obtained from analytical formula and from numerical simulation in free-electron laser
[DE88-000521] N88-12789
Controlling robots with spoken commands
[DE88-000537] N88-12801
Numerical modeling of slow shocks
[DE87-014768] N88-12808
A mineral reconnaissance sampling manual for Costa Rica: Central American energy and resource project
[DE87-014997] N88-12859

Latency differences and effects of selective attention to gratings in the central and right visual fields: 2
[DE87-014730] N88-12918
Visual evoked responses to sinusoidal gratings presented in central and right visual fields: 1
[DE87-014731] N88-12919
Parallel superconvergent multigrid
[DE87-013153] N88-12960
GOLD: Integration of model-based control systems with artificial intelligence and workstations
[DE88-000506] N88-12976
GOLD: Integration of model-based control systems with artificial intelligence and workstations
[DE88-000706] N88-12977
Future directions in interplays between particle and nuclear physics: Summary session
[DE87-011791] N88-13013
Increased gain of channel intensifier tubes by pulsed biasing
[DE88-000512] N88-13019
Transport simulations of the oscillating field current drive experiment in the ZT-40M reversed field pinch
[DE88-000538] N88-13027
Refueling and density control in the ZT-40M reversed field pinch
[DE88-000504] N88-13040
Soliton twin boundaries of the cubic-tetragonal martensitic transformations in ferroelastic materials
[DE87-014741] N88-13047
The Moessbauer effect of SnI4 at high pressure
[DE87-014771] N88-13048
Resistivity of EuBa2(Cu/sub 1-y/Zn/sub y/)3O/sub x/ as a ffunction of temperature, magnetic field, pressure and Zn concentration
[DE87-014740] N88-13069
Theory and simulations of Zone 2 microstructures in thin films
[DE87-014752] N88-13071
LOUISVILLE UNIV., KY.
Magnetic fields on K and M stars N88-13137
LOWELL OBSERVATORY, FLAGSTAFF, ARIZ.
Stellar cycle variability of solar-like stars: A sneak preview N88-13136
LOWER MISSISSIPPI RIVER FORECAST CENTER, SLIDELL, LA.
High latitude F-region drift studies
[AD-A184466] N88-12889

M

MADISON MAGNETICS, INC., WIS.
Repulsive force support system feasibility study
[NASA-CR-178400] N88-12497
MANKATO STATE COLL., MINN.
Infrared excesses of barium stars N88-13174
MARQUETTE UNIV., MILWAUKEE, WIS.
Analytical studies of axially symmetric motion of an incompressible viscous fluid between two concentric rotating spheres N88-12757
MARYLAND UNIV., BALTIMORE.
Microwave observations of red dwarf flare stars N88-13153
A VLA survey of dMe flare stars N88-13154
MARYLAND UNIV., COLLEGE PARK.
Two dimensional path planning with obstacles and shadows
[AD-A184075] N88-12474
A tight upper bound for the speed-up of parallel best-first branch-and-bound algorithms
[AD-A184246] N88-12939
MASSACHUSETTS INST. OF TECH., CAMBRIDGE.
Conductive polymers via reactive oligomer
[AD-A184270] N88-12597
Chemically modified microelectrode arrays. New kinds of electronic devices
[AD-A184389] N88-12724
Phase-coherent astrometric interferometry
[AD-A184428] N88-12725
On the recognition of curved objects
[AD-A184441] N88-12945
An approach to object recognition: Aligning pictorial descriptions
[AD-A184482] N88-12972
MASSACHUSETTS UNIV., AMHERST.
Molecular composites: Processing, post-treatment and mechanics
[AD-A184458] N88-12547
Thermoplastic elastomers as LOVA (Low Vulnerability Ammunition) binders
[AD-A184350] N88-12599
The modelling of orientation in planar polymer welding flows
[AD-A184404] N88-12793

MATERIALS RESEARCH LABS., MELBOURNE (AUSTRALIA).
Analysis of a series of electromagnetic launcher firings
[AR-005-131] N88-12516
Efficiency aspects of short, low velocity railguns
[AR-004-847] N88-12517
MCDONNELL-DOUGLAS ASTRONAUTICS CO., HOUSTON, TEX.
Spacecraft material flammability testing and configurations N88-12529
METEOROLOGICAL OFFICE, LONDON (ENGLAND).
Study of an airborne Doppler radar: Project Asterix
[BLL-MO-TRANS-1667-(0022.552)] N88-12675
MIAMI UNIV., FLA.
Mesoscale eddy dynamics by the method of point vortices N88-12663
MICHIGAN TECHNOLOGICAL UNIV., HOUGHTON.
Parallelization of hydrocodes on the Intel Hypercube, part 2
[DE88-001591] N88-12957
MINNESOTA UNIV., MINNEAPOLIS.
Applications of multivalent ionic conductors to polymeric electrolyte batteries
[AD-A184252] N88-12722
A dissipation principle and its consequences for structured shock waves in thermoelastic materials
[DE87-013723] N88-12813
Two-layer stratified flow analysis of gravity currents and turbidity currents in lakes, reservoirs and the ocean N88-12964
MOUND LAB., MIAMISBURG, OHIO.
Simultaneous TG/DSC (thermogravimetry/Differential Scanning Calorimetry) and TG/MS (thermogravimetry/Mass Spectrometry) analyses of polymeric and energetic materials
[DE88-000727] N88-12561
Metallography of maraging 350 steel
[DE87-013746] N88-12591
Optimization of dilatometer test procedures
[DE87-014666] N88-12769
Storing photomicrographs on optical laser disks
[DE87-013747] N88-12785

N

NAGOYA UNIV. (JAPAN).
Final (n,l) state-resolved electron capture by multiply charged ions from neutral atoms
[IPPJ-AM-54] N88-13030
Data base on the high heat flux behaviour of metals and carbon materials for plasma facing components: Experiments at the 10 MW neutral beam injection test stand of the IPP Nagoya
[IPPJ-AM-53] N88-13031
Confinement time of electrons and H(-)/D(-) ions in the Uramoto type sheet plasma
[IPPJ-852] N88-13032
Monte Carlo analysis of neoclassical transport for a compact helical system
[IPPJ-850] N88-13033
Magnetic fluctuation behaviour of current termination in reversed field pinch
[IPPJ-849] N88-13034
Monocrystal sputtering by the computer simulation code ACOCT
[IPPJ-848] N88-13035
Microstructural change of Al on H implantation
[IPPJ-847] N88-13036
Prompt simultaneous acceleration of protons and electrons to relativistic energies by shock waves in solar flares
[IPPJ-851] N88-13037
Proceedings of the Japan-US Workshop P-92 on Plasma Material Interaction/High Heat Flux Data Needs for the Next Step Ignition and Steady State Devices
[DE87-013568] N88-13042
NATIONAL AERONAUTICAL ESTABLISHMENT, OTTAWA (ONTARIO).
Access to microgravity: A technical description of the NAE T-33 microgravity facility
[NAE-AN-47] N88-12518
The effect of mass, wind angle and erection technique on the aeroelastic behaviour of a cable-stayed bridge model
[NAE-AN-46] N88-12819
NATIONAL AERONAUTICAL LAB., BANGALORE (INDIA).
Analysis of free cutting brass by A.C. polarography
[PD-MT-8728] N88-12587
Studies on estimation of nickel in zinc base die casting by D.C. polarography
[PD-MT-8729] N88-12588
Thermal expansion of some Ge-Se-Te glasses
[PD-MT-8722] N88-12606
Studies on some Ge-Se-Te glasses
[PD-MT-8721] N88-12607
Observations on the hydrodynamic flow visualization at ONERA
[PD-FM-8718] N88-12753
NCSU code: Validation and extension on NAL's UNIVAC 1100/60 system
[PD-FM-8716] N88-12931
A quadrature formula for a double-pole singular integral
[PD-FM-8725] N88-12990
NATIONAL AERONAUTICS AND SPACE ADMINISTRATION, WASHINGTON, D.C.
Aeronautical engineering: A continuing bibliography with indexes (supplement 219)
[NASA-SP-7037(219)] N88-12470
Aerospace medicine and biology: A continuing bibliography with indexes
[NASA-SP-7011(304)] N88-12922
NATIONAL AERONAUTICS AND SPACE ADMINISTRATION. AMES RESEARCH CENTER, MOFFETT FIELD, CALIF.
Some experiences with the viscous-inviscid interaction approach
[NASA-TM-100015] N88-12466
Digital-flight-control-system software written in automated-engineering-design language: A user's guide of verification and validation tools
[NASA-TM-88313] N88-12494
Flap-lag equations of motion of rigid, articulated rotor blades with three hinge sequences
[NASA-TM-100023] N88-12495
Research papers and publications (1981-1987): Workload research program
[NASA-TM-100016] N88-12924
CGI delay compensation
[NASA-TM-88703] N88-12932
INS3D: An incompressible Navier-Stokes code in generalized three-dimensional coordinates
[NASA-TM-100012] N88-12991
NATIONAL AERONAUTICS AND SPACE ADMINISTRATION. GODDARD SPACE FLIGHT CENTER, GREENBELT, MD.
Design concepts for the ASTROMAG cryogenic system
[NASA-CR-181505] N88-13060
Exploiting the IR: Solar and stellar spectroscopy in the IR N88-13102
The acceleration of winds by MHD waves in open magnetic structures N88-13109
The onset of chromospheric activity among the A- and F- type stars N88-13144
A flash spectrum of Cl I, C I, N I, and Ni II absorption in 31 Cygni: A direct observation of the reversing layer N88-13158
VLA observations of rapid 6 cm flux variations in alpha Ori N88-13169
The delta upsilon = 1 fundamental bands of carbon monoxide in late-type stars N88-13177
NATIONAL AERONAUTICS AND SPACE ADMINISTRATION. LYNDON B. JOHNSON SPACE CENTER, HOUSTON, TEX.
Space station internal environmental and safety concerns N88-12527
Interplanetary propulsion using inertial fusion
[NASA-TM-89661] N88-12540
Space suit extravehicular hazards protection development
[NASA-TM-100458] N88-12927
The VISTA spacecraft: Advantages of ICF (Inertial Confinement Fusion) for interplanetary fusions propulsion applications
[NASA-CR-181549] N88-13024
NATIONAL AERONAUTICS AND SPACE ADMINISTRATION. LANGLEY RESEARCH CENTER, HAMPTON, VA.
Planform effects on the supersonic aerodynamics of multibody configurations
[NASA-TP-2782] N88-12454
Effects of jet exhaust yaw vane installation and operation on the longitudinal and lateral-directional characteristics of the F-14 airplane
[NASA-TP-2769] N88-12455
Semiempirical method for prediction of aerodynamic forces and moments on a steadily spinning light airplane
[NASA-TM-4009] N88-12456
Aerodynamic sensitivities from subsonic, sonic and supersonic unsteady, nonplanar lifting-surface theory
[NASA-TM-100502] N88-12459
Effect of motion cues during complex curved approach and landing tasks: A piloted simulation study
[NASA-TP-2773] N88-12480
Effects of combining vertical and horizontal information into a primary flight display
[NASA-TP-2783] N88-12487
Analysis of 7- X 10-foot high speed wind tunnel shaft loads in support of fan blade failure investigation
[NASA-TM-100504] N88-12496
Structural analysis of a bolted joint concept for the space shuttle's solid rocket motor casing
[NASA-TM-89092] N88-12531
Effect of long-term thermal aging on coated Celion/LARC-160 composites
[NASA-TM-100495] N88-12544
Applications of the hybrid automated reliability predictor
[NASA-TP-2760] N88-12928
Comparing barrier algorithms
[NASA-CR-178377] N88-12934
Principles for problem aggregation and assignment in medium scale multiprocessors
[NASA-CR-178379] N88-12935
High resolution finite volume methods on arbitrary grids via wave propagation
[NASA-CR-178397] N88-12979
Measurement of velocity and vorticity fields in the wake of an airfoil in periodic pitching motion
[NASA-TP-2780] N88-13002
Results of the 1986 NASA/FAA/DFVLR main rotor test entry in the German-Dutch wind tunnel (DNW)
[NASA-TM-100507] N88-13003
Nuclear techniques in studies of condensed matter
[NASA-RP-1195] N88-13015
NATIONAL AERONAUTICS AND SPACE ADMINISTRATION. LEWIS RESEARCH CENTER, CLEVELAND, OHIO.
Application of Runge Kutta time marching scheme for the computation of transonic flows in turbomachines
[NASA-TM-86997] N88-12461
Experimental evidence for modifying the current physical model for ice accretion on aircraft surfaces
[NASA-TM-87184] N88-12473
Performance and combustion characteristics of direct-injection stratified-charge rotary engines
[NASA-TM-100134] N88-12490
Optical alignment of Centaur's inertial guidance system
[NASA-TM-88844] N88-12515
Spacecraft Fire Safety
[NASA-CP-2476] N88-12520
Microgravity combustion fundamentals N88-12528
Compatability of dispersion-strengthened platinum with resistojet propellants
[NASA-TP-2765] N88-12538
A two-dimensional finite difference program for thermal analysis of rocket thrust chambers
[NASA-TM-100191] N88-12539
High power ion thruster performance
[NASA-TM-100127] N88-12542
Surface catalytic degradation study of two linear perfluoropolyalkylethers at 345 C
[NASA-TP-2774] N88-12543
Free-edge delamination: Laminate width and loading conditions effects
[NASA-TM-100238] N88-12551
Composite mechanics for engine structures
[NASA-TM-100176] N88-12552
An analytical and experimental study of injection-locked two-port oscillators
[NASA-TM-100119] N88-12727
Similar solutions for viscous hypersonic flow over a slender three-fourths-power body of revolution
[NASA-TM-100205] N88-12752
Experimental study of thermocapillary flows in a thin liquid layer with heat fluxes imposed on the free surface
[NASA-TM-100252] N88-12763
Measured performance of the heat exchanger in the NASA icing research tunnel under severe icing and dry-air conditions
[NASA-TM-100116] N88-12796
On dynamic loads in parallel shaft transmissions. 1: Modelling and analysis
[NASA-TM-100180] N88-12797
On dynamic loads in parallel shaft transmissions. 2: Parameter study
[NASA-TM-100181] N88-12798
Creep life prediction based on stochastic model of microstructurally short crack growth
[NASA-TM-100245] N88-12825
Performance of GaAs and silicon concentrator cells under 37 MeV proton irradiation
[NASA-TM-100144] N88-12877
Radiation performance of AlGaAs concentrator cells and expected performance of cascade structures
[NASA-TM-100145] N88-12878
Small reactor power systems for manned planetary surface bases
[NASA-TM-100223] N88-13209

NATIONAL AERONAUTICS AND SPACE ADMINISTRATION. MARSHALL SPACE FLIGHT CENTER, HUNTSVILLE, ALA.
Development of optical modulators for measurements of solar magnetic fields
[NASA-TM-100315] N88-13018
FY 1985 scientific and technical reports, articles, papers and presentations
[NASA-TM-86521] N88-13083
Magnetic flux tubes as sources of wave generation N88-13108
MHD energy fluxes for late type dwarfs N88-13148

NATIONAL AERONAUTICS AND SPACE ADMINISTRATION. WHITE SANDS TEST FACILITY, N. MEX.
Ignition and combustion of metals in oxygen N88-12530

NATIONAL BUREAU OF STANDARDS, GAITHERSBURG, MD.
Techniques for fire detection N88-12521

NATIONAL BUREAU OF STANDARDS, WASHINGTON, D.C.
Fire-related standards and testing N88-12522

NATIONAL CENTER FOR ATMOSPHERIC RESEARCH, BOULDER, COLO.
User's guide to NCAR (National Center for Atmospheric Research) CCM1
[PB87-224366] N88-12899
National Center for Atmospheric Research
[PB87-226391] N88-12901
Atmospheres of stars in the limits of thick and thin convection zones: M giants N88-13105

NATIONAL OCEANIC AND ATMOSPHERIC ADMINISTRATION, BOULDER, COLO.
Measurements of vapor flux, liquid water contents, precipitation rates and riming in a Utah mountain cloud system
[PB87-224945] N88-12900

NATIONAL OPTICAL ASTRONOMY LAB. TUCSON, ARIZ.
Time series infrared spectroscopy of long period variables N88-13172

NATIONAL PHYSICAL LAB., TEDDINGTON (ENGLAND).
Input devices for tasks using interactive video
[PB87-220018] N88-12664

NATIONAL SOLAR OBSERVATORY, SUNSPOT, N. MEX.
Atmospheres of stars in the limits of thin and thick convection zones: The M dwarfs N88-13104

NATIONAL SOLAR OBSERVATORY, TUCSON, ARIZ.
Post-zero-age main sequence rotation N88-13100

NATIONAL TELECOMMUNICATIONS AND INFORMATION ADMINISTRATION, BOULDER, COLO.
General theory of radio propagation through a stratified atmosphere
[PB87-226197] N88-12662

NATIONAL WEATHER SERVICE, SILVER SPRING, MD.
NWS (National Weather Service) watch/warning verification flash flood, winter storm and high wind, January 1980 - June 1985
[PB87-223053] N88-12898

NAVAL OCEAN SYSTEMS CENTER, SAN DIEGO, CALIF.
Ground vehicle convoying
[DE88-000360] N88-13068

NAVAL OCEANOGRAPHY COMMAND CENTER/JOINT TYPHOON WARNING CENTER, FPO SAN FRANCISCO, CALIF.
Annual tropical cyclone report, 1986
[AD-A184082] N88-12903

NAVAL POSTGRADUATE SCHOOL, MONTEREY, CALIF.
Dynamic positioning at sea using the global positioning system
[AD-A184453] N88-12476
An inexpensive real-time interactive three-dimensional flight simulation system
[AD-A184340] N88-12499
A comparison of high damping shape memory alloys with Cu-Mn-based and Fe-Cr-based alloys
[AD-A184110] N88-12566
Meteor-burst communications: Is this what the Navy needs?
[AD-A184433] N88-12672
Numerical simulation of unsteady separated flows
[AD-A184132] N88-12741
A multibody dynamic analysis of the N-ROSS (Navy Remote Ocean Sensing System) satellite rotating flexible reflector using Kane's method
[AD-A184452] N88-12860
Coupled acoustic and ocean thermodynamic model
[AD-A184357] N88-12911
Effects of rainfall on the seasonal thermocline
[AD-A184432] N88-12912
A survey of object oriented languages in programming environments
[AD-A184127] N88-12937
An interactive computer graphics network monitor for a tactical communications network
[AD-A184131] N88-12938
A comparison of the basket method and the stratified random sampling for contract change order negotiations
[AD-A184170] N88-13060

NAVAL RESEARCH LAB., WASHINGTON, D.C.
Inerting and atmospheres N88-12524
The free electron laser sideband instability reconsidered
[AD-A184269] N88-12773
Variable collision frequency effects on hose and sausage instabilities in relativistic electron beams
[AD-A184206] N88-13021
Flux tube dynamics and solar/stellar redshift measurements N88-13095
Statistical properties of small high-velocity events in the solar transition region N88-13112

NAVAL SUBMARINE MEDICAL RESEARCH LAB., GROTON, CONN.
Fire-related medical science N88-12525
Performance and preference with various VDT (Video Display Terminal) phosphors
[AD-A184085] N88-12925

NAVAL SURFACE WEAPONS CENTER, SILVER SPRING, MD.
Corrosion behavior of P/M mechanically alloyed IN-9052.1: An electro-chemical investigation
[AD-A184191] N88-12567
On the stressing of annealed NITINOL: The electrical resistance and calorimetric effects
[AD-A184465] N88-12569
Automated microwave dielectric constant measurement
[AD-A184182] N88-12667

NEBRASKA UNIV., LINCOLN.
Design of source coders and joint source/channel coders for noisy channels
[NASA-CR-181547] N88-12678

NEW MEXICO STATE UNIV., LAS CRUCES.
Energy balance in laser-irradiated vaporizing droplets
[DE88-000525] N88-12782
X-rays, color, and the Vaughan-Preston gap N88-13135

NEW MEXICO UNIV., ALBUQUERQUE.
Thermomechanical cracking in coated media due to high speed asperity excitation
[AD-A184176] N88-12809
Spectral analysis of APT RS CVn binary light curves N88-13122
Starspots on the short-period RS CVn system SV Cam: 45 years of activity N88-13123

NEWCASTLE-UPON-TYNE UNIV. (ENGLAND).
Multicast gateway design considerations
[PB87-219960] N88-12663

NIELSEN ENGINEERING AND RESEARCH, INC., MOUNTAIN VIEW, CALIF.
Concepts for radically increasing the numerical convergence rate of the Euler equations
[NASA-CR-177456] N88-12463

NORTH CAROLINA STATE UNIV., RALEIGH.
Natural control of flexible space structures N88-12534

NORTH CAROLINA UNIV., CHARLOTTE.
Combined problem of slew maneuver control and vibration suppression
[NASA-CR-181537] N88-12617

NORTHWESTERN UNIV., EVANSTON, ILL.
Synthesis, NMR characterization and electrical properties of siloxane-based polymer electrolytes
[AD-A184184] N88-12596
Effect of sidechain length and crosslinking on ionic conductivity in polyphosphazene solid electrolytes
[AD-A184419] N88-13058

NUCLEAR REGULATORY COMMISSION, WASHINGTON, D. C.
PRAAGE: An interactive IBM-PC code for unreliability/aging analysis
[DE87-012124] N88-12803

O

OAK RIDGE GASEOUS DIFFUSION PLANT, TENN.
Evaluation of the sensidyne toxic gas sensor for HF (Hydrogen Fluoride) vapor
[DE88-000647] N88-12767
Calibration of a laser-pumped, thermographic phosphor remote thermometry system
[DE88-000452] N88-12781
Damping characteristics of a composite-reinforced stainless-steel plate
[DE88-000303] N88-12828
Increased gain of channel intensifier tubes by pulsed biasing
[DE88-000512] N88-13019

OAK RIDGE NATIONAL LAB., TENN.
Welding and weldability of ductile intermetallic alloys
[DE87-014061] N88-12562
Corrosion of ferritic steels by molten lithium: Influence of competing thermal gradient mass transfer and surface product reactions
[DE88-000334] N88-12585
The aging behavior of types 308 and 308CRE stainless steels and its effect on mechanical properties
[DE87-012541] N88-12590
Ceramic technology for advanced heat engines project
[DE88-001520] N88-12605
Pulsed eddy-current inspection of thin-walled stainless steel tubing
[DE88-001492] N88-12830
A study of the optimal transition temperatue of PCM (Phase Change Material) wallboard for solar energy storage
[DE88-001522] N88-12882
The pros and cons of using a CAI package on a central computer as opposed to a microprocessor: What's your CAI MO, mainframe or micro
[DE87-011123] N88-12929
A portable hypercube simulator
[DE87-013389] N88-12947
Statistical inference: Computer oriented algorithmic approach
[DE87-013874] N88-12948
Implementation of a 3-D nonlinear MHD calculation on the intel hypercube
[DE87-014637] N88-12949
QR factorization of a dense matrix on a shared-memory multiprocessor
[DE88-001506] N88-12956
User interface for a partially incompatible system software environment with non-ADP users
[DE88-001518] N88-12968
The linear characteristic method in XYZ geometry
[DE87-011668] N88-12984
Foundations of O-theory 2: Measurements and relation to fuzzy set theory
[DE88-000013] N88-12986
Magnetic diffuse scattering
[DE87-013539] N88-13014
The role of stellarators in the advanced toroidal program
[DE87-014815] N88-13025
A three-barrel repeating pneumatic pellet injector for plasma fueling of the Joint European Torus
[DE88-000330] N88-13026
Modular pump limiter systems for large tokamaks
[DE88-001487] N88-13045
Radiation induced collapse of the crystalline structure
[DE87-014407] N88-13064
Supertracks: The building blocks of chaos
[DE88-001513] N88-13207

OAK RIDGE Y-12 PLANT, TENN.
Development of an acoustic emission monitor and monitoring techniques for long-term monitoring of U-0.8Ti electron-beam weldments for postweld cracking
[DE88-000619] N88-12804
Computerized certification of digital ultrasonic instrumentation
[DE88-000820] N88-13008

OAKLAND UNIV., ROCHESTER, MICH.
Far-infrared spectra of lithium deposited on a gold electrode: Interpretation using a cluster model
[AD-A184231] N88-13050

OFFICE OF TECHNOLOGY ASSESSMENT, WASHINGTON, D.C.
Technology transfer to China
[PB87-223418] N88-13087

OHIO STATE UNIV., COLUMBUS.
Simulation of an enhanced TCAS 2 system in operation
[NASA-CR-181545] N88-12479
New main reflector, subreflector and dual chamber concepts for compact range applications
[NASA-CR-181506] N88-12498
On M-ARY sequential hypotheses testing for the classification of radar signals
[AD-A184094] N88-12666
Higher order theory analysis of a modified free-edge delamination specimen N88-12820
Vibration and buckling of geometrically imperfect laminated cylindrical shells N88-12822
Radial orbit error reduction and sea surface topography determination using satellite altimetry N88-12861
Accuracy potential of non-metric cameras in close-range photogrammetry N88-12862
An algorithmic approach to crustal deformation analysis N88-12891

OLD DOMINION UNIV., NORFOLK, VA.
Software reliability perspectives
[NASA-CR-181523] N88-12952
OPTIMETRICS, INC., BURLINGTON, MASS.
Review of inversion techniques for spaceborne lidar systems
[AD-A184164] N88-12772
OSLO UNIV. (NORWAY).
The Wilson-Bappu relationship: A barometric effect N88-13170
OSSERVATORIO ASTRONOMICO, TURIN (ITALY).
Neutron capture nucleosynthesis in low mass AGB stars N88-13178
IRAS and near IR observations of active binaries N88-13186
OXFORD UNIV. (ENGLAND).
A re-examination of the corona-wind dividing line: Diagnostics of non-coronal atmospheres N88-13101
Relations between chromospheric and coronal structure, flux-flux correlations and convective zone properties N88-13138
IUE observations of the hybrid K3 II star Iota Aurigae and constraints on the outer atmospheric structure N88-13171

P

PACIFIC NORTHWEST LABS., RICHLAND, WASH.
Retention processes in supercritical fluid chromatography
[DE88-000079] N88-12559
Real-time Raman detection of molecular changes in ceramics undergoing sliding friction
[DE88-000558] N88-12609
Low gravity fluid-thermal experiments
[DE88-000553] N88-12620
Noncontact temperature measurements of hot steel bodies using an electromagnetic acoustic transducer (EMAT)
[DE88-000560] N88-12765
Input turbulence features at a megawatt-size wind turbine, Medicine Bow, Wyoming
[DE88-000098] N88-12873
Performance analysis of solar thermal power systems
[DE88-000563] N88-12874
Using a new characterization of turbulent wind for accurate correlation of wind turbine response with wind speed
[DE88-001453] N88-12881
Variability of wind power near Oklahoma City and implications for siting of wind turbines
[DE88-000444] N88-12902
On computing environments in data analysis
[DE88-000076] N88-12961
The characterization of diagnostic tasks for engineering systems
[DE88-000093] N88-12973
PARAIBA UNIV., JOAO PESSOA (BRAZIL).
Canonical transformations and exact invariants for dissipative systems
[DE87-703683] N88-12985
PENNSYLVANIA STATE UNIV., UNIVERSITY PARK.
Characterization of catalysts with metal-support effects and of the species adsorbed on their surfaces
[DE87-014636] N88-12564
Proton abstraction as a route to conductive polymers
[AD-A184019] N88-12612
Effect of sidechain length and crosslinking on ionic conductivity in polyphosphazane solid electrolytes
[AD-A184419] N88-13058
Microwave observations of nonthermal phenomena in pre-main sequence stars N88-13107
Titanium oxide absorption and spot sizes in II Peg, HR 1099 and UX Ari N88-13126
Spectroscopic monitoring of RS CVn stars at Kitt Peak using the Penn State fiber optic echelle N88-13127
H alpha and Ca II emission line variability of FK comae N88-13128
PENNSYLVANIA UNIV., PHILADELPHIA.
Valence bond theory and superconductivity
[AD-A184274] N88-13052
The chemical bond and superconductivity
[AD-A184275] N88-13053
Valence bond cluster studies of alkali metal/semiconductor bonding
[AD-A184276] N88-13054
Tetrahedral carbon and interstitial electrons in Li cluster: CLi4 and (LiCH3)4
[AD-A184277] N88-13055
K-CO on transition metals: A local ionic interaction
[AD-A184342] N88-13056
PHYSICAL SCIENCES, INC., ANDOVER, MASS.
Experimental and theoretical study of condensation in multicomponent mixtures
[DE88-000897] N88-12563
PITTSBURGH UNIV., PA.
Pipe and bend erosion by pneumatic transport of solids at high temperature
[DE88-001345] N88-12658
PRESEARCH, INC., HOUSTON, TEX.
An assessment of clinical chemical sensing technology for potential use in space station health maintenance facility
[NASA-CR-172013] N88-12926
PRINCETON COMBUSTION RESEARCH LABS., INC., MONMOUTH JUNCTION, N.J.
High pressure strand burn rate tests of polyvinylnitrate/nitramine propellants
[AD-A184178] N88-12615
PRINCETON UNIV., N. J.
Solution of the two-dimensional Euler equations on unstructured triangular meshes N88-12469
An experimental investigation of unsteadiness in swept shock wave/turbulent boundary layer interactions N88-12760
Galaxy formation by gravitational collapse in a universe dominated by cold dark matter N88-13205
PUBLIC SERVICE CO. OF NEW MEXICO, ALBUQUERQUE.
Performance monitoring and analysis of electric van fleet vehicles
[DE88-900066] N88-13091

R

RICE UNIV., HOUSTON, TEX.
Gamma-ray optics of multi-beam Borrmann modes with possible applications to nuclear lasing N88-12784
Banded ion morphology N88-12892
The velocity structure and turbulence at the center of the Orion Nebula N88-13201
Model of solar-wind magnetosphere coupling N88-13211
Gamma ray lines from novae N88-13214
ROCKWELL INTERNATIONAL CORP., CANOGA PARK, CALIF.
Failure control techniques for the SSME
[NASA-CR-179224] N88-12537
Interplanetary propulsion using inertial fusion
[NASA-TM-89661] N88-12540
Space station resistojet system requirements and interface definition study
[NASA-CR-180832] N88-12541
The VISTA spacecraft: Advantages of ICF (Inertial Confinement Fusion) for interplanetary fusions propulsion applications
[NASA-CR-181549] N88-13024
ROCKWELL INTERNATIONAL CORP., GOLDEN, COLO.
Low-cost teleoperator-controlled vehicle for damage assessment and dose measurement
[DE88-000713] N88-12794
ROYAL NAVAL ENGINEERING COLL., MANADON (ENGLAND).
Determination of through-plane shear moduli for glass-reinforced plastics
[PB87-106274] N88-12592

S

SACRAMENTO PEAK OBSERVATORY, SUNSPOT, N. MEX.
Stellar activity and the rotation of Hyades stars N88-13139
SAN FRANCISCO STATE UNIV., CALIF.
Managing distributed derived data: A preliminary proposal
[DE88-000714] N88-12966
SANDIA NATIONAL LABS., ALBUQUERQUE, N. MEX.
The aerodynamics of supersonic parachutes
[DE87-014846] N88-12484
Ultimate velocities for induction launchers
[DE87-012360] N88-12513
Parachute materials
[DE87-014845] N88-12550
The effect of organic inhibitors on the atmospheric corrosion and solderability of copper
[DE88-000261] N88-12565
Molecular engineering of ceramics
[DE88-000174] N88-12603
High efficiency generation of 130-nm radiation from sum-frequency mixing in Hg
[DE87-013714] N88-12674
An excitation-term modification for a certain class of electromagnetic aperture-coupling problems
[DE88-000260] N88-12713
Impedance of passive lithium anodes in SOCl2 solutions under low-field polarization
[DE88-000922] N88-12726
Corrosion susceptibility study of candidate pin materials for ALTC (Active Lithium/Thionyl Chloride) batteries
[DE88-001449] N88-12734
Reliability of Li/SO2 cells for long-life applications
[DE88-001380] N88-12735
NACHOS 2: A finite element computer program for incompressible flow problems. Part 2: User's manual
[DE88-001451] N88-12750
Tracking through turbulence at the Tonopah Test Range
[DE88-001448] N88-12766
Ro-vibrational laser spectroscopy of ESD neutrals from chemisorbed species
[DE87-013011] N88-12770
Tribological properties of rf-sputtered MoS2 coatings
[DE88-000266] N88-12802
Mechanical shock test specification using nonstationary random excitation models
[DE87-013650] N88-12812
A dissipation principle and its consequences for structured shock waves in thermoelastic materials
[DE87-013723] N88-12813
The evolution of plastic strain in steady, plastic shock waves
[DE87-013812] N88-12826
Implementation of a new shock testing procedure using nonstationary random excitation
[DE87-014643] N88-12827
A comparison of structural frequency response functions measured with forces from 500 to 250,000 lb
[DE88-000666] N88-12829
A hydrogen/nickel oxide battery for remote applications
[DE87-009048] N88-12872
Measurements and calculations of aerodynamic torques for a vertical-axis wind turbine
[DE88-001783] N88-12876
International Energy Agency (IEA) Small Solar Power Systems (SSPS) sodium cavity and external receiver performance comparison
[DE88-001310] N88-12879
Characteristics of current solar central receiver projects
[DE88-001314] N88-12880
The developmental status of solar thermochemical hydrogen production
[DE88-001778] N88-12884
A data analysis environment for HP (Hewlett-Packard) 1000 computers
[DE87-010511] N88-12936
Two classes of preconditioners computed using block matrix factorization techniques
[DE88-001313] N88-12968
Reevaluating the worst-case radiation response of MOS transistors
[DE87-014157] N88-13059
Ground vehicle convoying
[DE88-000360] N88-13068
SANDIA NATIONAL LABS., LIVERMORE, CALIF.
TOPAZ: The transient one-dimensional pipe flow analyzer: An update on code improvements and increased capabilities
[DE88-001781] N88-12751
SANTA CATARINA UNIV., FLORIANOPOLIS (BRAZIL).
Mechanical behavior of a controlled rolled high-strength low alloy steeel plate, microalloyed with Nb and V
[DE87-703507] N88-12571
SAO PAULO UNIV. (BRAZIL).
Homogeneous space-time of Goedel type in higher-derivate gravity
[DE87-703690] N88-13077
SCHOOL OF AEROSPACE MEDICINE, BROOKS AFB, TEX.
F-16 control stick response during +Gz-induced loss of consciousness
[AD-A184107] N88-12491
SCIENCE AND ENGINEERING ASSOCIATES, INC., SEATTLE, WASH.
Aircraft engine exhaust plume dynamics
[AD-A184236] N88-12488
SCIENCE APPLICATIONS INTERNATIONAL CORP., ALBUQUERQUE, N. MEX.
Spectral analysis of APT RS CVn binary light curves N88-13122
SCIENCE APPLICATIONS INTERNATIONAL CORP., HUNTSVILLE, ALA.
Optimization techniques applied to passive measures for in-orbit spacecraft survivability
[NASA-CR-179216] N88-12532
SCIENTIFIC RESEARCH ASSOCIATES, INC., GLASTONBURY, CONN.
Numerical studies of the dual HEMT/algorithm development and numerical studies of Schrodinger's equation
[AD-A184471] N88-12948

SCRIPPS INSTITUTION OF OCEANOGRAPHY, LA JOLLA, CALIF.
Statistics of the geomagnetic secular variation for the past 5Ma
[NASA-CR-181558] N88-12890
SMITHSONIAN ASTROPHYSICAL OBSERVATORY, CAMBRIDGE, MASS.
Analytical investigation of the dynamics of tethered constellations in Earth orbit (phase 2)
[NASA-CR-179218] N88-12533
SOUTHWEST RESEARCH INST., SAN ANTONIO, TEX.
Experiments on densely-loaded non-Newtonian slurries in laminar and turbulent pipe flows
[DE88-000719] N88-12746
SPACE TELESCOPE SCIENCE INST., BALTIMORE, MD.
JHK photometry of CN-rich field giants N88-13175
SPARTA, INC., LAGUNA HILLS, CALIF.
An evaluation plan of bus architectures and protocols using the NASA Ames intelligent redundant actuation system
[NASA-CR-177458] N88-12482
ST SYSTEMS CORP., LANHAM, MD.
Radio continuum emission from the ionized stellar winds of the cool supergiants in zeta Aurigae-like systems N88-13160
STANFORD LINEAR ACCELERATOR CENTER, CALIF.
GOLD: Integration of model-based control systems with artificial intelligence and workstations
[DE88-000506] N88-12976
GOLD: Integration of model-based control systems with artificial intelligence and workstations
[DE88-000706] N88-12977
STANFORD UNIV., CALIF.
Research in VLSI (Very Large Scale Integration) systems
[AD-A184089] N88-12721
Estimation of a multivariate continuous variable panel model
[AD-A184472] N88-12982
Three-halves law in sunspot cycle shape
[NASA-CR-181520] N88-13210
STATE UNIV. OF NEW YORK, STONY BROOK.
The effects of minor trace gases on the transfer of thermal infrared radiation through the Earth's atmosphere N88-12893
Atomic and electronic structure of surfaces and chemisorbed layers
[DE87-014987] N88-13065
STERLING SOFTWARE, PALO ALTO, CALIF.
Software maintenance in scientific and engineering environments: An introduction and guide
[NASA-CR-177409] N88-12954
STUTTGART UNIV. (WEST GERMANY).
Plasma thruster development
[AD-A184173] N88-12536
SUNDSTRAND CORP., ROCKFORD, ILL.
A study of two-phase flow in a reduced gravity environment
[NASA-CR-172035] N88-12617
SYRACUSE UNIV., N. Y.
Comparative studies in the near-field of turbulent transports of heated and unheated jets normal to a cross stream N88-12758
SYSTEMS RESEARCH LABS., INC., DAYTON, OHIO.
Nitrogen energy transfer study
[AD-A184457] N88-12869
SYSTEMS TECHNOLOGY, INC., MOUNTAIN VIEW, CALIF.
Some data processing requirements for precision Nap-Of-the-Earth (NOE) guidance and control of rotorcraft
[NASA-CR-177453] N88-12493

T

TECHNICAL RESEARCH CENTRE OF FINLAND, ESPOO.
Design of digital filters for electronic instrumentation
[PB87-100418] N88-12716
Design of efficient FIR filters with minimal delay
[PB87-100434] N88-12717
Huurre expedition to the North Pole in 1984
[PB87-220935] N88-12858
TECHNICAL RESEARCH CENTRE OF FINLAND, HELSINKI.
Theory of one and two-pass cross-flow heat exchanger
[PB87-225157] N88-12736
TECHNISCHE HOGESCHOOL, DELFT (NETHERLANDS).
Programmable real-time digital video image processing
[PB87-104162] N88-12661
Programmable Logic Arrays (PLA's) design for testability
[PB87-102935] N88-12718
Total linearisation method for solving viscous free boundary flow problems by the finite element method
[PB87-222337] N88-12737
Technical evaluation of a solar-powered absorption cooling system (LiBr-H2O)
[PB87-108254] N88-12867
TEL-AVIV UNIV. (ISRAEL).
Gravity from symmetry breakdown of a gauge affine theory
[DE88-001671] N88-13079
TELEDYNE GEOTECHNICAL, ALEXANDRIA, VA.
Multichannel deconvolution of P waves at seismic arrays and three component stations
[AD-A184450] N88-12868
TEMPLE UNIV., PHILADELPHIA, PA.
Guest-host interactions in thermotropic and lyotropic liquid crystals
[AD-A184402] N88-13057
TENNESSEE UNIV., KNOXVILLE.
Nonlinear acoustics
[AD-A184271] N88-13004
TEXAS A&M UNIV., COLLEGE STATION.
Thermodynamic properties for natural gas binaries
[PB87-226833] N88-13074
TEXAS UNIV., AUSTIN.
A study of scattering from E-plane circuit elements
[AD-A184473] N88-12673
Plume mechanics and aerosol growth processes
[AD-A184467] N88-12742
Optimization of explicit time-stepping algorithms and Stream-Function-Coordinate (SFC) concept for fluid dynamics problems N88-12762
Closed-loop system analysis using Lyapunov stability theory N88-12978
Propagation of random initial conditions in time N88-12993
A supersymmetric Lagrangian for Poincare gauge theories of gravity
[DE88-001670] N88-13078
Gravity from symmetry breakdown of a gauge affine theory
[DE88-001671] N88-13079
A spectral survey of 26 G9-M6 flare stars in the solar neighborhood N88-13149
Cosmological applications of singular hypersurfaces in general relativity N88-13202
TEXTRON BELL HELICOPTER, FORT WORTH, TEX.
A 0.15-scale study of configuration effects on the aerodynamic interaction between main rotor and fuselage
[NASA-CR-166577] N88-12462
THEORY AND APPLICATIONS UNLIMITED CORP., LOS GATOS, CALIF.
GPS vertical axis performance enhancement for helicopter precision landing approach
[NASA-CR-177443] N88-12477
TOLEDO UNIV., OHIO.
Doppler snapshots N88-13125
A helium flare on the active G5 dwarf Kappa Ceti N88-13189
TORONTO UNIV. (ONTARIO).
Numerical prediction of propeller performance by vortex lattice method
[UTIAS-TN-265] N88-12489
Ideal-viscoplastic extrusion model with application to deforming pistons in light-gas guns
[UTIAS-TN-266] N88-12657
TRANSPORTATION SYSTEMS CENTER, CAMBRIDGE, MASS.
Corrosion control by composite material substitution with application to the M-939 5-ton truck N88-12654
TRW DEFENSE AND SPACE SYSTEMS GROUP, REDONDO BEACH, CALIF.
Study of Plasma Motor Generator (PMG) tether system for orbit reboost
[NASA-CR-172015] N88-12501

U

UNITED KINGDOM ATOMIC ENERGY AUTHORITY, ABINGDON (ENGLAND).
Ballooning modes or Fourier modes in a toroidal plasma?
[AD-A184299] N88-13022
UNITED KINGDOM ATOMIC ENERGY AUTHORITY, CULHAM (ENGLAND).
Negative ion beams for heating and current-drive in NET
[AD-A184390] N88-13012
Numerical simulation of the Reversed Field Pinch
[AD-A184353] N88-13023
UNITED TECHNOLOGIES CORP., EAST HARTFORD, CONN.
A full potential flow analysis with realistic wake influence for helicopter rotor airload prediction
[NASA-CR-4007] N88-12452
UNITED TECHNOLOGIES RESEARCH CENTER, EAST HARTFORD, CONN.
Carbon fiber reinforced glass matrix composites for space based applications
[AD-A184355] N88-12548
UNIVERSIDADE FEDERAL DE SAO CARLOS (BRAZIL).
Model for ultrasonic attenuation and elastic constant in chromium and its alloys
[DE87-703478] N88-12570
UNIVERSIDADE FEDERALE DO RIO DE JANEIRO (BRAZIL).
Mechanical properties of a microalloyed steel with high niobium content
[DE87-703545] N88-12572
Sintered steels of high resistance alloyed to Nb, Mo, Mn and Si
[DE87-703546] N88-12573
Mechanical properties of an acicular ferrite steel microalloyed to niobium and vanadium
[DE87-703547] N88-12574
Partial substitution of vanadium by niobium in AISI H13 steel
[DE87-703548] N88-12575
Progress in the development of niobium alloyed high speed steel
[DE87-703549] N88-12578
Hadfield steels with Nb and Ti carbides
[DE87-703706] N88-12579
Influence of some parameters on the stress corrosion of a ABNT 304 stainless steel in MgCl/sub 2/
[DE87-703707] N88-12580
UNIVERSITIES SPACE RESEARCH ASSOCIATION, HUNTSVILLE, ALA.
A multiple-time-scale turbulence model based on variable partitioning of turbulent kinetic energy spectrum
[NASA-CR-179222] N88-12754
UNIVERSITY OF NORTHERN ILLINOIS, DE KALB.
An approach to implementing state space searches on heterogeneous systems of multiprocessors
[DE88-001321] N88-12967
The attitudes of science policy, environmental, and utility leaders on US energy issues and fusion
[DE88-000784] N88-13041
UNIVERSITY OF SOUTHERN CALIFORNIA, MARINA DEL REY.
The ISI (Information Sciences Institute) grapher: A portable tool for displaying graphs pictorially
[AD-A184354] N88-12944
UNIVERSITY OF SOUTHERN MISSISSIPPI, HATTIESBURG.
Solid state C-13 NMR characterization of textiles: Qualitative and quantitative analysis
[AD-A184349] N88-12598
A low volume insert for solid state magic angle spinning NMR of small samples
[AD-A184359] N88-12601
UNIVERSITY OF WESTERN ONTARIO, LONDON.
An analysis of the photospheric line profiles in F, G, and K supergiants N88-13157
UTAH UNIV., SALT LAKE CITY.
Raman scattering as a diagnostic technique for cathode characterization
[AD-A184434] N88-12726

V

VIGYAN RESEARCH ASSOCIATES, INC., HAMPTON, VA.
The design and preliminary calibration of a boundary-layer flow channel
[NASA-CR-178399] N88-12457
VIRGINIA POLYTECHNIC INST. AND STATE UNIV., BLACKSBURG.
New feedback design methodologies for large space structures: A multi-criterion optimization approach N88-12535
Interfacial strength development in thermoplastic resins and fiber-reinforced thermoplastic composites
[NASA-CR-181525] N88-12549
Nonlinear axial stiffness characteristics of axisymmetric bolted joints N88-12799
A refined nonlinear analysis of laminated composite plates and shells
[AD-A184436] N88-12811
VIRGINIA UNIV., CHARLOTTESVILLE.
Microgravity nucleation and particle coagulation experiments support
[NASA-CR-181540] N88-12618

Microgravity nucleation and particle coagulation experiments support
[NASA-CR-181541] N88-12619
Computed neutron tomography and coded aperture holography from real time neutron images N88-12645
Calibration of a laser-pumped, thermographic phosphor remote thermometry system
[DE88-000452] N88-12781
Methods for design and evaluation of integrated hardware/software systems for concurrent computation
[NASA-CR-181522] N88-12953

W

WELLESLEY COLL., MASS.
Water masers associated with 2 carbon stars: EU Andromedae and V778 Cygni N88-13176
WESTERN RESEARCH CORP., TUCSON, ARIZ.
A search for X-ray luminous late type stars in NIPSS data N88-13143
WISCONSIN UNIV., MADISON.
On the interannual variability of South American climate and the Southern Oscillation N88-12905
Measurement of cirrus cloud optical properties by high spectral resolution lidar N88-12906
Inertial confinement fusion reactor cavity analysis
[DE88-000786] N88-13028
ICRF launcher studies
[DE88-001710] N88-13048

Y

YALE UNIV., NEW HAVEN, CONN.
Large scale solar and stellar magnetic fields N88-13117
Spin-up and spin-down on the way to the main sequence N88-13181

Typical Contract Number Index Listing

Listings in this index are arranged alphanumerically by contract number. Under each contract number the NASA accession numbers denoting documents that have been produced as a result of research done under that contract are arranged in ascending order. The NASA accession number denotes the number by which the citation is identified.

AF-AFOSR-0394-84 ..... N88-12536
ARPA ORDER 4395 ..... N88-13021
ARPA ORDER 4511 ..... N88-12888
ARPA ORDER 4952 ..... N88-13018
DA PROJ. R00-0001 ..... N88-12597
DAAA21-86-C-0067 ..... N88-12615
DAAG29-84-K-0036 ..... N88-13057
DAAG29-84-K-0076 ..... N88-12873
DAAG29-85-K-0007 ..... N88-12811
DAAG29-85-K-0208 ..... N88-12998
DAAG29-85-K-0239 ..... N88-12982
DAAK11-83-K-0008 ..... N88-12742
DAAL03-86-C-0013 ..... N88-12946
DAAL03-86-K-0064 ..... N88-12568
DACA76-84-C-0004 ..... N88-12474
N88-12939
DACA76-85-C-0002 ..... N88-12971
DACA76-85-C-0017 ..... N88-12475
DASG60-85-C-0051 ..... N88-12653
DE-AC02-76CH-00016 ..... N88-12558
N88-12738
N88-12803
N88-13009
N88-13010
N88-13011
N88-13020
N88-13197
DE-AC02-76CH-03000 ..... N88-12733
N88-12768
DE-AC02-76ER03077 ..... N88-12960
DE-AC02-76EV-03140 ..... N88-12921
DE-AC02-84ER-13154 ..... N88-12563
DE-AC02-84ER-13167 ..... N88-12764
DE-AC03-76SF-00098 ..... N88-12553
N88-12858
N88-12715
N88-12783
N88-12814
N88-12868
N88-12883
N88-12962
N88-12964
N88-12968
N88-12974
N88-13060
N88-13063
N88-13066
N88-13068
N88-13072
N88-13073
N88-13090
N88-13208
DE-AC03-76SF-00515 ..... N88-12977
DE-AC04-76DP-00053 ..... N88-12561
N88-12591
N88-12769
N88-12785
DE-AC04-76DP-00613 ..... N88-12815
DE-AC04-76DP-00789 ..... N88-12464
N88-12513
N88-12550
N88-12565
N88-12603
N88-12674
N88-12713
N88-12726
N88-12734
N88-12735
N88-12750
N88-12766
N88-12770
N88-12802
N88-12812
N88-12826
N88-12827
N88-12829
N88-12872
N88-12876
N88-12936
N88-12998
N88-13059
N88-13088
DE-AC04-76DP-03533 ..... N88-12794
DE-AC04-76DR-00789 ..... N88-12751
N88-12879
N88-12880
N88-12884
DE-AC05-84OR-21400 ..... N88-12582
N88-12585
N88-12590
N88-12604
N88-12605
N88-12738
N88-12813
N88-12830
N88-12882
N88-12929
N88-12947
N88-12948
N88-12949
N88-12956
N88-12968
N88-12984
N88-12986
N88-13014
N88-13025
N88-13026
N88-13045
N88-13064
N88-13207
DE-AC05-84OS-21400 ..... N88-12804
N88-13008
DE-AC05-84OT-21400 ..... N88-12767
N88-12781
N88-12828
DE-AC06-76RL-01830 ..... N88-12559
N88-12609
N88-12620
N88-12765
N88-12873
N88-12874
N88-12881
N88-12902
N88-12961
N88-12973
DE-AC07-76ID-01570 ..... N88-12957
DE-AC08-83NV-10282 ..... N88-12965
DE-AC09-76SR-00001 ..... N88-12796
N88-12800
N88-12933
DE-AC21-85MC-22045 ..... N88-12871
DE-AI05-84OR-21411 ..... N88-12600
DE-AI06-81RL-10336 ..... N88-12902
DE-AS09-77ER-01023 ..... N88-12564
DE-FG02-84ER-13276 ..... N88-12564
DE-FG02-84ER-45067 ..... N88-13070
DE-FG02-84ER-45088 ..... N88-12581
DE-FG02-85ER-13443 ..... N88-12562
DE-FG02-85ER-25001 ..... N88-12930
DE-FG02-86ER-13463 ..... N88-12560
DE-FG02-86ER-45239 ..... N88-13065
DE-FG02-86ER-45282 ..... N88-12989
DE-FG02-86ER-52133 ..... N88-13046
DE-FG02-87ER-25026 ..... N88-12987
N88-12994
DE-FG03-86ER-52134 ..... N88-13044
DE-FG03-86ER-53220 ..... N88-12731
DE-FG05-84ER-53176 ..... N88-13029
DE-FG05-85ER-40200 ..... N88-13078
N88-13079
DE-FG05-86OR-21702 ..... N88-13069
DE-FG22-85PC-80524 ..... N88-12658
DE-FG22-86PC-90958 ..... N88-12744
DE-FG22-86PC-90962 ..... N88-12746
F04701-85-C-0086 ..... N88-12943
F08606-86-C-0006 ..... N88-12888
F08635-85-C-0036 ..... N88-12488
F19628-83-C-0018 ..... N88-12904
F19628-83-C-0092 ..... N88-12889
F19628-85-C-0178 ..... N88-12772
F29601-83-C-0024 ..... N88-12774
F30602-82-C-0161 ..... N88-12726
F30602-84-C-0153 ..... N88-12726
F33615-83-K-2335 ..... N88-13051
F33615-83-K-5001 ..... N88-12547
F33615-84-C-2441 ..... N88-12889
F33615-84-C-5010 ..... N88-12548
F33615-84-K-1520 ..... N88-12971
F49620-84-C-0087 ..... N88-13018
GRI-5082-260-0591 ..... N88-13074
MDA903-81-C-0335 ..... N88-12944
MDA903-83-C-0335 ..... N88-12721
MDA903-84-K-0062 ..... N88-12721
NAGW-896 ..... N88-12865
NAG1-343 ..... N88-12549
NAG1-467 ..... N88-12953
NAG1-535 ..... N88-12817
NAG1-616 ..... N88-12458
NAG1-722 ..... N88-13005
NAG1-750 ..... N88-12952
NAG3-672 ..... N88-12539
NAG5-865 ..... N88-12818
N88-12819
NAG5-883 ..... N88-12890
NAG5-898 ..... N88-12908
NAG5-916 ..... N88-12878
NAG5-931 ..... N88-12712
NAG8-053 ..... N88-12748
NAG8-092 ..... N88-12748
NAG8-497 ..... N88-13182
NAG8-582 ..... N88-13182
NASA ORDER A-32501-C N88-13006
NASA ORDER W-30746 ..... N88-12747
NAS1-15759 ..... N88-12969
NAS1-17748 ..... N88-12897
NAS1-17919 ..... N88-12457
NAS1-18061 ..... N88-13000
NAS1-18107 ..... N88-12934
N88-12935
N88-12979
NAS1-18279 ..... N88-12497
NAS2-10850 ..... N88-12478
NAS2-11150 ..... N88-12452
NAS2-11268 ..... N88-12482
NAS2-11555 ..... N88-12954
NAS2-11601 ..... N88-12471
NAS2-11791 ..... N88-12477
NAS2-12039 ..... N88-12472
NAS2-12081 ..... N88-12482
NAS2-12129 ..... N88-12463
NAS2-12364 ..... N88-12493
NAS3-23862 ..... N88-12875
NAS3-24658 ..... N88-12541
NAS5-29381 ..... N88-13158
NAS7-918 ..... N88-12730
N88-12959
NAS8-35918 ..... N88-12754
NAS8-36305 ..... N88-12537
NAS8-36483 ..... N88-12870
NAS8-36606 ..... N88-12533
NAS8-37378 ..... N88-12532
NAS9-16581 ..... N88-12747
NAS9-17195 ..... N88-12617
NAS9-17594 ..... N88-12926
NAS9-17751 ..... N88-12501
NCA2-IR240-401 ..... N88-12453
NCC1-24 ..... N88-12457

NCG1-107 ..... N88-12480
NCC2-297 ..... N88-12557
NCC2-396 ..... N88-12486
NCC2-416 ..... N88-12483
NCC2-420 ..... N88-12485
NCC2-434 ..... N88-12484
NCC2-438 ..... N88-13084
NGL-05-020-272 ..... N88-13210
NGT01-008-803 ..... N88-12748
NSF AST-85-07029 ..... N88-13114
N88-13177
NSF ATM-82-17015 ..... N88-12901
NSF DMS-83-12229 ..... N88-12960
NSF ECS-84-04866 ..... N88-12941
N88-12942
NSF IST-83-12240 ..... N88-12972
NSF-ATM-82-17015 ..... N88-12899
NSG-1498 ..... N88-12479
NSG1-613 ..... N88-12498
N00014-77-C-0239 ..... N88-13050
N00014-80-C-0236 ..... N88-12971
N00014-80-C-0532 ..... N88-12596
N88-13058
N00014-81-K-0229 ..... N88-13004
N00014-83-D-0669 ..... N88-12669
N88-12671
N88-12997
N00014-84-C-0149 ..... N88-12723
N88-12941
N88-12942
N00014-84-K-0252 ..... N88-12809
N00014-84-K-0365 ..... N88-12998
N88-13049
N00014-84-K-0553 ..... N88-12724
N00014-85-C-0332 ..... N88-12546
N00014-85-K-0095 ..... N88-12975
N88-12980
N88-13075
N00014-85-K-0124 ..... N88-12945
N00014-85-K-0152 ..... N88-12971
N00014-85-K-0214 ..... N88-12972
N00014-85-K-0321 ..... N88-12666
N00014-85-K-0634 ..... N88-12722
N00014-85-K-0650 ..... N88-12920
N00014-85-K-0880 ..... N88-12599
N88-12793
N00014-85-K-0899 ..... N88-12612
N00014-86-C-2114 ..... N88-12725
N00014-86-K-0029 ..... N88-12668
N00014-86-K-0304 ..... N88-13052
N88-13053
N88-13054
N88-13055
N88-13056
N00014-86-K-0659 ..... N88-12598
N88-12601
N00014-86-K-0685 ..... N88-12945
N00014-86-K-0772 ..... N88-12595
N00039-82-C-0235 ..... N88-12940
N00039-84-C-0089 ..... N88-12940
N00039-85-C-0134 ..... N88-12971
N62269-85-C-0297 ..... N88-12597
RR0-4206 ..... N88-12975
N88-12980
N88-13075
W-31-109-ENG-38 ..... N88-12660
N88-12909
N88-12950
N88-12955
N88-12967
N88-12983
N88-12995
N88-13062
W-7405-ENG-36 ..... N88-12514
N88-12583
N88-12608
N88-12610
N88-12611
N88-12665
N88-12743
N88-12749
N88-12771
N88-12775
N88-12776
N88-12777
N88-12778
N88-12782
N88-12786
N88-12787
N88-12789
N88-12801
N88-12808
N88-12859
N88-12895
N88-12918
N88-12919
N88-12960
N88-12976
N88-13013
N88-13019
N88-13027
N88-13040
N88-13047
N88-13048
N88-13069
N88-13071
W-7405-ENG-48 ..... N88-12519
N88-12540
N88-12554
N88-12643
N88-12714
N88-12729
N88-12739
N88-12745
N88-12779
N88-12780
N88-12788
N88-12790
N88-12816
N88-12913
N88-12951
N88-12963
N88-13024
N88-13028
N88-13041
N88-13043
N88-13067
N88-13082
W-7405-ENG-82 ..... N88-12732
W-31109-ENG-38 ..... N88-12614
199-50-62-12-02 ..... N88-12711
307-04-02 ..... N88-12482
310-10-60-87-02 ..... N88-12683
310-10-60-87-04 ..... N88-12684
310-10-61-84-02 ..... N88-12682
310-10-61-84-04 ..... N88-12680
310-10-62-15-00 ..... N88-12685
310-10-62-34-00 ..... N88-12686
310-10-63-53-00 ..... N88-12681
310-20-60-09-00 ..... N88-12688
310-20-64-15-00 ..... N88-12687
310-20-66-09-00 ..... N88-12689
310-20-66-53-00 ..... N88-12690
310-20-67-59-00 ..... N88-12692
N88-12693
310-20-67-63-00 ..... N88-12691
310-30-70-84-02 ..... N88-12694
N88-12695
N88-12696
310-30-70-84-08 ..... N88-12697
N88-12699
N88-12700
310-30-71-87-02 ..... N88-12698
314-30-42-01-34 ..... N88-12708
314-30-51-38-66 ..... N88-12707
314-30-56-04-19 ..... N88-12701
N88-12702
N88-12706
314-30-57-23-32 ..... N88-12703
314-40-22-12-05 ..... N88-12730
314-40-32-10-11 ..... N88-12710
314-40-42-01-34 ..... N88-12709
314-40-50-28-22 ..... N88-12704
314-40-50-58-06 ..... N88-12705
481-02-02 ..... N88-12541
481-89-00-00-72 ..... N88-12927
505-31-04 ..... N88-12461
505-42-11 ..... N88-12452
505-42-71 ..... N88-12932
505-43-01 ..... N88-12453
505-60-01 ..... N88-12463
505-60-11 ..... N88-12471
505-60-21-02 ..... N88-12457
505-61-01-02 ..... N88-12497
505-61-01-07 ..... N88-12496
505-61-51 ..... N88-12495
505-61-51-06 ..... N88-13002
505-61-71-01 ..... N88-12454
505-61-71-02 ..... N88-12458
505-62-11 ..... N88-12490
505-62-21 ..... N88-12752
505-62-91-01 ..... N88-12455
505-63-01 ..... N88-12543
505-63-01-01 ..... N88-12544
505-63-11 ..... N88-12459
N88-12551
N88-12552
505-63-51 ..... N88-12797
N88-12798
505-63-51-06 ..... N88-13003
505-63-91-01 ..... N88-13015
505-65-11 ..... N88-12796
505-66-11 ..... N88-12477
N88-12478
505-66-21 ..... N88-12494
505-66-21-01 ..... N88-13000
505-66-21-02 ..... N88-12928
505-66-21-04 ..... N88-12897
505-66-41-04 ..... N88-12969
505-66-41-57 ..... N88-12480
505-67-41-02 ..... N88-12487
505-67-51 ..... N88-12924
505-68-11 ..... N88-12473
505-90-21-01 ..... N88-12934
N88-12935
N88-12979
506-41-11 ..... N88-12877
N88-12878
506-41-31 ..... N88-13209
506-42-21 ..... N88-12539
506-42-31 ..... N88-12538
N88-12542
506-43-41-04 ..... N88-12531
506-46-21-01 ..... N88-12456
506-49-3B N88-12520
506-63-1B N88-12825
532-08-11 ..... N88-12462
674-25-05 ..... N88-12763
679-40-00 ..... N88-12727
917-60-00 ..... N88-12515

REPORT/ACCESSION NUMBER INDEX

Typical Report Number Index Listing

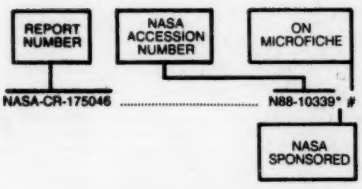

Listings in this index are arranged alphanumerically by report number. The NASA accession number denotes the number by which the citation is identified. An asterisk (*) indicates that the item is a NASA report. A pound sign (#) indicates that the item is available on microfiche.

A-86282 ..... N88-12494* #
A-87196 ..... N88-12924* #
A-87293 ..... N88-12991* #
A-87306 ..... N88-12466* #
A-87336 ..... N88-12495* #

ACT-79 ..... N88-12941 #
ACT-80 ..... N88-12942 #

AD-A184000 ..... N88-13066 #
AD-A184019 ..... N88-12612 #
AD-A184075 ..... N88-12474 #
AD-A184076 ..... N88-12740 #
AD-A184082 ..... N88-12903 #
AD-A184085 ..... N88-12925 #
AD-A184086 ..... N88-12595 #
AD-A184089 ..... N88-12721 #
AD-A184094 ..... N88-12666 #
AD-A184104 ..... N88-13049 #
AD-A184105 ..... N88-12960 #
AD-A184106 ..... N88-13075 #
AD-A184107 ..... N88-12491 #
AD-A184110 ..... N88-12566 #
AD-A184113 ..... N88-12975 #
AD-A184127 ..... N88-12937 #
AD-A184131 ..... N88-12938 #
AD-A184132 ..... N88-12741 #
AD-A184133 ..... N88-12996 #
AD-A184134 ..... N88-12920 #
AD-A184164 ..... N88-12772 #
AD-A184170 ..... N88-13060 #
AD-A184173 ..... N88-12536 #
AD-A184176 ..... N88-12809 #
AD-A184178 ..... N88-12615 #
AD-A184182 ..... N88-12667 #
AD-A184184 ..... N88-12596 #
AD-A184191 ..... N88-12567 #
AD-A184208 ..... N88-13021 #
AD-A184222 ..... N88-12904 #
AD-A184231 ..... N88-13050 #
AD-A184238 ..... N88-12486 #
AD-A184243 ..... N88-12475 #
AD-A184246 ..... N88-12939 #
AD-A184249 ..... N88-12940 #
AD-A184252 ..... N88-12722 #
AD-A184254 ..... N88-12723 #
AD-A184255 ..... N88-12668 #
AD-A184258 ..... N88-12997 #
AD-A184268 ..... N88-13051 #
AD-A184269 ..... N88-12773 #
AD-A184270 ..... N88-12597 #
AD-A184271 ..... N88-13004 #
AD-A184274 ..... N88-13052 #
AD-A184275 ..... N88-13053 #
AD-A184276 ..... N88-13054 #
AD-A184277 ..... N88-13055 #
AD-A184278 ..... N88-12941 #
AD-A184279 ..... N88-12942 #
AD-A184281 ..... N88-12981 #
AD-A184283 ..... N88-12791 #
AD-A184296 ..... N88-12792 #
AD-A184299 ..... N88-13022 #
AD-A184315 ..... N88-13018 #
AD-A184317 ..... N88-12669 #
AD-A184331 ..... N88-12971 #
AD-A184339 ..... N88-12943 #
AD-A184340 ..... N88-12499 #
AD-A184341 ..... N88-12810 #
AD-A184342 ..... N88-13056 #
AD-A184343 ..... N88-12670 #
AD-A184346 ..... N88-12556 #
AD-A184349 ..... N88-12598 #
AD-A184350 ..... N88-12599 #
AD-A184351 ..... N88-12671 #
AD-A184352 ..... N88-13210* #
AD-A184353 ..... N88-13023 #
AD-A184354 ..... N88-12944 #
AD-A184355 ..... N88-12546 #
AD-A184356 ..... N88-12600 #
AD-A184357 ..... N88-12911 #
AD-A184359 ..... N88-12601 #
AD-A184389 ..... N88-12724 #
AD-A184390 ..... N88-13012 #
AD-A184402 ..... N88-13057 #
AD-A184404 ..... N88-12793 #
AD-A184419 ..... N88-13058 #
AD-A184426 ..... N88-12725 #
AD-A184432 ..... N88-12912 #
AD-A184433 ..... N88-12672 #
AD-A184434 ..... N88-12726 #
AD-A184436 ..... N88-12811 #
AD-A184441 ..... N88-12945 #
AD-A184442 ..... N88-12887 #
AD-A184443 ..... N88-12492 #
AD-A184450 ..... N88-12888 #
AD-A184452 ..... N88-12860 #
AD-A184453 ..... N88-12476 #
AD-A184456 ..... N88-12774 #
AD-A184457 ..... N88-12969 #
AD-A184458 ..... N88-12547 #
AD-A184461 ..... N88-12500 #
AD-A184462 ..... N88-12972 #
AD-A184464 ..... N88-12568 #
AD-A184465 ..... N88-12569 #
AD-A184466 ..... N88-12889 #
AD-A184467 ..... N88-12742 #
AD-A184468 ..... N88-12548 #
AD-A184470 ..... N88-12998 #
AD-A184471 ..... N88-12946 #
AD-A184472 ..... N88-12982 #
AD-A184473 ..... N88-12673 #
AD-A184791 ..... N88-12644 #

AD-F000100 ..... N88-12724 #
AD-F000100 ..... N88-13012 #

AFAL-TR-87-053 ..... N88-12536 #

AFESC/ESL-TR-86-20 ..... N88-12488 #

AFGL-ERP-969 ..... N88-12670 #

AFGL-TR-86-0266 ..... N88-12772 #
AFGL-TR-87-0011 ..... N88-12904 #
AFGL-TR-87-0060 ..... N88-12670 #
AFGL-TR-87-0154 ..... N88-12889 #

AFWAL-TR-86-2031 ..... N88-13051 #
AFWAL-TR-87-2036 ..... N88-12969 #
AFWAL-TR-87-4001 ..... N88-12548 #
AFWAL-TR-87-4048 ..... N88-12547 #

AFWL-TR-85-140 ..... N88-12774 #

AGARD-AG-300-VOL-6 ..... N88-12481 #
AGARD-AG-304 ..... N88-12818 #
AGARD-AG-312 ..... N88-12923 #

AI-M-931 ..... N88-12972 #
AI-M-983 ..... N88-12945 #

ANL-87-23 ..... N88-12950 #
ANL-87-32 ..... N88-12909 #
ANL-87-36 ..... N88-12967 #
ANL-87-40 ..... N88-12955 #

ANL/MCS-TM-95 ..... N88-12995 #

AR-004-517 ..... N88-12992 #
AR-004-526 ..... N88-12495 #
AR-004-847 ..... N88-12517 #
AR-005-131 ..... N88-12516 #

ARL-AERO-TM-386 ..... N88-12485 #

ARL-STRUC-R-425 ..... N88-12992 #

ARO-21003.5-CH ..... N88-13057 #
ARO-21203.7-MA ..... N88-12811 #
ARO-21438.37-EL ..... N88-12673 #
ARO-22729.4-MA ..... N88-12982 #
ARO-22735.4-MA ..... N88-12996 #
ARO-23396.1-EL-5 ..... N88-12946 #
ARO-23474.16-MS ..... N88-12568 #

AVSCOM-TM-87-C-2 ..... N88-12797* #
AVSCOM-TM-87-C-3 ..... N88-12798* #

BBC-RD-1987/12 ..... N88-12676
BBC-RD-1987/13 ..... N88-12677

BDX-613-3710 ..... N88-12815 #

BLL-CE-TRANS-8256-(9022.09) ..... N88-12589 #
BLL-CE-TRANS-8258-(9022.09) ..... N88-12586 #
BLL-CE-TRANS-8265-(9022.09) ..... N88-12805 #
BLL-CE-TRANS-8281-(9022.09) ..... N88-12806 #

BLL-MO-TRANS-1667-(9022.552) N88-12675

BNL-NCS-39950 ..... N88-12558 #

BNL-NUREG-39923 ..... N88-12803 #

BNL-36225 ..... N88-12738 #
BNL-40156 ..... N88-13020 #
BNL-40210 ..... N88-13010 #
BNL-40211 ..... N88-13197 #
BNL-40216 ..... N88-13011 #
BNL-40217 ..... N88-13009 #

BRL-MR-3605 ..... N88-12981 #

BRL-TR-2810 ..... N88-12810 #

CAR-TR-255 ..... N88-12474 #
CAR-TR-290 ..... N88-12939 #

CBPF-NF-025/86 ..... N88-13198 #
CBPF-NF-029/86 ..... N88-13061 #
CBPF-NF-036/86 ..... N88-13199 #
CBPF-NF-042/86 ..... N88-13001 #
CBPF-NF-046/86 ..... N88-13076 #
CBPF-NF-048/86 ..... N88-12999 #
CBPF-NF-056/86 ..... N88-13213 #

CCMS-87-15 ..... N88-12549* #

CERL-TR-N-87-16 ..... N88-12556 #

CESAR-87/24 ..... N88-12988 #
CESAR-87/39 ..... N88-13207 #

CLM-P797 ..... N88-13022 #
CLM-P800 ..... N88-13012 #
CLM-P803 ..... N88-13023 #

CMU-RI-TR-87-16 ..... N88-12971 #

CONF-860778-VOL-3 ..... N88-12790 #
CONF-861299-3 ..... N88-12571 #
CONF-870102-29-REV-1 ..... N88-12540* #
CONF-870159-3 ..... N88-12739 #
CONF-870185 ..... N88-13042 #
CONF-870189-1 ..... N88-12554 #
CONF-870210-2 ..... N88-12873 #
CONF-870272-9 ..... N88-13062 #

CONF-870410-37 ..... N88-12559 #
CONF-870413-2 ..... N88-13013 #
CONF-870438-37 ..... N88-13066 #
CONF-870622-10 ..... N88-12789 #
CONF-870666-SUMMS ..... N88-12883 #
CONF-870691-3 ..... N88-12765 #
CONF-870719-5 ..... N88-12814 #
CONF-870725-12 ..... N88-12609 #
CONF-870734-3 ..... N88-12973 #
CONF-870739-2 ..... N88-13009 #
CONF-870753-73 ..... N88-12813 #
CONF-870753-77 ..... N88-12826 #
CONF-870799-3 ..... N88-13068 #
CONF-870802-20 ..... N88-13197 #
CONF-870802-23 ..... N88-13206 #
CONF-870808-1 ..... N88-13072 #
CONF-870825-1 ..... N88-13048 #
CONF-870832-6 ..... N88-12800 #
CONF-870873-6-REV ..... N88-13063 #
CONF-870873-15 ..... N88-12583 #
CONF-870878-1 ..... N88-12803 #
CONF-870881-3 ..... N88-13069 #
CONF-870883-1 ..... N88-13025 #
CONF-870908-7 ..... N88-13027 #
CONF-870908-8 ..... N88-13040 #
CONF-870909-2 ..... N88-13011 #
CONF-870981-2 ..... N88-12582 #
CONF-870984-4 ..... N88-12961 #
CONF-870988-3 ..... N88-12561 #
CONF-871007-2 ..... N88-13024* #
CONF-871007-3 ..... N88-12780 #
CONF-871007-9 ..... N88-12965 #
CONF-871027-8 ..... N88-12872 #
CONF-871027-34 ..... N88-12608 #
CONF-871027-35 ..... N88-12728 #
CONF-871027-37 ..... N88-12735 #
CONF-871036-5 ..... N88-12585 #
CONF-871101-34 ..... N88-12964 #
CONF-871101-51 ..... N88-12803 #
CONF-871125-1 ..... N88-13026 #
CONF-871125-3 ..... N88-13071 #
CONF-871134-1 ..... N88-12843 #
CONF-871136-1 ..... N88-12929 #
CONF-871142-1-REV ..... N88-12743 #
CONF-871163-4 ..... N88-13068 #
CONF-871164-1 ..... N88-12715 #
CONF-871207-11 ..... N88-12590 #
CONF-8610336-1 ..... N88-13062 #
CONF-8611137-3 ..... N88-12781 #
CONF-8611154-2 ..... N88-12777 #
CONF-8611184-2 ..... N88-12577 #
CONF-8611184-3 ..... N88-12578 #
CONF-8703157-1 ..... N88-12614 #
CONF-8704168-4 ..... N88-12745 #
CONF-8704205-1 ..... N88-13060 #
CONF-8704208-1 ..... N88-12749 #
CONF-8705168-2 ..... N88-13047 #
CONF-8705175-1 ..... N88-12602 #
CONF-8705176-1 ..... N88-12572 #
CONF-8705176-2 ..... N88-12573 #
CONF-8705176-3 ..... N88-12574 #
CONF-8705176-4 ..... N88-12575 #
CONF-8705176-5 ..... N88-12576 #
CONF-8705176-6 ..... N88-12579 #
CONF-8705176-7 ..... N88-12580 #
CONF-8705194-1 ..... N88-12770 #
CONF-8706125-13 ..... N88-13060* #
CONF-8706125-14 ..... N88-12553 #
CONF-8706155-2 ..... N88-12513 #
CONF-8706165-3 ..... N88-12464 #
CONF-8706165-4 ..... N88-12550 #
CONF-8706187 ..... N88-12660 #
CONF-8706199-3 ..... N88-12782 #
CONF-8706214-1 ..... N88-12620 #
CONF-8707113-1 ..... N88-12591 #
CONF-8707113-2 ..... N88-12785 #
CONF-8707114-1 ..... N88-12983 #
CONF-8707116-1 ..... N88-13090 #
CONF-8707117-1 ..... N88-12874 #
CONF-8708104-2 ..... N88-13084 #
CONF-8708105-4 ..... N88-12558 #
CONF-8708117-4 ..... N88-13014 #
CONF-8708121-1 ..... N88-12918 #
CONF-8708121-2 ..... N88-12919 #
CONF-8708134-2 ..... N88-12744 #
CONF-8708137-1 ..... N88-13059 #
CONF-8708141-1 ..... N88-12665 #
CONF-8708141-2 ..... N88-12895 #
CONF-8708141-3 ..... N88-12808 #
CONF-8708143-1 ..... N88-13010 #
CONF-8708145-1 ..... N88-12976 #
CONF-8708145-2 ..... N88-12977 #
CONF-8709110-4 ..... N88-12787 #
CONF-8709110-7 ..... N88-12771 #
CONF-8709110-8 ..... N88-12776 #
CONF-8709110-9 ..... N88-12775 #
CONF-8709110-10 ..... N88-12778 #
CONF-8709128-1 ..... N88-12948 #
CONF-8709136-1 ..... N88-12810 #
CONF-8709136-2 ..... N88-12611 #
CONF-8709139-1 ..... N88-13019 #
CONF-8709140-1 ..... N88-12786 #
CONF-8709143-1 ..... N88-12779 #
CONF-8709143-2 ..... N88-13067 #
CONF-8709143-3 ..... N88-13043 #
CONF-8709146-3 ..... N88-12674 #
CONF-8709153-1 ..... N88-12768 #
CONF-8710123-2 ..... N88-12581 #
CONF-8710132-5 ..... N88-12933 #
CONF-8710135-2 ..... N88-12827 #
CONF-8710135-3 ..... N88-12612 #
CONF-8710149-1 ..... N88-12936 #
CONF-8710150-1 ..... N88-12913 #
CONF-8710151-1 ..... N88-12801 #
CONF-8710157-1 ..... N88-12519 #
CONF-8710163-1 ..... N88-12951 #

CORR-86-00241 ..... N88-12795 #

CRDEC-CR-87084 ..... N88-12742 #

CRING-FRL-717-1 ..... N88-12458* #

CRPE/159 ..... N88-12675

CRREL-87-11 ..... N88-12887 #

CS-TR-1760 ..... N88-12474 #
CS-TR-1952 ..... N88-12939 #

CSSA-ASTRO-87-8 ..... N88-13210* #

CUED/B-ELECT/TR-73 ..... N88-12719 #

DE87-006518 ..... N88-12871 #
DE87-009048 ..... N88-12872 #
DE87-010511 ..... N88-12936 #
DE87-010873 ..... N88-12843 #
DE87-011123 ..... N88-12929 #
DE87-011393 ..... N88-12983 #
DE87-011504 ..... N88-12614 #
DE87-011512 ..... N88-13062 #
DE87-011868 ..... N88-12984 #
DE87-011756 ..... N88-12743 #
DE87-011791 ..... N88-13013 #
DE87-012124 ..... N88-12803 #
DE87-012243 ..... N88-13082 #
DE87-012360 ..... N88-12513 #
DE87-012541 ..... N88-12590 #
DE87-013011 ..... N88-12770 #
DE87-013153 ..... N88-12960 #
DE87-013369 ..... N88-12947 #
DE87-013539 ..... N88-13014 #
DE87-013557 ..... N88-12554 #
DE87-013568 ..... N88-13042 #
DE87-013650 ..... N88-12812 #
DE87-013714 ..... N88-12674 #
DE87-013723 ..... N88-12813 #
DE87-013746 ..... N88-12591 #
DE87-013747 ..... N88-12785 #
DE87-013812 ..... N88-12826 #
DE87-013874 ..... N88-12948 #
DE87-014061 ..... N88-12582 #
DE87-014078 ..... N88-13063 #
DE87-014157 ..... N88-13059 #
DE87-014342 ..... N88-12540* #
DE87-014357 ..... N88-12913 #
DE87-014397 ..... N88-12558 #
DE87-014407 ..... N88-13064 #
DE87-014636 ..... N88-12564 #
DE87-014637 ..... N88-12949 #
DE87-014643 ..... N88-12627 #
DE87-014683 ..... N88-13060* #
DE87-014730 ..... N88-12918 #
DE87-014731 ..... N88-12919 #
DE87-014740 ..... N88-13069 #
DE87-014741 ..... N88-13047 #
DE87-014752 ..... N88-13071 #
DE87-014754 ..... N88-12777 #
DE87-014783 ..... N88-12778 #
DE87-014786 ..... N88-12583 #
DE87-014788 ..... N88-12808 #
DE87-014771 ..... N88-13048 #
DE87-014801 ..... N88-12921 #
DE87-014812 ..... N88-12583 #
DE87-014815 ..... N88-13025 #
DE87-014837 ..... N88-12933 #
DE87-014839 ..... N88-12900 #
DE87-014845 ..... N88-12550 #
DE87-014846 ..... N88-12464 #
DE87-014868 ..... N88-13070 #
DE87-014899 ..... N88-12738 #
DE87-014910 ..... N88-13197 #
DE87-014917 ..... N88-13009 #
DE87-014920 ..... N88-13010 #
DE87-014921 ..... N88-13011 #
DE87-014987 ..... N88-13065 #
DE87-014997 ..... N88-12859 #
DE87-014998 ..... N88-12769 #
DE87-703357 ..... N88-13198 #
DE87-703360 ..... N88-13081 #
DE87-703364 ..... N88-13199 #
DE87-703368 ..... N88-13001 #
DE87-703371 ..... N88-13076 #
DE87-703372 ..... N88-12999 #
DE87-703376 ..... N88-13213 #
DE87-703478 ..... N88-12570 #
DE87-703500 ..... N88-12602 #
DE87-703507 ..... N88-12571 #
DE87-703545 ..... N88-12572 #
DE87-703546 ..... N88-12573 #
DE87-703547 ..... N88-12574 #
DE87-703548 ..... N88-12575 #
DE87-703549 ..... N88-12576 #
DE87-703663 ..... N88-12985 #
DE87-703690 ..... N88-13077 #
DE87-703692 ..... N88-12577 #
DE87-703693 ..... N88-12578 #
DE87-703706 ..... N88-12579 #
DE87-703707 ..... N88-12580 #
DE87-703765 ..... N88-13200 #
DE88-000013 ..... N88-12986 #
DE88-000065 ..... N88-12581 #
DE88-000078 ..... N88-12961 #
DE88-000079 ..... N88-12559 #
DE88-000093 ..... N88-12973 #
DE88-000098 ..... N88-12873 #
DE88-000137 ..... N88-12950 #
DE88-000147 ..... N88-12744 #
DE88-000160 ..... N88-13089 #
DE88-000166 ..... N88-12514 #
DE88-000174 ..... N88-12603 #
DE88-000188 ..... N88-13072 #
DE88-000191 ..... N88-12974 #
DE88-000207 ..... N88-12814 #
DE88-000210 ..... N88-13066 #
DE88-000216 ..... N88-12745 #
DE88-000219 ..... N88-13067 #
DE88-000220 ..... N88-12951 #
DE88-000242 ..... N88-12739 #
DE88-000260 ..... N88-12713 #
DE88-000261 ..... N88-12585 #
DE88-000266 ..... N88-12802 #
DE88-000303 ..... N88-12628 #
DE88-000328 ..... N88-12584 #
DE88-000330 ..... N88-13026 #
DE88-000334 ..... N88-12585 #
DE88-000360 ..... N88-13088 #
DE88-000413 ..... N88-12731 #
DE88-000417 ..... N88-13024* #
DE88-000420 ..... N88-12779 #
DE88-000423 ..... N88-12519 #
DE88-000425 ..... N88-12780 #
DE88-000444 ..... N88-12902 #
DE88-000451 ..... N88-12909 #
DE88-000452 ..... N88-12781 #
DE88-000459 ..... N88-13090 #
DE88-000460 ..... N88-12715 #
DE88-000463 ..... N88-13068 #
DE88-000483 ..... N88-12895 #
DE88-000494 ..... N88-12749 #
DE88-000496 ..... N88-12608 #
DE88-000501 ..... N88-12610 #
DE88-000503 ..... N88-12786 #
DE88-000504 ..... N88-13040 #
DE88-000506 ..... N88-12976 #
DE88-000507 ..... N88-12665 #
DE88-000510 ..... N88-12771 #
DE88-000512 ..... N88-13019 #
DE88-000514 ..... N88-12775 #
DE88-000515 ..... N88-12776 #
DE88-000521 ..... N88-12769 #
DE88-000525 ..... N88-12782 #
DE88-000527 ..... N88-12611 #
DE88-000532 ..... N88-12787 #
DE88-000537 ..... N88-12801 #
DE88-000538 ..... N88-13027 #
DE88-000553 ..... N88-12620 #
DE88-000558 ..... N88-12809 #
DE88-000560 ..... N88-12785 #
DE88-000583 ..... N88-12874 #
DE88-000636 ..... N88-12560 #
DE88-000641 ..... N88-12732 #
DE88-000647 ..... N88-12767 #
DE88-000649 ..... N88-12866 #
DE88-000668 ..... N88-12629 #
DE88-000672 ..... N88-12659 #
DE88-000675 ..... N88-12982 #

DE88-000678 ..... N88-12883 #
DE88-000682 ..... N88-12964 #
DE88-000696 ..... N88-12733 #
DE88-000706 ..... N88-12977 #
DE88-000713 ..... N88-12794 #
DE88-000714 ..... N88-12966 #
DE88-000715 ..... N88-12783 #
DE88-000719 ..... N88-12746 #
DE88-000727 ..... N88-12561 #
DE88-000732 ..... N88-12788 #
DE88-000755 ..... N88-13043 #
DE88-000779 ..... N88-12804 #
DE88-000784 ..... N88-13041 #
DE88-000788 ..... N88-13028 #
DE88-000805 ..... N88-12987 #
DE88-000807 ..... N88-12930 #
DE88-000809 ..... N88-12562 #
DE88-000810 ..... N88-12994 #
DE88-000819 ..... N88-12804 #
DE88-000820 ..... N88-13008 #
DE88-000831 ..... N88-12618 #
DE88-000833 ..... N88-12896 #
DE88-000835 ..... N88-12815 #
DE88-000897 ..... N88-12563 #
DE88-000922 ..... N88-12728 #
DE88-000964 ..... N88-12790 #
DE88-000997 ..... N88-12965 #
DE88-001310 ..... N88-12879 #
DE88-001313 ..... N88-12988 #
DE88-001314 ..... N88-12880 #
DE88-001320 ..... N88-12955 #
DE88-001321 ..... N88-12967 #
DE88-001323 ..... N88-13044 #
DE88-001324 ..... N88-12816 #
DE88-001326 ..... N88-12788 #
DE88-001328 ..... N88-12714 #
DE88-001345 ..... N88-12658 #
DE88-001360 ..... N88-12735 #
DE88-001367 ..... N88-12795 #
DE88-001393 ..... N88-13073 #
DE88-001395 ..... N88-12656 #
DE88-001448 ..... N88-12766 #
DE88-001449 ..... N88-12734 #
DE88-001451 ..... N88-12750 #
DE88-001453 ..... N88-12881 #
DE88-001457 ..... N88-12963 #
DE88-001458 ..... N88-12729 #
DE88-001461 ..... N88-13206 #
DE88-001464 ..... N88-13020 #
DE88-001475 ..... N88-13029 #
DE88-001477 ..... N88-12995 #
DE88-001479 ..... N88-12660 #
DE88-001487 ..... N88-13045 #
DE88-001492 ..... N88-12830 #
DE88-001506 ..... N88-12956 #
DE88-001513 ..... N88-13207 #
DE88-001518 ..... N88-12968 #
DE88-001520 ..... N88-12605 #
DE88-001522 ..... N88-12882 #
DE88-001591 ..... N88-12957 #
DE88-001670 ..... N88-13078 #
DE88-001671 ..... N88-13079 #
DE88-001687 ..... N88-12764 #
DE88-001706 ..... N88-12969 #
DE88-001710 ..... N88-13046 #
DE88-001778 ..... N88-12884 #
DE88-001781 ..... N88-12751 #
DE88-001783 ..... N88-12876 #
DE88-900066 ..... N88-13091 #
DE88-900082 ..... N88-12885 #

DOE/ER-0348 ..... N88-12659 #
DOE/ER-0349 ..... N88-12896 #
DOE/ER-01023/7 ..... N88-12584 #
DOE/ER-13154/11 ..... N88-12563 #
DOE/ER-13167/1 ..... N88-12764 #
DOE/ER-13276/T1 ..... N88-12584 #
DOE/ER-13443/2 ..... N88-12562 #
DOE/ER-13463/T1 ..... N88-12560 #
DOE/ER-25001/31 ..... N88-12930 #
DOE/ER-25026/12 ..... N88-12967 #
DOE/ER-25026/13 ..... N88-12994 #
DOE/ER-40200/117 ..... N88-13079 #
DOE/ER-40200/118 ..... N88-13078 #
DOE/ER-45067/T1 ..... N88-13070 #
DOE/ER-45239/2 ..... N88-13065 #
DOE/ER-45282/7 ..... N88-12969 #
DOE/ER-52133/2 ..... N88-13046 #
DOE/ER-53176/4 ..... N88-13029 #

DOE/EV-03140/10 ..... N88-12921 #
DOE/EV-06194/3-REV-3 ..... N88-12616 #

DOE/MC-22045/2364 ..... N88-12871 #

DOE/OR-21702/T1 ..... N88-13089 #

DOE/PC-80524/T8 ..... N88-12858 #
DOE/PC-90962/T4 ..... N88-12746 #

DOE/RL-10336/1 ..... N88-12902 #

DP-MS-87-6 ..... N88-12800 #
DP-MS-87-108 ..... N88-12933 #

DRD-TM-478T ..... N88-12617* #

DRL-T-1884 ..... N88-12617* #

DTIC/TR/86/14-VOL-1 ..... N88-13088 #
DTIC/TR/87/14-VOL-1 ..... N88-13088 #

D180-30473-1 ..... N88-12870* #

E-2543 ..... N88-12481* #
E-3226 ..... N88-12515* #
E-3395 ..... N88-12543* #
E-3484 ..... N88-12520* #
E-3658 ..... N88-12473* #
E-3661 ..... N88-12798* #
E-3663 ..... N88-12727* #
E-3676 ..... N88-12542* #
E-3684 ..... N88-12490* #
E-3696 ..... N88-12877* #
E-3697 ..... N88-12878* #
E-3736 ..... N88-12538* #
E-3750 ..... N88-12552* #
E-3758 ..... N88-12797* #
E-3756 ..... N88-12798* #
E-3773 ..... N88-12539* #
E-3803 ..... N88-12752* #
E-3831 ..... N88-12763* #
E-3839 ..... N88-13209* #
E-3862 ..... N88-12551* #
E-3867 ..... N88-12825* #

EEC/NOTE-15/86 ..... N88-12970 #

EGG-SPAG-7818-PT-2 ..... N88-12957 #

EMA-87-R-37 ..... N88-12897* #

EP-PATENT-APPL-SN-86300904.9 ..... N88-12642
EP-PATENT-APPL-SN-86301608.5 ..... N88-12594
EP-PATENT-APPL-SN-86303727.1 ..... N88-12593
EP-PATENT-APPL-SN-86305526.5 ..... N88-12607

EP-PATENT-0-191-623-A2 ..... N88-12642
EP-PATENT-0-199-444-A1 ..... N88-12594
EP-PATENT-0-204-453-A1 ..... N88-12593
EP-PATENT-0-210-794-A2 ..... N88-12607

ERIM-175900-11-T ..... N88-13018 #

ESL-716199-9 ..... N88-12479* #
ESL-717220-4 ..... N88-12666 #

ETL-0452 ..... N88-12474 #
ETL-0462 ..... N88-12939 #
ETL-0485 ..... N88-12475 #

ETN-87-90717 ..... N88-12545
ETN-87-90718 ..... N88-12607
ETN-87-90719 ..... N88-12593
ETN-87-90720 ..... N88-12642
ETN-87-90721 ..... N88-12594

EUR-9374-EN ..... N88-12666 #
EUR-10203-EN ..... N88-12666 #
EUR-10808-EN ..... N88-12885 #

FJSRL-TR-87-0005 ..... N88-12791 #

FNAL-TM-1468 ..... N88-12733 #

FNAL/C-87/127 ..... N88-12766 #

FOA-C-20621-2.1 ..... N88-12555 #
FOA-C-20660-2.1 ..... N88-12613 #

FR-667103 ..... N88-12969* #

GB-PATENT-APPL-SN-8621355 ..... N88-12545

GB-PATENT-2-180-251-A N88-12545

GK-1 ..... N88-12975 #
GK-2 ..... N88-13075 #
GK-3 ..... N88-12960 #

GMU/22461/103 ..... N88-12668 #

GRI-87/0136 ..... N88-13074 #

HV410-12 ..... N88-12532* #

ICASE-87-39 ..... N88-12935* #
ICASE-87-65 ..... N88-12934* #
ICASE-87-66 ..... N88-12979* #

ICOMP-87-7 ..... N88-12752* #

IFT-P-12/86 ..... N88-13001 #

IFUSP-P-604 ..... N88-13077 #

INIS-BR-701 ..... N88-12577 #
INIS-BR-702 ..... N88-12578 #
INIS-BR-726 ..... N88-12570 #
INIS-BR-749 ..... N88-12602 #
INIS-BR-757 ..... N88-12571 #
INIS-BR-802 ..... N88-12572 #
INIS-BR-803 ..... N88-12579 #
INIS-BR-804 ..... N88-12573 #
INIS-BR-805 ..... N88-12574 #
INIS-BR-806 ..... N88-12575 #
INIS-BR-807 ..... N88-12580 #
INIS-BR-808 ..... N88-12576 #

INPE-4070 ..... N88-13200 #

INT-PATENT-CLASS-B29C-37/00 ..... N88-12642
INT-PATENT-CLASS-B29C-45/16 ..... N88-12642
INT-PATENT-CLASS-B29C-45/57 ..... N88-12642

INT-PATENT-CLASS-C08J-5/00 ..... N88-12545
INT-PATENT-CLASS-C08K-5/54 ..... N88-12594
INT-PATENT-CLASS-C08L-23/04 ..... N88-12593
INT-PATENT-CLASS-C08L-33/08 ..... N88-12593
INT-PATENT-CLASS-C08L-61/06 ..... N88-12545

INT-PATENT-CLASS-G01N-27/84 ..... N88-12807

INT-PATENT-CLASS-H01B-3/44 ..... N88-12594
INT-PATENT-CLASS-H01B-3/46 ..... N88-12594
INT-PATENT-CLASS-H01B-7/28 ..... N88-12594

IOS/CRUISE-187 ..... N88-12910 #

IPPJ-AM-50 ..... N88-13042 #
IPPJ-AM-53 ..... N88-13031 #
IPPJ-AM-54 ..... N88-13030 #

IPPJ-847 ..... N88-13036 #
IPPJ-848 ..... N88-13035 #
IPPJ-849 ..... N88-13034 #
IPPJ-850 ..... N88-13033 #
IPPJ-851 ..... N88-13037 #
IPPJ-852 ..... N88-13032 #

IRS-87-P-10 ..... N88-12536 #

IS-4924 ..... N88-12732 #

ISBN-92-825-5307-8 ..... N88-12666 #
ISBN-92-835-0429-1 ..... N88-12618 #
ISBN-92-835-1559-5 ..... N88-12481 #
ISBN-92-835-1561-7 ..... N88-12923 #
ISBN-951-38-2580-9 ..... N88-12717 #
ISBN-951-38-2604-X ..... N88-12716 #
ISBN-951-38-2668-6 ..... N88-12858 #
ISBN-951-754-179-1 ..... N88-12736 #

ISI/RS-87-196 ..... N88-12944 #

ISSN-0082-5263 ..... N88-12489 #
ISSN-0082-5263 ..... N88-12657 #
ISSN-0469-4732 ..... N88-13032 #
ISSN-0469-4732 ..... N88-13033 #
ISSN-0469-4732 ..... N88-13034 #
ISSN-0469-4732 ..... N88-13035 #
ISSN-0469-4732 ..... N88-13036 #
ISSN-0469-4732 ..... N88-13037 #

JPL-PUB-87-22 ..... N88-12959* #
JPL-PUB-87-29 ..... N88-12730* #

JPL-TDA-PR-42-91 ..... N88-12679* #

JPRS-JST-87-025 ..... N88-12502 #

JPRS-UEQ-87-008 ..... N88-12621 #

JPRS-UES-86-006 ..... N88-12831 #

JPRS-ULS-87-009 ..... N88-12915 #

K/ETAC-8 ..... N88-12781 #
K/ETAC-31 ..... N88-12628 #

K/PS-5076 ..... N88-12767 #

L-15654 ..... N88-12456*
L-16302 ..... N88-12455*
L-16304 ..... N88-12928* #
L-16312 ..... N88-12454* #
L-16330 ..... N88-13002* #
L-16351 ..... N88-12480* #
L-16361 ..... N88-13015* #
L-16366 ..... N88-12487* #

LA-UR-87-1268 ..... N88-12789 #
LA-UR-87-1878 ..... N88-13013 #
LA-UR-87-2105-REV ..... N88-12743 #
LA-UR-87-2329 ..... N88-12960 #
LA-UR-87-2611 ..... N88-13047 #
LA-UR-87-2617 ..... N88-13069 #
LA-UR-87-2682-1 ..... N88-12919 #
LA-UR-87-2683-2 ..... N88-12918 #
LA-UR-87-2774 ..... N88-13048 #
LA-UR-87-2903 ..... N88-12808 #
LA-UR-87-2905 ..... N88-12583 #
LA-UR-87-2908 ..... N88-12778 #
LA-UR-87-2956 ..... N88-12777 #
LA-UR-87-2969 ..... N88-13071 #
LA-UR-87-2910 ..... N88-12776 #
LA-UR-87-2911 ..... N88-12775 #
LA-UR-87-2948 ..... N88-13019 #
LA-UR-87-2961 ..... N88-12771 #
LA-UR-87-2977 ..... N88-12665 #
LA-UR-87-2980 ..... N88-12976 #
LA-UR-87-2985 ..... N88-13040 #
LA-UR-87-3013 ..... N88-12786 #
LA-UR-87-3019 ..... N88-12610 #
LA-UR-87-3035 ..... N88-12787 #
LA-UR-87-3048 ..... N88-12611 #
LA-UR-87-3056 ..... N88-12782 #
LA-UR-87-3108 ..... N88-13027 #
LA-UR-87-3115 ..... N88-12801 #
LA-UR-87-3149 ..... N88-12608 #
LA-UR-87-3163 ..... N88-12749 #
LA-UR-87-3261 ..... N88-12895 #

LA-10945-M ..... N88-12859 #
LA-11087-MS ..... N88-12514 #

LBL-21522 ..... N88-12982 #
LBL-22361 ..... N88-12964 #
LBL-22903 ..... N88-13068 #
LBL-23037 ..... N88-13208 #
LBL-23244 ..... N88-13072 #
LBL-23453 ..... N88-12883 #
LBL-23495 ..... N88-12868 #
LBL-23531-REV ..... N88-13083 #
LBL-23544 ..... N88-12715 #
LBL-23604 ..... N88-12553 #
LBL-23742 ..... N88-13066 #
LBL-23795 ..... N88-12783 #
LBL-23811 ..... N88-12814 #
LBL-23822 ..... N88-13060* #
LBL-23833 ..... N88-13090 #
LBL-23852 ..... N88-12974 #
LBL-23861 ..... N88-12966 #
LBL-23880 ..... N88-12656 #
LBL-23937 ..... N88-13073 #

LC-87-619623 ..... N88-13087 #

ME-142(87)ONR-233-3 ..... N88-12809 #

MLM-3447(OP) ..... N88-12591 #
MLM-3449(OP) ..... N88-12785 #
MLM-3452 ..... N88-12769 #
MLM-3458(OP) ..... N88-12561 #

MR...-T-1029 ..... N88-12517 #
MRL-R-1053 ..... N88-12516 #

MTL-MS-86-3 ..... N88-12644 #

MTL-TR-87-28 ..... N88-12792 #
MTL-TR-87-29 ..... N88-12600 #

MW-87-P-5 ..... N88-12673 #

NADC-87036-60 ..... N88-12597 #

NAE-AN-46 ..... N88-12819 #
NAE-AN-47 ..... N88-12518 #

NAS 1.15:4009 ..... N88-12458*
NAS 1.15:86521 ..... N88-13083* #
NAS 1.15:86703 ..... N88-12932* #
NAS 1.15:86997 ..... N88-12461* #
NAS 1.15:87184 ..... N88-12473* #
NAS 1.15:88313 ..... N88-12494* #
NAS 1.15:88844 ..... N88-12515* #
NAS 1.15:89092 ..... N88-12531* #
NAS 1.15:89681 ..... N88-12540* #
NAS 1.15:100012 ..... N88-12991* #
NAS 1.15:100015 ..... N88-12486* #
NAS 1.15:100016 ..... N88-12924* #
NAS 1.15:100023 ..... N88-12495* #
NAS 1.15:100116 ..... N88-12796* #
NAS 1.15:100119 ..... N88-12727* #
NAS 1.15:100127 ..... N88-12542* #
NAS 1.15:100134 ..... N88-12490* #
NAS 1.15:100144 ..... N88-12877* #
NAS 1.15:100145 ..... N88-12878* #
NAS 1.15:100176 ..... N88-12552* #
NAS 1.15:100180 ..... N88-12797* #
NAS 1.15:100181 ..... N88-12798* #
NAS 1.15:100191 ..... N88-12539* #
NAS 1.15:100205 ..... N88-12752* #
NAS 1.15:100223 ..... N88-13209* #
NAS 1.15:100238 ..... N88-12551* #
NAS 1.15:100245 ..... N88-12625* #
NAS 1.15:100252 ..... N88-12763* #
NAS 1.15:100315 ..... N88-13016* #
NAS 1.15:100458 ..... N88-12927* #
NAS 1.15:100495 ..... N88-12544* #
NAS 1.15:100502 ..... N88-12459* #
NAS 1.15:100504 ..... N88-12496* #
NAS 1.15:100507 ..... N88-13003* #
NAS 1.21:7011(304) N88-12922*
NAS 1.21:7037(219) N88-12470*
NAS 1.26:4007 ..... N88-12452* #
NAS 1.26:4104 ..... N88-12897* #
NAS 1.26:4105 ..... N88-12458* #
NAS 1.26:4108 ..... N88-12969* #
NAS 1.26:166577 ..... N88-12482* #
NAS 1.26:172013 ..... N88-12928* #
NAS 1.26:172015 ..... N88-12501* #
NAS 1.26:172017 ..... N88-12747* #
NAS 1.26:172035 ..... N88-12617* #
NAS 1.26:177396 ..... N88-13006* #
NAS 1.26:177397 ..... N88-12472* #
NAS 1.26:177409 ..... N88-12954* #
NAS 1.26:177438 ..... N88-12478* #
NAS 1.26:177440 ..... N88-12453* #
NAS 1.26:177443 ..... N88-12477* #
NAS 1.26:177450 ..... N88-12471* #
NAS 1.26:177453 ..... N88-12493* #
NAS 1.26:177456 ..... N88-12463* #
NAS 1.26:177458 ..... N88-12482* #
NAS 1.26:178377 ..... N88-12934* #
NAS 1.26:178379 ..... N88-12935* #
NAS 1.26:178380 ..... N88-13000* #
NAS 1.26:178397 ..... N88-12979* #
NAS 1.26:178399 ..... N88-12457* #
NAS 1.26:178400 ..... N88-12497* #
NAS 1.26:179216 ..... N88-12532* #
NAS 1.26:179218 ..... N88-12533* #
NAS 1.26:179222 ..... N88-12754* #
NAS 1.26:179223 ..... N88-12870* #
NAS 1.26:179224 ..... N88-12537* #
NAS 1.26:179586 ..... N88-12875* #
NAS 1.26:180832 ..... N88-12541* #
NAS 1.26:181505 ..... N88-13060* #
NAS 1.26:181506 ..... N88-12498* #
NAS 1.26:181520 ..... N88-13210* #
NAS 1.26:181522 ..... N88-12953* #
NAS 1.26:181523 ..... N88-12952* #
NAS 1.26:181525 ..... N88-12549* #
NAS 1.26:181526 ..... N88-12748* #
NAS 1.26:181530 ..... N88-13005* #
NAS 1.26:181531 ..... N88-13084* #
NAS 1.26:181532 ..... N88-12484* #
NAS 1.26:181533 ..... N88-12483* #
NAS 1.26:181534 ..... N88-12465* #
NAS 1.26:181535 ..... N88-12557* #
NAS 1.26:181537 ..... N88-12817* #
NAS 1.26:181540 ..... N88-12618* #
NAS 1.26:181541 ..... N88-12619* #
NAS 1.26:181542 ..... N88-12665* #
NAS 1.26:181543 ..... N88-12712* #
NAS 1.26:181544 ..... N88-12908* #
NAS 1.26:181545 ..... N88-12479* #
NAS 1.26:181546 ..... N88-12679* #
NAS 1.26:181547 ..... N88-12678* #
NAS 1.26:181548 ..... N88-12486* #
NAS 1.26:181549 ..... N88-13024* #
NAS 1.26:181550 ..... N88-12959* #
NAS 1.26:181551 ..... N88-12730* #
NAS 1.26:181558 ..... N88-12890* #
NAS 1.55:2476 ..... N88-12520* #
NAS 1.60:2760 ..... N88-12928* #
NAS 1.60:2762 ..... N88-12454* #
NAS 1.60:2765 ..... N88-12538* #
NAS 1.60:2769 ..... N88-12455*
NAS 1.60:2773 ..... N88-12480* #
NAS 1.60:2774 ..... N88-12543* #
NAS 1.60:2780 ..... N88-13002* #
NAS 1.60:2783 ..... N88-12487* #
NAS 1.61:1195 ..... N88-13015* #

NASA-CP-2476 ..... N88-12520* #

NASA-CR-4007 ..... N88-12452* #
NASA-CR-4104 ..... N88-12897* #
NASA-CR-4105 ..... N88-12458* #
NASA-CR-4108 ..... N88-12969* #
NASA-CR-166577 ..... N88-12482* #
NASA-CR-172013 ..... N88-12928* #
NASA-CR-172015 ..... N88-12501* #
NASA-CR-172017 ..... N88-12747* #
NASA-CR-172035 ..... N88-12617* #
NASA-CR-177396 ..... N88-13006* #
NASA-CR-177397 ..... N88-12472* #
NASA-CR-177409 ..... N88-12954* #
NASA-CR-177438 ..... N88-12478* #
NASA-CR-177440 ..... N88-12453* #
NASA-CR-177443 ..... N88-12477* #
NASA-CR-177450 ..... N88-12471* #
NASA-CR-177453 ..... N88-12493* #
NASA-CR-177456 ..... N88-12463* #
NASA-CR-177458 ..... N88-12482* #
NASA-CR-178377 ..... N88-12934* #
NASA-CR-178379 ..... N88-12935* #
NASA-CR-178380 ..... N88-13000* #
NASA-CR-178397 ..... N88-12979* #
NASA-CR-178399 ..... N88-12457* #
NASA-CR-178400 ..... N88-12497* #
NASA-CR-179216 ..... N88-12532* #
NASA-CR-179218 ..... N88-12533* #
NASA-CR-179222 ..... N88-12754* #
NASA-CR-179223 ..... N88-12870* #
NASA-CR-179224 ..... N88-12537* #
NASA-CR-179586 ..... N88-12875* #
NASA-CR-180832 ..... N88-12541* #
NASA-CR-181505 ..... N88-13060* #
NASA-CR-181506 ..... N88-12498* #
NASA-CR-181520 ..... N88-13210* #
NASA-CR-181522 ..... N88-12953* #
NASA-CR-181523 ..... N88-12952* #
NASA-CR-181525 ..... N88-12549* #
NASA-CR-181526 ..... N88-12748* #
NASA-CR-181530 ..... N88-13005* #
NASA-CR-181531 ..... N88-13084* #
NASA-CR-181532 ..... N88-12484* #
NASA-CR-181533 ..... N88-12483* #
NASA-CR-181534 ..... N88-12465* #
NASA-CR-181535 ..... N88-12557* #
NASA-CR-181537 ..... N88-12817* #
NASA-CR-181540 ..... N88-12618* #
NASA-CR-181541 ..... N88-12619* #
NASA-CR-181542 ..... N88-12665* #
NASA-CR-181543 ..... N88-12712* #
NASA-CR-181544 ..... N88-12908* #
NASA-CR-181545 ..... N88-12479* #
NASA-CR-181546 ..... N88-12679* #
NASA-CR-181547 ..... N88-12678* #
NASA-CR-181548 ..... N88-12486* #
NASA-CR-181549 ..... N88-13024* #
NASA-CR-181550 ..... N88-12959* #
NASA-CR-181551 ..... N88-12730* #
NASA-CR-181558 ..... N88-12890* #

NASA-MPD-1683 ..... N88-12473* #

NASA-RP-1195 ..... N88-13015* #

NASA-SP-7011(304) N88-12922*
NASA-SP-7037(219) N88-12470*

NASA-TM-4009 ..... N88-12456*
NASA-TM-86521 ..... N88-13083* #
NASA-TM-86703 ..... N88-12932* #
NASA-TM-86997 ..... N88-12461* #
NASA-TM-87184 ..... N88-12473* #
NASA-TM-88313 ..... N88-12494* #
NASA-TM-88844 ..... N88-12515* #
NASA-TM-89092 ..... N88-12531* #
NASA-TM-89681 ..... N88-12540* #
NASA-TM-100012 ..... N88-12991* #
NASA-TM-100015 ..... N88-12486* #
NASA-TM-100016 ..... N88-12924* #
NASA-TM-100023 ..... N88-12495* #
NASA-TM-100116 ..... N88-12796* #
NASA-TM-100119 ..... N88-12727* #
NASA-TM-100127 ..... N88-12542* #
NASA-TM-100134 ..... N88-12490* #
NASA-TM-100144 ..... N88-12877* #
NASA-TM-100145 ..... N88-12878* #
NASA-TM-100176 ..... N88-12552* #
NASA-TM-100180 ..... N88-12797* #
NASA-TM-100181 ..... N88-12798* #
NASA-TM-100191 ..... N88-12539* #

NASA-TM-100205 ..... N88-12752* #
NASA-TM-100223 ..... N88-13209* #
NASA-TM-100236 ..... N88-12551* #
NASA-TM-100245 ..... N88-12825* #
NASA-TM-100252 ..... N88-12763* #
NASA-TM-100315 ..... N88-13016* #
NASA-TM-100458 ..... N88-12927* #
NASA-TM-100495 ..... N88-12544* #
NASA-TM-100502 ..... N88-12459* #
NASA-TM-100504 ..... N88-12496* #
NASA-TM-100507 ..... N88-13003* #

NASA-TP-2760 ..... N88-12928* #
NASA-TP-2762 ..... N88-12454* #
NASA-TP-2765 ..... N88-12538* #
NASA-TP-2769 ..... N88-12455*
NASA-TP-2773 ..... N88-12480* #
NASA-TP-2774 ..... N88-12543* #
NASA-TP-2780 ..... N88-13002* #
NASA-TP-2783 ..... N88-12487* #

NCAR/AR-86 ..... N88-12901 #

NCAR/TN-296/1A ..... N88-12899 #

NEAR-TR-360 ..... N88-12463* #

NMRDI-2-74-4610 ..... N88-13091 #

NOAA-TM-NWS-FCST-32 ..... N88-12898 #

NPL-DITC-87/87 ..... N88-12664 #

NPS52-87-034 ..... N88-12499 #

NRC-28207 ..... N88-12819 #
NRC-28342 ..... N88-12518 #

NRL-MR-6004 ..... N88-13021 #
NRL-MR-6028 ..... N88-12773 #

NSMRL-1093 ..... N88-12925 #

NSWC/TR-86-46 ..... N88-12667 #
NSWC/TR-86-412 ..... N88-12567 #
NSWC/TR-87-126 ..... N88-12569 #

NTIA-87-219 ..... N88-12662 #

NTU-CL/TRS-231 ..... N88-12663 #

OMI-181 ..... N88-12772 #

ORC-87-10 ..... N88-12998 #

ORNL-6335 ..... N88-12949 #
ORNL-6408 ..... N88-12830 #

ORNL/SUB-83-43369/01 ..... N88-12604 #

ORNL/TM-10164 ..... N88-13045 #
ORNL/TM-10210 ..... N88-12882 #
ORNL/TM-10410 ..... N88-12947 #
ORNL/TM-10469 ..... N88-12605 #
ORNL/TM-10486 ..... N88-12968 #
ORNL/TM-10493 ..... N88-12966 #
ORNL/TM-10550 ..... N88-13207 #
ORNL/TM-10581 ..... N88-12956 #

OSU-716148-22 ..... N88-12498* #

OTA-ISC-340 ..... N88-13087 #

PB87-100418 ..... N88-12716 #
PB87-100434 ..... N88-12717 #
PB87-102935 ..... N88-12718 #
PB87-104154 ..... N88-12555 #
PB87-104162 ..... N88-12661 #
PB87-106274 ..... N88-12592 #
PB87-106449 ..... N88-12970 #
PB87-107454 ..... N88-12886 #
PB87-107645 ..... N88-12666 #
PB87-108254 ..... N88-12867 #
PB87-110730 ..... N88-13193 #
PB87-123733 ..... N88-12719 #
PB87-123873 ..... N88-12720 #
PB87-217949 ..... N88-13017 #
PB87-219960 ..... N88-12663 #
PB87-220018 ..... N88-12664 #
PB87-220935 ..... N88-12858 #
PB87-222030 ..... N88-12910 #
PB87-222337 ..... N88-12737 #
PB87-223053 ..... N88-12896 #
PB87-223418 ..... N88-13087 #
PB87-224366 ..... N88-12899 #
PB87-224945 ..... N88-12900 #

PB87-225157 ..... N88-12736 #
PB87-226155 ..... N88-12613 #
PB87-226197 ..... N88-12662 #
PB87-226633 ..... N88-13074 #
PB87-228391 ..... N88-12901 #

PCRL-FR-87-004 ..... N88-12615 #

PD-FM-8716 ..... N88-12931 #
PD-FM-8718 ..... N88-12753 #
PD-FM-8725 ..... N88-12990 #

PD-MT-8721 ..... N88-12607 #
PD-MT-8722 ..... N88-12606 #
PD-MT-8726 ..... N88-12567 #
PD-MT-8729 ..... N88-12568 #

PNL-SA-14421 ..... N88-12559 #
PNL-SA-14517 ..... N88-12873 #
PNL-SA-14586 ..... N88-12874 #
PNL-SA-14674 ..... N88-12973 #
PNL-SA-14791 ..... N88-12785 #
PNL-SA-14794 ..... N88-12609 #
PNL-SA-15084 ..... N88-12620 #
PNL-SA-15189 ..... N88-12961 #

PNL-6283 ..... N88-12881 #
PNL-6293 ..... N88-12902 #

PSI-TR-154/710 ..... N88-12563 #

RADC-TR-87-67 ..... N88-12726 #

REPT-25 ..... N88-12736 #
REPT-86-30 ..... N88-12737 #
REPT-86/42 ..... N88-13193 #
REPT-015 ..... N88-12596 #
REPT-016 ..... N88-13058 #
REPT-1794 ..... N88-12588 #
REPT-1985-20 ..... N88-12661 #
REPT-7066-01 ..... N88-13006* #
REPT-85168 ..... N88-12932* #

RFP-4029 ..... N88-12794 #

RI/RD-87-211 ..... N88-12541* #

RI/RD86-165-REV ..... N88-12537* #

R86-915999-13 ..... N88-12452* #

S-565 ..... N88-12927* #

SAND-86-1817 ..... N88-12750 #
SAND-86-2164 ..... N88-12876 #
SAND-86-2825 ..... N88-12802 #
SAND-86-8056 ..... N88-12884 #
SAND-86-8058 ..... N88-12880 #
SAND-87-0165C ..... N88-12827 #
SAND-87-0166C ..... N88-12812 #
SAND-87-0454C ..... N88-12936 #
SAND-87-0632 ..... N88-12829 #
SAND-87-0642C ..... N88-12513 #
SAND-87-0644C ..... N88-12770 #
SAND-87-0707 ..... N88-12734 #
SAND-87-0797 ..... N88-12585 #
SAND-87-0889 ..... N88-12713 #
SAND-87-0903 ..... N88-12968 #
SAND-87-0924C ..... N88-12735 #
SAND-87-0966C ..... N88-12826 #
SAND-87-0967C ..... N88-12813 #
SAND-87-0998C ..... N88-12872 #
SAND-87-1001C ..... N88-13059 #
SAND-87-1106C ..... N88-12728 #
SAND-87-1111 ..... N88-12766 #
SAND-87-1395C ..... N88-12464 #
SAND-87-1398C ..... N88-12550 #
SAND-87-2098C ..... N88-12603 #
SAND-87-2383C ..... N88-13068 #
SAND-87-2383C ..... N88-12674 #
SAND-87-8021 ..... N88-12879 #
SAND-87-8225 ..... N88-12751 #

SD-TR-87-37 ..... N88-12943 #

SLAC-PUB-4398 ..... N88-12977 #

SR-2 ..... N88-12772 #
SR-7 ..... N88-12889 #

SRA-R930012F ..... N88-12948 #

ST-201 ..... N88-12867 #

TAUP/N-183/87 ..... N88-13079 #

TGAL-86-6 ..... N88-12888 #

TR-1 ..... N88-12612 #
TR-3 ..... N88-13054 #
TR-4 ..... N88-13055 #
TR-5 ..... N88-13056 #
TR-7 ..... N88-13052 #
TR-8 ..... N88-13053 #
TR-18 ..... N88-12724 #
TR-19 ..... N88-12962 #
TR-20 ..... N88-12793 #
TR-27 ..... N88-13004 #
TR-28 ..... N88-13050 #
TR-44 ..... N88-13049 #
TR-52 ..... N88-12996 #
TR-0086(6776)-2 ..... N88-12943 #
TR-1239-1 ..... N88-12493* #

UB/PSEEE-389 ..... N88-12720 #

UCB/ERL-M-87/51 ..... N88-12731 #

UCID-21062 ..... N88-12714 #
UCID-21152 ..... N88-12788 #
UCID-21188 ..... N88-12816 #
UCID-21189 ..... N88-12729 #
UCID-21193 ..... N88-12963 #

UCLA/PPG-1074 ..... N88-13044 #

UCRL-15894 ..... N88-13041 #
UCRL-15942 ..... N88-13029 #
UCRL-95275-REV-1 ..... N88-12540* #
UCRL-95577 ..... N88-12554 #
UCRL-96494 ..... N88-12779 #
UCRL-96632 ..... N88-12951 #
UCRL-96662 ..... N88-12780 #
UCRL-96676 ..... N88-13024* #
UCRL-96700 ..... N88-12643 #
UCRL-96911 ..... N88-13082 #
UCRL-97268 ..... N88-12739 #
UCRL-97278 ..... N88-12913 #
UCRL-97323 ..... N88-12745 #
UCRL-97325 ..... N88-13067 #
UCRL-97336 ..... N88-13043 #
UCRL-97378 ..... N88-12519 #

UFPB-DF-14/86 ..... N88-12985 #

UILU-ENG-87-1763 ..... N88-12987 #
UILU-ENG-87-1764 ..... N88-12994 #
UILU-ENG-87-2242 ..... N88-12941 #
UILU-ENG-87-2243 ..... N88-12942 #
UILU-ENG-87-2247 ..... N88-12723 #

UIUCDCS-R-87-1375 ..... N88-12987 #
UIUCDCS-R-87-1376 ..... N88-12994 #

ULRF-436/CAR ..... N88-12889 #

USAAEFA-86-02 ..... N88-12492 #

USAAVSCOM-TR-85-A-5 ..... N88-12954* #

USAFSAM-TR-86-26 ..... N88-12491 #

UTEC-MD-87-002 ..... N88-12726 #

UTIAS-TN-265 ..... N88-12489 #
UTIAS-TN-266 ..... N88-12657 #

UTRC/R87-917470-1 ..... N88-12546 #

UVA/528260/CHE88/101 ..... N88-12619* #
UVA/528260/CHE88/102 ..... N88-12618* #

UWFDM-725 ..... N88-13028 #

VPI-E-87-20 ..... N88-12549* #

VTT/PUB-30 ..... N88-12716 #

VTT/RN-665 ..... N88-12858 #

VTT/RR-403 ..... N88-12717 #

WES/MP/GL-87-16 ..... N88-12500 #

Y-2357 ..... N88-13008 #
Y-2387 ..... N88-12604 #

☆ U.S. GOVERNMENT PRINTING OFFICE: 1988— 202-150/80002

FEDERAL REGIONAL DEPOSITORY LIBRARIES

ALABAMA

AUBURN UNIV. AT MONTGOMERY LIBRARY
Documents Department
Montgomery, AL 36193
(205) 271-9650

UNIV. OF ALABAMA LIBRARY
Documents Dept.-Box S
University, AL 35486
(205) 348-6046

ARIZONA

DEPT. OF LIBRARY, ARCHIVES AND PUBLIC RECORDS
Third Floor—State Cap.
1700 West Washington
Phoenix, AZ 85007
(602) 255-4121

UNIVERSITY OF ARIZONA LIB.
Government Documents Dept.
Tucson, AZ 85721
(602) 621-6433

ARKANSAS

ARKANSAS STATE LIBRARY
One Capitol Mall
Little Rock, AR 72201
(501) 371-2326

CALIFORNIA

CALIFORNIA STATE LIBRARY
Govt. Publications Section
P.O. Box 2037
Sacramento, CA 95809
(916) 324-4863

COLORADO

UNIV OF COLORADO LIB.
Government Pub. Division
Campus Box 184
Boulder, CO 80309
(303) 492-8834

DENVER PUBLIC LIBRARY
Govt. Pub. Department
1357 Broadway
Denver, CO 80203
(303) 571-2131

CONNECTICUT

CONNECTICUT STATE LIBRARY
Government Documents Unit
231 Capitol Avenue
Hartford, CT 06106
(203) 566-7029

FLORIDA

UNIV. OF FLORIDA LIBRARIES
Library West
Documents Department
Gainesville, FL 32611
(904) 392-0367

GEORGIA

UNIV. OF GEORGIA LIBRARIES
Government Reference Dept.
Athens, GA 30602
(404) 542-8949

HAWAII

UNIV. OF HAWAII LIBRARY
Govt. Documents Collection
2550 The Mall
Honolulu, HI 96822
(808) 948-8230

IDAHO

UNIV. OF IDAHO LIBRARY
Documents Section
Moscow, ID 83843
(208) 885-6344

ILLINOIS

ILLINOIS STATE LIBRARY
Information Services Branch
Centennial Building
Springfield, IL 62756
(217) 782-5185

INDIANA

INDIANA STATE LIBRARY
Serials Documents Section
140 North Senate Avenue
Indianapolis, IN 46204
(317) 232-3686

IOWA

UNIV. OF IOWA LIBRARIES
Govt. Documents Department
Iowa City, IA 52242
(319) 353-3318

KANSAS

UNIVERSITY OF KANSAS
Doc. Collect—Spencer Lib.
Lawrence, KS 66045-2800
(913) 864-4662

KENTUCKY

UNIV. OF KENTUCKY LIBRARIES
Govt. Pub. Department
Lexington, KY 40506-0039
(606) 257-3139

LOUISIANA

LOUISIANA STATE UNIVERSITY
Middleton Library
Govt. Docs. Dept.
Baton Rouge, LA 70803
(504) 388-2570

LOUISIANA TECHNICAL UNIV. LIBRARY
Documents Department
Ruston, LA 71272-0046
(318) 257-4962

MAINE

UNIVERSITY OF MAINE
Raymond H. Fogler Library
Tri-State Regional Documents Depository
Orono, ME 04469
(207) 581-1680

MARYLAND

UNIVERSITY OF MARYLAND
McKeldin Lib.—Doc. Div.
College Park, MD 20742
(301) 454-3034

MASSACHUSETTS

BOSTON PUBLIC LIBRARY
Government Docs. Dept.
Boston, MA 02117
(617) 536-5400 ext.226

MICHIGAN

DETROIT PUBLIC LIBRARY
Sociology Department
5201 Woodward Avenue
Detroit, MI 48202-4093
(313) 833-1409

MICHIGAN STATE LIBRARY
P.O. Box 30007
Lansing, MI 48909
(517) 373-1593

MINNESOTA

UNIVERSITY OF MINNESOTA
Government Pubs. Division
409 Wilson Library
309 19th Avenue South
Minneapolis, MN 55455
(612) 373-7870

MISSISSIPPI

UNIV. OF MISSISSIPPI LIB.
Documents Department
University, MS 38677
(601) 232-5857

MONTANA

UNIV. OF MONTANA
Mansfield Library
Documents Division
Missoula, MT 59812
(406) 243-6700

NEBRASKA

UNIVERSITY OF NEBRASKA - LINCOLN
Love Library
Documents Department
Lincoln, NE 68588-0410
(402) 472-2562

NEVADA

UNIVERSITY OF NEVADA LIB.
Govt. Pub. Department
Reno, NV 89557-0044
(702) 784-6579

NEW JERSEY

NEWARK PUBLIC LIBRARY
5 Washington Street
Newark, NJ 07101-0630
(201) 733-7812

NEW MEXICO

UNIVERSITY OF NEW MEXICO
Zimmerman Library
Government Pub. Dept.
Albuquerque, NM 87131
(505) 277-5441

NEW MEXICO STATE LIBRARY
Reference Department
325 Don Gaspar Avenue
Santa Fe, NM 87503
(505) 827-3826

NEW YORK

NEW YORK STATE LIBRARY
Empire State Plaza
Albany, NY 12230
(518) 474-5563

NORTH CAROLINA

UNIVERSITY OF NORTH CAROLINA AT CHAPEL HILL
Davis Library
BA/SS Documents Division
Chapel Hill, NC 27515
(919) 962-1151

NORTH DAKOTA

UNIVERSITY OF NORTH DAKOTA
Chester Fritz Library
Documents Department
Grand Forks, ND 58202
(701) 777-4629
In cooperation with North Dakota State Univ. Library

OHIO

STATE LIBRARY OF OHIO
Documents Department
65 South Front Street
Columbus, OH 43266-0334
(614) 462-7051

OKLAHOMA

OKLAHOMA DEPT. OF LIB.
Government Documents
200 NE 18th Street
Oklahoma City, OK 73105
(405) 521-2502, ext. 252

OKLAHOMA STATE UNIV. LIB.
Documents Department
Stillwater, OK 74078
(405) 624-6546

OREGON

PORTLAND STATE UNIV. LIB.
Documents Department
P.O. Box 1151
Portland, OR 97207
(503) 229-3673

PENNSYLVANIA

STATE LIBRARY OF PENN.
Government Pub. Section
P.O. Box 1601
Harrisburg, PA 17105
(717) 787-3752

TEXAS

TEXAS STATE LIBRARY
Public Services Department
P.O. Box 12927—Cap. Sta.
Austin, TX 78711
(512) 475-2996

TEXAS TECH. UNIV. LIBRARY
Govt. Documents Department
Lubbock, TX 79409
(806) 742-2268

UTAH

UTAH STATE UNIVERSITY
Merrill Library, U.M.C. 30
Logan, UT 84322
(801) 750-2682

VIRGINIA

UNIVERSITY OF VIRGINIA
Alderman Lib.—Public Doc.
Charlottesville, VA 22903-2498
(804) 924-3133

WASHINGTON

WASHINGTON STATE LIBRARY
Documents Section
Olympia, WA 98504
(206) 753-4027

WEST VIRGINIA

WEST VIRGINIA UNIV. LIB.
Documents Department
Morgantown, WV 26506-6069
(304) 293-3640

WISCONSIN

MILWAUKEE PUBLIC LIBRARY
814 West Wisconsin Avenue
Milwaukee, WI 53233
(414) 278-3065

ST. HIST LIB. OF WISCONSIN
Government Pub. Section
816 State Street
Madison, WI 53706
(608) 262-4347

WYOMING

WYOMING STATE LIBRARY
Supreme Ct. & Library Bld.
Cheyenne, WY 82002
(307) 777-5919

National Aeronautics and
Space Administration
Code NTT-4
Washington, D.C.
20546

Official Business

Penalty for Private Use, $300

SPECIAL FOURTH-CLASS RATE
POSTAGE & FEES PAID
NASA
PERMIT No. G 27

NASA
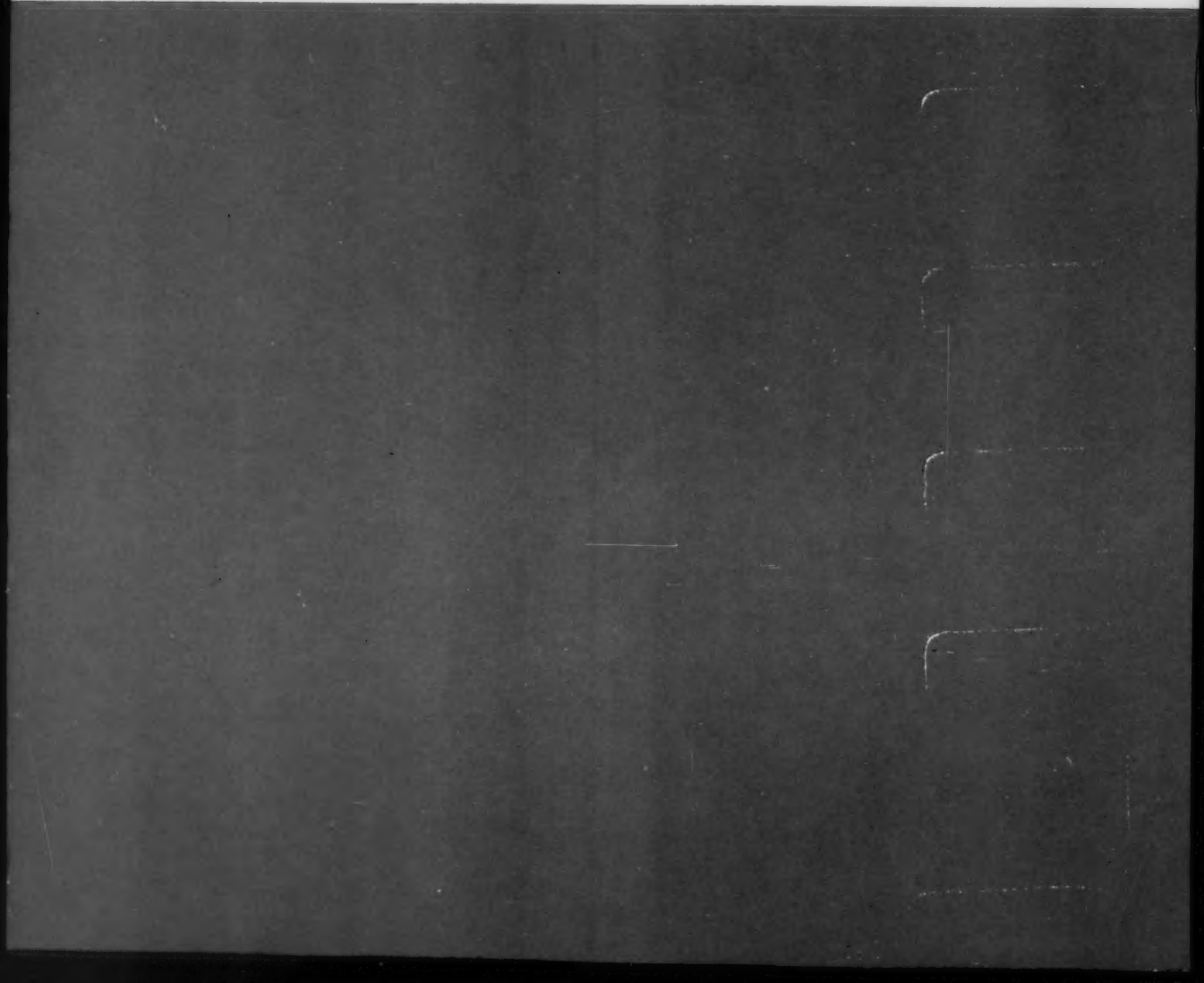
POSTMASTER: If Undeliverable (Section 158
Postal Manual) Do Not Return